

STRUCTURE, HEATS OF FORMATION, AND BOND DISSOCIATION ENERGIES
OF GROUP IIIA–GROUP IVA–GROUP VA MOLECULES
FOR CHEMICAL HYDROGEN STORAGE SYSTEMS

by

DANIEL JUSTIN GRANT

A DISSERTATION

Submitted in partial fulfillment of the requirements
for the degree of Doctor of Philosophy
in the Department of Chemistry
in the Graduate School of
The University of Alabama

TUSCALOOSA, ALABAMA

2010

Copyright Daniel Justin Grant 2010
ALL RIGHTS RESERVED

ABSTRACT

The potential of Group IIIA–IVA–VA compounds for chemical hydrogen storage have been evaluated from thermodynamic properties, heats of formation and bond dissociation energies (BDEs), from CCSD(T) calculations in conjunction with correlation consistent basis sets extrapolated to the complete basis set limit, including additional core-valence, scalar-relativistic, and atomic spin-orbit corrections. Geometry optimizations and frequencies were computed at the CCSD(T)/MP2 levels. Diatomic distances, frequencies, and anharmonic constants were obtained from a potential energy curve fit at the CCSD(T) level. Calculations show that $\text{AlH}_3\text{NH}_3(\text{g})$, $\text{AlH}_3\text{PH}_3(\text{g})$, $[\text{AlH}_4^-][\text{NH}_4^+](\text{s})$, $[\text{AlH}_4^-][\text{PH}_4^+](\text{s})$, and $[\text{BH}_4^-][\text{PH}_4^+](\text{s})$ can potentially serve as hydrogen storage systems, in addition to BH_3NH_3 and $[\text{BH}_4^-][\text{NH}_4^+](\text{s})$. Dehydrogenation of methyl-substituted ammonia boranes is most favorable across B-N where methylation at N reduces the reaction exothermicity, becoming more thermoneutral. The adiabatic π -bond energy is defined as the rotational barrier between the ground state and C_s transition state structures, the intrinsic π -bond energy as the adiabatic rotational barrier corrected for inversion, and σ -bond energy, as the adiabatic dissociation energy minus the adiabatic π -bond energy. Within the substituted boranes $\text{H}_{3-n}\text{BX}_n$ ($\text{X} = \text{F}, \text{Cl}, \text{Br}, \text{I}, \text{NH}_2, \text{OH}, \text{and SH}$), fluorines have the largest BDEs while the second and third largest are for hydroxyl and amino. Hydride and fluoride affinities have been predicted to judge the Lewis acidities with the highest affinities found for BI_3 , lowest for $\text{B}(\text{NH}_2)_3$, and within the boron trihalides, the acidity increases down the periodic table. Although the sequential dehydrogenation of diammoniosilane is exothermic, further dehydrogenation is largely endothermic, requiring an effective coupling process to

remove three hydrogen molecules thermoneutrally. Except for methylsilyl silane, methyl and halide substitution increases the Si-X and Si-C BDEs compared to the halosilanes and methylsilane, respectively. The differences in the adiabatic and diabatic BDEs in the PF_xO and SF_xO compounds are employed to explain trends in their stepwise BDEs. The adiabatic BDE for removal of fluorine from stable closed-shell SF_6 to give the unstable SF_5 radical is 2.8 times the BDE for removal of fluorine from the unstable SF_5 radical to give stable closed-shell SF_4 . Similar principles govern the BDEs of the phosphorous fluorides and the phosphoro and sulfur oxofluorides.

DEDICATION

This dissertation is dedicated to my parents, Daniel C. Grant and Susanna B. Grant, and my sister Danae N. Grant, who have never wavered in their love, prayers, and support; having shown me by their lives that with dedication, hard work, and perseverance that all things are possible.

LIST OF ABBREVIATIONS AND SYMBOLS

aug-cc-pVnZ	Augmented, correlation-consistent, polarized valence n zeta basis sets, where n = double (D), triple (T), quadruple (Q), quintuple (5), etc.
aug-cc-pV(n+d)Z	aug-cc-pVnZ basis sets with additional tight d functions for 2 nd row atoms
aug-cc-pVnZ-PP	aug-cc-pVnZ basis sets with pseudo-potentials for heavy atoms (\geq 3 rd row atoms)
aug-cc-pwCVZ	aug-cc-pVnZ basis sets with additional tight core-valence functions
aug-cc-pwCVZ-PP	aug-cc-pVnZ basis sets with additional core-valence functions and pseudo-potentials for heavy atoms (\geq 3 rd row atoms)
B3LYP	Becke 3-parameter (exchange), Lee, Yang and Parr (correlation) DFT functional
BDE	Bond dissociation energy
BE	Bond energy
CBS	Complete basis set
cc-pVnZ	Correlation-consistent, polarized valence n zeta basis sets, where n = double (D), triple (T), quadruple (Q), quintuple (5), etc.
CC	Coupled cluster theory
CCn	Coupled cluster singles, doubles, triples, where n = S, D, T, etc.
CCSD(T)	Coupled cluster singles, doubles, and perturbative triples
CI	Configuration interaction
CI n	Configuration interaction singles, doubles, triples, where n = S, D, T, etc.

CV	Core-valence
$D_{0,0K}$	Total Atomization or dissociation energy
DFT	Density functional theory
DKH	Douglas-Kroll-Hess
DZVP2	DFT-optimized double zeta basis set plus polarization
EA	Electron affinity
ΔE_{CBS}	Complete basis set valence electronic atomization energy
ΔE_{CV}	Core-valence energy correction to the total atomization energy
ΔE_{SO}	Atomic spin orbit energy correction to the total atomization energy
ΔE_{SR}	Scalar relativistic (Mass-velocity Darwin or Douglas-Kroll-Hess) energy correction to the total atomization energy
ΔE_{ZPE}	Zero point energy correction to the total atomization energy
FA	Fluoride affinity
G_n	Gaussian- n theory, $n = 2, 3$
$G_n(\text{MP2})$	G_n calculation using a reduced Møller-Plesset order (i.e., MP2)
HA	Hydride affinity
$\Delta H_{f,0K}$	Heat of formation at 0 K
$\Delta H_{f,298K}$	Heat of formation at 298 K
HF	Hartree-Fock
ΔH_{rxn}	Reaction enthalpy change
I	Ionic strength

MO	Molecular orbital
MBPT	Many-body perturbation theory
MP2	2 nd order Møller-Plesset perturbation theory
MVD	Mass-velocity Darwin
NBO	Natural bond order
NIST-JANAF	National Institute of Standards – Joint Army–Navy–Air Force
NMR	Nuclear magnetic resonance
PA	Proton affinity
PP	Pseudopotential
RECP	Relativistic effective core potential
ΔS	Entropy change
SCF	Self-consistent field
SO	Spin-orbit
SR	Scalar-relativistic
U_L	Lattice energy
V_m	Ion molecular volume of the lattice
V_+	Ion volume of the cation
V_-	Ion volume of the anion
ZPE	Zero-point energy

ACKNOWLEDGMENTS

I am pleased to have this opportunity to thank the many family, friends, faculty members, coworkers, and colleagues who have assisted me in completing the research projects encompassed in this dissertation. I am most indebted to Dr. David A. Dixon, chairman and academic research advisor, for sharing his expertise and wisdom regarding computational chemistry.

I am also grateful to my committee members, Dr. Anthony J. Arduengo III, Dr. Shane C. Street, Dr. Martin G. Bakker, and Dr. Heath C. Turner for their invaluable input, inspiring and challenging questions, guidance, patience, and continuous support and involvement through out my graduate school experience at The University of Alabama.

I would also like to extend a special thanks to the various collaborators who have contributed to the work presented in this dissertation: Karl O. Christe, Loker Hydrocarbon Research Institute and Department of Chemistry, University of Southern California; Myrna H. Matus, Unidad de Servicios de Apoyo en Resolución Analítica, Universidad Veracruzana, México; Anthony J. Arduengo III, Jackson R. Switzer, and Kevin D. Anderson, Department of Chemistry, The University of Alabama; Donald M. Camaioni and Robert G. Potter, Fundamental Sciences Division, Pacific Northwest National Laboratory; Joseph S. Francisco, Department of Chemistry, H. C. Brown Laboratory, Purdue University; Sharon R. Neufeldt and Clinton F. Lane, Department of Chemistry and Biochemistry, Northern Arizona University.

I am also truly thankful for the funding to accomplish this work, which was provided in part by the Department of Energy, Office of Energy Efficiency, and Renewable Energy under the

Hydrogen Storage Grand Challenge. The work was done as part of the Chemical Hydrogen Storage Center. This research was performed in part by using the Molecular Science Computing Facility in the William R. Wiley Environmental Molecular Sciences Laboratory, a national scientific user facility sponsored by the U.S. Department of Energy's Office of Biological and Environmental Research and located at the Pacific Northwest National Laboratory, which is operated for the Department of Energy by Battelle, and I would like to extend a special thanks as well.

Furthermore, this dissertation research would not have been possible had it not been for the continuous support of my friends, coworkers, fellow graduate students, and of course of my family, who have never stopped encouraging me to persist and persevere.

Finally, I would like to thank The University of Alabama and the Department of Chemistry for providing the means and the surroundings for an enjoyable and enlightening stay in Tuscaloosa, Alabama.

TABLE OF CONTENTS

ABSTRACT	ii
DEDICATION.....	iv
LIST OF ABBREVIATIONS AND SYMBOLS	v
ACKNOWLEDGMENTS	viii
LIST OF TABLES	xvi
LIST OF FIGURES	xx
CHAPTER 1 INTRODUCTION.....	1
1.1 Background.....	1
1.2 Hydrogen Production and Storage	2
1.3 Hydrogen Fuel Cells, Distribution, and Delivery	4
1.4 Chemical Hydrogen Storage.....	4
CHAPTER 2 COMPUTATIONAL METHODOLOGY	13
2.1 Introduction.....	13
2.2 Hartree–Fock Theory	14
2.3 Basis Sets	17
2.4 Electron Correlation Methods	22
2.4.1 Configuration Interaction Theory.....	23
2.4.2 Many–Body Perturbation Theory	24
2.4.3 Coupled Cluster Theory.....	26
2.5 Computational Thermochemistry.....	28

CHAPTER 3	THERMODYNAMIC PROPERTIES OF MOLECULAR BORANE PHOSPHINES, ALANE AMINES, AND PHOSPHINE ALANES AND THE $[\text{BH}_4^-][\text{PH}_4^+]$, $[\text{AlH}_4^-][\text{NH}_4^+]$, AND $[\text{AlH}_4^-][\text{PH}_4^+]$ SALTS FOR CHEMICAL HYDROGEN STORAGE SYSTEMS FROM AB INITIO ELECTRONIC STRUCTURE THEORY	33
	3.1 Introduction.....	33
	3.2 Computational Approach.....	36
	3.3 Results and Discussion	39
	3.4 Conclusions.....	46
	3.5 References.....	65
	3.5 Appendix.....	70
CHAPTER 4	σ - AND π -BOND STRENGTHS IN MAIN GROUP 3-5 COMPOUNDS	74
	4.1 Introduction.....	74
	4.2 Computational Approach.....	78
	4.3 Results and Discussion	80
	4.4 Conclusions.....	91
	4.5 References.....	104
	4.6 Appendix.....	108
CHAPTER 5	THERMOCHEMISTRY FOR THE DEHYDROGENATION OF METHYL SUBSTITUTED AMMONIA BORANE COMPOUNDS	115
	5.1 Introduction.....	115
	5.2 Experimental Methods.....	118
	5.2.1 Synthesis of Ammonia Borane	118

5.2.2	Synthesis of Methylamine Borane	119
5.2.3	Cosynthesis of Ammonia and Methylamine Borane.....	119
5.2.4	Melting of Ammonia Borane and Methylamine Borane Mixtures.....	120
5.3	Computational Methods	120
5.4	Experimental Results.....	123
5.5	Computational Results.....	124
5.5.1	Geometries and Frequencies	124
5.5.2	Heats of Formation.....	126
5.5.3	Dehydrogenation Reaction Energies	127
5.5.4	Bond Energies	129
5.5.5	Properties of Larger Compounds	135
5.6	Conclusions.....	137
5.7	References.....	157
5.8	Appendix.....	163
CHAPTER 6	HEATS OF FORMATION AND BOND ENERGY OF THE $H_{(3-n)}BX_n$ COMPOUNDS FOR (X = F, Cl, Br, I, NH ₂ , OH, and SH).....	183
6.1	Introduction.....	183
6.2	Computational Approach.....	185
6.3	Results and Discussion	190
6.3.1	Geometries	190

	6.3.2	Heats of Formation	190
	6.3.3	Bond Dissociation Energies	194
	6.3.4	Regeneration of Spent Fuel from Ammonia Borane.....	201
	6.4	Conclusions.....	202
	6.5	References.....	219
	6.6	Appendix.....	224
CHAPTER 7		LEWIS ACIDITIES AND HYDRIDE, FLUORIDE, AND X ⁻ AFFINITIES OF THE BH _{3-n} X _n COMPOUNDS (X = F, Cl, Br, I, NH ₂ , OH, and SH) FROM COUPLED CLUSTER THEORY	251
	7.1	Introduction.....	251
	7.2	Computational Approach.....	253
	7.3	Results and Discussion	256
	7.4	Conclusions.....	265
	7.5	References.....	291
	7.6	Appendix.....	294
CHAPTER 8		DIAMMONIOSILANE: COMPUTATIONAL PREDICTION OF THE THERMODYNAMIC PROPERTIES OF A POTENTIAL CHEMICAL HYDROGEN STORAGE SYSTEM.....	336
	8.1	Introduction.....	336
	8.2	Computational Methods	338
	8.3	Results and Discussion	340
	8.3.1	Geometries and Frequencies	341
	8.3.2	Energies and Heats of Formation	344

	8.4	Conclusions.....	347
	8.5	References.....	355
	8.6	Appendix.....	359
CHAPTER 9		HEATS OF FORMATION AND BOND DISSOCIATION ENERGIES OF THE HALOSILANES, METHYLHALOSILANES AND HALOMETHYLSILANES	368
	9.1	Introduction.....	368
	9.2	Computational Methods	370
	9.3	Results and Discussion	374
	9.3.1	Geometries and Frequencies	374
	9.3.2	Heats of Formation.....	375
	9.3.3	Bond Dissociation Energies.....	376
	9.4	Conclusions.....	380
	9.5	References.....	391
	9.6	Appendix.....	394
CHAPTER 10		BOND DISSOCIATION ENERGIES IN SECOND ROW COMPOUNDS	414
	10.1	Introduction.....	414
	10.2	Computational Approach.....	418
	10.3	Results and Discussion	421
	10.3.1	Geometries	421
	10.3.2	Vibrational Frequencies.....	423

10.3.3 Calculated Heats of Formation	424
10.3.4 Bond Dissociation Energies	427
10.4 Conclusions.....	433
10.5 References.....	455
10.6 Appendix.....	461
CHAPTER 11 CONCLUSIONS	481
REFERENCES.....	488

LIST OF TABLES

3.1.	Optimized CCSD(T) bond lengths (Å) and bond angles (°) for AlH _x and PH _x	48
3.2.	Optimized CCSD(T) bond lengths (Å) and bond angles (°) for BPH _x	49
3.3.	Optimized CCSD(T) bond lengths (Å) and bond angles (°) for AlNH _x	50
3.4.	Optimized CCSD(T) bond lengths (Å) and bond angles (°) for AlPH _x	51
3.5.	Calculated vibrational MP2/(CCSD(T)/aug-cc-pVDZ) frequencies (cm ⁻¹) for AlH _x and PH _x	52
3.6.	Calculated vibrational MP2/cc-pVTZ level frequencies (cm ⁻¹) for BPH _x	53
3.7.	Calculated vibrational MP2/(CCSD(T)/aug-cc-pVDZ) frequencies (cm ⁻¹) for AlNH _x	55
3.8.	Calculated vibrational MP2/(CCSD(T)/aug-cc-pVDZ) frequencies (cm ⁻¹) for AlPH _x	57
3.9.	Components for calculated atomization energies in kcal/mol.....	59
3.10.	Calculated heats of formation (kcal/mol) at 0 K and 298 K.....	61
3.11.	Calculated entropies (cal/mol K) at the MP2/cc-pVTZ level.....	63
3.12.	TΔS corrections for reactions 3.3 to 3.11 in kcal/mol.....	64
4.1.	Donor σ–bond strengths in AH ₃ XH ₃ compounds in kcal/mol.....	93
4.2.	Optimized CCSD(T) bond lengths (Å) and bond angles (°) for the rotated structures of AH ₂ XH ₂ in C _s and C _{2v} symmetries	94
4.3.	Calculated imaginary vibrational MP2/(cc-pVTZ) frequencies (cm ⁻¹).....	95
4.4.	Components for calculated atomization energies in kcal/mol.....	96
4.5.	Calculated heats of formation (kcal/mol) at 0 K and 298 K.....	97
4.6.	Rotation barriers (π–bond energies) and inversion barriers at N or P in kcal/mol	98

4.7.	Adiabatic ($\sigma + \pi$) total dissociation energies in kcal/mol.....	99
4.8.	AH ₂ -H and XH ₂ -H σ -bond energies in kcal/mol.....	100
5.1.	Components for CCSD(T) atomization energies (kcal/mol).....	140
5.2.	Calculated heats of formation in kcal/mol. Experimental values at 298 K in parentheses.....	141
5.3.	Dehydrogenation reactions (kcal/mol)	143
5.4.	Calculated imaginary vibrational frequencies (cm ⁻¹) at the MP2/VTZ level	144
5.5.	Adiabatic rotation barriers (π -bond energies) at 0 K at the MP2/VTZ level (kcal/mol).....	146
5.6.	Adiabatic ($\sigma + \pi$) total dissociation energies and adiabatic σ -bond energies 0 K at the CCSD(T) level (kcal/mol).....	147
5.7.	Adiabatic σ -bond energies (B. E.) in kcal/mol.....	148
5.8.	Calculated G3(MP2) heats of formation (kcal/mol)	150
5.9.	Dehydrogenation reactions at the G3(MP2) level (kcal/mol)	152
6.1.	Optimized CCSD(T) bond lengths (Å) and bond angles (°) for BX, HBX, BX ₂ , and H _{3-n} BX _n for (X = F, Cl, Br, I, NH ₂ , OH, and SH)	205
6.2.	Components for calculated atomization energies in kcal/mol.....	209
6.3.	Heats of formation (kcal/mol) at 0 K and 298 K	212
6.4.	B-X and B-H bond dissociation energies (BDE) in kcal/mol at 0 K	215
6.5.	Disproportionation reactions in kcal/mol at 0 K and 298 K.....	218
7.1.	Components for calculated atomization energies in kcal/mol.....	269
7.2.	Enthalpies of formation (kcal/mol) at 0 K and 298 K.....	273
7.3.	Calculated hydride (HA) and fluoride (FA) affinities in kcal/mol at 0 K and 298 K.....	276

7.4.	Calculated X^- affinities (XA ; $X = Cl, Br, I, NH_2, OH,$ and SH) in kcal/mol at 0 K and 298 K.....	277
7.5.	Calculated electron affinities at 0 K at the CCSD(T)/CBS and B3LYP/aVTZ levels....	279
7.6.	Calculated $BH_{3-n}X_n-A^-$ bond dissociation energies in kcal/mol at 0 K	280
7.7.	Distortion energies at 0 K in kcal/mol at the B3LYP/aVDZ and CCSD(T)/aVTZ levels.....	283
8.1.	CCSD(T) atomization and reaction energies in kcal/mol.....	349
8.2.	Calculated CCSD(T) heats of formation (kcal/mol)	350
8.3.	Dehydrogenation and NH_3 stabilization reactions at 0 K and 298 K (kcal/mol).....	351
8.4.	Calculated Si NMR chemical shifts for SiH_4 (T_d), SiH_4 (D_{4h}) and $H_4Si(NH_3)_2$ (C_i) at the B3LYP/Alrichs-VTZ+P level (ppm)	352
9.1.	CCSD(T) atomization and reaction energies in kcal/mol.....	382
9.2.	Calculated heats of formation (kcal/mol)	384
9.3.	Calculated bond dissociation energies (BDEs) at 0 K (kcal/mol)	385
9.4.	Calculated Si-X and Si-C stretching frequencies at the CCSD(T)/aVTZ-PP level (cm^{-1})	386
10.1.	Experimental and calculated bond dissociation energies in kcal/mol at 0 K	437
10.2.	Optimized bond lengths (\AA) and angles (degrees) for PF_xO_y equilibrium geometries.....	439
10.3.	Optimized bond lengths (\AA) and angles (degrees) for SF_xO_y equilibrium geometries.....	441
10.4.	Components for calculating the atomization energies in kcal/mol.....	444
10.5.	Heats of formation (kcal/mol) at 0 K and 298 K	446

10.6. Electronic contribution to the CCSD(T) singlet-triplet splitting (kcal/mol) for SF _x O _y and PF _x O _y compounds.....	448
--	-----

LIST OF FIGURES

4.1.	Optimized molecular structures for BH_2NH_2 , AlH_2NH_2 , BH_2PH_2 , AlH_2PH_2 , and the corresponding rotated structures	102
4.2.	HOMO for the ground state and rotated structures of BH_2NH_2 , AlH_2NH_2 , BH_2PH_2 , and AlH_2PH_2	103
5.1.	Melting temperature ranges in $^\circ\text{C}$ of ammonia borane/methylamine borane mixtures as a function of the weight percent of ammonia borane	155
5.2.	Optimized molecular structures for $\text{H}_2\text{B}=\text{NH}_2$, $(\text{CH}_3)\text{HB}=\text{NH}_2$, $(\text{CH}_3)\text{HN}=\text{BH}_2$, $(\text{NH}_3)\text{HB}=\text{CH}_2$, $(\text{BH}_3)\text{HN}=\text{CH}_2$, $(\text{CH}_3)_2\text{B}=\text{NH}_2$, $(\text{CH}_3)_2\text{N}=\text{BH}_2$, $\text{H}_3\text{B}-\text{NH}_3$, $(\text{CH}_3)_2\text{B}-\text{NH}_3$, $(\text{CH}_3)_2\text{N}-\text{BH}_3$, $(\text{CH}_3)_2\text{HB}-\text{NH}_3$, $(\text{CH}_3)_2\text{HN}-\text{BH}_3$, $(\text{CH}_3)_3\text{B}-\text{NH}_3$, and $(\text{CH}_3)_3\text{N}-\text{BH}_3$	156
7.1.	(a) Three step thermodynamic cycle for the A^- ion affinities of $\text{BH}_{3-n}\text{X}_n$. (b) Representative three step thermodynamic cycle for the hydride affinity of BH_3 . (c) Thermodynamic cycle relating the hydride affinity of X_2BA to the anion affinity of X_2BH	286
7.2.	Hydride and fluoride affinities of the $\text{BH}_{3-n}\text{X}_n$ compounds in kcal/mol at 0 K show a linear correlation with the proton affinity of X^-	287
7.3.	The I^- , Br^- , Cl^- , SH^- , OH^- , and NH_2^- anion affinities of BH_3 in kcal/mol at 0 K correlate linearly with the PAs of these anions.....	288
7.4.	Plots of the homolytic B-X BDEs for BH_2X and BH_3X^- against the homolytic HX BDEs for the halogen series	289
7.5.	Born-Haber cycles for the FAs of BF_3 and BI_3	290
8.1.	Optimized molecular structures for SiH_4 , $\text{H}_2\text{Si}=\text{NH}$, $\text{HN}=\text{Si}=\text{NH}$, $\text{H}_3\text{Si}(\text{NH}_2)$, $\text{HN}=\text{SiH}(\text{NH}_2)$, $\text{H}_2\text{Si}(\text{NH}_2)_2$, $\text{H}_4\text{Si}(\text{NH}_3)$, $\text{H}_3\text{Si}(\text{NH}_2)(\text{NH}_3)$, and $\text{H}_4\text{Si}(\text{NH}_3)_2$	354
9.1.	Plot of the calculated adiabatic BDE (kcal/mol) at 0 K as a function of the electronegativity of the halogen substituent	388
9.2.	Plot of the calculated adiabatic BDE (kcal/mol) at 0 K as a function of the covalent radii (\AA) of the halogen substituent.....	389

9.3.	Plot of the magnitude of the energy difference between the calculated $\Delta H_f(\text{CH}_3\text{SiH}_2\text{X})$ and $\Delta H_f(\text{SiH}_3\text{CH}_2\text{X})$ of the different isomers in kcal/mol at 0 K as a function of the electronegativity of the halogen substituent	390
10.1.	Adiabatic and diabatic BDEs for PF_x in kcal/mol. Unique diabatic BDEs in red. Spin density contour levels obtained with density functional theory at the B3LYP/DZVP2 level	450
10.2.	Adiabatic and diabatic BDEs for PF_xO in kcal/mol. See Figure 10.1 caption	451
10.3.	Adiabatic and diabatic BDEs for SF_x in kcal/mol. See Figure 10.1 caption	452
10.4.	Adiabatic and diabatic BDEs for SF_xO in kcal/mol. See Figure 10.1 caption	453
10.5.	Adiabatic and diabatic BDEs for SF_xO_2 in kcal/mol. See Figure 10.1 caption	454

CHAPTER 1

INTRODUCTION

1.1. Background

The research described in this dissertation is primarily focused on understanding the structure and thermodynamics of compounds of the main group elements with a focus on their use in the development and design of new materials to chemically store hydrogen for ultimate application to fuel cell technology in the automobile industry. In his 2003 State of the Union address, President Bush briefly outlined his plan for a transportation sector fueled by hydrogen to provide for the energy and national security standards of the United States by “committing \$1.2 billion in research funding so that America could lead the world in developing clean, hydrogen-powered automobiles”.¹ The development of hydrogen fuel cells for the transportation sector clearly promises economic, energy, and environmental security benefits to the U.S. and involves far-reaching collaborative efforts of the automotive and energy industries, academia (universities), national laboratories, and federal and international agencies. Diversification of our energy resources, particularly through the expansion of a domestic resource such as hydrogen, will significantly strengthen U.S. flexibility and economic resiliency in all sectors, as well as meet specific national security needs. In addition to the popular political justification of “freedom from dependence on foreign oil”, hydrogen fuel cell technology has the potential to significantly benefit the environment through the development of zero-emissions vehicles that emit only water vapor as the sole byproduct, leading to the reduction and elimination of

greenhouse gas (carbon/CO₂) emissions from the fuel cycle.^{1,2} However, there are key challenges involved in using hydrogen as the energy transfer agent for the transportation sector, and these include reducing the cost of hydrogen production; developing safe, reliable, compact, cost-effective, and technologically feasible hydrogen storage materials; and developing cost-effective, reliable, high-performing, and durable fuel cells.^{3,4,5,6}

1.2. Hydrogen Production and Storage

Hydrogen is produced from a variety of diverse and domestic resources such as fossil fuels, biomass, nuclear energy, and renewable energies (wind, solar, geothermal, and hydroelectric). The pertinent technologies that have been developed for its production include natural gas reforming, renewable electrolysis, gasification, renewable liquid reforming, nuclear high-temperature electrolysis, high-temperature thermochemical water-splitting, and photobiological and photochemical processes.³ In addition to production requirements, hydrogen storage will be required both on- and off-board the vehicle at refueling stations, production sites, and power sites. The physical approaches currently practiced for storing hydrogen include the physical storage of compressed hydrogen gas in pressurized tanks or as cryogenic liquid hydrogen in insulated-pressurized tanks. The chemical approaches include adsorption on the surfaces of solids, absorption within solids, and storage within molecular structures where chemical reactions are needed to release the hydrogen.⁵ Absorptive hydrogen storage incorporates hydrogen directly into the bulk of the material, for example into the interstitial sites of crystal lattice structures.⁵ The chemical reaction approach potentially allows for hydrogen generation and storage on-board the vehicle through reversible reactions, which arise from modest changes in temperature and pressure and by employing Le Châtelier's principle.⁷ Although the energy content of hydrogen is ~3 times that of gasoline, its energy content by

volume is ~4 times less (low volumetric energy density), creating a challenge given the size and weight constraints of a vehicle that requires ~13 kg of on-board hydrogen storage for a conventional driving range of 300 miles. However, the material-based approach conveniently allows for storage of larger quantities of hydrogen in smaller volumes, at lower pressures, and near room temperature, and several different materials are being considered as possible sources including metal hydrides, carbon-based materials, and chemical hydrides. The metal hydrides and carbon-based materials are reversible solid-state materials allowing for on-board storage and regeneration at low temperatures and pressures within the typical operating window for vehicular application of 1–10 atm and 25–120 °C. In general, chemical hydrides are non-reversible under the required modest operating temperatures and pressures, and the spent fuel needs to be regenerated off-board.⁸ The metal hydrides currently being studied as possible storage materials include the sodium alanates (NaAlH_4), lithium amides (Li_2NH), magnesium amides (MgNH), and lanthanum-nickel hydrides (LaNi_5H_6) where the main issues are low H_2 weight percent storage, slow kinetics for hydrogenation (storage) and dehydrogenation (release), and cost. Under the carbon-based category, carbon and metal-doped hybrid nanotubes, aerogels, nanofibers, microporous metal-organic frameworks (high-surface area sorbents composed of metal oxide complexes linked by organic molecules), conducting polymers, and clathrates (e.g. hydrogen-bonded water frameworks) are being investigated to address the main challenges of reproducibility, low H_2 weight percent, cost, and system volume capacity. Chemical hydrogen storage encompasses technologies that generate hydrogen through a chemical reaction, for example hydrolysis and alcoholysis of sodium borohydrides and magnesium hydrides or hydrogenation–dehydrogenation of ammonia boranes (solid) and methylammonia boranes

(liquid). Additional challenges include the system weight, volume, and complexity; cost; and off-board regeneration requirements.

1.3. Hydrogen Fuel Cells, Distribution, and Delivery

Having produced and stored hydrogen, the stored chemical energy in hydrogen must be converted to electricity, which ultimately powers the vehicle's motor, through the use of fuel cells. Compared to gasoline engines, hydrogen fuel cells emit no greenhouse gas pollutants, are ~2–3 times more efficient in converting chemical energy into electricity, and operate under quieter conditions.⁶ In addition, the distribution and delivery infrastructure of hydrogen must be considered. Current methods for hydrogen transport include land pipelines (least expensive but limited availability), high-pressure tube trailers (expensive and short delivery distances), barges, and cryogenic liquid tankers (long delivery distances but costly liquefaction requirements).⁹ The major challenges facing distribution and delivery are reducing costs through more reliable hydrogen compression, liquefaction, and bulk storage technologies; new and inexpensive materials for pipelines; safety considerations; preventing permeation, leakage, embrittlement of seals and pipe metals; and ultimately integrating production, delivery, and end-use technologies.

1.4. Chemical Hydrogen Storage

The technical objective of the U.S. Department of Energy states: “By 2010, develop and verify on-board hydrogen storage systems achieving 1.5 kWh/kg (4.5 wt%), 0.9 kWh/L, and \$3-7/gge; and by 2015, 1.8 kWh/kg (5.5 wt%), 2.7 kWh/L, and \$2-6/gge”.¹⁰ Our approach to meeting this objective is focused on the development and design of novel chemical hydrogen storage materials that can readily store and release hydrogen under controlled conditions. In this manner, safety concerns are alleviated as hydrogen is never stored in high pressurized tanks. Besides being beneficial from a safety standpoint, chemical hydrogen storage will assist in

developing economic processes for the regeneration of the spent fuel (hydrogen depleted material). Unlike gasoline, which is converted to CO₂ and emitted from the exhaust system into the atmosphere where it has adverse environmental impacts,¹¹ chemical hydrogen storage materials after they have released hydrogen for use in a fuel cell never leave the automobile and only need to be regenerated. Consequently, there is a critical need to develop new chemical hydrogen storage materials and novel approaches for the release and uptake of H₂ for use in on-board transportation systems.¹² Specifically, there is substantial interest in discovering new materials that hydrogenate–dehydrogenate in thermoneutral processes (heat of reaction near zero kcal/mol) in order to minimize the heat and energy requirements for hydrogen release and regeneration.

Due to their low molecular weights and polar bonds, boron hydride derivatives, specifically the borane amines, are being considered for development as potential materials for chemical hydrogen storage, and there have been a number of efforts focused on its use for H₂ storage.^{13,14,15,16,17,18,19,20,21} Interest in ammonia borane (BH₃NH₃) and the ammonium borohydride salt initially stemmed from the military's efforts to develop clean sources of H₂ for use in HF laser systems.^{22,23} BH₃NH₃ and the derived salt [BH₄⁻][NH₄⁺] have an excellent weight percent storage of H₂ having 19 and 24% if 3 and 4 molecules of H₂ are released, respectively, which both meet DOE's 2015 requirement for realistic H₂ storage–release materials of 5.5% weight storage. In addition, the NH_xBH_x ($x = 1 - 4$) compounds have been studied using theoretical methods as solid sources for hydrogen storage.²⁴ Although ammonia borane can be considered to be an inorganic analog of the hydrocarbon ethane, it is a solid and not a gas at ambient temperatures.^{25,26,27} The solid nature arises due to the greater polarity of the BN unit, which is derived from the different electronegativities of B and N,²⁸ and the stronger

intermolecular interactions as compared to the organic gaseous analogues. Calculations show that $\text{BH}_3\text{NH}_3(\text{g})$, $\text{BH}_3\text{NH}_3(\text{s})$, and the $[\text{BH}_4^-][\text{NH}_4^+](\text{s})$ salt can serve as good hydrogen storage systems releasing hydrogen by thermoneutral reactions within 10 kcal/mol.^{24,29} These theoretical results are consistent with experimental work that has shown the first dehydrogenation reaction of BH_3NH_3 to be exothermic by 5 kcal/mol.³⁰ The thermoneutrality of dehydrogenation from solid NH_xBH_x compounds is significantly different from hydrolysis pathways of boron-based hydrogen storage materials.³¹ The release of hydrogen from ammonia boranes has been shown to be mediated by nano-scaffolds, displaying more favorable kinetics and thermodynamics.³²

In Chapter 3, the molecular systems isoelectronic to the ammonia boranes, (BH_3PH_3 , AlH_3NH_3 , and AlH_3PH_3)³³ are investigated as alternative sources for chemical hydrogen storage systems that may be easier to synthesize or for which new catalysts can be effectively designed and developed. On the basis of the calculated heats of formation, $\text{AlH}_3\text{NH}_3(\text{g})$, the $[\text{AlH}_4^-][\text{NH}_4^+](\text{s})$ salt, $\text{AlH}_3\text{PH}_3(\text{g})$, the $[\text{AlH}_4^-][\text{PH}_4^+](\text{s})$ salt, and the $[\text{BH}_4^-][\text{PH}_4^+](\text{s})$ salt have the potential to serve as chemical hydrogen storage systems in terms of the energetics for H_2 release.

In Chapter 4, the novel electronic structure of these isoelectronic ammonia borane compounds led to the study of their bond dissociation energies (BDEs), which will allow an improved understanding of their chemistry in terms of stability, reactivity, and thermodynamic forces driving H_2 release. The energetics for H_2 release for BH_3NH_3 is predicted to be substantially different from that of C_2H_6 in that loss of H_2 from $\text{BH}_3\text{NH}_3(\text{g})$ is exothermic, whereas the comparable organic reaction of C_2H_6 is substantially endothermic.³⁴ We show that this difference in energetic requirements is due to a low energy dative σ -bond in BH_3NH_3 that readily loses H_2 to form a strong B-N σ -bond and a dative π -bond in BH_2NH_2 . Thus, the driving force for H_2 loss from BH_3NH_3 is the transition from a B-N Lewis acid-base donor-acceptor

bond to a strong sp^2 - sp^2 σ -bond in BH_2NH_2 , which is stronger than the experimental C-C σ -bond in C_2H_4 .³⁵ The B-N dative bond in H_3B-NH_3 is predicted to be 27.2 kcal/mol,²⁴ compared to the experimental covalent C-C σ -bond of 90.1 kcal/mol for C_2H_6 .³⁴

In order to evaluate σ -bond strengths of the AH_2XH_2 compounds, one must first be able to evaluate the π -bond strength as discussed in Chapter 4. Several methods exist in literature for determining the π -bond strengths of molecules, including the use of hydrogenation thermochemical cycles and BDEs of singly and doubly bonded compounds.³⁶ However, to predict the π -bond strength, we employ the rotational barrier approach in which rotation by 90° about the A-X bond axis in the AH_2X_2 (A = B, Al; X = N, P) molecule breaks the dative π -bond interaction between the electron lone pair on the XH_2 moiety with the vacant p -orbital on the AH_2 moiety. In C_2H_4 , this is equivalent to breaking the covalent interaction between the two $2p$ -orbitals, putting one electron on each CH_2 group and forming a diradical. Consequently, the adiabatic σ -bond energy is then evaluated as the difference between the adiabatic (dissociation to the ground states of the separated species) total dissociation energy of the AH_2XH_2 compound, which equals the sum of the σ - and π -bond energies, and the rotational barrier, which equals the adiabatic π -bond energy. These bond energies can be compared to the σ - and π -bond energies in C_2H_4 ,^{37,38} having a covalent π -bond unlike the dative π -bond found in the AH_2X_2 compounds. The adiabatic σ -bond of $H_2B=NH_2$ is predicted to be 109.8 kcal/mol, and is comparable to that of $H_2C=CH_2$ of 106 kcal/mol, given the experimental π -bond energy of 65 kcal/mol^{38,39} and C=C BDE of 171 kcal/mol.³⁴ We define the intrinsic π -bond energy as the adiabatic π -bond energy corrected for pyramidalization at N or P in the ground and rotated transition state structures. The adiabatic σ -bonds for $H_2B=NH_2$ and $H_2Al=NH_2$ do not change substantially when considering the intrinsic π -bonds due to the small inversion barriers at N in the rotated transition state

structures but do for the P derivatives as the inversion barrier at P is much higher. These bond energies are critical design concepts for main group chemical hydrogen storage materials, and we were the first to quantify the Lewis acid-base donor-acceptor σ -bond strengths in the AH_3XH_3 compounds and the σ -bond and dative π -bond strengths in the AH_2X_2 compounds, and to differentiate between adiabatic and diabatic π -bond energies for these types of compounds.

Ammonia borane is a solid at room temperature due to the moderate strength intermolecular $H\cdots H$ bonds that form between the $H^{\delta+}$ on N and the $H^{\delta-}$ on B,^{25,26,27} consequently requiring substantial infrastructural changes as the use of solid fuels is not currently extensively practiced. The presence of alkyl groups lowers the melting point of ammonia borane,⁴⁰ due to fewer $H\cdots H$ interactions, and experimental results have shown solubility in methyl-substituted ammonia borane,⁴¹ which would enable the generation of a liquid fuel. As there is a weight penalty associated with additional components, in Chapter 5, we have investigated the methyl-substituted ammonia boranes as possible hydrogen sources, in terms of their thermodynamics for hydrogen release, with methylammonia borane having 9.8% weight storage compared to ammonia borane's 14.9% weight storage if 2 molecules of H_2 are produced. Sequentially methylating ammonia borane at N, in contrast to B, reduces the exothermicity of the dehydrogenation reaction and becomes more thermoneutral, facilitating both H_2 release and regeneration. Similarly, to further understand their chemistry in terms of reactivity and stability, the various BDEs have been investigated following our previous procedures for determining the σ - and π -bonds in the main Group IIIA–Group VA $H_2A=XH_2$ compounds⁴² that employ the rotational barrier to estimate the π -bond energies as presented in Chapter 4. Expanding efforts have also led to the reliable prediction of the thermochemistry and dehydrogenation of the BN analogues of the methylated cycloborazane molecules.⁴³

In addition to their potential relevance to the dehydrogenation process, the energetics, specifically heats of formation and BDEs, of the substituted boranes have been investigated as intermediates in regeneration cycles of spent fuel derived from ammonia borane in Chapter 6. The difficulty in experimentally measuring BDEs offers high-level theoretical calculations a unique opportunity to obtain accurate self-consistent values of these processes, and we have predicted the heats of formation and BDEs in the $\text{BH}_{3-n}\text{X}_n$ compounds, where $\text{X} = \text{F}, \text{Cl}, \text{Br}, \text{I}, \text{NH}_2, \text{OH},$ and SH , as well as the BX_2 and HBX radicals. Although there have been some measurements of the heats of formation and BDEs, most are inaccurate and unreliable,⁴⁴ and our calculated values dramatically improve the estimates of these important thermodynamic quantities, particularly for the radicals, and are to be preferred over the experimental values.

We have also addressed the appropriate description of BDEs when considering the step-wise dissociation of substituents in these substituted boranes, following our work⁴⁵ on BDEs in the PF_xO_y and SF_xO_y compounds described in Chapter 10. The diabatic BDE is defined as dissociation to the configurations most closely representing the bonding configuration in the reactant, and the adiabatic BDE is defined as dissociation to the ground state of the separated species. The adiabatic BDE will always be equal to or less than the diabatic BDE. For the diabatic BDE, the spin states are likely to be conserved whereas in the adiabatic BDE, they may not be conserved. Compared to the other substituents, the B-F BDE in BF and the $\text{H}_{3-n}\text{BF}_n$ compounds is the highest BDE predicted, while the second and third highest are for the OH and NH_2 substituents, respectively. The substituents have a minimal effect on the B-H BDE in the HBX_2 and H_2BX compounds compared to that of borane. The differences in the adiabatic and diabatic BDEs, which represents the reorganization or relaxation energy of the product atom or

molecule, can be estimated from the singlet-triplet splittings and accounts for the large fluctuations in the adiabatic BDEs, specifically in the BX_2 and HBX radicals.

In Chapter 7, to further understand the chemistry of the substituted boranes, we have also predicted the hydride (HA), fluoride (FA), and X^- (XA) affinities. The fluoride⁴⁶ or hydride⁴⁷ affinity offers a unique measure of the strength of a Lewis acid and provides significant insight into their reactivity and periodic behavior. Vianello and Maksic⁴⁷ have previously calculated the HAs of BH_3 and the fluoro, chloro, bromo, hydroxo, and methyl-substituted boranes at the G2(MP2) level, writing a three step thermodynamic cycle that involves, for BH_3 , the electron affinity (EA) of H, the negative EA of BH_3 , and the chemical homolytic bond formation of BH_3^- and H radicals. However, an issue with their approach was the inclusion of negative EAs, instead of the more appropriate value of zero since the electron is unbound when the $EA \leq 0$. They showed that F, OH, and CH_3 and Cl and Br substitution reduces and enhances the HA, respectively, and that BBr_3 was the most acidic compound studied. Our study expanded the scope of the previous investigation for the HA by including the additional ligands, I, NH_2 , and SH, as well as calculating the FAs and the Cl^- , Br^- , I^- , NH_2^- , OH^- , and SH^- affinities. We determined that the HA correlates linearly with the proton affinity (PA) of X^- , except for H and F, in turn allowing the HA of $BH_{3-n}X_n$ compounds with other X groups to be estimated since the PAs for a number of anions are experimentally known or readily calculated.

In Chapter 8, we have continued our efforts to discover potential candidates for chemical hydrogen storage systems by studying a potential class of hydrogen storage molecules based on diammoniosilane, $SiH_4(NH_3)_2$. Diammoniosilane has an excellent weight percent storage of hydrogen at 26% if 8 molecules of H_2 are produced as compared to the ammonia borane having 19% if 3 molecules of H_2 are produced. The thermodynamics for H_2 release have been predicted

based on calculated heats of formation, where the dehydrogenation reaction yielding two hydrogen molecules is exothermic with the sequential release of three and four hydrogen molecules being largely endothermic. However, effectively coupling the exothermic and endothermic reactions would enable the removal of three hydrogen molecules. The study of diammoniosilane also provided a platform to a further understanding of the chemistry of the edge inversion process, i.e., the formation of square planar AX_4 structures from tetrahedral AX_4 structures given that the amine complex forms from the addition of NH_3 to SiH_4 to make a square planar SiH_4 with two NH_3 molecules coordinated in the apical positions. This is equivalent to stabilization of the edge inversion transition state for SiH_4 by two amines.^{48,49}

In Chapter 9, the energetics of silane-based compounds have been studied for possible regeneration schemes for chemical hydrogen storage systems, as well as, for use in technological applications such as precursors for chemical vapor deposition. The limited experimental thermodynamic data available for the halosilanes, the methylhalosilanes, and the halomethylsilanes prompted our study to obtain accurate heats of formation and BDEs, both of which are important in assessing the thermochemistry involved in the regeneration process.

The research presented in Chapter 10 expanded our understanding of chemical BDEs, specifically in compounds containing second and higher row main group elements with coordination numbers beyond the standard values for a Lewis octet. Measurements of experimental BDEs are often very difficult to make, especially when radicals are formed as products in the bond breaking process, and this in turn largely limits their availability and accuracy.⁴⁴ Therefore, the various BDEs in the PF_x , PF_xO , SF_x , SF_xO and SF_xO_2 compounds have been predicted from high-level *ab initio* calculations to within chemical accuracy. Compared to diatomic molecules, the bond dissociation process in polyatomic molecules is a bit more

complicated as each BDE for the stepwise dissociation process maybe be very different depending on the relative stabilities of the starting reactant and the final products. They can also differ largely from the average bond energy, which is defined as the molecular total atomization energy divided by the number of bonds present in the molecule. The results show significant differences in the adiabatic and diabatic BDEs and that when interpreting molecular structures and vibrational spectra near the minimum, it is more appropriate to compare diabatic BDEs, especially in developing correlations and when addressing bond distances, stretching frequencies and bond force constants.

CHAPTER 2

COMPUTATIONAL METHODOLOGY

2.1. *Introduction*

Advanced *ab initio* electronic structure methods performed on high-performance computer architectures are employed to study main group compounds. The calculations enable the reliable prediction of molecular properties such as vibrational spectra, geometrical structures, and energetics to within chemical accuracy of ± 1 kcal/mol, and consequently allow for the prediction of the thermodynamics and kinetics of chemical reactions, i.e., how much energy is required or released by the reaction and how fast a reaction can proceed, respectively. Such accuracy is critical for chemical hydrogen storage systems that have very narrow operating parameters within which to operate due to the fact that the energy storage systems need to be compatible with how automobiles are currently operated, and there cannot be a high-energy cost to release or regenerate hydrogen.

In addition, such data is essential in designing not only the release process but also the regeneration process, the addition of hydrogen back to the hydrogen depleted material. Moreover, the experimental measurements of the individual steps in the various bond dissociation processes of these materials are very difficult and challenging to obtain under comparable and reliable conditions due to the formation of radical species. Modern computational chemistry methods implemented on high-performance computer architectures can now provide reliable predictions of total atomization energies, heats of formation, bond dissociation energies, and hydride and

fluoride affinities to within ~ 1 kcal/mol for most compounds that are not dominated by multireference character.⁵⁰ We use the approach that the Dixon research group has been developing with collaborators at Washington State University and Pacific Northwest Laboratory for the prediction of the accurate molecular thermochemistry⁵¹ of these compounds. The approach is based on calculating the total atomization energy of a molecule at 0 K and using this value with the known heats of formation of the atoms to calculate the heat of formation at 0 K. The approach starts with coupled cluster theory with single and double excitations and including a perturbative triples correction (CCSD(T)),^{52,53,54} combined with the correlation-consistent basis sets^{55,56} extrapolated to the complete basis set (CBS) limit⁵⁷ to treat the correlation energy of the valence electrons. A number of smaller additive corrections need to be included: core-valence interactions and relativistic effects, both scalar and spin-orbit. The zero point energy is obtained either from experiment, theory, or a combination of the two. Corrections to the heats of formation from 0 K to 298 K are calculated by using standard thermodynamic and statistical mechanics expressions in the rigid rotor-harmonic oscillator approximation⁵⁸ and appropriate thermal corrections for the heat of formation of the atoms.⁵⁹ We first describe the foundations on which our applications of quantum mechanics are based.

2.2. *Hartree-Fock Theory*

Hartree-Fock (HF) theory is an approximate solution to the time-independent Schrödinger equation (2.1) for the description of the stationary state of an atom or molecule, its electronic structure,

$$\hat{H}\Psi = E\Psi \tag{2.1}$$

where \hat{H} is the total Hamiltonian operator, Ψ is the total wavefunction, and E is the total energy of the system. The total Hamiltonian operator can be written as the sum of the kinetic and potential energies of the nuclei and electrons.

$$\hat{H}_{total} = T_n + T_e + V_{ne} + V_{ee} + V_{nn} \quad 2.2$$

The Schrödinger equation to a good approximation can be separated into two parts, one describing the electronic wave function for a fixed nuclear geometry and the other describing the nuclear wave function, and this separation is the Born-Oppenheimer approximation.⁶⁰ The Born-Oppenheimer approximation reduces the solution of 2.2 solely to that of the electronic Schrödinger equation for a fixed set of nuclear geometries based on the fact that the mass of the proton is much larger (~1800 times) than of the electron resulting in its slower movement as compared to those of the electron. The electronic Hamiltonian operator is written as

$$\hat{H}_e = T_e + V_{ne} + V_{ee} + V_{nn} \quad 2.3$$

and more explicitly as,

$$\hat{H}_e = \sum_i \left(-\frac{1}{2} \nabla_i^2 - \sum_A \frac{Z_A}{r_{iA}} + \sum_{i>j} \frac{1}{r_{ij}} \right) \quad 2.4$$

where the terms represented are (1) first sum – electron kinetic energy, (2) second sum – electron-nuclear attraction energy, and (3) third sum – electron-electron repulsion energy, with A – the nuclei, r – nuclear and electronic coordinates, i and j – respective electrons, and Z – the atomic number. Solving the electronic Schrödinger equation yields the total electronic energy and solving for all possible nuclear geometries (and possibly for several electronic states) maps the potential energy surface (PES) of the system. Energy minima on the PES correspond to the molecular structures and the second derivatives of the energy with respect to the nuclear coordinates can be transformed into the harmonic molecular vibrational modes. Solutions to the

time-independent Schrödinger equation without reference to experimental data are referred to as *ab initio* methods.

A fundamental approximation many electronic structure methods make is the independent electron or HF approximation, where the electron moves in the mean field of the nuclei and the other $(n - 1)$ electrons. The total electronic wavefunction is antisymmetric (change sign) with respect to interchanging any two electrons given that the electrons are fermions having a spin of $\frac{1}{2}$. The Pauli principle, which states that two electrons cannot have all quantum numbers equal, is a direct result of this antisymmetry requirement. Thus, the wavefunction of the system is built from Slater determinants – the columns are single electron wave functions called orbitals and the rows are the electron coordinates – and are written as an antisymmetrized product of molecular orbitals.

$$\Psi = \frac{1}{\sqrt{N!}} \begin{vmatrix} \chi_1(1) & \chi_1(2) & \dots & \chi_1(N) \\ \chi_1(2) & \chi_2(2) & \dots & \chi_2(N) \\ \vdots & \vdots & \ddots & \vdots \\ \chi_1(N) & \chi_2(N) & \dots & \chi_N(N) \end{vmatrix} \quad 2.5$$

For the molecular orbital $\chi_a(i)$, a is the orbital number and i represents the electron in that specific orbital. The molecular orbitals are determined from the HF equation containing terms for the Coulomb operator, \hat{J}_b , which represents the classical repulsion between two charge distributions; the exchange operator, \hat{K}_b , which reflects the reduced probability of finding two electrons of the same spin (Pauli principle) close to one another with a “Fermi-hole” surrounding each electron; and the energy of the orbital, ε_a .

$$\left\{ -\frac{1}{2} \nabla_1^2 - \sum_A \frac{Z_A}{r_{1A}} + \sum_b [\hat{J}_b(1) - \hat{K}_b(1)] \right\} \chi_a(1) = \varepsilon_a \chi_a(1), \quad 2.6$$

$$\hat{J}_b(1)\chi_a(1) = \left[\int \partial\tau_2 \frac{\chi_b^*(2)\chi_b(2)}{r_{12}} \right] \chi_a(1), \quad 2.7$$

$$\hat{K}_b(1)\chi_a(1) = \left[\int \partial\tau_2 \frac{\chi_b^*(2)\chi_a(2)}{r_{12}} \right] \chi_b(1) \quad 2.8$$

The HF equation is solved by the iterative self-consistent field method, and the molecular orbitals are approximated as a linear combination of atomic orbitals (LCAO), i.e., as a linear combination of atomic basis functions.

2.3. Basis Sets

Another inherent approximation of most *ab initio* molecular electronic structure methods is the introduction of an atomic orbital basis set, of which there are typically two types: Slater Type Orbitals (STOs) and Gaussian Type Orbitals (GTOs). STOs are essentially solutions for the hydrogen atom of the form

$$\chi_{\zeta,n,l,m}(r, \theta, \varphi) = NY_{l,m}(\theta, \varphi)r^{(n-1)}e^{-\zeta r} \quad 2.9$$

where N is a normalization constant and $Y_{l,m}$ are spherical harmonic functions. STOs do not have radial nodes, and the exponential dependence allows rapid convergence with increasing number of functions. However, they suffer from the significant limitation that there is no analytical solution for the general four-index integral. GTOs in terms of polar or cartesian coordinates are of the form

$$\chi_{\zeta,n,l,m}(r, \theta, \varphi) = NY_{l,m}(\theta, \varphi)r^{(2n-2-1)}e^{-\zeta r^2} \quad 2.10$$

$$\chi_{\zeta,l_x,l_y,l_z}(x, y, z) = Nx^{l_x}y^{l_y}z^{l_z}e^{-\zeta r^2} \quad 2.11$$

where l_x , l_y , and l_z determines the orbital type ($l_x + l_y + l_z = 1$ is a p -orbital). The r^2 dependence renders two disadvantages in that at the nucleus, GTOs have a zero slope compared to a “cusp” in STOs, not representing the proper behavior near the nucleus. The other problem arises due to

the rapid fall off of GTOs away from the nucleus, leading to a poorer representation of the wavefunction tail. Although more GTOs are necessary to achieve the same accuracy as STOs, the computational efficiency of integral evaluation more than compensates for the increase in the number of orbitals. In addition, there is also the possibility of using plane waves as basis sets in periodic boundary conditions in condensed-phase simulations.⁶¹

An important factor to consider is the number of basis functions due to the computational scaling with the number of orbitals and electrons. The smallest number of basis functions required to represent all of the electrons of the neutral atom is referred to as a minimum basis set. For hydrogen and helium, this is a single $1s$ function, for a first row atom, these are two s functions ($1s$ and $2s$) and a set of p functions ($2p_x$, $2p_y$, and $2p_z$), and for a second row atom, these are three s functions ($1s$, $2s$, and $3s$) and two sets of p functions ($2p$ and $3p$). The next improvement doubles the number of basis functions required to represent all the electrons in a neutral atom, referred to as a double zeta (DZ) basis set, allocating two s functions for hydrogen and helium, four s functions and two p functions for a first row atom, and six s functions and four p functions for a second row atom. Doubling just the number of valence orbitals that are involved in chemical bonding produces a split valence basis set, referred to as valence double zeta (VDZ). Further improvement in basis set size is triple zeta (TZ), which contains three times as many functions as a minimum basis set; splitting the core and valence orbitals for the TZ basis set gives the valence triple zeta basis set (VTZ). Next in the sequence are the valence quadruple (VQZ) and quintuple (V5Z) basis sets that have four and five times as many basis functions as the minimum basis set.

The next level in basis set quality is to add higher angular momentum functions to the VnZ ($n = D, T, Q, 5$) basis sets called polarization functions, where the first set adds p functions

to hydrogen and d functions to heavy atoms, denoted as valence n zeta plus polarization. Adding two sets of polarization functions gives a valence n zeta plus double polarization. Furthermore, the polarized valence basis sets can be augmented with diffuse functions, which consists of adding one extra function with a smaller exponent per angular momentum, i.e. an additional set of $1s1p1d$ and $1s1p1d1f$ functions to the valence double, triple, and quadruple zeta basis sets, respectively. Diffuse functions are basis sets with small exponents describing the shape of the wavefunction far away from the nucleus, and are necessary for studying systems with more loosely bound electrons as in anions, excited states, molecules with electron lone pairs, hydrogen-bonded systems, transition states, or when investigating molecular properties that are dependent on the wavefunction tail, such as the polarizability. These diffuse functions are referred to as augmented polarized valence basis sets and denoted as aug-cc-pVnZ.

There are various available basis sets in literature such as the Pople,⁶² Dunning-Huzinaga,⁶³ and Atomic Natural Orbital⁶⁴ basis sets. The basis sets employed in this research are the correlation consistent (cc) basis sets, which were initially designed to recover the correlation energy of the valence electrons. The design of the basis set is based on adding functions that contribute similar amounts of correlation energy at the same stage irrespective of function type. Improving the quality of the basis set increases the specific type of basis function and adds a new type of higher-order polarization function, and are sequentially added in the order $1d$, $2d1f$, and $3d2f1g$ to the valence double, triple, and quadruple basis sets, respectively. The basis sets are referred to as the correlation consistent polarized valence basis sets and denoted as cc-pVnZ, $n = D, T, Q,$ and 5 for the atoms for which they are available. In addition, the cc basis sets are augmented by additional diffuse functions, and are referred to as augmented correlation consistent basis sets and denoted as aug-cc-pVnZ or in shorthand as aVnZ. The current research

has employed the use of the augmented correlation consistent basis sets developed by Dunning and coworkers,^{55,56} $aVnZ$ ($n = D, T, Q,$ and 5) for H, B, C, N, O, F, and Br, in calculating the valence electronic energies. In addition, the inclusion of tight d functions are necessary for calculating accurate total atomization energies for 2nd row elements;⁶⁵ therefore, we included additional tight d functions in our calculations of the valence electronic energies, giving the aug-cc-pV($n+d$)Z basis set on the 2nd row atoms Al, Si, P, S, and Cl, and are denoted as aV($n+d$)Z.

The cc basis sets can also be augmented with additional tight functions (large exponents) that are necessary in recovering core-valence electron correlation in order to achieve thermochemical properties within ± 1 kcal/mol of experiment, and are referred to as the augmented correlation consistent polarized weighted core-valence basis sets aug-cc-pwCV nZ and denoted as awCV nZ .⁶⁶ The wCVTZ basis set (employed for core-valence corrections to the total atomization energies) adds a set of $2s2p1d$ tight functions to the VTZ basis set.⁶⁶ The core-valence correction is then taken as the difference in energy between the valence electron correlation calculation and that with the appropriate core electrons included using the additional weighted functions.

For atoms of the third (Br) and fourth row (I) that have large atomic numbers, a pseudopotential (PP) or relativistic effective core potential (RECP)⁶⁷ is employed to account for the electronic contributions of the core electrons, which are chemically inert compared to the valence electrons, and to include relativistic effects due to the higher atomic number. For molecules containing I, we used a different approach due to issues described in our recent study of the iodofluorides⁶⁸ that led to further improvements of our total atomization procedure. We found it necessary to correlate the core electrons with the awCV nZ basis sets in order to extrapolate these quantities to the CBS limit to predict accurate heats of formation. For I, our

calculations used the new RECP-correlation consistent basis sets developed by Peterson and co-workers.⁶⁷ These basis sets were developed in combination with the small core RECP from the Stuttgart-Köln group, and are typically represented as aug-cc-pVnZ-PP and denoted as aVnZ-PP. The RECP for I subsumes the ($1s^2$, $2s^2$, $2p^6$, $3s^2$, $3p^6$, and $3d^{10}$) orbital space into the 28-electron core set, leaving the ($4s^2$, $4p^6$, $5s^2$, $4d^{10}$, and $5p^5$) space with 25 electrons to be handled explicitly. Our calculations were performed with the awCVnZ basis sets for $n = D, T,$ and Q with 25 active electrons on each I atom, automatically including the core-valence correction upon extrapolating to the CBS limit. The combination of the aVnZ basis sets on H, B, C, N, O, F, and Br and aV($n+d$)Z basis sets on the 2nd row atoms Al, Si, P, S, and Cl are typically represented as aVnZ. For molecules containing Br, additional calculations were performed using the new RECP-correlation consistent basis sets developed by Peterson and co-workers.⁶⁷ For Br, the RECP subsumes the ($1s^2$, $2s^2$, and $2p^6$) orbital space into the 10-electron core set, leaving the ($3s^2$, $3p^6$, $4s^2$, $3d^{10}$, and $4p^5$) space with 25 electrons to be handled explicitly, and only the ($4s^2$ and $4p^5$) electrons are active in the valence correlation treatment.

The main advantage in using the cc basis sets is the ability to generate a sequence of basis sets (aVnZ, $n = D, T, Q$) that converges toward the CBS limit,⁵⁷ to eliminate the basis set one electron function approximation, and the calculation accuracy should then solely be limited by the electron correlation method. Our principle for achieving thermochemical properties within chemical accuracy (± 1 kcal/mol) uses the high level CCSD(T) method^{52,53,54} to perform a series of correlation energy calculations with systematically larger correlation consistent basis sets in order to extrapolate the valence electronic energies to the CBS limit.⁵⁷ In this regard, several approaches exist for extrapolation to the CBS limit:⁵⁷

$$A + Be^{-CL} \quad (L = 2, 3, 4, 5) \tag{2.12}$$

$$A + Be^{-(L-1)} + Ce^{-(L-1)(L-1)} \quad 2.13$$

$$A + B(L + 1/2)^{-4+} \quad 2.14$$

The present research employs a mixed exponential–Gaussian function of the form

$$E(n) = E_{CBS} + Ae^{-(n-1)} + Be^{-(n-1)^2} \quad 2.15$$

where $n = 2$ (aVDZ), 3 (aVTZ), and 4 (aVQZ), as first proposed by Peterson *et al.*,⁵⁷ to extrapolate the CCSD(T) total valence electronic energies to the CBS limit. This extrapolation method has been shown when combined with the other corrections (core-valence and relativistic, both scalar and atomic spin-orbit) to yield total atomization energies in the closest agreement with experiment as compared to other extrapolation approaches up through $n = 4$.⁵¹ In some instances where computationally affordable, CCSD(T) calculations were performed with the aV5Z basis set, and the total atomization energies at the CCSD(T)/CBS limit were obtained by extrapolating solely the aVQZ and aV5Z valence electronic energies using a formula incorporating the inverse of the angular momentum function, l .

$$E(l_{\max}) = E_{CBS} + \frac{B}{l_{\max}^3} \quad 2.16$$

The CBS extrapolation derived from former equation is henceforth referred to as the DTQ extrapolation and that with latter as the Q5 extrapolation.

2.4. *Electron Correlation Methods*

Given a sufficiently large basis set, the HF equation accounts for ~99% of the total energy of the system; however, the remaining ~1%, unaccounted due to the neglect of the instantaneous electron interactions, is critical in describing chemical phenomena. The difference in energy between the HF and the lowest possible energy in a given basis set is called the electron correlation energy, and physically corresponds to the motion of a pair of electrons in an orbital being correlated due to the classical repulsion energy. The electron correlation energy can

be recovered from several methods including configuration interaction (CI),⁶⁹ many-body perturbation theory (MBPT n),⁷⁰ and coupled cluster (CC) theory,^{52,53,54} upon which the foundation of this research is based and will be discussed more in depth over the former two methods.

2.4.1. Configuration Interaction Theory

The CI method⁶⁹ is based on the variation principle with the CI wavefunction written as a linear combination of determinants with the expansion coefficients determined by requiring the energy of the system to be a minimum or at least stationary. In the simplest approach, the MOs that are used to build the excited Slater determinants are determined from a HF calculation and are held fixed. The CI wavefunction is written as

$$\Psi_{CI} = a_0\Psi_0 + \sum_S a_S\Psi_S + \sum_D a_D\Psi_D + \sum_T a_T\Psi_T + \dots = \sum_i a_i\Psi_i \quad 2.17$$

where Ψ_0 is the reference HF determinant; Ψ_S , Ψ_D , Ψ_T , etc. are the determinants, which are singly, doubly, and triply, etc. excited relative to the HF configuration; and a_0 , a_D , a_S , a_T , etc. are the expansion coefficients determined by the variational principle. If all the possible determinants are included, the full CI wave function is obtained, and there is no truncation in the many-electron expansion besides that generated by the finite one-electron expansion and 100% of the correlation energy is recovered for the given basis set. However, the number of excited determinants grows factorially with the size of the basis set, and this makes the full CI method infeasible for but the very smallest systems and only with a modest sized basis set.

Developing a computationally applicable model calls for reducing the number of excited determinants in the CI expansion. Truncating the excitation at the singles level (CIS) for a closed shell molecule offers no improvement over the HF result due to Brillouin's theorem,⁷¹ and the lowest level yielding improvement includes the doubly excited states, giving the CID method.

Compared to the doubly excited determinants, the singly excited determinants are relatively few in number and their inclusion gives the CISD method,⁶⁹ which renders only a marginal increase in computational effort over the CID model. The CISD method is iterative and formally scales as M^6 (M = number of basis functions of the system). Although full CI is size consistent (method is additive for infinitely separated and non-interacting particles with separation of ~ 100 Å) and size extensive (method scales linearly with the number of particles that can be interacting with a separation of ~ 5 Å),⁶¹ the any lower level CI energy is not size-consistent and the lack of size extensivity results in a decreased recovery of the electron correlation as the size of the system grows larger. Including the triply and quadruply excited determinants gives the CISDT and CISDTQ models, scaling as M^8 and M^{10} , respectively. In our calculations, the CISD method in conjunction with a VTZ basis set is used, in some cases, for calculating the scalar relativistic correction to the total atomization energy of the molecule.

2.4.2. Many-Body Perturbation Theory

The MBPT method⁷⁰ is based on the hypothesis that the desired wavefunction only differs slightly from a simpler wavefunction that has been solved either exactly or approximately, so the desired solution should be close to the solution of the known system. The Hamiltonian operator is divided into two parts,

$$H = H_0 + \lambda H' \quad 2.18$$

where H_0 is the reference operator and H' is the perturbation operator, which in some sense is small compared to the H_0 operator, and can be represented as follows

$$H_0 \Psi_i = E_i \Psi_i, i = 0, 1, 2, \dots, \infty, \quad 2.19$$

$$H_0 = \sum_i \left\{ -\frac{1}{2} \nabla_i^2 - \sum_A \frac{Z_A}{r_{iA}} + \sum_b \left(\hat{J}_b(i) - \hat{K}_b(i) \right) \right\}, \quad 2.20$$

$$H' = \sum_i \sum_{i>j} \frac{1}{r_{ij}} - \sum_i \sum_b [\hat{J}_b(i) - \hat{K}_b(i)] \quad 2.21$$

Given that the Schrödinger equation for the reference Hamilton operator is solved, solutions for the unperturbed Hamilton operator form a complete set and λ is a variable parameter determining the strength of the perturbation. The perturbed Schrödinger equation is

$$H\Psi = W\Psi \quad 2.22$$

If $\lambda = 0$, then $H = H_0$, $\Psi = \Psi_0$, and $W = E_0$, and these yield the unperturbed or zero-order wavefunction and energy. However, as the perturbation is increased to a finite value, the energy and wavefunction change, and that change can be expressed as a Taylor expansion in powers of the perturbation parameter λ .

$$W = \lambda^0 W_0 + \lambda^1 W_1 + \lambda^2 W_2 + \lambda^3 W_3 + \dots + \lambda^n W_n \quad 2.23$$

$$\Psi = \lambda^0 \Psi_0 + \lambda^1 \Psi_1 + \lambda^2 \Psi_2 + \lambda^3 \Psi_3 + \dots + \lambda^n \Psi_n \quad 2.24$$

$\Psi_1, \Psi_2, \dots, \Psi_n$ and W_1, W_2, \dots, W_n are the first-, second-, and n^{th} -order corrections to the wavefunction and energy, respectively. The λ parameter will eventually be set to 1, and the n th order energy or wavefunction then become a sum of all terms up to order n .

The common notation MPn is used to denote total energies corrected up to the n th order, and $MP2^{70}$ is the most widely applied *ab initio* MBPT method for the treatment of electron correlation. The MPn method is size-extensive to any given order and the energy is non-variational. $MP2$ typically accounts for ~80 – 90% of the correlation energy. The $MP2$ method formally scales as M^5 due to the integral transformation step and has the lowest computational cost compared to the other electron correlation methods. In this research, the $MP2$ method in conjunction with the either the VTZ or aVTZ basis set is utilized for geometry optimizations to get molecular structures and vibrational harmonic frequencies (zero point energies) from the

analytic first and second derivatives, respectively. Even though the MP2 method produces reasonable results in terms of the energetics and molecular properties, structures, and frequencies, accurate energy results require a higher level method.

2.4.3. Coupled Cluster Theory

In coupled cluster theory,^{52,53,54} the coupled cluster wavefunction of the system is written as

$$\Psi_{CC} = e^T \Psi_0 \quad 2.25$$

$$e^T = 1 + T + \frac{1}{2}T^2 + \frac{1}{6}T^3 + \dots = \sum_{k=0}^{\infty} \frac{1}{k!} T^k \quad 2.26$$

where Ψ_0 is the reference HF wavefunction, e^T is the exponential operator, and T is the cluster operator.

$$T = T_1 + T_2 + T_3 + T_4 + \dots + T_N \quad 2.27$$

The coupled cluster method includes all corrections of a given type to infinite order. The T_i operator acting on the HF reference wave function generates all i th excited Slater determinants, where the expansion coefficients, t , are the amplitudes. The exponential operator is written as

$$e^T = 1 + T_1 + \left(T_2 + \frac{1}{2}T_1^2 \right) + \left(T_3 + T_2T_1 + \frac{1}{6}T_1^3 \right) + \left(T_4 + T_3T_1 + \frac{1}{2}T_2^2 + \frac{1}{2}T_2T_1^2 + \frac{1}{24}T_1^4 \right) + \dots \quad 2.28$$

The first and second term generate the HF and all singly excited states. The first parenthesis generates all doubly excited states that are considered as either connected (T_2) or disconnected (T_1), the second parenthesis generates all triply excited states, which are either connected T_3 or disconnected triples (T_2T_1 or T_1^3), while the fourth parenthesis generates all quadruply excited states composed of five terms, a true quadruple (T_4) and four product terms (T_3T_1 , T_2^2 , $T_2T_1^2$, and

T_1^4). The connected T_4 corresponds to the simultaneous interaction of four electrons while the disconnected term T_2^2 corresponds to two non-interacting pairs of interacting electrons.

For feasibility in application to moderate-sized systems, the cluster operator must be truncated at some excitation level. If all excitations are included, the CC wavefunction is equivalent to the full CI for a given basis set, and as previously stated, full CI is too computationally expensive for all but the smallest systems. Including only the T_1 operator does not give improvement over the HF result because the single excitations are zero due to Brillouin's theorem, and the lowest level of approximation is $T = T_2$, referred to as coupled cluster doubles (CCD). Truncation of T at $T = T_1 + T_2$ gives the coupled cluster singles and doubles (CCSD). The CC wavefunction and energy are solved iteratively, and both CCD and CCSD scale as iterative M^6 . The next higher level has $T = T_1 + T_2 + T_3$, giving the coupled cluster singles doubles and triples model CCSDT, which involves a computational effort scaling as iterative M^8 , and is often impractical but for small-sized systems. However, the contributions from triples excitation are essential for the very accurate treatment of the electron correlation energy, and alternatively can be evaluated by perturbation theory and added to the CCSD result. The most common method accounts for the triples contribution non-iteratively and is calculated from MP4 (MP4SDTQ), using the CCSD amplitudes instead of the perturbation coefficients for the wavefunction corrections, and is denoted to as CCSD(T).^{52,53,54} The CCSD(T) method is non-iterative and scales as M^7 , and like all CC methods, is size-consistent and size-extensive. When combined with a relatively large basis set, typically extrapolation to the CBS limit, CCSD(T) is one of the most accurate electronic structure methods of the day and is often considered the "gold" standard.⁵¹

All of the CCSD(T) calculations in this research were performed with the MOLPRO package of programs.⁷² The open-shell CCSD(T) calculations were carried out at the R/UCCSD(T) level. In this approach, a restricted open shell HF (ROHF) calculation was initially performed, and then the spin constraint was relaxed in the coupled cluster calculation.^{73,74,75} The various calculations were done on several computer architectures, including an Opteron-based Cray XD-1 and Itanium 2-based Altix computer systems at the Alabama Supercomputer Center, a local single processor of an SGI Origin computer, a Xeon-based Dell Linux cluster at the University of Alabama, a local Opteron-based Parallel Quantum Solutions Linux Cluster, and a massively parallel Itanium 2-based HP Linux cluster in the Molecular Sciences Computing Facility in the William R. Wiley Environmental Molecular Sciences Laboratory at Pacific Northwest National Laboratory.

2.5. *Computational Thermochemistry*

We now examine the various additive components that are required for predicting the thermodynamic properties of these molecules to within chemical accuracy of ± 1 kcal/mol. The geometries were optimized numerically with a convergence threshold on the gradient of $\sim 10^{-4}$ E_h/bohr or smaller at the frozen core CCSD(T) level with the aVDZ and aVTZ correlation-consistent basis sets. The CCSD(T)/aVTZ geometries were then used in single point CCSD(T)/aVQZ calculations. The diatomic molecules were further optimized at the CCSD(T)/aVQZ level, and the bond distances, harmonic frequencies, and anharmonic corrections were obtained from a 5th order fit of the PES at this level.⁷⁶ For the molecules containing I as a substituent, geometry optimizations were performed at the CCSD(T) level with the aVDZ-PP and aVTZ-PP basis sets and additionally with the aVQZ-PP basis set for the diatomics with a fit of the PES performed at the this level. The CCSD(T)/aVTZ-PP geometry

was then used in single point CCSD(T)/aVnZ ($n = D, T,$ and Q) calculations. For polyatomic molecules where CCSD(T) optimizations would have been too computationally expensive, geometry optimizations were performed at either the MP2/VTZ or MP2/aVTZ levels,⁷⁰ and the MP2 geometry was then consequently used in single point CCSD(T)/aVnZ ($n = D, T,$ and Q) calculations.

The harmonic vibrational frequencies of the polyatomic molecules were typically calculated at the MP2 level⁷⁰ with either the VTZ or aVTZ basis set or at the CCSD(T) level with the aVDZ or aVTZ basis set, where computationally feasible, in order to obtain zero point energies, except in the case for the diatomics, thermal corrections at 298 K, and entropies. The zero point energies (ΔE_{ZPE}) were calculated from the formula $\frac{1}{2} \sum \omega_i$, where ω_i are the vibrational frequencies obtained either directly from the experimental (anharmonic) or calculated (harmonic) values, if experimental values were not available. In some cases, our calculated harmonic frequencies for the M-H ($M = B, C, N, Al,$ and P) stretches were scaled to the experimental values to account for anharmonic effects and obtain better agreement. The MP2 calculations were performed with the Gaussian program system.⁷⁷

In order to achieve thermochemical properties within ± 1 kcal/mol of experiment, core-valence (CV) correlation energy effects must be accounted for. CV calculations employed the cc-pwCVTZ⁷⁸ basis set, except for I and Br. CV calculations for Br utilized the wCVTZ-PP basis set, which is based on the VTZ-PP basis set and the accompanying small core RECP,⁶⁷ involving all 25 electrons outside the RECP core. For Br, the wCVTZ-PP basis set includes up through g -functions to provide a consistent degree of angular correlation for the active $4d$ electrons. The CV correction (ΔE_{CV}) is taken as the energy difference between the valence electron correlation calculation and that with the appropriate core electrons included using basis sets with additional

tight functions. For I, we correlated the core electrons with the awCVnZ basis sets in order to extrapolate these quantities to the CBS limit using the new RECP-correlation consistent basis sets developed by Peterson and co-workers.⁶⁷ The RECP subsumes the ($1s^2$, $2s^2$, $2p^6$, $3s^2$, $3p^6$, and $3d^{10}$) orbital space into the 28-electron core set, leaving the ($4s^2$, $4p^6$, $5s^2$, $4d^{10}$, and $5p^5$) space with 25 active electrons on each I atom, automatically including the core-valence correction upon extrapolating to the CBS limit.

Two adjustments to the total atomization energy (TAE, $\Sigma D_{0,0K}$) are necessary in order to account for relativistic effects in atoms and molecules. The first correction lowers the sum of the atomic energies, decreasing the TAE, by replacing energies that correspond to an average over the available spin multiplets with energies for the lowest multiplets as most electronic structure codes produce only spin multiplet averaged wavefunctions. The atomic spin-orbit corrections are $\Delta E_{SO}(B) = 0.03$ kcal/mol, $\Delta E_{SO}(C) = 0.09$ kcal/mol, $\Delta E_{SO}(O) = 0.22$ kcal/mol, $\Delta E_{SO}(F) = 0.39$ kcal/mol, $\Delta E_{SO}(Al) = 0.21$ kcal/mol, $\Delta E_{SO}(S) = 0.56$ kcal/mol, $\Delta E_{SO}(Si) = 0.43$ kcal/mol, $\Delta E_{SO}(Cl) = 0.84$ kcal/mol, $\Delta E_{SO}(Br) = 3.50$ kcal/mol, and $\Delta E_{SO}(I) = 7.24$ kcal/mol obtained from the excitation tables of Moore.⁷⁹ A second relativistic correction to the atomization energy accounts for molecular scalar relativistic effects, ΔE_{SR} . ΔE_{SR} is taken as the sum of the mass-velocity and 1-electron Darwin (MVD) terms in the Breit-Pauli Hamiltonian.⁸⁰ We evaluated ΔE_{SR} by using expectation values for the two dominant terms in the Breit-Pauli Hamiltonian, the so-called mass-velocity and one-electron Darwin (MVD) corrections from CISD calculations. The quantity ΔE_{SR} was obtained from CISD wavefunction with a VTZ basis set at the optimized CCSD(T) or MP2 geometry. The CISD(MVD) approach generally yields ΔE_{SR} values in good agreement (± 0.3 kcal/mol) with more accurate values from, for example, Douglas-Kroll-Hess calculations, for most molecules.⁵¹ A potential problem arises in computing the scalar relativistic

corrections for the molecules in this study as there is the possibility of “double counting” the relativistic effect on I when applying a MVD correction to an energy, which already includes most of the relativistic effects via the RECP. Since the MVD operators mainly sample the core region where the pseudo-orbitals are small, we assume any double counting to be small. For the molecules containing Br, the molecular scalar relativistic correction ΔE_{SR} was calculated using the spin-free, one-electron Douglas-Kroll-Hess (DKH) Hamiltonian.^{81,82,83} ΔE_{SR} was defined as the difference in the atomization energy between the results obtained from basis sets recontracted for DKH calculations⁸² and the atomization energy obtained with the normal valence basis set of the same quality. DKH calculations were carried out at the CCSD(T)/VTZ and the CCSD(T)/VTZ-DK levels of theory.

The total atomization energies of the molecules at 0 K ($\Sigma D_{0,0K}$) were calculated as the energy difference between the ground states of the atoms and those of the molecule, following the procedures of our previous work given in the references above,

$$\sum D_{0,0K} = \Delta E_{CBS} - \Delta E_{ZPE} + \Delta E_{CV} + \Delta E_{SR} + \Delta E_{SO} \quad 2.29$$

The heat of formation of the molecule ($A_x B_y$) at 0 K is calculated by combining our computed total atomization energies, $\Sigma D_{0,0K}$, and the experimental heats of formation of the atoms.⁸⁴

$$\Delta H_{f,0K}(A_x B_y) = x\Delta H_{f,0K}(A) + y\Delta H_{f,0K}(B) - \sum D_{0,0K}(A_x B_y) \quad 2.30$$

The heats of formation of the elements in the gas-phase employed in this research are $\Delta H_{f,0K}(H) = 51.63$ kcal/mol, $\Delta H_{f,0K}(B) = 135.1 \pm 0.2$ kcal/mol,⁸⁵ $\Delta H_{f,0K}(C) = 169.98$ kcal/mol, $\Delta H_{f,0K}(N) = 112.53$ kcal/mol, $\Delta H_{f,0K}(O) = 58.99$ kcal/mol, $\Delta H_{f,0K}(F) = 18.47$ kcal/mol, $\Delta H_{f,0K}(Al) = 78.2 \pm 1.0$ kcal/mol, $\Delta H_{f,0K}(P) = 75.42 \pm 0.24$ kcal/mol, $\Delta H_{f,0K}(S) = 65.66$ kcal/mol, $\Delta H_{f,0K}(Si) = 107.4 \pm 0.6$ kcal/mol, $\Delta H_{f,0K}(Cl) = 28.59$ kcal/mol, $\Delta H_{f,0K}(Br) = 28.19$ kcal/mol, and $\Delta H_{f,0K}(I) = 25.61$ kcal/mol, and we can derive $\Delta H_{f,0K}$ values for the molecules under study in the gas-phase. We

employ what we consider to be the best heat of formation⁸⁵ of the boron atom, which has changed over time.^{85,86,87,88} This value is based on W4 calculations of the TAEs of BF₃ and B₂H₆ and their experimental heats of formation.^{89,90} The value for Si is also not well-established, and we use $\Delta H_{f,0K}(\text{Si}) = 107.4 \pm 0.6$ kcal/mol from the work of Feller and Dixon on small Si-containing molecules.⁹¹ This value is within the error bars of the NIST value of $\Delta H_{f,0K}(\text{Si}) = 106.6 \pm 1.9$ kcal/mol.⁸⁴ The heats of formation at 298 K, $\Delta H_{f,298K}$, are obtained by following the procedures outlined by Curtiss *et al.*⁵⁹ The experimental $H_{0,298K} - H_{0,0K}$ values (thermal corrections) for the elements in their standard states and employed in this research are 1.01 (H), 0.29 (B), 0.25 (C), 1.04 (N), 1.04 (O), 1.05 (F), 1.08 (Al), 0.76 (Si), 1.28 (P), 1.05 (S), 1.10 (Cl), 2.93 (Br), and 1.58 (I) kcal/mol, respectively. The $\Delta H_{f,298K}$ values are obtained as follows

$$\begin{aligned} \Delta H_{f,298K}(A_x B_y) = & \Delta H_{f,0K}(A_x B_y) + [H_{0,298K}(A_x B_y) - H_{0,0K}(A_x B_y)] - x[H_{0,298K}(A) - H_{0,0K}(A)] \\ & - y[H_{0,298K}(B) - H_{0,0K}(B)] \end{aligned} \quad 2.31$$

CHAPTER 3

THERMODYNAMIC PROPERTIES OF MOLECULAR BORANE PHOSPHINES, ALANE AMINES, AND PHOSPHINE ALANES AND THE $[\text{BH}_4^-][\text{PH}_4^+]$, $[\text{AlH}_4^-][\text{NH}_4^+]$, AND $[\text{AlH}_4^-][\text{PH}_4^+]$ SALTS FOR CHEMICAL HYDROGEN STORAGE SYSTEMS FROM AB INITIO ELECTRONIC STRUCTURE THEORY

From: Grant, D. J.; Dixon, D. A *J. Phys. Chem. A.* **2005**, *109*, 10138-10147.

3.1 Introduction

There is clear interest in the development of H_2 -based fuel cells to provide economic, energy, and environmental security benefits to the United States. There is a critical need to develop new chemical H_2 storage materials and novel approaches for the release/uptake of H_2 for use in on-board transportation systems.¹ The amine boranes have excellent weight percent storage for H_2 with BH_3NH_3 having 19% if 3 molecules of H_2 are produced, and the salt $(\text{NH}_4)(\text{BH}_4)$ having 24% if 4 molecules of H_2 are produced. The suitability of the NH_xBH_x ($x = 1-4$) compounds for hydrogen storage has recently been evaluated using theoretical methods.^{2,3,4} The calculations showed that both $\text{BH}_3\text{NH}_3(\text{g})$, $\text{BH}_3\text{NH}_3(\text{s})$, and $[\text{BH}_4^-][\text{NH}_4^+](\text{s})$ can serve as good hydrogen storage systems. The energetics for release of H_2 were calculated and the energetics for release of H_2 from BH_3NH_3 is predicted to be substantially different than the energetics for release of H_2 from C_2H_6 . In addition, calculations on the solid materials show that they may all be good systems for H_2 storage. These prior results show that the thermoneutrality of hydrogen release from the NH_xBH_x compounds is in significant contrast to hydrolysis pathways of boron based hydrogen storage materials.⁵ In addition, recent work has shown that

nano-scaffolds can be used to mediate the release of hydrogen from amine boranes.⁶ Our current interest is to search for other candidates for H₂ storage systems in order to identify alternatives that may be easier to synthesize and for which we can design new catalysts. We have chosen to study the molecular systems isoelectronic to the previously studied amine boranes, BH₃NH₃, BH₂NH₂, and HBNH, those compounds containing Al, P, B, and N.

An important need for understanding these materials and their performance are accurate thermodynamic data. Such data is needed in designing not only the release process, but also for the regeneration system, i.e., addition of H₂ back to the H₂ depleted material. We have been developing an approach^{7,8,9,10,11,12,13,14,15,16,17,18,19,20} to the reliable calculation of molecular thermodynamic properties, notably heats of formation, based on *ab initio* molecular orbital theory. Our approach is based on calculating the total atomization energy of a molecule and using this with known heats of formation of the atoms to calculate the heat of formation at 0 K. This approach starts with coupled cluster theory with single and double excitations and including a perturbative triples correction (CCSD(T)),^{21,22,23} combined with the correlation-consistent basis sets^{24,25} extrapolated to the complete basis set limit to treat the correlation energy of the valence electrons. This is followed by a number of smaller additive corrections including core-valence interactions and relativistic effects, both scalar and spin-orbit. Finally, one must include the zero point energy obtained either from experiment, theory, or some combination. The standard heats of formation of compounds at 298 K can then be calculated by using standard thermodynamic and statistical mechanics expressions in the rigid rotor-harmonic oscillator approximation²⁶ and the appropriate corrections for the heat of formation of the atoms.²⁷

In the present study, we present data for the molecular compounds BH₃PH₃, BH₂PH₂, HBPH, AlH₃NH₃, AlH₂NH₂, HAlNH, AlH₃PH₃, AlH₂PH₂, HAlPH, AlH₄⁻, PH₃, PH₄, and PH₄⁺,

as well as the diatomics BP, AlN, and AlP. We have recently used a combined computational chemistry/empirical modeling approach²⁸ to predict the lattice energy of the $N_3^-N_5^+$ and $N_5^-N_5^+$ salts²⁹ and that of $[BH_4^-][NH_4^+](s)$.⁴ We employ this same approach to calculate the lattice energy for the $[BH_4^-][PH_4^+](s)$, $[AlH_4^-][NH_4^+](s)$, and $[AlH_4^-][PH_4^+](s)$ salts.

There have been previous experimental and computational studies of a number of the molecules under study. The molecule BH_3PH_3 has been shown to be the monomer in the molten state at 37 °C and in the solid based on nmr, infrared and Raman studies.³⁰ Jungwirth and Zahradnik³¹ calculated the geometries for BH_3NH_3 , BH_3PH_3 , AlH_3NH_3 , and AlH_3PH_3 at the MP2/6-31G* level and evaluated bond energies at the QCISD(T)/6-31G* level with a BSSE (basis set superposition error) correction. They find X-Y bond distances of 1.661, 1.944, 2.083, and 2.544 Å, respectively, and X-Y bond energies of 20.9, 15.6, 22.4, and 8.8 kcal/mol, respectively. The dissociation energy to form $BH_3 + PH_3$ has been calculated to be 18.0 kcal/mol at the MP4(STDQ)/6-31++G(d,p)//MP2/6-31++G(d,p) level.³² The bond distance for the B-P bond has been calculated to be 1.947 Å. Similarly, AlH_3PH_3 has been calculated to have a bond distance of 2.555 Å and an Al-P bond energy of 12.8 kcal/mol. The structures and frequencies of AlH_3PH_3 have been calculated at the CISD/DZP level and for AlH_2PH_2 at the CISD/TZ2P level. The geometries were also calculated at the CCSD/TZ2P level, and the Al-P bond is 2.576 Å for AlH_3PH_3 and 2.335 Å for AlH_2PH_2 with a decidedly nonplanar structure for the latter. The AlHPH isomer has been predicted to be 13 kcal/mol higher in energy than the AlPH₂ isomer at the CCSD/TZ2P level.³³ The Al-P bond distance for $Me_3Al-PMe_3$ has been found to be 2.53(4) Å based on an electron diffraction study.³⁴ The best calculated value for D_0 for the Al-P bond energy in AlH_3PH_3 is the CCSD/TZ2P value of 11.0 kcal/mol.³³ This group also calculated a dehydrogenation energy of 3.3 kcal/mol at the CCSD/TZ2P level with zero point corrections for

loss of H₂ from AlH₃PH₃ to form AlH₂PH₂. The structures and energetics of AlNH_y have been calculated at the CISD and CCSD levels with basis sets up to TZ2P.³⁵ The heat of hydrogenation of AlH₂NH₂ is -4 kcal/mol and for AlHNH is -62 kcal/mol at the CCSD/DZP level. The bond energy of AlH₃NH₃ has been calculated to be 26 kcal/mol at the CCSD/DZP level.³⁶ At the MP2/cc-pVDZ level, the bond distance in AlH₃NH₃ has been calculated to be 2.116 Å and 2.111 Å at the B3LYP/cc-pVDZ level. These values were obtained in a study of the dimers.³⁷ Watts *et al.*³⁸ studied the molecule HB=PH and found a cis structure to be the global minimum with a variety of methods up through CCSD(T) with the cc-pVTZ basis set. The cis structure is best described as an H bridging the B and P although it is not described as such in the reference. Kerrins *et al.*³⁹ also found a similar cisoid structure to be the most stable with geometries optimized at the HF/6-31G** level and energies obtained at the MP4/6-31++G** level. Their cisoid structure has less P-H bond bridging than the correlated one. The AlN molecule has been studied by Langhoff *et al.*⁴⁰ at the CASSCF and MRCI levels with a focus on the spectrum. The AlN bond energy for the ³Π state has been calculated to be 63.2 kcal/mol at the density functional theory level with the Becke exchange and Perdew-Wang correlation functional (BPW) and the DNP basis set.⁴¹ Costales *et al.* used the same method to calculate the properties of AlP for the ³Σ⁻ state.⁴²

3.2 Computational Approach

For the current study, we used the augmented correlation consistent basis sets aug-cc-pVnZ for H, B, and N ($n = D, T, Q$).^{24,25} For the sake of brevity, we abbreviate the names to aVnZ. Only the spherical components (5-*d*, 7-*f*, 9-*g* and 11-*h*) of the Cartesian basis functions were used. All of the current work was performed with the MOLPRO suite of programs.⁴³ The open-shell CCSD(T) calculations for the atoms were carried out at the R/UCCSD(T) level. In

this approach, a restricted open shell Hartree-Fock (ROHF) calculation was initially performed, and the spin constraint was relaxed in the coupled cluster calculation.^{44,45,46} All of the calculations were done on a massively parallel HP Linux cluster with 1970 Itanium-2 processors in the Molecular Sciences Computing Facility in the William R. Wiley Environmental Molecular Sciences Laboratory or on the 144 processor Cray XD-1 computer system at the Alabama Supercomputer Center.

The geometries were optimized numerically at the frozen core CCSD(T) level with the aug-cc-pVDZ and aug-cc-pVTZ correlation-consistent basis sets. The CCSD(T)/aug-cc-pVTZ geometries were then used in single point CCSD(T)/aug-cc-pVQZ calculations. Harmonic frequencies and anharmonic constants for the diatomic molecules were obtained from a 5th order fit of the potential energy surface at the CCSD(T)/aug-cc-pV(Q+d)Z level. For a few molecules, the harmonic frequencies were calculated at the CCSD(T)/aug-cc-pVDZ to get scaling parameters for the zero point energies. All of the vibrational frequencies were calculated at the MP2/cc-pVTZ level⁴⁷ using the Gaussian program system.⁴⁸ These were used for the zero point energies, except for the diatomics and for the thermal corrections and entropies.

It has recently been found that tight *d* functions are necessary for calculating accurate atomization energies for 2nd row elements,⁴⁹ so we also included additional tight *d* functions in our calculations. Basis sets containing extra tight *d* functions are denoted aug-cc-pV(*n*+*d*)Z in analogy to the original augmented correlation consistent basis sets. We will use aug-cc-pV(*n*+*d*)Z to represent the combination of aug-cc-pV(*n*+*d*)Z (on the 2nd row atoms Al and P) and aug-cc-pV*n*Z (on H, B, and N) basis sets and abbreviate this as aV(*n*+*d*)Z. The CCSD(T) total energies were extrapolated to the CBS limit by using a mixed exponential/Gaussian function of the form:

$$E(n) = E_{\text{CBS}} + A \exp[-(n-1)] + B \exp[-(n-1)^2] \quad (1)$$

with $n = 2$ (DZ), 3 (TZ) and 4 (QZ), as first proposed by Peterson *et al.*⁵⁰ This extrapolation method has been shown to yield atomization energies in the closest agreement with experiment (by a small amount) as compared to other extrapolation approaches up through $n = 4$.

Core-valence corrections, ΔE_{CV} , were obtained at the CCSD(T)/cc-pwCVTZ level of theory.⁵¹ Scalar relativistic corrections (ΔE_{SR}), which account for changes in the relativistic contributions to the total energies of the molecule and the constituent atoms, were included at the CI-SD (configuration interaction singles and doubles) level of theory using the cc-pVTZ basis set. ΔE_{SR} is taken as the sum of the mass-velocity and 1-electron Darwin (MVD) terms in the Breit-Pauli Hamiltonian.⁵² Most calculations using available electronic structure computer codes do not correctly describe the lowest energy spin multiplet of an atomic state as spin-orbit in the atom is usually not included. Instead, the energy is a weighted average of the available multiplets. For N or P in the ^4S state, no spin-orbit correction is needed, but a correction of 0.03 kcal/mol is needed for B and one of 0.21 kcal/mol for Al, taken from the excitation energies of Moore.⁵³

By combining our computed ΣD_0 (total atomization energies) values with the known heats of formation at 0 K for the elements ($\Delta H_f^0(\text{N}) = 112.53 \pm 0.02$ kcal mol⁻¹, $\Delta H_f^0(\text{B}) = 136.2 \pm 0.2$ kcal mol⁻¹, $\Delta H_f^0(\text{P}) = 75.42 \pm 0.24$ kcal mol⁻¹, $\Delta H_f^0(\text{Al}) = 78.23 \pm 1.0$ kcal mol⁻¹, and $\Delta H_f^0(\text{H}) = 51.63$ kcal mol⁻¹,⁵⁴ we can derive ΔH_f^0 values for the molecules under study in the gas phase. We obtain heats of formation at 298 K by following the procedures outlined by Curtiss *et al.*²⁷

In order to predict the lattice energies needed for predicting the heat of formation of a salt, we can use the empirical expression²⁸

$$U_L = 2 I [\alpha V_m^{-1/3} + \beta] \quad (2)$$

to estimate the lattice energy, U_L , of the salt where I is the ionic strength ($I = 1$), V_m is the molecular (formula unit) volume of the lattices involved, which is equal to the sum of the individual ion volumes of the cation, V_+ and anion, V_- and $\alpha = 28.0 \text{ kcal mol}^{-1} \text{ nm}$ and $\beta = 12.4 \text{ kcal mol}^{-1}$ for 1:1 salts. Most of the individual ion volumes for can be taken from an ion volume database and are $V(\text{BH}_4^-) = 0.066 \pm 0.15$, $V(\text{NH}_4^+) = 0.021 \pm 0.15$, $V(\text{AlH}_4^-) = 0.067 \text{ nm}^3$.²⁸ The volume for PH_4^+ was calculated based on the volumes that we have used in free energy of solvation calculations.⁵⁵ The electron densities were calculated at the B3LYP/6-31+G* level,⁵⁶ and the volume was taken to be that inside the 0.001 a.u. contour of the electron density giving $V(\text{PH}_4^+) = 0.025 \text{ nm}^3$. The empirical expression is probably good to $\pm 5 \text{ kcal/mol}$ based on comparing lattice energies from it with those obtained from experimental data based on a Born-Haber cycle. For example, for NH_4CN , KI , and LiF the values are essentially identical within 1 kcal/mol as shown by Jenkins *et al.*²⁸ based on the values reported by Jenkins.⁵⁷

3.3 Results and Discussion

The calculated geometries are given in Tables 3.1 to 3.4 and the calculated vibrational frequencies in Tables 3.5 to 3.8. The molecular structures are shown in Figure 3.1. The calculated geometries show some interesting behavior. The molecules BH_3PH_3 , AlH_3NH_3 , and AlH_3PH_3 all have long dative bonds between the Group IIIA and Group VA atoms. As a consequence, the HPH angles become a little less pyramidal than in PH_3 , and the HAlH and HBH bond angles become more pyramidal and move away from the D_{3h} angle of 120.0° . The molecule AlH_2NH_2 remains planar as found for BH_2NH_2 , but the molecules BH_2PH_2 and AlH_2PH_2 become non-planar. The non-planarity occurs at the PH_2 - moiety and is consistent with the much higher inversion barrier in PH_3 as compared to NH_3 .⁵⁸ The non-planar form of BH_2PH_2

is 6.5 kcal/mol more stable than the planar structure at the CBS valence electronic energy level, and the non-planar form of AlH_2PH_2 is 5.0 more stable than the planar structure at the same level. The molecules BHPH and AlHPH are clearly bent with the bent structures 28.4 and 25.9 kcal/mol more stable than the linear structures at the CBS valence electronic energy level, respectively. The bent structure HBPH forms a BHP bridge-bond with a PH distance of 1.529 Å, which is slightly larger than the PH bond distance obtained for PH_3 of 1.419 Å. Also, the $\angle\text{BHP}$ of 70.1° is smaller than the $\angle\text{BHB}$ of 84.3° obtained in diborane. This structure for the minimum is essentially the same as the one predicted by Watts *et al.*³⁸ The molecule AlHNH has more complicated energetics with the bent and linear forms having the same energy at the CBS valence electronic energy level. The bent AlHNH molecule has a trans-structure with a $\angle\text{HNAI}$ of 147.2° further from linear compared to the $\angle\text{HAIN}$ of 161.4°. The bent structure HAIPH has a $\angle\text{HPAI}$ of 78.0° with the HAIP angle remaining linear. The PH bond distance of 1.449 Å is larger than the PH bond distance obtained in PH_3 of 1.419 Å.

Huber and Herzberg⁵⁹ report a bond length of 1.786 Å for the bond length of the $^3\Pi$ state for AlN, and our best calculated value is a little long by 0.02 Å. The calculated and experimental values for ω_e are in excellent agreement with each other for the $^3\Pi$ state. Langhoff *et al.*⁴⁰ calculated a number of states for AlN at the CASSCF and MRCI levels and suggest that the ground state is $^3\Pi$ with the $^3\Sigma^-$ slightly higher in energy. Their spectroscopic constants of $R_e = 1.817$ Å and $\omega_e = 737$ cm^{-1} for the $^3\Pi$ state are in good agreement with ours, and our values of $R_e = 1.8031$ Å and $\omega_e = 745$ cm^{-1} for the $^3\Pi$ state show a slightly shorter bond distance and higher frequency as a consequence. Costales *et al.*⁴² calculated the properties of AlP for the $^3\Sigma^-$ state at the BPW/DNP level and obtain $R_e = 2.46$ Å and $\omega_e = 348$ cm^{-1} in qualitative agreement with our values as their bond length is too long and their frequency too low.

The calculated frequencies for the molecules under consideration are given in Tables 3.5 to 3.8. Where comparisons can be made, the values are in reasonable agreement with the experimental values.^{60,61,62} Based on our previous calculations on BNH_x compounds,⁴ as well as those of others,⁶³ the largest error in the calculated frequencies would be in the bond between the Group IIIA and Group VA atoms in the compound $\text{H}_3\text{X}-\text{YH}_3$. However, because the bonds are longer in the compounds under consideration, the error is smaller in an absolute sense. In order to calculate the zero point energy correction, we scaled the M-H frequencies by the factors 0.96 for $\text{M} = \text{B}$ and $\text{M} = \text{N}$, 0.95 for $\text{M} = \text{P}$, and 0.954 for $\text{M} = \text{Al}$. These scale factors were obtained by taking the average of the CCSD(T)/aug-cc-pVTZ values and the experimental values for the M-H stretches for the MH_3 compounds and dividing them by the MP2/cc-pVTZ value. Thus, we estimate that the error introduced in the heats of formation due to the zero point energies is a maximum of ± 0.5 kcal/mol.

The calculated total valence CCSD(T) energies as a function of basis set are given as Supplementary Material, and the calculated energy components for the total atomization energies in Table 3.9. The relativistic corrections are all negative and reasonably small ranging from 0 to -1 kcal/mol. The core-valence corrections are positive for the BPH_x series and range from 1 to 1.6 kcal/mol. For the AlNH_x series, the core-valence corrections are negative and range for 0 to -1 kcal/mol. For the AlPH_x series, the core-valence corrections are positive for the compounds containing PH_3 and are negative for the remaining compounds. The calculated heats of formation are given in Table 3.10. The calculated value for $\Delta H_f(\text{PH}_3)$ is in excellent agreement with the experimental value. Our estimated error bars for the heats of formation are ± 1.0 kcal/mol.

The diatomic BN molecule has a $^3\Pi$ ground state with the $^1\Sigma^+$ 0.54 kcal/mol higher in energy.⁶⁴ The diatomic BP has a $^3\Pi$ ground state with the $^1\Sigma^+$ 7.5 kcal/mol higher in energy and

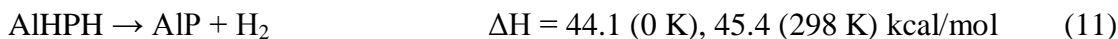
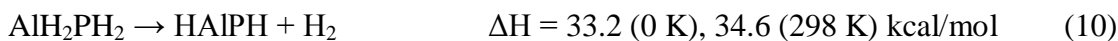
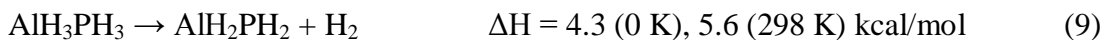
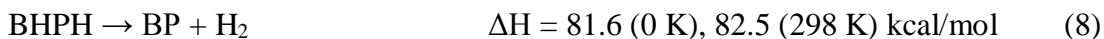
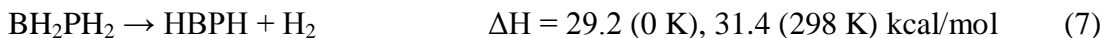
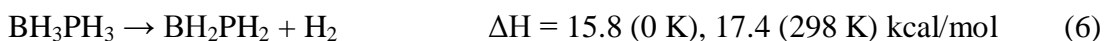
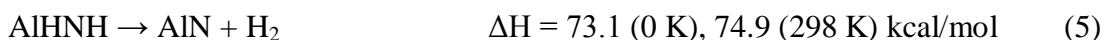
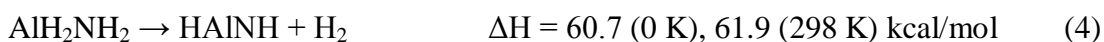
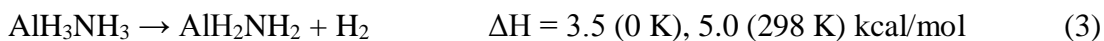
the $^3\Sigma^-$ 20.9 kcal/mol higher in energy. The AlN molecule has a near degeneracy between the $^3\Pi$ and the $^3\Sigma^-$, and we predict the $^3\Sigma^-$ to be slightly lower in energy. The $^1\Sigma^+$ state is 9.5 kcal/mol higher in energy. Both the $^3\Pi$ and $^1\Sigma^+$ states have substantial multi-reference character as noted by the large T_1 diagnostics.⁶⁵ The $^3\Sigma^-$ state does not have substantial multi-reference character. The AlP molecule is very similar to the AlN molecules with the two triplet states essentially isoenergetic, and the $^3\Sigma^-$ is the ground state. The $^1\Sigma^+$ state is 12.0 kcal/mol higher in energy than the ground state. Although the AlP $^1\Sigma^+$ state does have some multireference character, it is substantially smaller than in BN or AlN. The $^3\Pi$ state for AlP has a little multireference character, but it is not large, and the $^3\Sigma^-$ has very little. The BP bond energy is substantially higher than the AlN or AlP bond energies. The multireference character in the three states for BP is like that in AlP.

The dissociation energy for AlN has been measured spectroscopically to be 66 ± 9 kcal/mol.^{54,66} Our value of 57.3 kcal/mol is consistent with the lower range of the experimental value. The higher experimental dissociation energy leads to a value of $\Delta H_f^0(\text{AlN}) = 125.0$ kcal/mol, lower than our calculated value as expected based on the difference in dissociation energies. Our value of $D_e = 58.1$ kcal/mol for the $^3\Pi$ state is consistent with the value calculated by Langhoff *et al.*⁴⁰ of 54.2 kcal/mol at the MRCI+Q level with a [5s4p2d1f(N)/6s5p2d1f(Al)] basis set. Langhoff *et al.*⁴⁰ find the $^1\Sigma^+$ state to be 13.3 kcal/mol above the $^3\Pi$, a few kcal/mol higher than our energy difference. At the BPW/DNP level, the bond energy for AlN is calculated to be about 6 kcal/mol higher than our more accurately calculated value.⁴¹ The BP bond energy has been measured to be 82.0 ± 4 kcal/mol based on Knudsen cell measurements in reasonable agreement with our value of 76.4 kcal/mol.⁶⁷ The dissociation energy for AlP has been measured to be 50.8 ± 3 kcal/mol in excellent agreement with our calculated value of 50.7 kcal/mol.⁶⁸

The calculated heat of formation of PH₃ of 1.4 kcal/mol at 298 K is in excellent with the experimental value of 1.3 kcal/mol.⁵⁴ Similarly, the calculated heat of formation of AlH₃ of 30.3 kcal/mol at 298 K is in excellent agreement with the experimental value of 30.8 kcal/mol,⁵⁴ especially considering the error bars for the heat of formation of the Al atom. We have previously shown that the calculated heats of formation of BH₃ and NH₃ are in good agreement with experiment.^{4,19,20}

The dissociation energy of AlH₃NH₃ to form AlH₃ + NH₃ is calculated to be 26.1 kcal/mol, comparable to the calculated value of 25.9 kcal/mol for BH₃NH₃.⁴ The dissociation energy of BH₃PH₃ is calculated to be somewhat lower at 21.1 kcal/mol, and the dissociation energy of AlH₃PH₃ is calculated to be even lower at 14.0 kcal/mol. These values are in general higher than those obtained by workers using lower level methods.³¹⁻³⁶

Based on the calculated values, we can calculate the energy for the sequential release of H₂ from these molecules in the gas phase



Based simply on the value of ΔH , reaction (3) involving AlH_3NH_3 and reaction (9) involving AlH_3PH_3 might be possible sources for H_2 release as they are close to thermoneutral. However, one must also consider the values of the free energy. The formation of two gas phase products will lead to a substantial $T\Delta S$ term, which will make H_2 generation more favorable. The values of S for each molecule are given in Table 3.11, and the values of $-T\Delta S$ at $T = 298\text{K}$ for reactions (3) – (11) are given in Table 3.12. These values clearly show that reactions (3) and (9) are potential sources for H_2 .

Another possibility for an H_2 storage system are the salts $[\text{BH}_4^-][\text{PH}_4^+]$, $[\text{AlH}_4^-][\text{NH}_4^+]$, and $[\text{AlH}_4^-][\text{PH}_4^+]$. We⁴ and others^{2,3} have previously predicted that the salt $[\text{BH}_4^-][\text{NH}_4^+]$ can readily release H_2 to form either solid or gaseous BH_3NH_3 exothermically. We can estimate the lattice energy of the salts from equation (2) by using the volumes given above. Use of these values in equation (2) gives lattice energies for $[\text{BH}_4^-][\text{PH}_4^+]$, $[\text{AlH}_4^-][\text{NH}_4^+]$, and $[\text{AlH}_4^-][\text{PH}_4^+]$ of 149.3, 150.7, and 148.9 kcal/mol, respectively, and calculated heats of formation of the salts at 0 K of 21.8, -0.5, and 30.4 kcal/mol, respectively. We note that the error bars for using Eq. (2) are probably ± 5 kcal/mol. The reaction energies starting from the ionic solid to form the gas phase products are:



All of the reactions involving the salts releasing H_2 are predicted to be exothermic as found for $[\text{BH}_4^-][\text{NH}_4^+]$. Thus, they may serve as H_2 storage systems. The reaction starting from $[\text{AlH}_4^-][\text{NH}_4^+](\text{s})$ is close to thermoneutral so this salt might be a good source of H_2 as it will be easier to manage the heat release.

In order for the salt to be stable, we need to look at the possibility of electron transfer. The electron affinity (EA) of NH_4^+ is very low as NH_4 is a Rydberg molecule with only a weak binding of H to NH_3 if at all. Thus, we estimate the $\text{EA}(\text{NH}_4^+)$ as the energy of the reaction



giving -111.6 kcal/mol (4.84 eV). The ionization potential of BH_4^- can be estimated from the reaction



as BH_4 is a weakly bonded system with a predicted dissociation energy of 12.9 kcal/mol to form $\text{BH}_3 + \text{H}$ and a dissociation energy to form $\text{BH}_2 + \text{H}_2$ of 14.8 kcal/mol at the UMP4/6-311G(df,p) level.⁶⁹ The electron affinity of BH_3 is very small (0.038 ± 0.015 eV = 0.88 ± 0.35 kcal/mol).⁷⁰ The ionization potential of BH_4^- is thus predicted to quite low, 76.7 kcal/mol (3.33 eV).⁷¹ The fact that the electron affinity of NH_4^+ and the ionization potential of BH_4^- are comparable within 1.5 eV of each other is consistent with the fact that this salt can be produced as we have previously reported.

The molecule AlH_4 is predicted to be only weakly bound by 1 kcal/mol (without zero point energy (ZPE) corrections and unbound with ZPE corrections included) with respect to $\text{AlH}_2 + \text{H}_2$ at the UMP4/6-311+G(MC)(2df,p) level and is predicted to be bound by 17.9 kcal/mol with respect to $\text{AlH}_3 + \text{H}$.⁷² The ionization potential of AlH_4^- can be estimated by the reaction



giving a value of 69.0 kcal/mol (2.99 eV), which is similar to the value found for BH_4^- . The EA of PH_4^+ is given by



where the 1st half of the reaction gives 127.8 kcal/mol (5.54 eV), which is reduced by 4.4 kcal/mol (0.19 eV) by the ability of PH₃ to bind H to give a final value of 5.35 eV. PH₄ (²A₁) is thus barely stable with a P-H bond energy of 4.4 kcal/mol with respect to PH₃ + H.

Use of these ionization and electron attachment values for reactions (12) to (14) gives electron transfer energies of 2.02, 1.85, and 2.36 eV, respectively. These values are substantially less than the lattice energies so that electron transfer is unlikely to occur and the salts are expected to be stable in terms of their ionic components.

From the heats of formation of AlH₄⁻ and AlH₃ together with the heat of formation of H⁻ (34.2 kcal/mol at 298 K), we can calculate the hydride affinity of AlH₃ defined as -ΔH for the reaction AlH₃ + H⁻ → AlH₄⁻. This value is 70.4 kcal/mol, which shows that AlH₃ is a good hydride acceptor as expected. There is a very recent experimental value⁷³ (published after our paper was initially submitted) based on a flowing afterglow mass spectrometric measurement for the hydride affinity of 75 ± 4 kcal/mol, in reasonable agreement with our computational value. The value⁴ for the hydride affinity of BH₃ of 72.2 kcal/mol is very similar to that for AlH₃. From the heats of formation of PH₄⁺ and PH₃ together with the heat of formation of H⁺ (367.2 kcal/mol at 298K), we calculate the proton affinity of PH₃ to be 187.8 kcal/mol, in excellent agreement with the experimental value of 188 kcal/mol.⁷⁴

3.4 Conclusions

Ab initio molecular orbital theory at the CCSD(T)/CBS level plus additional corrections has been used to predict the heats of formation of a number of borane phosphines, alane amines, and phosphine alanes. The heat of formation of the salts [BH₄⁻][PH₄⁺], [AlH₄⁻][NH₄⁺], and [AlH₄⁻][PH₄⁺](s) has been estimated by using an empirical expression for the lattice energy and the calculated heats of formation of the two component ions. The calculations show that both

$\text{AlH}_3\text{NH}_3(\text{g})$ and $[\text{AlH}_4^-]\text{NH}_4^+(\text{s})$ can serve as good hydrogen storage systems. In addition, AlH_3PH_3 and the salts $[\text{AlH}_4^-][\text{PH}_4^+]$ and $[\text{BH}_4^-][\text{PH}_4^+]$ have the potential to serve as H_2 storage systems. The hydride affinity for AlH_3 and the proton affinity for PH_3 were also calculated, and the latter value is found to be in good agreement with the available experimental result. The P-H bond energy in PH_4 of 4.4 kcal/mol shows that PH_4 is only weakly bound with respect to the $\text{H} + \text{PH}_3$ asymptote.

Acknowledgements Funding provided in part by the Department of Energy, Office of Energy Efficiency and Renewable Energy under the Hydrogen Storage Grand Challenge, Solicitation No. DE-PS36-03GO93013. The Robert Ramsay Fund of the University of Alabama is thanked for support. This work was done as part of the Chemical Hydrogen Storage Center. This research was performed in part using the Molecular Science Computing Facility (MSCF) in the William R. Wiley Environmental Molecular Sciences Laboratory, a national scientific user facility sponsored by the U.S. Department of Energy's Office of Biological and Environmental Research and located at the Pacific Northwest National Laboratory. Pacific Northwest National Laboratory is operated for the Department of Energy by Battelle.

Appendix Total CCSD(T) energies (E_h) as a function of basis set. This material is available free of charge via the Internet at <http://pubs.acs.org>.

Table 3.1. Optimized CCSD(T) Bond Lengths (\AA) and Bond Angles ($^\circ$) for AlH_x and PH_x .

Molecule	Basis Set	r_{MH}	$\angle\text{HMH}$
AlH_3	aVDZ	1.5921	120.0
	aVTZ	1.5855	120.0
AlH_4^-	aVDZ	1.6547	109.5
	aVTZ	1.6482	109.5
PH_3 ($^1\text{A}_1$)	aVDZ	1.4343	93.5
	aVTZ	1.4195	93.5
	expt	1.413	93.5
PH_4 (C_{2v})	aVDZ	1.5488 _{ax}	170.7 _{ax}
		1.4238 _{eq}	99.1 _{eq}
	aVTZ	1.5241 _{ax}	170.6 _{ax}
		1.4091 _{eq}	99.8 _{eq}
PH_4^+	aVDZ	1.4103	109.5
	aVTZ	1.3972	109.5

Table 3.2. Optimized CCSD(T) Bond Lengths (Å) and Bond Angles (°) for BPH_x.

Molecule	Basis Set	r _{PH}	∠HPH	∠HPB	r _{BH}	∠HBH	∠HBP	r _{BP}
BP (³ Π)	aVDZ							1.7858
	aVTZ							1.7602
	aVQZ							1.7521
BP (³ Σ ⁻)	aVDZ							1.9976
	aVTZ							1.9728
	aVQZ							1.9643
BP (¹ Σ ⁺)	aVDZ							1.7133
	aVTZ							1.6880
	aVQZ							1.6799
HBPH (linear)	aVDZ	1.3967			1.1841			1.6701
	aVTZ	1.3855			1.1717			1.6507
HBPH (non-linear)	aVDZ	1.5454		52.70	1.1910		176.38	1.7307
	aVTZ	1.5288		52.57	1.1778		176.49	1.7066
BH ₂ PH ₂ (planar)	aVDZ	1.4071	109.23		1.2029	124.61		1.8140
	aVTZ	1.3939	109.03		1.1888	124.69		1.7943
BH ₂ PH ₂ (non-planar)	aVDZ	1.4101	100.16	102.53	1.2056	120.86	119.65	1.8997
	aVTZ	1.4101	100.16	103.18	1.1913	120.86	119.57	1.8783
BH ₃ PH ₃	aVDZ	1.4205	99.98		1.2215	115.01		1.9818
	aVTZ	1.4062	99.99		1.2079	114.87		1.9491

Table 3.3. Optimized CCSD(T) Bond Lengths (Å) and Bond Angles (°) for AlNH_x.

Molecule	Basis Set	r _{NH}	∠HNH	∠HNAI	r _{AlH}	∠HAIH	∠HAIN	r _{AIN}
AlN (³ Π)	aVDZ							1.8597
	aVTZ							1.8141
	aVQZ							1.8031
AlN (³ Σ ⁻)	aVDZ							1.9894
	aVTZ							1.9400
	aVQZ							1.9287
AlN (¹ Σ ⁺)	aVDZ							1.7186
	aVTZ							1.6863
	aVQZ							1.6771
HAINH (linear)	aVDZ	1.0080			1.5630			1.6530
	aVTZ	0.9990			1.5590			1.6312
HAINH (non-linear)	aVDZ	1.0175		137.67	1.5730		157.30	1.6974
	aVTZ	1.0046		147.21	1.5646		161.37	1.6579
AlH ₂ NH ₂ (planar)	aVDZ	1.0168	110.02		1.5888	124.78		1.8087
	aVTZ	1.0090	109.77		1.5833	124.38		1.7812
AlH ₃ NH ₃	aVDZ	1.0238	107.09		1.6087	117.71		2.1220
	aVTZ	1.0164	107.36		1.6038	117.51		2.0714

Table 3.4. Optimized CCSD(T) Bond Lengths (Å) and Bond Angles (°) for AlPH_x .

Molecule	Basis Set	r_{PH}	$\angle\text{HPH}$	$\angle\text{HPAl}$	r_{AlH}	$\angle\text{HAlH}$	$\angle\text{HAIP}$	r_{AlP}
AlP ($^3\Pi$)	aVDZ							2.2743
	aVTZ							2.2366
	aVQZ							2.2197
AlP ($^3\Sigma^-$)	aVDZ							2.4773
	aVTZ							2.4374
	aVQZ							2.4232
AlP ($^1\Sigma^+$)	aVDZ							2.1399
	aVTZ							2.1108
	aVQZ							2.0967
HAIPH (linear)	aVDZ	1.4013			1.5623			2.0532
	aVTZ	1.3890			1.5576			2.0315
HAIPH (non-linear)	aVDZ	1.4592		80.04	1.5881		180.0	2.1865
	aVTZ	1.4487		78.01	1.5817		180.0	2.1585
AlH ₂ PH ₂ (planar)	aVDZ	1.4097	107.28		1.5835	127.82		2.2573
	aVTZ	1.3971	106.95		1.5775	127.50		2.2373
AlH ₂ PH ₂ (non-planar)	aVDZ	1.4352	95.16	94.02	1.5919	121.34	119.33	2.3651
	aVTZ	1.4213	95.01	93.55	1.5855	121.09	119.46	2.3402
AlH ₃ PH ₃	aVDZ	1.4229	98.44		1.6033	118.75		2.6231
	aVTZ	1.4087	98.63		1.5979	118.65		2.5673

Table 3.5. Calculated Vibrational MP2/(CCSD(T)/aug-cc-pVDZ) Frequencies (cm^{-1}) for AlH_x and PH_x .^a

Molecule	Symmetry	Calc.	Expt.
AlH_3	a_1'	1894.0/1904.5	
	a_2''	732.1/721.7	697.8 ⁶⁰
	e'	1896.2/1911.2	1882.8
	e'	807.3/787.0	783.4
AlH_4^-	a	1692.5/1702.8	
	e	778.3 (750.5)	750.0 ⁶⁰
	t	1614.0 (1620.4)	1609.3
	t	802.9/767.9	766.6
PH_3	a_1	2352.6 (2385.0)	2323 ⁶¹
	a_1	1020.4 (1005.0)	992
	e	2364.5 (2398.1)	2328
	e	1161.6 (1133.4)	1118
PH_4	a_1	2402.7	
	a_1	1791.2	
	a_1	1027.7	
	a_1	919.4	
	a_2	1218.8	
	b_1	2418.7	
	b_1	856.7	
	b_2	1441.5	
PH_4^+	a	2449.9	
	e	1166.5	
	t	2502.5	
	t	1020.1	

^a Calculated values at the CCSD(T)/aug-cc-pVDZ level are given after the “/”.

Table 3.6. Calculated Vibrational MP2/cc-pVTZ Level Frequencies (cm^{-1}) for BPH_x .^a

Molecule	Symmetry	Calc.
$\text{BP } (^3\Pi)^b$	σ	941.1
		6.21 ($\omega_e\chi_e$)
$\text{BP } (^3\Sigma^-)^b$	σ	638.7
		4.41 ($\omega_e\chi_e$)
$\text{BP } (^1\Sigma^+)^b$	σ	1043.4
		6.26 ($\omega_e\chi_e$)
HBPH (linear)	σ	2749.0
	σ	2551.0
	σ	1145.4
	π	650.7
	π	574.9i
HBPH (non-linear)	a_1	2708.0
	a_1	1978.7
	a_1	1068.9
	a_1	1050.0
	a_1	759.0
	a_2	658.5
BH_2PH_2 (planar)	a_1	2550.0
	a_1	2485.9
	a_1	1194.6
	a_1	1088.2
	a_1	828.5
	a_2	720.4
	b_1	891.4
	b_1	340.8i
	b_2	2656.3
	b_2	2518.4
	b_2	823.8
b_2	438.8	
BH_2PH_2 (non-planar)	a_1	2540.3

	a ₁	2398.5
	a ₁	1224.3
	a ₁	1136.5
	a ₁	950.7
	a ₁	750.2
	a ₁	403.5
	a ₂	2633.8
	a ₂	2419.4
	a ₂	896.5
	a ₂	536.8
	a ₂	491.3
BH ₃ PH ₃	a ₁	2442.6
	a ₁	2403.0
	a ₁	1118.2
	a ₁	1037.4
	a ₁	547.7
	a ₂	245.4
	e	2492.5
	e	2430.1
	e	1186.7
	e	1163.4
	e	850.7
	e	385.3

^a Calculated values at the CCSD(T)/aug-cc-pVDZ level are given after the “/”. ^b Diatomic molecule frequencies calculated at the CCSD(T)/aug-cc-pV(Q+d)Z level with a 5th order fit.

Table 3.7. Calculated Vibrational MP2/(CCSD(T)/aug-cc-pVDZ) Frequencies (cm^{-1}) for AlNH_x .^a

Molecule	Symmetry	Calc.	Expt.
AlN ($^3\Pi$)	σ	745.06	746.9 ⁵⁹
		5.65 ($\omega_e\chi_e$)	
AlN ($^3\Sigma^-$)	σ	622.54	
		4.54 ($\omega_e\chi_e$)	
AlN ($^1\Sigma^+$)	σ	970.7	
		6.04 ($\omega_e\chi_e$)	
HAlNH (linear)	σ	3630.7	
	σ	2000.8	
	σ	1106.2	
	π	531.5	
	π	216.1i	
HAlNH (non-linear)	a_1	3563.5	
	a_1	1977.0	
	a_1	1051.3	
	a_1	486.2	
	a_1	296.8	
	a_2	517.4	
AlH_2NH_2 (planar)	a_1	3469.5/3499.7	3558.1 ⁶²
	a_1	1897.9/1891.0	1921.5
	a_1	1573.0/1541.6	1566.6
	a_1	839.3/801.4	818.7
	a_1	764.8/742.8	755.0
	a_2	498.8	
	b_1	629.8/627.2	608.7
	b_1	427.8/411.7	518.3
	b_2	3567.6/3657.7	
	b_2	1900.1/1925.9	1899.3
b_2	735.0/745.1	769.8	

AlH ₃ NH ₃	b ₂	424.1/435.1
	a ₁	3354.9
	a ₁	1827.4
	a ₁	1263.5
	a ₁	791.2
	a ₁	422.3
	a ₂	125.6
	e	3483.4
	e	1808.8
	e	1664.8
	e	800.2
	e	709.6
e	373.2	

^a Calculated values at the CCSD(T)/aug-cc-pVDZ level are given after the “/”. ^b Diatomic molecule frequencies calculated at the CCSD(T)/aug-cc-pV(Q+d)Z level with a 5th order fit.

Table 3.8. Calculated Vibrational MP2/(CCSD(T)/aug-cc-pVDZ) Frequencies (cm^{-1}) for AlPH_x ^a

Molecule	Symmetry	Calc.
AlP ($^3\Pi$)	σ	466.7
		0.85 ($\omega_e\chi_e$)
AlP ($^3\Sigma^-$)	σ	372.76
		1.67 ($\omega_e\chi_e$)
AlP ($^1\Sigma^+$)	σ	560.1
		2.93 ($\omega_e\chi_e$)
HAlPH (linear)	σ	2521.2
	σ	1996.0
	σ	687.9
	π	441.1
	π	565.3i
HAlPH (non-linear)	a_1	2155.8
	a_1	1905.8
	a_1	636.8
	a_1	534.2
	a_1	300.5
	a_2	391.1
AlH ₂ PH ₂ (planar)	a_1	2463.8
	a_1	1910.3
	a_1	1079.8
	a_1	747.2
	a_1	494.5
	a_2	440.2
	b_1	594.9
	b_1	413.8i
	b_2	2493.0
	b_2	1926.0
b_2	546.5	
b_2	318.6	

AlH ₂ PH ₂ (non-planar)	a ₁	2337.5	
	a ₁	1884.1	
	a ₁	1105.4	
	a ₁	791.9	
	a ₁	632.1	
	a ₁	432.1	
	a ₁	417.0	
	a ₂	2351.5	
	a ₂	1893.4	
	a ₂	665.4	
	a ₂	373.4	
	a ₂	203.9	
	AlH ₃ PH ₃	a ₁	2430.5
		a ₁	1842.2
a ₁		1016.7	
a ₁		730.6	
a ₁		241.1	
a ₂		125.2	
e		2424.1	
e		1833.2	
e		1153.6	
e		777.8	
e	515.95		
e	220.6		

^a Calculated values at the CCSD(T)/aug-cc-pVDZ level are given after the “/”. ^b Diatomic molecule frequencies calculated at the CCSD(T)/aug-cc-pV(Q+d)Z level with a 5th order fit.

Table 3.9. Components for Calculated Atomization Energies in kcal/mol.^a

Molecule	CBS ^b	$\Delta E_{\text{ZPE}}^{\text{c}}$	$\Delta E_{\text{CV}}^{\text{d}}$	$\Delta E_{\text{SR}}^{\text{e}}$	$\Delta E_{\text{SO}}^{\text{f}}$	$\Sigma D_0(\text{OK})^{\text{g}}$
BP ($^3\Pi$)	77.19	1.34	0.78	-0.16	-0.03	76.44
BP ($^3\Sigma^-$)	56.24	0.91	0.35	-0.07	-0.03	55.58
BP ($^1\Sigma^+$)	69.83	1.50	0.81	-0.13	-0.03	68.98
AlN ($^3\Pi$)	58.23	1.06	0.24	-0.13	-0.21	57.07
AlN ($^3\Sigma^-$)	58.51	0.89	-0.01	-0.14	-0.21	57.26
AlN ($^1\Sigma^+$)	49.94	1.40	-0.42	-0.13	-0.21	47.78
AlP ($^3\Pi$)	51.63	0.67	0.12	-0.13	-0.21	50.74
AlP ($^3\Sigma^-$)	51.72	0.53	0.07	-0.12	-0.21	50.93
AlP ($^1\Sigma^+$)	40.53	0.81	-0.46	-0.16	-0.21	38.90
HBPH (linear)	243.35	11.07	1.23	-0.64	-0.03	232.84
HBPH (non-linear)	271.79	11.75	1.48	-0.23	-0.03	261.26
HAlNH (linear)	245.89	11.14	-0.29	-0.63	-0.21	233.62
HAlNH (non-linear)	245.88	11.27	-0.27	-0.57	-0.21	233.56
HAlPH (linear)	181.89	8.70	-0.88	-1.00	-0.21	171.10
HAlPH (non-linear)	207.80	8.46	-0.31	-0.48	-0.21	198.34
BH ₂ PH ₂ (planar)	409.82	23.14	1.39	-0.66	-0.03	387.38
BH ₂ PH ₂ (non-planar)	416.31	23.40	1.35	-0.53	-0.03	393.70
AlH ₂ NH ₂ (planar)	422.57	23.90	-0.21	-0.69	-0.21	397.56
AlH ₂ PH ₂ (planar)	345.97	18.59	-0.74	-0.96	-0.21	325.42
AlH ₂ PH ₂ (non-planar)	354.92	18.70	-0.60	-0.72	-0.21	334.73
BH ₃ PH ₃	547.28	35.45	1.57	-0.61	-0.03	512.76
AlH ₃ NH ₃	541.80	36.38	-0.15	-0.73	-0.21	504.33
AlH ₃ PH ₃	472.00	28.91	0.27	-0.86	-0.21	442.29
AlH ₃	214.27	11.48	-1.00	-0.33	-0.21	201.25
AlH ₄ ⁻	304.76	15.00	-0.99	-0.48	-0.21	288.10
PH ₃	242.01	14.89	0.27	-0.36	0.00	227.03
PH ₄	250.81	18.86	0.09	-0.61	0.00	231.43
PH ₄ ⁺	121.89	21.93	-0.08	-0.62	0.00	99.26

^a The energies of the atomic asymptotes and the open shell states of the diatomics were calculated with the R/UCCSD(T) method. ^b Extrapolated by using Equation (1) with aug-cc-PVnZ, $n = D, T, Q$. ^c The zero point energies were obtained as described in the text. ^d Core/valence corrections were obtained with the cc-pwCVTZ basis sets at the optimized geometries. ^e The scalar relativistic correction is based on a CISD(FC)/cc-pVTZ MVD calculation. ^f Correction due to the incorrect treatment of the atomic asymptotes as an average of spin multiplets. Values are based on C. Moore's Tables, ref. [53]. ^g The theoretical value of the dissociation energy to atoms $\Sigma D_0(0 \text{ K})$.

Table 3.10. Calculated Heats of Formation (kcal/mol) at 0 K and 298 K.^a

Molecule	$\Delta H_f(0\text{ K})_{\text{theory}}$	$\Delta H_f(298\text{ K})_{\text{theory}}$
BP ($^3\Pi$) ^b	135.2	135.7
AlN ($^3\Pi$) ^c	133.7	133.7
AlN ($^3\Sigma^-$)	133.5	133.5
AlP ($^3\Pi$) ^d	102.9	102.8
AlP ($^3\Sigma^-$)	102.7	102.6
HBPH (non-linear) ^e	53.6	53.2
HAlNH (non-linear) ^f	60.4	58.6
HAlPH (non-linear) ^g	58.6	57.2
BH ₂ PH ₂ (non-planar) ^h	24.4	21.8
AlH ₂ NH ₂ (planar)	-0.3	-3.3
AlH ₂ PH ₂ (non-planar) ⁱ	25.4	22.6
BH ₃ PH ₃	8.6	4.4
AlH ₃ NH ₃	-3.8	-8.3
AlH ₃ PH ₃	21.1	17.0
AlH ₃	31.9	30.3
AlH ₄ ⁻	-3.4	-5.9
PH ₃	3.28	1.4
PH ₄	50.5	47.7
PH ₄ ⁺	182.7	179.8
BH ₃	26.4	25.5
BH ₄ ⁻	-11.6	-13.5
NH ₃	-9.6	-11.3
NH ₄ ⁺	153.6	150.9

^a Values for BH₃, BH₄⁻, NH₃, and NH₄⁺ from Ref. 4. ^b $\Delta H_f(0\text{ K})$ BP ($^3\Sigma^-$) = 156.0 kcal/mol, $\Delta H_f(0\text{ K})$ BP ($^1\Sigma^+$) = 142.6 kcal/mol. ^c $\Delta H_f(0\text{ K})$ AlN ($^1\Sigma^+$) = 143.0 kcal/mol. ^d $\Delta H_f(0\text{ K})$ AlP ($^1\Sigma^+$) = 114.8 kcal/mol. ^e $\Delta H_f(0\text{ K})$ HBPH (linear) = 82.0 kcal/mol. ^f $\Delta H_f(0\text{ K})$ HAlNH (linear) =

60.4 kcal/mol. ^g $\Delta H_f(0 \text{ K})$ HAlPH (linear) = 86.1 kcal/mol. ^h $\Delta H_f(0 \text{ K})$ BH₂PH₂ (planar) = 31.0 kcal/mol. ⁱ $\Delta H_f(0 \text{ K})$ AlH₂PH₂ (planar) = 35.4 kcal/mol.

Table 3.11. Calculated Entropies (cal/mol·K) at the MP2/cc-pVTZ level.

Molecule	S(298 K)_{theory}
BP ($^3\Pi$)	52.64
AlN ($^3\Pi$)	53.28
AlN ($^3\Sigma^-$)	53.28
AlP ($^3\Pi$)	56.40
AlP ($^3\Sigma^-$)	56.40
HBPH (non-linear)	56.74
HAlNH (non-linear)	52.38
HAlPH (non-linear)	62.40
BH ₂ PH ₂ (non-planar)	60.88
AlH ₂ NH ₂ (planar)	60.11
AlH ₂ PH ₂ (non-planar)	66.87
BH ₃ PH ₃	61.79
AlH ₃ NH ₃	64.50
AlH ₃ PH ₃	70.66
AlH ₃	49.49
AlH ₄ ⁻	49.87
PH ₃	50.16
PH ₄	53.76
PH ₄ ⁺	48.52
BH ₃	44.96
BH ₄ ⁻	45.17
NH ₃	45.94
NH ₄ ⁺	44.39
H ₂	31.23

Table 3.12. T Δ S corrections for reactions 3 to 11 in kcal/mol.

Reaction	-TΔS (298K)
3	8.0
4	7.0
5	9.6
6	9.0
7	8.1
8	8.1
9	8.2
10	8.0
11	7.5

3.5 References

- ¹ “Basic Energy Needs for the Hydrogen Economy,” Dresselhaus, M.; Crabtree, G.; Buchanan, M., Eds., Basic Energy Sciences, Office of Science, U.S. Department of Energy, Washington, D.C., 2003; Maelund, A.J.; Hauback, B.C. in “Advanced Materials for the Energy Conversion II,” Ed. Chandra, D.; Bautista, R.G.; Schlapbach, L. The Minerals, Metals and Material Society, 2004.
- ² Gutowski, M.; Autrey, T. *Prepr. Pap. –Am. Chem. Soc., Div. Fuel Chem.* **2004**, *49*, 275.
- ³ Gutowski, M.; Autrey, T.; Linehan, J. *J. Phys. Chem. B.* accepted, 2005.
- ⁴ Dixon, D. A.; Gutowski, M. *J. Phys. Chem. A* **2005**, *109*, 5129.
- ⁵ Amendola, S. C.; Sharp-Goldman, S. L.; Janjua, M. S.; Spencer, N. C.; Kelly, M. T.; Petillo, P. J.; Binder, Michael. *Int. J. Hydrogen Energy*, 2000, *25*, 969.
- ⁶ Gutowska, A.; Li, L.; Shin, Y.; Wang, Ch.; Li, S.; Linehan, J.; Smith, R. S.; Kay, B.; Schmid, B.; Shaw, W.; Gutowski, M.; Autrey, T. *Angew. Chem. Int. Ed.* **2005**, *44*, 2.
- ⁷ Peterson, K. A.; Xantheas, S. S.; Dixon, D. A.; Dunning, T. H. Jr. *J. Phys. Chem. A* **1998**, *102*, 2449.
- ⁸ Feller, D.; Peterson, K. A. *J. Chem. Phys.* **1998**, *108*, 154.
- ⁹ Dixon, D. A.; Feller, D. *J. Phys. Chem. A* **1998**, *102*, 8209.
- ¹⁰ Feller, D.; Peterson, K. A. *J. Chem. Phys.* **1999**, *110*, 8384.
- ¹¹ Feller, D.; Dixon, D. A. *J. Phys. Chem. A* **1999**, *103*, 6413.
- ¹² Feller, D. *J. Chem. Phys.* 1999, *111*, 4373.
- ¹³ Feller, D.; Dixon, D. A. *J. Phys. Chem. A* **2000**, *104*, 3048.
- ¹⁴ Feller, D.; Sordo, J. A. *J. Chem. Phys.* **2000**, *113*, 485.
- ¹⁵ Feller, D.; Dixon, D. A. *J. Chem. Phys.* **2001**, *115*, 3484.
- ¹⁶ Dixon, D. A.; Feller, D.; Sandrone, G. *J. Phys. Chem. A* **1999**, *103*, 4744.
- ¹⁷ Ruscic, B.; Feller, D.; Dixon, D. A.; Peterson, K. A.; Harding, L. B.; Asher, R. L.; Wagner, A. *J. Phys. Chem. A* **2001**, *105*, 1.

-
- ¹⁸ Ruscic, B.; Wagner, A. F.; Harding, L. B.; Asher, R. L.; Feller, D.; Dixon, D. A.; Peterson, K. A.; Song, Y.; Qian, X.; Ng, C.; Liu, J.; Chen, W.; Schwenke, D. W. *J. Phys. Chem. A* **2002**, *106*, 2727.
- ¹⁹ Feller, D.; Dixon, D. A.; Peterson, K. A. *J. Phys. Chem. A* **1998**, *102*, 7053.
- ²⁰ Dixon, D. A.; Feller, D.; Peterson, K. A. *J. Chem. Phys.* **2001**, *115*, 2576.
- ²¹ Purvis, G. D. III; Bartlett, R. J. *J. Chem. Phys.* **1982**, *76*, 1910.
- ²² Raghavachari, K.; Trucks, G. W.; Pople, J. A.; Head-Gordon, M. *Chem. Phys. Lett.* **1989**, *157*, 479.
- ²³ Watts, J. D.; Gauss, J.; Bartlett, R. J. *J. Chem. Phys.* **1993**, *98*, 8718.
- ²⁴ Dunning, T. H., Jr. *J. Chem. Phys.* **1989**, *90*, 1007.
- ²⁵ Kendall, R. A.; Dunning, T. H., Jr.; Harrison, R. J. *J. Chem. Phys.* **1992**, *96*, 6796.
- ²⁶ McQuarrie, D.A. "Statistical Mechanics," University Science Books, Sausalito, CA, 2001.
- ²⁷ Curtiss, L. A.; Raghavachari, K.; Redfern, P. C.; Pople, J. A. *J. Chem. Phys.* **1997**, *106*, 1063.
- ²⁸ Jenkins, H. D. B.; Roobottom, H. K.; Passmore, J.; Glasser, L. *Inorg. Chem* **1999**, *38*, 3609; Jenkins, H. D. B.; Tudela, D.; Glasser, L. *Inorg. Chem* **2002**, *41*, 2364.
- ²⁹ Dixon, D. A.; Feller, D.; Christe, K. O.; Wilson, W. W.; Vij, A.; Vij, V.; Jenkins, H. D. B.; Olson, R. M.; Gordon, M. S. *J. Am. Chem. Soc.* **2004**, *126*, 834.
- ³⁰ Rudolph, R.W.; Parry, R.W.; Farran, C. F. *Inorg. Chem.* **1966**, *5*, 723.
- ³¹ Jungwirth, P.; Zahradnik, J. *Mol. Struct. (Theochem)* **1993**, *283*, 317.
- ³² Kulkarni, S. A.; Srivastava, A. K. *J. Phys. Chem. A* **1999**, *103*, 2836.
- ³³ Davy, R. D.; Schaeffer, H. F., III. *J. Phys. Chem. A* **1997**, *101*, 3135.
- ³⁴ Almenningen, A.; Fernhalt, L.; Haaland, A.; Weidlen, J. *J. Organomet. Chem.* **1987**, *145*, 109.
- ³⁵ Davy, R. D.; Jaffrey, K. L. *J. Phys. Chem.* **1994**, *98*, 8930.
- ³⁶ Marsh, C. M. B.; Hamilton, T. P.; Xie, Y.; Schaeffer, H.F., III. *J. Chem. Phys.* **1992**, *96*, 5310.
- ³⁷ Cramer, C. J.; Gladfelter, W. L. *Inorg. Chem.* **1997**, *36*, 5358.

-
- ³⁸ Watts, J. D.; Van Zant, L. C. *Chem. Phys. Lett.* **1996**, *251*, 119.
- ³⁹ Kerins, M. C.; Fitzpatrick, N. J.; Nguyen, M. T. *Polyhedron* **1989**, *7*, 969.
- ⁴⁰ Langhoff, S. R.; Bauschlicher, C. W.; Petterson, L. G. M. *J. Chem. Phys.* **1988**, *89*, 7354.
- ⁴¹ Kandalam, A. K.; Pandey, R.; Blanco, M. A.; Costales, A.; Recio, J. M.; Newsam, J. H. *J. Phys. Chem. B* **2000**, *104*, 4361.
- ⁴² Costales, A.; Kandalam, A. K.; Franco, R.; Pandey, R. *J. Phys. Chem. B* **2002**, *106*, 1940.
- ⁴³ Werner, H.-J.; Knowles, P. J.; Amos, R. D.; Bernhardsson, A.; Berning, A.; Celani, P.; Cooper, D. L.; Deegan, M. J. O.; Dobbyn, A. J.; Eckert, F.; Hampel, C.; Hetzer, G.; Korona, T.; Lindh, R.; Lloyd, A. W.; McNicholas, S. J.; Manby, F. R.; Meyer, W.; Mura, M. E.; Nicklass, A.; Palmieri, P.; Pitzer, R. M.; Rauhut, G.; Schütz, M.; Stoll, H.; Stone, A. J.; Tarroni, R.; Thorsteinsson, T. MOLPRO-2002, a package of initio programs written by, Universität Stuttgart, Stuttgart, Germany, University of Birmingham, Birmingham, United Kingdom, 2002.
- ⁴⁴ Rittby, M.; Bartlett, R. J. *J. Phys. Chem.* **1988**, *92*, 3033.
- ⁴⁵ Knowles, P. J.; Hampel, C.; Werner, H. –J. *J. Chem. Phys.* **1994**, *99*, 5219.
- ⁴⁶ Deegan, M. J. O.; Knowles, P. J. *Chem. Phys. Lett.* **1994**, *227*, 321.
- ⁴⁷ (a) Møller, C.; Plesset, M. S. *Phys. Rev.* **1934**, *46*, 618; (b) Pople, J. A.; Binkley, J. S.; Seeger, R. *Int. J. Quantum Chem. Symp.* **1976**, *10*, 1.
- ⁴⁸ Gaussian 03, Revision C.02, Frisch, M. J.; Trucks, G. W.; Schlegel, H. B.; Scuseria, G. E.; Robb, M. A.; Cheeseman, J. R.; Montgomery, Jr., J. A.; Vreven, T.; Kudin, K. N.; Burant, J. C.; Millam, J. M.; Iyengar, S. S.; Tomasi, J.; Barone, V.; Mennucci, B.; Cossi, M.; Scalmani, G.; Rega, N.; Petersson, G. A.; Nakatsuji, H.; Hada, M.; Ehara, M.; Toyota, K.; Fukuda, R.; Hasegawa, J.; Ishida, M.; Nakajima, T.; Honda, Y.; Kitao, O.; Nakai, H.; Klene, M.; Li, X.; Knox, J. E.; Hratchian, H. P.; Cross, J. B.; Bakken, V.; Adamo, C.; Jaramillo, J.; Gomperts, R.; Stratmann, R. E.; Yazyev, O.; Austin, A. J.; Cammi, R.; Pomelli, C.; Ochterski, J. W.; Ayala, P. Y.; Morokuma, K.; Voth, G. A.; Salvador, P.; Dannenberg, J. J.; Zakrzewski, V. G.; Dapprich, S.; Daniels, A. D.; Strain, M. C.; Farkas, O.; Malick, D. K.; Rabuck, A. D.; Raghavachari, K.; Foresman, J. B.; Ortiz, J. V.; Cui, Q.; Baboul, A. G.; Clifford, S.; Cioslowski, J.; Stefanov, B. B.; Liu, G.; Liashenko, A.; Piskorz, P.; Komaromi, I.; Martin, R. L.; Fox, D. J.; Keith, T.; Al-Laham, M. A.; Peng, C. Y.; Nanayakkara, A.; Challacombe, M.; Gill, P. M. W.; Johnson, B.; Chen, W.; Wong, M. W.; Gonzalez, C.; and Pople, J. A.; Gaussian, Inc., Wallingford CT, 2004.
- ⁴⁹ Dunning, T. H., Jr., Peterson, K. A.; Wilson, A. K. *J. Chem. Phys.* **2001**, *114*, 9244.
- ⁵⁰ Peterson, K. A.; Woon, D. E.; Dunning, T. H., Jr. *J. Chem. Phys.* **1994**, *100*, 7410.

-
- ⁵¹ Peterson, K. A.; Dunning, T. H., Jr. *J. Chem. Phys.* **2002**, *117*, 10548; Woon, D. E.; Dunning, T. H., Jr. *J. Chem. Phys.* **1993**, *98*, 1358.
- ⁵² Davidson, E. R.; Ishikawa, Y.; Malli, G. L. *Chem. Phys. Lett.* **1981**, *84*, 226.
- ⁵³ Moore, C. E. "Atomic energy levels as derived from the analysis of optical spectra, Volume 1, H to V," U.S. National Bureau of Standards Circular 467, U.S. Department of Commerce, National Technical Information Service, COM-72-50282, Washington, D.C.; **1949**.
- ⁵⁴ Chase, M. W., Jr. NIST-JANAF Tables (4th Edition), *J. Phys. Chem. Ref. Data*, Mono. 9, Suppl. 1, **1998**.
- ⁵⁵ Zhan, C. -G.; Dixon, D. A. *J. Phys. Chem. A* **2001**, *105*, 11534; Zhan, C. -G.; Dixon, D. A. *J. Phys. Chem. A* **2002**, *106*, 9737; Zhan, C. -G.; Bentley, J.; Chipman, D. M. *J. Chem. Phys.* **1998**, *108*, 177; Zhan, C. -G.; Chipman, D. M. *J. Chem. Phys.* **1998**, *109*, 10543.
- ⁵⁶ Becke, A. D. *J. Chem. Phys.* **1993**, *98*, 5648; Lee, C.; Yang, W.; Parr, R. G. *Phys. Rev. B* **1988**, *37*, 785; Stephens, P. J.; Devlin, F. J.; Chabalowski, C. F.; Frisch, M. J. *J. Phys. Chem.* **1994**, *98*, 11623.
- ⁵⁷ Jenkins, H. D. B. "Lattice Energies," in *Handbook of Chemistry and Physics*, 79th Ed.; Lide, D. R., Ed.; CRC Press: Boca Raton FL, 1998; Chapter 9, p. 1222.
- ⁵⁸ Marynick, D. S.; Dixon D. A. *J. Phys. Chem.* **1982**, *86*, 914.
- ⁵⁹ Huber, K. P.; Herzberg, G. "Constants of Diatomic Molecules" (data prepared by Gallagher J.W.; Johnson, R.D., III) in NIST Chemistry WebBook, NIST Standard Reference Database Number 69, Eds. Linstrom, P. J.; Mallard, W. G.; June 2005, National Institute of Standards and Technology, Gaithersburg MD, 20899 (<http://webbook.nist.gov>); Huber K. P.; Herzberg, G. *Molecular Spectra and Molecular Structure. IV. Constants of Diatomic Molecules* (Van Nostrand Reinhold, New York, 1979).
- ⁶⁰ Wang, X.; Andrews, L.; Tam, S.; DeRose, M. E.; Fajardo, M. E. *J. Am. Chem. Soc.* **2003**, *125*, 9218.
- ⁶¹ Shimanouchi, T. "Tables of Molecular Vibrational Frequencies. Consolidated Volume I," NSRDS-NBS 39, National Bureau of Standards, U.S. Department of Commerce, National Technical Information Service, Washington, D.C., **1972**.
- ⁶² Himmel, H.-J.; Downs, A. J.; Greene, T. M. *J. Am. Chem. Soc.* **2000**, *122*, 9793.
- ⁶³ Jagielska, A.; Moszynski, R.; Piela, L. *J. Chem. Phys.* **1999**, *110*, 947.
- ⁶⁴ Peterson, K. A. *J. Chem. Phys.* **1995**, *102*, 262.

-
- ⁶⁵ Lee, T. J.; Rice, J. E.; Scuseria, G. E.; Schaefer, H. F., III. *Theor. Chim. Acta* **1989**, 75, 81.
- ⁶⁶ Simmons, J. D.; McDonald, J. K. *J. Mol. Spectrosc.* **1972**, 41, 584.
- ⁶⁷ Gingerich, K. *J. Chem. Phys.* **1972**, 56, 4239.
- ⁶⁸ De Maria, G.; Gingerich, K. A.; Malaspina, L.; Piacente, V. *J. Chem. Phys.* **1966**, 44, 2531.
- ⁶⁹ Paddon-Row, M. N.; Wong, S. S. *J. Mole Struct. (Theochem)* **1988**, 180, 353.
- ⁷⁰ Wickham-Jones, C. T.; Moran, S.; Ellison, G. B., *J. Chem. Phys.*, **1989**, 90, 795.
- ⁷¹ Note that this value is lower than used by us (see Ref. 4) previously because we neglected the ability of H to bond to BH₃.
- ⁷² Wong, S. S.; Li, W. -K.; Paddon-Row, M. N. *J. Mole Struct. (Theochem)* **1991**, 226, 285.
- ⁷³ Goebbert, D. J.; Hernandez, H.; Francisco, J. S.; Wenthold, P. G. *J. Am. Chem. Soc.* **2005**, 127, 11684.
- ⁷⁴ Hunter, E. P.; Lias, S. G., *J. Phys. Chem. Ref. Data*, **1998**, 27, 3, 413.

3.5 Appendix

Table A3.1. Total CCSD(T) Energies (E_h) as a Function of Basis Set.^a

System	Basis Set	E_h
BH ₃ PH ₃	aVDZ	-369.201258
	aVTZ	-369.276040
	aVQZ	-369.295558
	CBS (DTQ)	-369.306160
BH ₂ PH ₂	aVDZ	-367.997055
	aVTZ	-368.063771
	aVQZ	-368.081682
	CBS (DTQ)	-368.087105
BH ₂ PH ₂ (non-planar)	aVDZ	-368.004147
	aVTZ	-368.069915
	aVQZ	-368.087698
	CBS (DTQ)	-368.097440
HBPH	aVDZ	-366.736952
	aVTZ	-366.796333
	aVQZ	-366.812763
	CBS (DTQ)	-366.821812
HBPH (bent)	aVDZ	-366.782991
	aVTZ	-366.842158
	aVQZ	-366.858283
	CBS (DTQ)	-366.867133
BP (³ Π)	aVDZ	-365.490881
	aVTZ	-365.536502
	aVQZ	-365.549691
	CBS (DTQ)	-365.557027
BP (³ Σ ⁻)	aVDZ	-365.464050
	aVTZ	-365.505387
	aVQZ	-365.517131
	CBS (DTQ)	-365.523638

BP ($^1\Sigma^+$)	aVDZ	-365.476230
	aVTZ	-365.523753
	aVQZ	-365.537595
	CBS (DTQ)	-365.545306
AlH ₄ ⁻	aVDZ	-244.388107
	aVTZ	-244.415730
	aVQZ	-244.423389
	CBS (DTQ)	-244.427609
AlH ₃	aVDZ	-243.744475
	aVTZ	-243.766774
	aVQZ	-243.773034
	CBS (DTQ)	-243.776493
PH ₃	aVDZ	-342.654442
	aVTZ	-342.699004
	aVQZ	-342.710864
	CBS (DTQ)	-342.717337
PH ₄	aVDZ	-343.162949
	aVTZ	-343.211818
	aVQZ	-343.224484
	CBS (DTQ)	-343.231352
PH ₄ ⁺	aVDZ	-342.961209
	aVTZ	-342.006527
	aVQZ	-343.019018
	CBS (DTQ)	-343.025891
AlH ₃ PH ₃	aVDZ	-586.420208
	aVTZ	-586.489619
	aVQZ	-586.508504
	CBS (DTQ)	-586.518864
AlH ₂ PH ₂	aVDZ	-585.225357
	aVTZ	-585.290019
	aVQZ	-585.308069
	CBS (DTQ)	-585.318030

AlH ₂ PH ₂ (non-planar)	aVDZ	-585.241102
	aVTZ	-585.304948
	aVQZ	-585.322586
	CBS (DTQ)	-585.332296
AlHPH	aVDZ	-583.971332
	aVTZ	-584.030447
	aVQZ	-584.047246
	CBS (DTQ)	-584.056554
AlHPH (non-linear)	aVDZ	-584.015940
	aVTZ	-584.073328
	aVQZ	-584.089142
	CBS (DTQ)	-584.097843
AlP (³ Π)	aVDZ	-582.782821
	aVTZ	-582.829004
	aVQZ	-582.841867
	CBS (DTQ)	-582.848962
AlP (³ Σ ⁻)	aVDZ	-582.788200
	aVTZ	-582.831031
	aVQZ	-582.842701
	CBS (DTQ)	-582.849106
AlP (¹ Σ ⁺)	aVDZ	-582.760777
	aVTZ	-582.809522
	aVQZ	-582.823508
	CBS (DTQ)	-582.831273
AlH ₃ NH ₃	aVDZ	-300.214694
	aVTZ	-300.294392
	aVQZ	-300.316389
	CBS (DTQ)	-300.328497
AlH ₂ NH ₂	aVDZ	-299.030430
	aVTZ	-299.105899
	aVQZ	-299.126909
	CBS (DTQ)	-299.138496

AlH ₂ NH	aVDZ	-297.757170
	aVTZ	-297.826740
	aVQZ	-297.846202
	CBS (DTQ)	-297.856947
AlH ₂ NH (bent)	aVDZ	-297.758602
	aVTZ	-297.827092
	aVQZ	-297.846307
	CBS (DTQ)	-297.856923
AlN (³ Π)	aVDZ	-296.481143
	aVTZ	-296.534561
	aVQZ	-296.549580
	CBS (DTQ)	-296.557882
AlN (³ Σ ⁻)	aVDZ	-296.485796
	aVTZ	-296.535806
	aVQZ	-296.550286
	CBS (DTQ)	-296.558341
AlN (¹ Σ ⁺)	aVDZ	-296.461771
	aVTZ	-296.518929
	aVQZ	-296.535471
	CBS (DTQ)	-296.544673

^a Complete basis set limit (CBS) from equation (1). See text.

CHAPTER 4

σ - AND π -BOND STRENGTHS IN MAIN GROUP 3-5 COMPOUNDS

From: Grant, D. J.; Dixon, D. A *J. Phys. Chem. A* **2006**, *110*, 12955-12962.

4.1 Introduction

The suitability of NH_xBH_x ($x = 1-4$) compounds for hydrogen storage has recently been evaluated using theoretical methods.^{1,2,3} The calculations showed that $\text{BH}_3\text{NH}_3(\text{g})$, $\text{BH}_3\text{NH}_3(\text{s})$, and $[\text{BH}_4^-][\text{NH}_4^+](\text{s})$ can potentially serve as hydrogen storage systems based on the thermodynamics. In addition, molecular systems isoelectronic to the amine boranes were studied computationally as alternative candidates for H_2 storage systems.⁴ On the basis of the calculated heats of formation, $\text{AlH}_3\text{NH}_3(\text{g})$, $[\text{AlH}_4^-][\text{NH}_4^+](\text{s})$, $\text{AlH}_3\text{PH}_3(\text{g})$, $[\text{AlH}_4^-][\text{PH}_4^+](\text{s})$, and $[\text{BH}_4^-][\text{PH}_4^+](\text{s})$ have the potential to serve as H_2 storage systems in terms of the reaction energetics for H_2 release.

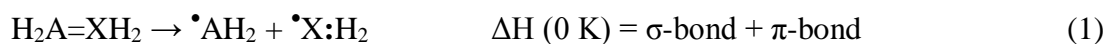
We are interested in the chemistry of these species in terms of their stability and reactivity. Because of the novel electronic structure of these species, we are interested in their bond energies. We have previously provided the best estimates of the Lewis acid-base donor-acceptor σ -bond strengths in AH_3XH_3 compounds as shown in Table 4.1.^{3,4} These values are quite low as compared to a covalent C-C σ -bond energy, for example, the value of 90.1 kcal/mol at 298 K for C_2H_6 .⁵ The AH_3XH_3 molecules can eliminate H_2 to form AH_2XH_2 molecules. The resulting AH_2XH_2 molecules have σ -bonds formed between the AH_2 and XH_2 groups with

approximate sp^2 - sp^2 hybridization and π -bonds formed by donation of the lone pair on the Group VA XH_2 group to the vacant p orbital on the Group IIIA AH_2 group. The strengths of the π -bond and the resulting σ -bond are questions that need to be addressed. We are particularly interested in the inherent bond energies of the σ - and π -bonds to better understand the thermodynamic driving forces for H_2 release. The bond energies in these systems can be compared to the σ - and π -bond strengths in C_2H_4 , which has a covalent π bond.⁶

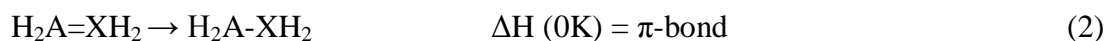
Several methods exist in the literature for determining π -bond strengths. A general procedure is to compare the bond dissociation energies of double, $D^\circ(X=Y)$, and single, $D^\circ(X-Y)$, bonds. The issue here is the proper description of how to define the π -bond energy.^{7,8,9} One method involves the use of hydrogenation thermochemical cycles and bond dissociation energies. The energy required to dehydrogenate a singly bonded compound to produce a double bond can be used to estimate the strength of the double bond provided that the overall heat of the dehydrogenation reaction and the bond dissociation energies are known.^{6,10} One can also look at the barrier to rotation about the A-X bond as rotation about the σ -bond by 90° breaks the π -bond interaction of the molecule. This can be done, for example, by measuring the kinetics for cis-trans isomerization.¹¹ Borden⁷ has discussed various approaches to calculating the π -bond energy in olefins and has shown that relaxation of the orthogonal diradical is important in determining the π -bond energy in C_2F_4 , as compared to C_2H_4 , as well as issues related to diabatic (dissociation to the configuration most closely representing the bonding configuration in the molecule) vs. adiabatic (dissociation to the ground state of the separated species) dissociation energies. Carter and Goddard have provided a similar discussion for substituted olefins.⁸

In order to calculate the σ -bond energy, one has to evaluate the π -bond strength. We have chosen to use the rotation barrier approach as the hydrogenation method could lead to very

different types of radicals than found in carbon based systems, and it is not possible to determine which end to hydrogenate first. We can write the following process:



where A is the Group 3A atom and X is the group 5A atom. The total dissociation energy for this reaction is the sum of the σ - and π -bond energies. Given the energies of the three species, one can calculate the sum of the σ - and π -bond energies. The sum of the bond energies at the adiabatic limit is for dissociation to the ground states, which are $^2\text{A}_1$ for AH_2 (orbital with unpaired electron in the plane) and $^2\text{B}_1$ for XH_2 (orbital with unpaired electron out of the plane and orbital with the lone pair in the plane). In order to calculate the π -bond energy, one can rotate about the A-X bond by 90° so that there is no interaction between the lone pair on the XH_2 with the vacant orbital on AH_2 .



In C_2H_4 , this is equivalent to breaking the covalent interaction between the p orbitals and putting one electron on each CH_2 group to form a diradical. For the Group 3-5 binary compounds $\text{H}_2\text{A}=\text{XH}_2$ with A = B, Al and X = N, P, the rotation process stays on the closed shell singlet potential energy surface so there is no need to be concerned with accessing an open shell species. In the rotated structure, the pair of electrons involved in the rotation localize as the lone pair on the Group 5A atom. An issue that arises in these compounds is the structure in the rotated state.

There have been several previous theoretical studies of the σ - and π -bond energies of the molecules presented here. Allen and Fink¹² predicted that aminoborane, BH_2NH_2 , has two rotational transition states at the CISD+Q/DZ+P level, one of C_s symmetry at 32.4 kcal/mol and one of C_{2v} symmetry at 37.9 kcal/mol, both with respect to the planar ground state configuration. This type of energy difference is consistent with relaxation of the geometry in the rotated

structure as discussed by Borden,⁷ as well as the size of the inversion barrier in NH_3 .¹³ McKee¹⁴ predicted the rotational barrier in BH_2NH_2 to be 32.1 kcal/mol at the MP4/6-31+G(2d,p) level of theory. Allen *et al.*¹⁵ and Allen and Fink¹⁶ also investigated the internal rotational energy barrier of borylphosphine at the level described above. They predicted that the BH_2PH_2 molecule can undergo internal rotation through either a low-energy transition state of C_s symmetry 10.0 kcal/mol above the ground state structure, or a high-energy transition state of C_{2v} symmetry, 46.4 kcal/mol above the ground state. The difference in the two rotation barriers is consistent with the inversion barrier in PH_3 .¹⁷ Coolidge and Borden¹⁸ have also studied the rotation barrier in BH_2PH_2 and find a barrier of 10.4 kcal/mol passing through a C_s transition state and a barrier of 44.6 kcal/mol passing through a C_{2v} rotated structure at the MP4 level. For alane amine, AlH_2NH_2 , Fink *et al.*¹⁹ predicted the rotational energy barrier to be 11.2 kcal/mol at the RHF/6-31+G** level. Davy and Jaffrey²⁰ obtained a value of 11.0 kcal/mol for the rotational barrier energy of AlH_2NH_2 at the HF/DZP level.

We use the approach developed for accurate molecular thermochemistry²¹ and for the heats of formation of the parent compounds^{3,4} to predict the bond energies. This approach is based on calculating the total atomization energy of a molecule and using this with known heats of formation of the atoms to calculate the heat of formation at 0 K. The approach starts with coupled cluster theory with single and double excitations and including a perturbative triples correction (CCSD(T)),^{22,23,24} combined with the correlation-consistent basis sets^{25,26} extrapolated to the complete basis set limit to treat the correlation energy of the valence electrons. This is followed by a number of smaller additive corrections including core-valence interactions and relativistic effects, both scalar and spin-orbit. Finally, one must include the zero point energy obtained either from experiment, theory, or some combination. Corrections to 298 K can then be

calculated by using standard thermodynamic and statistical mechanics expressions in the rigid rotor-harmonic oscillator approximation²⁷ and appropriate corrections for the heat of formation of the atoms.²⁸

4.2 *Computational Approach*

We used the augmented correlation consistent basis sets aug-cc-pVnZ for H, B, and N ($n = D, T, Q$).^{25,26} For the sake of brevity, we abbreviate the names to aVnZ. Only the spherical components (5-*d*, 7-*f*, and 9-*g*) of the Cartesian basis functions were used. All of the current work was performed with the MOLPRO suite of programs.²⁹ The open-shell CCSD(T) calculations for the atoms were carried out at the R/UCCSD(T) level. In this approach, a restricted open shell Hartree-Fock (ROHF) calculation was initially performed, and the spin constraint was relaxed in the coupled cluster calculation.^{30,31,32} All of the calculations were done on a massively parallel HP Linux cluster with 1970 Itanium-2 processors in the Molecular Sciences Computing Facility in the William R. Wiley Environmental Molecular Sciences Laboratory or on the 144 processor Cray XD-1 computer system at the Alabama Supercomputer Center.

The geometries were optimized numerically at the frozen core CCSD(T) level with the aug-cc-pVDZ and aug-cc-pVTZ correlation-consistent basis sets. The CCSD(T)/aug-cc-pVTZ geometries were then used in single point CCSD(T)/aug-cc-pVQZ calculations. For the planar and rotated C_{2v} structures, geometry optimizations were only done at the CCSD(T)/aug-cc-pVDZ level, as the energies of the ground state structure or the lowest energy rotated structure only decreased by a few tenths of a kcal/mol upon optimization at the CCSD(T)/aug-cc-pVTZ level. All of the vibrational frequencies were calculated at the MP2/cc-pVTZ level³³ using the

Gaussian program system.³⁴ These were used for the zero point energies and for the thermal corrections and entropies.

It has recently been found that tight d functions are necessary for calculating accurate atomization energies for 2nd row elements,³⁵ so we also included additional tight d functions in our calculations. Basis sets containing extra tight d functions are denoted aug-cc-pV(n+d)Z in analogy to the original augmented correlation consistent basis sets. We use aug-cc-pV(n+d)Z to represent the combination of aug-cc-pV(n+d)Z (on the 2nd row atoms Al and P) and aug-cc-pVnZ (on H, B, and N) basis sets and abbreviate this as aV(n+d)Z. The CCSD(T) total energies were extrapolated to the CBS limit by using a mixed exponential/Gaussian function of the form:

$$E(n) = E_{\text{CBS}} + A \cdot \exp[-(n-1)] + B \cdot \exp[-(n-1)^2] \quad (3)$$

with $n = 2$ (DZ), 3 (TZ) and 4 (QZ), as first proposed by Peterson *et al.*³⁶ This extrapolation method has been shown to yield atomization energies in the closest agreement with experiment (by a small amount) as compared to other extrapolation approaches up through $n = 4$.

Core-valence corrections, ΔE_{CV} , were obtained at the CCSD(T)/cc-pwCVTZ level of theory.³⁷ Scalar relativistic corrections (ΔE_{SR}), which account for changes in the relativistic contributions to the total energies of the molecule and the constituent atoms, were included at the CI-SD (configuration interaction singles and doubles) level of theory using the cc-pVTZ basis set. ΔE_{SR} is taken as the sum of the mass-velocity and 1-electron Darwin (MVD) terms in the Breit-Pauli Hamiltonian.³⁸ Most calculations using available electronic structure computer codes do not correctly describe the lowest energy spin multiplet of an atomic state as spin-orbit in the atom is usually not included. Instead, the energy is a weighted average of the available multiplets. For N or P in the ⁴S state, no spin-orbit correction is needed, but a correction of 0.03

kcal/mol is needed for B and one of 0.21 kcal/mol for Al, taken from the excitation energies of Moore.³⁹

In order to calculate the zero point energy correction, we scaled the M-H frequencies by the factors 0.96 for M=B and M=N, 0.95 for M=P, and 0.954 for M=Al. These scale factors were obtained by taking the average of the CCSD(T)/aug-cc-pVTZ values and the experimental values for the M-H stretches for the MH₃ compounds and dividing them by the MP2/cc-pVTZ value. Thus, we estimate that the error introduced in the heats of formation due to the zero point energies is a maximum of ± 0.5 kcal/mol.

By combining our computed ΣD_0 (total atomization energies) values with the known heats of formation at 0 K for the elements $\Delta H_f^0(\text{N}) = 112.53 \pm 0.02$ kcal mol⁻¹, $\Delta H_f^0(\text{B}) = 136.2 \pm 0.2$ kcal mol⁻¹, $\Delta H_f^0(\text{P}) = 75.42 \pm 0.24$ kcal mol⁻¹, $\Delta H_f^0(\text{Al}) = 78.23 \pm 1.0$ kcal mol⁻¹, and $\Delta H_f^0(\text{H}) = 51.63$ kcal mol⁻¹,⁴⁰ we can derive ΔH_f^0 values for the molecules under study in the gas phase. We obtain heats of formation at 298 K by following the procedures outlined by Curtiss *et al.*²⁸

4.3 Results and Discussion

The calculated geometries of the orthogonal transition state structures, corresponding to rotation about the AX bond, and the C_{2v} structures obtained by rotating about the A-X bond and planarizing the AH₂ and XH₂ groups are given in Table 4.2. In addition, structures for planar NH₃ and PH₃, and the triatomic molecules BH₂, AlH₂, and PH₂ are provided as Supporting Information. The calculated vibrational frequencies for all of the structures have been included in the Supporting Information. For the rotated structures and the rotated-planar C_{2v} structures, the unique imaginary frequencies associated with each molecule, are given in Table 4.3. The C_s structures are characterized by one imaginary frequency corresponding to rotation about the A-X

bond and the C_{2v} structures by two imaginary frequencies with the second imaginary frequency corresponding to inversion at X. The molecular structures for the optimized ground states and the lowest energy transition states for rotation are shown in Figure 4.1.

The rotation process leads to breaking the π -bond and a consequent lengthening of the XY bond. The BN bond length of BH_2NH_2 increases by 0.084 Å in going from the planar ground state configuration to the 90°-rotated C_s symmetry transition state structure. For the rotated-planar C_{2v} structure of BH_2NH_2 , the XY bond shows a smaller increase of 0.067 Å. A similar increase was found for BH_2PH_2 with the BP bond lengthening of 0.082 Å from the ground state to the rotated structure. There was decrease in the XY bond distance of 0.017 Å going from the rotated to the planar-rotated C_{2v} structure. Upon rotation, a smaller increase of 0.040 Å was found for the AlN bond of AlH_2NH_2 from the planar ground state to the C_s transition state structure. In going from the rotated C_s structure to the planar-rotated C_{2v} structure, a similar decrease of 0.018 Å was predicted as found for the other molecules. The AlP bond of AlH_2PH_2 had a similar small increase of 0.027 Å on rotation to the C_s structure. In going from the rotated C_s structure to the rotated-planar C_{2v} structures, there was a considerable decrease in AlP bond distance of 0.070 Å. In comparison, Dobbs and Hehre⁹ calculated a much larger increase of 0.15 Å in C-C bond length in going from the planar to the twisted form of ethylene at the UHF/6-31G* level. We note that the rotated form of C_2H_4 is a diradical, as compared to the closed shell with a lone pair structure found in rotated AH_2XH_2 .

The total valence CCSD(T) energies as a function of basis set are given in the Supporting Information. The calculated energy components for the total atomization energies are given in Table 4.4, and the calculated heats of formation at 0 K and 298 K are given in Table 4.5. The previously reported results for the ground states are reported for completeness, and the results for

planar (C_{2v}) BH_2PH_2 and AlH_2PH_2 are also given in Table 4.5.^{3,4} The relativistic corrections for the structures investigated are all negative and reasonably small, ranging from -0.06 to -1.04 kcal/mol. The core-valence corrections are positive for the BH_2 , PH_2 , BH_2NH_2 , and BH_2PH_2 and range from 0.2 to 1.6 kcal/mol. For AlH_2 , AlH_2NH_2 , and AlH_2PH_2 , the core valence corrections are negative and range from -0.3 to -1.0 kcal/mol.

The π -bond energies can be estimated from the magnitude of the energies of the rotation barriers. There are three values for the rotation barrier given in Table 4.6. The adiabatic rotation energy barriers were calculated as the energy difference between the equilibrium ground state configuration and the C_s transition state for torsion about the A-X bond. The values from the C_s or C_{2v} ground state to the rotated C_{2v} structure were calculated, as were the values for the rotation barrier from a C_{2v} planar structure to a C_{2v} rotated structure.

The adiabatic rotation barrier of borane amine is 29.9 kcal/mol, which is much larger than found for the other molecules and indicative of a strong dative π -bond between B and N. This value is much lower than the π -bond strength of 65 kcal/mol¹¹ in ethylene¹¹ obtained from the rate of cis-trans isomerization in 1,2-dideuterioethylene. Our value for BH_2NH_2 is in good agreement with that of Allen and Fink,¹² who predicted a rotational barrier (C_s symmetry transition state) of 32.4 kcal/mol at the CISD+Q/DZ+P level and of Mckee,¹⁴ who predicted 32.1 kcal/mol at the MP4/6-31+G(2d,p) level of theory.

The adiabatic dative π -bond energy of H_2AlNH_2 is about one third that of borane amine, 10.5 kcal/mol, consistent with the smaller change in bond distance on rotation and the lower π -bond energy expected for a bond between a 1st and 2nd row metal. The lower level values calculated by Fink¹⁹ and Davy²⁰ of 11.2 kcal/mol and 11.0 kcal/mol, respectively, are in excellent agreement with our higher-level calculation. Borylphosphine, H_2BPH_2 , has a similar adiabatic π -

bond energy of 9.2 kcal/mol. Surprisingly, the B-P bond distance increases by an amount comparable to that of BH_2NH_2 on rotation even though the latter has a much higher barrier. Borden¹⁸ calculated the adiabatic barrier to rotation in BH_2PH_2 to be 10.4 kcal/mol at the MP4 level of theory, in good agreement with our value. Allen *et al.*¹⁶ also calculated the rotational barrier in BH_2PH_2 through a transition state of C_s symmetry at 10.0 kcal/mol. The rotational energy barrier for the phosphine alane was considerably smaller than the others indicating a very weak adiabatic π -bond between AlP. The adiabatic π -bond energy of H_2AlPH_2 was about one third that of borane phosphine's at 2.7 kcal/mol.

We provide plots of the HOMO at the Hartree-Fock level for the ground state and the transition state for rotation in Figure 4.2. The HOMO in the planar structures corresponds essentially to a lone pair on N or P that can delocalize to the B or Al. The largest delocalization is found for BH_2NH_2 as expected from this compound having the highest barrier. The other molecules, which have much lower rotation barriers, show less delocalization from the lone pair on X toward the empty orbital on A with the smallest change in the orbitals found for AlH_2PH_2 , the compound with the lowest barrier. There is a small interaction of the lone pair on N with the A-H orbitals in the rotated transition state. The orbital plots confirm that the π -bond in these AH_2XH_2 compounds is best described as a dative bond, just as found for the σ -bond in the AH_3XH_3 compounds.

We also calculated a rotation barrier as the energy difference between the ground state and the rotated-planar C_{2v} structures. This information can be used to provide insights into the heights of the barriers. The rotation barrier for BH_2NH_2 is 33.8 kcal/mol going from the C_{2v} ground state to the rotated C_{2v} structure, similar to the value of 37.9 kcal/mol of Allen and Fink.¹² A much smaller value of 10.9 kcal/mol was obtained for the $C_{2v} - C_{2v}$ rotational barrier in

AlH₂NH₂. The barrier to rotation in going from the ground state non-planar BH₂PH₂ C_s structure to the rotated C_{2v} structure is 42.3 kcal/mol, similar to the values obtained by Borden¹⁸ of 44.6 kcal/mol and by Allen and Fink¹⁶ of 46.4 kcal/mol. In AlH₂PH₂, the C_s – C_{2v} rotation barrier is 24.2 kcal/mol. The final rotation barrier to be considered is the barrier to rotation between the planar C_{2v} structure and the rotated-planar C_{2v} structure for BH₂PH₂ and AlH₂PH₂, with respective values of 35.7 kcal/mol and 14.2 kcal/mol.

In order to better understand the rotation energies, we need to consider the inversion barriers at N and P. The molecular structures of most BY₃ and AlY₃ compounds are planar so inversion does not occur at them. We calculate a barrier height for the inversion of ammonia of 5.1 kcal/mol at the CCSD(T)/CBS limit, about 0.7 kcal/mol below the experimental¹³ barrier height of 2020 ± 12 cm⁻¹ (5.77 kcal/mol). Including the zero-point contribution, we obtain a value of 5.0 kcal/mol for the inversion of NH₃. We calculate the inversion barrier of PH₃ to be 33.6 kcal/mol, which decreases to 32.9 kcal/mol with the zero-point correction included. This value is similar to that of Marynick and Dixon,¹⁷ who calculated a barrier for PH₃ of 34.4 kcal/mol at the SCF-CI/DZ+P level including an estimate for quadruple excitations.

We calculated the inversion of the non-planar –PH₂ moiety in the ground state structures of BH₂PH₂ and AlH₂PH₂ to be 6.6 kcal/mol and 10.0 kcal/mol, respectively, both considerably less than the inversion barrier of PH₃. This is consistent with the fact that the BH₂ and AlH₂ groups are electropositive, which is known to decrease the inversion barrier. In addition, the presence of the dative π-bond can lower the inversion barrier. Borden¹⁸ finds a smaller barrier to planarity in BH₂PH₂ of 4.5 kcal/mol at the MP4/6-31G* level.

The barriers to inversion of the –NH₂ and –PH₂ moieties in the rotated structures at the CCSD(T)/CBS level were also calculated. This provides an estimate of the electropositive effect

as no π -bond is present. For BH_2NH_2 , the barrier to invert NH_2 in the rotated structure is 3.9 kcal/mol, slightly lower than our calculated value of 5.0 kcal/mol for the inversion barrier of NH_3 , showing a small effect of substitution of BH_2 for H when there is no overlap of the lone pair on N with the vacant orbital on B. For rotated AlH_2NH_2 , the barrier to inversion was 0.4 kcal/mol, considerably less than that in BH_2NH_2 , and consistent with the fact that AlH_2 is more electropositive than BH_2 . For rotated BH_2PH_2 , the barrier to inversion of the $-\text{PH}_2$ moiety was 33.1 kcal/mol, showing essentially no effect of substituting BH_2 for H, just as found for the nitrogen analog. For rotated AlH_2PH_2 , the barrier to inversion was 21.5 kcal/mol, considerably less than that in BH_2PH_2 . The decrease of 11.4 kcal/mol on substitution of AlH_2 for H is again consistent with AlH_2 being more electropositive than BH_2 or H.

On the basis of these values, we can now re-examine the π -bond strengths. For BH_2NH_2 and AlH_2NH_2 , the differences between the rotation barrier proceeding through the rotated C_s and C_{2v} structures are similar due to the relatively small inversion barrier at N. For BH_2PH_2 and AlH_2PH_2 , the difference between the rotation barrier proceeding through the rotated C_s and C_{2v} structures is due to the much larger inversion barrier at P. The tendency for the phosphorus atom to pyramidalize serves to weaken the π -bond energy because there is reduced overlap between the lone pair on P and the vacant orbital at B or Al. We can estimate this effect by comparing the inversion barriers in the unrotated and rotated states, which corresponds to the $C_{2v} - C_{2v}$ energy difference. For BH_2PH_2 , this value is 35.7 kcal/mol and, in AlH_2PH_2 , this value is 14.2 kcal/mol.

The adiabatic π -bond energies are the ground state (G. S.) to C_s values given in Table 4.6. The intrinsic π -bond energies are given by the adiabatic bond energy plus the energy used to invert the N or P atom or the $C_{2v} \rightarrow C_{2v}$ rotation energies. The intrinsic $\text{B}=\text{N}$ π -bond energy is thus 34 kcal/mol, and the intrinsic $\text{Al}=\text{N}$ π -bond energy is 11 kcal/mol, both similar to the

adiabatic values. The intrinsic B=P π -bond energy is 36 kcal/mol, and the intrinsic Al=P π -bond energy is 14 kcal/mol. The intrinsic π -bond energies for the latter two are substantially different from the adiabatic values because of the high inversion barrier at P. Comparing the intrinsic values, we see that the B=N and B=P values are quite similar, and the Al=N and Al=P values are also similar and substantially smaller.

On the basis of the calculated heats of formations given in Table 4.5, the adiabatic dissociation energies, which correspond to the sum of the σ - and π -bond energies are given in Table 4.7. The adiabatic reaction energies show that BH₂NH₂ has the largest binding energy at 139.7 kcal/mol, which can be compared with the C-C bond dissociation energy of 171.0 kcal/mol in ethylene.⁶ AlH₂NH₂ has a binding energy approximately 20 kcal/mol lower than that of BH₂NH₂, 109.3 kcal/mol. Both the BH₂PH₂ and AlH₂PH₂ have lower binding energies of 86.8 kcal/mol and 71.0 kcal/mol, respectively.

The adiabatic σ -bond energies of the molecules can be calculated as the difference between the binding energy of the optimized ground state structure, representing the σ -bond + π -bond energies, and the corresponding adiabatic rotational energy barrier, representing the π -bond energy. The adiabatic σ -bond strengths for the molecules BH₂NH₂, AlH₂NH₂, BH₂PH₂, and AlH₂PH₂ from the (σ + π) adiabatic asymptote using the adiabatic rotation barriers are 109.8, 98.8, 77.4, and 68.3 kcal/mol, respectively. The adiabatic σ -bond strength for BH₂NH₂ is comparable to the adiabatic σ -bond strength in ethylene of 106 kcal/mol given the experimentally determined π -bond strength of 65 kcal/mol¹¹ and an adiabatic C=C bond dissociation energy of 171 kcal/mol.⁵ The fact that it is slightly higher is consistent with the fact that the bond in BH₂NH₂ includes some ionic character. If we use the intrinsic π -bond strengths, we lower the adiabatic σ -bond strength to 106 kcal/mol for BH₂NH₂. For AlH₂NH₂, use of the

intrinsic π -bond strength results in very little change, a σ -bond strength of 98 kcal/mol. For BH_2PH_2 and AlH_2PH_2 , use of the intrinsic π -bond strengths leads to substantially lower σ -bond strengths of 51.1 and 56.8 kcal/mol, respectively.

The adiabatic σ -bond energies can be compared to the bond dissociation energies of the diatomics BN, AlN, BP, and AlP are 102.4, 57.3, 76.4, and 50.9 kcal/mol at 0 K.^{3,4} Thus, the σ -bond energies are stronger in the molecular systems than in the diatomics. In contrast, the dissociation energy⁴¹ of C_2 is 148 kcal/mol, much higher than the C-C σ -bond energies in most organic compounds.

The σ -bond energies for the AH_2XH_2 compounds can be compared to the dative σ -bond energies in the corresponding AH_3XH_3 compound (Table 4.1). The σ -bond energies for the AH_2XH_2 compounds are substantially higher than the dative σ -bond energies. As a consequence, the reaction $\text{AH}_3\text{XH}_3 \rightarrow \text{AH}_2\text{XH}_2 + \text{H}_2$ becomes closer to thermoneutral than in the hydrocarbon case for $\text{CH}_3\text{CH}_3 \rightarrow \text{CH}_2\text{CH}_2 + \text{H}_2$, which is substantially endothermic. Only for the BH_3PH_3 reaction is a substantial endothermicity found, and this is consistent with the relatively low σ -bond energy.

Carter and Goddard⁸ have shown that most of the decrease in dissociation energy of C_2F_4 to 2CF_2 , as compared to dissociation of C_2H_4 to 2CH_2 , is due to the difference in the ground states of CF_2 and CH_2 . The singlet ground state of CF_2 is not optimal for forming the σ - and π -bonds in C_2F_4 so the total dissociation energy is substantially reduced by the promotion energy to the triplet configuration, which is optimal for forming C_2F_4 . In C_2H_4 , the triplet ground state of CH_2 is optimal for forming C_2H_4 so there is no reduction in the total bond dissociation energy. Borden⁷ has suggested that the same types of arguments need to be considered in comparing the

strengths of the π -bonds in C_2H_4 and $HCCH$. This is because the optimal state of CH for forming $HCCH$ is the $^4\Sigma^-$, which is 16.7 kcal/mol above the $^2\Pi$ ground state.

This approach can be applied to analyze the bonding of AH_2XH_2 compounds to derive an intrinsic total ($\sigma + \pi$) bond dissociation energy. The bonding in the molecules at equilibrium corresponds to BH_2 or AlH_2 in the ground state and the NH_2 or PH_2 in the excited state. The excited state for XH_2 is the 2A_1 with the unpaired electron in the plane and the lone pair orbital out of the plane. For NH_2 , $T_0 (^2B_1 \rightarrow ^2A_1)$ is 31.8 kcal/mol and for PH_2 T_0 is 52.2 kcal/mol.⁴² To a first approximation, the bonding in $H_2A=XH_2$ can be described as arising from the 2A_1 configurations of both fragments. Thus, the sum of the bond energies in the diabatic limit or the intrinsic total ($\sigma + \pi$) bond dissociation energy would be increased by 31.8 kcal/mol for BH_2NH_2 and AlH_2NH_2 , and by 52.2 kcal/mol for BH_2PH_2 and AlH_2PH_2 giving respective values of 171.5, 141.1, 139.0, and 123.2 kcal/mol. If the intrinsic total ($\sigma + \pi$) bond dissociation energy is used, then BH_2NH_2 has a σ -bond strength of 142 kcal/mol using the adiabatic rotation barrier and one of 138 kcal/mol using the intrinsic π -bond energy. For AlH_2NH_2 the σ -bond strengths are 131 and 130 kcal/mol using the two definitions of the π -bond energy. For BH_2PH_2 , the σ -bond energies would be 130 kcal/mol with the adiabatic π -bond energy and 103 kcal/mol with the intrinsic the π -bond energy. For AlH_2PH_2 , the σ -bond energies would be 121 kcal/mol with the adiabatic π -bond energy and 109 kcal/mol with the intrinsic π -bond energy. These values seem to be somewhat high and are not consistent with other chemical concepts.

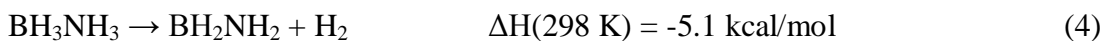
This analysis suggested another way to analyze the bonding in these molecules. As the π -bond is best described as a dative bond (see Figure 4.2), it is appropriate to compare breaking the σ -bond in these compounds to breaking an AH_2-R or XH_2-R bond. The simplest comparison is to consider R as H and compare the A-H or X-H bond energies to the A-X bond energies. Dixon *et*

*al.*⁴³ calculated the heats of formation of some simple boron compounds and predicted $\Delta H_f^0(\text{BH}_2, 0 \text{ K}) = 78.4 \text{ kcal/mol}$ and $\Delta H_f^0(\text{BH}, 0 \text{ K}) = 106.2 \text{ kcal/mol}$ at the CCSD(T)/CBS level. These values for BH_2 and BH are in good agreement with our current value of 78.5 kcal/mol and 106.2 kcal/mol, respectively, where we have included scalar-relativistic and spin-orbit corrections, which were not included previously. Given the heat of formation of BH_3 of 26.4 kcal/mol at 0 K,³ we calculate a B-H bond energy of 103.7 kcal/mol (see Table 4.8). In the present study, we have calculated the heats for formation at 0 K of the triatomics AlH_2 and PH_2 , giving values of 63.7 kcal/mol and 32.7 kcal/mol, respectively, and the corresponding diatomics AlH and PH , giving values of 58.9 kcal/mol and 57.0 kcal/mol, respectively. Given $\Delta H_f^0(\text{AlH}_3, 0 \text{ K}) = 31.9 \text{ kcal/mol}$ and $\Delta H_f^0(\text{PH}_3, 0 \text{ K}) = 3.3 \text{ kcal/mol}$ ⁴, the resulting Al-H bond energy in AlH_3 is 83.4 kcal/mol while the P-H bond energy in PH_3 is 81.0 kcal/mol. These can be compared to the B-H bond energy of 103.7 kcal/mol in BH_3 and the N-H bond energy of 106.5 kcal/mol in NH_3 .³ The bond energies for HAl-H and HP-H in going to the corresponding diatomic species are 46.8 kcal/mol at 0 K and 75.9 kcal/mol at 0 K, respectively, and can be compared to the value of the H-BH bond energy of 79.3 kcal/mol and the H-NH bond energy of 92.3 kcal/mol at 0 K.^{21m}

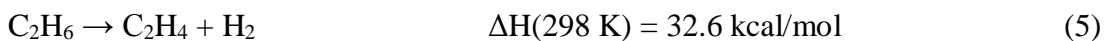
Comparison of the AH_3 and XH_3 bond energies in Table 4.8 with the A-B adiabatic σ -bond energies in Table 4.7 shows that the X-H bond energies track the A-B bond energies. The σ -bond energy in BH_2NH_2 is larger than the N-H bond energy in NH_3 by only 3 kcal/mol. The σ -bond energy in AlH_2NH_2 is less than that in BH_2NH_2 by 11 kcal/mol, as expected as Al is a 2nd row atom, and the bond energy is only 8 kcal/mol less than the N-H bond energy in NH_3 . For $\text{BH}_2=\text{PH}_2$ and $\text{AlH}_2=\text{PH}_2$, the σ -bond energies are 3 and 13 kcal/mol less than the P-H bond energy in PH_3 , essentially the same trend found in comparing the σ -bond energies in $\text{BH}_2=\text{NH}_2$ and $\text{AlH}_2=\text{NH}_2$ with the N-H bond energy in NH_3 . Thus, the σ -bond energies resemble very

closely the XH_3 bond energies, and it is not appropriate to compare with the diabatic limit approximation given above. The bonding in these compounds is much closer to that in a normal NH_2R or PH_2R compound with a delocalized lone pair (dative π -bond) from N or P, as compared to a model which describes the bonding as a fully shared π -bond as found in C_2H_4 . This result is consistent with Pauling's electroneutrality rule⁴⁴ as one would have to write the structure of BH_2NH_2 as $\text{H}_2\text{B}=\text{NH}_2^+$ with formal charges which puts the negative charge on the least electronegative atom B and the positive charge on the more electronegative atom N, which is the reverse of where the charges want to be.

The bond energies for the H_2AXH_2 compounds provide us with some useful insights into the differences in the donor-acceptor chemistry and covalent bond carbon-based chemistry. The elimination reaction (4) for loss of H_2 from BH_3NH_3 in the gas phase is exothermic



whereas the comparable organic reaction (5) is substantially endothermic.³



This difference in energetic requirements for H_2 release is due to the fact that a weak B-N dative σ -bond is broken in BH_3NH_3 and a strong $\text{sp}^2\text{-sp}^2$ σ -bond is formed in BH_2NH_2 , whereas a strong σ -bond is broken in C_2H_6 and a σ -bond of comparable strength to that in BH_2NH_2 is formed in C_2H_4 . Even though the adiabatic π -bond energy of BH_2NH_2 is only 30 kcal/mol as compared to the value of 65 kcal/mol in C_2H_4 , the difference of 35 kcal/mol is much smaller than the difference of 63 kcal/mol for the σ -bond strengths in BH_3NH_3 and C_2H_6 . Thus, the difference in the reactant σ -bond strengths is more important than the differences in the product π -bond strengths because of the strength of the σ -bonds in the product are comparable. The differences in the σ - and π -bond strengths can also be observed in the bond distances. The change in the C-C

bond length⁴⁵ from C₂H₆ to C₂H₄ is 0.20 Å, whereas the difference in the B-N bond lengths between BH₃NH₃ and BH₂NH₂ is 0.26 Å. The larger difference in the latter pair is consistent with the larger change in the σ-bond strengths in the boron amines even though the π-bond strength is lower in the boron amines. The π-bond shortens the B-N bond length by 0.08 Å, obtained by comparing the ground state and rotated structures for BH₂NH₂. In C₂H₄, the difference has been calculated⁹ to be 0.15 Å at the UHF/6-31G* level (C₂H₄ vs twisted •CH₂CH₂•), a larger difference consistent with the stronger π-bond in C₂H₄. The value of 1.465 Å for the diradical sp²-sp² σ-bond is consistent with the experimental⁴⁶ and calculated⁴⁷ values of 1.45 to 1.47 Å for the C-C sp²-sp² σ-bond in s-trans-1,3-butadiene.

4.4 Conclusions

Ab initio molecular orbital theory at the CCSD(T)/CBS level plus additional corrections has been used to predict the σ- and π-bond energies of BH₂NH₂, AlH₂NH₂, BH₂PH₂, and AlH₂PH₂. The adiabatic π-bond energy was defined as the barrier to rotation between the ground state and C_s transition state structures, and the intrinsic π-bond energy was defined as the adiabatic π-bond energy corrected for inversion at N or P. Using the adiabatic dissociation energies for AH₂XH₂ to AH₂ + XH₂, the adiabatic σ- and π-bond energies respectively, for BH₂NH₂ are 109.8 and 29.9 kcal/mol; for, AlH₂NH₂ 98.8 and 10.5 kcal/mol; for BH₂PH₂, 77.6 and 9.2 kcal/mol; and for AlH₂PH₂, 68.3 and 2.7 kcal/mol. These results are consistent with the binding being best described as breaking a σ-bond in an NH₂R or PH₂R molecule, which contains a delocalized lone pair (a dative π-bond). The energy differences between the weak dative σ-bond energies in AH₃XH₃ compounds and the strong sp²-sp² σ-bonds in the AH₂XH₂ compounds are an important reason why H₂ can readily be released from AH₃XH₃ compounds (except for BH₃PH₃) in contrast to C₂H₆ where loss of H₂ is substantially endothermic.

Acknowledgements We thank Prof. A. Arduengo, III, for helpful discussions. Funding provided in part by the Department of Energy, Office of Energy Efficiency and Renewable Energy under the Hydrogen Storage Grand Challenge, Solicitation No. DE-PS36-03GO93013. The Robert Ramsay Fund of the University of Alabama is thanked for support. This work was done as part of the Chemical Hydrogen Storage Center. This research was performed in part using the Molecular Science Computing Facility (MSCF) in the William R. Wiley Environmental Molecular Sciences Laboratory, a national scientific user facility sponsored by the U.S. Department of Energy's Office of Biological and Environmental Research and located at the Pacific Northwest National Laboratory. Pacific Northwest National Laboratory is operated for the Department of Energy by Battelle.

Appendix Optimized CCSD(T) geometry parameters for AH_2 , XH_2 , and planar NH_3 and PH_3 , calculated vibrational frequencies, and total CCSD(T) energies (E_h) as a function of basis set extrapolated to the complete basis set limit. This material is available free of charge via the Internet at <http://pubs.acs.org>.

Table 4.1. Donor σ -Bond Strengths in AH_3XH_3 Compounds in kcal/mol.

Molecule	σ-Bond Energy (0K)	σ-Bond Energy (298K)
$\text{H}_3\text{BNH}_3^{\text{a}}$	25.9	27.2
$\text{H}_3\text{AlNH}_3^{\text{b}}$	26.1	27.3
$\text{H}_3\text{BPH}_3^{\text{b}}$	21.1	22.5
$\text{H}_3\text{AlPH}_3^{\text{b}}$	14.0	14.7

^a Reference 3. ^b Reference 4.

Table 4.2. Optimized CCSD(T) Bond Lengths (Å) and Bond Angles (°) for the Rotated Structures of AH₂XH₂ in C_s and C_{2v} Symmetries.

Molecule	Basis Set	R _{XH}	∠HXH	∠HXA	R _{AH}	∠HAH	∠HAX	R _{XA}
BH ₂ NH ₂ (rot)	aVDZ	1.031	101.34	108.25	1.2172	118.63	122.22	1.4912
	aVTZ	1.022	101.86	108.87	1.2032	118.58	122.12	1.4793
BH ₂ NH ₂ (rot-planar)	aVDZ	1.012	113.64	123.18	1.2475	117.36	121.32	1.4735
BH ₂ PH ₂ (rot)	aVDZ	1.442	90.76	91.85	1.2067	119.00	120.77	1.9813
	aVTZ	1.428	90.71	91.87	1.1920	119.13	120.62	1.9627
BH ₂ PH ₂ (rot-planar)	aVDZ	1.401	115.20	122.40	1.2044	119.65	120.17	1.9646
AlH ₂ NH ₂ (rot)	aVDZ	1.022	105.84	118.61	1.5967	119.17	122.67	1.8491
	aVTZ	1.011	107.37	122.35	1.5899	118.44	122.37	1.8066
AlH ₂ NH ₂ (rot-planar)	aVDZ	1.016	109.18	125.41	1.5937	118.68	120.66	1.8313
AlH ₂ PH ₂ (rot)	aVDZ	1.442	91.84	90.46	1.5933	119.77	120.74	2.3924
	aVTZ	1.397	91.71	90.02	1.5867	119.55	120.77	2.3645
AlH ₂ PH ₂ (rot-planar)	aVDZ	1.407	109.18	125.41	1.5868	119.98	120.01	2.3227

Table 4.3. Calculated Imaginary Vibrational MP2/cc-pVTZ Frequencies (cm^{-1}).

Molecule	Symmetry	Calc.	Type
BH ₂ NH ₂ (rot)	a''	778.9i	Rotation
BH ₂ PH ₂ (rot)	a''	393.1i	Rotation
AlH ₂ NH ₂ (rot)	a''	516.2i	Rotation
AlH ₂ PH ₂ (rot)	a''	186.5i	Rotation
BH ₂ NH ₂ (rot-planar)	a ₂	1186.2i	Rotation
	b ₂	631.5i	Inversion
BH ₂ PH ₂ (rot-planar)	a ₂	1150.7i	Rotation
	b ₂	870.7i	Inversion
AlH ₂ NH ₂ (rot-planar)	a ₂	549.3i	Rotation
	b ₂	164.2i	Inversion
AlH ₂ PH ₂ (rot-planar)	b ₂	641.8i	Inversion
	a ₂	532.7i	Rotation

Table 4.4. Components for Calculated Atomization Energies in kcal/mol.

Molecule	CBS ^a	ΔE_{ZPE} ^b	ΔE_{CV} ^c	ΔE_{SR} ^d	ΔE_{SO} ^e	$\Sigma D_0(0\text{ K})$ ^f
BH ₂	169.28	8.97	0.72	-0.06	-0.03	160.95
AlH ₂	125.53	6.36	-0.91	-0.28	-0.21	117.76
PH ₂	154.32	8.32	0.19	-0.22	0.00	145.96
BH ₂ NH ₂ (rot)	467.89	27.75	1.55	-0.36	-0.03	441.30
BH ₂ NH ₂ (rot-planar)	463.38	27.13	1.59	-0.42	-0.03	437.39
BH ₂ PH ₂ (rot)	406.37	22.67	1.28	-0.43	-0.03	384.52
BH ₂ PH ₂ (rot-planar)	373.49	22.20	0.97	-0.79	-0.03	351.44
AlH ₂ NH ₂ (rot)	411.19	22.85	-0.31	-0.70	-0.21	387.12
AlH ₂ NH ₂ (rot-planar)	410.67	22.58	-0.45	-0.73	-0.21	386.70
AlH ₂ PH ₂ (rot)	351.94	18.36	-0.59	-0.69	-0.21	332.08
AlH ₂ PH ₂ (rot-planar)	330.91	18.10	-0.99	-1.04	-0.21	310.57

^a Extrapolated by using Equation (1) with aug-cc-PVnZ, $n = D, T, Q$. ^b The zero point

energies were obtained as described in the text. ^c Core/valence corrections were obtained with the cc-pwCVTZ basis sets at the aVTZ optimized geometries for the transition states for rotation and at the aVDZ optimized geometries for the rotated-planar structures.

^d The scalar relativistic correction is based on a CISD(FC)/cc-pVTZ MVD calculation at the aVTZ optimized geometries for the transition states for rotation and at the aVDZ optimized geometries for the rotated-planar structures. ^e Correction due to the incorrect treatment of the atomic asymptotes as an average of spin multiplets. Values are based on C. Moore's Tables, ref. 39. ^f The theoretical value of the dissociation energy to atoms, $\Sigma D_0(0\text{ K})$.

Table 4.5. Calculated Heats of Formation (kcal/mol) at 0 K and 298 K.

Molecule	$\Delta H_f(0\text{ K})_{\text{theory}}$	$\Delta H_f(298\text{ K})_{\text{theory}}$
BH ₂	78.5	78.6
AlH ₂	63.7	63.0
PH ₂	32.7	31.8
BH ₂ NH ₂ (rot)	14.0	11.1
BH ₂ NH ₂ (rot-planar)	17.9	15.0
BH ₂ PH ₂ (rot)	33.6	30.7
BH ₂ PH ₂ (rot-planar)	66.7	63.8
AlH ₂ NH ₂ (rot)	10.2	7.1
AlH ₂ NH ₂ (rot-planar)	10.6	7.2
AlH ₂ PH ₂ (rot)	28.1	24.8
AlH ₂ PH ₂ (rot-planar)	49.6	46.2
BH ₂ NH ₂ (G.S. C _{2v}) ^a	-15.9	-18.6
AlH ₂ NH ₂ (G.S. C _{2v}) ^b	-0.3	-3.3
BH ₂ PH ₂ (G.S. C _s) ^b	24.4	21.8
BH ₂ PH ₂ (planar C _{2v}) ^b	31.0	28.2
AlH ₂ PH ₂ (G.S. C _s) ^b	25.4	22.6
AlH ₂ PH ₂ (planar C _{2v}) ^b	35.4	32.2

^a Reference 3. ^b Reference 4.

Table 4.6. Rotation Barriers (π -Bond Energies) and Inversion Barriers at N or P in kcal/mol

Molecule	Rotation	Rotation	Rotation	Inversion	Inversion
	(G. S. \rightarrow C_s)	($C_s \rightarrow C_{2v}$)	($C_{2v} \rightarrow C_{2v}$)	(Ground State)	(Rotated)
	Adiabatic ^a	Inherent ^b			
H ₂ B=NH ₂	29.9	33.8	33.8	0 ^c	3.9
H ₂ Al=NH ₂	10.5	10.9	10.9	0 ^c	0.4
H ₂ B=PH ₂	9.2	42.3	35.7	6.6	33.1
H ₂ Al=PH ₂	2.7	24.2	14.2	10.0	21.5

^a Adiabatic π -bond energy. ^b Intrinsic π -bond energy. ^c Planar ground state structure.

Table 4.7. Adiabatic ($\sigma + \pi$) Total Dissociation Energies in kcal/mol.

Molecule	Adiabatic Total Dissociation Energy	Adiabatic σ-bond Energy
H ₂ B=NH ₂	139.7	109.8
H ₂ Al=NH ₂	109.3	98.8
H ₂ B=PH ₂	86.8	77.6
H ₂ Al=PH ₂	71.0	68.3

Table 4.8. AH₂-H and XH₂-H σ -Bond Energies in kcal/mol.

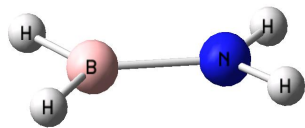
Molecule	Adiabatic σ-bond Energy
BH ₃	103.7
NH ₃	106.5
AlH ₃	83.4
PH ₃	81.0

Figure Captions

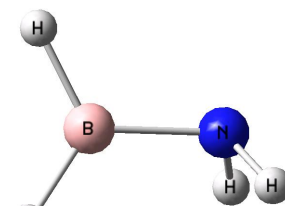
Figure 4.1. Optimized molecular structures for BH_2NH_2 , AlH_2NH_2 , BH_2PH_2 , AlH_2PH_2 , and the corresponding rotated structures.

Figure 4.2. HOMO for the ground state and rotated structures of BH_2NH_2 , AlH_2NH_2 , BH_2PH_2 , and AlH_2PH_2 .

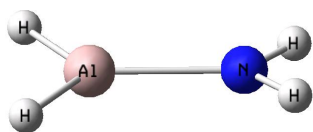
Figure 4.1.



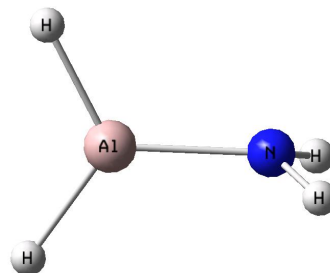
BH_2NH_2



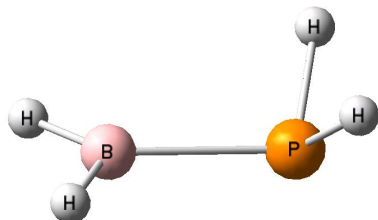
Rotated BH_2NH_2



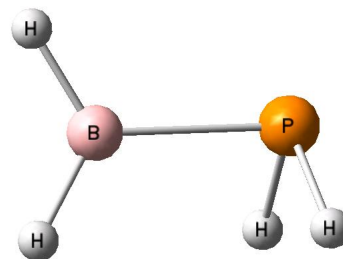
AlH_2NH_2



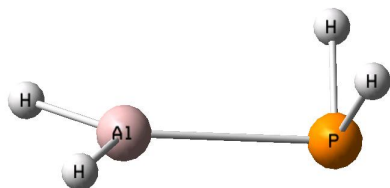
Rotated AlH_2NH_2



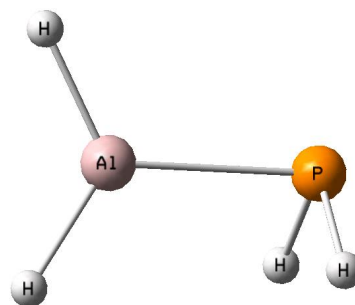
BH_2PH_2



Rotated BH_2PH_2

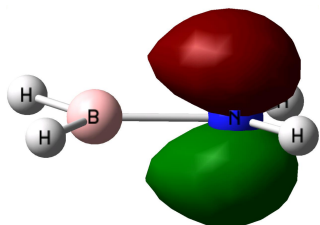


AlH_2PH_2

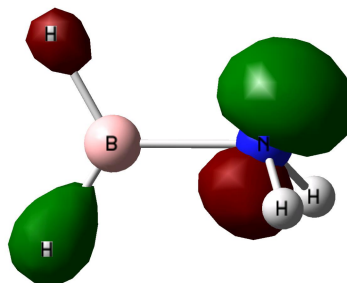


Rotated AlH_2PH_2

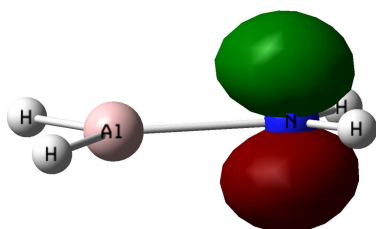
Figure 4.2.



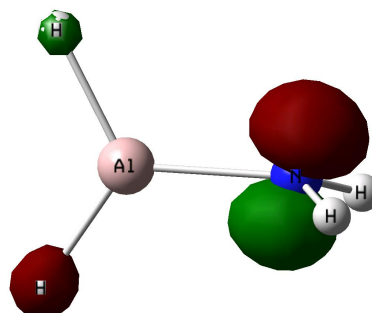
BH₂NH₂



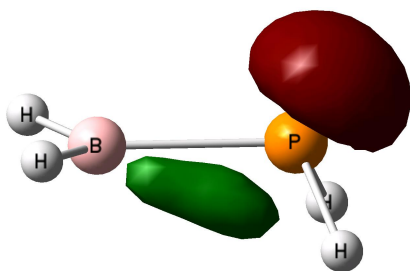
Rotated BH₂NH₂



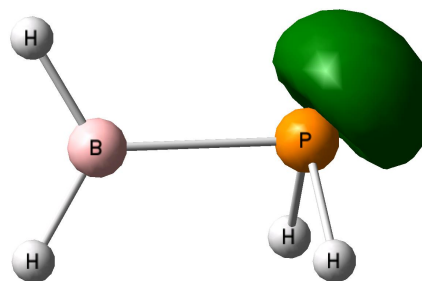
AlH₂NH₂



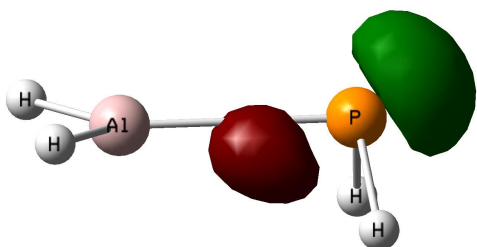
Rotated AlH₂NH₂



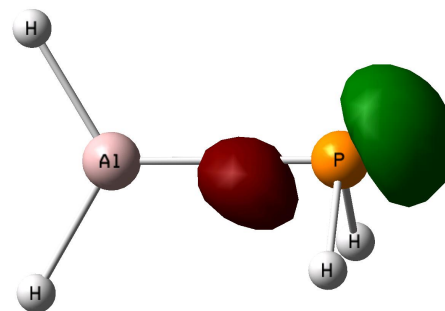
Non-planar BH₂PH₂



Rotated BH₂PH₂



Non-planar AlH₂PH₂



Rotated AlH₂PH₂

4.5 References

-
- ¹ Gutowski, M.; Autrey, T. Prepr. Pap. –Am. Chem. Soc., Div. Fuel Chem. **2004**, *49*, 275.
- ² Gutowski, M.; Autrey, T.; Linehan, J. *J. Phys. Chem. B.* accepted, 2005.
- ³ Dixon, D.A.; Gutowski, M. *J. Phys. Chem. A*, **2005**, *109*, 5129.
- ⁴ Dixon, D.A.; Grant, D.J. *J. Phys. Chem. A* **2005**, *109*, 10138.
- ⁵ Sander, S. P.; Friedl, R. R.; Ravishankara, A. R.; Golden, D. M.; Kolb, C. E.; Kurylo, M. J.; Huie, R. E.; Orkin, V. L.; Molina, M. J.; Moortgat, G. K.; Finlayson-Pitts, B. J. *Chemical Kinetics and Photochemical Data for Use in Atmospheric Studies: Evaluation Number 14*; JPL Publication 02-25, National Aeronautics and Space Administration, Jet Propulsion Laboratory, California Institute of Technology: Pasadena, California 2003. http://jpldataeval.jpl.nasa.gov/pdf/JPL_02-25_rev02.pdf.
- ⁶ Ervin, K.M.; Gronert, S.; Barlow, S.E.; Gilles, M.K.; Harrison, A.G.; Bierbaum, V.M.; DePuy, C.H.; Lineberger, W.C.; Ellison, G.B. *J. Am. Chem. Soc.* **1990**, *112*, 5750.
- ⁷ Nicolaidis, A.; Borden, W.T. *J. Am. Chem. Soc.* **1991**, *113*, 6750; Wang, S.Y.; Borden, W.T. *J. Am. Chem. Soc.* **1989**, *111*, 7282.
- ⁸ Carter, E.A.; Goddard, W.A., III, *J. Am. Chem. Soc.* **1988**, *110*, 4077; Carter, E.A.; Goddard, W.A., III, *J. Phys. Chem.* **1986**, *90*, 998.
- ⁹ Dobbs, K.D.; Hehre, W.J. *Organometallics* **1986**, *5*, 2057.
- ¹⁰ Schimdt, M.W.; Truong, P.N.; Gordon, M.S. *J. Am. Chem. Soc.* **1987**, 5217.
- ¹¹ Douglas, J.E.; Rabinovitch, B.S.; Looney, F.S. *J. Chem. Phys.* 1955, *23*, 315.
- ¹² Allen, T.L.; Fink, W.H. *Inorg. Chem.* **1993**, *32*, 4230.
- ¹³ Swallen, J.D., Ibers, J.A., *J. Chem. Phys.* **1962**, *36*, 1914.
- ¹⁴ McKee, M.I. *J. Phys. Chem.* **1992**, *96*, 5380.
- ¹⁵ Allen, T.L.; Scheiner, A.C.; Schaefer, H.F. *Inorg. Chem.* **1990**, *29*, 1930.
- ¹⁶ Allen, T.L.; Fink, W.H. *Inorg. Chem.* **1992**, *31*, 1703.
- ¹⁷ Marynick, D.S., Dixon, D.A., *J. Phys. Chem.* **1982**, *86*, 914.
- ¹⁸ Coolidge, M.B.; Borden, W.T. *J. AM. Chem. Soc.* 1990, *112*, 1704.

-
- ¹⁹ Fink, W.H.; Power, P.P.; Allen, T.L. *Inorg. Chem.* **1997**, *36*, 1431.
- ²⁰ Davy, R. D.; Jaffrey, K.L. *J. Phys. Chem.* **1994**, *98*, 8930.
- ²¹ (a) Peterson, K. A.; Xantheas, S. S.; Dixon, D. A.; Dunning, T. H. Jr, *J. Phys. Chem. A* **1998**, *102*, 2449; (b) Feller, D.; Peterson, K. A. *J. Chem. Phys.* **1998**, *108*, 154; (c) Dixon, D. A.; Feller, D. *J. Phys. Chem. A* **1998**, *102*, 8209; (d) Feller, D.; Peterson, K. A. *J. Chem. Phys.* **1999**, *110*, 8384; (e) Feller, D.; Dixon, D. A. *J. Phys. Chem. A* **1999**, *103*, 6413; (f) Feller, D. *J. Chem. Phys.* **1999**, *111*, 4373; (g) Feller, D.; Dixon, D. A. *J. Phys. Chem. A* **2000**, *104*, 3048; (h) Feller, D.; Sordo, J. A. *J. Chem. Phys.* **2000**, *113*, 485; (i) Feller, D.; Dixon, D. A. *J. Chem. Phys.* **2001**, *115*, 3484; (j) Dixon, D. A.; Feller, D.; Sandrone, G. *J. Phys. Chem. A* **1999**, *103*, 4744; (k) Ruscic, B.; Wagner, A. F.; Harding, L. B.; Asher, R. L.; Feller, D.; Dixon, D. A.; Peterson, K. A.; Song, Y.; Qian, X.; Ng, C.; Liu, J.; Chen, W.; Schwenke, D. W. *J. Phys. Chem. A* **2002**, *106*, 2727; (l) Feller, D.; Dixon, D.A.; Peterson, K.A. *J. Phys. Chem. A*, **1998**, *102*, 7053; (m) Dixon, D.A.; Feller, D.; Peterson, K.A. *J. Chem. Phys.*, **2001**, *115*, 2576.
- ²² Purvis, G. D. III; Bartlett, R. J. *J. Chem. Phys.* **1982**, *76*, 1910.
- ²³ Raghavachari, K.; Trucks, G. W.; Pople, J. A.; Head-Gordon, M. *Chem. Phys. Lett.* **1989**, *157*, 479.
- ²⁴ Watts, J. D.; Gauss, J.; Bartlett, R. J. *J. Chem. Phys.* **1993**, *98*, 8718.
- ²⁵ Dunning, T. H., Jr. *J. Chem. Phys.* **1989**, *90*, 1007.
- ²⁶ Kendall, R. A.; Dunning, T. H., Jr.; Harrison, R. J. *J. Chem. Phys.* **1992**, *96*, 6796.
- ²⁷ McQuarrie, D. A. "Statistical Mechanics," University Science Books, Sausalito, CA, 2001.
- ²⁸ Curtiss, L. A.; Raghavachari, K.; Redfern, P.C.; Pople, J.A. *J. Chem. Phys.* **1997**, *106*, 1063.
- ²⁹ Werner, H.-J.; Knowles, P. J.; Amos, R. D.; Bernhardsson, A.; Berning, A.; Celani, P.; Cooper, D. L.; Deegan, M. J. O.; Dobbyn, A. J.; Eckert, F.; Hampel, C.; Hetzer, G.; Korona, T.; Lindh, R.; Lloyd, A. W.; McNicholas, S. J.; Manby, F. R.; Meyer, W.; Mura, M. E.; Nicklass, A.; Palmieri, P.; Pitzer, R. M.; Rauhut, G.; Schütz, M.; Stoll, H.; Stone, A. J.; Tarroni, R.; Thorsteinsson, T. MOLPRO-2002, a package of initio programs written by, Universität Stüttgart, Stüttgart, Germany, University of Birmingham, Birmingham, United Kingdom, 2002.
- ³⁰ Rittby, M.; Bartlett, R. J. *J. Phys. Chem.* **1988**, *92*, 3033.
- ³¹ Knowles, P. J.; Hampel, C.; Werner, H. -J. *J. Chem. Phys.* **1994**, *99*, 5219.

-
- ³² Deegan, M. J. O.; Knowles, P. J. *Chem. Phys. Lett.* **1994**, *227*, 321.
- ³³ (a) Møller, C.; Plesset, M.S. *Phys. Rev.* **1934**, *46*, 618; (b) Pople, J.A.; Binkley, J.S.; Seeger, R. *Int. J. Quantum Chem. Symp.* **1976**, *10*, 1.
- ³⁴ Gaussian 03, Revision C.02, Frisch, M. J.; Trucks, G. W.; Schlegel, H. B.; Scuseria, G. E.; Robb, M. A.; Cheeseman, J. R.; Montgomery, Jr., J. A.; Vreven, T.; Kudin, K. N.; Burant, J. C.; Millam, J. M.; Iyengar, S. S.; Tomasi, J.; Barone, V.; Mennucci, B.; Cossi, M.; Scalmani, G.; Rega, N.; Petersson, G. A.; Nakatsuji, H.; Hada, M.; Ehara, M.; Toyota, K.; Fukuda, R.; Hasegawa, J.; Ishida, M.; Nakajima, T.; Honda, Y.; Kitao, O.; Nakai, H.; Klene, M.; Li, X.; Knox, J. E.; Hratchian, H. P.; Cross, J. B.; Bakken, V.; Adamo, C.; Jaramillo, J.; Gomperts, R.; Stratmann, R. E.; Yazyev, O.; Austin, A. J.; Cammi, R.; Pomelli, C.; Ochterski, J. W.; Ayala, P. Y.; Morokuma, K.; Voth, G. A.; Salvador, P.; Dannenberg, J. J.; Zakrzewski, V. G.; Dapprich, S.; Daniels, A. D.; Strain, M. C.; Farkas, O.; Malick, D. K.; Rabuck, A. D.; Raghavachari, K.; Foresman, J. B.; Ortiz, J. V.; Cui, Q.; Baboul, A. G.; Clifford, S.; Cioslowski, J.; Stefanov, B. B.; Liu, G.; Liashenko, A.; Piskorz, P.; Komaromi, I.; Martin, R. L.; Fox, D. J.; Keith, T.; Al-Laham, M. A.; Peng, C. Y.; Nanayakkara, A.; Challacombe, M.; Gill, P. M. W.; Johnson, B.; Chen, W.; Wong, M. W.; Gonzalez, C.; and Pople, J. A.; Gaussian, Inc., Wallingford CT, 2004.
- ³⁵ Dunning, T. H. Jr., Peterson, K. A. Wilson, A. K. *J. Chem. Phys.* **2001**, *114*, 9244.
- ³⁶ Peterson, K. A.; Woon, D. E.; Dunning, T. H., Jr. *J. Chem. Phys.* **1994**, *100*, 7410.
- ³⁷ Peterson, K. A.; Dunning, T. H., Jr., *J. Chem. Phys.* **2002**, *117*, 10548; Woon, D. E.; Dunning, T. H., Jr., *J. Chem. Phys.* **1993**, *98*, 1358.
- ³⁸ Davidson, E. R.; Ishikawa, Y.; Malli, G. L. *Chem. Phys. Lett.* **1981**, *84*, 226.
- ³⁹ Moore, C. E. "Atomic energy levels as derived from the analysis of optical spectra, Volume 1, H to V," U.S. National Bureau of Standards Circular 467, U.S. Department of Commerce, National Technical Information Service, COM-72-50282, Washington, D.C.; **1949**.
- ⁴⁰ Chase, M.W., Jr.; NIST-JANAF Tables (4th Edition), *J. Phys. Chem. Ref. Data*, Mono. **9**, Suppl. 1, **1998**.
- ⁴¹ Urdahl, R. S.; Bao, Y.; Jackson, W. M. *Chem. Phys. Lett.* **1991**, *178*, 425.
- ⁴² Jacox, M.E., *J. Phys. Chem. Ref. Data, Monograph 3*, 1994.
- ⁴³ Feller, D., Dixon, D.A., Peterson, K.A. *J. Phys. Chem. A* **1998**, *102*, 7053

⁴⁴ Pauling, L. "The Nature of the Chemical Bond," Cornell University Press, Ithaca NY, 3rd Edition, 1960. For example, see pp. 271ff.

⁴⁵ Kutchitsu, K. (Ed.) "Structure of Free Polyatomic Molecules – Basic Data," Springer-Verlag, Berlin, 1998.

⁴⁶ Kveseth, K.; Seip, R.; Kohl, D. *Acta Chem. Scand. A* **1980**, *34*, 31; Craig, N. C.; McKean, D. C.; Groner, P. *J. Phys. Chem. A* **2006**, *110*, 7461.

⁴⁷ McKean, D. C.; Craig, N. C.; Panchenko, Y.N. *J. Phys. Chem. A* **2006**, *110*, 8044.

4.6 Appendices

Table 4.1. Optimized CCSD(T) Bond Lengths (Å) and Bond Angles (°) for AH₂, XH₂, and planar NH₃ and PH₃.

Molecule	Basis Set	r_{M(VA)H}	∠H_{NH}	r_{M(III A)H}	∠H_{BH}
BH ₂	aVDZ			1.2059	128.3
	aVTZ			1.1893	128.9
AlH ₂	aVDZ			1.6090	118.7
	aVTZ			1.6010	118.5
PH ₂	aVDZ	1.4103	122.2		
	aVTZ	1.3981	122.1		
NH ₃ (planar)	aVDZ	1.0055	120.0		
	aVTZ	0.9975	120.0		
PH ₃ (planar)	aVDZ	1.3943	120.0		
	aVTZ	1.3820	120.0		

Table 4.2. Calculated Vibrational MP2/cc-pVTZ Frequencies (cm⁻¹).

Molecule	Symmetry	Calculated	Experiment ^a
BH ₂	a ₁	2538.7	
	a ₁	1042.6	
	b ₂	2697.0	
AlH ₂	a ₁	1818.4	1766
	a ₁	786.5	760
	b ₂	1844.8	1799
PH ₂	a ₁	2459.3	2310
	a ₁	1143.2	1101.9
	b ₂	2470.4	
BH ₂ NH ₂ (rot)	a'	3342.1	
	a'	2562.4	
	a'	2478.4	
	a'	1561.4	
	a'	1331.2	
	a'	1082.6	
	a'	1021.5	
	a'	727.7	
	a''	3410.6	
	a''	1178.0	
	a''	778.9i	
	a''	728.4	
	BH ₂ NH ₂ (rot-planar)	a ₁	3522.6
a ₁		2463.4	
a ₁		1560.3	
a ₁		1348.4	
a ₁		1124.9	
a ₂		1186.2i	
b ₁		3625.4	
b ₁		1168.8	
b ₁		651.0	

	b ₂	2516.7
	b ₂	1009.6
	b ₂	631.5i
BH ₂ PH ₂ (rot)	a'	2626.8
	a'	2535.6
	a'	2308.5
	a'	1244.9
	a'	1068.5
	a'	851.7
	a'	675.2
	a'	586.1
	a''	2313.5
	a''	1024.7
	a''	632.7
	a''	393.1i
BH ₂ PH ₂ (rot-planar)	a ₁	2542.5
	a ₁	2507.6
	a ₁	1264.0
	a ₁	1035.5
	a ₁	700.7
	a ₂	1150.7i
	b ₁	2548.8
	b ₁	1021.3
	b ₁	460.8
	b ₂	2635.4
	b ₂	825.3
	b ₂	870.7i
AlH ₂ NH ₂ (rot)	a'	3454.4
	a'	1891.5
	a'	1870.5
	a'	1566.9
	a'	846.4

	a'	772.5
	a'	571.9
	a'	238.8
	a''	3541.5
	a''	727.9
	a''	516.2i
	a''	514.4
AlH ₂ NH ₂ (rot-planar)	a ₁	3478.9
	a ₁	1883.6
	a ₁	1565.9
	a ₁	851.1
	a ₁	784.3
	a ₂	549.3i
	b ₁	3568.6
	b ₁	719.0
	b ₁	507.2
	b ₂	1871.4
	b ₂	578.4
	b ₂	164.2i
AlH ₂ PH ₂ (rot)	a'	2303.8
	a'	1889.3
	a'	1879.8
	a'	1089.5
	a'	804.6
	a'	610.8
	a'	431.9
	a'	381.6
	a''	2311.7
	a''	673.5
	a''	477.2
	a''	186.5i
AlH ₂ PH ₂ (rot-planar)	a ₁	2481.7

a ₁	1901.5
a ₁	1059.4
a ₁	819.4
a ₁	464.2
a ₂	532.7i
b ₁	2502.6
b ₁	631.3
b ₁	378.0
b ₂	1903.2
b ₂	525.3
b ₂	641.8i

^a Jacox, M. E., *J. Phys. Chem. Ref. Data*, Monograph 3, 1994.

Table A4.3. Total CCSD(T) Energies (E_h) as a Function of Basis Set and Extrapolations to the CBS Limit Using Equation 3.

System	Basis Set	E_h
BH ₂ NH ₂ (rot)	aVDZ	-81.76893
	aVTZ	-81.845504
	aVQZ	-81.866507
	CBS (DTQ)	-81.878051
BH ₂ NH ₂ (rot-planar)	aVDZ	-81.761047
	aVTZ	-81.837999
	aVQZ	-81.859204
	CBS (DTQ)	-81.870871
BH ₂ PH ₂ (rot)	aVDZ	-367.989422
	aVTZ	-368.054623
	aVQZ	-368.072073
	CBS (DTQ)	-368.081609
BH ₂ PH ₂ (rot-planar)	aVDZ	-367.930755
	aVTZ	-367.999761
	aVQZ	-368.018339
	CBS (DTQ)	-368.028506
AlH ₂ NH ₂ (rot)	aVDZ	-299.011641
	aVTZ	-299.087723
	aVQZ	-299.108769
	CBS (DTQ)	-299.120359
AlH ₂ NH ₂ (rot-planar)	aVDZ	-299.011384
	aVTZ	-299.086965
	aVQZ	-299.107958
	CBS (DTQ)	-299.119530
AlH ₂ PH ₂ (rot)	aVDZ	-585.236575
	aVTZ	-585.300398
	aVQZ	-585.317912
	CBS (DTQ)	-585.327540

AlH ₂ PH ₂ (rot-planar)	aVDZ	-585.201306
	aVTZ	-585.266256
	aVQZ	-585.284172
	CBS (DTQ)	-585.294032
NH ₃ (planar)	aVDZ	-56.416255
	aVTZ	-56.471739
	aVQZ	-56.487220
	CBS (DTQ)	-56.495762
AlH	aVDZ	-242.534088
	aVTZ	-242.547218
	aVQZ	-242.550697
	CBS (DTQ)	-242.552594
AlH ₂	aVDZ	-243.109759
	aVTZ	-243.127383
	aVQZ	-243.13233
	CBS (DTQ)	-243.135063
PH	aVDZ	-341.404295
	aVTZ	-341.436111
	aVQZ	-341.444275
	CBS (DTQ)	-341.448692
PH ₂ (² B ₁)	aVDZ	-342.023126
	aVTZ	-342.061892
	aVQZ	-342.072059
	CBS (DTQ)	-342.077588
PH ₃ (planar)	aVDZ	-342.599972
	aVTZ	-342.645620
	aVQZ	-342.657892
	CBS (DTQ)	-342.664605

CHAPTER 5

THERMOCHEMISTRY FOR THE DEHYDROGENATION OF METHYL SUBSTITUTED AMMONIA BORANE COMPOUNDS

From: Grant, D. J.; Matus, M. H.; Anderson, K. D.; Camaioni, D. M.; Neufeldt, S. R.; Lane, C. F.; Dixon, D. A. *J. Phys. Chem. A* **2009**, *113*, 6121-6132.

5.1 Introduction

There is substantial interest in the discovery of new molecules for chemical hydrogen storage systems in which dehydrogenation (hydrogen release) and hydrogenation (regeneration of spent fuel) from these molecules are near thermoneutral processes. The need for a thermoneutral reaction arises because one wants to minimize the heat needed for the reaction to release hydrogen and to minimize the energy requirements of the regeneration process. An important potential chemical hydrogen storage material is ammonia borane, and there are a number of efforts focused on its use for H₂ storage.^{1,2,3,4,5,6,7,8,9} High level *ab initio* molecular orbital theory has been used to predict reliably the gas phase thermochemistry of ammonia borane and various dehydrogenation processes,¹⁰ as well as for the heats of formation of larger B_xN_yH_z compounds.¹¹

An issue with ammonia borane is that it is a solid at room temperature, and this may make use of the fuel in the transportation sector difficult as the use of solids as a fuel is not currently practiced. Solid fuels would require substantial changes to the infrastructure. Ammonia borane is a solid due to the large number of moderate strength intermolecular H...H bonds formed between the H^{δ+} on the N and the H^{δ-} on the B.^{12,13,14} Alkyl substituted ammonia boranes

have lower melting points than does ammonia borane,¹⁵ presumably because there are fewer H···H interactions due to the presence of the alkyl groups. It has recently been found that borane amine can be solubilized in methyl substituted ammonia borane (see below).¹⁶ Dimethylamine borane has a melting point of 36 °C,¹⁷ and a melt of the neat compound can be kept at 45 °C for 7 days with no observed decomposition.¹⁸ The vapor pressures of the *N*-methyl substituted methylamine boranes have been reported, and the heat of sublimation for the *N*-mono and *N,N*-dimethyl derivatives are higher than the *N,N,N*-trimethyl derivative.¹⁹ Thus, addition of methyl substituted ammonia boranes could enable the generation of a liquid fuel and potentially enable use of portions of the current infrastructure. As there is a weight penalty associated with any additional components, we wished to determine if the substituted ammonia boranes can also act as a hydrogen source in terms of their thermodynamic properties. *N*-methylammonia borane and ammonia *B*-methylborane have a weight percent storage for hydrogen of 9.8% if 2 molecules of H₂ are produced as compared to the amine boranes having 14.9% if 2 molecules of H₂ are produced. This requires that we know the thermochemistry for the dehydrogenation of *N*-methylammonia borane and ammonia *B*-methylborane to see if the weight issues can be improved. As the thermodynamic properties are not known, we have used high-level molecular orbital theory to predict the critical heats of formation. The heats of formation of these simple model compounds are also needed accurately for use in isodesmic reaction schemes in order to predict the heat of formation of larger molecules. In the current work, we have calculated the heats of formation for the *N*-methylammonia borane and ammonia *B*-methylborane, as well as various molecules involved in the dehydrogenation processes ((CH₃)₂N-BH₃, (CH₃)₂B-NH₃, (CH₃)HN=BH₂, (BH₃)HN=CH₂, (CH₃)HB=NH₂, and (NH₃)HB=CH₂), at the CCSD(T)/CBS level (coupled cluster with an approximate triples correction²⁰ at the complete basis set limit). In

addition, we report G3(MP2) calculations on the alkylated dehydrogenated products derived from cyclodi-, cyclotri-, and cyclotetrazaborazane.

In order to further understand the chemistry of these compounds in terms of their reactivity and stability, we are also interested in the various σ - and π -bond dissociation energies (BDEs). The B-N dative bond in $\text{H}_3\text{B-NH}_3$ is 27.2 kcal/mol,¹⁰ as compared to the covalent C-C σ -bond energy of 90.1 kcal/mol at 298 K for C_2H_6 .²¹ We have previously investigated the σ - and π -bonds in the main Group IIIA–Group VA $\text{H}_2\text{A=XH}_2$ compounds and calculated the rotation barrier to estimate the π -bond energies.²² The bond energies can then be compared to the σ - and π -bond energies in C_2H_4 , which has a covalent π -bond.²³ We predicted that the adiabatic σ -bond strength of $\text{H}_2\text{B=NH}_2$ of 109.8 kcal/mol was comparable to the adiabatic σ -bond strength in $\text{H}_2\text{C=CH}_2$ of 106 kcal/mol, given the experimentally determined π -bond strength of 65 kcal/mol²⁴ and an adiabatic C=C BDE of 171 kcal/mol.²¹ In addition, we defined intrinsic π -bond strengths that are corrected for pyramidalization in the ground state and rotated transition state structures. The adiabatic σ -bond strengths for $\text{H}_2\text{B=NH}_2$ and $\text{H}_2\text{Al=NH}_2$ did not change substantially when considering the intrinsic π -bond strength due to the rather small inversion barriers at N in the rotated transition state structures.

There have been a number of experimental investigations of the structures of the *N*-methyl substituted ammonia boranes. Bauer²⁵ used electron diffraction to study the structure of *N*-trimethylamine borane. Later, Taylor *et al.*²⁶ used microwave spectroscopy to obtain the B-N and C-N bond distances and the CNB angle of trimethylamine-borane. The best molecular structure of trimethylamine-borane was obtained from a combination of gas-phase electron diffraction and microwave spectroscopy data by Shibata *et al.*²⁷ Bowden *et al.* reported the crystal structure of methylamine borane and showed that thermal decomposition of the melt

starting at ~100 °C leads to liberation of H₂;²⁸ a second H₂ is lost near 190 °C. Most recently, Wann *et al.*²⁹ reported an elaborate detailed study of the structures of methylamine-borane and dimethylamine-borane by x-ray diffraction of the crystal and gas-phase electron diffraction aided by quantum chemical calculations. Anane *et al.* reported G2(MP2) B-N bond energies for the (CH₃)_nH_{3-n}BNH₃ and BH₃N(CH₃)_nH_{3-n} (n = 0-3) complexes.^{30, 31} Gilbert compared density functional theory (DFT) with different exchange correlation functionals with MP2 all with the 6-311++G(d,p) basis set and experiment for different BR₃-NR₃' compounds. He found that MP2 gives the best agreement with experiment.³² Very recently, Sun *et al.* reported the B-N BDEs for BH₃NH₃, BH₃NH₂CH₃ and BH₃NH(CH₃)₂ at the B3LYP/6-311G** and MP2/6-31G** levels, as well as the barrier height for the unimolecular loss of H₂. The barrier heights are predicted to increase slightly on methylation at the MP2/6-31G* level.³³

5.2 Experimental Methods

5.2.1 *Synthesis of Ammonia Borane. Procedure 1: Addition of BH₃•THF to NH₃.* Ammonia (8 mL, 320 mmol) was condensed into a cold (-78 °C) graduated cylinder and then allowed to warm slowly. The NH₃ gas was bubbled into THF (50 mL) in a flask held at -40 °C under N₂. To this solution was added 1 M BH₃•THF (100 mL, 100 mmol), and the reaction mixture was cooled to -78 °C and stirred for 1 h. After slow warming to ambient temperature, the reaction mixture was concentrated by using a rotary evaporator and dried under vacuum to yield an oily white solid. This was stirred in isopropyl alcohol, filtered, and dried under vacuum to yield 2.04 g (66%) of a white solid.

Procedure 2: Addition of NH₃ to BH₃•THF. Ammonia (5 mL, 200 mmol) was condensed into a cold (-78 °C) graduated cylinder and then allowed to warm slowly. The gas was bubbled into 1 M BH₃•THF (100 mL, 100 mmol) in a flask held at -20 °C under N₂. The reaction mixture

was stirred for 1 h at -20 °C, then allowed to warm to ambient temperature and stirred overnight. The reaction mixture was filtered through diatomaceous earth and concentrated by using a rotary evaporator, then dried under vacuum to yield an oily white solid. This was stirred in isopropyl alcohol, filtered, and dried under vacuum to yield 1.23 g (40%) of a white solid.

5.2.2 Synthesis of Methylamine Borane. Methylamine (21.3 mL, 480 mmol) was condensed into a cold (-78 °C) graduated cylinder and then allowed to warm slowly. The gas was bubbled into 1 M BH₃•THF (400 mL, 400 mmol) in a flask held at -20 °C under N₂. The reaction mixture was then allowed to slowly warm to ambient temperature and stirred for 2 h. The reaction mixture was concentrated by using a rotary evaporator and dried under vacuum to yield an oily white solid. This was stirred in *n*-heptane, filtered, and dried under vacuum to yield 16.34 g (91%) of a white solid.

5.2.3 Co-synthesis of Ammonia and Methylamine Borane. The ratios of ammonia and methylamine used in the co-synthesis were chosen to yield a mixture of 20-40% ammonia borane in methylamine borane. The experimental yields from the procedures described above for the individual syntheses of ammonia borane and methylamine borane indicated that the reaction of the two amines with BH₃•THF did not proceed to the same degree of completion. Ammonia (1.8 mL, 70 mmol) was condensed into a cold (-78 °C) graduated cylinder and then allowed to warm slowly. The gas was bubbled into 1 M BH₃•THF (100 mL, 100 mmol) in a flask held at -40 °C under N₂. Methylamine (3.2 mL, 72 mmol) was then condensed into a cold (-78 °C) graduated cylinder and allowed to warm slowly. The gas was bubbled into the reaction mixture at -15 °C under N₂. The reaction mixture was allowed to warm slowly to ambient temperature and stirred for 1 h. The reaction mixture was concentrated by using a rotary evaporator, and then dried under vacuum to yield an oily white solid. The solid melted completely in a 30 °C water bath, and

separated into two liquid layers. The top layer was isolated and determined to be a mixture of about 30–40% ammonia borane in methylamine borane by ^1H NMR. The bottom layer was mainly impurities and side products (including *n*-butanol due to ring-opening of the THF) by NMR.

5.2.4 Melting of Ammonia Borane and Methylamine Borane Mixtures. Eleven mixtures of ammonia borane (AB) and methyl amine borane (MeAB) were prepared in weight ratios ranging from 0:1 to 1:0 of AB:MeAB, respectively. One gram of each mixture was prepared by combining the appropriate amount of AB and MeAB in a test tube; each mixture was then suspended in THF (10 mL) and poured into a crystallizing dish. After evaporation of the THF, the resulting white solid was dried under vacuum. Multiple melting point capillary tubes were prepared for each mixture. Each tube was evacuated and refilled with N_2 (3x) and sealed with paraffin wax. Melting ranges were obtained by using a Meltemp device set to a specific temperature. Melting was observed 15 sec after insertion of the capillary tube. Multiple temperatures were tested for each AB/MeAB mixture, using a different capillary tube for each temperature setting.

5.3 Computational Methods

We have been developing a composite approach^{34, 35} to the prediction of the thermodynamic properties of molecules based on molecular orbital theory using coupled cluster methods at the CCSD(T) level. In most CCSD(T) calculations of atomization energies (or heats of formation), the largest source of error typically arises from the finite basis set approximation, unless there is significant multireference character to the wavefunction. Our composite approach for predicting atomization energies makes use of the systematic convergence properties of the valence correlation consistent family of basis sets including additional diffuse functions.³⁶ These

basis sets are conventionally denoted aug-cc-pVnZ, with $n = D, T,$ and Q . The standard aug-cc-pVnZ basis sets were used for H, B, C, and N. We use the shorthand notation of aVnZ and VnZ to denote the aug-cc-pVnZ and cc-pVnZ basis sets, respectively, on H, B, C, and N. Only the spherical component subset (e.g., 5-term d functions, 7-term f functions, etc.) of the Cartesian polarization functions were used. All CCSD(T) calculations were performed with the MOLPRO-2002 program system³⁷ on the Cray XD-1, Altix, or DMC at the Alabama Supercomputer Center or with a Dell Cluster at the University of Alabama.

For the open shell atomic calculations, we used the restricted method for the starting Hartree-Fock wavefunction and then relaxed the spin restriction in the coupled cluster portion of the calculation. This method is conventionally labeled R/UCCSD(T). Our CBS estimates use a mixed exponential/Gaussian function of the form³⁸

$$E(n) = E_{\text{CBS}} + Be^{-(n-1)} + Ce^{-(n-1)^2} \quad (1)$$

where $n = 2$ (aVDZ), 3 (aVTZ), and 4 (aVQZ). This extrapolation method has been shown to yield atomization energies in the closest agreement with experiment (by a small amount) as compared to other extrapolation approaches up through $n = 4$.

Most correlated electronic structure calculations based on molecular orbital theory are done in the frozen core approximation with the energetically lower lying orbitals, e.g., the $1s$ in carbon, excluded from the correlation treatment. In order to achieve thermochemical properties within ± 1 kcal/mol of experiment, it is necessary to account for core-valence correlation energy effects. Core-valence (CV) calculations were carried out with the weighted core-valence basis set cc-pwCVTZ.³⁹

Two adjustments to the total atomization energy ($\text{TAE} = \Sigma D_0$) are necessary in order to account for relativistic effects in atoms and molecules. The first correction lowers the sum of the

atomic energies (decreasing TAE) by replacing energies that correspond to an average over the available spin multiplets with energies for the lowest multiplets as most electronic structure codes produce only spin multiplet averaged wavefunctions. The atomic spin-orbit corrections are $\Delta E_{\text{SO}}(\text{B}) = 0.03$ kcal/mol and $\Delta E_{\text{SO}}(\text{C}) = 0.09$ kcal/mol from the tables of Moore.⁴⁰ A second relativistic correction to the atomization energy accounts for molecular scalar relativistic effects, ΔE_{SR} . We evaluated ΔE_{SR} by using expectation values for the two dominant terms in the Breit-Pauli Hamiltonian, the so-called mass-velocity and one-electron Darwin (MVD) corrections from configuration interaction singles and doubles (CISD) calculations.⁴¹ The quantity ΔE_{SR} was obtained from CISD wavefunction with a VTZ basis set at the appropriate CCSD(T) or MP2 optimized geometry. The CISD(MVD) approach generally yields ΔE_{SR} values in good agreement (± 0.3 kcal/mol) with more accurate values from, for example, Douglas-Kroll-Hess calculations,⁴² for most molecules.

Geometries for the smaller molecules (HBNH_2 , HNBH_2 , HBCH_2 , and HNCH_2) were optimized at the CCSD(T) level with the aVDZ and aVTZ basis sets. The geometry obtained with the aVTZ basis set was then used in a single point aVQZ calculation. For the larger molecules, geometries were optimized at the MP2/VTZ level.^{43,44} Geometries obtained with the VTZ basis set were then used in CCSD(T) single point calculations with the aVDZ, aVTZ, and aVQZ basis sets. The impact of the use of the different geometries is on the order of a few tenths of a kcal/mol for these well-behaved systems. The zero point energies (ΔE_{ZPE}) were obtained at the MP2 level with the VTZ basis set. To calculate the zero point correction and account for anharmonic effects, the calculated harmonic A-H stretching frequencies were scaled by factors of 0.974 (B), 0.972 (C), and 0.973 (N), obtained by taking the average of the MP2/VTZ and

experimental values^{45,46,47} for the A-H stretches of BH₃, CH₄, and NH₃ and dividing the average by the theoretical value, respectively.

By combining our computed ΣD_0 values given by the following expression

$$\Sigma D_0 = \Delta E_{\text{elec}}(\text{CBS}) - \Delta E_{\text{ZPE}} + \Delta E_{\text{CV}} + \Delta E_{\text{SR}} + \Delta E_{\text{SO}} \quad (2)$$

with the known⁴⁸ heats of formation at 0 K for the elements, $\Delta H_f^0(\text{H}) = 51.63$ kcal/mol, $\Delta H_f^0(\text{B}) = 135.10$ kcal/mol,⁴⁹ $\Delta H_f^0(\text{C}) = 169.98$ kcal/mol, and $\Delta H_f^0(\text{N}) = 112.53$ kcal/mol, we can derive ΔH_f^0 values for the molecules under study. We employ what we consider to be the best heat of formation⁴⁹ of the boron atom, which has changed over time.^{48,50,51,52} This value is based on W4 calculations of the total atomization energies of BF₃ and B₂H₆ and their experimental heats of formation.^{53,54} Heats of formation at 298 K were obtained by following the procedures outlined by Curtiss *et al.*⁵⁵

We have also calculated heats of formation and dehydrogenation energies employing a computationally less intensive approach by using the G3(MP2) level of theory,⁵⁶ as it can be used for much larger molecules, and we wish to test it.

5.4 *Experimental Results*

Various mixtures of CH₃NH₂BH₃ and NH₃BH₃ were made and their melting points were measured as described above. The results are shown in Figure 5.1 (Detailed values are given in Supporting Information). The lowest melting mixture contained ~35% NH₃BH₃ by weight and melted at 35-37 °C. As shown in Figure 5.1, a range of NH₃BH₃ weight percents from 20% to 50% in CH₃NH₂BH₃ will melt between 35 and 42 °C. The pure NH₃BH₃ melted at 118-120 °C and pure CH₃NH₂BH₃ melted at 58-59 °C.

5.5 Computational Results

The calculated geometries for the molecules under study are given as Supporting Information in Tables A5.2 and A5.3, respectively, and the calculated harmonic frequencies are given in Table A5.4 of the Supporting Information, where they are compared with the available experimental values. The total energies used in this study are also given as Supporting Information (Table A5.5). Optimized structures for the compounds with 1 B and N are shown in Figure 5.2.

5.5.1 *Geometries and Frequencies.* Structural data are available for a few of the molecules under study, and our calculated values are in excellent agreement with the reported values. We use the values calculated at the MP2/VTZ level in our discussion below unless specified otherwise. The lower level MP2(full)/6-31 G(d) values from the G2(MP2) calculations^{30,31} for the free methylboranes and methylamines are in good agreement with our higher level values. The C-N bond distance in H₂C=NH is calculated to be 0.002 Å longer than the experimental value of 1.273 Å,⁵⁷ consistent with our prior calculations.⁵⁸

For the free methyl substituted boranes, the B-C bond distance in methylborane is predicted to increase by 0.007 and 0.002 Å, respectively, for dimethylborane and trimethylborane. A small decrease in the B-C bond distance is predicted for the dimethylborane radical B(CH₃)₂ of 0.003 Å.

In the free methyl substituted amines, the C-N bond distance in methylamine is calculated to be slightly shorter by 0.008 Å than the experimental value of 1.471 Å,⁵⁷ consistent with our prior calculations.⁵⁹ The C-N bond distance in dimethylamine and trimethylamine are predicted to be shorter by 0.01 and 0.001 Å than the experimental values of 1.464 and 1.451 Å, respectively.⁵⁷ Sequential methylation of methylamine leads to a further decrease in the C-N

bond distance by 0.009 and 0.013 Å for $\text{HN}(\text{CH}_3)_2$ and $\text{N}(\text{CH}_3)_3$, respectively. An even larger decrease in C-N bond distance is predicted for the dimethylamine radical $\text{N}(\text{CH}_3)_2$ of 0.025 Å.

The effect of mono- and dimethyl substitution in $\text{H}_2\text{B}=\text{NH}_2$ at B for $(\text{CH}_3)\text{HB}=\text{NH}_2$ and $(\text{CH}_3)_2\text{B}=\text{NH}_2$ is predicted to increase the B-N bond distance by 0.005 and 0.010 Å, respectively, compared to the B-N bond distance in $\text{H}_2\text{B}=\text{NH}_2$. Sequential methylation at N leads to decreases in the B-N bond distance of 0.002 and 0.001 Å for $(\text{CH}_3)\text{HN}=\text{BH}_2$ and $(\text{CH}_3)_2\text{N}=\text{BH}_2$. The effect of ammoniation on the B-C bond distance in $(\text{NH}_3)\text{HB}=\text{CH}_2$ increases the bond distance by 0.043 Å as compared to $\text{HB}=\text{CH}_2$. We predict the equivalent borane substituent to have essentially no effect on the N-C bond distance in $(\text{BH}_3)\text{HN}=\text{CH}_2$, as compared to that of $\text{HN}=\text{CH}_2$.

Similarly, we can examine the effect of methylation at B and N on the B-N bond distance of $\text{H}_3\text{B}-\text{NH}_3$. Our calculated MP2/VTZ parameters for $(\text{CH}_3)\text{H}_2\text{N}-\text{BH}_3$ and $(\text{CH}_3)_2\text{HN}-\text{BH}_3$, are in reasonable agreement with the new experimental²⁹ data and the other MP2 optimizations.^{29,30,31} The B-N bond distances of $(\text{CH}_3)\text{H}_2\text{N}-\text{BH}_3$ and $(\text{CH}_3)_2\text{HN}-\text{BH}_3$ are predicted to be 0.033 and 0.015 Å longer than the gas-phase electron diffraction (GED) refined values ($r_{\text{a3,1}}$) of 1.602(7) and 1.615(4) Å, respectively.²⁹ The N-C bond distances are also predicted to be slightly longer than the GED $r_{\text{a3,1}}$ values²⁹ by 0.025 and 0.0064 Å, respectively. Our calculated geometry parameters are also in excellent agreement with the MP2/aVQZ²⁹ values. For $(\text{CH}_3)\text{H}_2\text{N}-\text{BH}_3$ and $(\text{CH}_3)_2\text{HN}-\text{BH}_3$, our VTZ B-N and N-C bond distances are longer than the aVQZ values by an average of 0.011 and 0.006 Å, respectively. Our calculated parameters for trimethylamineborane, $(\text{CH}_3)_3\text{N}-\text{BH}_3$, are consistent with the experimental structural data.^{25,26,27,29,57} The experimental B-N bond distances vary over ~0.04 Å, and our calculated value is 0.022 Å shorter, 0.004 Å shorter, and 0.0144 Å longer than the experimental

values of 1.656 ± 0.002 ($r_{a3,1}$),²⁷ 1.638 ± 0.01 ,^{26,57} and 1.62 ± 0.15^{25} Å determined from GED and spectroscopic data, microwave (MW) spectroscopy, and electron diffraction, respectively. The C-N and B-H bond distances are in good agreement with the recent experimental values.^{25,26,27,57} Sequential methylation at B in $(\text{CH}_3)\text{H}_2\text{B-NH}_3$, $(\text{CH}_3)_2\text{HB-NH}_3$, and $(\text{CH}_3)_3\text{B-NH}_3$ leads to respective increases of 0.005, 0.013, and 0.021 Å in the B-N bond distance compared to that of $\text{H}_3\text{B-NH}_3$. Sequential methylation of $\text{H}_3\text{B-NH}_3$ at N leads to respective decreases in the B-N bond distance of 0.016, 0.021, and 0.017 Å for $(\text{CH}_3)\text{H}_2\text{N-BH}_3$, $(\text{CH}_3)_2\text{HN-BH}_3$, and $(\text{CH}_3)_3\text{N-BH}_3$ compared to that of $\text{H}_3\text{B-NH}_3$. Thus, the B-N bond distance in $(\text{CH}_3)_3\text{N-BH}_3$ is longer than that in $(\text{CH}_3)_2\text{HN-BH}_3$ consistent with the MP2(full)/6-311++G**²⁹ and MP2(full)/6-31 G(*d*)^{30,31} calculations. The available experimental data²⁹ suggests that methylation at N will decrease the B-N bond distance for the first methyl group and then subsequent methylation at N will increase the B-N bond distance. Further experimental results are needed to explain the discrepancy in the trend.

5.5.2 Heats of Formation. The energetic components for predicting the total molecular dissociation energies are given in Table 5.1. The electronic states and symmetry labels are included in Tables 5.1 and 5.2. The core-valence corrections are positive and range from 1.12 [$\text{HB}(\text{NH}_3)$] to 3.02 [$(\text{CH}_3)\text{H}_2\text{B-NH}_3$] kcal/mol. The scalar relativistic corrections are all negative and range from -0.23 [HBCH_2] to -0.61 [$(\text{CH}_3)\text{H}_2\text{N-BH}_3$] kcal/mol. We estimate that the error bars for the calculated heats of formation are ± 1.0 kcal/mol considering errors in the energy extrapolation, frequencies, and other electronic energy components. The largest error is most likely in the valence contribution and extrapolation to the complete basis set limit followed by the prediction of the zero point energy.^{35k} An estimate of the potential for significant multireference character in the wavefunction can be obtained from the T_1 diagnostic⁶⁰ for the

CCSD calculation. The values for the T_1 diagnostics are small (<0.03) showing that the wavefunctions are dominated by a single configuration. The T_1 diagnostics are given as Supporting Information (Table A5.7).

The calculated CCSD(T)/CBS heats of formation for the molecules are given in Table 5.2 and compared to experimental data where available.^{61,62,63,64,65} In general, the heats of formation calculated at the G3(MP2) level are within 2 kcal/mol of the more accurate CCSD(T) value, except for $\text{H}_3\text{B-NH}_3$, where the difference is predicted to be 2.9 kcal/mol. The heats of formation of the methyl amines are known from experiment. The CCSD(T)/CBS value for CH_3NH_2 is within 1 kcal/mol of experiment as expected. The heats of formation of $(\text{CH}_3)_2\text{NH}$ and $(\text{CH}_3)_3\text{N}$ were calculated at the G3(MP2) level using isodesmic reaction schemes. The G3(MP2) isodesmic values are similar to the G3(MP2) values calculated from the atomization energies. The differences of the calculated values for the amines from experiment are less than 2 kcal/mol, and the calculated values are less negative than the experimental values. The calculated values for $\text{B}(\text{CH}_3)_3$, $\text{B}(\text{CH}_3)_3\text{NH}_3$, and $\text{N}(\text{CH}_3)_3\text{BH}_3$ are in reasonable agreement with the experimental values.^{62,64,65}

5.5.3 Dehydrogenation Reaction Energies. We can predict the heats of reaction for the dehydrogenation of *N*-methylammonia borane and ammonia *B*-methylborane (Table 5.3), and we use the CCSD(T) values at 298 K in our discussions below unless specified otherwise. The dehydrogenation of *N*-methylammonia borane can occur via two possible pathways. One is the removal of H_2 from across B-N bond resulting in the formation of $(\text{CH}_3)\text{HN}=\text{BH}_2$. This pathway is exothermic by -3.5 and -5.2 (G3(MP2)) kcal/mol, showing reasonable agreement of the G3(MP2) value with the more accurate CCSD(T) result. This value can be compared to the dehydrogenation of ammonia borane of $\Delta\text{H} = -5.1$ kcal/mol.¹⁰ The effect of the methyl

substituent at N is to decrease the exothermicity of the dehydrogenation reaction by 1.6 kcal/mol, making the reaction closer to thermoneutral. Dehydrogenation of *N*-methylammonia borane can also occur by the removal of H₂ from across C-N bond leading to the formation of a C=N double bond in (BH₃)HN=CH₂. This reaction is predicted to be endothermic by 28.0 and 26.3 (G3(MP2)) kcal/mol. This value is ~1 kcal/mol more endothermic than the dehydrogenation of (CH₃)NH₂ to give H₂C=NH of 26.7 kcal/mol. Substitution of the -BH₃ group has a minimal effect on the dehydrogenation reaction across the C-N bond. This value can also be compared to the experimental value^{48,66} of 32.6 kcal/mol for the dehydrogenation of C₂H₆. The latter pathway for the dehydrogenation process is unlikely due to its large endothermicity.

The dehydrogenation of ammonia *B*-methylborane can also occur via two pathways. Dehydrogenation across the B-N bond leads to the product (CH₃)HB=NH₂; this reaction is predicted to be exothermic by -9.4 and -11.0 (G3(MP2)) kcal/mol, again showing reasonable agreement of the G3(MP2) value with the more accurate CCSD(T) value. The dehydrogenation reaction at the B-N bond is more exothermic for methyl substitution on B as compared to methyl substitution on N. Dehydrogenation across the B-C bond leads to (NH₃)HB=CH₂, and this reaction is endothermic by 38.3 and 36.3 (G3(MP2)) kcal/mol. This value is ~6 kcal/mol less than the dehydrogenation enthalpy of (CH₃)BH₂ to give H₂C=BH of 44.5 kcal/mol. This value is ~12 kcal/mol more endothermic than the dehydrogenation of C₂H₆.^{48,66}

We predicted the heats of formation of *N*-dimethylammonia borane and ammonia *B*-dimethylborane, their thermodynamically favorable dehydrogenated derivatives, (CH₃)₂N=BH₂ and (CH₃)₂B=NH₂, and *N*-trimethylammonia borane and ammonia *B*-trimethylborane on the basis of isodesmic reactions at the G3(MP2) level (Table A5.6). The calculated heats of formation at 0 K and 298 K are given in Table 5.2. Although the dehydrogenation of *N*-

dimethylammonia borane can occur via two possible pathways, we have chosen to focus only on the removal of H₂ from across the B-N bond, as the dehydrogenation reaction across the N-C bond is substantially endothermic. The dehydrogenation pathway forming (CH₃)₂N=BH₂ is predicted to be exothermic by only -1.8 (isodesmic G3(MP2)) and -3.6 (standard G3(MP2)) kcal/mol. The additional methyl substituent further decreases the exothermicity of the dehydrogenation reaction by 1.7 kcal/mol and becomes even closer to thermoneutral.

Similarly, we consider dehydrogenation of ammonia *B*-dimethylborane across the B-N bond, as the dehydrogenation across the B-C bond is highly endothermic. The dehydrogenation pathway forming (CH₃)₂B=NH₂ is calculated to be -11.7 (isodesmic G3(MP2)) and -13.3 (standard G3(MP2)) kcal/mol. The second methyl substituent further increases the exothermicity by 2.3 kcal/mol compared to its monomethyl analogue and by 6.6 kcal/mol compared to ammonia borane, leading to a more exothermic dehydrogenation reaction.

5.5.4 Bond Energies. We first examine the effect of sequentially methylating ammonia borane at both B and N on the B-N dative σ -bond energy (Table 5.7), and use the values calculated at 0 K in our discussion below. Monomethylation of ammonia borane at N leads to a predicted 5.6 kcal/mol increase in the B-N dative σ -bond energy compared to that of ammonia borane.¹⁰ The substitution of the second methyl group to form *N*-dimethylammonia borane leads to an additional 3.4 kcal/mol increase in the B-N dative σ -bond energy compared to the monomethyl analogue and 9.0 kcal/mol increase compared to that of ammonia borane.¹⁰ The B-N dative σ -bond energy of (CH₃)₃N-BH₃ shows a smaller increase of 1.1 kcal/mol compared to that of the dimethyl substituted analogue and a total 10.1 kcal/mol increase compared to that of ammonia borane.¹⁰ The calculated values for the B-N dative bond energies for methyl substitution at N can be compared to experimental estimates^{67, 68} at 298 K as shown in Table 5.7. The largest

difference was found for BH_3NH_3 where Haaland⁶⁷ estimated the value. We note that the calculations predict that methylation at N increases the B-N bond energy in contrast to Haaland's experimental prediction of an increase through dimethylation and a decrease for trimethylation. If one uses more modern values^{62,64} for $\Delta H_f(\text{N}(\text{CH}_3)_3)$ and $\Delta H_f(\text{N}(\text{CH}_3)_3\text{BH}_3)$ and our best calculated value for BH_3 , one obtains a value of 39.2 kcal/mol for the B-N dative bond energy for $\text{N}(\text{CH}_3)_3\text{BH}_3$, which is completely consistent with the predicted trends. In contrast, methylation of ammonia borane at B is predicted to have the opposite effect, and the B-N dative σ -bond energy of $(\text{CH}_3)_{(3-n)}\text{H}_n\text{B}-\text{NH}_3$ for $n = 2, 1,$ and 0 are predicted to be 5.8, 9.9, and 13.1 kcal/mol less than that in $\text{H}_3\text{B}-\text{NH}_3$, respectively (Table 5.7). The calculated value for the B-N dative bond in $\text{NH}_3\text{B}(\text{CH}_3)_3$ can be compared with the experimental value^{67,69} of 13.8 kcal/mol and good agreement is found.

Our calculated dative bond energies can be compared with previous theoretical calculations. The G2(MP2) B-N dative bond energies at 0 K are in good agreement with our values and the MP2/TZ2P values⁷⁰ are too large by 2 to 3 kcal/mol. The MP2(full)6-311++G** and MP2/6-311++G** values are in reasonable agreement with our values, but how the ZPE was included and the temperature of the results were not given.^{29,32} Calculations at the HF/6-31G* level⁷¹ using isodesmic reactions give methylated boron-nitrogen bond energies that are too large and methylated nitrogen-boron bond energies that are too small. The HF/6-31G* methylated boron-nitrogen bond energies do have the correct qualitative trend of decreasing bond energy with increasing degrees of methylation, but the HF/6-31G* level does not get the correct trend for an increase in the dative bond energy with methylation at N and, in fact, HF/6-31G* does not predict any real methylation effect.

We estimate the π - and σ -bond energies of the various “double” bonds following the procedures we recently used for the Group IIIA–Group VA $\text{H}_2\text{A}=\text{XH}_2$ compounds based on rotation barriers.²² The molecular structures for the optimized ground state as well as the transition state for rotation about the $\text{A}=\text{X}$ bond are shown in Figures A5.1 and A5.2 of the Supporting Information. For the $\text{B}=\text{N}$ bond, the transition state lies on the singlet surface as a dative π -bond is being broken. For the $\text{C}=\text{N}$ and $\text{B}=\text{C}$ bonds, a covalent π -bond is broken so we estimate the rotation barrier by calculating the energy of the triplet rotated transition state. For the rotated structures, the unique imaginary frequencies associated with each molecule are given in Table 5.4. The π -bond energies can be estimated from the magnitude of the energies of the rotation barrier, and the values for the rotation barriers are presented in Table 5.5. The adiabatic rotation energy barrier was calculated as the energy difference between the equilibrium ground state configuration and the transition state structure of C_s symmetry for torsion by 90 degrees about the central $\text{A}=\text{X}$ bond. In addition, we also calculated an intrinsic π -bond energy, which is defined as the adiabatic bond energy plus the energy used to invert the N atom in the rotated transition state structure or the $C_{2v} \rightarrow C_{2v}$ rotation energies. The rotation barrier calculated at the MP2/VTZ level should be an excellent estimate of the CCSD(T)/CBS value, as in BH_2NH_2 , the adiabatic and intrinsic π -bond energies were within 0.2 kcal/mol of each other at the CCSD(T)/CBS and MP2/VTZ levels.

The adiabatic rotation barriers of $(\text{CH}_3)\text{HB}=\text{NH}_2$ and $(\text{CH}_3)\text{HN}=\text{BH}_2$ are predicted to be 3.4 kcal/mol less and 7.1 kcal/mol more than that of $\text{H}_2\text{B}=\text{NH}_2$. The higher rotational barrier for $(\text{CH}_3)\text{HN}=\text{BH}_2$ can be rationalized in terms of electron donating ability of the methyl group at N, leading to further delocalization of the increased electron density toward the empty p orbital on B and a stronger dative π -bond. The adiabatic rotation barriers of $(\text{NH}_3)\text{HB}=\text{CH}_2$ and

$(\text{BH}_3)\text{HN}=\text{CH}_2$ are much larger, consistent with the former two molecules having only a dative π -bond and the latter two molecules having a covalent π -bond. In comparison, the measured rotational barriers for systems substituted with 3 alkyls and a phenyl on either B or N, e.g. $(\text{CH}_3)_2\text{NB}(\text{R})\text{Ph}$ and $\text{Ph}(\text{R})\text{NB}(\text{CH}_3)_2$, are lower, ranging from 10-19 kcal/mol.⁷² Such low barriers are consistent with expected steric interactions, which destabilize the planar ground states along with stabilizing resonance effects with the phenyl ring in the transition structures. The adiabatic π -bond energies of $(\text{NH}_3)\text{HB}=\text{CH}_2$ and $(\text{BH}_3)\text{HN}=\text{CH}_2$ are predicted to be comparable to the π -bond strength of C_2H_4 of 65 kcal/mol.²⁴ Our calculated value for the rotation barrier of C_2H_4 is 65.8 kcal/mol.⁷³ Similarly, we predict the adiabatic rotation barriers $(\text{CH}_3)_2\text{B}=\text{NH}_2$ and $(\text{CH}_3)_2\text{N}=\text{BH}_2$ to be 1.0 and 4.0 kcal/mol less, respectively, than those of their monomethyl analogues.

We also calculated a rotation barrier defined as the energy difference between the ground state and the rotated transition state structure that is corrected for any pyramidalization that may have occurred upon rotation. For $\text{H}_2\text{B}=\text{NH}_2$, the rotational barrier difference is 4.0 kcal/mol (3.9 kcal/mol at the CCSD(T)/CBS level) due to the inversion barrier of the $-\text{NH}_2$ moiety in the rotated structure. Similarly for $(\text{CH}_3)_2\text{N}=\text{BH}_2$ and $(\text{CH}_3)_2\text{B}=\text{NH}_2$, we predict an intrinsic π -bond strength of 38.1 and 29.1 kcal/mol, a difference of 5.3 and 3.8 kcal/mol due to the inversion barrier at N. The inversion barriers in methyl-substituted amines has been previously calculated using the approximate PRDDO method and *ab initio* levels employing a DZP basis set giving barriers of 4.7, 5.1, 5.4, and 9.6 kcal/mol for NH_3 , CH_3NH_2 , $(\text{CH}_3)_2\text{NH}$, and $(\text{CH}_3)_3\text{N}$, respectively.⁷⁴ The inversion barrier of $(\text{CH}_3)_2\text{N}=\text{BH}_2$ is essentially the same as that of $(\text{CH}_3)_2\text{NH}$ indicating no substituent effect of the $=\text{BH}_2$ group. Similarly, the inversion barriers of $(\text{CH}_3)_2\text{B}=\text{NH}_2$ and $\text{H}_2\text{B}=\text{NH}_2$ are the essentially the same indicating no effect of the $-\text{CH}_3$ groups

on the inversion barrier at N, indicating that inversion is not as important as delocalization. The orbital diagrams (obtained at the density functional theory B3LYP/DZVP2 level,^{75, 76} see Supporting Information) are consistent with these effects.

The adiabatic BDEs (Tables 5.6 and 5.7) correspond to the sum of the σ - and π -bond energies (doubly bonded compounds) or to the σ -bond energies (singly bonded compounds). The C-N adiabatic BDE of $(\text{CH}_3)\text{HN}=\text{BH}_2$ is equal to the diabatic BDE as the ground state of the separated species can be directly derived from the bonding configuration in the molecule. The C-N adiabatic BDE (value of $\Delta H_f(\text{CH}_3)$ from Reference⁷⁷) can be compared to the value of 82.4 kcal/mol in $\text{H}_3\text{C}-\text{NH}_2$, showing a substituent effect of 9.3 kcal/mol for the $-\text{BH}_2$ group. The B=N adiabatic BDE of $(\text{CH}_3)\text{HN}=\text{BH}_2$ is 3.6 kcal/mol less than the adiabatic ($\sigma + \pi$) total dissociation energy of $\text{H}_2\text{B}=\text{NH}_2$,²² showing a small effect of the methyl substituent on the B=N BDE. This value is substantially less than the C=C BDE in ethylene of 171.0 kcal/mol.²³

We consider the B-N and N=C BDEs of $(\text{BH}_3)\text{HN}=\text{CH}_2$, the dehydrogenated product of *N*-methylammonia borane from dehydrogenation across the N-C bond, that has a dative B-N bond. The $=\text{CH}_2$ group increases the B-N dative BDE by 4.3 kcal/mol as compared to the B-N donor σ -bond in $\text{H}_3\text{B}-\text{NH}_3$.¹⁰ The N=C bond dissociates to ground state $^3\text{B}_1 \text{CH}_2$ and $^3\text{A} \text{HN}-\text{BH}_3$ so the adiabatic and diabatic BDEs are the same. This BDE is comparable to the C=N adiabatic BDE in $\text{H}_2\text{C}=\text{NH}$ of 155.5 kcal/mol, showing a minimal substitution effect of 2.7 kcal/mol for the $-\text{BH}_3$ group on the C=N diabatic BDE. This value is about 13 kcal/mol less than the C=C BDE in ethylene.²³

The B-C adiabatic BDE in $(\text{CH}_3)\text{HB}=\text{NH}_2$ (Table 5.7) is about the same as the B-C adiabatic BDE in $\text{H}_3\text{C}-\text{BH}_2$ of 102.2 kcal/mol, showing no substituent effect for the $=\text{NH}_2$ group. The B=N adiabatic BDE is slightly less than the adiabatic ($\sigma + \pi$) BDE in $\text{H}_2\text{B}=\text{NH}_2$,²² showing a

minimal substituent effect for the $-\text{CH}_3$ group. It is also slightly higher by ~ 1 kcal/mol than the B=N BDE in $(\text{CH}_3)\text{HN}=\text{BH}_2$.

The B-N dative BDE in $(\text{NH}_3)\text{HB}=\text{CH}_2$ is approximately equal to the B-N donor σ -bond in $\text{H}_3\text{B}-\text{NH}_3$,¹⁰ and is ~ 4 kcal/mol less than that in $(\text{BH}_3)\text{HN}=\text{CH}_2$. The B=C adiabatic BDE can be compared to that in $\text{H}_2\text{C}=\text{BH}$ of 145.0 kcal/mol, showing a 13.9 kcal/mol substituent effect of the $-\text{NH}_3$ group. We can define a diabatic B=C BDE with dissociation occurring to the excited triplet state of $\text{HB}-\text{NH}_3$ and the $^3\text{B}_1$ ground state of CH_2 that more closely represents the bonding electron configuration in the molecule. The diabatic B=C BDE in $(\text{NH}_3)\text{HB}=\text{CH}_2$ is 166.6 kcal/mol. The analogous diabatic BDE in $\text{H}_2\text{C}=\text{BH}$, in which dissociation occurs to the excited $^3\Pi$ state of BH , is 174.6 kcal/mol, 8.0 kcal/mol higher than the B=C diabatic BDE in $(\text{NH}_3)\text{HB}=\text{CH}_2$. (The experimental singlet-triplet splitting of the BH radical is $10,410\text{ cm}^{-1}$ (29.7 kcal/mol)⁷⁸) The diabatic BDE in $\text{H}_2\text{C}=\text{BH}$ is 3.6 kcal/mol higher than the C=C BDE in ethylene.²³

For the dimethyl substituted compounds, the B=N adiabatic BDEs in $(\text{CH}_3)_2\text{N}=\text{BH}_2$ and $(\text{CH}_3)_2\text{B}=\text{NH}_2$ are 7.4 and 4.3 kcal/mol less, respectively, than that in $\text{H}_2\text{B}=\text{NH}_2$,²² consistent with an approximately additive methyl substituent effect as these BDEs are less than those of their respective monomethyl analogues by 3.8 and 1.8 kcal/mol.

The adiabatic σ -bond energies of the doubly bonded molecules are calculated as the difference between the adiabatic BDE of the optimized ground state structure, representing the sum of the $(\sigma + \pi)$ bond energies, and the corresponding adiabatic rotational energy barrier, representing the π -bond energy. The adiabatic σ -bond strengths for $(\text{CH}_3)\text{HN}=\text{BH}_2$, $(\text{BH}_3)\text{HN}=\text{CH}_2$, $(\text{CH}_3)\text{HB}=\text{NH}_2$, $(\text{NH}_3)\text{HB}=\text{CH}_2$, $(\text{CH}_3)_2\text{N}=\text{BH}_2$, and $(\text{CH}_3)_2\text{B}=\text{NH}_2$ from the $(\sigma + \pi)$ adiabatic asymptote using the adiabatic rotation barriers are given in Table 5.5. The

adiabatic σ -bond strengths for $(\text{CH}_3)\text{HN}=\text{BH}_2$, $(\text{CH}_3)\text{HB}=\text{NH}_2$, $(\text{CH}_3)_2\text{N}=\text{BH}_2$, and $(\text{CH}_3)_2\text{B}=\text{NH}_2$ can be compared to the adiabatic B-N σ -bond strength in $\text{H}_2\text{B}=\text{NH}_2$ of 109.8 kcal/mol.²² Comparing the adiabatic σ -bond strengths for $(\text{CH}_3)\text{HN}=\text{BH}_2$ versus $(\text{CH}_3)_2\text{N}=\text{BH}_2$ and $(\text{CH}_3)\text{HB}=\text{NH}_2$ versus $(\text{CH}_3)_2\text{B}=\text{NH}_2$, we note that sequential methylation essentially has no effect on the B-N σ -bond to within 1 kcal/mol (Table 5.6). The adiabatic B-N σ -bond strengths for $(\text{CH}_3)\text{HB}=\text{NH}_2$ and $(\text{CH}_3)_2\text{B}=\text{NH}_2$ are also comparable to the adiabatic C-C σ -bond strength in C_2H_4 of 106 kcal/mol based on the experimentally determined π -bond strength of 65 kcal/mol,²⁴ as well as the calculated value⁷³ of 65.8 kcal/mol and the adiabatic C=C BDE.²³ The fact that they are slightly more stable is consistent with the fact that the bonds in $(\text{CH}_3)\text{HB}=\text{NH}_2$ and $(\text{CH}_3)_2\text{B}=\text{NH}_2$ include some ionic character. The adiabatic B-C σ -bond strength of $(\text{NH}_3)\text{HB}=\text{CH}_2$ is slightly less endothermic by an average of 6.2 kcal/mol compared to those in $\text{H}_3\text{C}-\text{BH}_2$ and $(\text{CH}_3)\text{HB}=\text{NH}_2$ of 102.2 and 102.0 kcal/mol, respectively. The adiabatic N-C σ -bond strength of $(\text{BH}_3)\text{HN}=\text{CH}_2$ compares well with the adiabatic N-C σ -bond strengths in $\text{H}_3\text{C}-\text{NH}_2$ and $(\text{CH}_3)\text{HN}=\text{BH}_2$ of 82.4 and 91.4 kcal/mol, respectively, being slightly more and slightly less endothermic by 4.5 kcal/mol, respectively.

5.5.5 Properties of Larger Compounds. The G3(MP2) method predicts reasonable BDEs and dehydrogenation energies so we can use this method for larger B-C-N compounds, which would be too computationally expensive to calculate at the CCSD(T) level. We have used the G3(MP2) method to predict the heats of formation (Table 5.8) and dehydrogenation energies (Table 5.9) of the methylated cyclodi-, cyclotri- and cyclotetrazaborazanes and use the 298 K values in our discussion below. The experimental heat of formation of the N-methylated *c*- $\text{B}_3\text{N}_3\text{H}_3(\text{CH}_3)_3$ compound has been reported to be -217 ± 1 kcal/mol, which is clearly incorrect.^{63,79} The *cis* and *trans* isomers of *N*-dimethyl cyclodiborazane, *c*- $\text{B}_2\text{N}_2\text{H}_6(\text{CH}_3)_2$, are calculated to be the same at

298 K, slightly favoring the *trans* isomer at 0 K. Dehydrogenation of *c*-B₂N₂H₆(CH₃)₂ to give *c*-B₂N₂H₂(CH₃)₂ + 2H₂ is calculated to be 4.6 kcal/mol more endothermic than the equivalent non-methylated reaction *c*-B₂N₂H₈ → *c*-B₂N₂H₄ + 2H₂,¹¹ showing that methylation at N in the cyclodiborazane compound increases the endothermicity of the dehydrogenation reaction. Dehydrogenation of *c*-B₃N₃H₉(CH₃)₃ to give 3 H₂ molecules is calculated to be 12.4 kcal/mol less exothermic than the equivalent reaction of *c*-B₃N₃H₁₂ (twist-boat),¹¹ indicating a larger substituent effect of the -CH₃ groups on reducing the exothermicity of the dehydrogenation reaction. Dehydrogenation of *c*-B₄N₄H₁₂(CH₃)₄ to give *c*-B₄N₄H₄(CH₃)₄ + 4H₂ is calculated to be near thermoneutral and 28.8 kcal/mol more endothermic than the equivalent non-methylated cyclotetaborazane reaction *c*-B₄N₄H₁₆ → *c*-B₄N₄H₈ + 4H₂.

We also studied the effect of substituting NH₂BH₃ and BH₂NH₃ for H in C₂H₆. Dehydrogenation of (H₃BH₂N)H₂C-CH₂(NH₂BH₃) (**A**) and (H₃NH₂B)H₂C-CH₂(BH₂NH₃) (**B**) can occur by several pathways. The most thermodynamically favorable pathway is dehydrogenation across the dative B-N bond with the first dehydrogenation step predicted to be 2.2 and 0.4 kcal/mol more exothermic than the equivalent dehydrogenation reactions of (CH₃)H₂N-BH₃ and (CH₃)H₂B-NH₃ of -5.2 and -11.0 kcal/mol, respectively. The other possible dehydrogenation pathways are predicted to be largely endothermic. The first dehydrogenation reaction across the C-N and B-C bonds yielding (H₃B)HN=CH-CH₂(NH₂BH₃) and (H₃N)HB=CH-CH₂(BH₂NH₃) are essentially the same (within 0.4 kcal/mol) as the equivalent dehydrogenation reaction of (CH₃)H₂N-BH₃ and (CH₃)H₂B-NH₃ of 26.3 and 36.3 kcal/mol, respectively. The dehydrogenation energies of **A** and **B** across the C-C bond are calculated to be 2 and 11 kcal/mol less endothermic, respectively, than the experimental value of 32.6 kcal/mol for the dehydrogenation of C₂H₆.^{48,66} We obtain values of 32.8^{34e} and 30.8 kcal/mol for the

equivalent reaction at the CCSD(T) and G3(MP2) levels, respectively. The second dehydrogenation step is most favorable across the second available B-N dative bond, and the resulting reaction energies are slightly less exothermic by 0.6 and 1.2 kcal/mol than the equivalent first dehydrogenation step, respectively. We also considered a third dehydrogenation step occurring across the C-C bond with the consequent energies for $(\text{H}_2\text{B}=\text{NH})\text{H}_2\text{C}-\text{CH}_2(\text{HN}=\text{BH}_2)$ and $(\text{H}_2\text{N}=\text{BH})\text{H}_2\text{C}-\text{CH}_2(\text{HB}=\text{NH}_2)$ predicted to be endothermic, indicating that this avenue for dehydrogenation is not likely unless one can couple the exothermicity of the loss of H_2 across the B-N bonds with that of the endothermicity of elimination across the C-C bond.

5.6 Conclusions

Ammonia borane and methylamine borane melt at 35-42 °C over a weight range of 20 to 50% of the former in the latter. The melt temperature of these mixtures are lower than that of the pure materials by up to 25 °C for methylamine borane and by up to 80-85 °C for ammonia borane. We have predicted the heats of formation of *N*-methylammonia borane and ammonia *B*-methylborane and their various dehydrogenated derivatives, as well as various molecules involved in the bond breaking processes, at the CCSD(T)/CBS level plus additional corrections. We considered the possibility of several dehydrogenation pathways, and find that dehydrogenation across the B-N bond is more favorable as opposed to dehydrogenation across the B-C and C-N bonds. Dehydrogenation of *N*-methylammonia borane is exothermic by -3.5 kcal/mol at the CCSD(T) level at 298 K, whereas for ammonia *B*-methylborane, it was slightly more exothermic, -9.4 kcal/mol at the CCSD(T) level at 298 K. The effects of methyl substitution on the dehydrogenation of BH_3NH_3 were studied. Dehydrogenation of *N*-dimethylammonia borane is exothermic by -1.8 kcal/mol at the CCSD(T) level at 298 K, showing a decreased exothermicity of 3.3 kcal/mol compared to that of BH_3NH_3 . Methyl substitution at N improves

the thermodynamics as the dehydrogenation reactions are closer to thermoneutral. Dehydrogenation of ammonia *B*-dimethylborane is exothermic by -11.7 kcal/mol at the CCSD(T) level at 298 K, showing an increase in the exothermicity compared to that of ammonia borane. Methyl substitution at B leads to unfavorable thermodynamics as the dehydrogenation reactions move further away from thermoneutral. Methyl substitution at N in the cycloborazane rings increases the endothermicity of the dehydrogenation reactions and for *c*-B₄N₄H₁₂(CH₃)₄, the thermodynamics for dehydrogenation reaction become favorable as it is near thermoneutral. Dehydrogenation of *c*-B₂N₂H₆(CH₃)₂, *c*-B₃N₃H₉(CH₃)₃, and *c*-B₄N₄H₁₂(CH₃)₄ producing two, three, and four molecules of H₂ are 26.2, -13.0, and 3.4 kcal/mol at the G3(MP2) level at 298 K, respectively.

Acknowledgments Funding provided in part by the Department of Energy, Office of Energy Efficiency and Renewable Energy under the Hydrogen Storage Grand Challenge, Solicitation No. DE-PS36-03GO93013. This work was done as part of the Chemical Hydrogen Storage Center. DAD is indebted to the Robert Ramsay Endowment of the University of Alabama. Part of this work was performed at the W. R. Wiley Environmental Molecular Sciences Laboratory, a national scientific user facility sponsored by DOE's Office of Biological and Environmental Research and located at Pacific Northwest National Laboratory, operated for the DOE by Battelle.

Appendix. Melt temperatures as a function of weight percent; calculated geometry parameters at the MP2/VTZ level; calculated MP2/VTZ frequencies, total CCSD(T) energies as a function of basis set; isodesmic reaction energies at the G3(MP2) level; *T*₁ diagnostics. HOMOs of (CH₃)HN=BH₂, (CH₃)HB=NH₂, (CH₃)₂N=BH₂, and (CH₃)₂B=NH₂ at the B3LYP/DZVP2 level;

and HOMOs of $(\text{BH}_3)\text{HN}=\text{CH}_2$ and $(\text{NH}_3)\text{HB}=\text{CH}_2$ at the B3LYP/DZVP2 level. This material is available free of charge via the internet at <http://pubs.acs.org>.

Table 5.1. Components for CCSD(T) Atomization Energies (kcal/mol).^a

Molecule	CBS ^b	ΔE_{ZPE} ^c	ΔE_{CV} ^d	ΔE_{SR} ^e	ΔE_{SO} ^f	$\Sigma D_0(0\text{ K})$ ^g
HBCH ₂ ($C_{2v} - ^1A_1$)	425.62	20.68	2.12	-0.23	-0.12	406.74
HBNH ₂ ($C_s - ^2A'$)	387.92	22.83	1.66	-0.38	-0.03	366.34
HNBH ₂ ($C_1 - ^2A$)	377.03	19.24	1.79	-0.31	-0.03	359.24
HNCH ₂ ($C_s - ^1A'$)	437.76	24.86	1.39	-0.38	-0.09	413.81
HBCH ₃ ($C_1 - ^2A$)	476.35	27.78	1.97	-0.26	-0.12	450.16
HBNH ₃ ($C_1 - ^1A$)	399.87	29.14	1.12	-0.33	-0.03	371.48
HBNH ₃ ($C_s - ^3A''$)	392.86	30.19	1.56	-0.40	-0.03	363.80
HNBH ₃ ($C_1 - ^3A$)	392.74	23.55	1.84	-0.26	-0.03	370.73
HNCH ₃ ($C_s - ^2A''$)	472.95	30.74	1.37	-0.39	-0.09	443.10
H ₂ BCH ₃ ($C_s - ^1A'$)	586.05	34.87	2.15	-0.26	-0.12	552.95
(CH ₃)HB=NH ₂ ($C_s - ^1A'$)	803.56	47.93	2.99	-0.59	-0.12	757.91
(NH ₃)HB=CH ₂ ($C_s - ^1A'$)	755.99	48.07	2.94	-0.57	-0.12	710.16
(CH ₃)HN=BH ₂ ($C_s - ^1A'$)	785.93	48.01	2.95	-0.60	-0.12	740.16
(BH ₃)HN=CH ₂ ($C_s - ^1A'$)	752.61	46.16	2.89	-0.53	-0.12	708.69
(CH ₃)H ₂ B-NH ₃ ($C_s - ^1A'$)	909.48	61.73	3.02	-0.59	-0.12	850.06
(CH ₃)H ₂ N-BH ₃ ($C_s - ^1A'$)	897.94	61.84	2.98	-0.61	-0.12	838.24

^a The atomic asymptotes were calculated with the R/UCCSD(T) method. ^b Extrapolated by using eq. (1) with the aVDZ, aVTZ, and aVQZ basis sets. ^c The zero point energies were taken as 0.5 the sum of the MP2 scaled frequencies. ^d Core-valence corrections were obtained with the cc-pwCVTZ (B, C, N) basis sets at the optimized CCSD(T)/aVTZ or MP2/VTZ geometries. ^e The scalar relativistic correction is based on a CISD(FC)/VTZ MVD calculation and is expressed relative to the CISD result without the MVD correction, i.e. including the existing relativistic effects resulting from the use of a relativistic effective core potential. ^f Correction due to the incorrect treatment of the atomic asymptotes as an average of spin multiplets. Values are based on C. Moore's Tables, reference 40. ^g The theoretical value of $\Delta D_0(0\text{ K})$ was computed with the CBS estimates.

Table 5.2. Calculated Heats of Formation in kcal/mol. Experimental values at 298 K in Parentheses.

Molecule	CCSD(T) Unless Noted		G3(MP2)	
	Theory (0 K)	Theory (298 K)	Theory (0 K)	Theory (298 K)
HBCH ₂ ($C_{2v} - ^1A_1$)	53.2	52.4	54.1	53.2
HBNH ₂ ($C_s - ^2A'$)	36.2	34.4	37.8	36.1
HNBH ₂ ($C_1 - ^2A$)	43.3	42.1	44.8	43.5
HNCH ₂ ($C_s - ^1A'$)	23.6	21.7	23.2	21.3
HBCH ₃ ($C_1 - ^2A$)	61.4	59.8	62.3	60.9
HBNH ₃ ($C_1 - ^1A$)	82.7	80.4	83.1	81.2
HBNH ₃ ($C_s - ^3A''$)	90.3	87.9	92.1	89.7
HNBH ₃ ($C_1 - ^3A$)	83.4	81.3	85.0	82.7
HNCH ₃ ($C_s - ^2A''$)	45.9	43.3	45.9	43.3
H ₂ BCH ₃ ($C_s - ^1A'$)	10.3	7.7	11.6	9.1
H ₂ NCH ₃ ($C_s - ^1A'$)	-1.4 ^a	-4.7 ^a (-5.6 ± 0.2 ^b)	-0.5	-4.1
H ₂ B=NH ₂ ($C_{2v} - ^1A_1$)	-17.0 ^c	-19.7 ^c	-15.1	-17.8
(CH ₃)HB=NH ₂ ($C_s - ^1A'$)	-30.5	-34.7	-29.2	-33.3
(NH ₃)HB=CH ₂ ($C_s - ^1A'$)	17.2	13.0	18.1	14.0
(CH ₃)HN=BH ₂ ($C_s - ^1A'$)	-12.8	-17.1	-11.4	-15.7
(BH ₃)HN=CH ₂ ($C_s - ^1A'$)	18.7	14.4	20.1	15.9
H ₃ B-NH ₃ ($C_{3v} - ^1A_1$)	-10.2 ^c	-14.6 ^c	-7.4	-11.7
(CH ₃)H ₂ B-NH ₃ ($C_s - ^1A'$)	-19.4	-25.3	-17.8	-23.5

$(\text{CH}_3)_2\text{N-BH}_3$ ($C_s - ^1A'$)	-7.6	-13.7	-5.7	-11.6
$\text{B}(\text{CH}_3)_2$ ($C_2 - ^2A$)	45.8 ^d	42.6 ^d	46.4	43.5
$\text{HB}(\text{CH}_3)_2$ ($C_2 - ^1A$)	-5.2 ^d	-9.2 ^d	-4.3	-8.1
$\text{N}(\text{CH}_3)_2$ ($C_{2v} - ^1A_1$)	43.6 ^d	39.9 ^d	43.1	39.1
$\text{HN}(\text{CH}_3)_2$ ($C_s - ^1A'$)	1.8 ^d	-2.8 ^c (-4.5 ± 0.4 ^b)	2.3	-2.9
$(\text{CH}_3)_2\text{B=NH}_2$ ($C_{2v} - ^1A_1$)	-44.4 ^d	-49.8 ^d	-43.4	-48.6
$(\text{CH}_3)_2\text{HB-NH}_3$ ($C_s - ^1A'$)	-30.9 ^d	-38.1 ^d	-29.5	-36.5
$(\text{CH}_3)_2\text{N=BH}_2$ ($C_{2v} - ^1A_1$)	-11.3 ^d	-16.9 ^d	-10.4	-16.2
$(\text{CH}_3)_2\text{HN-BH}_3$ ($C_s - ^1A'$)	-7.8 ^d	-15.1 ^d	-6.3	-13.8
$\text{B}(\text{CH}_3)_3$ ($C_1 - ^1A$)	-20.6 ^d	-25.7 ^d 9 (-29.7, ^e -29.2 ± 3.0 ^f)	-20.0	-24.8
$\text{N}(\text{CH}_3)_3$ ($C_{3v} - ^1A_1$)	1.5 ^d	-4.4 ^d (-5.6 ± 0.3 ^b)	1.5	-5.2
$(\text{CH}_3)_3\text{B-NH}_3$ ($C_{3v} - ^1A_1$)	-43.0 ^d	-51.5 ^d (-54.1 ^e)	-42.0	-50.2
$(\text{CH}_3)_3\text{N-BH}_3$ ($C_{3v} - ^1A_1$)	-9.2 ^d	-17.8 ^d (-20.3, ^e -20.4 ± 0.6 ^f)	-8.0	-17.2

^a Reference 35c. ^b Reference 61. ^c Reference 10. Corrected for the new heat of formation of the B atom. ^d Calculated based on isodesmic reactions at the G3(MP2) level. ^e Reference 62. ^f Reference 64.

Table 5.3. Dehydrogenation Reactions (kcal/mol).

Reaction	CCSD(T)		G3(MP2)	
	(0 K)	(298 K)	(0 K)	(298 K)
$\text{H}_3\text{B-NH}_3 \rightarrow \text{H}_2\text{B=NH}_2 + \text{H}_2$	-6.8 ^a	-5.1 ^a	-8.9	-7.3
$(\text{CH}_3)_2\text{N-BH}_3 \rightarrow (\text{CH}_3)\text{HN=BH}_2 + \text{H}_2$	-5.2	-3.5	-6.9	-5.2
$(\text{CH}_3)_2\text{N-BH}_3 \rightarrow (\text{BH}_3)\text{HN=CH}_2 + \text{H}_2$	26.3	28.0	24.5	26.3
$(\text{CH}_3)_2\text{B-NH}_3 \rightarrow (\text{CH}_3)\text{HB=NH}_2 + \text{H}_2$	-11.1	-9.4	-12.6	-11.0
$(\text{CH}_3)_2\text{B-NH}_3 \rightarrow (\text{NH}_3)\text{HB=CH}_2 + \text{H}_2$	36.6	38.3	34.7	36.3
$(\text{CH}_3)_2\text{HN-BH}_3 \rightarrow (\text{CH}_3)_2\text{N=BH}_2 + \text{H}_2$	-3.5	-1.8	-5.3	-3.6
$(\text{CH}_3)_2\text{HB-NH}_3 \rightarrow (\text{CH}_3)_2\text{B=NH}_2 + \text{H}_2$	-13.5	-11.7	-15.1	-13.3

^a Reference 10.

Table 5.4. Calculated Imaginary Vibrational Frequencies (cm^{-1}) at the MP2/VTZ Level.

Molecule	Symmetry	Calc.	Type
$\text{H}_2\text{B}=\text{NH}_2$ rot ($C_s - {}^1\text{A}'$) ^a	a''	$778.9i$	NH ₂ Rotation
$\text{H}_2\text{B}=\text{NH}_2$ rot-planar ($C_{2v} - {}^1\text{A}_1$) ^a	a_2	$1186.2i$	NH ₂ Rotation
	b_2	$631.5i$	N Inversion
$(\text{CH}_3)\text{HN}=\text{BH}_2$ rot ($C_s - {}^1\text{A}'$)	a''	$1028.4i$	BH ₂ Rotation + NH Wag
	a''	$374.3i$	NH Wag + BH ₂ Rotation
	a''	$71.9i$	CH ₃ Rotation
$(\text{BH}_3)\text{HN}=\text{CH}_2$ rot ($C_s - {}^3\text{A}''$)	a''	$192.0i$	BH ₃ Rotation
$(\text{CH}_3)\text{HB}=\text{NH}_2$ rot ($C_s - {}^1\text{A}'$)	a''	$601.5i$	NH ₂ Rotation
	a''	$99.6i$	CH ₃ Rotation
$(\text{NH}_3)\text{HB}=\text{CH}_2$ rot ($C_s - {}^3\text{A}''$)	a''	$555.5i$	BH Wag
	a''	$81.1i$	NH ₃ Rotation
$(\text{CH}_3)_2\text{N}=\text{BH}_2$ rot ($C_s - {}^1\text{A}'$)	a''	$497.2i$	BH ₂ Rotation
$(\text{CH}_3)_2\text{N}=\text{BH}_2$ rot ($C_{2v} - {}^1\text{A}_1$)	a_2	$858.7i$	BH ₂ Rotation
	b_1	$254.0i$	N Inversion
$(\text{CH}_3)_2\text{B}=\text{NH}_2$ rot ($C_s - {}^1\text{A}'$)	a''	$545.6i$	NH ₂ Rotation
	a''	$155.0i$	asymm. CH ₃ Rotation
	a''	$115.4i$	symm. CH ₃ Rotation
$(\text{CH}_3)_2\text{B}=\text{NH}_2$ rot ($C_{2v} - {}^1\text{A}_1$)	a_2	$852.6i$	NH ₂ Rotation
	b_2	$623.1i$	N Inversion

a_2	$170.8i$	asymm. CH ₃ Rotation
b_1	$145.3i$	symm. CH ₃ Rotation

^a Reference 22.

Table 5.5. Adiabatic Rotation Barriers (π -Bond Energies) at 0 K at the MP2/VTZ level (kcal/mol).

Molecule	Rotation (G. S. \rightarrow C_s)
H ₂ B=NH ₂ ^a	29.7 (29.9)
(CH ₃)HN=BH ₂	36.8
(BH ₃)HN=CH ₂	71.3
(CH ₃)HB=NH ₂	26.3
(NH ₃)HB=CH ₂	63.0
(CH ₃) ₂ N=BH ₂	32.8
(CH ₃) ₂ B=NH ₂	25.3

^a Value in parenthesis was calculated at the CCSD(T)/CBS level. Reference 22.

Table 5.6. Adiabatic ($\sigma + \pi$) Total Dissociation Energies and Adiabatic σ -Bond Energies 0 K at the CCSD(T) level (kcal/mol).^a

Reaction	Bond Type	Total Dissociation Energy	σ -Bond Energy
$\text{H}_2\text{B}=\text{NH}_2 (^1\text{A}_1) \rightarrow \text{BH}_2 (^2\text{A}_1) + \text{NH}_2 (^2\text{B}_1)$	B=N	139.7 ^b	109.8 ^b
$(\text{CH}_3)\text{HN}=\text{BH}_2 (^1\text{A}') \rightarrow \text{BH}_2 (^2\text{A}_1) + \text{H}\cdot\text{N}\cdot\text{CH}_3 (^2\text{A}'')$	B=N	136.1	99.3
$(\text{BH}_3)\text{HN}=\text{CH}_2 (^1\text{A}') \rightarrow \text{:CH}_2 (^3\text{B}_1) + \text{HN}\cdot\text{BH}_3 (^3\text{A})$	N=C	158.2	86.9
$(\text{CH}_3)\text{HB}=\text{NH}_2 (^1\text{A}') \rightarrow \text{NH}_2 (^2\text{B}_1) + \text{H}\cdot\text{B}\cdot\text{CH}_3 (^2\text{A})$	B=N	137.2	110.9
$(\text{NH}_3)\text{HB}=\text{CH}_2 (^1\text{A}') \rightarrow \text{:CH}_2 (^3\text{B}_1) + \text{HB}\cdot\text{NH}_3 (^1\text{A})$	B=C	158.9	95.9
$(\text{CH}_3)_2\text{N}=\text{BH}_2 (^1\text{A}_1) \rightarrow \text{BH}_2 (^2\text{A}_1) + \text{N}(\text{CH}_3)_2 (^2\text{A}_1)$	B=N	132.3	99.5
$(\text{CH}_3)_2\text{B}=\text{NH}_2 (^1\text{A}_1) \rightarrow \text{NH}_2 (^2\text{B}_1) + \text{B}(\text{CH}_3)_2 (^2\text{A})$	B=N	135.4	110.1

^a $\Delta\text{H}_f(\text{BH}_2) = 78.5$ kcal/mol,²² $\Delta\text{H}_f(\text{NH}_2) = 45.3$ kcal/mol,^{34m} and $\Delta\text{H}_f(\text{CH}_2) = 93.5$ kcal/mol.^{34e} ^b Reference 22.

Table 5.7. Adiabatic σ -Bond Energies (B. E.) in kcal/mol.^a

Reaction	Bond Type	B. E. Calc. (0 K)	B. E. Calc. (298 K)	B.E. Expt. (298 K)	B. E. Other Calc. (0 or 298 K) ^b
$\text{H}_3\text{B-NH}_3 (^1\text{A}_1) \rightarrow \text{BH}_3 (^1\text{A}_1') + \text{:NH}_3 (^1\text{A}_1)$	B-N dative	25.9 ^c	27.7	$31.1 \pm 1.0^{\text{d}}$	26.0 G2(MP2) ^e 28.3 MP2/TZ2P ^f (28.5) MP4 ^g 27.9 MP2 ^h 26.5 MP2 ⁱ 29.6 MP2 ^m
$(\text{CH}_3)\text{HN=BH}_2 (^1\text{A}') \rightarrow \text{CH}_3 (^2\text{A}_2'') + \text{H}\cdot\text{N=BH}_2 (^2\text{A})$	C-N covalent	91.7	94.2		
$(\text{BH}_3)\text{HN=CH}_2 (^1\text{A}') \rightarrow \text{BH}_3 (^1\text{A}_1') + \text{H}\cdot\text{N=CH}_2 (^1\text{A}')$	B-N dative	30.2	31.7		
$(\text{CH}_3)\text{HB=NH}_2 (^1\text{A}') \rightarrow \text{CH}_3 (^2\text{A}_2'') + \text{H}\cdot\text{B=NH}_2 (^2\text{A}')$	B-C covalent	102.4	104.1		
$(\text{NH}_3)\text{HB=CH}_2 (^1\text{A}') \rightarrow \text{:NH}_3 (^1\text{A}_1) + \text{HB=CH}_2 (^1\text{A}_1)$	B-N dative	26.4	28.1		
$(\text{CH}_3)\text{H}_2\text{N-BH}_3 (^1\text{A}') \rightarrow \text{BH}_3 (^1\text{A}_1') + \text{NH}_2(\text{CH}_3) (^1\text{A}')$	B-N dative	31.5	33.4	$35.0 \pm 0.8^{\text{d}}$	31.9 G2(MP2) ^e (31.3) HF/6-31G* ^g 33.1 MP2 ^h 32.3 MP2 ⁱ 34.7 MP2 ^m
$(\text{CH}_3)\text{H}_2\text{B-NH}_3 (^1\text{A}') \rightarrow \text{BH}_2(\text{CH}_3) (^1\text{A}') + \text{:NH}_3 (^1\text{A}_1)$	B-N dative	20.1	21.7		(23.5) HF/6-31G* ^g

$(\text{CH}_3)_2\text{HN-BH}_3 (^1\text{A}') \rightarrow \text{BH}_3 (^1\text{A}_1') + \text{HN}(\text{CH}_3)_2 (^1\text{A}')$	B-N dative	34.9	36.7	$36.4 \pm 1.0^{\text{d}}$	35.2 G2(MP2) ^e (31.8) HF/6-31G** ^g 35.9 MP2 ^h 35.6 MP2 ⁱ 37.3 MP2 ^m
$(\text{CH}_3)_2\text{HB-NH}_3 (^1\text{A}') \rightarrow \text{HB}(\text{CH}_3)_2 (^1\text{A}) + \text{:NH}_3 (^1\text{A}_1)$	B-N dative	16.0	17.6		(19.0) HF/6-31G** ^g
$(\text{CH}_3)_3\text{N-BH}_3 (^1\text{A}_1) \rightarrow \text{BH}_3 (^1\text{A}_1') + \text{N}(\text{CH}_3)_3 (^1\text{A}_1)$	B-N dative	36.0	37.8	$34.8 \pm 0.5^{\text{d}}$	36.2 G2(MP2) ^e 39.2 ^j 38.7 MP2/TZ2P ^g 31.5 ^k (30.6) HF/6-31G** ^g 36.6 MP2 ^h 36.8 MP2 ⁱ
$(\text{CH}_3)_3\text{B-NH}_3 (^1\text{A}_1) \rightarrow \text{B}(\text{CH}_3)_3 (^1\text{A}_1') + \text{:NH}_3 (^1\text{A}_1)$	B-N dative	12.8	14.5	$13.8 \pm 0.3^{\text{l}}$	(14.9) HF/6-31G** ^g 15.4 MP2 ⁱ

^a $\Delta\text{H}_f(\text{BH}_3) = 25.3 \pm 0.7 \text{ kcal/mol}^{10}$ recalculated with the new heat of formation of B of $135.1 \pm 0.2 \text{ kcal/mol}$,⁴⁹ $\Delta\text{H}_f(\text{CH}_3) = 35.7 \text{ kcal/mol}$,⁷⁷ and $\Delta\text{H}_f(\text{NH}_3) = -9.6 \pm 0.5 \text{ kcal/mol}$,¹⁰ all at 0 K. 298 K values are $\Delta\text{H}_f(\text{BH}_3) = 24.4$, $\Delta\text{H}_f(\text{NH}_3) = -11.3$, and $\Delta\text{H}_f(\text{CH}_3) = 35.0 \text{ kcal/mol}$. ^b Values in parentheses at 298 K. ^c Reference 10. ^d Reference 67. ^e References 30 and 31. ^f Reference 70. ^g Reference 71. ^h Reference 29. MP2(full)/6-311++G**. ⁱ Reference 32. MP2/6-311++G**. ^j Re-evaluated from literature. See text. ^k Reference 68. ^l References 67 and 69. ^m Reference 33. MP2/6-311G** at 0 K with ZPE included.

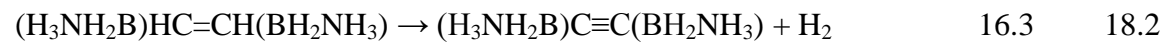
Table 5.8. Calculated G3(MP2) Heats of Formation (kcal/mol).

Molecule	Theory (0 K)	Theory (298 K)
<i>c</i> -B ₂ N ₂ H ₄ (<i>D</i> _{2h})	-23.6	-27.1
<i>c</i> -B ₂ N ₂ H ₈ (<i>D</i> _{2h}) ^a	-43.9	-50.9
<i>c</i> -B ₃ N ₃ H ₆ (<i>D</i> _{3h}) ^a	-106.5	-112.4
<i>c</i> -B ₃ N ₃ H ₁₂ twist boat (<i>C</i> ₃) ^a	-82.6	-93.5
<i>c</i> -B ₄ N ₄ H ₈ (<i>D</i> _{4h})	-123.3	-131.0
<i>c</i> -B ₄ N ₄ H ₁₆ (<i>C</i> _{4v})	-95.2	-110.0
<i>c</i> -B ₂ N ₂ H ₂ (CH ₃) ₂ <i>trans</i> (<i>C</i> _i)	-16.1	-21.6
<i>c</i> -B ₂ N ₂ H ₆ (CH ₃) ₂ <i>trans</i> (<i>C</i> _{2h})	-40.2	-50.0
<i>c</i> -B ₃ N ₃ H ₃ (CH ₃) ₃ (<i>C</i> _{3h})	-94.2	-103.5
<i>c</i> -B ₃ N ₃ H ₉ (CH ₃) ₃ (<i>C</i> _{3v})	-78.4	-93.6
<i>c</i> -B ₄ N ₄ H ₄ (CH ₃) ₄ (<i>S</i> ₄)	-99.4	-111.8
<i>c</i> -B ₄ N ₄ H ₁₂ (CH ₃) ₄ (<i>C</i> ₁)	-99.2	-119.6
(H ₃ BH ₂ N)H ₂ C-CH ₂ (NH ₂ BH ₃) (<i>C</i> _s)	0.3	-10.5
(H ₂ B=NH)H ₂ C-CH ₂ (NH ₂ BH ₃) (<i>C</i> ₁)	-7.6	-16.8
(H ₃ B)HN=CH-CH ₂ (NH ₂ BH ₃) (<i>C</i> ₁)	24.3	17.4
(H ₃ BH ₂ N)HC=CH(NH ₂ BH ₃) (<i>C</i> _i)	30.4	21.5
(H ₂ B=NH)H ₂ C-CH ₂ (HN=BH ₂) (<i>C</i> _i)	-14.8	-22.4
(H ₃ B)HN=CHHC=NH(BH ₃) (<i>C</i> _{2h})	47.2	40.0
(H ₃ BH ₂ N)C≡C(NH ₂ BH ₃) (<i>C</i> ₂)	88.2	81.4
(H ₂ B=NH)HC=CH(NH ₂ BH ₃) (<i>C</i> ₁)	20.6	13.2
(H ₂ B=NH)HC=CH(HN=BH ₂) (<i>C</i> _{2h})	7.3	1.4
(H ₃ NH ₂ B)H ₂ C-CH ₂ (BH ₂ NH ₃) (<i>C</i> _s)	-19.0	-29.3
(H ₂ N=BH)H ₂ C-CH ₂ (BH ₂ NH ₃) (<i>C</i> ₁)	-30.8	-39.6
(H ₃ N)HB=CH-CH ₂ (BH ₂ NH ₃) (<i>C</i> ₁)	16.6	7.9
(H ₃ NH ₂ B)HC=CH(BH ₂ NH ₃) (<i>C</i> _i)	2.0	-6.6
(H ₂ N=BH)H ₂ C-CH ₂ (HB=NH ₂) (<i>C</i> _i)	-41.4	-48.6
(H ₃ N)HB=CH-HC=BH(NH ₃) (<i>C</i> _{2h})	47.8	40.7
(H ₃ NH ₂ B)C≡C(BH ₂ NH ₃) (<i>C</i> ₂)	19.5	12.7
(H ₂ N=BH)HC=CH(BH ₂ NH ₃) (<i>C</i> ₁)	-8.5	-15.7
(H ₂ N=BH)HC=CH(HB=NH ₂) (<i>C</i> _{2h})	-21.0	-26.6

^a Taken from Reference 11 and recalculated with new heat of formation of B of 135.1 ± 0.2 kcal/mol.⁴⁹

Table 5.9. Dehydrogenation Reactions at the G3(MP2) level (kcal/mol).

1st Dehydrogenation Step	(0 K)	(298 K)
$c\text{-B}_2\text{N}_2\text{H}_8 \rightarrow c\text{-B}_2\text{N}_2\text{H}_4 + 2\text{H}_2$	17.9	21.6
$c\text{-B}_3\text{N}_3\text{H}_{12}$ twist boat $\rightarrow c\text{-B}_3\text{N}_3\text{H}_6 + 3\text{H}_2$	-27.5 ^a	-22.2 ^a
$c\text{-B}_4\text{N}_4\text{H}_{16} \rightarrow c\text{-B}_4\text{N}_4\text{H}_8 + 4\text{H}_2$	-33.0	-25.4
$c\text{-B}_2\text{N}_2\text{H}_6(\text{CH}_3)_2 \rightarrow c\text{-B}_2\text{N}_2\text{H}_2(\text{CH}_3)_2 + 2\text{H}_2$	21.6	26.2
$c\text{-B}_3\text{N}_3\text{H}_9(\text{CH}_3)_3 \rightarrow c\text{-B}_3\text{N}_3\text{H}_3(\text{CH}_3)_3 + 3\text{H}_2$	-19.4	-13.0
$c\text{-B}_4\text{N}_4\text{H}_{12}(\text{CH}_3)_4 \rightarrow c\text{-B}_4\text{N}_4\text{H}_4(\text{CH}_3)_4 + 4\text{H}_2$	-7.3	3.4
$(\text{H}_3\text{BH}_2\text{N})\text{H}_2\text{C}-\text{CH}_2(\text{NH}_2\text{BH}_3) \rightarrow (\text{H}_2\text{B}=\text{NH})\text{H}_2\text{C}-\text{CH}_2(\text{NH}_2\text{BH}_3) + \text{H}_2$	-9.0	-7.4
$(\text{H}_3\text{BH}_2\text{N})\text{H}_2\text{C}-\text{CH}_2(\text{NH}_2\text{BH}_3) \rightarrow (\text{H}_3\text{B})\text{HN}=\text{CH}-\text{CH}_2(\text{NH}_2\text{BH}_3) + \text{H}_2$	22.9	26.7
$(\text{H}_3\text{BH}_2\text{N})\text{H}_2\text{C}-\text{CH}_2(\text{NH}_2\text{BH}_3) \rightarrow (\text{H}_3\text{BH}_2\text{N})\text{HC}=\text{CH}(\text{NH}_2\text{BH}_3) + \text{H}_2$	29.0	30.8
$(\text{H}_3\text{NH}_2\text{B})\text{H}_2\text{C}-\text{CH}_2(\text{BH}_2\text{NH}_3) \rightarrow (\text{H}_2\text{N}=\text{BH})\text{H}_2\text{C}-\text{CH}_2(\text{BH}_2\text{NH}_3) + \text{H}_2$	-13.0	-11.4
$(\text{H}_3\text{NH}_2\text{B})\text{H}_2\text{C}-\text{CH}_2(\text{BH}_2\text{NH}_3) \rightarrow (\text{H}_3\text{N})\text{HB}=\text{CHC}-\text{H}_2(\text{BH}_2\text{NH}_3) + \text{H}_2$	34.4	36.1
$(\text{H}_3\text{NH}_2\text{B})\text{H}_2\text{C}-\text{CH}_2(\text{BH}_2\text{NH}_3) \rightarrow (\text{H}_3\text{NH}_2\text{B})\text{HC}=\text{CH}(\text{BH}_2\text{NH}_3) + \text{H}_2$	19.8	21.6
2nd Dehydrogenation Step		
$(\text{H}_2\text{B}=\text{NH})\text{H}_2\text{C}-\text{CH}_2(\text{NH}_2\text{BH}_3) \rightarrow (\text{H}_2\text{B}=\text{NH})\text{H}_2\text{CCH}_2(\text{HN}=\text{BH}_2) + \text{H}_2$	-8.4	-6.8
$(\text{H}_3\text{B})\text{HN}=\text{CH}-\text{CH}_2(\text{NH}_2\text{BH}_3) \rightarrow (\text{H}_3\text{B})\text{HN}=\text{CHHC}=\text{NH}(\text{BH}_3) + \text{H}_2$	21.7	21.5
$(\text{H}_3\text{BH}_2\text{N})\text{HC}=\text{CH}(\text{NH}_2\text{BH}_3) \rightarrow (\text{H}_3\text{BH}_2\text{N})\text{C}\equiv\text{C}(\text{NH}_2\text{BH}_3) + \text{H}_2$	56.6	58.8
$(\text{H}_2\text{B}=\text{NH})\text{H}_2\text{C}-\text{CH}_2(\text{NH}_2\text{BH}_3) \rightarrow (\text{H}_2\text{B}=\text{NH})\text{HC}=\text{CH}(\text{NH}_2\text{BH}_3) + \text{H}_2$	27.0	28.9
$(\text{H}_2\text{N}=\text{BH})\text{H}_2\text{C}-\text{CH}_2(\text{BH}_2\text{NH}_3) \rightarrow (\text{H}_2\text{N}=\text{BH})\text{H}_2\text{C}-\text{CH}_2(\text{HB}=\text{NH}_2) + \text{H}_2$	-11.8	-10.2
$(\text{H}_3\text{N})\text{HB}=\text{CH}-\text{CH}_2(\text{BH}_2\text{NH}_3) \rightarrow (\text{H}_3\text{N})\text{HB}=\text{CH}-\text{HC}=\text{BH}(\text{NH}_3) + \text{H}_2$	30.0	31.6



3rd Dehydrogenation Step



^a Taken from Reference 11 and recalculated with new heat of formation of B of 135.1 ± 0.2 kcal/mol.⁴⁹

Figure Captions

Figure 5.1. Melting temperature ranges in °C of ammonia borane/methylamine borane mixtures as a function of the weight percent of ammonia borane.

Figure 5.2. Optimized molecular structures for $\text{H}_2\text{B}=\text{NH}_2$, $(\text{CH}_3)\text{HB}=\text{NH}_2$, $(\text{CH}_3)\text{HN}=\text{BH}_2$, $(\text{NH}_3)\text{HB}=\text{CH}_2$, $(\text{BH}_3)\text{HN}=\text{CH}_2$, $(\text{CH}_3)_2\text{B}=\text{NH}_2$, $(\text{CH}_3)_2\text{N}=\text{BH}_2$, $\text{H}_3\text{B}-\text{NH}_3$, $(\text{CH}_3)\text{H}_2\text{B}-\text{NH}_3$, $(\text{CH}_3)\text{H}_2\text{N}-\text{BH}_3$, $(\text{CH}_3)_2\text{HB}-\text{NH}_3$, $(\text{CH}_3)_2\text{HN}-\text{BH}_3$, $(\text{CH}_3)_3\text{B}-\text{NH}_3$, and $(\text{CH}_3)_3\text{N}-\text{BH}_3$.

Figure 5.1.

Melting Ranges of AB and MeAB Mixtures

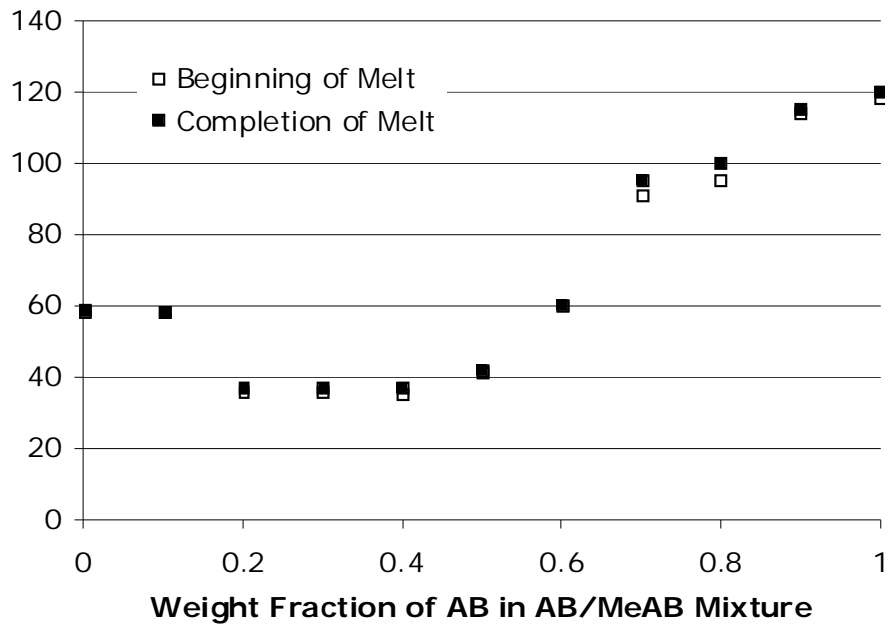
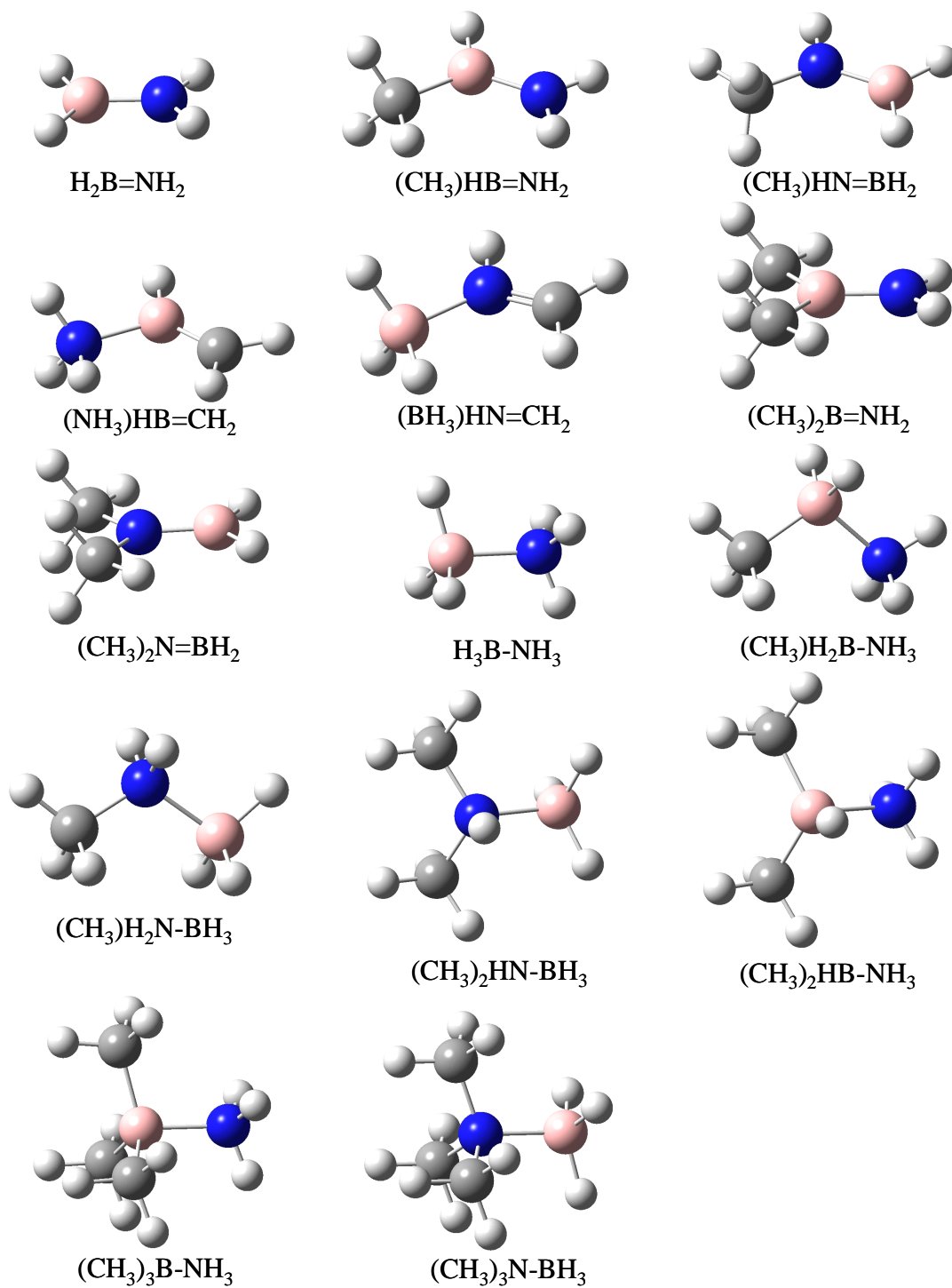


Figure 5.2.



5.7 References

-
- ¹ Stephens, F. H.; Pons, V.; Baker, R. T. *Dalton Trans.*, **2007**, 2613
- ² Karkamkar, A. J., Aardahl, C. L.; Autrey, T. *Material Matters*, **2007**, 2, 6.
- ³ (a) Wolf, G.; van Miltenburg, R. A.; Wolf, U. *Thermochim. Acta* **1998**, 317, 111. (b) Wolf, G.; Baumann, J.; Baitalow, F.; Hoffmann, F. P. *Thermochim. Acta* **2000**, 343, 19. (c) Baitalow, F.; Baumann, J.; Wolf, G.; Jaenicke-Rlobler, K.; Leitner, G. *Thermochim. Acta* **2002**, 391, 159.
- ⁴ Parvanov, V. M.; Schenter, G. K.; Hess, N. J.; Daemen, L. L.; Hartl, A.; Stowe, A. C.; Camaioni, D. M.; Autrey, T. *Dalton Trans.* **2008**, 4514.
- ⁵ Stowe, A. C.; Shaw, W. J.; Linehan, J. C.; Schmid, B.; Autrey, T., *Phys. Chem. Chem. Phys.*, **2007**, 9, 1831.
- ⁶ Shaw, W. J.; Linehan, J. C.; Szymczak, N. K.; Heldebrant, D. J.; Yonker, C.; Camaioni, D. M.; Baker, R. T.; Autrey, T., *Angew. Chem. Int. Ed.* **2008**, 47, 7493.
- ⁷ Stephens, F. H.; Baker, R. T.; Matus, M. H.; Grant, D. J.; Dixon, D. A. *Angew Chem. Int. Ed.*, **2007**, 46, 746.
- ⁸ Pons, V.; Baker, R. T.; Szymczak, N. K.; Heldebrant, D. J.; Linehan, J. C.; Matus, M. H.; Grant, D. J.; Dixon, D. A. *Chem Comm.*, **2008**, 6597.
- ⁹ Gutowska, A.; Li, L.; Shin, Y.; Wang, Ch.; Li, S.; Linehan, J.; Smith, R. S.; Kay, B.; Schmid, B.; Shaw, W.; Gutowski, M.; Autrey, T. *Angew. Chem. Int. Ed.* **2005**, 44, 2.
- ¹⁰ Gutowski, M.; Dixon, D. A. *J. Chem. Phys. A* **2005**, 109, 5129.
- ¹¹ Matus, M. H.; Anderson, K. A.; Camaioni, D. M.; Autrey, S. T.; Dixon, D. A. *J. Phys. Chem. A* **2007**, 111, 4411.
- ¹² Klooster, W. T.; Koetzle, T. F. Siegbahn, P. E. M.; Richardson, T. B.; Crabtree, R. H. *J. Am. Chem. Soc.* **1999**, 121, 6337.
- ¹³ Morrison, C. A.; Siddick, M. M. *Angew. Chem.-Int. Edit.* **2004**, 43, 4780.
- ¹⁴ Richardson, T. B.; de Gala, S.; Crabtree, R. H.; Siegbahn, P. E. M. *J. Am. Chem. Soc.* **1995**, 117, 12875.
- ¹⁵ (a) Geanangel, R. A.; Shore, S. G. *Prep. Inorg. React.* **1966**, 3, 123; (b) Framery, E.; Vaultier, M. *Heteroatom Chem.* **2000**, 11, 218; (c) See also Lane, C.F. *Ammonia-Borane*

and Related N-B-H Compounds and Materials: Safety Aspects, Properties and Applications, (2005).

http://www1.eere.energy.gov/hydrogenandfuelcells/pdfs/nbh_h2_storage_survey.pdf

¹⁶ Lane, C.; Baker, S.; "Applied Research on the Use of Amine-Borane Materials for Hydrogen Storage," DOE Hydrogen Program Annual Merit Review, Project ID # STP8, May 2007, Arlington, Va.

http://www.hydrogen.energy.gov/pdfs/review07/stp_8_lane.pdf; Lane, C. F., "Safety Analysis and Applied Research on the Use of Borane-Amines for Hydrogen Storage," DOE Hydrogen Program Annual Progress Report, Contract No. DE-FC36-05GO15060, November 2007, Washington, D.C.

http://www.hydrogen.energy.gov/pdfs/progress07/iv_b_5j_lane.pdf

¹⁷ Geanangel, R. A.; Shore, S. G. *Prep. Inorg. React.* **1966**, 3, 123.

¹⁸ Jaska, C. A.; Temple, K.; Lough, A. J.; Manners, I. *Chem. Commun.* **2001**, 962.

¹⁹ Alton, E. R.; Brown, R. D.; Carter, J. C.; Taylor, R. C. *J. Am. Chem. Soc.*, **1959**, 81, 3550

²⁰ Bartlett, R. J.; Musial, M. *Rev. Mod. Phys.* **2007**, 79, 291.

²¹ Sander, S. P.; Friedl, R. R.; Ravishankara, A. R.; Golden, D. M.; Kolb, C. E.; Kurylo, M. J.; Huie, R. E.; Orkin, V. L.; Molina, M. J.; Moortgat, G. K.; Finlayson-Pitts, B. J. *Chemical Kinetics and Photochemical Data for Use in Atmospheric Studies: Evaluation Number 14*; JPL Publication 02-25, National Aeronautics and Space Administration, Jet Propulsion Laboratory, California Institute of Technology: Pasadena, California 2003. http://jpldataeval.jpl.nasa.gov/pdf/JPL_02-25_rev02.pdf.

²² Grant, D. J.; Dixon, D. A. *J. Phys. Chem. A.* **2006**, 110, 12955.

²³ Ervin, K. M.; Gronert, S.; Barlow, S. E.; Gilles, M. K.; Harrison, A. G.; Bierbaum, V. M.; DePuy, C. H.; Lineberger, W. C.; Ellison, G. B. *J. Am. Chem. Soc.* **1990**, 112, 5750.

²⁴ Douglas, J. E.; Rabinovitch, B. S.; Looney, F. S. *J. Chem. Phys.* **1955**, 23, 315.

²⁵ Bauer, S. H. *J. Am. Chem. Soc.* **1937**, 59, 1823.

²⁶ Cassoux, P.; Kuczkowski, R. L.; Bryan, P. S.; Taylor, R. C. *Inorg. Chem.* **1975**, 14, 126.

²⁷ Iijima, K.; Adachi, N.; Shibata, S. *Bull. Chem. Soc. Jpn.* **1984**, 57, 3269.

²⁸ Bowden, M. E.; Brown, I. W. M.; Gainsford, G. J.; Wong, H., *Inorganica Chimica Acta* 2008, 361, (7), 2147.

-
- ²⁹ Aldridge, S.; Downs, A. J.; Tang, C. Y.; Parsons, S.; Clarke, M. C.; Johnstone, R. D.; Robertson, H. E.; Rankin, D. W.; Wann, D. A. *J. Am. Chem. Soc.* **2009**, *131*, 2231.
- ³⁰ Anane, H.; Abdellah, J.; Boutalib, A.; Nebot-Gil, I.; Tomás, F. *J. Molec. Structure; THEOCHEM.* **1998**, *455*, 51.
- ³¹ Anane, H.; Boutalib, A.; Nebot-Gil, I.; Tomás, F. *Chem. Phys. Lett.* **1998**, *287*, 575.
- ³² Gilbert, T. M. *J Phys Chem A* **2004**, *108*, 2550
- ³³ Sun, C.-H.; Yao, Z.-D.; Du, A.-J.; Smith, S.; Lu, G.-Q. *Phys. Chem. Chem. Phys.*, **2008**, *10*, 6104.
- ³⁴ (a) Feller, D.; Peterson, K. A. *J. Chem. Phys.* **1998**, *108*, 154; (b) Feller, D.; Peterson, K. A. *J. Chem. Phys.* **1999**, *110*, 8384; (d) Feller, D. *J. Chem. Phys.* **1999**, *111*, 4373; (f) Feller, D.; Sordo, J. A. *J. Chem. Phys.* **2000**, *113*, 485.
- ³⁵ (a) Feller, D.; Dixon, D. A. *J. Phys. Chem. A* **1999**, *103*, 6413; (b) Feller, D.; Dixon, D. A. *J. Phys. Chem. A* **2000**, *104*, 3048; (c) Feller, D.; Dixon, D. A. *J. Chem. Phys.* **2001**, *115*, 3484; (d) Dixon, D. A.; Feller, D. *J. Phys. Chem. A* **1998**, *102*, 8209; (e) Dixon, D. A.; Feller, D.; Sandrone, G. *J. Phys. Chem. A* **1999**, *103*, 4744; (f) Ruscic, B.; Wagner, A. F.; Harding, L. B.; Asher, R. L.; Feller, D.; Dixon, D. A.; Peterson, K. A.; Song, Y.; Qian, X.; Ng, C.-Y.; Liu, J.; Chen, W.; Schwenke, D. W. *J. Phys. Chem. A* **2002**, *106*, 2727; (g) Dixon, D. A.; Feller, D.; Peterson, K. A. *J. Chem. Phys.* **2001**, *115*, 2576; (h) Dixon, D. A.; Feller, D.; Peterson, K. A. *J. Phys. Chem. A* **1998**, *102*, 7053; (i) Ruscic, B.; Wagner, A. F.; Harding, L. B.; Asher, R. L.; Feller, D.; Dixon, D. A.; Peterson, K. A.; Song, Y.; Qian, X.; Ng, C.-Y.; Liu, J.; Chen, W.; Schwenke, D. W. *J. Phys. Chem.* **2002**, *106*, 2727; (j) Pollack, L.; Windus, T. L.; de Jong, W. A.; Dixon, D. A. *J. Phys. Chem. A* **2005**, *109*, 6934; (k) Feller, D.; Peterson, K. A.; Dixon, D. A. *J. Chem. Phys.*, **2008**, *129* 204015.
- ³⁶ (a) Dunning, T. H., Jr. *J. Chem. Phys.* **1989**, *90*, 1007; (b) Kendall, R. A.; Dunning, T. H., Jr.; Harrison, R. J. *J. Chem. Phys.* **1992**, *96*, 6796; (c) Woon, D.E.; Dunning, T. H., Jr., *J. Chem. Phys.* **1993**, *98*, 1358; (d) Dunning, T. H., Jr.; Peterson, K. A.; Wilson, A. K. *J. Chem. Phys.* **2001**, *114*, 9244; (e) Wilson, A. K.; Woon, D.E.; Peterson, K. A.; Dunning, T. H., Jr., *J. Chem. Phys.* **1999**, *110*, 7667.
- ³⁷ MOLPRO a package of *ab initio* programs designed by Werner, H.-J.; and Knowles, P. J. version 2002.6, Universität Stuttgart, Stuttgart, Germany, University of Birmingham, Birmingham, United Kingdom, Amos, R. D.; Bernhardsson, A.; Berning, A.; Celani, P.; Cooper, D. L.; Deegan, M. J. O.; Dobbyn, A. J.; Eckert, F.; Hampel, C.; Hetzer, G.; Knowles, P. J.; Korona, T.; Lindh, R.; Lloyd, A. W.; McNicholas, S. J.; Manby, F. R.; Meyer, W.; Mura, M. E.; Nicklass, A.; Palmieri, P.; Pitzer, R.; Rauhut, G.; Schütz, M.; Schumann, U.; Stoll, H.; Stone, A. J.; Tarroni, R.; Thorsteinsson, T.; Werner, H.-J.

-
- ³⁸ Peterson, K. A.; Woon, D. E.; Dunning, T. H., Jr. *J. Chem. Phys.* **1994**, *100*, 7410.
- ³⁹ Peterson, K. A.; Dunning, T. H., Jr., *J. Chem. Phys.* **2002**, *117*, 10548.
- ⁴⁰ Moore, C. E. "Atomic energy levels as derived from the analysis of optical spectra, Volume 1, H to V," U.S. National Bureau of Standards Circular 467, U.S. Department of Commerce, National Technical Information Service, COM-72-50282, Washington, D.C.; 1949.
- ⁴¹ Davidson, E. R.; Ishikawa, Y.; Malli, G. L. *Chem. Phys. Lett.* **1981**, *84*, 226.
- ⁴² (a) Douglas, M.; Kroll, N. M. *Ann. Phys.* **1974**, *82*, 89. (b) Hess, B. A. *Phys. Rev. A* **1985**, *32*, 756. (c) Hess, B. A. *Phys. Rev. A* **1986**, *33*, 3742.
- ⁴³ Pople, J. A.; Binkley, J. S.; Seeger, R. *Int. J. Quant. Chem., Quantum Chem. Symp.* **1976**, *10*, 1.
- ⁴⁴ Gaussian 03, Revision C.01, Frisch, M. J.; Trucks, G. W.; Schlegel, H. B.; Scuseria, G. E.; Robb, M. A.; Cheeseman, J. R.; Montgomery, Jr., J. A.; Vreven, T.; Kudin, K. N.; Burant, J. C.; Millam, J. M.; Iyengar, S. S.; Tomasi, J.; Barone, V.; Mennucci, B.; Cossi, M.; Scalmani, G.; Rega, N.; Petersson, G. A.; Nakatsuji, H.; Hada, M.; Ehara, M.; Toyota, K.; Fukuda, R.; Hasegawa, J.; Ishida, M.; Nakajima, T.; Honda, Y.; Kitao, O.; Nakai, H.; Klene, M.; Li, X.; Knox, J. E.; Hratchian, H. P.; Cross, J. B.; Bakken, V.; Adamo, C.; Jaramillo, J.; Gomperts, R.; Stratmann, R. E.; Yazyev, O.; Austin, A. J.; Cammi, R.; Pomelli, C.; Ochterski, J. W.; Ayala, P. Y.; Morokuma, K.; Voth, G. A.; Salvador, P.; Dannenberg, J. J.; Zakrzewski, V. G.; Dapprich, S.; Daniels, A. D.; Strain, M. C.; Farkas, O.; Malick, D. K.; Rabuck, A. D.; Raghavachari, K.; Foresman, J. B.; Ortiz, J. V.; Cui, Q.; Baboul, A. G.; Clifford, S.; Cioslowski, J.; Stefanov, B. B.; Liu, G.; Liashenko, A.; Piskorz, P.; Komaromi, I.; Martin, R. L.; Fox, D. J.; Keith, T.; Al-Laham, M. A.; Peng, C. Y.; Nanayakkara, A.; Challacombe, M.; Gill, P. M. W.; Johnson, B.; Chen, W.; Wong, M. W.; Gonzalez, C.; Pople, J. A.; Gaussian, Inc., Wallingford CT, 2004.
- ⁴⁵ Jacox, M. E. *J. Phys. Chem. Ref. Data* **1994**, *Monograph 3*.
- ⁴⁶ Kawaguchi, K., *J. Chem. Phys.*, **1992**, *96*, 3411.
- ⁴⁷ Shimanouchi, T. "Molecular Vibrational Frequencies" in NIST Chemistry WebBook, NIST Standard Reference Database Number 69, Eds. P.J. Linstrom and W.G. Mallard, National Institute of Standards and Technology, Gaithersburg MD, 20899. <http://webbook.nist.gov>, (retrieved December 11, 2008).
- ⁴⁸ Chase, M.W., Jr.; NIST-JANAF Tables (4th Edition), *J. Phys. Chem. Ref. Data*, Mono. **9**, Suppl. 1, 1998.

-
- ⁴⁹ Karton, A.; Martin, J. M. L. *J. Phys. Chem. A* **2007**, *111*, 5936.
- ⁵⁰ Storms E.; Mueller, B. *J. Phys. Chem.* **1977**, *81*, 318.
- ⁵¹ Ruscic, B.; Mayhew, C. A.; Berkowitz, J. J. *Chem. Phys.* **1988**, *88*, 5580.
- ⁵² Martin, J. M. L.; Taylor, P. R. *J. Phys. Chem. A* **1998**, *102*, 2995.
- ⁵³ Cox, J. D.; Wagman, D. D.; Medvedev, V. A., *CODATA Key Values for Thermodynamics*, Hemisphere Publishing Corp., New York, 1989.
- ⁵⁴ Gurvich, L. V.; Veyts, I. V.; Alcock, C. B. *Thermodynamic Properties of Individual Substances*, Vol. 3, Begell House, New York, 1996.
- ⁵⁵ Curtiss, L. A.; Raghavachari, K.; Redfern, P. C.; Pople, J. A. *J. Chem. Phys.* **1997**, *106*, 1063.
- ⁵⁶ Curtis, L. A.; Redfern, P. C.; Raghavachari, K.; Rassolov, V.; Pople, J. A. *J. Chem. Phys.* **1999**, *110*, 4703.
- ⁵⁷ Harmony, M. D.; Laurie, V. W.; Kuczkowski, R. L.; Schwendeman, R. H.; Ramsey, D. A.; Lovas, F. J.; Lafferty, W. J.; Maki, A. G. *J. Phys. Chem. Ref. Data* **1979**, *8*, 619.
- ⁵⁸ Dixon, D. A.; Arduengo, A. J., III *J. Phys. Chem. A* **2006**, *110*, 1968.
- ⁵⁹ Gutowski, K. E.; Rogers, R. D.; Dixon, D. A., *J. Phys. Chem. A* **2006**, *110*, 11890.
- ⁶⁰ Lee, T. J.; Taylor, P. R. *Int. J. Quantum Chem. Symp.* **1989**, *23*, 199.
- ⁶¹ Pedley, J. B. *Thermochemical Data and Structures of Organic Compounds*, TRC Data Series, Thermodynamics Research Center; College Station: Texas, 1994.
- ⁶² Wagman, D. D.; Evans, W. H.; Parker, V. B.; Schumm, R. H.; Halow, I.; Bailey, S. M.; Churley, K. L.; Nuttall, R. L. *J. Phys. Chem. Ref. Data*, **1982**, *11*, Supplement 2.
- ⁶³ Lias, S. G.; Bartmess, J. E.; Liebman, J. F.; Holmes, J. L.; Levin, R. D.; Mallard, W. G. *J. Phys. Chem. Ref. Data*, **1988**, *17*, Supplement 1.
- ⁶⁴ Cox, J. D.; Pilcher, G. *Thermochemistry of Organic and Organometallic Compounds*; Academic Press: London, 1970.
- ⁶⁵ Guest, M. F.; Pedley, J. B.; Horn, M. J. *Chem. Thermo.* **1969**, *1*, 345.

-
- ⁶⁶ Frenkel, M.; Marsh, K. N.; Wilhoit, R. C.; Kabo, G. J.; Roganov, G. N. *Thermodynamics of Organic Compounds in the Gas State, Vol 1*; TRC Data Series; Thermodynamic Research Center: Texas A&M University, College Station: Texas, 1944.
- ⁶⁷ Haalane, A. *Angew. Chem. Int. Ed. Engl.* **1989**, *28*, 992.
- ⁶⁸ McCoy, R. E.; Bauer, S. H. *J. Am. Chem. Soc.*, **1956**, *78*, 2061.
- ⁶⁹ Brown, H. C.; Bartholomay, H. Jr.; Taylor, M. D. *J. Am. Chem. Soc.* **1944**, *66*, 435.
- ⁷⁰ Jonas, V.; Frenking, Reetz, M. *J. Am. Chem. Soc.* **1994**, *116*, 8741.
- ⁷¹ Sana, M.; Leroy, G.; Wilante, C. *Organometallics*, **1992**, *11*, 781.
- ⁷² Beall, H.; Bushwell. *Ch. Chem. Rev.* **1973**, *73*, 465
- ⁷³ Nguyen, M. T.; Matus, M. H.; Lester, Jr., W. A.; Dixon, D. A. *J. Phys. Chem. A*, **2008**, *112*, 2082.
- ⁷⁴ Eades, R. A.; Well, D. A.; Dixon, D. A.; Douglass, Jr., C. H. *J. Phys. Chem.* **1981**, *85*, 976.
- ⁷⁵ (a) Becke, A. D. *J. Chem. Phys.* **1993**, *98*, 5648; (b) Lee, C.; Yang, W.; Parr, R. G. *Phys. Rev. B*, **1988**, *37*, 785.
- ⁷⁶ Godbout, N.; Salahub, D. R.; Andzelm, J.; Wimmer, E. *Can. J. Chem.* **1992**, *70*, 560.
- ⁷⁷ Feller, D.; Peterson, K. A.; Dixon, D. A. *J. Chem. Phys.*, **2008**, *129*, 204015.
- ⁷⁸ Brazier, C. R. *J. Molec. Spec.* **1996**, *177*, 90.
- ⁷⁹ Tel'noi, V.I.; Rabinovich, I.B. *Russ. Chem. Rev.* **1980**, *49*, 603 (Engl. translation, *49*, 1134).

5.8 *Appendices*

Table A5.1. Melting Temperature Ranges in °C of Ammonia Borane/Methylamine Borane Mixtures as a Function of the Weight Percent of Ammonia Borane.

Weight Fraction of NH₃BH₃	Melting Range (°C)
0.0	58-59
0.1	58
0.2	36-37
0.3	36-37
0.4	35-37
0.5	41-42
0.6	60
0.7	91-95
0.8	95-100
0.9	114-115
1.0	118-120

Table A5.2. Calculated Geometry Parameters for the $\text{BH}_m(\text{CH}_n)_{3-m}$, BH_mNH_n , and $\text{NH}_m\text{N}(\text{CH}_3)_{3-n}$ $m, n = 0-3$. Molecules at the MP2/VTZ level. Bond Distances in Å and Bond Angles in Degrees. Given in the order X-Y as shown in the first column.

Molecule	$R_{\text{B-H}}$	$R_{\text{N-H}}$	$R_{\text{C-H}}$	$R_{\text{X-Y}}$	$\angle \text{HXY}$	$\angle \text{HYX}$	$\angle \text{HXYH}$
$\text{HBCH}_2 (C_{2v} - ^1A_1)^a$	1.1700		1.0825	1.3825	180.0	122.1	0.0
$\text{HBNH}_2 (C_s - ^2A')^a$	1.1889	1.0079		1.3827	124.2	123.3	0.0
$\text{HNBH}_2 (C_1 - ^2A)^a$	1.1921	0.9982		1.3474	161.7	120.0	163.7
$\text{HNCH}_2 (C_s - ^1A')^a$		1.0199	1.0896	1.2751	109.5	124.7	0.0
$\text{HBCH}_3 (C_1 - ^2A)$	1.1894		1.0859	1.5473	127.2	115.7	167.7
			1.0914			112.6	40.2
			1.0981			104.8	-74.3
$\text{HBNH}_3 (C_1 - ^1A)$	1.2266	1.0197		1.6939	96.7	118.5	36.1
		1.0113				103.4	-82.5
		1.0209				110.5	163.6
$\text{HBNH}_3 (C_s - ^3A'')$	1.1891	1.0140		1.6063	115.1	109.5	180.0
		1.0169				112.6	60.9
$\text{HNBH}_3 (C_1 - ^3A)$	1.2047	1.0095		1.4453	151.2	112.2	180.0
	1.2244					103.9	58.2
$\text{HNCH}_3 (C_s - ^2A'')$	1.0208		1.0857	1.4426	160.2	110.5	180.0
			1.0940			111.2	59.2
$\text{H}_2\text{BCH}_3 (C_s - ^1A')$	1.1918		1.1003	1.5577	120.8	103.5	88.1
						114.9	27.0
calc. ^c	1.196			1.561			

B(CH ₃) ₂ (C ₂ - ² A) ^b		1.0866	1.5544		115.1	-154.3
		1.0925			113.3	-26.9
		1.0973			104.9	88.9
HB(CH ₃) ₂ (C ₂ - ¹ A)	1.1970	1.0883	1.5644	118.7	114.1	33.8
		1.0883			114.6	162.1
		1.0984			104.9	-81.3
calc. ^c	1.202		1.567			
B(CH ₃) ₃ (C ₁ - ¹ A) ^b		1.0884	1.5733		114.7	154.8
		1.0895	1.5734		113.6	27.5
		1.0973	1.5729		105.8	-88.2
calc. ^c			1.575			
N(CH ₃) ₂ (C _{2v} - ² B ₁) ^b		1.0859	1.4383		110.6	180.0
		1.0960			110.8	59.1
HN(CH ₃) ₂ (C _s - ¹ A')	1.0117	1.0878	1.4541	108.8	110.0	56.2
		1.0896			109.0	174.1
		1.0984			113.8	-65.8
calc. ^c	1.018		1.456			
N(CH ₃) ₃ (C _{3v} - ¹ A ₁) ^b		1.0887	1.4503		109.8	-178.9
		1.1023			112.3	60.7
calc. ^c			1.453			

^a Geometry parameters were calculated at the CCSD(T)/aVTZ level. ^b ∠ HAXH = ∠ HXAX. ^c Anane, H.; Abdellah, J.; Boutalib, A.;

Nebot-Gil, I.; Tomás, F. *J. Molec. Structure; THEOCHEM.* **1998**, *455*, 51; Anane, H.; Boutalib, A.; Nebot-Gil, I.; Tomás, F. *Chem.*

Phys. Lett. **1998**, *287*, 575.

Table A5.3. Calculated Geometry Parameters for $(\text{CH}_3)_{2-n}\text{H}_n\text{X}=\text{YH}_2$ and $(\text{CH}_3)_{3-n}\text{H}_n\text{X}-\text{YH}_3$ (X, Y = B and N; n = 0, 1, 2) and $(\text{NH}_3)\text{HB}=\text{CH}_2$ and $(\text{BH}_3)\text{HN}=\text{CH}_2$ at the MP2/VTZ level. Bond Distances in Å and Bond Angles in Degrees. X is the 1st atom of B or N and Y is the 2nd atom of B or N in the 1st column.

Molecule	R _{C-H}	R _{X-H}	R _{Y-H}	R _{X-Y}	R _{X-C}	∠ HXY	∠ HYX	∠ CXY	∠ HXYH	∠ HCXH
(CH ₃)HB=NH ₂	1.0897	1.1955	1.0051	1.3969	1.5744	117.1	123.0	121.6	180.0	180.0
(C _s - ¹ A')	1.0913		1.0040				123.2		0.0	58.2
(CH ₃)HB=NH ₂ rot	1.0860	1.2036	1.0184	1.4797	1.5621	120.8	108.8	121.3	55.1	180.0
(C _s - ¹ A')	1.0935									57.0
(NH ₃)HB=CH ₂	1.0156	1.1929	1.0878	1.4258	1.6139	134.2	123.6	114.9	180.0	180.0
(C _s - ¹ A') ^a	1.0150		1.0823				122.7		0.0	60.6
(NH ₃)HB=CH ₂ rot	1.0153	1.1877	1.0866	1.5578	1.6201	132.3	123.9	115.7	87.1	180.0
(C _s - ³ A'') ^a	1.0160									60.7
(CH ₃)HN=BH ₂	1.0858	1.0075	1.1925	1.3902	1.4518	119.2	118.6	126.7	180.0	180.0
(C _s - ¹ A')	1.0894		1.1911				118.7		0.0	60.5
(CH ₃)HN=BH ₂ rot	1.0901	1.0023	1.2022	1.4547	1.4501	122.6	121.5	121.0	91.1	180.0
(C _s - ¹ A')	1.0920									61.5
(BH ₃)HN=CH ₂	1.2069	1.0156	1.0805	1.2750	1.5902	115.2	117.6	127.7	180.0	180.0
(C _s - ¹ A') ^a	1.2077		1.0816				121.5		0.0	59.0
(BH ₃)HN=CH ₂ rot	1.1970	1.0141	1.0795	1.3989	1.5002	115.7	117.2	126.3	103.1	180.0
(C _s - ³ A'') ^a	1.2257									53.7
(CH ₃)H ₂ B-NH ₃	1.0905	1.2103	1.0135	1.6569	1.6111	103.6	111.2	106.3	58.8	66.2
(C _s - ¹ A')	1.0942		1.0143				110.8		61.4	52.6

calc. ^b		1.213	1.020	1.667	1.609					
(CH ₃) ₂ N-BH ₃	1.0875	1.0145	1.2076	1.6350	1.4744	108.5	105.4	113.5	57.6	58.4
(C _s - ¹ A')	1.0848		1.2082				104.9		62.6	63.0
expt. ^c	1.112	1.025	1.208	1.602	1.449	108.9	103.9	111.4	57.8	58.8
	(7)	(10)	(10)	(7)	(3)		(9)		61.2	61.8
calc. ^c	1.083	1.012	1.205	1.624	1.468	108.3	105.5	113.4	57.5	58.4
							105.0		62.7	63.0
calc. ^b		1.021	1.211	1.646	1.478					
(CH ₃) ₂ B=NH ₂	1.0897		1.0047	1.4021	1.5815		123.0	119.6	0.0	0.0
(C _{2v} - ¹ A ₁) ^d	1.0915									121.6
(CH ₃) ₂ B=NH ₂ rot	1.0880		1.0187	1.4874	1.5742		108.9	118.8	124.8	0.0
(C _s - ¹ A') ^d	1.0929									122.3
(CH ₃) ₂ B=NH ₂ rot	1.0863		1.022	1.4680	1.5812		123.4	121.3	90.0	0.0
(C _{2v} - ¹ A ₁) ^d	1.0934									122.5
(CH ₃) ₂ HB-NH ₃	1.0939	1.2147	1.0154	1.6643	1.6134	102.7	110.4	105.2	180.0	-52.1
(C _s - ¹ A')	1.0910		1.0142				111.1		60.2	67.0
	1.0956									-174.6
calc. ^c		1.218	1.021	1.671	1.612					
(CH ₃) ₂ N=BH ₂	1.0850		1.1921	1.3915	1.4520		118.7	123.6	0.0	0.0
(C _{2v} - ¹ A ₁) ^d	1.0918									120.3
(CH ₃) ₂ N=BH ₂ rot	1.0895		1.1929	1.4667	1.4632		121.2	109.4	120.3	-59.9
(C _s - ¹ A') ^d	1.0901									-178.0

	1.1001									61.6
CH ₃) ₂ N=BH ₂ rot	1.0904		1.2038	1.4542	1.4387		121.5	121.9	90.0	0.0
(C _{2v} - ¹ A ₁) ^d	1.0965									119.5
(CH ₃) ₂ HN-BH ₃	1.0848	1.0165	1.2101	1.6304	1.4734	106.2	104.7	111.6	180.0	-59.2
(C _s - ¹ A')	1.0894		1.2086				105.5		60.1	62.6
	1.0863									-177.0
expt. ^c	1.080	1.023	1.216	1.615	1.467	106.2	105.8	112.4	180.0	-57.1
	(2)	(9)	(7)	(4)	(2)				59.3	60.2
										-180.0
calc. ^c	1.084	1.014	1.206	1.619	1.467	106.1	104.7	111.5	180.0	-59.1
							105.6		60.2	62.7
										-176.9
calc. ^b		1.023	1.212	1.642	1.478					
(CH ₃) ₃ B-NH ₃	1.0907		1.0151	1.6723	1.6172		110.8	104.4	60.0	180.0
(C _{3v} - ¹ A ₁) ^d	1.0950									61.3
calc. ^c			1.022	1.677	1.615					
(CH ₃) ₃ N-BH ₃	1.0909		1.2093	1.6344	1.4754		105.2	110.2	60.0	180.0
(C _{3v} - ¹ A ₁) ^d	1.0857							108.5		59.2
expt. ^e	1.108		1.261	1.656	1.485					
	± 0.006		± 0.006	± 0.002	± 0.001					
expt. ^f				1.638	1.483			109.9		
				± 0.01	± 0.01			± 1		

expt. ^g		1.62	1.53
		± 0.15	± 0.06
calc. ^b	1.212	1.646	1.479

^a For the molecules (NH₃)HB=CH₂ and (BH₃)HN=CH₂, the NH₃ and BH₃ substituent corresponds to CH₃ and the B=C and N=C bonds correspond to the X=Y bond with respect to the (CH₃)_{2-n}H_nX=YH₂ (n = 1) notation. ^b Anane, H.; Abdellah, J.; Boutalib, A.; Nebot-Gil, I.; Tomás, F. *J. Molec. Structure; THEOCHEM.* **1998**, 455, 51; Anane, H.; Boutalib, A.; Nebot-Gil, I.; Tomás, F. *Chem. Phys. Lett.* **1998**, 287, 575. ^c Aldridge, S.; Downs, A. J.; Tang, C. Y.; Parsons, S.; Clarke, M. C.; Johnstone, R. D.; Robertson, H. E.; Rankin, D. W.; Wann, D. A. *J. Am. Chem. Soc.* **2009**, in press. ^d ∠ HXYH = ∠ HXYC and ∠ HCXH = ∠ HCXY. ^e Iijima, K.; Adachi, N.; Shibata, S. *Bull. Chem. Soc. Jpn.* **1984**, 57, 3269. ^f Cassoux, P.; Kuczkowski, R. L.; Bryan, P. S.; Taylor, R. C. *Inorg. Chem.* **1975**, 14, 126. ^g Bauer, S. H. *J. Am. Chem. Soc.* **1937**, 59, 1823.

Table A5.4. Calculated MP2/VTZ Frequencies (cm⁻¹).^a

Molecule	Symmetry	Calculated
HBCH ₂ (<i>C</i> _{2v} - ¹ A ₁)	a ₁	3182.6 (3093.5)
	a ₁	2869.2 (2794.6)
	a ₁	1498.5
	a ₁	1280.5
	b ₁	724.4
	b ₁	627.2
	b ₂	3261.5 (3170.2)
	b ₂	916.3
	b ₂	373.1
HBNH ₂ (<i>C</i> _s - ² A')	a'	3712.8 (3612.6)
	a'	3594.7 (3497.6)
	a'	2678.3 (2608.7)
	a'	1626.5
	a'	1334.2
	a'	1084.7
	a'	759.9
	a''	858.7
	a''	599.1
HNBH ₂ (<i>C</i> ₁ - ² A)	a	3800.0 (3697.4)
	a	2664.4 (2595.1)
	a	2571.4 (2504.5)
	a	1371.2
	a	1140.8
	a	966.3
	a	812.1
	a	321.4
	a	56.8
HNCH ₂ (<i>C</i> _s - ¹ A')	a'	3482.8 (3388.8)
	a'	3197.7 (3108.2)
	a'	3092.0 (3005.4)

	a'	1679.4
	a'	1494.5
	a'	1377.4
	a'	1074.4
	a''	1176.7
	a''	1100.2
HBNH ₃ (C ₁ - ¹ A)	a	3621.8 (3524.0)
	a	3535.7 (3440.2)
	a	3410.2 (3318.1)
	a	2394.8 (2332.5)
	a	1671.9
	a	1621.0
	a	1291.8
	a	1165.3
	a	720.2
	a	630.9
	a	504.8
	a	180.1
HBNH ₃ (C _s - ³ A'')	a'	3598.7 (3501.5)
	a'	3447.9 (3354.8)
	a'	2672.3 (2602.8)
	a'	1665.6
	a'	1347.3
	a'	1047.4
	a'	773.1
	a''	3535.4 (3439.9)
	a''	1660.5
	a''	834.3
	a''	691.1
	a''	216.2
HNBH ₃ (C ₁ - ³ A)	a	3664.6 (3565.7)
	a	2499.6 (2434.6)

	a	2455.4 (2391.6)
	a	2263.1 (2204.3)
	a	1076.2
	a	1039.0
	a	964.6
	a	869.9
	a	786.5
	a	700.2
	a	352.9
	a	99.3
HBCH ₃ (C ₁ - ² A)	a	3180.9 (3091.8)
	a	3118.3 (3031.0)
	a	3034.7 (2949.7)
	a	2679.5 (2609.8)
	a	1474.9
	a	1440.0
	a	1311.1
	a	1029.2
	a	1020.6
	a	692.2
	a	591.7
	a	200.9
HNCH ₃ (C _s - ² A'')	a'	3478.6 (3384.7)
	a'	3174.6 (3085.7)
	a'	3032.7 (2947.8)
	a'	1505.5
	a'	1416.3
	a'	1349.6
	a'	1070.6
	a'	1015.9
	a''	3095.0 (3008.3)
	a''	1508.8

	a''	965.7
	a''	256.1
H ₂ BCH ₃ (C _s - ¹ A')	a'	3137.6 (3049.7)
	a'	3025.1 (2940.4)
	a'	2622.2 (2554.0)
	a'	1493.8
	a'	1335.4
	a'	1277.3
	a'	1101.9
	a'	982.6
	a'	553.1
	a''	3193.7 (3104.3)
	a''	2698.0 (2627.9)
	a''	1447.7
	a''	1076.3
	a''	688.3
	a''	174.0
(CH ₃)HB=NH ₂ (C _s - ¹ A')	a'	3742.0 (3641.0)
	a'	3628.0 (3530.0)
	a'	3156.6 (3068.2)
	a'	3063.2 (2977.4)
	a'	2631.0 (2562.6)
	a'	1643.7
	a'	1494.1
	a'	1402.8
	a'	1322.1
	a'	1170.1
	a'	1057.3
	a'	840.6
	a'	788.7
	a'	355.5
	a''	3142.8 (3054.8)

	a''	1479.9
	a''	983.0
	a''	844.8
	a''	577.6
	a''	529.5
	a''	141.4
(NH ₃)HB=CH ₂ (C _s - ¹ A')	a'	3600.0 (3502.8)
	a'	3470.3 (3376.6)
	a'	3233.1 (3142.6)
	a'	3134.5 (3046.7)
	a'	2654.0 (2585.0)
	a'	1667.2
	a'	1519.3
	a'	1347.2
	a'	1334.8
	a'	1078.4
	a'	956.0
	a'	725.6
	a'	692.4
	a'	337.9
	a''	3591.6 (3494.6)
	a''	1656.8
	a''	903.7
	a''	818.7
	a''	774.2
	a''	510.2
	a''	180.9
(CH ₃)HN=BH ₂ (C _s - ¹ A')	a'	3637.9 (3539.7)
	a'	3189.9 (3100.6)
	a'	3072.7 (2986.7)
	a'	2699.6 (2629.4)
	a'	2614.7 (2546.7)

	a'	1566.0
	a'	1512.4
	a'	1464.9
	a'	1349.5
	a'	1224.5
	a'	1184.9
	a'	998.0
	a'	906.7
	a'	399.5
	a''	3144.3 (3056.3)
	a''	1514.2
	a''	1165.6
	a''	1013.4
	a''	819.3
	a''	440.0
	a''	185.5
(BH ₃)HN=CH ₂ (C _s - ¹ A')	a'	3550.3 (3454.4)
	a'	3298.1 (3205.8)
	a'	3175.2 (3086.3)
	a'	2550.7 (2484.4)
	a'	2478.0 (2413.6)
	a'	1696.8
	a'	1487.5
	a'	1423.2
	a'	1216.3
	a'	1193.4
	a'	1165.3
	a'	935.4
	a'	687.5
	a'	368.5
	a''	2537.7 (2471.7)
	a''	1199.6

	a''	1110.0
	a''	1077.7
	a''	961.6
	a''	470.2
	a''	201.1
(CH ₃)H ₂ B-NH ₃ (C _s - ¹ A')	a'	3622.3 (3524.5)
	a'	3483.7 (3389.6)
	a'	3139.9 (3052.0)
	a'	3034.3 (3046.5)
	a'	2480.3 (2415.8)
	a'	1670.0
	a'	1491.3
	a'	1334.9
	a'	1319.8
	a'	1244.1
	a'	1193.1
	a'	991.7
	a'	851.5
	a'	706.8
	a'	637.1
	a'	284.5
	a''	3613.6 (3516.0)
	a''	3103.5 (3016.6)
	a''	2515.5 (2450.1)
	a''	1668.6
	a''	1494.7
	a''	1097.3
	a''	1069.3
	a''	697.0
	a''	619.0
	a''	227.6
	a''	202.7

(CH ₃)H ₂ N-BH ₃ (C _s - ¹ A')	a'	3510.3 (3415.5)
	a'	3198.4 (3108.8)
	a'	3099.9 (3013.1)
	a'	2541.1 (2475.0)
	a'	2474.2 (2409.9)
	a'	1653.7
	a'	1527.1
	a'	1464.0
	a'	1291.3
	a'	1223.1
	a'	1215.9
	a'	1152.1
	a'	1058.0
	a'	902.2
	a'	694.6
	a'	323.7
	a''	3590.3 (3493.4)
	a''	3218.4 (3128.3)
	a''	2537.2 (2471.2)
	a''	1519.8
	a''	1358.5
	a''	1222.1
	a''	1130.4
	a''	951.6
	a''	652.8
	a''	256.1
a''	178.2	

^a Scaled A-H frequencies given in parenthesis. See text for further details.

Table A5.5. CCSD(T) Total Energies (E_h) as a Function of the Basis Set.^{a,b}

Molecule	Basis Set	Energy
HBCH ₂ ($C_{2v} - ^1A_1$)	aVDZ	-64.488518
	aVTZ	-64.546244
	aVQZ	-64.561768
	CBS (DTQ)	-64.570262
HBNH ₂ ($C_s - ^2A'$)	aVDZ	-81.147462
	aVTZ	-81.218880
	aVQZ	-81.239293
	CBS (DTQ)	-81.250618
HNBH ₂ ($C_1 - ^2A$)	aVDZ	-81.130701
	aVTZ	-81.202053
	aVQZ	-81.222144
	CBS (DTQ)	-81.233253
HNCH ₂ ($C_s - ^1A'$)	aVDZ	-94.397419
	aVTZ	-94.480534
	aVQZ	-94.504177
	CBS (DTQ)	-94.517280
HBCH ₃ ($C_1 - ^2A$)	aVDZ	-65.067260
	aVTZ	-65.127352
	aVQZ	-65.142746
	CBS (DTQ)	-65.151069
HBNH ₃ ($C_1 - ^1A$)	aVDZ	-81.665220
	aVTZ	-81.739023
	aVQZ	-81.758826
	CBS (DTQ)	-81.769654
HBNH ₃ ($C_s - ^3A''$)	aVDZ	-81.654055
	aVTZ	-81.727848
	aVQZ	-81.747657
	CBS (DTQ)	-81.758490
HNBH ₃ ($C_1 - ^3A$)	aVDZ	-81.655190
	aVTZ	-81.727870

	aVQZ	-81.747523
	CBS (DTQ)	-81.758289
HNCH ₃ ($C_s - ^2A''$)	aVDZ	-94.950875
	aVTZ	-95.037106
	aVQZ	-95.060518
	CBS (DTQ)	-95.073355
H ₂ BCH ₃ ($C_s - ^1A'$)	aVDZ	-65.735522
	aVTZ	-65.800559
	aVQZ	-65.817016
	CBS (DTQ)	-65.825886
(CH ₃)HB=NH ₂ ($C_s - ^1A'$)	aVDZ	-121.038661
	aVTZ	-121.154283
	aVQZ	-121.185490
	CBS (DTQ)	-121.202577
(NH ₃)HB=CH ₂ ($C_s - ^1A'$)	aVDZ	-120.963762
	aVTZ	-121.079085
	aVQZ	-121.109917
	CBS (DTQ)	-121.126762
(CH ₃)HN=BH ₂ ($C_s - ^1A'$)	aVDZ	-121.010902
	aVTZ	-121.126238
	aVQZ	-121.157399
	CBS (DTQ)	-121.174489
(BH ₃)HN=CH ₂ ($C_s - ^1A'$)	aVDZ	-120.959751
	aVTZ	-121.073680
	aVQZ	-121.104495
	CBS (DTQ)	-121.121378
(CH ₃)H ₂ B-NH ₃ ($C_s - ^1A'$)	aVDZ	-122.199490
	aVTZ	-122.322166
	aVQZ	-122.354063
	CBS (DTQ)	-122.371373
(CH ₃)H ₂ N-BH ₃ ($C_s - ^1A'$)	aVDZ	-122.181752
	aVTZ	-122.303828

aVQZ	-122.335587
CBS (DTQ)	-122.352823

^a Dissociation is with respect to RCCSD(T) atoms for closed shell atoms and R/UCCSD(T) for open shell atoms. Symmetry equivalency of the p_x , p_y , and p_z orbitals was not imposed in the atomic calculations. ^b CBS (DTQ) values from Eq. 1 (see text) obtained with the $aVnZ$ basis sets with $n = D, T, Q$.

Table A5.6. Isodesmic Reaction Energies at the G3(MP2) Level in kcal/mol.

Molecule	Isodesmic Reaction	ΔH_{rxn}	
		(0 K)	(298 K)
$\text{B}(\text{CH}_3)_2$ ($C_2 - ^2A$)	$\text{HB}(\text{CH}_3) + \text{H}_2\text{B}-\text{CH}_3 \rightarrow \text{B}(\text{CH}_3)_2 + \text{BH}_3$	-0.6	-0.5
$\text{HB}(\text{CH}_3)_2$ ($C_2 - ^1A$)	$2\text{H}_2\text{B}-\text{CH}_3 \rightarrow \text{HB}(\text{CH}_3)_2 + \text{BH}_3$	-0.5	-0.2
$\text{B}(\text{CH}_3)_3$ ($C_1 - ^1A$)	$\text{H}_2\text{B}-\text{CH}_3 + \text{HB}(\text{CH}_3)_2 \rightarrow \text{B}(\text{CH}_3)_3 + \text{BH}_3$	-0.3	0.2
$\text{N}(\text{CH}_3)_2$ ($C_{2v} - ^2B_1$)	$\text{HN}(\text{CH}_3) + \text{H}_2\text{N}-\text{CH}_3 \rightarrow \text{N}(\text{CH}_3)_2 + \text{NH}_3$	-10.5	-10.1
$\text{HN}(\text{CH}_3)_2$ ($C_s - ^1A'$)	$2\text{H}_2\text{N}-\text{CH}_3 \rightarrow \text{HN}(\text{CH}_3)_2 + \text{NH}_3$	-5.0	-4.7
$\text{N}(\text{CH}_3)_3$ ($C_{3v} - ^1A_1$)	$\text{H}_2\text{N}-\text{CH}_3 + \text{HN}(\text{CH}_3)_2 \rightarrow \text{N}(\text{CH}_3)_3 + \text{NH}_3$	-8.5	-8.2
$(\text{CH}_3)_2\text{B}=\text{NH}_2$ ($C_{2v} - ^1A_1$)	$\text{H}_2\text{B}-\text{CH}_3 + (\text{CH}_3)\text{HB}=\text{NH}_2 \rightarrow (\text{CH}_3)_2\text{B}=\text{NH}_2 + \text{BH}_3$	1.2	1.6
$(\text{CH}_3)_2\text{HB}-\text{NH}_3$ ($C_s - ^1A'$)	$\text{H}_2\text{B}-\text{CH}_3 + (\text{CH}_3)\text{H}_2\text{B}-\text{NH}_3 \rightarrow (\text{CH}_3)_2\text{HB}-\text{NH}_3 + \text{BH}_3$	3.6	3.9
$(\text{CH}_3)_2\text{N}=\text{BH}_2$ ($C_{2v} - ^1A_1$)	$\text{H}_2\text{N}-\text{CH}_3 + (\text{CH}_3)\text{HN}=\text{BH}_2 \rightarrow (\text{CH}_3)_2\text{N}=\text{BH}_2 + \text{NH}_3$	-6.8	-6.4
$(\text{CH}_3)_2\text{HN}-\text{BH}_3$ ($C_s - ^1A'$)	$\text{H}_2\text{N}-\text{CH}_3 + (\text{CH}_3)\text{H}_2\text{N}-\text{BH}_3 \rightarrow (\text{CH}_3)_2\text{HN}-\text{BH}_3 + \text{NH}_3$	-8.4	-8.1
$(\text{CH}_3)_3\text{B}-\text{NH}_3$ ($C_{3v} - ^1A_1$)	$\text{H}_2\text{B}-\text{CH}_3 + (\text{CH}_3)_2\text{HB}-\text{NH}_3 \rightarrow (\text{CH}_3)_3\text{B}-\text{NH}_3 + \text{BH}_3$	2.9	3.3
$(\text{CH}_3)_3\text{N}-\text{BH}_3$ ($C_{3v} - ^1A_1$)	$\text{H}_2\text{N}-\text{CH}_3 + (\text{CH}_3)_2\text{HN}-\text{BH}_3 \rightarrow (\text{CH}_3)_3\text{N}-\text{BH}_3 + \text{NH}_3$	-9.6	-9.3

Table A5.7. T_1 Diagnostics Calculated at the CCSD(T)/aVQZ level.

Molecule	T_1 Diagnostics
HBCH ₂ ($C_{2v} - ^1A_1$)	0.0144
HBNH ₂ ($C_s - ^2A'$)	0.0148
HNBH ₂ ($C_1 - ^2A$)	0.0310
HNCH ₂ ($C_s - ^1A'$)	0.0125
HBCH ₃ ($C_1 - ^2A$)	0.0126
HBNH ₃ ($C_1 - ^1A$)	0.0124
HBNH ₃ ($C_s - ^3A''$)	0.0118
HNBH ₃ ($C_1 - ^3A$)	0.0502
HNCH ₃ ($C_s - ^2A''$)	0.0141
H ₂ BCH ₃ ($C_s - ^1A'$)	0.0093
(CH ₃)HB=NH ₂ ($C_s - ^1A'$)	0.0112
(NH ₃)HB=CH ₂ ($C_s - ^1A'$)	0.0113
(CH ₃)HN=BH ₂ ($C_s - ^1A'$)	0.0123
(BH ₃)HN=CH ₂ ($C_s - ^1A'$)	0.0141
(CH ₃)H ₂ B-NH ₃ ($C_s - ^1A'$)	0.0087
(CH ₃)H ₂ N-BH ₃ ($C_s - ^1A'$)	0.0087

CHAPTER 6

HEATS OF FORMATION AND BOND ENERGY OF THE $H_{(3-n)}BX_n$ COMPOUNDS FOR (X = F, Cl, Br, I, NH₂, OH, and SH)

From: Grant, D. J.; Dixon, D. A. *J. Phys. Chem. A* **2009**, *113*, 777-787.

6.1 *Introduction*

There is substantial interest in the energetics of borane compounds as intermediates in regeneration cycles for chemical hydrogen storage systems. We are especially interested in the B-X and B-H bond dissociation energies (BDEs) in the BX_3 , HBX_2 , and H_2BX compounds, as well as the radicals BX_2 and HBX , which are products of varying bond breaking processes, where X = F, Cl, Br, I, NH₂, OH, and SH, for use in the investigation of the thermodynamics of regeneration schemes for spent fuel derived from ammonia borane. These compounds have other applications and are of substantial interest as model systems.¹ Following our recent work² on the BDEs in the PF_xO_y and SF_xO_y compounds, we define the diabatic BDE as dissociation to the configurations most closely representing the bonding configuration in the reactant and the adiabatic BDE as dissociation to the ground state of the separated species. The adiabatic BDE will always be equal to or less than the diabatic BDE. Because it can be difficult to measure BDEs, high-level theoretical calculations of these quantities offer a unique opportunity to obtain accurate self-consistent values for these processes.

There have been a number of measurements of BDEs for these borane compounds, but many of them have not been as accurate as one would hope for.³ The experimental dissociation

energies for the diatomic haloboranes have been summarized by Huber and Herzberg.⁴ The experimental heats of formation for the hydrogen halides,⁵ the haloboranes,⁶ the dihaloboranes (with the exception of diiodoborane),⁶ the dihaloboryl radicals⁶, the trihaloboranes,^{5,6} trihydroxyborane,⁶ and the dihydroxyboryl radical⁶ have been reported. The bond dissociation energies of the borane compounds $B(H)_x-H$ for $x = 0, 1,$ and 2 have been reported.^{7,8,9}

Modern computational chemistry methods implemented on high performance computer architectures can now provide reliable predictions of chemical bond energies to within about 1 kcal/mol for most compounds that are not dominated by multireference character.¹⁰ We can use the approach that we have been developing with collaborators at Pacific Northwest Laboratory and Washington State University for the prediction of accurate molecular thermochemistry¹¹ to predict BDEs in these boron compounds. Our approach is based on calculating the total atomization energy of a molecule and using this value with known heats of formation of the atoms to calculate the heat of formation at 0 K. The approach starts with coupled cluster theory with single and double excitations and including a perturbative triples correction (CCSD(T)),^{12,13,14} combined with the correlation-consistent basis sets^{15,16} extrapolated to the complete basis set limit to treat the correlation energy of the valence electrons. This is followed by a number of smaller additive corrections including core-valence interactions and relativistic effects, both scalar and spin-orbit. The zero point energy can be obtained from experiment, theory, or a combination of the two. Corrections to 298 K can then be calculated by using standard thermodynamic and statistical mechanics expressions in the rigid rotor-harmonic oscillator approximation¹⁷ and appropriate corrections for the heat of formation of the atoms.¹⁸

There have been several theoretical investigations into a couple of the molecules under study. The heats of formation of some small halogenated compounds, including the hydrogen

halides, have been previously calculated using a similar approach at the CCSD(T)/CBS level plus additional corrections.¹⁹ The authors noted that the largest errors in the calculated heats of formation were found for the molecules containing the I atom. In our recent study of the iodofluorides,²⁰ we found that it was necessary to correlate the core electrons with the aug-cc-pwCVnZ basis sets for $n = D, T, Q$ in order to extrapolate these quantities to the CBS limit to predict accurate heats of formation. The molecular atomization energies of BF_3 and BCl_3 have previously been reported at a comparable composite CCSD(T)/CBS level.¹¹ⁱ Martin and Taylor have reported on the atomization energies of BF and BF_3 using the CCSD(T) method and used these results in an analysis of the heat of formation of the boron atom.²¹ Bauschlicher and Ricca have reported CCSD(T)/CBS heats of formation on the basis of the atomization energies obtained with the cc-pVnZ basis sets up through $n = 5$ for BF_n , BF_n^+ , BCl , and BCl_n^+ for $n = 1 - 3$.²² Schlegel and Harris have reported the heats of formation of the BH_mCl_n species at the G-2 level of theory.²³ Rablen and Hartwig have reported on the sequential BDEs of borane compounds at the G-2 and CBS-4 levels of theory.²⁴ Baeck and Bartlett have studied BCl_3 , BCl_2 , BCl , and their anions and cations using the coupled-cluster and MBPT levels of theory and looked at their structure, spectra, and decomposition paths.²⁵

6.2 Computational Approach

For the current study, we used the augmented correlation consistent basis sets aug-cc-pVnZ ($n = D, T, Q$) for H, B, N, O, F, and Br.^{15,16} It has recently been found that tight d functions are necessary for calculating accurate atomization energies for 2nd row elements,²⁶ so we also included additional tight d functions in our calculations giving the aug-cc-pV($n+d$)Z basis set on the 2nd row atoms S and Cl. The CCSD(T) total energies were extrapolated in the normal way to the CBS limit by using a mixed exponential/Gaussian function of the form:

$$E(n) = E_{\text{CBS}} + A \exp[-(n-1)] + B \exp[-(n-1)^2] \quad (1)$$

with $n = 2$ (aVDZ), 3 (aVTZ), and 4 (aVQZ), as first proposed by Peterson *et al.*²⁷

In order to achieve thermochemical properties within ± 1 kcal/mol of experiment, it is necessary to account for core-valence correlation energy effects. Core-valence (CV) calculations were carried out with the weighted core-valence basis set cc-pwCVTZ.²⁸ The core-valence correction is then taken as the difference in energy between the valence electron correlation calculation and that with the appropriate core electrons included using basis sets with additional functions.

For molecules containing I as a substituent, we used a different approach due to issues described elsewhere.²⁰ For I, we used the new effective core potential/correlation consistent basis sets developed by Peterson and co-workers.²⁹ These basis sets were developed in combination with the small core relativistic effective core potentials (RECPs) from the Stuttgart/Köln group. The RECP for I subsumes the ($1s^2$, $2s^2$, $2p^6$, $3s^2$, $3p^6$, and $3d^{10}$) orbital space into the 28-electron core set, leaving the ($4s^2$, $4p^6$, $5s^2$, $4d^{10}$, and $5p^5$) space with 25 electrons to be handled explicitly. We performed our complete basis set extrapolation with the aug-cc-pwCV n Z basis sets for $n =$ D, T, Q with 25 active electrons on each I atom so the core-valence correction is automatically included in the CBS extrapolation. We use aV n Z to represent the combination of aug-cc-pV n Z on H, B, N, O, F, and Br and aug-cc-pV($n+d$)Z on the 2nd row atoms S and Cl. For the molecules containing I as a substituent, we also use aV n Z to represent the combination of aug-cc-pwCV n Z on the other atoms and aug-cc-pwCV n Z-PP on I.

We also performed additional calculations for molecules containing Br using the new effective core potential/correlation consistent basis sets developed by Peterson and co-workers.²⁹ The RECP subsumes the ($1s^2$, $2s^2$, and $2p^6$) orbital space into the 10-electron core set, leaving the

($3s^2$, $3p^6$, $4s^2$, $3d^{10}$, and $4p^5$) space with 25 electrons to be handled explicitly, and only the (ns^2 , np^5) electrons are active in our valence correlation treatment. In these calculations, we will use aVnZ-PP to represent the combination of aug-cc-pVnZ basis set on H and B and the aug-cc-pVnZ-PP basis set on Br. Core-valence (CV) calculations were also carried out with the weighted core-valence basis set cc-pwCVTZ for H and B²⁸ and the cc-pwCVTZ-PP basis set for Br, which is based on the cc-pVTZ-PP basis set and accompanying small core RECP. For Br, the cc-pwCVTZ-PP basis set includes up through *g*-functions in order to provide a consistent degree of angular correlation for the active $4d$ electrons. The core-valence calculations for Br involve all 25 electrons outside the RECP core.

All of the current work was performed with the MOLPRO suite of programs.³⁰ The open-shell CCSD(T) calculations for the atoms were carried out at the R/UCCSD(T) level. In this approach, a restricted open shell Hartree-Fock (ROHF) calculation was initially performed and the spin constraint was relaxed in the coupled cluster calculation.^{31,32,33} All of the calculations were done on the 144 processor Cray XD-1 computer system at the Alabama Supercomputer Center or a Dell cluster at the University of Alabama.

The geometries were optimized numerically for most of the molecules at the frozen core CCSD(T) level with the aVDZ and aVTZ correlation-consistent basis sets. The CCSD(T)/aVTZ geometries were then used in single point CCSD(T)/aVQZ calculations. Diatomics were further optimized at the CCSD(T)/aVQZ level, and bond distances, harmonic frequencies, and anharmonic corrections were obtained from a 5th order fit of the potential energy surface (PES) at this level. For the molecules containing I as a substituent, geometry optimizations were performed at the CCSD(T) level with the aVDZ-PP and aVTZ-PP basis sets and additionally with the aVQZ-PP basis set for the diatomic with a fit of the PES performed at the this level. The

CCSD(T)/aVTZ-PP geometry was then used in single point CCSD(T)/aVnZ ($n = D, T, Q$) calculations. For $H_{(3-n)}BX_n$ ($X = OH$ and NH_2), geometry optimizations were performed at the MP2/aVTZ level,³⁴ and the MP2/aVTZ geometry was consequently used in single point CCSD(T)/aVnZ ($n = D, T, Q$) calculations.

The vibrational frequencies of the polyatomic molecules were calculated at the MP2/aVTZ level³⁴ using the Gaussian program system³⁵ in order to obtain the zero point energies and the thermal corrections at 298 K.

Two adjustments to the total atomization energy ($TAE = \Sigma D_0$) are necessary in order to account for relativistic effects in atoms and molecules. The first correction lowers the sum of the atomic energies (decreasing TAE) by replacing energies that correspond to an average over the available spin multiplets with energies for the lowest multiplets as most electronic structure codes produce only spin multiplet averaged wavefunctions. The atomic spin-orbit corrections are $\Delta E_{SO}(B) = 0.03$ kcal/mol, $\Delta E_{SO}(O) = 0.22$ kcal/mol, $\Delta E_{SO}(F) = 0.39$ kcal/mol, $\Delta E_{SO}(S) = 0.56$ kcal/mol, $\Delta E_{SO}(Cl) = 0.84$ kcal/mol, $\Delta E_{SO}(Br) = 3.50$ kcal/mol, and $\Delta E_{SO}(I) = 7.24$ kcal/mol from the tables of Moore.³⁶ A second relativistic correction to the atomization energy accounts for molecular scalar relativistic effects, ΔE_{SR} . ΔE_{SR} is taken as the sum of the mass-velocity and 1-electron Darwin (MVD) terms in the Breit-Pauli Hamiltonian.³⁷ We evaluated ΔE_{SR} by using expectation values for the two dominant terms in the Breit-Pauli Hamiltonian, the so-called mass-velocity and one-electron Darwin (MVD) corrections from configuration interaction singles and doubles (CISD) calculations. The quantity ΔE_{SR} was obtained from CISD wavefunction with a VTZ basis set at the CCSD(T)/aVTZ, CCSD(T)/aVTZ-PP or MP2/aVTZ geometry. The CISD(MVD) approach generally yields ΔE_{SR} values in good agreement (± 0.3 kcal/mol) with more accurate values from, for example, Douglas-Kroll-Hess calculations, for

most molecules. A potential problem arises in computing the scalar relativistic corrections for the molecules in this study as there is the possibility of “double counting” the relativistic effect on I when applying a MVD correction to an energy which already includes most of the relativistic effects via the RECP. Because the MVD operators mainly sample the core region where the pseudo-orbitals are small, we assume any double counting to be small. For the molecules containing Br, the molecular scalar relativistic correction ΔE_{SR} was calculated using the spin-free, one-electron Douglas-Kroll-Hess (DKH) Hamiltonian.^{38,39,40} ΔE_{SR} was defined as the difference in the atomization energy between the results obtained from basis sets recontracted for DKH calculations³⁹ and the atomization energy obtained with the normal valence basis set of the same quality. DKH calculations were carried out at the CCSD(T)/cc-pVTZ and the CCSD(T)/cc-pVTZ-DK levels of theory.

By combining our computed ΣD_0 values with the known heats of formation at 0 K for the elements⁶ $\Delta H_f^0(\text{H}) = 51.63 \text{ kcal mol}^{-1}$, $\Delta H_f^0(\text{B}) = 135.1 \pm 0.2 \text{ kcal mol}^{-1}$,⁴¹ $\Delta H_f^0(\text{N}) = 112.53 \text{ kcal mol}^{-1}$, $\Delta H_f^0(\text{O}) = 58.99 \text{ kcal mol}^{-1}$, $\Delta H_f^0(\text{F}) = 18.47 \text{ kcal mol}^{-1}$, $\Delta H_f^0(\text{S}) = 65.66 \text{ kcal mol}^{-1}$, $\Delta H_f^0(\text{Cl}) = 28.59 \text{ kcal mol}^{-1}$, $\Delta H_f^0(\text{Br}) = 28.19 \text{ kcal mol}^{-1}$, and $\Delta H_f^0(\text{I}) = 25.61 \text{ kcal mol}^{-1}$, we can derive ΔH_f^0 values for the molecules under study in the gas phase. The heat of formation of the boron atom has changed over time. The original JANF value⁶ was $\Delta H_f^0(0 \text{ K}, \text{B}) = 132.7 \pm 2.9 \text{ kcal/mol}$. Storms and Mueller⁴² recommended a much larger value of $136.2 \pm 0.2 \text{ kcal/mol}$, which based on the analysis of Ruscic and co-workers,⁴³ we have used in our previous work.^{44,45,46} Martin and Taylor⁴⁷ calculated the atomization energies of BF and BF₃ using a composite approach based on CCSD(T), used these results to analyze the heat of formation of the boron atom, and came to a similar conclusion as that of Ruscic.⁴³ More recently, Karton and Martin⁴¹ revised their heat of formation of the B atom to $135.1 \pm 0.2 \text{ kcal/mol}$ on the basis of the

experimental heats of formation of BF_3 ⁵ and B_2H_6 ⁴⁸ coupled with W4 calculations of their total atomization energies, and this is the value we have used. We obtain heats of formation at 298 K by following the procedures outlined by Curtiss *et al.*¹⁸

6.3 *Results and Discussion*

6.3.1 *Geometries* The calculated geometry parameters with the aVTZ basis set are given in Table 6.1 and are in excellent agreement with the available structural data.⁴⁹ The electronic states and symmetry of the molecules are also given in Table 6.1 and consequently have been excluded from the other tables. The bond distance for the halide acids calculated with the aVDZ and aVTZ basis sets are given as Supporting Information (Table A6.1), and those for the remaining molecules calculated with the aVDZ basis set are also given in the Supporting Information (Table A6.2). The total CCSD(T) energies as a function of the aVnZ and aVnZ-PP ($n = \text{D, T, Q}$) basis sets are given in the Supporting Information in Tables A6.3 and A6.4, respectively. The calculated harmonic vibrational frequencies are also given as Supporting Information (Table A6.5). Finally, the components for the calculated atomization energies for the halide acids are given as Supporting Information (Table A6.6).

6.3.2 *Heats of Formation* The energetic components for predicting the total molecular dissociation energies are given in Table 6.2, and we first describe some trends in the different components. The core-valence corrections for the molecules are all positive and range from 0.42 (BCl) to 3.44 kcal/mol ($\text{B}(\text{NH}_2)_3$). The scalar relativistic corrections are all small and negative, and range in values from -0.01 (BI) to -1.18 ($\text{B}(\text{OH})_3$) kcal/mol, except for BBr with a 0.01 kcal/mol correction. We estimate that the error bars for the calculated heats of formation are ± 1.5 kcal/mol considering errors in the energy extrapolation, frequencies, and other electronic energy components. An estimate of the potential for significant multireference character in the

wavefunction can be obtained from the T_1 diagnostic⁵⁰ for the CCSD calculation. The value for the T_1 diagnostics are small (<0.03) showing that the wavefunction is dominated by a single configuration. The T_1 diagnostics for the molecules are given as Supporting Information (Table A6.9).

The calculated heats of formation⁵¹ at 0 K and 298 K are given in Table 6.3, where they are compared with available experimental data. We use the calculated values at 298 K in our discussions below unless specified otherwise. Our calculated heats of formation for the hydrogen halides HX (X = F, Cl, Br, and I) are in excellent agreement with the previously calculated¹⁹ and experimental values.⁵ Including the core electrons in the correlation and employing the weighted core basis sets for the CBS extrapolation, our calculated $\Delta H_f(\text{HI})$ overestimates the experimental value by 0.5 kcal/mol.⁵ Using the new heat of formation of the boron atom, we recalculated the values of $\Delta H_f(\text{BH})$,⁴⁵ $\Delta H_f(\text{BH}_2)$,⁴⁵ $\Delta H_f(\text{BH}_3)$,⁴⁴ and $\Delta H_f(\text{BH}_2\text{NH}_2)$,⁴⁴ as given in Table 6.3.

Our calculated value for the $\Delta H_f(\text{BF})$ is in excellent agreement with the value from a spectroscopic measurement,⁴ the experimental value derived from a mass spectrometry study of the BF_2 radical,⁵² and the JANAF⁶ value (within the ± 3.3 kcal/mol error bars of the latter). Our calculated value is in excellent agreement with the high-level theoretical values^{21,22} at the CCSD(T)/CBS level using basis sets up through aug-cc-pV6Z. The $\Delta H_f(\text{BF})$ at the lower G-2 and CBS-4 levels²⁴ are in good agreement with our CCSD(T)/CBS value. Our calculated value for the $\Delta H_f(\text{BCl})$ is in excellent agreement with the experimental value derived from a thermochemical analysis of the dissociation energy of BCl ,⁵³ but differs from the JANAF value⁶ by 9.6 kcal/mol and from the spectroscopically derived value⁴ by 5.8 kcal/mol. The JANAF value was derived from the $\text{Cl}_2\text{B-Cl}$ BDE and employing a ratio of the $D_0^0(\text{B-F})$ /average bond energy of BF_3 . Our value should be accurate to ± 1.0 kcal/mol and supports the thermochemical

value⁵³ as the preferred experimental one. Our calculated value is also in excellent agreement with the CCSD(T)/CBS (VnZ) theoretical value,²² and the G-2 value is in agreement with our more accurately calculated value.²³ Our calculated values for the $\Delta H_f(\text{BBr})$ and $\Delta H_f(\text{BI})$ are in excellent agreement with the JANAF values⁶ within the rather large error bar limits of ± 10.0 kcal/mol, and we expect our values to be accurate to within ± 1.5 kcal/mol. Our $\Delta H_f(\text{BBr})$ differs by 2.5 and 8.8 kcal/mol, respectively, from the spectroscopically derived values from Huber and Herzberg⁴ and an infrared diode laser spectroscopy study of the vibrational levels, which were used to construct a potential energy curve.⁵⁴

Our calculated values for the $\Delta H_f(\text{BF}_3)$, $\Delta H_f(\text{BCl}_3)$, and $\Delta H_f(\text{BBr}_3)$ are in excellent agreement with the reported experimental values,⁶ within 0.5 kcal/mol. Two high-level calculated values^{11i,21} from similar CCSD(T)/CBS approaches are in agreement with our $\Delta H_f(\text{BF}_3)$ value. Our $\Delta H_f(\text{BCl}_3)$ is within 0.5 kcal/mol of the previously reported value at the RCCSD(T)/CBS level.¹¹ⁱ The G2 value²³ for the $\Delta H_f(\text{BCl}_3)$ is in good agreement with our higher level CCSD(T)/CBS value. Our $\Delta H_f(\text{BI}_3)$ is in agreement with the experimental value,⁶ determined from measuring the appearance potential of the B^+ ion from BI_3 , within the rather large error bar limits of ± 12.0 kcal/mol. The $\Delta H_f(\text{B(OH)}_3)$ is calculated to be within 2.6 kcal/mol of the experimental value obtained from the heat of formation of the crystal and an average of the enthalpy of sublimation.⁶

Our calculated values for the $\Delta H_f(\text{HBF}_2)$ and $\Delta H_f(\text{HBCl}_2)$ are within 0.3 kcal/mol of the experimental values,⁶ while the $\Delta H_f(\text{HBBR}_2)$ differs by 2.2 kcal/mol. The G2 values²³ for $\Delta H_f(\text{HBCl}_2)$ and $\Delta H_f(\text{H}_2\text{BCl})$ are in good agreement with our CCSD(T)/CBS values.

For our calculations on molecules containing Br, we note that there is a difference of ~ 0.5 kcal/mol per Br atom in the valence electronic energy extrapolated to the CBS limit based on the

aVnZ and aVnZ-PP (Table A6.7) basis sets, respectively. However, much of the difference is recovered in the various components of the atomization energy and the largest difference in the calculated heats of formation based on both approaches was 0.7 kcal/mol for BBr₃. The predicted heat of formation of BBr₃ (aVnZ-PP) of -47.6 kcal/mol shows a larger difference of 1.2 kcal/mol from the experimental value.⁶ For the heats of formation for the I containing molecules, the inclusion of the core electrons and the CBS extrapolation with the weighted core basis sets yields calculated values for the heats of formation that are on average within 0.3 kcal/mol of the heats of formation calculated using the aVnZ-PP basis sets and just correlating the valence electrons. The largest difference between the predicted heats of formation based on both approaches was 0.5 kcal/mol for BI₃, where the heats of formation were predicted to be 8.6 (awCVnZ) and 9.1 (aVnZ-PP) kcal/mol, respectively, at 0 K.

Our calculated $\Delta H_f(\text{BF}_2)$ is in excellent agreement with the experimental value obtained from the thermochemical analysis of the BF₂ radical by mass spectrometry, differing by 1.3 kcal/mol and within the error bar limits.⁵² The JANAF value differs by 22 kcal/mol and is clearly incorrect.⁶ The JANAF value⁶ was calculated based on combining the appearance potential of BF₂⁺ from BF₃ and the ionization potential for BF₂. Using the same method, Margrave⁵⁵ obtained a value of $\Delta_f H^0(\text{BF}_2, \text{g}) \leq -124 \pm 9$ kcal/mol in better agreement with our reliably calculated value. Our $\Delta H_f(\text{BF}_2)$ is in excellent agreement with the CCSD(T)/CBS (VnZ) value.²² For the $\Delta H_f(\text{BCl}_2)$, there is a large difference of 12 kcal/mol between the JANAF⁶ and our calculated theoretical value. The JANAF value was determined based on an analysis of the equilibrium constants, which were obtained from ion intensity data, for the reaction $\text{BCl}_3 (\text{g}) + \text{BCl} (\text{g}) = 2\text{BCl}_2 (\text{g})$ in combination with the experimental enthalpies of formation for BCl₃ (g) and BCl (g).⁶ Our calculated value for the $\Delta H_f(\text{BCl}_2)$ is in excellent agreement with the CCSD(T)/CBS

(VnZ)²² and G2 values.²³ Our $\Delta H_f(\text{BBr}_2)$ and $\Delta H_f(\text{BI}_2)$ differ by 9.2 and 1.8 kcal/mol from the estimated experimental values, which were based on an analogy with BF_3 , employing the ratio $\Delta_f H^0(\text{BX}_3 \rightarrow \text{BX}_2 + \text{X})/\Delta_f H^0(\text{BX}_3 \rightarrow \text{B} + 3\text{X})$.⁶ Our $\Delta H_f(\text{B}(\text{OH})_2)$ differs from the estimated experimental value by 15 kcal/mol, which was calculated using the bond energy, $D_0^0(\text{B-OH})$, of 132.7 kcal/mol and the enthalpies of formation of B (g) and OH (g) as 132.80 and 9.33 kcal/mol, respectively.⁶ We recalculated the “experimental” $\Delta H_f(\text{B}(\text{OH})_2)$ using the new value for $\Delta H_f^0(\text{B})$ of 135.1 ± 0.2 kcal/mol⁴¹ and $\Delta H_f^0(\text{OH}) = 8.85$ kcal/mol,^{11k} and obtain a value of -112.6 kcal/mol, and still do not find agreement with our value. On the basis of extensive comparisons with experiment for a wide range of compounds, our calculated values for these radicals should be good to ± 1.5 kcal/mol, and thus are to be preferred over the experimental values when there are large differences.

6.3.3 Bond Dissociation Energies From the calculated heats of formation, we can predict the various B-X and B-H adiabatic BDEs at 0 K for BX_3 , HBX_2 , H_2BX , BX , and HX as well as the various radicals involved in the bond breaking processes. The results are presented in Table 6.4 for comparison with the available experimental data, which is largely compiled by Luo³ and references therein. On the basis of the results for the heats of formation of the BX_2 radicals, we expect that there are large errors in the experimental BDEs. We define the calculated BDE as the adiabatic value at 0 K. We first examine the BDEs in the diatomics (B-X) as they are representative of the strength of a single bond in these compounds. Our calculated value for the BDE of $\text{BF} (^1\Sigma^+)$ is in excellent agreement with the value from Huber and Herzberg,⁴ the reported experimental value of Hildebrand and Lau,⁵² and other calculations (CCSD(T)/CBS, G2, and CBS-4)^{21,22,24} The B-F BDE is the largest B-X bond energy. Our calculated $\text{BCl} (^1\Sigma^+)$ BDE differs by 1.2 kcal/mol from the thermochemical value,⁵³ 5.8 kcal/mol from that of Huber

and Herzber,⁴ and 8.0 kcal/mol from the JANAF value.⁶ Our calculated value is within 0.5 kcal/mol of another CCSD(T)/CBS value.²² The BDE of BBr ($^1\Sigma^+$) falls within the range of the available experimental BDEs.^{6,54,56} The predicted BI ($^1\Sigma^+$) BDE differs from the experimental value by 8 kcal/mol.³ Given the previously calculated $\Delta H_f(\text{NH}_2)^{11\text{m}}$ and the experimental $\Delta H_f(\text{OH})^{11\text{k}}$ and $\Delta H_f(\text{SH})$,⁶ the B-X BDE in the pseudo-diatomic molecules B(NH₂), B(OH), and B(SH) are calculated with the predicted B-OH BDE lying just outside the error bar limits of the reported experimental value.⁴⁸

BF₃ is predicted to have the largest X₂B-X BDE and this B-F BDE is slightly less stable than the calculated BF ($^1\Sigma^+$) BDE. Our calculated F₂B-F BDE is in excellent agreement with the experimental value derived from a mass spectrometry study,⁵² but differs by 20 kcal/mol from the other available experimental values,^{57,6} due to errors in the experimental $\Delta H_f(\text{BF}_2)$. The F₂B-F BDE is 9.6 kcal/mol less than the BDE of BF ($^1\Sigma^+$). The strong bond is consistent with back-bonding from the F lone pairs to the vacant B out-of-plane p orbital.⁵⁸ Our calculated value is in good agreement with previous calculations.^{22,24} The Cl₂B-Cl BDE is calculated to be 12 and 8 kcal/mol larger, respectively, than the reported experimental values^{6,57} and 3.1 kcal/mol less than the BDE of BCl ($^1\Sigma^+$). Our calculated value is within 0.6 kcal/mol of a previously reported CCSD(T)/CBS value.²² The Br₂B-Br and I₂B-I BDEs are calculated to be 8.6 and 10.8 kcal/mol larger than the JANAF values⁶ and only 2.6 and 1.2 kcal/mol smaller than the BBr ($^1\Sigma^+$) and BI ($^1\Sigma^+$) BDEs, respectively, showing that the other halide substituents have only a small effect on the B-X BDE. The I₂B-I BDE is predicted to be 93 kcal/mol smaller than the F₂B-F BDE. For the Group VIIA substituents, there is the expected decrease in X₂B-X BDE as one increases the atomic number.

The second highest B-X BDE of the BX_3 compounds is predicted for the hydroxyl substituent, which is isoelectronic with fluorine. The $(HO)_2B-OH$ BDE is 15.7 kcal/mol larger than the JANAF value.⁶ The $(HO)_2B-OH$ BDE is 7.4 kcal/mol less than the B-OH BDE and 23 kcal/mol less than the F_2B-F BDE. The $(H_2N)_2B-NH_2$ and $(HS)_2B-SH$ BDEs are predicted to be 4 kcal/mol lower and 6 kcal/mol higher than the B- NH_2 and B-SH BDEs, respectively, and 47 and 71 kcal/mol lower, respectively, than the F_2B-F BDE.

Similar trends were found in the HBX-X BDE of the HBX_2 molecules. Substitution of H for X to form HBX_2 leads to an average increase of 3 kcal/mol in the HBX-X BDE of the HBX_2 molecules relative to the BX_3 molecules. The HBF-F BDE is again the largest HBX-X BDE and is calculated to be slightly larger than the F_2B-F BDE and 7.4 kcal/mol less than the BDE in BF ($^1\Sigma^+$). The G-2 and CBS-4 values are in good agreement with our calculated value for the HBF-F BDE.²⁴ The HBCl-Cl and HBr-Br BDEs are calculated to be 1 kcal/mol more stable than the corresponding diatomic BDEs. There is a decrease in the HBX-X BDE with halide substitution with the HBI-I BDE predicted to be the lowest, 91 kcal/mol less than the HBF-F BDE. The HBI-I BDE is 4 and 3 kcal/mol more stable than the first B-I BDE in BI_3 and BI ($^1\Sigma^+$), respectively.

The HB(OH)-OH BDE is calculated to be slightly higher than the $(HO)_2B-OH$ BDE, 7 kcal/mol less than the B-OH BDE, and 24 kcal/mol less than the HBF-F BDE. The HB(NH_2)- NH_2 and HB(SH)-SH BDEs are predicted to be 4 kcal/mol larger than the analogous first BDE in $B(NH_2)_3$ and $B(SH)_3$, respectively. The HB(NH_2)- NH_2 BDE is predicted to be approximately the same as the BDE in B- NH_2 , while the HB(SH)-SH BDE is 10 kcal/mol larger than the B-SH BDE. The HB(NH_2)- NH_2 and HB(SH)-SH BDEs are calculated to be 45 and 69 kcal/mol less than the HBF-F BDE, respectively.

The highest and lowest B-H BDEs for the HBX_2 compounds were calculated for H-BF_2 and H-BI_2 respectively, bracketing the H-BH_2 BDE obtained from the calculated $\Delta H_f(\text{BH}_3)$ and $\Delta H_f(\text{BH}_2)$, indicating only a small substituent effect on the B-H BDEs. Our calculated value for the H-BF_2 BDE is in good agreement with the lower level G-2 and CBS-4 values.²⁴ For all of the HBX_2 molecules, the HBX-X BDE is larger than the $\text{X}_2\text{B-H}$ BDE, except in HBBr_2 where the $\text{Br}_2\text{B-H}$ and HBBr-Br BDEs are the same and in HBI_2 where the $\text{I}_2\text{B-H}$ BDE is larger than the HBI-I BDE by 18 kcal/mol.

The B-X BDEs in the H_2BX molecules were calculated using our revised $\Delta H_f(\text{BH}_2)$ ⁴⁵ with the new heat of formation of the B atom. The substitution of a second H for X to form H_2BX leads to an increase in the $\text{H}_2\text{B-X}$ BDE compared to the HBX-X BDE except for $\text{X} = \text{F}$ where a decrease of 4 kcal/mol is predicted for the $\text{H}_2\text{B-F}$ BDE compared to the HBF-F BDE. There is also a general increase in the $\text{H}_2\text{B-X}$ BDE compared to the B-X BDE in the diatomic molecules except for $\text{X} = \text{F}$ and OH with a predicted decrease of 12 and 5 kcal/mol in the $\text{H}_2\text{B-F}$ and $\text{H}_2\text{B-OH}$ BDEs compared to the analogous BDEs in $\text{BF} (^1\Sigma^+)$ and B(OH) , respectively. The $\text{H}_2\text{B-F}$ BDE differs by 24 kcal/mol from the reported experimental value. The $\text{H}_2\text{B-F}$ BDE is the highest BDE predicted for the H_2BX molecules, and similar trends are noted as found for the BDEs of BX_3 and HBX_2 . Our calculated value for the $\text{H}_2\text{B-F}$ BDE is in good agreement with the lower level G-2 and CBS-4 values.²⁴ There is a general decrease in the $\text{H}_2\text{B-X}$ BDE down the group for the halide substituents, with that of iodine predicted to have the smallest $\text{H}_2\text{B-X}$ BDE, 83 kcal/mol less than the $\text{H}_2\text{B-F}$ BDE but 7 kcal/mol more stable than the BDE of $\text{BI} (^1\Sigma^+)$. The $\text{H}_2\text{B-NH}_2$ and $\text{H}_2\text{B-SH}$ BDEs are calculated to be 29 and 58 kcal/mol smaller than the $\text{H}_2\text{B-F}$ BDE, respectively, and 12 and 17 kcal/mol larger than the corresponding BDEs in $\text{B(NH}_2)$ and B(SH) , respectively.

As for the HBX_2 compounds, the effect of the substituent on the first B-H BDE in H_2BX is small when compared to the first B-H BDE in BH_3 . The largest difference is predicted for the HBI-H BDE, which is only 1.6 kcal/mol less than the H-BH₂ BDE. The HBF-H BDE has been calculated at the G-2 and CBS-4 levels,²⁴ and show good agreement with our higher level CCSD(T)/CBS value. For the H_2BX molecules, the $\text{H}_2\text{B-X}$ BDE is larger than the HBX-H BDE, except for H_2BI where the $\text{H}_2\text{B-I}$ BDE is 17 kcal/mol less than the HBI-H BDE.

We also predicted the B-X and B-H BDEs in the BX_2 and HBX radicals. Although the XB-X and HB-X BDEs follow similar trends to those discussed above, there is a considerable decrease in the strength of both compared to the corresponding $\text{X}_2\text{B-X}$, HBX-X, $\text{H}_2\text{B-X}$, and B-X BDEs. Our calculated FB-F BDE is in excellent agreement with the experimental value derived from a mass spectrometry study of the BF_2 radical,⁵² but differs from the other experimental values,^{3,6} due to errors in $\Delta H_f(\text{BF}_2)$. Our calculated value is in good agreement with other calculated values.^{22,24} The FB-F BDE is significantly lower than the BDE in $\text{BF} (^1\Sigma^+)$ by 70 kcal/mol. The calculated ClB-Cl BDE is within 3.4 kcal/mol of one of the reported experimental value and 15 kcal/mol of the other reported value,³ and smaller than the $\text{BCl} (^1\Sigma^+)$ BDE by 43 kcal/mol. Our calculated value is in excellent agreement with the reported CCSD(T)/CBS value.²² The BrB-Br and IB-I BDEs differ by 5 and 7 kcal/mol from the reported experimental values, respectively,³ and are predicted to be 38 and 31 kcal/mol less stable than the analogous BDEs in $\text{BBr} (^1\Sigma^+)$ and $\text{BI} (^1\Sigma^+)$, respectively. Our calculated value for the (HO)B-OH BDE is not in agreement with the reported experimental value.⁶

The first B-F adiabatic BDEs of all the fluoroboranes are large except for BF_2 , which is much lower due to the relative instability of the BF_2 radical and the stability of the closed-shell singlet diatomic BF. The adiabatic B-F BDE for $^2\text{BF}_2$ produces $\text{BF} (^1\Sigma^+)$ and $\text{F} (^2\text{P})$. Following

our previous study on the BDEs in the PF_xO_y and SF_xO_y compounds,² in order to compare the BDEs, it may be more appropriate to consider the diabatic BDE with the formation of ^3BF where there are two unpaired electrons, one from the unpaired electron on BF_2 and one from the B-F bond that was broken. Inclusion of the singlet-triplet splitting for BF obtained at the CCSD(T)/CBS//MP2/aVTZ level (Supporting Information, Table A6.8) provides an estimate of the reorganization energy. We then obtain a diabatic BDE of 193.4 kcal/mol, which is more consistent with the other B-F BDEs, 23 and 14 kcal/mol larger than the first B-F BDE in BF_3 and BF ($^1\Sigma^+$) respectively. The reorganization energy in this case is the pairing of the two electrons to form the lone pair on BF to give the singlet structure. Our calculated diabatic BF-F BDE is in good agreement with the G-2 and CBS-4 diabatic BF-F BDEs of 195.5 and 193.2 kcal/mol, respectively.²⁴ For the other molecules, we can also consider dissociation to the diabatic limit given by the reaction $^2\text{BX}_2 \rightarrow ^3\text{BX} + ^2\text{X}$. We calculated the single-triplet splitting for the BX molecules at the CCSD(T)/CBS//MP2/aVTZ level (Supporting Information, Table A6.8). Use of the singlet-triplet splitting in the BX molecules leads to diabatic BX-X BDEs of 136.3, 116.1, 94.5, 137.0, 165.7, and 109.5 kcal/mol for X = Cl, Br, I, NH_2 , OH, and SH, respectively. These values are comparable and on average about 16 kcal/mol larger than the corresponding first B-X BDE in BX_3 .

The HB-F BDE is the largest for the HBX molecules and is in excellent agreement with the reported experimental⁴⁸ and G-2 and CBS-4 theoretical values.²⁴ The B-X BDE decreases down the group, and the HB-I BDE is calculated to be 82 kcal/mol smaller than the HB-F BDE. The HB-X BDEs where X = OH, NH_2 , and SH are calculated to be 18, 30, and 57 kcal/mol smaller than the HB-F BDE, respectively.

The HB-F BDE is 24 and 36 kcal/mol smaller than the H₂B-F and B-F BDEs, respectively. Again, it is appropriate to consider dissociation of the products to the diabatic limit. We define the diabatic B-F BDE in HBF as occurring with dissociation to the excited ³Π state of BH, which has two unpaired electrons, one from the unpaired electron on HBF and one from the B-F bond that was broken. The experimental singlet-triplet splitting of the BH radical is 10,410 cm⁻¹ (29.7 kcal/mol)⁵⁹ giving a diabatic B-F BDE in HBF of 173.9 kcal/mol, consistent with the predicted B-F BDEs in BF₃, HBF₂, H₂BF, and BF. The HB-F diabatic BDE has been calculated at the G-2 and CBS-4 levels, and the results are in good agreement with our CCSD(T)/CBS value.²⁴ We predict the HB-X diabatic BDEs for X = Cl, Br, I, NH₂, OH, and SH to be 129.0, 111.6, 92.3, 143.6, 156.4, and 117.0 kcal/mol. These diabatic HB-X BDEs are on average 6 kcal/mol larger than the analogous H₂B-X BDE.

The corresponding B-H BDEs of the HBX molecules are also considerably less than the B-H BDE in BH₃. The smallest H-BX BDE is predicted for H-BF, 58 kcal/mol less than the H-BH₂ BDE. Our calculated value the H-BF BDE is in good agreement with the lower level G-2 and CBS-4 values.²⁴ We consider dissociation to the diabatic asymptote defined by the reaction ²HBX → ³BX + ²H. Use of the single-triplet splittings (Table A6.7) yields diabatic B-H BDEs that are considerably larger than the B-H BDE in BH₃ by as much as 26 kcal/mol in HBF, which suggests that use of this diabatic model may not be appropriate. Our calculated diabatic H-BF BDE of 129.3 kcal/mol is in good agreement with the G-2 and CBS-4 values of 130.3 and 128.2 kcal/mol, respectively.²⁴ For HB(SH), we find the B-H diabatic BDE to be only 5 kcal/mol larger than the H-BH₂ BDE. Comparison of the B-X and B-H BDEs in the HBX molecules shows that the HB-X BDE is larger than the XB-H BDE, except for HBI where the HB-I BDE is smaller than the H-BI BDE by 6.1 kcal/mol.

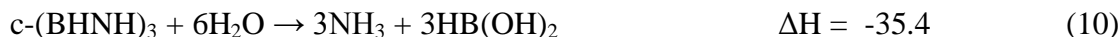
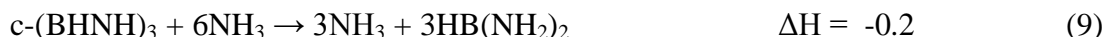
6.3.4 *Regeneration of Spent Fuel From Ammonia Borane* On the basis of the BDEs, it is unlikely that B-X to B-H conversion will occur for any of the substituted HBX₂, H₂BX, and HBX molecules studied. The iodine derivatives were the most favorable for B-X to B-H conversion as the B-H BDEs in HBI₂, H₂BI, and BHI were more stable than the corresponding B-I BDEs, respectively, and the B-I BDE in BI₃ was the smallest.

We can calculate the heats of reaction for the disproportionation step in proposed reprocessing schemes for the regeneration of ammonia borane. The results are in Table 6.5. The generic disproportionation reactions are:



The disproportionation reactions involving the halide and hydroxyl derivatives are all relatively close to thermoneutral. Reaction (4) involving the F substituent was the only exothermic reaction. These are model reactions for these processes, and BH₃ and BH₂Cl may form dimers in an actual system depending on the temperature. For example, Christie has demonstrated the chemical transformation of B₂H₅Cl to B₂H₆ and BCl₃ ($6\text{B}_2\text{H}_5\text{Cl} \leftrightarrow 5\text{B}_2\text{H}_6 + 2\text{BCl}_3$) in the gas phase using a platinum catalyst at temperatures between 200 and 520 °C.⁶⁰ Another group has reported similar transformations for boron trihalides over Group IB metals at even higher temperatures, 550 to 750 °C.⁶¹

We can predict the thermodynamics for the digestion reaction of borazine with the halide acids at 298 K in kcal/mol given the recalculated heat of formation of borazine⁴⁶ (using the new value for the heat of formation of the boron atom) of -118.8 kcal/mol at 298 K in the gas phase. The reactions with NH₃,⁴⁴ H₂O,⁶ and SH₂⁶ are also given for comparison.



We predict the reaction of borazine with hydrofluoric acid to be considerably more exothermic as compared to the other halide acids. In order to better understand the digestion chemistry and the energetics for the borazine reactions, one can compare the various bond energies for the respective halide acid reactants and the HBX_2 products. Breaking an HF bond compared to an HCl bond is more endothermic by 33 kcal/mol; however, much of this energy difference in the HF/ BF_3 system is gained back on forming HBF_2 . More notably, there is a difference of 96 kcal/mol in the cumulative reaction sequence $\text{BH} + \text{X} \rightarrow \text{HBX} + \text{X} \rightarrow \text{HBX}_2$ between $\text{X} = \text{F}$ and $\text{X} = \text{Cl}$. Similarly, breaking an HBr bond is about 49 kcal/mol less endothermic than breaking an HF bond; however, the cumulative reaction to form HBBr_2 ($\text{BH} + \text{Br} \rightarrow \text{HBBr} + \text{Br} \rightarrow \text{HBBr}_2$) is only exothermic by 184 kcal/mol as compared to 317 kcal/mol for the analogous fluorine reaction. Although breaking an HI bond is considerably less endothermic than breaking an HF bond by 66 kcal/mol, only 144 kcal/mol is regained in forming HBI_2 , and this value is less than half the equivalent reaction for the fluoride derivatives. The digestion reaction involving H_2O is also exothermic, but is ~21 kcal/mol less compared to the reaction with HF. The reactions involving NH_3 are thermoneutral, and the reactions involving SH_2 are endothermic.

6.4 Conclusions

The heats of formation at 0 K and 298 K are predicted for a range of substituted borane compounds, BX_3 , HBX_2 , and H_2BX , and the radicals, BX_2 and HBX , for $\text{X} = \text{F}, \text{Cl}, \text{Br}, \text{I}, \text{NH}_2, \text{OH},$ and SH , on the basis of coupled cluster theory (CCSD(T)) calculations extrapolated to the complete basis set limit. The calculated values should be good to ± 1.5 kcal/mol. The calculated heats of formation are in excellent agreement with the available experimental data for the closed shell molecules, but show larger differences with the reported experimental values for the BX_2 radicals. However, on the basis of extensive comparisons with experiment for a wide range of compounds, our calculated values for these radicals are to be preferred over the experimental values. Our calculated heats of formation allow us to predict the adiabatic BDEs for all of the compounds to within ± 1.5 kcal/mol, dramatically improving the estimates of these important quantities, particularly for the radicals.

The calculated BDEs provide insights into the reactivity of these molecules. The B-F BDE is the largest B-X BDE predicted for BX_2 , HBX_2 , and H_2BX , and for the halogens, there is the expected decrease in B-X BDE with increasing atomic number. For ammonia borane spent fuel regeneration processes, B-X to B-H conversion will most likely not occur for any of the substituted HBX_2 , H_2BX , and HBX molecules studied, except for the iodine derivatives, which were the most favorable with the B-H BDEs in HBI_2 , H_2BI , and HBI larger than the corresponding B-I BDEs, respectively, and the B-I BDE in BI_3 being the lowest for all of the substituents studied.

Acknowledgments We thank Prof. Karl Christe (USC) for helpful discussions and comments. Funding provided in part by the Department of Energy, Office of Energy Efficiency and Renewable Energy under the Hydrogen Storage Grand Challenge, Solicitation No. DE-PS36-

03GO93013. This work was done as part of the Chemical Hydrogen Storage Center. David A. Dixon is indebted to the Robert Ramsay Endowment of the University of Alabama. Part of this work was performed at the W. R. Wiley Environmental Molecular Sciences Laboratory, a national scientific user facility sponsored by DOE's Office of Biological and Environmental Research and located at Pacific Northwest National Laboratory, operated for the DOE by Battelle.

Appendix Geometry parameters for HX (X = F, Cl, Br, and I). Geometry parameters for BX, HBX, BX₂, and H_{3-n}BX_n for (X = F, Cl, Br, I, NH₂, OH, and SH) at the CCSD(T)/aVDZ level. Total CCSD(T) energies as a function of basis set. Total CCSD(T)/aVnZ-PP energies as a function of basis set. Calculated MP2/aVTZ frequencies (cm⁻¹). Components for calculated atomization energies for HX (X = F, Cl, Br, and I). Components for calculated atomization energies for BX, HBX, BX₂, and H_{3-n}BX_n for (X = Br and I). Electronic contribution to the CCSD(T) singlet-triplet splitting for the HBX compounds. *T*₁ diagnostics calculated at the CCSD(T)/aVQZ level. This material is available free of charge via the Internet at <http://pubs.acs.org>.

Table 6.1. Optimized CCSD(T) Bond Lengths (Å) and Bond Angles (°) for BX, HBX, BX₂, and H_(3-n)BX_n for (X = F, Cl, Br, I, NH₂, OH, and SH).

Molecule	Basis Set	R _{HX}	R _{HB}	R _{BX}	∠HBX	∠HXB	∠XBX
BF (¹ Σ ⁺ – C _{∞v})	aVTZ			1.2747			
	aVQZ			1.2686			
	expt. ^a			1.2625 ₉			
HBf (² A' – C _s)	aVTZ		1.2027	1.3094	121.0		
H ₂ Bf (¹ A ₁ – C _{2v})	aVTZ		1.1933	1.3250	117.8		
HBf ₂ (¹ A ₁ – C _{2v})	aVTZ		1.1861	1.3190	121.0		118.0
	expt. ^b		1.189(10)	1.311(5)			118.3(10)
Bf ₂ (² A ₁ – C _{2v})	aVTZ			1.3124			121.1
Bf ₃ (¹ A' – D _{3h})	aVTZ			1.3153			120.0
	expt. ^b			1.3070(1)			
Bcl (¹ Σ ⁺ – C _{∞v})	aVTZ			1.7283			
	aVQZ			1.7239			
	expt. ^a			1.715 ₉			
HBcl (² A' – C _s)	aVTZ		1.1909	1.7238	123.3		
H ₂ Bcl (¹ A ₁ – C _{2v})	aVTZ		1.1869	1.7435	118.1		
HBcl ₂ (¹ A ₁ – C _{2v})	aVTZ		1.1826	1.7423	119.7		120.7
	expt. ^b		1.13(20)	1.75			119.7(30)

BCl ₂ (² A ₁ - C _{2v})	aVTZ		1.7291			125.5
BCl ₃ (¹ A ₁ ' - D _{3h})	aVTZ		1.7446			120.0
	expt ^b		1.7421(44)			
BBr (¹ Σ ⁺ - C _{∞v})	aVTZ		1.9062			
	aVQZ		1.9044			
	expt. ^a		1.888 ₂			
HBBr (² A' - C _s)	aVTZ	1.1900	1.8804	123.6		
H ₂ BBr (¹ A ₁ - C _{2v})	aVTZ	1.9035	1.1856	117.9		
HBBr ₂ (¹ A ₁ - C _{2v})	aVTZ	1.1819	1.9026	119.3		121.4
	expt ^b	1.20	1.87			119.3(20)
BBr ₂ (² A ₁ - C _{2v})	aVTZ		1.8910			126.2
BBr ₃ (¹ A ₁ ' - D _{3h})	aVTZ		1.9081			120.0
	expt ^b		1.8932(54)			
BI (¹ Σ ⁺ - C _{∞v})	aVTZ		2.1501			
	aVQZ		2.1484			
HBI (² A' - C _s)	aVTZ	1.1902	2.0943	124.3	124.3	
H ₂ BI (¹ A ₁ - C _{2v})	aVTZ	1.1853	2.1182	117.8	117.8	
HBI ₂ (¹ A ₁ - C _{2v})	aVTZ	1.1830	2.1200	118.7	118.7	
BI ₂ (² A ₁ - C _{2v})	aVTZ		2.1087			128.2
BI ₃ (¹ A ₁ ' - D _{3h})	aVTZ		2.1315			120.0
	expt ^b		2.118(5)			

B(NH ₂) (¹ A ₁ - C _{2v})	aVTZ	1.0115		1.3875		122.8	
HB(NH ₂) (² A' - C _s)	aVTZ	1.0071	1.1941	1.3872	124.3	123.2	
		1.0111				123.4	
HB(NH ₂) ₂ (¹ A ₁ - C _{2v}) ^c	aVTZ	1.0012	1.1932	1.4143	118.6	121.9	122.7
		1.0033				124.4	
	expt ^b	1.000(1)	1.193(1)	1.414(1)		121.1(1)	122.0(3)
		1.002(2)				123.7(6)	
B(NH ₂) ₂ (¹ A ₁ - C _{2v}) ^c	aVTZ	1.0081		1.4075		124.0	126.2
		1.0023				122.4	
B(NH ₂) ₃ (¹ A' - C _s) ^c	aVTZ	1.0031		1.4341		120.7	119.9
		1.0023		1.4309		121.6	120.2
B(OH) (¹ A' - C _s)	aVTZ	0.9653		1.3130		120.7	
HB(OH) (² A' - C _s)	aVTZ	0.9626	1.1976	1.3466	120.7	113.6	
H ₂ B(OH) (¹ A' - C _s) ^c	aVTZ	0.9620	1.1887	1.3607	116.6	112.5	
			1.1941		120.5		
	expt ^b	0.967(14)	1.200	1.352(4)	117.2(8)	112.0(17)	
			1.200		121.8(8)		
HB(OH) ₂ (¹ A' - C _s) ^c	aVTZ	0.9641	1.1898	1.3635	118.5	111.5	119.1
		0.9605		1.3741	122.4	112.4	
	expt ^b	0.9590(8)	1.1972(3)	1.359(9)	118.2(12)	111.8(13)	119.1(13)
		0.9498(4)		1.365(9)	122.8(12)	113.3(17)	

B(OH) ₂ (² A' - C _s) ^c	aVTZ	0.9610		1.3662		112.6	122.6
		0.9673		1.3536		112.4	
B(OH) ₃ (¹ A' - C _{3h}) ^c	aVTZ	0.9614		1.3745		111.5	120.0
B(SH) (¹ A' - C _s)	aVTZ	1.3492		1.8213		86.3	
HB(SH) (² A' - C _s)	aVTZ	1.3432	1.1878	1.7571	124.4	99.0	
H ₂ B(SH) (¹ A' - C _s)	aVTZ	1.3411	1.1893	1.7782	123.0	98.5	
			1.1882				116.1
HB(SH) ₂ (¹ A' - C _s)	aVTZ	1.3431	1.1873	1.7960	116.7	98.2	122.1
		1.3400		1.7988	121.2	96.8	
B(SH) ₂ (² A' - C _s) ^c	aVTZ	1.3439		1.7675		99.1	129.9
		1.3360		1.7714		97.0	
B(SH) ₃ (¹ A' - C _{3h})	aVTZ	1.3418		1.8121		97.2	120.0

^a Reference 4. ^b Reference 49. ^c Geometry parameters were obtained at the MP2 level.

Table 6.2. Components for Calculated Atomization Energies in kcal/mol.

Molecule	CBS ^a	ΔE_{ZPE}^b	ΔE_{CV}^c	ΔE_{SR}^d	ΔE_{SO}^e	$\Sigma D_0(0\text{ K})^f$
BF	182.05	1.98	0.54	-0.24	-0.42	179.92
BCl	122.70	1.19	0.42	-0.07	-0.87	120.99
BBr	104.72	1.01	0.92	0.01	-3.53	101.11
BI	86.56	0.82		-0.01	-7.27	78.47
B(NH ₂)	313.47	15.75	1.17	-0.31	-0.03	298.54
B(OH)	264.99	8.34	0.87	-0.34	-0.25	256.92
B(SH)	184.30	5.70	0.59	-0.23	-0.59	178.37
HBF	232.76	7.08	0.92	-0.35	-0.42	225.83
HBCl	187.47	6.40	0.95	-0.24	-0.87	180.91
HBBr	172.52	6.16	1.38	-0.48	-3.53	163.73
HBI	157.52	5.92		-0.07	-7.27	144.25
HB(NH ₂)	387.92	23.13	1.66	-0.38	-0.03	366.04
HB(OH)	324.59	15.15	1.24	-0.40	-0.25	310.03
HB(SH)	265.77	12.41	1.19	-0.39	-0.59	253.56
H ₂ BF	343.22	14.40	1.13	-0.37	-0.42	329.16
H ₂ BCl	298.01	13.51	1.18	-0.27	-0.87	284.54
H ₂ BBr	282.05	13.22	1.66	-0.54	-3.53	266.42
H ₂ BI	266.57	12.87		-0.08	-7.27	246.35
H ₂ B(OH)	434.32	22.42	1.45	-0.40	-0.25	412.69

H ₂ B(SH)	374.88	18.97	1.42	-0.39	-0.59	356.36
HBF ₂	409.82	11.36	1.33	-0.69	-0.81	398.29
HBCl ₂	313.02	9.48	1.40	-0.44	-1.71	302.80
HBBr ₂	280.49	8.88	2.40	-0.88	-7.03	266.11
HBI ₂	248.87	8.27		-0.10	-14.51	225.99
HB(NH ₂) ₂	704.14	41.91	2.71	-0.72	-0.03	664.19
HB(OH) ₂	586.17	26.80	1.89	-0.78	-0.47	560.00
HB(SH) ₂	462.06	20.23	1.81	-0.74	-1.15	441.74
BF ₂	295.71	4.42	1.11	-0.67	-0.81	290.92
BCl ₂	203.18	2.86	1.17	-0.40	-1.71	199.38
BBr ₂	172.11	2.33	2.05	-0.75	-7.03	164.04
BI ₂	142.64	2.05		-0.09	-14.51	125.99
B(NH ₂) ₂	591.19	34.62	2.49	-0.73	-0.03	558.31
B(OH) ₂	473.28	19.60	1.68	-0.77	-0.47	454.12
B(SH) ₂	353.20	13.83	1.64	-0.73	-1.15	339.13
BF ₃	469.75	7.80	1.53	-1.05	-1.20	461.23
BCl ₃	323.71	4.88	1.61	-0.60	-2.55	317.30
BBr ₃	275.04	3.86	3.14	-1.16	-10.53	262.63
BI ₃	228.36	3.16		-0.11	-21.75	203.34
B(NH ₂) ₃	902.25	52.00	3.44	-1.07	-0.03	852.60
B(OH) ₃	733.80	30.59	2.33	-1.18	-0.69	703.67

B(SH) ₃	545.23	21.37	2.17	-1.09	-1.71	523.22
--------------------	--------	-------	------	-------	-------	--------

^a Extrapolated by using Equation (1) with aVnZ, $n = D, T, Q$. ^b The zero point energies were obtained as described in the text. ^c Core-valence corrections were obtained with the cc-pwCVTZ (B, N, O, F, S, Cl) and cc-pwCVTZ-PP (Br and I) basis sets at the optimized CCSD(T)/aVTZ or MP2/aVTZ geometries. ^d The scalar relativistic correction is based on a CISD(FC)/VTZ MVD calculation and is expressed relative to the CISD result without the MVD correction, i.e. including the existing relativistic effects resulting from the use of a relativistic effective core potential. ^e Correction due to the incorrect treatment of the atomic asymptotes as an average of spin multiplets. Values are based on C. Moore's Tables, ref. [36]. ^f The theoretical value of the dissociation energy to atoms $\Sigma D_0(0\text{ K})$.

Table 6.3. Heats of Formation (kcal/mol) at 0 K and 298 K.^a

Molecule	$\Delta H_f(0\text{ K})_{\text{theory}}$	$\Delta H_f(298\text{ K})_{\text{theory}}$	$\Delta H_f(298\text{ K})_{\text{expt}}$	$\Delta H_f(298\text{ K})_{\text{other}}$
HF ($^1\Sigma^+$)	-65.5	-64.8	-65.32 ± 0.17^b	-65.2^c
HCl ($^1\Sigma^+$)	-22.1	-22.1	-22.06 ± 0.024^b	-22.6^c
HBr ($^1\Sigma^+$)	-6.6	-8.5	-8.674 ± 0.038^b	-8.6^c
HI ($^1\Sigma^+$)	7.3	6.8	6.334 ± 0.024^b	5.5^c
BH ($^1\Sigma^+$) ^d	105.1	105.9	105.8 ± 2.0^e	
BF ($^1\Sigma^+$)	-26.4	-25.6	-27.7 ± 3.3^e $-25.3,^f (-26.5)^g$	$(-25.5),^h -25.9,^i$ $(-26.1),^j (-24.1)^j$
BCl ($^1\Sigma^+$)	42.7	43.4	33.8 ± 4.0^e $(36.9),^g (43.5)^k$	$44.9,^i 42.5^l$
BBr ($^1\Sigma^+$)	62.2	61.1	55.9 ± 10.0^e $(59.7),^g (71.0)^m$	
BI ($^1\Sigma^+$)	82.2	82.5	72.9 ± 10.0^e	
B(NH ₂)	52.3	51.7		
B(OH)	-11.2	-11.1		
B(SH)	74.0	74.2		
HBF	-20.6	-20.6		
HBCl	34.4	34.4		34.5^l
HBBr	51.2	51.2		
HBI	68.1	67.7		

HB(NH ₂)	36.5	34.7		
HB(OH)	-12.7	-13.6		
HB(SH)	50.5	49.7		
H ₂ B ^d	77.4	77.5	48.0 ± 15.1 ^e	
H ₂ BF	-72.3	-73.3		
H ₂ BCl	-17.6	-18.5		-19.0 ^l
H ₂ BBr	0.1	-2.6		
H ₂ BI	17.6	16.3		
H ₂ B(NH ₂) ⁿ	-17.0	-19.7		
H ₂ B(OH)	-63.7	-65.6		
H ₂ B(SH)	-0.7	-2.4		
HBF ₂	-174.6	-175.5	-175.4 ± 0.8 ^e	
HBCl ₂	-58.9	-59.6	-59.3 ± 1.0 ^e	-60.7 ^l
HBBr ₂	-23.0	-27.2	-25.0 ± 1.2 ^e	
HBI ₂	12.0	10.6		
HB(NH ₂) ₂	-45.9	-49.9		
HB(OH) ₂	-152.0	-154.6		
HB(SH) ₂	-20.4	-22.5		
BF ₂	-118.9	-118.7	-141.0 ± 3.1, ^e -120.0 ± 4, ^f ≤ -124 ± 9 ^o	-118.9, ⁱ -118.2 ^p
BCl ₂	-7.1	-6.9	-19.0 ± 3.0 ^e	-5.9, ⁱ -6.8, ^l -6.8 ^p

BBr ₂	27.4	24.2	15.0 ± 3.6 ^e	
BI ₂	60.3	59.9	58.1 ± 15.1 ^e	
B(NH ₂) ₂	8.4	5.5		
B(OH) ₂	-97.8	-99.3	-114.00 ± 3.6 ^e	-97.4 ^p
B(SH) ₂	30.5	29.5		
BH ₃ ⁿ	25.3	24.4	25.5 ± 2.4 ^e	
BF ₃	-270.7	-271.4	-271.4 ± 0.4 ^e	(-271.0), ^h (-269.8) ^q
BCl ₃	-96.4	-96.7	-96.3 ± 0.5 ^e	-98.6, ^l (-95.8) ^q
BBr ₃	-43.0	-48.3	-48.8 ± 0.05 ^e	
BI ₃	8.6	7.6	17.0 ± 12.0 ^e	
B(NH ₂) ₃	-70.1	-74.9		
B(OH) ₃	-236.7	-239.8	-237.2 ± 0.6 ^e	
B(SH) ₃	-36.3	-38.4		

^a Values given in parenthesis are at 0 K. ^b Reference 5. ^c Reference 19. ^d Reference 45. ^e Reference 6. ^f Reference 52. ^g Reference 4. ^h Reference 21. ⁱ Reference 22. ^j Reference 24. ^k Reference 53. ^l Reference 23. ^m Reference 54. ⁿ Reference 44. ^o Reference 55. ^p Calculated at the G3(MP2) level in this work. Reference ⁶². ^q Reference 11i.

Table 6.4 B-X and B-H Bond Dissociation Energies (BDE) in kcal/mol at 0 K.

Bond	BDE _{calc} This work	BDE _{expt}	BDE _{other theory}
BF ₃ → BF ₂ + F	170.3	150.0, ^a 149.4, ^b 169 ^c	170.2, ^d 172.0, ^e 171.0 ^e
BCl ₃ → BCl ₂ + Cl	117.9	106.3, ^b 110.0 ^a	118.5 ^d
BBr ₃ → BBr ₂ + Br	98.3	89.7 ^b	
BI ₃ → BI ₂ + I	77.3	66.5 ^b	
B(NH ₂) ₃ → B(NH ₂) ₂ + NH ₂	123.8		
B(OH) ₃ → B(OH) ₂ + OH	147.8	132.1 ± 7 ^b	
B(SH) ₃ → B(SH) ₂ + SH	99.4		
HBF ₂ → HBF + F	172.5		174.0, ^e 172.2 ^e
HBCl ₂ → HBCl + Cl	121.9		
HBBr ₂ → HBBr + Br	102.1		
HBI ₂ → HBI + I	81.7		
HB(NH ₂) ₂ → HB(NH ₂) + NH ₂	127.6		
HB(OH) ₂ → HB(OH) + OH	148.2		
HB(SH) ₂ → HB(SH) + SH	103.5		
BF ₂ → BF + F	111.0	136, ^a 132.3, ^b 110 ^c	110.9 ^d , 109.7, ^e 110.2 ^e
BCl ₂ → BCl + Cl	78.4	81.8, ^b 93 ^a	78.9 ^d
BBr ₂ → BBr + Br	62.7	67.7 ^b	
BI ₂ → BI + I	47.5	40.5 ^b	
B(NH ₂) ₂ → B(NH ₂) + NH ₂	89.2		
B(OH) ₂ → B(OH) + OH	95.4	121.3 ± 7 ^b	
B(SH) ₂ → B(SH) + SH	76.1		
H ₂ BF → BH ₂ + F	168.2	144.4 ± 6 ^f	169.9, ^e 167.8 ^e
H ₂ BCl → BH ₂ + Cl	123.6		
H ₂ BBr → BH ₂ + Br	105.2		
H ₂ BI → BH ₂ + I	85.4		
H ₂ B(NH ₂) → BH ₂ + NH ₂	139.7		
H ₂ B(OH) → BH ₂ + OH	150.0		

$\text{H}_2\text{B}(\text{SH}) \rightarrow \text{BH}_2 + \text{SH}$	110.7		
$\text{HBF} \rightarrow \text{BH} + \text{F}$	144.2	$145.5 \pm 6^{\text{f}}$	$142.5,^{\text{e}} 143.3^{\text{e}}$
$\text{HBCl} \rightarrow \text{BH} + \text{Cl}$	99.3		
$\text{HBBr} \rightarrow \text{BH} + \text{Br}$	81.9		
$\text{HBI} \rightarrow \text{BH} + \text{I}$	62.6		
$\text{HB}(\text{NH}_2) \rightarrow \text{BH} + \text{NH}_2$	113.9		
$\text{HB}(\text{OH}) \rightarrow \text{BH} + \text{OH}$	126.6		
$\text{HB}(\text{SH}) \rightarrow \text{BH} + \text{SH}$	87.3		
$\text{BF} \rightarrow \text{B} + \text{F}$	179.9	$180.0,^{\text{c}} 180.1^{\text{g}}$	$181.0 \pm 0.2,^{\text{h}} 179.9,^{\text{d}}$ $180.8,^{\text{e}} 178.8^{\text{e}}$
$\text{BCl} \rightarrow \text{B} + \text{Cl}$	121.0	$122.2 \pm 1.1,^{\text{i}} 126.8,^{\text{g}}$ 129^{b}	121.5^{d}
$\text{BBr} \rightarrow \text{B} + \text{Br}$	100.9	$104.6,^{\text{b}} 103.5,^{\text{g}}$ $93.4 \pm 0.1,^{\text{j}} 94.6^{\text{k}}$	
$\text{BI} \rightarrow \text{B} + \text{I}$	78.5	86.4^{b}	
$\text{B}(\text{NH}_2) \rightarrow \text{B} + \text{NH}_2$	128.0		
$\text{B}(\text{OH}) \rightarrow \text{B} + \text{OH}$	155.2	$144.3 \pm 7^{\text{f}}$	
$\text{B}(\text{SH}) \rightarrow \text{B} + \text{SH}$	93.7		
$\text{BH} \rightarrow \text{B} + \text{H}$	81.6	$83.9,^{\text{l}} 81.3,^{\text{m}} 82.5 \pm 0.6^{\text{n}}$	
$\text{HF} \rightarrow \text{F} + \text{H}$	135.6	$135.2 \pm 0.2^{\text{b}}$	
$\text{HCl} \rightarrow \text{Cl} + \text{H}$	102.3	$102.23 \pm 0.05^{\text{b}}$	
$\text{HBr} \rightarrow \text{Br} + \text{H}$	86.3	$86.64 \pm 0.04^{\text{b}}$	
$\text{HI} \rightarrow \text{I} + \text{H}$	69.9	$70.42 \pm 0.05^{\text{b}}$	
$\text{BH}_3 \rightarrow \text{BH}_2 + \text{H}$	103.7	$74.6,^{\text{b}} 82.6^{\text{l}}$	
$\text{NH}_3 \rightarrow \text{NH}_2 + \text{H}$	106.5		
$\text{H}_2\text{O} \rightarrow \text{OH} + \text{H}$	117.6		
$\text{H}_2\text{S} \rightarrow \text{SH} + \text{H}$	88.5		
$\text{HBF}_2 \rightarrow \text{BF}_2 + \text{H}$	107.4	86.5^{b}	$108.8,^{\text{e}} 107.1^{\text{e}}$
$\text{HBCl}_2 \rightarrow \text{BCl}_2 + \text{H}$	103.4		
$\text{HBBr}_2 \rightarrow \text{BBr}_2 + \text{H}$	102.1		
$\text{HBI}_2 \rightarrow \text{BI}_2 + \text{H}$	100.0		
$\text{HB}(\text{NH}_2)_2 \rightarrow \text{B}(\text{NH}_2)_2 + \text{H}$	105.9		
$\text{HB}(\text{OH})_2 \rightarrow \text{B}(\text{OH})_2 + \text{H}$	105.9		

$\text{HB}(\text{SH})_2 \rightarrow \text{B}(\text{SH})_2 + \text{H}$	102.6		
$\text{H}_2\text{BF} \rightarrow \text{HBF} + \text{H}$	103.3		104.8, ^e 103.4 ^e
$\text{H}_2\text{BCl} \rightarrow \text{HBCl} + \text{H}$	103.6		
$\text{H}_2\text{BBr} \rightarrow \text{HBBr} + \text{H}$	102.7		
$\text{H}_2\text{BI} \rightarrow \text{HBI} + \text{H}$	102.1		
$\text{H}_2\text{B}(\text{NH}_2) \rightarrow \text{HB}(\text{NH}_2) + \text{H}$	105.1		
$\text{H}_2\text{B}(\text{OH}) \rightarrow \text{HB}(\text{OH}) + \text{H}$	102.7		
$\text{H}_2\text{B}(\text{SH}) \rightarrow \text{HB}(\text{SH}) + \text{H}$	102.8		
$\text{BH}_2 \rightarrow \text{BH} + \text{H}$	79.3	109.9, ^b 89.9 ^l	
$\text{HBF} \rightarrow \text{BF} + \text{H}$	45.9		44.5, ^e 45.2 ^e
$\text{HBCl} \rightarrow \text{BCl} + \text{H}$	59.9		
$\text{HBBr} \rightarrow \text{BBr} + \text{H}$	62.6		
$\text{HBI} \rightarrow \text{BI} + \text{H}$	65.8		
$\text{HB}(\text{NH}_2) \rightarrow \text{BNH}_2 + \text{H}$	67.5		
$\text{HB}(\text{OH}) \rightarrow \text{BOH} + \text{H}$	53.1		
$\text{HB}(\text{SH}) \rightarrow \text{BSH} + \text{H}$	75.2		

^a Reference 57. ^b Reference 6. ^c Reference 52. ^d Reference 22. ^e Reference 24. ^f

Reference 48. ^g Reference 4. ^h Reference 21. ⁱ Reference 53. ^j Reference 54. ^k Reference

56. ^l Reference 7. ^m Reference 8. ⁿ Reference 9.

Table 6.5. Disproportionation Reactions in kcal/mol at 0 K and 298 K.

Disproportionation Reactions	$\Delta H_{\text{rxn}}(0 \text{ K})_{\text{theory}}$	$\Delta H_{\text{rxn}}(298 \text{ K})_{\text{theory}}$
$2\text{HBF}_2 \rightarrow \text{H}_2\text{BF} + \text{BF}_3$	6.2	6.3
$\text{H}_2\text{BF} + \text{HBF}_2 \rightarrow \text{BH}_3 + \text{BF}_3$	1.5	2.7
$2\text{H}_2\text{BF} \rightarrow \text{BH}_3 + \text{HBF}_2$	-4.7	-3.6
$2\text{HBCl}_2 \rightarrow \text{H}_2\text{BCl} + \text{BCl}_3$	3.7	4.0
$\text{H}_2\text{BCl} + \text{HBCl}_2 \rightarrow \text{BH}_3 + \text{BCl}_3$	5.4	6.7
$2\text{H}_2\text{BCl} \rightarrow \text{BH}_3 + \text{HBCl}_2$	1.6	2.8
$2\text{HBBr}_2 \rightarrow \text{H}_2\text{BBr} + \text{BBr}_3$	3.3	3.6
$\text{H}_2\text{BBr} + \text{HBBr}_2 \rightarrow \text{BH}_3 + \text{BBr}_3$	5.3	6.8
$2\text{H}_2\text{BBr} \rightarrow \text{BH}_3 + \text{HBBr}_2$	2.0	3.3
$2\text{HBI}_2 \rightarrow \text{H}_2\text{BI} + \text{BI}_3$	2.3	2.7
$\text{H}_2\text{BI} + \text{HBI}_2 \rightarrow \text{BH}_3 + \text{BI}_3$	4.3	6.0
$2\text{H}_2\text{BI} \rightarrow \text{BH}_3 + \text{HBI}_2$	2.0	3.3
$2\text{HB}(\text{NH}_2)_2 \rightarrow \text{H}_2\text{B}(\text{NH}_2) + \text{B}(\text{NH}_2)_3$	4.6	5.1
$\text{H}_2\text{B}(\text{NH}_2) + \text{HB}(\text{NH}_2)_2 \rightarrow \text{BH}_3 + \text{B}(\text{NH}_2)_3$	18.0	19.0
$2\text{H}_2\text{B}(\text{NH}_2) \rightarrow \text{BH}_3 + \text{HB}(\text{NH}_2)_2$	13.4	13.9
$2\text{HB}(\text{OH})_2 \rightarrow \text{H}_2\text{B}(\text{OH}) + \text{B}(\text{OH})_3$	3.6	3.8
$\text{H}_2\text{B}(\text{OH}) + \text{HB}(\text{OH})_2 \rightarrow \text{BH}_3 + \text{B}(\text{OH})_3$	4.3	5.6
$2\text{H}_2\text{B}(\text{OH}) \rightarrow \text{BH}_3 + \text{HB}(\text{OH})_2$	0.7	1.9
$2\text{HB}(\text{SH})_2 \rightarrow \text{H}_2\text{B}(\text{SH}) + \text{B}(\text{SH})_3$	3.9	4.2
$\text{H}_2\text{B}(\text{SH}) + \text{HB}(\text{SH})_2 \rightarrow \text{BH}_3 + \text{B}(\text{SH})_3$	10.2	11.9
$2\text{H}_2\text{B}(\text{SH}) \rightarrow \text{BH}_3 + \text{HB}(\text{SH})_2$	6.3	7.7

6.5 References

-
- ¹ Greenwood, N. N.; Earnshaw, A. *Chemistry of the Elements*, Pergamon Press, Oxford, 1984.
- ² Grant, D. J.; Matus, M. H.; Switzer, J. S.; Dixon, D. A.; Francisco, J. S.; Christe, K. O. *J. Phys Chem.*, web released, May. 2008.
- ³ Luo, T. -R. *Comprehensive Handbook of Chemical Bond Energies*; CRC Press, Taylor & Francis Group: Boca Raton, FL, 2007.
- ⁴ Huber, K. P.; Herzberg, G. *Molecular Spectra and Molecular Structure. IV. Constants of Diatomic Molecules*, Van Nostrand Reinhold Co., 1979.
- ⁵ Cox, J. D.; Wagman, D. D.; Medvedev, V. A. *CODATA Key Values for Thermodynamics*, Hemisphere Publishing Corp., New York, **1989**.
- ⁶ Chase, M.W., Jr. *NIST-JANAF Thermochemical Tables, Fourth Edition*, J. Phys. Chem. Ref. Data, Monograph 9, **1998**, 1-1951; Mallard, W. G., Eds., *NIST Chemistry WebBook*, NIST Standard Reference Database Number 69, August 1996, National Institute of Standards and Technology, Gaithersburg MD, 20899, (<http://webbook.nist.gov/chemistry/>).
- ⁷ Litzow, M. R.; Spalding, T. R. *Physical Inorganic Chemistry, Monograph No. 2. Mass Spectrometry of Inorganic and Organometallic Compounds* Elsevier, New York, 1973.
- ⁸ Pinalto, F. S.; O'Brien, L. C.; Keller, P. C.; Bernath, P. F. *J. Molec. Spec.* **1988**, *129*, 348.
- ⁹ Bauschlicher Jr., C. H.; Langhoff, S. R.; Taylor, P. R. *J. Chem. Phys.* **1990**, *93*, 502.
- ¹⁰ Dunning, T. H., Jr. *J. Phys. Chem.* **2000**, *104*, 9062.
- ¹¹ (a) Peterson, K. A.; Xantheas, S. S.; Dixon, D. A.; Dunning, T. H. Jr., *J. Phys. Chem. A* **1998**, *102*, 2449; (b) Feller, D.; Peterson, K. A. *J. Chem. Phys.* **1998**, *108*, 154; (c) Dixon, D. A.; Feller, D. *J. Phys. Chem. A* **1998**, *102*, 8209; (d) Feller, D.; Peterson, K. A. *J. Chem. Phys.* **1999**, *110*, 8384; (e) Feller, D.; Dixon, D. A. *J. Phys. Chem. A* **1999**, *103*, 6413; (f) Feller, D. *J. Chem. Phys.* 1999, *111*, 4373; (g) Feller, D.; Dixon, D. A. *J. Phys. Chem. A* **2000**, *104*, 3048; (h) Feller, D.; Sordo, J. A. *J. Chem. Phys.* **2000**, *113*, 485; (i) Feller, D.; Dixon, D. A. *J. Chem. Phys.* **2001**, *115*, 3484; (j) Dixon, D. A.; Feller, D.; Sandrone, G. *J. Phys. Chem. A* **1999**, *103*, 4744; (k) Ruscic, B.; Wagner, A. F.; Harding, L. B.; Asher, R. L.; Feller, D.; Dixon, D. A.; Peterson, K. A.; Song, Y.; Qian, X.; Ng, C.; Liu, J.; Chen, W.; Schwenke, D. W. *J. Phys. Chem. A* **2002**, *106*, 2727; (l) Feller, D.; Dixon, D.A.; Peterson, K.A. *J. Phys. Chem. A*, **1998**, *102*, 7053; (m) Dixon, D.A.; Feller, D. ; Peterson, K.A. *J. Chem. Phys.*, **2001**, *115*, 2576.

-
- ¹² Purvis III, G. D.; Bartlett, R. J. *J. Chem. Phys.* **1982**, *76*, 1910.
- ¹³ Raghavachari, K.; Trucks, G. W.; Pople, J. A.; Head-Gordon, M. *Chem. Phys. Lett.* **1989**, *157*, 479.
- ¹⁴ Watts, J. D.; Gauss, J.; Bartlett, R. J. *J. Chem. Phys.* **1993**, *98*, 8718.
- ¹⁵ Dunning, T. H. *J. Chem. Phys.* **1989**, *90*, 1007.
- ¹⁶ Kendall, R. A.; Dunning Jr., T. H.; Harrison, R. J. *J. Chem. Phys.* **1992**, *96*, 6796.
- ¹⁷ McQuarrie, D. A. *Statistical Mechanics*, University Science Books: Sausalito, CA, 2001.
- ¹⁸ Curtiss, L. A.; Raghavachari, K.; Redfern, P. C.; Pople, J. A. *J. Chem. Phys.* **1997**, *106*, 1063.
- ¹⁹ Feller, D.; Peterson, K. A.; Jong, W. A. de; Dixon, D. A., *J. Chem. Phys.* **2003**, *118*, 3510.
- ²⁰ Dixon, D. A.; Grant, D. J.; Christe, K. O.; Peterson, K. A. *Inorg. Chem.* **2008**, *47*, 5485
- ²¹ Martin, J. M. L.; Taylor, P. R. *J. Phys. Chem.* **1998**, *102*, 2995.
- ²² Bauschlicher Jr., C. W.; Ricca, A. *J. Phys. Chem. A* **1999**, *103*, 4313.
- ²³ Schlegel, H. B.; Harris, S. J. *J. Phys. Chem.* **1994**, *98*, 11178.
- ²⁴ Rablen, P. R.; Hartwig, J. F. *J. Am. Chem. Soc.* **1996**, *118*, 4648.
- ²⁵ Baeck, K. K.; Bartlett, R. J. *J. Chem. Phys.* **1997**, *106*, 4604.
- ²⁶ Dunning, T. H. Jr., Peterson, K. A. Wilson, A. K. *J. Chem. Phys.* **2001**, *114*, 9244.
- ²⁷ Peterson, K. A.; Woon, D. E.; Dunning, T. H., Jr. *J. Chem. Phys.* **1994**, *100*, 7410.
- ²⁸ Peterson, K. A.; Dunning, T. H., Jr., *J. Chem. Phys.* **2002**, *117*, 10548.
- ²⁹ (a) Peterson, K. A. *J. Chem. Phys.* **2003**, *119*, 11099; (b) Peterson, K. A.; Figgien, D.; Goll, E.; Stoll, H.; Dolg, M. *J. Chem. Phys.* **2003**, *119*, 11113.
- ³⁰ Werner, H.-J.; Knowles, P. J.; Amos, R. D.; Bernhardsson, A.; Berning, A.; Celani, P.; Cooper, D. L.; Deegan, M. J. O.; Dobbyn, A. J.; Eckert, F.; Hampel, C.; Hetzer, G.; Korona, T.; Lindh, R.; Lloyd, A. W.; McNicholas, S. J.; Manby, F. R.; Meyer, W.; Mura,

M. E.; Nicklass, A.; Palmieri, P.; Pitzer, R. M.; Rauhut, G.; Schütz, M.; Stoll, H.; Stone, A. J.; Tarroni, R.; Thorsteinsson, T. MOLPRO-2002, a package of initio programs written by, Universität Stüttgart, Stüttgart, Germany, University of Birmingham, Birmingham, United Kingdom, 2002.

³¹ Rittby, M.; Bartlett, R. J. *J. Phys. Chem.* **1988**, *92*, 3033.

³² Knowles, P. J.; Hampel, C.; Werner, H. –J. *J. Chem. Phys.* **1994**, *99*, 5219.

³³ Deegan, M. J. O.; Knowles, P. J. *Chem. Phys. Lett.* **1994**, *227*, 321.

³⁴ (a) Møller, C.; Plesset, M.S. *Phys. Rev.* **1934**, *46*, 618; (b) Pople, J.A.; Binkley, J.S.; Seeger, R. *Int. J. Quantum Chem. Symp.* **1976**, *10*, 1.

³⁵ Gaussian 03, Revision C.02, Frisch, M. J.; Trucks, G. W.; Schlegel, H. B.; Scuseria, G. E.; Robb, M. A.; Cheeseman, J. R.; Montgomery, Jr., J. A.; Vreven, T.; Kudin, K. N.; Burant, J. C.; Millam, J. M.; Iyengar, S. S.; Tomasi, J.; Barone, V.; Mennucci, B.; Cossi, M.; Scalmani, G.; Rega, N.; Petersson, G. A.; Nakatsuji, H.; Hada, M.; Ehara, M.; Toyota, K.; Fukuda, R.; Hasegawa, J.; Ishida, M.; Nakajima, T.; Honda, Y.; Kitao, O.; Nakai, H.; Klene, M.; Li, X.; Knox, J. E.; Hratchian, H. P.; Cross, J. B.; Bakken, V.; Adamo, C.; Jaramillo, J.; Gomperts, R.; Stratmann, R. E.; Yazyev, O.; Austin, A. J.; Cammi, R.; Pomelli, C.; Ochterski, J. W.; Ayala, P. Y.; Morokuma, K.; Voth, G. A.; Salvador, P.; Dannenberg, J. J.; Zakrzewski, V. G.; Dapprich, S.; Daniels, A. D.; Strain, M. C.; Farkas, O.; Malick, D. K.; Rabuck, A. D.; Raghavachari, K.; Foresman, J. B.; Ortiz, J. V.; Cui, Q.; Baboul, A. G.; Clifford, S.; Cioslowski, J.; Stefanov, B. B.; Liu, G.; Liashenko, A.; Piskorz, P.; Komaromi, I.; Martin, R. L.; Fox, D. J.; Keith, T.; Al-Laham, M. A.; Peng, C. Y.; Nanayakkara, A.; Challacombe, M.; Gill, P. M. W.; Johnson, B.; Chen, W.; Wong, M. W.; Gonzalez, C.; and Pople, J. A.; Gaussian, Inc., Wallingford CT, 2004.

³⁶ C. E. Moore "Atomic energy levels as derived from the analysis of optical spectra, Volume 1, H to V," U.S. National Bureau of Standards Circular 467, U.S. Department of Commerce, National Technical Information Service, COM-72-50282, Washington, D.C.; **1949**.

³⁷ Davidson, E. R.; Ishikawa, Y.; Malli, G. L. *Chem. Phys. Lett.* **1981**, *84*, 226.

³⁸ (a) Douglas, M.; Kroll, N. M. *Ann. Phys.* **1974**, *82*, 89-155. (b) Hess, B. A. *Phys. Rev. A* **1985**, *32*, 756-763. (c) Hess, B. A. *Phys. Rev. A* **1986**, *33*, 3742-3748.

³⁹ de Jong, W.A.; Harrison, R.J.; Dixon, D.A. *J. Chem. Phys.* **2001**, *114*, 48.

⁴⁰ EMSL basis set library. <http://www.emsl.pnl.gov/forms/basisform.html>

⁴¹ Karton, A.; Martin, J. M. L. *J. Phys. Chem. A* **2007**, *111*, 5936.

-
- ⁴² Storms E.; Mueller, B. *J. Phys. Chem.* **1977**, *81*, 318.
- ⁴³ Ruscic, B.; Mayhew, C. A.; Berkowitz, J. *J. Chem. Phys.* **1988**, *88*, 5580.
- ⁴⁴ Gutowski, M.; Dixon, D. *J. Phys. Chem. A* **2005**, *109*, 5129.
- ⁴⁵ Grant, D. J.; Dixon, D. A. *J. Phys. Chem. A* **2006**, *110*, 12955.
- ⁴⁶ Matus, M. H.; Anderson, K. A.; Camaioni, D. M.; Autrey, S. T.; Dixon, D. A. *J. Phys. Chem. A* **2007**, *111*, 4411.
- ⁴⁷ Martin, J. M. L.; Taylor, P. R. *J. Phys. Chem. A* **1998**, *102*, 2995.
- ⁴⁸ Gurvich, L. V.; Veyts, I. V.; Alcock, C. B. *Thermodynamic Properties of Individual Substances*, Vol. 3, Begell House, New York, 1996.
- ⁴⁹ Kuchitsu, K. Ed. *Structure of Free Polyatomic Molecules - Basic Data*; Springer: Berlin, 1998.
- ⁵⁰ Lee, T. J.; Taylor, P. R. *Int. J. Quantum Chem. Symp.* **1989**, *23*, 199
- ⁵¹ Our present values for the molecular atomization energies of BF₃ and BCl₃ of 461.2 and 317.3 kcal/mol are in excellent agreement with the previously reported theoretical values of 461.4 and 137.8 kcal/mol respectively,¹¹ⁱ as well as the value of 462.6 kcal/mol reported by Martin and Taylor.²¹
- ⁵² Lau, K. H.; Hildebrand, D. L. *J. Chem. Phys.* **1980**, *72*, 4928.
- ⁵³ Hildenbrand, D. L. *J. Chem. Phys.* **1996**, *105*, 10507.
- ⁵⁴ Hunt, N. T.; Fan, W. Y.; Liu, Z.; Davies, P. B. *J. Mol. Spec.* **1998**, *191*, 326.
- ⁵⁵ Margrave, J. L. *J. Phys. Chem.* **1962**, *66*, 1209.
- ⁵⁶ Bharate, N. S.; Bhartiya, J. B.; Behere, S. H. *Proc. Indian Natl. Sci. Acad. Part A* **1991**, *419*.
- ⁵⁷ Hildenbrand, D. L.; Lau, K. H.; Baglio, J. W.; Struck, C. W. *J. Phys. Chem. A* **2001**, *105*, 4114.
- ⁵⁸ Hall Jr., J. H.; Halgren, T. A.; Kleier, D. A.; Lipscomb, W. N. *J. Inorg. Chem.* **1974**, *103*, 2520.
- ⁵⁹ Brazier, C. R. *J. Molec. Spec.* **1996**, *177*, 90.

⁶⁰ Christe, K. Diplomarbeit, *Über die katalytische Hydrierung von Borsäuremethylester und Borontrichlorid*, Anorganisches Institut der Technologie Hochschule, Stuttgart, 1959.

⁶¹ Murib, J.H.; Bonecutter, C.A. *Preparation of Boron Compounds*, U.S. Patent, 3216797, Nov. 9, 1965; *Verfahren zur Herstellung von Borhydriden*, German patent, 1094248, May 25, 1961.

⁶² Curtiss, L. A.; Redfern, P. C.; Raghavachari, K.; Rassolov, V.; Pople, J. A. *J. Chem. Phys.* **1999**, *110*, 4703.

6.6 *Appendix***Table A6.1.** Optimized CCSD(T) Bond Lengths (\AA) for HX for (X = F, Cl, Br, and I).

Molecule	Basis Set	R_{HX}
HF (${}^1\Sigma^+ - C_{\infty v}$)	aVDZ	0.9242
	aVTZ	0.9210
	aVQZ	0.9177
HCl (${}^1\Sigma^+ - C_{\infty v}$)	aVDZ	1.2872
	aVTZ	1.2760
	aVQZ	1.2760
HBr (${}^1\Sigma^+ - C_{\infty v}$)	aVDZ	1.4288
	aVTZ	1.4196
	aVQZ	1.4189
HI (${}^1\Sigma^+ - C_{\infty v}$)	aVDZ	1.6235
	aVTZ	1.6198
	aVQZ	1.6178

Table A6.2. Optimized CCSD(T) Bond Lengths (Å) and Bond Angles (°) for BX, HBX, BX₂, and H_(3-n)BX_n for (X = F, Cl, Br, I, NH₂, OH, and SH).

Molecule	Basis Set	R _{HX}	R _{HB}	R _{BX}	∠HBX	∠HXB	∠XBX
BF (¹ Σ ⁺ - C _{∞v})	aVDZ			1.3101			
HBF (² A' - C _s)	aVDZ		1.2166	1.3429	120.5	120.5	
H ₂ BF (¹ A ₁ - C _{2v})	aVDZ		1.2063	1.3558	117.4	117.4	
HBFB ₂ (¹ A ₁ - C _{2v})	aVDZ		1.1970	1.3449	121.2	121.2	
BF ₂ (² A ₁ - C _{2v})	aVDZ			1.3411			120.3
BF ₃ (¹ A' ₁ - D _{3h})	aVDZ			1.3370			120.0
BCl (¹ Σ ⁺ - C _{∞v})	aVDZ			1.7496			
HBCl (² A' - C _s)	aVDZ		1.2063	1.7463	122.7	122.7	
H ₂ BCl (¹ A ₁ - C _{2v})	aVDZ		1.2011	1.7592	118.1	118.1	
HBCl ₂ (¹ A ₁ - C _{2v})	aVDZ		1.1963	1.7569	119.6	119.6	
BCl ₂ (² A ₁ - C _{2v})	aVDZ			1.7465			125.3
BCl ₃ (¹ A' ₁ - D _{3h})	aVDZ			1.7581			120.0
BBr (¹ Σ ⁺ - C _{∞v})	aVDZ			1.9278			
HBBR (² A' - C _s)	aVDZ		1.2059	1.8975	123.1	123.1	
H ₂ BBr (¹ A ₁ - C _{2v})	aVDZ		1.2002	1.9165	117.9	117.9	
HBBR ₂ (¹ A ₁ - C _{2v})	aVDZ		1.1964	1.9146	119.2	119.2	
BBr ₂ (² A ₁ - C _{2v})	aVDZ			1.9066			126.3

BBr_3 (${}^1\text{A}'_1 - D_{3h}$)	aVDZ			1.9196			120.0
BI (${}^1\Sigma^+ - C_{\infty v}$)	aVDZ			2.1693			
HBI (${}^2\text{A}' - C_s$)	aVDZ	1.2057		2.1115	124.2	124.2	
H_2BI (${}^1\text{A}_1 - C_{2v}$)	aVDZ		1.1999	2.1316	118.0	118.0	
HBI_2 (${}^1\text{A}_1 - C_{2v}$)	aVDZ		1.1975	2.1333	118.6	118.6	
BI_2 (${}^2\text{A}_1 - C_{2v}$)	aVDZ			2.1256			128.3
BI_3 (${}^1\text{A}'_1 - D_{3h}$)	aVDZ			2.1462			120.0
$\text{B}(\text{NH}_2)$ (${}^1\text{A}_1 - C_{2v}$)	aVDZ	1.0193		1.3997		122.6	
$\text{HB}(\text{NH}_2)$ (${}^2\text{A}' - C_s$)	aVDZ	1.0148/1.0191	1.2080	1.3975	124.0	123.1/123.4	
$\text{B}(\text{OH})$ (${}^1\text{A}' - C_s$)	aVDZ	0.9704		1.3295		118.9	
$\text{HB}(\text{OH})$ (${}^2\text{A}' - C_s$)	aVDZ	0.9676	1.2120	1.3621	120.3	112.8	
$\text{B}(\text{SH})$ (${}^1\text{A}' - C_s$)	aVDZ	1.3590		1.8402		86.9	
$\text{HB}(\text{SH})$ (${}^2\text{A}' - C_s$)	aVDZ	1.3544	1.2035	1.7757	123.6	98.8	
$\text{H}_2\text{B}(\text{SH})$ (${}^1\text{A}' - C_s$)	aVDZ	1.3522	1.2035/1.2023	1.7930	122.8/116.1	98.6	
$\text{HB}(\text{SH})_2$ (${}^1\text{A}' - C_s$)	aVDZ	1.3541/1.3509	1.2013	1.8095/1.8127	116.5/121.1	98.4/96.7	122.3
$\text{B}(\text{SH})_3$ (${}^1\text{A}' - C_{3h}$)	aVDZ	1.3526		1.8252		97.3	120.0

Table A6.3. CCSD(T) Total Energies (E_h) as a Function of the Basis Set.^{a,b}

Molecule	Basis Set	E_h
HF	aVDZ	-100.263641
	aVTZ	-100.349577
	aVQZ	-100.377384
	CBS (DTQ)	-100.393207
HCl	aVDZ	-460.279700
	aVTZ	-460.345710
	aVQZ	-460.365829
	CBS (DTQ)	-460.377143
HBr	aVDZ	-2573.126878
	aVTZ	-2573.252497
	aVQZ	-2573.271275
	CBS (DTQ)	-2573.279602
HI	aVDZ	-295.759015
	aVTZ	-296.166874
	aVQZ	-296.352160
	CBS (DTQ)	-296.463334
BF	aVDZ	-124.404497
	aVTZ	-124.509794
	aVQZ	-124.541670
	CBS (DTQ)	-124.559572
BCl	aVDZ	-484.390708
	aVTZ	-484.466045
	aVQZ	-484.490162
	CBS (DTQ)	-484.503857
BBr	aVDZ	-2597.232148
	aVTZ	-2597.366396
	aVQZ	-2597.388952
	CBS (DTQ)	-2597.399536
BI	aVDZ	-319.886087
	aVTZ	-320.317928

	aVQZ	-320.511227
	CBS (DTQ)	-320.626986
B(NH ₂)	aVDZ	-80.535312
	aVTZ	-80.601842
	aVQZ	-80.621190
	CBS (DTQ)	-80.631964
B(OH)	aVDZ	-100.405366
	aVTZ	-100.489204
	aVQZ	-100.514653
	CBS (DTQ)	-100.528952
B(SH)	aVDZ	-422.97651
	aVTZ	-423.041127
	aVQZ	-423.060226
	CBS (DTQ)	-423.070898
HBF	aVDZ	-124.981158
	aVTZ	-125.089645
	aVQZ	-125.122166
	CBS (DTQ)	-125.140392
HBCl	aVDZ	-484.980146
	aVTZ	-485.066351
	aVQZ	-485.092433
	CBS (DTQ)	-485.107079
HBBr	aVDZ	-2597.832147
	aVTZ	-2597.972736
	aVQZ	-2597.996443
	CBS (DTQ)	-2598.007585
HBI	aVDZ	-320.490516
	aVTZ	-320.929537
	aVQZ	-321.123862
	CBS (DTQ)	-321.240064
HB(NH ₂)	aVDZ	-81.147462
	aVTZ	-81.218880

	aVQZ	-81.239293
	CBS (DTQ)	-81.250618
HB(OH)	aVDZ	-100.995257
	aVTZ	-101.083048
	aVQZ	-101.109261
	CBS (DTQ)	-101.123940
HB(SH)	aVDZ	-423.598094
	aVTZ	-423.668974
	aVQZ	-423.689388
	CBS (DTQ)	-423.700732
H ₂ BF	aVDZ	-125.650880
	aVTZ	-125.764191
	aVQZ	-125.797692
	CBS (DTQ)	-125.816414
H ₂ BCl	aVDZ	-485.654953
	aVTZ	-485.742082
	aVQZ	-485.768429
	CBS (DTQ)	-485.783222
H ₂ BBr	aVDZ	-2598.499257
	aVTZ	-2598.645607
	aVQZ	-2598.670433
	CBS (DTQ)	-2598.682132
H ₂ BI	aVDZ	-321.156760
	aVTZ	-321.601732
	aVQZ	-321.797129
	CBS (DTQ)	-321.913849
H ₂ B(OH)	aVDZ	-101.662709
	aVTZ	-101.756208
	aVQZ	-101.783552
	CBS (DTQ)	-101.798798
H ₂ B(SH)	aVDZ	-424.265003
	aVTZ	-424.341412

	aVQZ	-424.362804
	CBS (DTQ)	-424.374617
HBF ₂	aVDZ	-224.794050
	aVTZ	-224.994841
	aVQZ	-225.055564
	CBS (DTQ)	-225.089658
HBCl ₂	aVDZ	-944.792619
	aVTZ	-944.940467
	aVQZ	-944.986867
	CBS (DTQ)	-945.013113
HBBr ₂	aVDZ	-5170.480063
	aVTZ	-5170.746485
	aVQZ	-5170.789876
	CBS (DTQ)	-5170.809952
HBI ₂	aVDZ	-615.765406
	aVTZ	-616.612984
	aVQZ	-616.993093
	CBS (DTQ)	-617.220781
HB(NH) ₂	aVDZ	-137.099872
	aVTZ	-137.228113
	aVQZ	-137.264476
	CBS (DTQ)	-137.284614
HB(OH) ₂	aVDZ	-176.810363
	aVTZ	-176.969919
	aVQZ	-177.018071
	CBS (DTQ)	-177.045095
HB(SH) ₂	aVDZ	-822.005327
	aVTZ	-822.131765
	aVQZ	-822.168167
	CBS (DTQ)	-822.188393
BF ₂	aVDZ	-224.117464
	aVTZ	-224.314126

	aVQZ	-224.374083
	CBS (DTQ)	-224.407803
BCl ₂	aVDZ	-944.124497
	aVTZ	-944.266983
	aVQZ	-944.312341
	CBS (DTQ)	-944.338069
BBr ₂	aVDZ	-5169.814369
	aVTZ	-5170.075418
	aVQZ	-5170.117709
	CBS (DTQ)	-5170.137228
BI ₂	aVDZ	-615.103115
	aVTZ	-615.945125
	aVQZ	-616.324265
	CBS (DTQ)	-616.551491
B(NH ₂) ₂	aVDZ	-136.426791
	aVTZ	-136.549525
	aVQZ	-136.584930
	CBS (DTQ)	-136.604610
B(OH) ₂	aVDZ	-176.136506
	aVTZ	-176.291572
	aVQZ	-176.338706
	CBS (DTQ)	-176.365197
B(SH) ₂	aVDZ	-821.337370
	aVTZ	-821.459517
	aVQZ	-821.495092
	CBS (DTQ)	-821.514909
BF ₃	aVDZ	-323.928009
	aVTZ	-324.214740
	aVQZ	-324.302722
	CBS (DTQ)	-324.352267
BCl ₃	aVDZ	-1403.923303
	aVTZ	-1404.131839

	aVQZ	-1404.198366
	CBS (DTQ)	-1404.236117
BBr ₃	aVDZ	-7742.454187
	aVTZ	-7742.841032
	aVQZ	-7742.903067
	CBS (DTQ)	-7742.931561
BI ₃	aVDZ	-910.369067
	aVTZ	-911.619742
	aVQZ	-912.184587
	CBS (DTQ)	-912.523241
B(NH ₂) ₃	aVDZ	-192.373244
	aVTZ	-192.551232
	aVQZ	-192.602145
	CBS (DTQ)	-192.630395
B(OH) ₃	aVDZ	-251.953120
	aVTZ	-252.177163
	aVQZ	-252.245944
	CBS (DTQ)	-252.284679
B(SH) ₃	aVDZ	-1219.739166
	aVTZ	-1219.915703
	aVQZ	-1219.967127
	CBS (DTQ)	-1219.995773

^a Dissociation is with respect to RCCSD(T) atoms for closed shell atoms and R/UCCSD(T) for open shell atoms. Symmetry equivalencing of the p_x , p_y , and p_z orbitals was not imposed in the atomic calculations. The I RECP has a 28 electron core leaving 25 electrons to be explicitly treated. ^b CBS (DTQ) values from Eq. 1 (see text) obtained with the aVnZ basis sets with $n = D, T, Q$.

Table A6.4. CCSD(T)/aVnZ-PP ($n = D, T, Q$) Total Energies (E_h) as a Function of the BasisSet.^{a,b}

Molecule	Basis Set	E_h
HBr	aVDZ-PP	-416.230147
	aVTZ-PP	-416.298131
	aVQZ-PP	-416.315603
	CBS (DTQ-PP)	-416.325057
HI	aVDZ-PP	-295.369811
	aVTZ-PP	-295.423675
	aVQZ-PP	-295.441408
	CBS (DTQ-PP)	-295.451530
BBr	aVDZ-PP	-440.336703
	aVTZ-PP	-440.413079
	aVQZ-PP	-440.434273
	CBS (DTQ-PP)	-440.445954
BI	aVDZ-PP	-319.467324
	aVTZ-PP	-319.529677
	aVQZ-PP	-319.550841
	CBS (DTQ-PP)	-319.562990
HBBr	aVDZ-PP	-440.935945
	aVTZ-PP	-441.018655
	aVQZ-PP	-441.041047
	CBS (DTQ-PP)	-441.053306
HBI	aVDZ-PP	-320.071343
	aVTZ-PP	-320.140257
	aVQZ-PP	-320.162511
	CBS (DTQ-PP)	-320.175170
H ₂ BBr	aVDZ-PP	-441.602844
	aVTZ-PP	-441.691411
	aVQZ-PP	-441.714942
	CBS (DTQ-PP)	-441.727779

H ₂ BI	aVDZ-PP	-320.737180
	aVTZ-PP	-320.811863
	aVQZ-PP	-320.835221
	CBS (DTQ-PP)	-320.848425
HBBr ₂	aVDZ-PP	-856.687532
	aVTZ-PP	-856.838352
	aVQZ-PP	-856.879134
	CBS (DTQ-PP)	-856.901476
HBI ₂	aVDZ-PP	-614.956166
	aVTZ-PP	-615.079505
	aVQZ-PP	-615.119943
	CBS (DTQ-PP)	-615.143009
BBr ₂	aVDZ-PP	-856.022289
	aVTZ-PP	-856.167591
	aVQZ-PP	-856.207189
	CBS (DTQ-PP)	-856.228920
BI ₂	aVDZ-PP	-614.294607
	aVTZ-PP	-614.412500
	aVQZ-PP	-614.451905
	CBS (DTQ-PP)	-614.474463
BBr ₃	aVDZ-PP	-1271.765737
	aVTZ-PP	-1271.979143
	aVQZ-PP	-1272.037184
	CBS (DTQ-PP)	-1272.069022
BI ₃	aVDZ-PP	-909.170019
	aVTZ-PP	-909.342589
	aVQZ-PP	-909.400121
	CBS (DTQ-PP)	-909.433040

^a Dissociation is with respect to RCCSD(T) atoms for closed shell atoms and R/UCCSD(T) for open shell atoms. Symmetry equivalencing of the p_x, p_y, and p_z orbitals was not imposed in the atomic calculations. The Br and I RECP have a 10 and 28 electron core respectively, leaving 25

electrons to be explicitly treated. ^b CBS (DTQ) values from Eq. 1 (see text) obtained with the aVnZ-PP basis sets with $n = D, T, Q$.

Table A6.5. Calculated Vibrational MP2/aVTZ Frequencies (cm⁻¹).

Molecule	Symmetry	Calculated
HF ($C_{\infty v}$) ^a	ω_e	4256.1
	$\omega_e X_e$	6.01
BF ($C_{\infty v}$) ^a	ω_e	1390.7
	$\omega_e X_e$	11.9
HBF (C_s)	a'	2614.9
	a'	1317.1
	a'	1023.5
H ₂ BF (C_{2v})	a_1	2638.4
	a_1	1363.9
	a_1	1189.0
	b_1	1105.6
	b_2	2741.5
	b_2	1035.6
HBF ₂ (C_{2v})	a_1	2759.7
	a_1	1169.6
	a_1	535.9
	b_1	944.4
	b_2	1421.7
	b_2	1116.5
BF ₂ (C_{2v})	a_1	1157.8
	a_1	518.0
	b_2	1417.7
BF ₃ (D_{3h})	e'	1463.9
	e'	1463.9
	e'	474.9
	e'	474.9
	a_1'	887.9
	a_2''	691.1
HCl ($C_{\infty v}$) ^a	ω_e	3039.7
	$\omega_e X_e$	4.30

BCl ($C_{\infty v}$) ^a	ω_e	834.5
	$\omega_e X_e$	5.4
HBCl (C_s)	a'	2697.9
	a'	922.6
	a'	857.0
H ₂ BCl (C_{2v})	a_1	2666.3
	a_1	1256.5
	a_1	840.9
	b_1	1021.9
	b_2	2778.9
	b_2	883.8
HBCl ₂ (C_{2v})	a_1	2748.9
	a_1	749.6
	a_1	293.7
	b_1	803.2
	b_2	1114.7
	b_2	919.1
BCl ₂ (C_{2v})	a_1	711.0
	a_1	285.4
	b_2	1004.8
BCl ₃ (D_{3h})	e'	977.3
	e'	977.3
	e'	256.2
	e'	256.2
	a_1'	482.4
	a_2''	460.8
HBr ($C_{\infty v}$) ^a	ω_e	2678.2
	$\omega_e X_e$	3.79
BBr ($C_{\infty v}$) ^a	ω_e	680.1
	$\omega_e X_e$	3.7
HBBr (C_s)	a'	2707.8
	a'	864.3

	a'	738.6
H ₂ BBr (C _{2v})	a ₁	2674.2
	a ₁	1237.1
	a ₁	711.3
	b ₁	996.7
	b ₂	2792.5
	b ₂	838.5
HBBR ₂ (C _{2v})	a ₁	2753.0
	a ₁	614.7
	a ₁	183.7
	b ₁	755.8
	b ₂	1068.4
	b ₂	811.0
BBr ₂ (C _{2v})	a ₁	567.7
	a ₁	178.3
	b ₂	889.0
BBr ₃ (D _{3h})	e'	850.3
	e'	850.3
	e'	155.8
	e'	155.8
	a ₁ '	291.5
	a ₂ "	394.5
HI (C _{∞v}) ^a	ω _e	2324.7
	ω _e X _e	39.0
BI (C _{∞v}) ^a	ω _e	573.5
	ω _e X _e	2.7
HBI (C _s)	a'	2707.8
	a'	790.9
	a'	644.9
H ₂ BI (C _{2v})	a ₁	2673.0
	a ₁	1200.0
	a ₁	619.4

	b ₁	959.6
	b ₂	2794.3
	b ₂	760.4
HBI ₂ (C _{2v})	a ₁	2740.5
	a ₁	515.3
	a ₁	125.1
	b ₁	694.1
	b ₂	993.0
	b ₂	720.1
BI ₂ (C _{2v})	a ₁	509.8
	a ₁	121.6
	b ₂	799.9
BI ₃ (D _{3h})	e'	738.3
	e'	738.3
	e'	104.5
	e'	104.5
	a ₁ '	202.4
	a ₂ ''	323.7
B(NH ₂) (C _{2v}) ^b	a ₁	3539.6
	a ₁	1572.1
	a ₁	1251.9
	b ₁	401.9
	b ₂	3651.6
	b ₂	610.7
HB(NH ₂) (C _s)	a'	3698.8
	a'	3581.9
	a'	2676.0
	a'	1627.4
	a'	1320.2
	a'	1078.6
	a'	753.8
	a''	851.3

	a''	590.3
HB(NH ₂) ₂ (C _{2v})	a ₁	3771.7
	a ₁	3655.6
	a ₁	2650.5
	a ₁	1638.5
	a ₁	1199.8
	a ₁	928.5
	a ₁	394.5
	b ₁	941.6
	b ₁	605.1
	b ₁	355.7
	b ₂	3773.0
	b ₂	3655.9
	b ₂	1642.1
	b ₂	1441.2
	b ₂	1109.7
	b ₂	816.4
	a ₂	460.1
a ₂	310.6	
B(NH ₂) ₂ (C _{2v})	a ₁	3737.5
	a ₁	3595.2
	a ₁	1624.7
	a ₁	1157.2
	a ₁	926.0
	a ₁	370.0
	b ₁	573.2
	b ₁	361.6
	b ₂	3738.2
	b ₂	3597.4
	b ₂	1623.6
	b ₂	1416.8
b ₂	837.5	

	a ₂	348.9
	a ₂	306.9
B(NH ₂) ₃ (C _s)	a'	3768.4
	a'	3660.4
	a'	3650.3
	a'	1648.1
	a'	1638.8
	a'	1406.8
	a'	608.7
	a'	480.3
	a'	377.6
	a'	326.7
	a'	286.4
	a''	3768.8
	a''	3756.6
	a''	3659.7
	a''	1636.9
	a''	1412.1
	a''	940.6
	a''	843.7
	a''	376.2
	a''	175.4
	a''	114.7
B(OH) (C _s) ^b	a'	3824.0
	a'	1391.7
	a'	621.4
HB(OH) (C _s)	a'	3849.2
	a'	2648.1
	a'	1330.7
	a'	114.7
	a'	885.3
	a''	768.9

$\text{H}_2\text{B}(\text{OH})$ (C_s)	a'	3835.9
	a'	2705.0
	a'	2601.6
	a'	1338.2
	a'	1187.1
	a'	1161.2
	a'	884.3
	a''	1066.7
	a''	779.6
$\text{HB}(\text{OH})_2$ (C_s)	a'	3887.7
	a'	3886.3
	a'	2688.7
	a'	1439.6
	a'	1236.2
	a'	1122.4
	a'	1003.3
	a'	968.3
	a'	470.1
	a''	939.9
	a''	627.2
	a''	530.1
$\text{B}(\text{OH})_2$ (C_s)	a'	3838.9
	a'	3776.1
	a'	1426.9
	a'	1203.3
	a'	969.4
	a'	965.1
	a'	448.9
	a''	569.5
	a''	468.6
$\text{B}(\text{OH})_3$ (C_{3h})	e'	3876.7
	e'	3876.7

	e'	1455.6
	e'	1455.6
	e'	1019.9
	e'	1019.9
	e'	423.6
	e'	423.6
	e''	532.2
	e''	532.2
	a'	3876.5
	a'	1021.1
	a'	875.6
	a''	669.5
	a''	443.2
B(SH) (C_s) ^b	a'	2649.7
	a'	771.9
	a'	568.7
HB(SH) (C_s)	a'	2739.9
	a'	2725.6
	a'	922.9
	a'	877.6
	a'	693.6
	a''	723.7
H ₂ B(SH) (C_s)	a'	2715.8
	a'	2667.2
	a'	2615.8
	a'	1206.4
	a'	971.9
	a'	807.1
	a'	676.0
	a''	950.8
	a''	656.1
HB(SH) ₂ (C_s)	a'	2681.6

	a'	2671.7
	a'	2650.6
	a'	1117.6
	a'	935.0
	a'	849.3
	a'	797.3
	a'	618.4
	a'	238.3
	a''	807.4
	a''	426.2
	a''	361.0
B(SH) ₂ (C _s)	a'	2752.2
	a'	2679.2
	a'	1034.6
	a'	892.7
	a'	791.3
	a'	585.6
	a'	215.3
	a''	402.7
	a''	320.5
B(SH) ₃ (C _{3h})	e'	2752.7
	e'	2752.7
	e'	1032.0
	e'	1032.0
	e'	776.9
	e'	776.9
	e'	212.1
	e'	212.1
	e''	369.2
	e''	369.2
	a'	2748.7
	a'	830.0

a'	448.6
a''	416.3
a''	219.4

^a Diatomic molecule frequencies calculated at the CCSD(T) level with either the aVTZ or aVTZ-PP basis sets with a 5th order fit. ^b Frequencies calculated at the CCSD(T) level with either the aVTZ or aVTZ-PP basis sets.

Table A6.6. Components for Calculated Atomization Energies in kcal/mol for HX (X = F, Cl, Br, and I).

Molecule	CBS ^a	ΔE_{ZPE} ^b	ΔE_{CV} ^c	ΔE_{SR} ^d	ΔE_{SO} ^e	$\Sigma D_0(0\text{ K})$ ^f
HF	141.88	5.85	0.16	-0.22	-0.38	135.58
HCl	107.42	4.24	0.18	-0.19	-0.84	103.44
HBr	93.69	3.76	0.56	-0.57	-3.50	86.41
HI	79.38	3.29	0.83	0.01	-7.24	69.69

^a Extrapolated by using Equation (1) with $aVnZ$, $n = D, T, Q$. ^b The zero point energies were obtained as described in the text. ^c Core-valence corrections were obtained with the cc-pwCVTZ (F, Cl and Br) and cc-pwCVTZ-PP (I) basis sets at the optimized CCSD(T)/aVTZ or CCSD(T)/aVTZ-PP geometries. ^d The scalar relativistic correction is based on a CISD(FC)/VTZ MVD calculation and is expressed relative to the CISD result without the MVD correction, i.e. including the existing relativistic effects resulting from the use of a relativistic effective core potential. For HBr, the relativistic calculation was calculated using the DKH method as described in the text. ^e Correction due to the incorrect treatment of the atomic asymptotes as an average of spin multiplets. Values are based on C. Moore's Tables, ref. [36]. ^f The theoretical value of the dissociation energy to atoms $\Sigma D_0(0\text{ K})$.

Table A6.7. Components for Calculated Atomization Energies in kcal/mol for BX, HBX, BX₂, and H_(3-n)BX_n for (X = Br and I).

Molecule	CBS ^a	ΔE_{ZPE} ^b	ΔE_{CV} ^c	ΔE_{SR} ^d	ΔE_{SO} ^e	$\Sigma D_0(0\text{ K})$ ^f
BBr	104.65	0.97	0.85	-0.09	-3.53	100.91
BI	85.10	0.82	1.35	-0.01	-7.27	78.35
HBBr	172.02	6.16	1.32	-0.13	-3.53	163.52
HBI	155.49	5.92	1.82	-0.07	-7.27	144.04
H ₂ BBr	281.50	13.23	1.60	-0.15	-3.53	266.19
H ₂ BI	264.21	12.87	2.16	-0.08	-7.27	246.15
HBBr ₂	279.54	8.87	2.28	-0.25	-7.03	265.67
HBI ₂	245.11	8.27	3.41	-0.10	-14.51	225.64
BBr ₂	171.26	2.34	1.93	-0.22	-7.03	163.60
BI ₂	139.34	2.05	2.93	-0.09	-14.51	125.63
BBr ₃	273.71	3.89	2.95	-0.36	-10.53	261.88
BI ₃	223.15	3.16	4.68	-0.11	-21.75	202.81

^a Extrapolated by using Equation (1) with aVnZ-PP, $n = D, T, Q$. ^b The zero point energies were obtained as described in the text. ^c Core-valence corrections were obtained with the cc-pwCVTZ (B, N, O, F, S, Cl) and cc-pwCVTZ-PP (Br and I) basis sets at the optimized MP2/aVTZ-PP geometries. ^d The scalar relativistic correction is based on a CISD(FC)/VTZ MVD calculation and is expressed relative to the CISD result without the MVD correction, i.e. including the existing relativistic effects resulting from the use of a relativistic effective core potential. ^e Correction due to the incorrect treatment of the atomic asymptotes as an average of spin multiplets. Values are based on C. Moore's Tables, ref. [36]. ^f The theoretical value of the dissociation energy to atoms $\Sigma D_0(0\text{ K})$.

Table A6.8. Electronic Contribution to the CCSD(T)/CBS Singlet-Triplet Splitting (kcal/mol) in the BX compounds where X = F, Cl, Br, I, NH₂, OH, and SH.

Molecule	aVDZ	aVTZ	aVQZ	CBS (DTQ)
BF	81.3	82.8	83.2	83.4
BCl	58.5	57.9	57.9	57.9
BBr	54.2	53.4	53.4	53.4
BI	48.0	46.9	47.0	47.0
B(NH ₂)	46.8	47.5	47.7	47.8
B(OH)	68.4	69.6	70.0	70.3
B(SH)	34.4	33.7	33.5	33.4

Table A6.9. T_1 Diagnostics calculated at the CCSD(T)/aVQZ level.

Molecule	T_1 Diagnostics
BF	0.0157
HBF	0.0171
H ₂ BF	0.0128
HBF ₂	0.0127
BF ₂	0.0156
BF ₃	0.0118
BCl	0.0161
HBCl	0.0168
H ₂ BCl	0.0113
HBCl ₂	0.0112
BCl ₂	0.0157
BCl ₃	0.0107
BBr	0.0186
HBBr	0.0192
H ₂ BBr	0.0132
HBBr ₂	0.0134
BBr ₂	0.0188
BBr ₃	0.0129
BI	0.0227
HBI	0.0229
H ₂ BI	0.0162
HBI ₂	0.0166
BI ₂	0.0229
BI ₃	0.0161
B(NH ₂)	0.0137
HB(NH ₂)	0.0148
HB(NH ₂) ₂	0.0105
B(NH ₂) ₂	0.0127
B(NH ₂) ₃	0.0102
B(OH)	0.0157

HB(OH)	0.0169
H ₂ B(OH)	0.0134
HB(OH) ₂	0.0126
B(OH) ₂	0.0154
B(OH) ₃	0.0115
B(SH)	0.0188
HB(SH)	0.0197
H ₂ B(SH)	0.0147
HB(SH) ₂	0.0142
B(SH) ₂	0.0176
B(SH) ₃	0.0137

CHAPTER 7

LEWIS ACIDITIES AND HYDRIDE, FLUORIDE, AND X⁻ AFFINITIES OF THE BH_{3-n}X_n COMPOUNDS (X = F, Cl, Br, I, NH₂, OH, and SH) FROM COUPLED CLUSTER THEORY

From: Grant, D. J.; Dixon, D. A.; Camaioni, D.; Potter, R. G.; Christe, K. O. *Inorg. Chem.* **2009**, *48*, 8811-8821.

7.1 Introduction

We have recently reported the calculated enthalpies of formation and the B-X and B-H bond dissociation energies (BDEs) for the BX₃, HBX₂, and H₂BX compounds with X = F, Cl, Br, I, NH₂, OH, and SH together with the different radicals involved in the bond breaking process¹ as part of an effort to predict the thermodynamics of regeneration schemes for spent fuel derived from loss of H₂ from ammonia borane. In addition, these compounds have many practical applications and are of substantial interest as model systems.² To further understand the chemistry of these compounds, we investigated the hydride (HA) and fluoride (FA) affinities as well as the X⁻ affinities (XA) of these substituted borane compounds. Furthermore, the fluoride ion³ or hydride⁴ affinities offer unique measures of the strength as a Lewis acid.

The most thorough and relevant previous study on this subject was carried out by Vianello and Maksic,⁴ who calculated the H⁻ affinities of BH₃ and the fluoro, chloro, bromo, hydroxo, and methyl substituted boranes using the G2(MP2) method. They wrote a three step thermodynamic cycle (shown in Figures 7.1(a) for the general case and in 7.1(b) for the H⁻ affinities. For BH₃, this is (1) the pruning of an electron from H⁻, which equals to 17.4 kcal/mol, the first ionization potential of H⁻ (or the electron affinity (EA) of H), (2) the attachment of the

electron to BH_3 (the negative of the EA of BH_3), and (3) the homolytic chemical bond formation resulting from the combination of the BH_3^- and H radicals. For compounds with a calculated negative EA, they used these negative values, not the more appropriate value of 0 in the cycle. Since the electron is not bound when the $\text{EA} \leq 0$, such an approach is non-physical and somewhat arbitrary as the size of the negative EA is strongly method and basis set dependent. They showed that F, OH, and CH_3 substitution reduces the hydride affinity (Lewis acidity) of the boranes, whereas Cl and Br substitution enhances the acidity, and that BBr_3 was the most acidic one of the compounds studied. Vianello and Maksic⁴ also reported that the HA of the $\text{BH}_{3-n}\text{X}_n$ compounds with X = halogen, OH, and Me show a correlation with the EA with the inclusion of negative electron affinities.

In our present study, the scope of the previous investigation⁴ for the HA was expanded by including the additional ligands, I, NH_2 , and SH, and all calculations were done at a higher level. The F^- affinities for all compounds were also calculated and compared to the H^- values. Furthermore, the Cl^- , Br^- , I^- , NH_2^- , OH^- , and SH^- affinities were determined for the BX_3 , HBX_2 , H_2BX , and BH_3 series. It was found that H^- affinities correlate linearly with the proton affinities (PA) of X^- , except for H and F. The reasons for the correlation and the deviations from it are discussed. Since PAs for a number of anions are known or readily calculated, the H^- affinity of $\text{BH}_{3-n}\text{X}_n$ compounds with other X groups may be readily estimated.

Modern computational chemistry methods implemented on high performance computer architectures can now provide reliable predictions of chemical bond energies to within about 1 kcal/mol for most compounds that are not dominated by multireference character. We use the approach that we have been developing with collaborators at Pacific Northwest Laboratory and Washington State University for the prediction of accurate molecular thermochemistry⁵ to

determine accurate thermodynamic data for these compounds, including total atomization energies ($TAE = \Sigma D_0$), enthalpies of formation, BDEs, HAs, and FAs. As we have shown previously,¹ the experimental enthalpies of formation for a number of the molecules under study, specifically the neutral analogs, are available allowing for comparison to our calculated theoretical values. The experimental enthalpies of formation for the hydrogen halides,⁶ the haloboranes,⁷ the dihaloboranes (with the exception of diiodoborane),⁷ the dihaloboryl radicals,⁷ the trihaloboranes,^{6,7} trihydroxyborane,⁷ and the dihydroxyboryl radical⁷ have been reported. Our theoretical calculations on the enthalpies of formation show excellent agreement with the reported experimental values.

7.2 *Computational Approach*

Our approach is based on calculating the TAE of a molecule and using this value with known enthalpies of formation of the atoms to calculate the enthalpy of formation at 0 K. The approach starts with coupled cluster theory with single and double excitations and including a perturbative triples correction (CCSD(T)),^{8,9,10} combined with the correlation-consistent basis sets^{11,12} extrapolated to the complete basis set (CBS) limit to treat the correlation energy of the valence electrons. This is followed by a number of smaller additive corrections including core-valence interactions and relativistic effects, both scalar and spin-orbit. The zero point energy is obtained from experiment, theory, or a combination of the two. Corrections to 298 K can then be calculated by using standard thermodynamic and statistical mechanics expressions in the rigid rotor-harmonic oscillator approximation¹³ and appropriate corrections for the enthalpy of formation of the atoms.¹⁴ All of the current work was performed with the MOLPRO suite of programs.¹⁵ The open-shell CCSD(T) calculations for the atoms were carried out at the R/UCCSD(T) level.^{16,17,18} All of the calculations were done on the 144 processor Cray XD-1

computer system at the Alabama Supercomputer Center or a Dell Cluster at the University of Alabama.

For the current study, we used the augmented correlation consistent basis sets aug-cc-pVnZ ($n = D, T, Q$) for H, B, N, O, F, and Br.¹² In addition, it has recently been found that tight d functions are necessary for calculating accurate atomization energies for 2nd row elements,¹⁹ so we also included additional tight d functions in our calculations giving the aug-cc-pV($n+d$)Z basis set on the 2nd row atoms S and Cl. We use aVnZ to represent the combination of aug-cc-pVnZ on H, B, N, O, F, and Br, and aug-cc-pV($n+d$)Z on the 2nd row atoms S and Cl. Only the spherical components of the cartesian basis functions were used. The CCSD(T) total energies were extrapolated to the CBS limit by using a mixed exponential/Gaussian function of the form:

$$E(n) = E_{\text{CBS}} + A \exp[-(n-1)] + B \exp[-(n-1)^2] \quad (1)$$

with $n = 2$ (aVDZ), 3 (aVTZ), and 4 (aVQZ), as first proposed by Peterson *et al.*²⁰

Core-valence (CV) calculations were carried out with the weighted core-valence basis set cc-pwCVTZ.²¹ The core-valence correction is then taken as the difference in energy between the valence electron correlation calculation and that with the appropriate core electrons included using basis sets with additional functions. For molecules containing I as a substituent, we used a different approach due to issues described elsewhere.²² We used the new effective core potential/correlation consistent basis sets developed by Peterson and co-workers.²³ These basis sets were developed in combination with the small core relativistic effective core potentials (RECPs) from the Stuttgart/Köln group. The RECP for I subsumes the ($1s^2, 2s^2, 2p^6, 3s^2, 3p^6,$ and $3d^{10}$) orbital space into the 28-electron core set, leaving the ($4s^2, 4p^6, 5s^2, 4d^{10},$ and $5p^5$) space with 25 electrons to be handled explicitly. We performed our CBS extrapolation with the aug-cc-pwCVnZ basis sets for $n = D, T, Q$ with 25 active electrons on each I atom so the core-

valence correction is automatically included in the CBS extrapolation. We use aVnZ to represent the combination of aug-cc-pwCVnZ on the other atoms and aug-cc-pwCVnZ-PP on I.

For Br, we also performed additional calculations using the new effective core potential/correlation consistent basis sets.²³ For Br, the RECP subsumes the (1s², 2s², and 2p⁶) orbital space into the 10-electron core set, leaving the (3s², 3p⁶, 4s², 3d¹⁰, and 4p⁵) space with 25 electrons to be handled explicitly. Only the (4s², 4p⁵) electrons are active in our valence correlation treatment. We use aVnZ-PP to represent the combination of aug-cc-pVnZ basis set on the other atoms and the aug-cc-pVnZ-PP basis set on Br. Core-valence (CV) calculations (all 25 electrons outside the RECP core) were also carried out with the weighted core-valence basis set cc-pwCVTZ for H and B²¹ and the cc-pwCVTZ-PP basis set for Br.

Geometry optimizations were performed at the MP2/aVTZ or MP2/aVTZ-PP level.²⁴ The vibrational frequencies were calculated at the same MP2/aVTZ level in order to obtain the zero point energies and the thermal corrections at 298 K and were used without scaling, except for calculating the electron affinity of BH₃. For the calculation of the electron affinity of BH₃, the zero point corrections for BH₃ and BH₃⁻ were obtained from the calculated harmonic stretching frequencies scaled by a factor of 0.96, (the average of the CCSD(T)/aVTZ and experimental values²⁵ of BH₃ divided by the average by the theoretical value).²⁶ The Gaussian program system²⁷ was used for the MP2 calculations. The MP2/aVTZ geometries were used in the single point CCSD(T)/aVnZ (*n* = D, T, Q) calculations.

Two adjustments to the TAE are necessary in order to account for relativistic effects in atoms and molecules. The atomic spin-orbit corrections are $\Delta E_{\text{SO}}(\text{B}) = 0.03$ kcal/mol, $\Delta E_{\text{SO}}(\text{O}) = 0.22$ kcal/mol, $\Delta E_{\text{SO}}(\text{F}) = 0.39$ kcal/mol, $\Delta E_{\text{SO}}(\text{S}) = 0.56$ kcal/mol, $\Delta E_{\text{SO}}(\text{Cl}) = 0.84$ kcal/mol, $\Delta E_{\text{SO}}(\text{Br}) = 3.50$ kcal/mol, and $\Delta E_{\text{SO}}(\text{I}) = 7.24$ kcal/mol from the tables of Moore.²⁸ A second

relativistic correction to the TAE accounts for molecular scalar relativistic effects, ΔE_{SR} . ΔE_{SR} is taken as the sum of the mass-velocity and 1-electron Darwin (MVD) terms in the Breit-Pauli Hamiltonian.²⁹ For the molecules containing Br, the molecular scalar relativistic correction ΔE_{SR} was calculated using the spin-free, one-electron Douglas-Kroll-Hess (DKH) Hamiltonian.^{30,31,32} ΔE_{SR} was defined as the difference in the atomization energy between the results obtained from basis sets recontracted for DKH calculations³¹ and the atomization energy obtained with the normal valence basis set of the same quality. DKH calculations were carried out at the CCSD(T)/cc-pVTZ and the CCSD(T)/cc-pVTZ-DK levels of theory.

By combining our computed ΣD_0 values with the best available enthalpies of formation at 0 K for the elements, $\Delta H_f^0(\text{H}) = 51.63 \text{ kcal mol}^{-1}$, $\Delta H_f^0(\text{B}) = 135.1 \pm 0.2 \text{ kcal mol}^{-1}$,³³ $\Delta H_f^0(\text{N}) = 112.53 \text{ kcal mol}^{-1}$, $\Delta H_f^0(\text{O}) = 58.99 \text{ kcal mol}^{-1}$, $\Delta H_f^0(\text{F}) = 18.47 \text{ kcal mol}^{-1}$, $\Delta H_f^0(\text{S}) = 65.66 \text{ kcal mol}^{-1}$, $\Delta H_f^0(\text{Cl}) = 28.59 \text{ kcal mol}^{-1}$, $\Delta H_f^0(\text{Br}) = 28.19 \text{ kcal mol}^{-1}$, and $\Delta H_f^0(\text{I}) = 25.61 \text{ kcal mol}^{-1}$, we can derive ΔH_f^0 values for the molecules under study in the gas phase.

7.3 Results and Discussion

The calculated geometry parameters, total energies and vibrational frequencies are given in the Supporting Information (Tables A7.1, A7.2, A7.3, and A7.4). The energetic components for predicting the TAE are given in Table 7.1 along with the point groups and ground-state symmetry labels. We first describe some trends in the various components for the TAE. The ΔE_{CV} corrections are all positive and range from 1.13 (BH_3^-) to 4.16 (BBr_4^-) kcal/mol. The ΔE_{SR} corrections are all negative and range from -0.09 (BH_3^-) to -1.86 kcal/mol (BBr_4^-). We estimate that the error bars for the calculated enthalpies of formation are ± 1.5 kcal/mol considering errors in the energy extrapolation, frequencies, and other electronic energy components. Quantities such as the fluoride affinities should be good to ± 1.0 kcal/mol as the errors in adding F^- are

smaller. An estimate of the potential for significant multireference character in the wavefunction can be obtained from the T_1 diagnostic³⁴ for the CCSD calculation. The value for the T_1 diagnostics are small (<0.02) for most molecules showing that the wavefunction is dominated by a single configuration. The T_1 diagnostics for BH_3^- , BH_2F^- , and BHF_2^- are all substantially higher. In the case of BH_2F^- and BHF_2^- , this is not surprising, because as discussed below, the parent neutral does not bind an electron. BH_3 does have a positive electron affinity so the large T_1 diagnostic was somewhat surprising. However, the predicted small electron affinity is within 0.01 eV of the experimental value³⁵ so this is not a serious issue for BH_3^- . The T_1 diagnostics for the molecules are given as Supporting Information (Table A7.6).

The calculated enthalpies of formation of the borane-derived anions are given in Table 7.2 at 0 K and 298 K, together with those of the neutral parent molecules¹ for completeness. For our calculations on molecules containing Br, we note a ~ 0.8 kcal/mol difference per Br atom in the valence electronic energy extrapolated to the CBS limit based on the $aVnZ$ and $aVnZ\text{-PP}$ basis sets, respectively. The largest difference in the calculated enthalpies of formation based on both approaches was 1.4 kcal/mol for BBr_3^- (Table A7.5). For the enthalpies of formation for the I containing molecules, the inclusion of the core electrons into the treatment of the correlation energy and employing the weighted core basis sets for the CBS extrapolation yields calculated values for the enthalpies of formation that are on average within 0.2 kcal/mol of the calculated value for the enthalpies of formation using the $aVnZ\text{-PP}$ basis sets and just correlating the valence electrons (Table A7.5). In general, the agreement between calculated and experimental enthalpies of formation is excellent. The only significant deviation, 9 kcal/mol, was found for BI_3 , which is attributed to the very large uncertainty of 12 kcal/mol in the experimental value.

Given the calculated enthalpies of formation and the experimental enthalpies of formation of the hydride ($\Delta H_f^0(\text{H}^-)$ (298 K) = 34.7 kcal mol⁻¹) and fluoride ($\Delta H_f^0(\text{F}^-)$ (298 K) = 59.5 kcal mol⁻¹) anions, we can predict the HA and FA of the neutral molecules. We use the values of the ions without any energy attached to the electron. We define the HA and FA as $-\Delta H$ for the following respective reactions:



The calculated HAs and FAs are summarized in Table 7.3 and depicted in Figure 7.2. The values at 298 K are used in our discussion below, except as noted. The HA of BH_3 has been previously reported using the same approach as here.³⁶ The highest H^- and F^- affinities are found for BI_3 and the lowest ones for $\text{B}(\text{NH}_2)_3$, and within the boron trihalide series, the Lewis acidity increases monotonically with increasing atomic weight of the halogen, i.e., BI_3 is a considerably stronger Lewis acid than BF_3 .

In addition, we predict the chloride, bromide, iodide, amide, hydroxide, and bisulfide anion affinities, XA , where $\text{X} = \text{Cl}, \text{Br}, \text{I}, \text{NH}_2, \text{OH},$ and SH , respectively. We define the XA as $-\Delta H$ for the reaction:



The calculated XA values are presented in Table 7.4. For the X^- affinities in the BX_3 , HBX_2 , and H_2BX series, the fluorides show the highest values, while the amides, iodides, and bisulfides show the lowest ones. If X is a halogen, the X^- affinity increases with increasing X content of the molecule, i.e., from H_2BX to HBX_2 and BX_3 . However, if X is OH , the OH^- affinity decreases from $\text{H}_2\text{B}(\text{OH})$ to $\text{B}(\text{OH})_3$ with $\text{HB}(\text{OH})_2$ and $\text{B}(\text{OH})_3$ having essentially the same value. For $\text{X} =$

SH, there is a substantial increase from H_2BX to HBX_2 and only a small increase to BX_3 . For $\text{X} = \text{NH}_2$, the X^- affinity is a maximum for $\text{HB}(\text{NH}_2)_2$ with respect to $\text{H}_2\text{B}(\text{NH}_2)$ and $\text{B}(\text{NH}_2)_3$.

As can be seen from the data in Table 7.3, the FAs and HAs have similar values. The largest differences are observed for the boranes substituted with the strongly electron withdrawing and backdonating fluorine and hydroxyl ligands. These compounds exhibit large distortion energies upon addition of an electron to BX_3 or HBX_2 .⁴ In the case of F^- addition, this distortion energy loss can be recovered to a large extent by the high energy of the newly formed B-F bond, which is not the case for the weaker and more polar B-H bond. Therefore, the HAs for the fluoro- or hydroxo-boranes are considerably lower than the corresponding FAs. The largest differences in the opposite direction, i.e., the HA being significantly higher than the FA, is seen for BH_3 . In BH_4^- , all four ligands are identical and form strong covalent bonds, whereas in BH_3F^- , the B-F bond becomes highly polar and, therefore, weaker. A comparison of our HAs with the less comprehensive data set of reference 4 shows very good agreement with the deviations being 2 kcal/mol or less, except for $\text{B}(\text{OH})_3$ where the difference is 3.4 kcal/mol. Furthermore, the range of the previously reported acidities for the boranes has been extended at both ends of the scale, BI_3 becoming the strongest acid and $\text{B}(\text{NH}_2)_3$ becoming the weakest one.

As discussed in the Introduction, Vianello and Maksic⁴ provided a thermodynamic scheme for the HAs with three steps, the ionization of H^- to a hydrogen radical and an electron (step 1), the capture of the electron by the Lewis acid (LA), including the reorganization energy resulting from the structural change from LA to LA^- (step 2), and the subsequent formation of the $[\text{LA-H}]^-$ bond (step 3). As described above, there are issues with the use of the appropriate value for step 2. For the thermodynamic cycle depicted in Figure 7.1(a), we predicted the electron affinities of all of the compounds in our study (Table 7.5) at the density functional

theory level with the B3LYP exchange-correlation functional³⁷ and the aVTZ basis set, and, for some, at the CCSD(T)/CBS level. We employ the usual convention that a positive EA signifies that a molecule will bind an extra electron and a negative EA that it will not. In a thermodynamic cycle, this means that if a molecule has a positive EA that the detachment energy is positive and the attachment energy is negative. The DFT values are in good agreement with the CCSD(T)/CBS values for the larger positive EAs and differ somewhat more for negative EAs or weakly positive EAs. BH_3 is predicted to weakly bind an electron with a very small positive EA value of 0.8 kcal/mol, about 1 kcal/mol less than that for CH_3 .³⁸ This value is in excellent agreement with experiment within 0.01 eV.³⁵ Substitution of one to three H atoms by F atoms to form H_2BF , HBF_2 , and BF_3 yields negative EAs, so these boranes will not bind a free electron, and the appropriate value for use in step 2 is thus 0. The EAs of the BX_3 compounds for $\text{X} = \text{Cl}$, Br , and I are all positive so they will bind an electron. The calculated EAs for BCl_3 and BBr_3 are in good agreement with the experimental values³⁹ considering the rather large error bars. For BCl_3 , we would recommend a value at the higher end of the experimental range. The EA increases with increasing atomic number of the substituent, with BI_3 having the highest EA. The EAs of the BX_3 compounds for $\text{X} = \text{halogen}$ correlate directly with the B-X bond order, which decreases with increasing atomic number. The decrease in bond order is due to decreasing back-donation of electron density from the halogen ligand to boron so that the vacant orbital on the B is more available to add a negatively charged species such as an electron, H^- , or F^- . The changes in the relative HA and FA values mirror the changes in the positive EAs so step 2 in the cycles 1(a) and 1(b) of Figure 7.1 is important in providing the relative ordering the HA or FA values if the borane binds an electron.

We searched for other possible energetic properties that would correlate with the HA and FA in order to develop qualitative predictors. Properties such as atomic charges and molecular orbital energies of the $\text{BH}_{3-n}\text{X}_n$ compounds were found to be generally poor predictors of HA, probably, because such properties of either the initial A or final HA^- are inadequate to capture the effects of R substitution on both initial and final states.

We did observe that the HA and FA of $\text{BH}_{3-n}\text{X}_n$ tended to correlate linearly with the PA of the substituent X^- (the enthalpic component of the gas phase acidity), which equates directly to the enthalpy for dissociation of HX into H^+ and X^- (the enthalpic component of the gas phase acidity of HX). Figure 7.2 shows the HA and FA from Table 7.3 plotted against literature values⁴⁰ for $\text{PA}(\text{X})$. Different lines (6 in all) are obtained for the HA and FA and for different values of n. Each line is a linear fit to the data except for $\text{X} = \text{F}$ and $\text{X} = \text{H}$. The data points for $\text{X} = \text{F}$ (i.e., $\text{BH}_{3-n}\text{F}_n$) deviate from the respective lines and the deviation increases with n. The data points for $\text{X} = \text{H}$ corresponding to HA and FA of BH_3 are not plotted in Figure 7.2 as they deviate significantly from the trend lines. Like the data for $\text{X} = \text{F}$, the affinity of BH_3 for H^- is greater than predicted by the PA of H^- . The acidity of HX can be considered in part to be a measure of the ability of a group X to stabilize negative charge. From this perspective, the F when attached to B, as a group, is better at stabilizing negative charge than when it is by itself. This is also the case for H and Me. We will comment on this after discussing reasons for the observed correlation.

The thermodynamic cycle shown in Figure 7.1(a) shows that we can calculate the BDE for the B-A bond in $\text{BH}_{3-n}\text{X}_n\text{-A}^-$ by use of the other quantities in the cycle, which we already have. These BDEs are given in Table 7.6 where we set the $\text{EA} = 0$ if the corresponding Lewis acid repels an electron, i.e., the EA is negative. From the data in Table 7.6, it is clear that the

dominant component of determining the absolute magnitude of the hydride, fluoride, or X^- affinities of the boranes is the $BH_{3-n}X_n-A^-$ bond dissociation energy.

We looked for but did not find a thermodynamic cycle to equate the HA of $BH_{3-n}X_n$ with the PA of the X^- group. We did observe, however, that the HA of $BH_{3-n}X_n$ ($n = 0, 1, 2,$ or 3) can be related to the anion affinity (AA) of $BH_{3-n}X_n$ via the thermodynamic cycle shown in Figure 7.1(c). Therefore, since the proton is a Lewis acid, it seems reasonable that the affinities of anions for protons and for the $BH_{3-n}X_n$ Lewis acids may exhibit a good correlation. Anane, Boutalib and coworkers have demonstrated correlations of B dative bond energies with the PA of Lewis base ligands.⁴¹ Consistent with this relationship, the plot in Figure 7.3 shows that the AAs of BH_3 and the PA of these anions, $PA(X^-)$, are well correlated; the only exception being F^- for which the reaction with BH_3 releases more energy than expected.

As shown by the cycle of Figure 7.1(c), the difference between the HA of $BH_{3-n}X_n$ and the AA of $BH_{3-n}X_n$ amounts to the differences in the homolytic B-X and B-H BDEs and the EAs of X and H. Therefore, the goodness of the correlation between HA or FA of $BH_{3-n}X_n$ and the PA of X^- depends on how well the differences between the BDE and EA changes exhibit the same trends as the PAs of X^- .

In the plots shown in Figures 7.2 and 7.3, the compounds with $X = F$ deviate from the trends followed by the other atoms and groups. This deviation might be caused by anomalies in the homolytic B-F BDEs and/or the EA of F that determine the PA of F^- .⁴² As can be seen from Figure 7.4, which shows plots of the EAs of the halogen atoms and of the B-X BDEs of BH_2X and BHX_2 against the homolytic BDEs of the corresponding acids, $D(HX)$, the main culprit for the deviation is the anomalously low EA of F^- .⁴³ The EAs of the halogens increase linearly with $D(HX)$ for I, Br, and Cl, but falls considerably below the trend line for F. For the EA of F to be

on the trend line, the BDE of HF would have to be close to that of HBr. As we had calculated the homolytic BDEs of the $[\text{BH}_3\text{-X}]^-$ and $\text{BH}_2\text{-X}$ compounds,¹ we also plotted them against the HX BDEs in Figure 7.4. The values including those for the F-substituted compounds follow linear trends suggesting that the B-F BDEs are normal. Finally, we note that the HAs of BH_3 and BMe_3 ⁴ also deviate significantly from the trend lines plotted in Figure 7.2. The values deviate upward from the lines indicating that the PAs of H^- and Me^- also are not good predictors. As with F, the EAs of H and CH_3 are also low, whereas the B-H and B-C bond dissociation energies follow the expected trend lines. The low values for the EAs show that the free gas phase radicals H and CH_3 do not stabilize excess negative charge as well as when bonded as substituents to boron.

One of the more interesting results is that the fluoride affinities of the boron trihalides BX_3 increase with increasing atomic number of X, so that BF_3 has the lowest FA and BI_3 has the highest FA. This trend has been discussed previously⁴⁴ for other Lewis acid strength descriptors, such as the NH_3 affinities of BF_3 and BCl_3 , and several authors have offered different explanations for this observation. These include the energy of the BX_3 LUMO⁴⁵ and the distortion energy for the BX_3 to form the complex BH_3A (ligand close packing).⁴⁶ Brinck *et al.*⁴⁷ suggested that the larger BDE for NH_3BCl_3 is due to increased charge capacity in BCl_3 and not to the stronger overlap of the out of plane p orbitals on F with the vacant p orbital on B. Hirao *et al.*⁴⁸ argue that the backbonding to the unoccupied p orbital on B is not the major factor but that the LUMO is more stable, and thus, more available (lower acidic hardness) leading to a larger BDE. Branchadell and Oliva⁴⁹ used charge density analysis to predict that the increase in Lewis acidity from BF_3 to BBr_3 is due to the EA differences and the nature of the boron-halogen bond.

They calculated the distortion energy to reach an angle of 113.5° and showed that BF_3 requires more energy than BBr_3 .

Our analysis shows that, based on the charge distributions alone, BF_3 should have the highest FA as it has the largest positive natural orbital⁵⁰ charge on B (BF_3 (1.53 e), BCl_3 (0.41 e), BBr_3 (0.05 e), and BI_3 (-0.40 e)) and BI_3 the smallest one. However, the calculated EAs (Table 7.5) show that BF_3 cannot bind an electron and that the EAs increase from BCl_3 to BI_3 . The NBO charge distribution tends to exaggerate the ionic character of a bond. The large positive charge on the B in BF_3 can be explained by the strong electron withdrawing inductive effect of the highly electronegative fluorine ligands (sigma effect). However, for the electron affinity, this sigma effect is outweighed by the strong back donation from the out-of-plane p orbital of fluorine into the empty p orbital on B, which has the opposite effect and leads to an inability to bind an electron. As shown in the orbital diagrams in the Supporting Information, the amount of back donation in BF_3 is stronger than that in BI_3 . Using average covalent atomic radii,⁵¹ we find that the B-F bond distance¹ (1.315 Å) in BF_3 is 10% shorter than the sum of the covalent radii (1.46 Å). The B-Cl (1.745 Å), B-Br (1.908 Å), and B-I (2.132 Å) bond distances¹ are shorter by 7%, 6%, and 4% in BCl_3 , BBr_3 , and BI_3 , respectively, than the sum of the covalent radii. This is consistent with the larger pi backbonding in BF_3 .

A second energetic effect that plays an important role is the energy needed to distort the geometry at the boron from planar BX_3 to tetrahedral BX_3F^- . This distortion energy can be broken down into two components. The first component is the energy required to distort BX_3 from its planar structure to a pyramidal structure having the same geometry as in BX_3^- . The second component is the distortion from pyramidal to tetrahedral BX_3^- , which has the same geometry as the BX_3 part of BX_3F^- . These distortion energies were calculated and are

summarized in Table 7.7. Using these values, additional components can be included in the various steps in the Born-Haber cycles we have written for the F^- affinities of BF_3 and BI_3 (see Figure 7.5 for $X = F$ and I). This allows a quantitative analysis of the relative contributions of EAs, BDEs and distortion energies to the Lewis acidities of BF_3 and BI_3 , thus, providing more detailed energetic insight as to why BI_3 is a stronger Lewis acid than BF_3 .

As can be seen from Figure 7.5, the energies of step 1 (the ionization potential of F^-) are identical for both $X = F$ and $X = I$. The energies of step 3 (conceptually the sum of an “undistorted” B-F BDE in BX_3^-F and the distortion energy from the pyramidal to the tetrahedral geometry of BX_3^-) are also comparable. The major difference between the cycle for $X = F$ and that for $X = I$ arises from step 2, which is the EA of BX_3 (conceptually the sum of the undistorted EA of BX_3 and the associated distortion energy from planar to pyramidal BX_3). For the purpose of the Born-Haber cycles, step 2 of the BF_3 cycle was set equal to zero because a negative EA (positive value for the reaction enthalpy due to a repulsive interaction between BF_3 and the electron) is physically not meaningful. Thus, step 2 is responsible for the higher Lewis acidity of BI_3 , and the EA of BX_3 makes by far the largest contribution to the relative differences in the acidities. The fact that the EA of BI_3 is higher than that of BF_3 can be explained by the fact that fluorine is a better π -backdonor than iodine, resulting in a higher occupation of the empty p_z orbital (LUMO) of boron. The calculations show that the large distortion energy in BF_3 is important in preventing BF_3 from readily binding an electron. Although, the energetics of step 2 govern the relative acidities, the overall magnitudes are governed by the strength of the X_3B^-F bonds, which are quite large, consistent with the large value for the BF_2-F bond energy of 170.3 kcal/mol at 0 K.¹

7.4 Conclusions

The enthalpies of formation at 0 K and 298 K are predicted for a range of anionic substituted borane compounds, $\text{BH}_{4-n}\text{X}_n^-$ and $\text{BH}_{3-n}\text{X}_n\text{F}^-$ for $\text{X} = \text{F}, \text{Cl}, \text{Br}, \text{I}, \text{NH}_2, \text{OH},$ and SH , on the basis of coupled cluster theory (CCSD(T)) calculations extrapolated to the complete basis set limit. The calculated enthalpies of formation allow the prediction of the H^- , F^- , and X^- affinities to within ± 1.0 kcal/mol, dramatically improving the previous estimates of these important quantities. The hydride affinity is defined as $-\Delta\text{H}$ for the reaction $\text{BH}_{3-n}\text{X}_n + \text{H}^- \rightarrow \text{BH}_{4-n}\text{X}_n^-$, with similar considerations for the fluoride and X^- affinities. For the BX_3 series, the highest hydride and fluoride affinities are predicted for BI_3 at 112.6 and 105.9 kcal/mol, respectively, and the lowest ones for $\text{B}(\text{NH}_2)_3$ at 19.8 and 28.1 kcal/mol, respectively, at 298 K. The highest X^- affinity within the BX_3 series to form BX_4^- is found for BF_3 at 82.1 kcal/mol and the lowest one for $\text{B}(\text{NH}_2)_3$ at 33.3 kcal/mol, at 298 K. For the HBX_2 compounds, HBI_2 has the highest hydride and fluoride affinities at 106.0 and 99.9 kcal/mol, respectively, and $\text{HB}(\text{NH}_2)_2$ has the lowest ones at 24.0 and 29.0 kcal/mol, respectively, at 298 K. The highest X^- affinity is predicted for HBF_2 at 72.1 kcal/mol at 298 K, while HBI_2 is predicted to have the lowest one at 34.4 kcal/mol at 298 K. Similar trends were observed for the H_2BX compounds with the highest H^- and F^- affinities predicted for H_2BI at 94.3 and 89.9 kcal/mol, respectively, and the lowest ones for H_2BNH_2 at 37.8 and 39.7 kcal/mol, respectively, at 298 K, while H_2BF and H_2BNH_2 are predicted to have the highest and lowest X^- affinities at 67.9 and 16.0 kcal/mol, respectively, at 298 K.

The dominant component of determining the absolute magnitude of the hydride, fluoride, or X^- affinities of the boranes is the $\text{BH}_{3-n}\text{X}_n\text{-A}^-$ bond dissociation energy. The H^- and F^- affinities of $\text{BH}_{3-n}\text{X}_n$, i.e., their Lewis acidities, correlate linearly with the proton affinities of the substituent X^- , i.e., their gas phase Brønsted acidities. A decreasing proton affinity of the

corresponding base, X^- , corresponds to an increase in the Brønsted acidity of HX and in the Lewis acidities of $BH_{3-n}X_n$ although the absolute values go in opposite directions due to their different definitions. This correlation also accounts for the fact that BI_3 is the strongest Lewis acid in our series, in the same way as HI is the strongest gas phase Brønsted acid. The only deviations from this correlation are observed for X being H and F. These deviations can be attributed to the anomalous values of the electron affinities of the F and H atoms relative to the homolytic bond dissociation energies of the B-F and B-H bonds, respectively, that determine the proton affinities of the corresponding X^- anions. The fact that BI_3 is a stronger Lewis acid than BF_3 is primarily due to its higher electron affinity, which is influenced to some extent by the distortion energy from planar to pyramidal BX_3 . The roles of the X_3B^- -F bond dissociation energy and the concomitant distortion energy from pyramidal to tetrahedral BX_3^- in determining the relative acidities are considerably smaller. Since the electron affinity of BX_3 is strongly influenced by the charge density in the empty p_z LUMO of boron, the π -back donation from the halogen to boron plays a very important role.

Acknowledgments Funding provided in part by the Department of Energy, Office of Energy Efficiency and Renewable Energy under the Hydrogen Storage Grand Challenge, Solicitation No. DE-PS36-03GO93013. This work was done as part of the Chemical Hydrogen Storage Center. DAD is indebted to the Robert Ramsay Endowment of the University of Alabama. KOC thanks the Air Force Office of Scientific Research, the National Science Foundation, the Defense Threat Reduction Agency, and the Office of Naval Research for financial support.

Appendix Full author citations for References 15 and 27. Optimized MP2/aVTZ geometry parameters for the $BH_{4-n}X_n^-$, $BH_{3-n}X_nF$, and $BH_{3-n}X_{n+1}^-$ compounds. Total CCSD(T) energies as

a function of basis set. Total CCSD(T)/aVnZ-PP energies as a function of basis set. Calculated MP2/aVTZ frequencies (cm^{-1}). Enthalpies of formation (kcal/mol) at 0 K and 298 K for the BH_4 , ${}_{n-1}\text{X}_n^-$, $\text{BH}_{3-n}\text{X}_n\text{F}^-$ and $\text{BH}_{3-n}\text{X}_{n+1}^-$ compounds where X = Br and I based on CCSD(T)/aVnZ-PP extrapolation. T_1 diagnostics calculated at the CCSD(T)/aVQZ level. Natural bond orbital analysis of the trihaloboranes at the B3LYP/aug-cc-pVDZ Level. Top view of occupied out-of-plane lone pair orbital on BX_3 and side view of empty p orbital on BX_3 for X a halogen. This material is available free of charge via the Internet at <http://pubs.acs.org>.

Table 7.1. Components for Calculated Atomization Energies in kcal/mol.

Molecule	CBS ^a	$\Delta E_{\text{ZPE}}^{\text{b}}$	$\Delta E_{\text{CV}}^{\text{c}}$	$\Delta E_{\text{SR}}^{\text{d}}$	$\Delta E_{\text{SO}}^{\text{e}}$	$\Sigma D_0(0\text{K})^{\text{f}}$
$\text{BH}_3^- (^2A_2'' - D_{3h})$	278.80	14.31 ^h	1.13	-0.09	-0.03	265.51
$\text{BH}_4^- (^1A_1 - T_d)^{\text{g}}$	373.88	20.69	1.28	-0.09	-0.03	354.35
$\text{H}_2\text{BF}^- (^2B_1 - C_{2v})$	330.18	12.55	1.31	-0.41	-0.42	318.12
$\text{H}_3\text{BF}^- (^1A_1 - C_{3v})$	426.60	18.66	1.23	-0.42	-0.42	408.33
$\text{H}_2\text{BF}_2^- (^1A_1 - C_{2v})$	490.62	16.08	1.30	-0.75	-0.81	474.28
$\text{H}_2\text{BCl}^- (^2A' - C_s)$	297.73	11.73	1.21	-0.38	-0.87	285.95
$\text{H}_3\text{BCl}^- (^1A_1 - C_{3v})$	400.11	18.69	1.31	-0.38	-0.87	381.48
$\text{H}_2\text{BClF}^- (^1A' - C_s)$	457.55	15.58	1.33	-0.70	-1.26	441.34
$\text{H}_2\text{BBr}^- (^2A' - C_s)$	287.59	11.62	1.58	-0.93	-3.53	273.33
$\text{H}_3\text{BBr}^- (^1A_1 - C_{3v})$	390.98	18.56	1.77	-0.88	-3.53	369.78
$\text{H}_2\text{BBrF}^- (^1A' - C_s)$	447.17	15.40	1.83	-0.98	-3.92	428.69
$\text{H}_2\text{BI}^- (^2A' - C_s)$	278.35	11.46		-0.09	-7.27	259.53
$\text{H}_3\text{BI}^- (^1A_1 - C_{3v})$	382.49	18.37		-0.09	-7.27	356.76
$\text{H}_2\text{BIF}^- (^1A' - C_s)$	437.32	15.23		-0.67	-7.66	413.77
$\text{H}_3\text{B}(\text{NH}_2)^- (^1A' - C_s)$	557.49	33.72	1.73	-0.38	-0.03	525.09
$\text{H}_2\text{B}(\text{NH}_2)\text{F}^- (^1A' - C_s)$	618.56	30.99	1.79	-0.71	-0.42	588.23
$\text{H}_3\text{B}(\text{OH})^- (^1A - C_1)$	502.57	26.02	1.45	-0.43	-0.25	477.33
$\text{H}_2\text{B}(\text{OH})\text{F}^- (^1A - C_1)$	566.72	23.33	1.50	-0.77	-0.64	543.49
$\text{H}_3\text{B}(\text{SH})^- (^1A' - C_s)$	465.78	23.70	1.51	-0.49	-0.59	442.51

$\text{H}_2\text{B}(\text{SH})\text{F}^- (^1\text{A} - \text{C}_1)$	521.89	20.64	1.53	-0.80	-0.98	500.99
$\text{HBF}_2^- (^2\text{A}' - \text{C}_s)$	388.47	9.10	1.39	-0.73	-0.81	379.21
$\text{HBF}_2^- (^2\text{B}_1 - \text{C}_{2v})$	386.54	10.67	1.51	-0.76	-0.81	375.80
$\text{HBF}_3^- (^1\text{A}_1 - \text{C}_{3v})$	561.43	12.74	1.42	-1.11	-1.20	547.80
$\text{HBCl}_2^- (^2\text{A}' - \text{C}_s)$	317.91	8.27	1.28	-0.62	-1.71	308.59
$\text{H}_2\text{BCl}_2^- (^1\text{A}_1 - \text{C}_{2v})$	422.99	14.99	1.42	-0.63	-1.71	407.07
$\text{HBCl}_2\text{F}^- (^1\text{A}' - \text{C}_s)$	482.06	11.23	1.47	-0.94	-2.10	469.27
$\text{HBBr}_2^- (^2\text{A}' - \text{C}_s)$	294.86	7.83	2.32	-1.47	-7.03	281.21
$\text{H}_2\text{BBr}_2^- (^1\text{A}_1 - \text{C}_{2v})$	400.03	14.56	2.48	-1.40	-7.03	379.52
$\text{HBBr}_2\text{F}^- (^1\text{A}' - \text{C}_s)$	456.48	10.72	2.61	-1.43	-7.42	439.52
$\text{HBI}_2^- (^2\text{A}' - \text{C}_s)$	272.08	7.44		-0.10	-14.51	250.03
$\text{H}_2\text{BI}_2^- (^1\text{A}_1 - \text{C}_{2v})$	376.86	14.09		-0.11	-14.51	348.15
$\text{HBI}_2\text{F}^- (^1\text{A}' - \text{C}_s)$	430.32	11.32		-0.67	-14.90	403.44
$\text{H}_2\text{B}(\text{NH}_2)_2^- (^1\text{A}' - \text{C}_s)$	748.21	45.54	2.25	-0.68	-0.03	704.21
$\text{HB}(\text{NH}_2)_2\text{F}^- (^1\text{A}' - \text{C}_s)$	811.82	41.89	2.30	-1.02	-0.42	770.79
$\text{H}_2\text{B}(\text{OH})_2^- (^1\text{A} - \text{C}_2)$	643.16	30.61	1.69	-0.78	-0.47	612.99
$\text{HB}(\text{OH})_2\text{F}^- (^1\text{A} - \text{C}_1)$	712.39	27.10	1.80	-1.14	-0.86	685.10
$\text{H}_2\text{B}(\text{SH})_2^- (^1\text{A} - \text{C}_2)$	556.26	25.24	1.80	-0.87	-1.15	530.81
$\text{HB}(\text{SH})_2\text{F}^- (^1\text{A}' - \text{C}_s)$	610.93	21.33	1.84	-1.18	-1.54	588.72
$\text{BF}_3^- (^2\text{A}_1 - \text{C}_{3v})$	453.58	6.14	1.38	-1.07	-1.20	446.55
$\text{BF}_4^- (^1\text{A}_1 - \text{T}_d)$	631.23	8.90	1.58	-1.50	-1.59	620.82

$\text{BCl}_3^- (^2\text{A}_1 - \text{C}_{3v})$	335.80	3.86	1.45	-0.81	-2.55	330.04
$\text{HBCl}_3^- (^1\text{A}_1 - \text{C}_{3v})$	441.60	10.47	1.56	-0.83	-2.55	429.32
$\text{BCl}_3\text{F}^- (^1\text{A}_1 - \text{C}_{3v})$	499.68	6.22	1.64	-1.15	-2.94	491.01
$\text{BCl}_4^- (^1\text{A}_1 - \text{T}_d)$	455.10	5.33	1.73	-0.99	-3.39	447.12
$\text{BBr}_3^- (^2\text{A}_1 - \text{C}_{3v})$	297.52	3.08	3.30	-1.75	-10.53	285.46
$\text{HBBR}_3^- (^1\text{A}_1 - \text{C}_{3v})$	402.29	9.67	3.30	-1.72	-10.53	383.68
$\text{BBr}_3\text{F}^- (^1\text{A}_1 - \text{C}_{3v})$	457.37	5.31	3.44	-1.75	-10.92	442.82
$\text{BBr}_4^- (^1\text{A}_1 - \text{T}_d)$	398.42	4.10	4.16	-1.86	-14.03	382.58
$\text{BI}_3^- (^2\text{A}_1 - \text{C}_{3v})$	260.33	2.59		-0.11	-21.75	235.88
$\text{HBI}_3^- (^1\text{A}_1 - \text{C}_{3v})$	363.00	9.04		-0.12	-21.75	332.09
$\text{BI}_3\text{F}^- (^1\text{A}_1 - \text{C}_{3v})$	414.65	4.73		-0.67	-22.14	387.11
$\text{BI}_4^- (^1\text{A}_1 - \text{T}_d)$	342.84	3.36		-0.14	-28.99	310.36
$\text{HB}(\text{NH}_2)_3^- (^1\text{A}' - \text{C}_s)$	943.30	57.14	2.80	-0.98	-0.03	887.95
$\text{B}(\text{NH}_2)_3\text{F}^- (^1\text{A}' - \text{C}_s)$	1010.16	53.59	2.92	-1.34	-0.42	957.72
$\text{B}(\text{NH}_2)_4^- (^1\text{A}_1 - \text{D}_{2d})$	1139.00	68.67	3.38	-1.30	-0.03	1072.38
$\text{HB}(\text{OH})_3^- (^1\text{A} - \text{C}_3)$	785.95	33.72	2.00	-1.16	-0.69	752.38
$\text{B}(\text{OH})_3\text{F}^- (^1\text{A} - \text{C}_3)$	857.05	30.39	2.15	-1.54	-1.08	826.19
$\text{B}(\text{OH})_4^- (^1\text{A} - \text{S}_4)$	933.82	38.04	2.34	-1.56	-0.91	895.64
$\text{HB}(\text{SH})_3^- (^1\text{A} - \text{C}_3)$	641.63	26.04	2.13	-1.19	-1.71	614.82
$\text{B}(\text{SH})_3\text{F}^- (^1\text{A} - \text{C}_3)$	697.99	21.99	2.06	-1.52	-2.10	674.43
$\text{B}(\text{SH})_4^- (^1\text{A} - \text{S}_4)$	726.49	26.63	2.48	-1.54	-2.27	698.53

^a Extrapolated by using Equation (1) with aVnZ, $n = D, T, Q$. ^b The zero point energies were obtained as described in the text. ^c Core-valence corrections were obtained with the cc-pwCVTZ (B, N, O, F, S, Cl, and Br) and cc-pwCVTZ-PP (I) basis sets at the optimized MP2/aVTZ geometries. ^d The scalar relativistic correction is based on a CISD(FC)/VTZ MVD calculation and is expressed relative to the CISD result without the MVD correction, i.e. including the existing relativistic effects resulting from the use of a relativistic effective core potential. For molecules containing Br, the scalar relativistic correction was calculated using the DKH method as described in the text. ^e Correction due to the incorrect treatment of the atomic asymptotes as an average of spin multiplets. Values are based on C. Moore's Tables, Reference 28. ^f The theoretical value of the dissociation energy to atoms $\Sigma D_0(0\text{ K})$. ^g Reference 36. ^h Unscaled ZPE is 14.73 kcal/mol.

Table 7.2. Enthalpies of Formation (kcal/mol) at 0 K and 298 K.^a

Molecule	$\Delta H_f(0\text{ K})_{\text{theory}}$	$\Delta H_f(298\text{ K})_{\text{theory}}$
BH ₃ ^b	25.3	24.4 [25.5 ± 2.4 ^c]
BH ₃ ⁻	24.5	23.7
BH ₄ ^{-b}	-12.7	-14.6
H ₃ BF ⁻	-99.9	-101.7
H ₂ BF	-72.3	-73.3
H ₂ BF ⁻	-61.3	-62.2
H ₂ BF ₂ ⁻	-199.0	-200.7
H ₂ BCl	-17.6	-18.5
H ₂ BCl ⁻	-19.0	-19.7
H ₃ BCl ⁻	-62.9	-64.7
H ₂ BClF ⁻	-155.9	-157.5
H ₂ BBr	0.1	-2.6
H ₂ BBr ⁻	-6.8	-9.3
H ₃ BBr ⁻	-51.6	-55.2
H ₂ BBrF ⁻	-143.7	-147.0
H ₂ BI	17.6	16.3
H ₂ BI ⁻	4.4	3.3
H ₃ BI ⁻	-41.2	-43.3
H ₂ BIF ⁻	-131.3	-133.2
H ₂ B(NH ₂) ^b	-17.0	-19.7
H ₃ B(NH ₂) ⁻	-19.3	-22.8
H ₂ B(NH ₂)F ⁻	-115.6	-118.9
H ₂ B(OH)	-63.7	-65.6
H ₃ B(OH) ⁻	-76.7	-79.2
H ₂ B(OH)F ⁻	-176.0	-178.4
H ₂ B(SH)	-0.7	-2.4
H ₃ B(SH) ⁻	-35.2	-37.6
H ₂ B(SH)F ⁻	-126.9	-129.0
HBF ₂	-174.6	-175.5 [-175.4 ± 0.8 ^c]
HBF ₂ ⁻	-155.5	-156.3

HBF_3^-	-305.7	-307.1
HBCl_2	-58.9	-59.6 $[-59.3 \pm 1.0^c]$
HBCl_2^-	-64.7	-65.2
H_2BCl_2^-	-111.5	-113.0
HBCl_2F^-	-206.9	-208.0
HBBr_2	-23.0	-27.2 $[-25.0 \pm 1.2^c]$
HBBr_2^-	-38.1	-42.1
H_2BBr_2^-	-84.8	-89.8
HBBr_2F^-	-178.0	-182.5
HBI_2	12.0	10.6
HBI_2^-	-12.1	-13.3
H_2BI_2^-	-58.6	-60.7
HBI_2F^-	-147.0	-148.8
$\text{HB}(\text{NH}_2)_2$	-45.9	-49.9
$\text{H}_2\text{B}(\text{NH}_2)_2^-$	-34.3	-39.1
$\text{HB}(\text{NH}_2)_2\text{F}^-$	-134.0	-138.4
$\text{HB}(\text{OH})_2$	-152.0	-154.6
$\text{H}_2\text{B}(\text{OH})_2^-$	-153.4	-156.5
$\text{HB}(\text{OH})_2\text{F}^-$	-258.7	-261.4
$\text{HB}(\text{SH})_2$	-20.4	-22.5
$\text{H}_2\text{B}(\text{SH})_2^-$	-57.9	-60.5
$\text{HB}(\text{SH})_2\text{F}^-$	-148.9	-151.0
BF_3	-270.7	-271.4 $[-271.5 \pm 0.2^d]$
BF_3^-	-256.0	-256.5
BF_4^-	-411.8	-413.0
BCl_3	-96.4	-96.7 $[-96.3 \pm 0.5^c]$
BCl_3^-	-109.2	-109.2
HBCl_3^-	-156.8	-157.8
BCl_3F^-	-251.7	-252.2
BCl_4^-	-197.7	-198.0
BBr_3	-43.0	-48.3 $[-48.8 \pm 0.05^c]$
BBr_3^-	-65.8	-71.0

HBBr ₃ ⁻	-112.4	-118.5
BBr ₃ F ⁻	-204.7	-210.3
BBr ₄ ⁻	-134.7	-141.8
BI ₃	8.6	7.6 [17 ± 12 ^c]
BI ₃ ⁻	-23.9	-24.8
HBI ₃ ⁻	-68.5	-70.3
BI ₃ F ⁻	-156.7	-157.9
BI ₄ ⁻	-72.8	-74.7
B(NH ₂) ₃	-70.1	-74.9
HB(NH ₂) ₃ ⁻	-53.9	-60.0
B(NH ₂) ₃ F ⁻	-156.8	-162.5
B(NH ₂) ₄ ⁻	-74.1	-81.5
B(OH) ₃	-236.7	-239.8 [-237.2 ± 0.6 ^c]
HB(OH) ₃ ⁻	-233.8	-236.9
B(OH) ₃ F ⁻	-340.8	-343.7
B(OH) ₄ ⁻	-318.1	-321.9
B(SH) ₃	-36.3	-38.4
HB(SH) ₃ ⁻	-76.2	-78.8
B(SH) ₃ F ⁻	-169.0	-171.2
B(SH) ₄ ⁻	-94.3	-96.9

^a Experimental values are given in square brackets. ^b Reference 36. ^c Reference 7. ^d Reference 6.

Table 7.3. Calculated Hydride (HA) and Fluoride (FA) Affinities in kcal/mol at 0 K and 298 K.

Molecule	HA		FA	
	(0 K)	(298 K)	(0 K)	(298 K)
H ₃ B	72.3	73.7	65.2	66.6
H ₂ BF	61.8	63.2	66.7	67.9
H ₂ BCl	79.5	80.9	78.3	79.4
H ₂ BBr	86.0	87.3	83.8	84.9
H ₂ BI	93.0	94.3	88.9	89.9
H ₂ BNH ₂	36.6	37.8	38.6	39.7
H ₂ BOH	47.2	48.4	52.3	53.3
H ₂ BSH	68.8	69.8	66.2	67.0
HBF ₂	58.6	60.0	71.0	72.1
HBCl ₂	86.9	88.1	88.0	88.9
HBBr ₂	96.0	97.3	95.0	95.8
HBI ₂	104.8	106.0	99.0	99.9
HB(NH ₂) ₂	22.6	24.0	28.1	29.0
HB(OH) ₂	35.6	36.6	46.6	47.3
HB(SH) ₂	71.7	72.7	68.5	69.0
BF ₃	69.2	70.5	81.1	82.1
BCl ₃	94.6	95.8	95.2	96.0
BBr ₃	103.6	104.9	101.7	102.4
BI ₃	111.4	112.6	105.3	105.9
B(NH ₂) ₃	18.0	19.8	26.7	28.1
B(OH) ₃	31.3	31.8	44.1	44.4
B(SH) ₃	74.2	75.2	72.7	73.3

Table 7.4. Calculated X^- Affinities (XA; X = Cl, Br, I, NH₂, OH, and SH) in kcal/mol at 0 K and 298 K.

Molecule	X	(0 K)	(298 K)
H ₃ B	Cl	33.4	33.2
H ₃ B	Br	27.5	27.2
H ₃ B	I	21.5	21.2
H ₃ B	NH ₂	72.0	73.9
H ₃ B	OH	69.2	69.3
H ₃ B	SH	39.7	41.2
H ₂ BF	Cl	28.8	28.3
H ₂ BF	Br	21.9	21.4
H ₂ BF	I	14.1	13.4
H ₂ BF	NH ₂	70.7	72.4
H ₂ BF	OH	70.9	70.9
H ₂ BF	SH	33.8	35.0
H ₂ BCl	Cl	39.1	38.6
H ₂ BBr	Br	35.5	34.8
H ₂ BI	I	31.3	30.5
H ₂ BNH ₂	NH ₂	15.8	16.0
H ₂ BOH	OH	56.8	56.6
H ₂ BSH	SH	16.7	17.2
HBCl ₂	Cl	43.1	42.3
HBBr ₂	Br	39.3	38.3
HBI ₂	I	35.6	34.4
HB(NH ₂) ₂	NH ₂	35.4	36.9
HB(OH) ₂	OH	48.9	48.0
HB(SH) ₂	SH	35.0	35.6
BCl ₃	Cl	46.4	45.4
BBr ₃	Br	42.3	41.1
BI ₃	I	36.9	36.2
B(NH ₂) ₃	NH ₂	31.4	33.3

B(OH) ₃	OH	48.5	47.7
B(SH) ₃	SH	37.2	37.7

Table 7.5. Calculated Electron Affinities at 0 K at the CCSD(T)/CBS and B3LYP/aVTZ Levels.

Molecule	CCSD(T)	CCSD(T)	B3LYP	B3LYP	Expt.
	kcal/mol	eV	kcal/mol	eV	
BH ₃	0.8	0.031	4.5	0.17	0.038 ± 0.015 ^a
H ₂ BF	-11.0	-0.42	-15.9	-0.61	
H ₂ BCl	1.4	0.05	4.7	0.18	
H ₂ BBr	6.6	0.26	8.6	0.33	
H ₂ BI	13.2	0.51	14.7	0.56	
HBF ₂	-19.1	-0.73	-13.4	-0.51	
HBCl ₂	5.8	0.22	9.0	0.35	
HBBr ₂	14.8	0.57	15.7	0.60	
HBI ₂	24.0	0.92	25.0	0.96	
BF ₃	-14.7	-0.56	-8.9	-0.34	
BCl ₃	12.7	0.49	14.4	0.55	0.33 ± 0.20 ^b
BBr ₃	22.5	0.86	23.2	0.89	0.82 ± 0.20 ^b
BI ₃	32.5	1.25	33.0	1.27	
H ₂ BNH ₂			-8.6	-0.33	
H ₂ BOH			-8.8	-0.34	
H ₂ BSH			-4.6	-0.17	
HB(NH ₂) ₂			-7.9	-0.30	
HB(OH) ₂			-6.2	-0.24	
HB(SH) ₂			-4.6	-0.18	
B(NH ₂) ₃			-6.1	-0.24	
B(OH) ₃			-5.3	-0.20	
B(SH) ₃			1.8	0.07	

^a Reference 35. Laser photoelectron spectroscopy. ^b Reference 39. Neutral beam ionization potentials.

Table 7.6. Calculated $\text{BH}_{3-n}\text{X}_n\text{-A}^-$ Bond Dissociation Energies in kcal/mol at 0 K.^a

Molecule	A	(0 K)
H ₃ B	H	88.8
H ₂ BF	H	79.2 (90.2)
H ₂ BCl	H	92.3
H ₂ BBr	H	96.7
H ₂ BI	H	97.2
H ₂ BNH ₂	H	53.9
H ₂ BOH	H	64.6
H ₂ BSH	H	86.2
HBF ₂	H	76.0 (95.1)
HBCl ₂	H	98.5
HBBr ₂	H	98.6
HBI ₂	H	98.1
HB(NH ₂) ₂	H	40.0
HB(OH) ₂	H	53.0
HB(SH) ₂	H	89.1
BF ₃	H	86.6 (101.2)
BCl ₃	H	99.3
BBr ₃	H	98.6
BI ₃	H	96.3
B(NH ₂) ₃	H	35.4
B(OH) ₃	H	48.7
B(SH) ₃	H	91.6
H ₃ B	F	142.8
H ₂ BF	F	145.1 (156.1)
H ₂ BCl	F	155.4
H ₂ BBr	F	155.6
H ₂ BI	F	154.2
H ₂ BNH ₂	F	117.0
H ₂ BOH	F	130.8
H ₂ BSH	F	144.6

HB F_2	F	149.5 (168.5)
HBCl $_2$	F	160.6
HBBr $_2$	F	158.6
HBI $_2$	F	153.4
HB(NH $_2$) $_2$	F	106.6
HB(OH) $_2$	F	125.1
HB(SH) $_2$	F	146.9
BF $_3$	F	159.5 (174.2)
BCl $_3$	F	160.9
BBr $_3$	F	157.7
BI $_3$	F	151.3
B(NH $_2$) $_3$	F	105.1
B(OH) $_3$	F	122.5
B(SH) $_3$	F	151.2
H $_3$ B	Cl	115.9
H $_2$ BF	Cl	112.1 (123.1)
H $_2$ BCl	Cl	121.0
HBCl $_2$	Cl	120.6
BCl $_3$	Cl	117.0
H $_3$ B	Br	104.2
H $_2$ BF	Br	99.5 (110.5)
H $_2$ BBr	Br	106.4
HBBr $_2$	Br	102.1
BBr $_3$	Br	97.4
H $_3$ B	I	91.3
H $_2$ BF	I	84.6 (95.7)
H $_2$ BI	I	88.6
HBI $_2$	I	82.1
BI $_3$	I	74.9
H $_3$ B	NH $_2$	89.0
H $_2$ BF	NH $_2$	88.5 (99.5)
H $_2$ BNH $_2$	NH $_2$	33.6

HB(NH ₂) ₂	NH ₂	53.1
B(NH ₂) ₃	NH ₂	49.1
H ₃ B	OH	110.5
H ₂ BF	OH	113.0 (124.1)
H ₂ BOH	OH	99.0
HB(OH) ₂	OH	91.1
B(OH) ₃	OH	90.7
H ₃ B	SH	92.4
H ₂ BF	SH	87.2 (98.2)
H ₂ BSH	SH	70.1
HB(SH) ₂	SH	88.4
B(SH) ₃	SH	90.7

^a Values in parenthesis include calculated negative EA values of the fluoroboranes.

Table 7.7. Distortion Energies at 0 K in kcal/mol at the B3LYP/aVDZ and CCSD(T)/aVTZ levels.

Molecule	$\Delta E_{\text{distort}1}(\text{BX}_3^-)^{\text{a}}$	$\Delta E_{\text{distort}1}(\text{BX}_3^-)^{\text{a}}$	$\Delta E_{\text{distort}2}(\text{BX}_3\text{F}^-)^{\text{b}}$	$\Delta E_{\text{distort}2}(\text{BX}_3\text{F}^-)^{\text{b}}$
	B3LYP	CCSD(T)	B3LYP	CCSD(T)
BF ₃	34.4	38.1	42.6	47.1
BCl ₃	26.6	29.1	37.8	40.9
BBr ₃	20.2	22.1	31.1	33.5
BI ₃	14.7	16.3	26.9	29.0

^a Distortion Energy1 = E(distorted Structure BX₃⁻ geometry) - E(planar, ground state minimum BX₃). ^b Distortion Energy2 = E(distorted Structure BX₃F⁻ geometry) - E(planar, ground state minimum BX₃))

Figure Captions

Figure 7.1. (a) Three step thermodynamic cycle for the A^- ion affinities of $BH_{3-n}X_n$: (1) the first ionization potential of A^- , (2) the electron affinity of $BH_{3-n}X_n$, and (3) the homolytic BDE of the B-A bond in the corresponding $BH_{3-n}X_nA^-$ anion. (b) Representative three step thermodynamic cycle for the hydride affinity of BH_3 : (1) the electron affinity of the H radical, (2) the electron affinity of BH_3 , and (3) the homolytic BDE of the B-H bond in BH_4^- . Energies in kcal/mol. (c) Thermodynamic cycle relating the hydride affinity of X_2BA to the anion affinity of X_2BH . The two reactions are linked by a metathesis reaction for which the energetics can be related to the homolytic bond energies of X_2B-A and X_2B-H and the electron affinities of A and H.

Figure 7.2. Hydride and fluoride affinities of the $BH_{3-n}X_n$ compounds in kcal/mol at 0 K show a linear correlation with the proton affinity of X^- . Values for $X = F$ deviate from the trend line drawn through the points for I, Br, Cl, SH, OH, and NH_2 .

Figure 7.3. The I^- , Br^- , Cl^- , SH^- , OH^- , and NH_2^- anion affinities of BH_3 in kcal/mol at 0 K correlate linearly with the PAs of these anions, but the point for F^- deviates from the trend line.

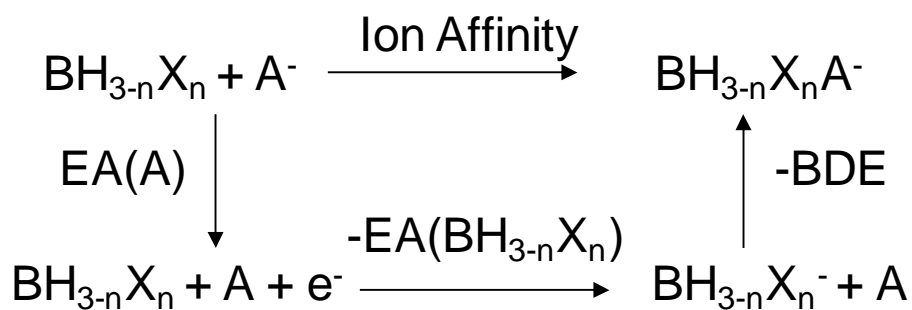
Figure 7.4. Plots of the homolytic B-X BDEs for BH_2X and BH_3X^- against the homolytic HX BDEs for the halogen series. For I, Br, and Cl, the EAs increase linearly with the homolytic HX BDEs, however, the EA for F falls way below the trend line suggesting that it is anomalously low.

Figure 7.5. Born-Haber cycles for the FAs of BF_3 and BI_3 . For each step, the total energies and the energies of each component are given in kcal/mol. The values for the overall reaction are the sums of steps 1-3 given by the values inside the square defined by the arrows. The values outside the square defined by the arrows are the conceptual values, which include the effect of the distortion energies calculated for BX_3 at the BX_3^- and BX_3F^- geometries (CCSD(T) values from

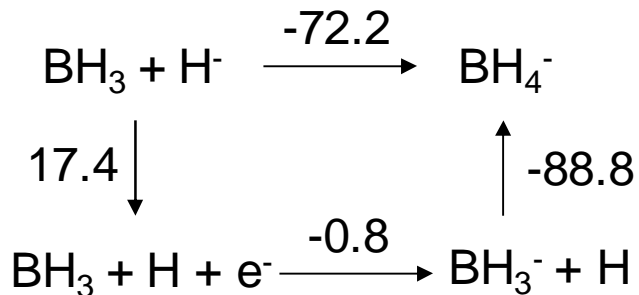
Table 7). These values are provided as guidelines for understanding the roles of the various terms. The EA of BF_3 is negative so it is set to 0.

Figure 7.1.

(a)



(b)



(c)

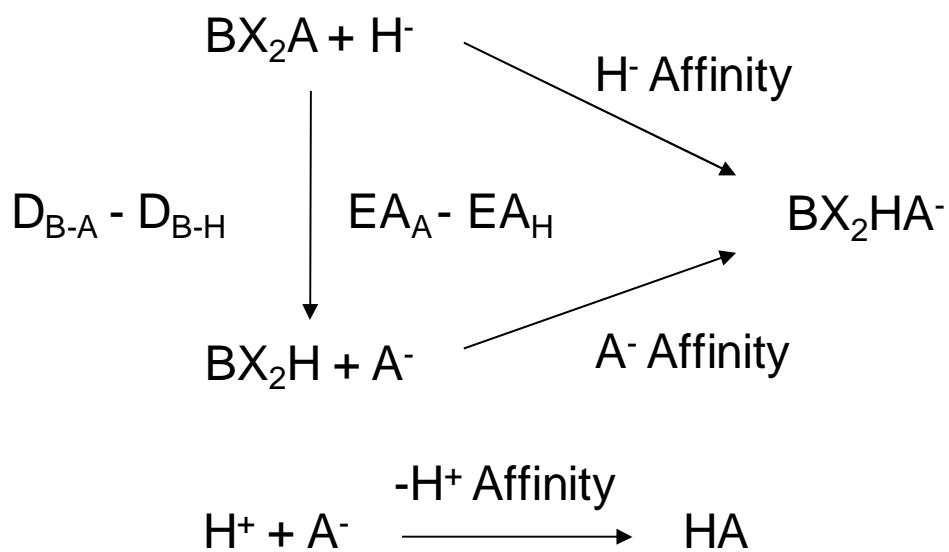


Figure 7.2.

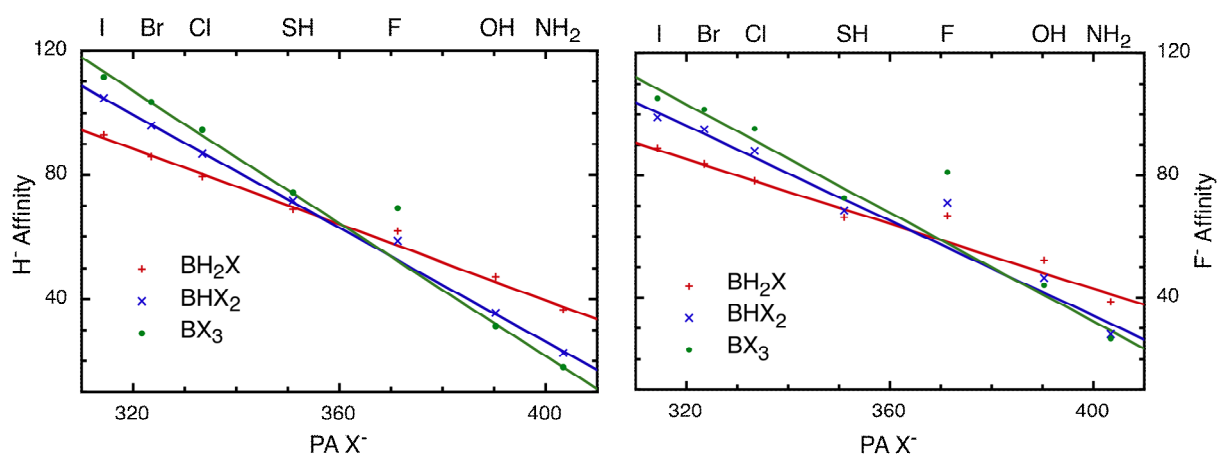


Figure 7.3.

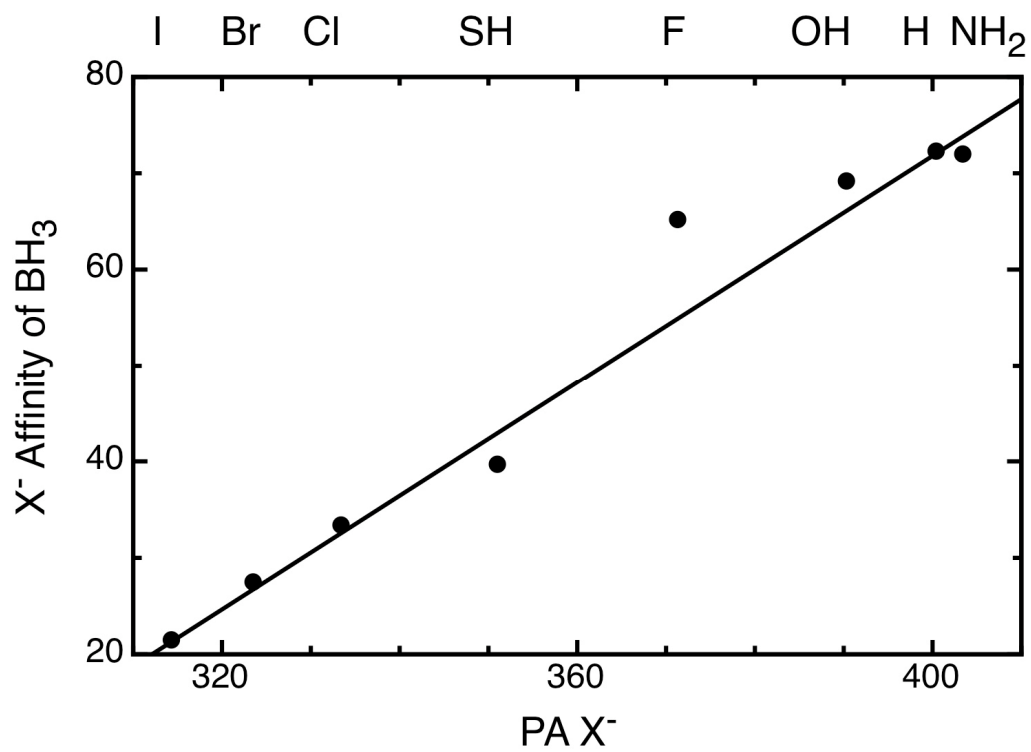


Figure 7.4.

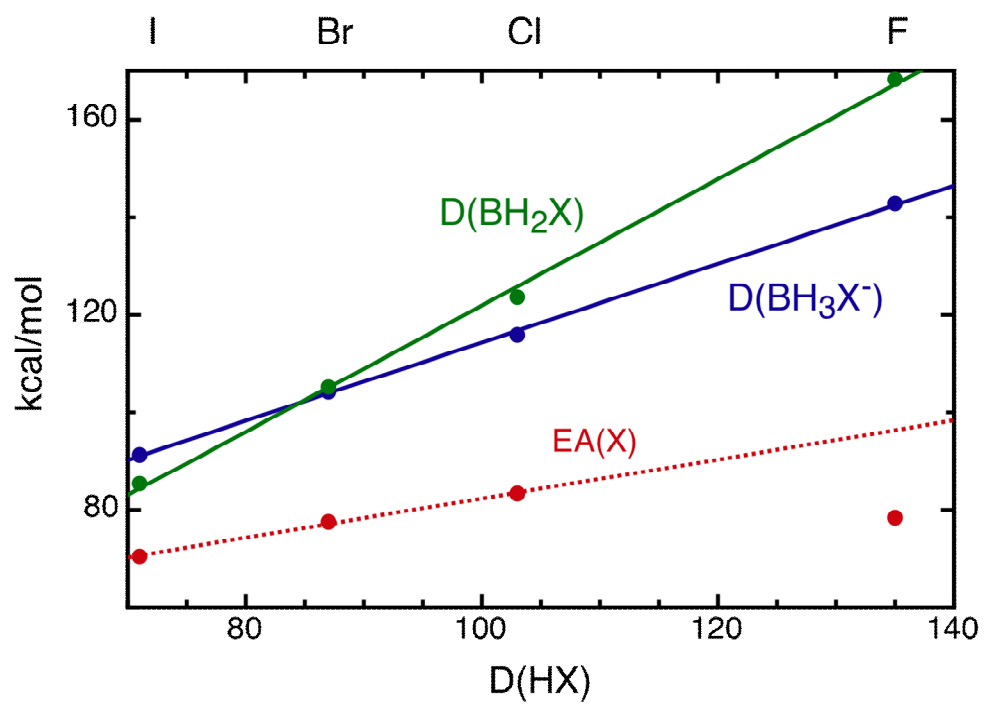
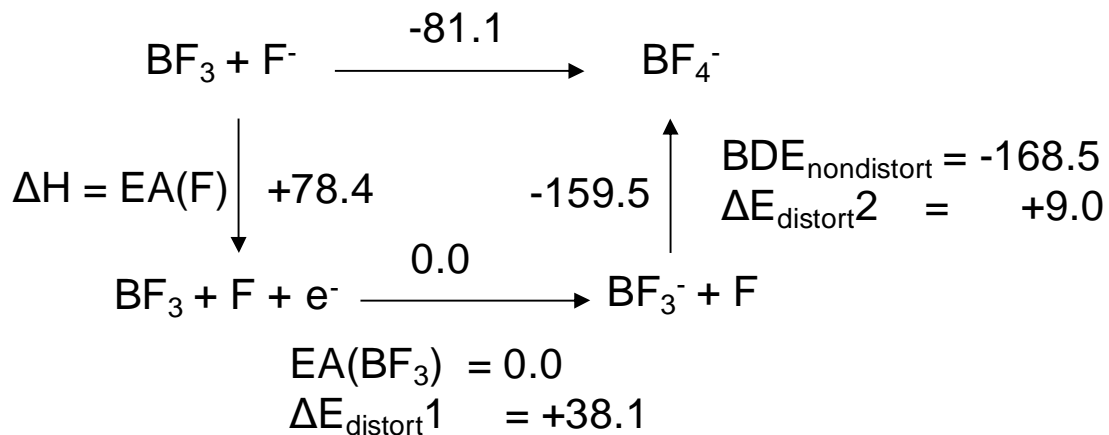
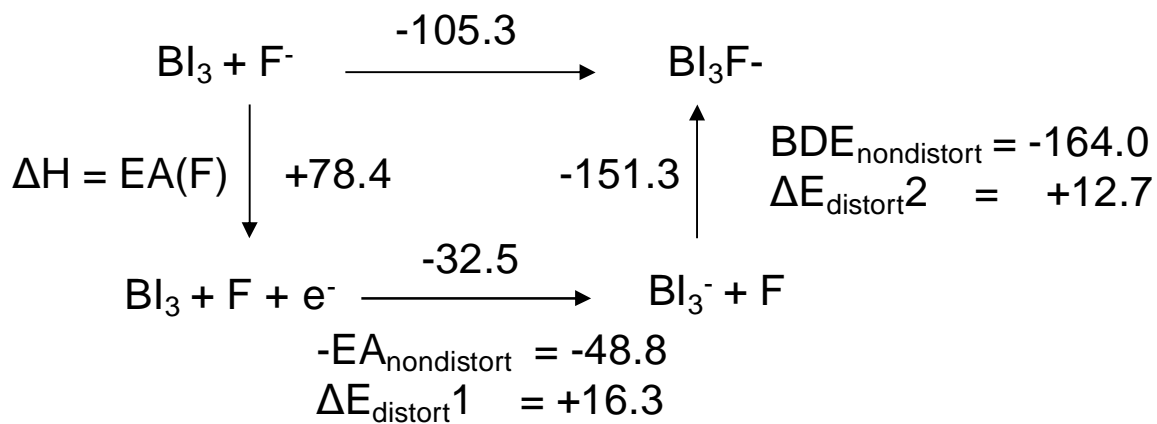


Figure 7.5

(a)



(b)



7.5 References

-
- ¹ Grant, D. J.; Dixon, D. A. *J. Phys. Chem. A*, **2009**, *113*, 777.
- ² Greenwood, N. N.; Earnshaw, A. *Chemistry of the Elements*, Pergamon Press, Oxford, 1984.
- ³ Christe, K. O.; Dixon, D. A.; McLemore, D.; Wilson, W. W.; Sheehy, J. A.; Boatz, J. A., *J. Fluor. Chem.* **2000**, *101*, 151.
- ⁴ Vianello, R.; Maccis, Z. B. *Inorg. Chem.* **2005**, *44*, 1095, and references cited therein.
- ⁵ (a) Peterson, K. A.; Xantheas, S. S.; Dixon, D. A.; Dunning, T. H. Jr., *J. Phys. Chem. A* **1998**, *102*, 2449; (b) Feller, D.; Peterson, K. A. *J. Chem. Phys.* **1998**, *108*, 154; (c) Dixon, D. A.; Feller, D. *J. Phys. Chem. A* **1998**, *102*, 8209; (d) Feller, D.; Peterson, K. A. *J. Chem. Phys.* **1999**, *110*, 8384; (e) Feller, D.; Dixon, D. A. *J. Phys. Chem. A* **1999**, *103*, 6413; (f) Feller, D. *J. Chem. Phys.* **1999**, *111*, 4373; (g) Feller, D.; Dixon, D. A. *J. Phys. Chem. A* **2000**, *104*, 3048; (h) Feller, D.; Sordo, J. A. *J. Chem. Phys.* **2000**, *113*, 485; (i) Feller, D.; Dixon, D. A. *J. Chem. Phys.* **2001**, *115*, 3484; (j) Dixon, D. A.; Feller, D.; Sandrone, G. *J. Phys. Chem. A* **1999**, *103*, 4744; (k) Ruscic, B.; Wagner, A. F.; Harding, L. B.; Asher, R. L.; Feller, D.; Dixon, D. A.; Peterson, K. A.; Song, Y.; Qian, X.; Ng, C.; Liu, J.; Chen, W.; Schwenke, D. W. *J. Phys. Chem. A* **2002**, *106*, 2727; (l) Feller, D.; Dixon, D. A.; Peterson, K. A. *J. Phys. Chem. A*, **1998**, *102*, 7053; (m) Dixon, D. A.; Feller, D.; Peterson, K. A. *J. Chem. Phys.*, **2001**, *115*, 2576.
- ⁶ Cox, J. D.; Wagman, D. D.; Medvedev, V. A. *CODATA Key Values for Thermodynamics*, Hemisphere Publishing Corp., New York, **1984**, 1.
- ⁷ Chase, M.W., Jr. *NIST-JANAF Thermochemical Tables, Fourth Edition*, J. Phys. Chem. Ref. Data, Monograph 9, **1998**, 1-1951.
- ⁸ Purvis III, G. D.; Bartlett, R. J. *J. Chem. Phys.* **1982**, *76*, 1910.
- ⁹ Raghavachari, K.; Trucks, G. W.; Pople, J. A.; Head-Gordon, M. *Chem. Phys. Lett.* **1989**, *157*, 479.
- ¹⁰ Watts, J. D.; Gauss, J.; Bartlett, R. J. *J. Chem. Phys.* **1993**, *98*, 8718.
- ¹¹ Dunning, T. H. *J. Chem. Phys.* **1989**, *90*, 1007.
- ¹² Kendall, R. A.; Dunning Jr., T. H.; Harrison, R. J. *J. Chem. Phys.* **1992**, *96*, 6796.
- ¹³ McQuarrie, D. A. *Statistical Mechanics*, University Science Books: Sausalito, CA, 2001.
- ¹⁴ Curtiss, L. A.; Raghavachari, K.; Redfern, P. C.; Pople, J. A. *J. Chem. Phys.* **1997**, *106*, 1063.

-
- ¹⁵ Werner, H. -J.; Knowles, P. J.; *et al.* MOLPRO, version 2006.1, a package of ab initio programs, Universität Stuttgart, Stuttgart, Germany, University of Birmingham, Birmingham, United Kingdom, 2006. See <http://www.molpro.net>.
- ¹⁶ Rittby, M.; Bartlett, R. J. *J. Phys. Chem.* **1988**, *92*, 3033.
- ¹⁷ Knowles, P. J.; Hampel, C.; Werner, H. -J. *J. Chem. Phys.* **1994**, *99*, 5219.
- ¹⁸ Deegan, M. J. O.; Knowles, P. J. *Chem. Phys. Lett.* **1994**, *227*, 321.
- ¹⁹ Dunning, T. H. Jr., Peterson, K. A. Wilson, A. K. *J. Chem. Phys.* **2001**, *114*, 9244.
- ²⁰ Peterson, K. A.; Woon, D. E.; Dunning, T. H., Jr. *J. Chem. Phys.* **1994**, *100*, 7410.
- ²¹ Peterson, K. A.; Dunning, T. H., Jr., *J. Chem. Phys.* **2002**, *117*, 10548.
- ²² Dixon, D. A.; Grant, D. J.; Christe, K. O.; Peterson, K. A. *Inorg. Chem.* **2008**, *47*, 5485
- ²³ (a) Peterson, K. A. *J. Chem. Phys.* **2003**, *119*, 11099; (b) Peterson, K. A.; Figgien, D.; Goll, E.; Stoll, H.; Dolg, M. *J. Chem. Phys.* **2003**, *119*, 11113.
- ²⁴ (a) Møller, C.; Plesset, M.S. *Phys. Rev.* **1934**, *46*, 618; (b) Pople, J.A.; Binkley, J.S.; Seeger, R. *Int. J. Quantum Chem. Symp.* **1976**, *10*, 1.
- ²⁵ Jacox, M. E. *J. Phys. Chem. Ref. Data* **1994**, *Monograph 3*.
- ²⁶ Grant, D. J.; Dixon D. A. *J. Phys. Chem., A* **2005**, *109*, 10138
- ²⁷ Gaussian 03, Revision E.01, Frisch, M. J., et al. Gaussian, Inc., Wallingford CT, 2004
- ²⁸ C.E. Moore "Atomic energy levels as derived from the analysis of optical spectra, Volume 1, H to V," U.S. National Bureau of Standards Circular 467, U.S. Department of Commerce, National Technical Information Service, COM-72-50282, Washington, D.C.; **1949**.
- ²⁹ Davidson, E. R.; Ishikawa, Y.; Malli, G. L. *Chem. Phys. Lett.* **1981**, *84*, 226.
- ³⁰ (a) Douglas, M.; Kroll, N. M. *Ann. Phys.* **1974**, *82*, 89. (b) Hess, B. A. *Phys. Rev. A* **1985**, *32*, 756. (c) Hess, B. A. *Phys. Rev. A* **1986**, *33*, 3742.
- ³¹ de Jong, W. A.; Harrison, R. J.; Dixon, D. A. *J. Chem. Phys.* **2001**, *114*, 48.
- ³² EMSL basis set library. <http://www.emsl.pnl.gov/forms/basisform.html>
- ³³ Karton, A.; Martin, J. M. L. *J. Phys. Chem. A* **2007**, *111*, 5936.

-
- ³⁴ Lee, T. J.; Taylor, P. R. *Int. J. Quantum Chem. Symp.* **1989**, *23*, 199
- ³⁵ Wickham-Jones, C. T.; Moran, S.; Ellison, G. B. *J. Chem. Phys.* **1989**, *90*, 795.
- ³⁶ Gutowski, M.; Dixon, D. *J. Phys. Chem. A* **2005**, *109*, 5129.
- ³⁷ Becke, A. D., *J. Chem. Phys.*, **1993**, *98*, 5648; Lee, C. T., Yang, W. T.; Parr, R. G., *Phys. Rev. B*, **1988**, *37*, 785.
- ³⁸ Dixon, D. A.; Feller, D. F.; Peterson, K. A. *J. Phys. Chem. A* **1997**, *101*, 9405.
- ³⁹ Rothe, E. W.; Mathur, B. P.; Reck, G. P. *Inorg. Chem.* **1980**, *19*, 829.
- ⁴⁰ Bartmess, J. E. "Negative Ion Energetics Data" in NIST Chemistry WebBook, NIST Standard Reference Database Number 69, Eds. Linstrom, P. J.; Mallard, W. G.; National Institute of Standards and Technology, Gaithersburg MD, 20899, <http://webbook.nist.gov>, (retrieved April 20, 2009).
- ⁴¹ Anane, H.; Boutalib, A.; Tomas, F. *J. Phys. Chem. A* **1997**, *101*, 7879; Anane, H.; El Houssame, S.; El Guerraze, A.; Guermoune, A.; Boutalib, A.; Jarid, A.; Nebot-Gil, I.; Tomas, F., *Cent. Eur. J. Chem.* **2008**, *6*, 400.
- ⁴² $PA(X^-) = D(X-H) - EA(X) + IP(H)$ where $D(X-H)$ is the enthalpy for homolysis, of the X-H bond, $EA(X)$ is the electron affinity of X, and IP is the ionization energy of H; by convention EA is a positive number if the electron is bound.
- ⁴³ Cox, J. D.; Wagman, D. D.; Medvedev, V. A. CODATA Key Values for Thermodynamics, Hemisphere Publishing Corp., New York, 1984, 1.
- ⁴⁴ Klapötke, T. M.; Tornieporth-Oetting, I. C. *Nichtmetallchemie*, VCH, Weinheim 1994, pp 187 – 190.
- ⁴⁵ Bessac, F.; Frenking, G. *Inorg. Chem.*, **2003**, *42*, 7990.
- ⁴⁶ Rowsell, B. D.; Gillespie, R. J.; Heard, G. L. *Inorg. Chem.*, **1999**, *38*, 4659.
- ⁴⁷ Brinck, T.; Murray, J. S.; Politzer, P. *Inorg. Chem.* **1993**, *32*, 2622.
- ⁴⁸ Hirao, H.; Omoto, K.; Fujimoto, H. *J. Phys. Chem. A* **1999**, *103*, 5807.
- ⁴⁹ Branchadell, V.; Oliva, A. *J. Mol. Struct.: THEOCHEM* **1991**, *236*, 75.
- ⁵⁰ Reed, A. E., Curtiss, L. A.; Weinhold, F. *Chem. Rev.*, **1988**, *88*, 899; Reed, A. E., Weinstock, R. B.; Weinhold, F., *J. Chem. Phys.* **1985**, *83*, 735.
- ⁵¹ Emsley, J. *The Elements*, 2nd Edition, Clarendon Press, Oxford, 1994.

7.6 Appendix

Full author citations for References 15 and 27

15. MOLPRO, version 2006.1, a package of ab initio programs, Werner, H.-J.; Knowles, P. J.; Lindh, R.; Manby, F. R.; Schütz, M.; Celani, P.; Korona, T.; Rauhut, G.; Amos, R. D.; Bernhardsson, A.; Berning, A.; Cooper, D. L.; Deegan, M. J. O.; Dobbyn, A. J.; Eckert, F.; Hampel, C.; Hetzer, G.; Lloyd, A. W.; McNicholas, S. J.; Meyer, W.; Mura, M. E.; Nicklass, A.; Palmieri, P.; Pitzer, R.; Schumann, U.; Stoll, H.; Stone, A. J.; Tarroni, R.; Thorsteinsson, T. See <http://www.molpro.net>.

27. Gaussian 03, Revision E.01, Frisch, M. J.; Trucks, G. W.; Schlegel, H. B.; Scuseria, G. E.; Robb, M. A.; Cheeseman, J. R.; Montgomery, Jr., J. A.; Vreven, T.; Kudin, K. N.; Burant, J. C.; Millam, J. M.; Iyengar, S. S.; Tomasi, J.; Barone, V.; Mennucci, B.; Cossi, M.; Scalmani, G.; Rega, N.; Petersson, G. A.; Nakatsuji, H.; Hada, M.; Ehara, M.; Toyota, K.; Fukuda, R.; Hasegawa, J.; Ishida, M.; Nakajima, T.; Honda, Y.; Kitao, O.; Nakai, H.; Klene, M.; Li, X.; Knox, J. E.; Hratchian, H. P.; Cross, J. B.; Bakken, V.; Adamo, C.; Jaramillo, J.; Gomperts, R.; Stratmann, R. E.; Yazyev, O.; Austin, A. J.; Cammi, R.; Pomelli, C.; Ochterski, J. W.; Ayala, P. Y.; Morokuma, K.; Voth, G. A.; Salvador, P.; Dannenberg, J. J.; Zakrzewski, V. G.; Dapprich, S.; Daniels, A. D.; Strain, M. C.; Farkas, O.; Malick, D. K.; Rabuck, A. D.; Raghavachari, K.; Foresman, J. B.; Ortiz, J. V.; Cui, Q.; Baboul, A. G.; Clifford, S.; Cioslowski, J.; Stefanov, B. B.; Liu, G.; Liashenko, A.; Piskorz, P.; Komaromi, I.; Martin, R. L.; Fox, D. J.; Keith, T.; Al-Laham, M. A.; Peng, C. Y.; Nanayakkara, A.; Challacombe, M.; Gill, P. M. W.; Johnson, B.; Chen, W.; Wong, M. W.; Gonzalez, C.; and Pople, J. A.; Gaussian, Inc., Wallingford CT, 2004.

Table A7.1. Optimized MP2/aVTZ Bond Lengths (Å) and Bond Angles (°).

Molecule	R_{HX}	R_{HB}	R_{BX}	R_{BF}	$\angle\text{HBH}$	$\angle\text{HBX}$	$\angle\text{HXB}$	$\angle\text{FBX}$	$\angle\text{XBX}$
$\text{H}_3\text{B}^- (^2\text{A}_2'' - D_{3h})^a$		1.2110			120.0				
$\text{H}_2\text{BF}^- (^1\text{A}_1 - C_{3v})^a$		1.2038	1.3817			117.3			
$\text{H}_3\text{BF}^- (^1\text{A}_1 - C_{3v})^a$		1.2430	1.4663		109.4	109.7			
$\text{H}_3\text{B-FH} (^1\text{A}' - C_s)$	0.9257	1.1921		2.1898	119.4		103.5		
		1.1867							
$\text{H}_2\text{BF}_2^- (^1\text{A}_1 - C_{2v})$		1.2368	1.4439		112.1	109.1			108.1
$\text{H}_2\text{BF-FH} (^1\text{A}' - C_s)$	0.9251	1.1874	1.3371	2.5268	124.7	117.6	92.2	85.8	
$\text{H}_2\text{BCl}^- (^2\text{A}' - C_s)^a$		1.2045	1.8886			113.3			
$\text{H}_3\text{BCl}^- (^1\text{A}_1 - C_{3v})$		1.2155	1.9638		112.2	106.6			
$\text{H}_2\text{BClF}^- (^1\text{A}' - C_s)$		1.2154	1.9687	1.4177	114.5	105.2		107.8	
$\text{H}_2\text{BBr}^- (^2\text{A}' - C_s)^a$		1.2032	2.0714			111.6			
$\text{H}_3\text{BBr}^- (^1\text{A}_1 - C_{3v})$		1.2116	2.1198		113.1	105.6			
$\text{H}_2\text{BBrF}^- (^1\text{A}' - C_s)$		1.2113	2.1423	1.4097	115.5	103.8		107.6	
$\text{H}_2\text{BI}^- (^2\text{A}' - C_s)^a$		1.2019	2.2955			110.3			
$\text{H}_3\text{BI}^- (^1\text{A}_1 - C_{3v})$		1.2069	2.3574		114.4	103.9			
$\text{H}_2\text{BIF}^- (^1\text{A}' - C_s)$		1.2057	2.4288	1.3964	117.2	101.2		107.1	
$\text{H}_3\text{B}(\text{NH}_2)^- (^1\text{A}' - C_s)$	1.0164	1.2348	1.5817		109.3	108.9	109.8		
		1.2482			108.1	113.5			
$\text{H}_2\text{B}(\text{NH}_2)\text{F}^- (^1\text{A}' - C_s)$	1.0153	1.2350	1.5433	1.4800	111.7	109.0	110.7	111.8	

$\text{H}_3\text{B}(\text{OH})^- (^1\text{A} - \text{C}_1)$	0.9595	1.2453	1.5224		107.8	111.5	106.7	
		1.2312			109.1			
$\text{H}_2\text{B}(\text{OH})\text{F}^- (^1\text{A} - \text{C}_1)$	0.9599	1.2314	1.4895	1.4635	111.9	107.6	107.0	110.1
		1.2442				111.0		
$\text{H}_3\text{B}(\text{SH})^- (^1\text{A}' - \text{C}_s)$	1.3361	1.2189	1.9812		111.9	109.3	99.3	-
		1.2195			111.2	103.5		
$\text{H}_2\text{B}(\text{SH})\text{F}^- (^1\text{A} - \text{C}_1)$	1.3359	1.2213	1.9796	1.4343	113.1	103.2	98.5	110.7
		1.2195				107.6		
$\text{HBF}_2^- (^2\text{A}' - \text{C}_s)^{\text{a}}$		1.2117	1.3842			116.0		
$\text{HBF}_3^- (^1\text{A}_1 - \text{C}_{3v})$		1.2286	1.4242			110.5		108.5
$\text{HBF}_2\text{-FH} (^1\text{A} - \text{C}_1)$	0.9323	1.1808	1.3435	2.5283		121.1	107.1	88.3
			1.3356			121.6		96.3
$\text{HBCl}_2^- (^2\text{A}' - \text{C}_s)^{\text{a}}$		1.2017	1.8740			112.5		
$\text{H}_2\text{BCl}_2^- (^1\text{A}_1 - \text{C}_{2v})$		1.2023	1.9082		115.4	108.0		109.2
$\text{HBCl}_2\text{F}^- (^1\text{A}' - \text{C}_s)$		1.2022	1.9072	1.3903		108.3		108.9
$\text{HBBr}_2^- (^2\text{A}' - \text{C}_s)^{\text{a}}$		1.1981	2.0422			111.8		
$\text{H}_2\text{BBr}_2^- (^1\text{A}_1 - \text{C}_{2v})$		1.1973	2.0511		116.5	107.6		109.8
$\text{HBBr}_2\text{F}^- (^1\text{A}' - \text{C}_s)$		1.1978	2.0584	1.3824		107.6		108.9
$\text{HBI}_2^- (^2\text{A}' - \text{C}_s)^{\text{a}}$		1.1966	2.2553			111.4		
$\text{H}_2\text{BI}_2^- (^1\text{A}_1 - \text{C}_{2v})$		1.1929	2.2700		117.8	107.1		110.5
$\text{HBI}_2\text{F}^- (^1\text{A}' - \text{C}_s)$		1.1952	2.2991	1.3735		106.5		109.0
								108.5

H ₂ B(NH ₂) ₂ ⁻ (¹ A' - C _s)	1.0154	1.2486	1.5632		107.9	106.6	111.1		106.5
	1.0164						110.0		
HB(NH ₂) ₂ F ⁻ (¹ A' - C _s)	1.0154	1.2368	1.5613	1.4436		107.7	110.1	106.3	116.8
	1.0182						110.2		
H ₂ B(OH) ₂ ⁻ (¹ A - C ₂)	0.9664	1.2413	1.5177		111.3	106.1	105.8		110.6
HB(OH) ₂ F ⁻ (¹ A - C ₁)	0.9602	1.2320	1.4644	1.4637		109.1	106.3	106.6	108.4
	0.9622						105.5		
H ₂ B(SH) ₂ ⁻ (¹ A - C ₂)	1.3361	1.2099	1.9461	-	112.9	111.3	98.2	-	112.6
HB(SH) ₂ F ⁻ (¹ A' - C _s)	1.3366	1.2129	1.9506	1.4137		105.5	97.3	110.3	112.0
BF ₃ ⁻ (² A ₁ - C _{3v})			1.3977						111.3
BF ₄ ⁻ (¹ A ₁ - T _d)			1.4101						109.5
F ₃ B-FH (¹ A' - C _s)	0.9246		1.3235	2.4804			108.8	88.1	119.7
			1.3171						
BCl ₃ ⁻ (² A ₁ - C _{3v})			1.8476	-					112.0
HBCl ₃ ⁻ (¹ A ₁ - C _{3v})		1.1935	1.8761	-		109.6			109.4
BCl ₃ F ⁻ (¹ A ₁ - C _{3v})			1.8751	1.3759				109.8	109.1
Cl ₃ B-FH (¹ A' - C _s)	0.9237		1.7489	2.8799			97.7	86.7	119.7
			1.7350						
BCl ₄ ⁻ (¹ A ₁ - T _d)			1.8588						109.5
BBr ₃ ⁻ (² A ₁ - C _{3v})			1.9906						112.6
HBBr ₃ ⁻ (¹ A ₁ - C _{3v})		1.1888	2.0169			109.0			110.0

$\text{BBr}_3\text{F}^- (^1\text{A}_1 - \text{C}_{3v})$			2.0235	1.3691			109.6	109.3
$\text{Br}_3\text{B-FH} (^1\text{A}' - \text{C}_s)$	0.9277		1.9033	3.3503		45.8	71.9	119.3
			1.8720					
$\text{BBr}_4^- (^1\text{A}_1 - \text{T}_d)$			2.0028					109.5
$\text{BI}_3^- (^2\text{A}_1 - \text{C}_{3v})$			2.2076					113.5
$\text{HBI}_3^- (^1\text{A}_1 - \text{C}_{3v})$		1.1858	2.2361		108.2			110.7
$\text{BI}_3\text{F}^- (^1\text{A}_1 - \text{C}_{3v})$			2.2571	1.3628			109.5	109.4
$\text{I}_3\text{B-FH} (^1\text{A}' - \text{C}_s)$	0.9279		2.1244	3.4589		45.4	74.5	119.4
			2.0939					
$\text{BI}_4^- (^1\text{A}_1 - \text{T}_d)$			2.2301					109.5
$\text{HB}(\text{NH}_2)_3^- (^1\text{A}' - \text{C}_s)$	1.0156	1.2477	1.5647		106.3	111.1		117.8
	1.0182		1.5503		116.3	109.5		105.3
	1.0141					110.8		
$\text{B}(\text{NH}_2)_3\text{F}^- (^1\text{A}' - \text{C}_s)$	1.0152		1.5565	1.4592		110.5	105.1	118.6
	1.0145		1.5318			110.4	114.9	106.8
	1.0134					110.4		
$\text{B}(\text{NH}_2)_4^- (^1\text{A}_1 - \text{D}_{2d})$	1.0150		1.5600			110.4	-	119.1
								104.5
$\text{HB}(\text{OH})_3^- (^1\text{A} - \text{C}_3)$	0.9605	1.2608	1.4849		110.0	106.6		109.0
$\text{B}(\text{OH})_3\text{F}^- (^1\text{A} - \text{C}_3)$	0.9600		1.4668	1.4692		106.8	108.5	110.4

B(OH)_4^- ($^1\text{A} - S_4$)	0.9603		1.4863			105.8		115.2
								106.7
HB(SH)_3^- ($^1\text{A} - C_3$)	1.3384	1.2027	1.9317		111.2	96.9		107.6
$\text{B(SH)}_3\text{F}^-$ ($^1\text{A} - C_3$)	1.3383		1.9338	1.4007		95.7	111.3	107.6
B(SH)_4^- ($^1\text{A} - S_4$)	1.3382		1.9224			96.4		113.6
								107.4

^a Optimized at the CCSD(T)/aVTZ level.

Table A7.2. CCSD(T) Total Energies (E_h) as a Function of the Basis Set.^{a,b}

Molecule	Basis Set	E_h
H ₃ B ⁻	aVDZ	-26.508589
	aVTZ	-26.536183
	aVQZ	-26.542996
	CBS (DTQ)	-26.546645
H ₂ BF ⁻	aVDZ	-125.629074
	aVTZ	-125.741979
	aVQZ	-125.776328
	CBS (DTQ)	-125.795637
H ₃ BF ⁻	aVDZ	-126.281967
	aVTZ	-126.395489
	aVQZ	-126.429935
	CBS (DTQ)	-126.449288
H ₂ BF ₂ ⁻	aVDZ	-225.423829
	aVTZ	-225.622610
	aVQZ	-225.683876
	CBS (DTQ)	-225.718407
H ₂ BCl ⁻	aVDZ	-485.652299
	aVTZ	-485.740144
	aVQZ	-485.767398
	CBS (DTQ)	-485.782780
H ₃ BCl ⁻	aVDZ	-486.309326
	aVTZ	-486.401848
	aVQZ	-486.430062
	CBS (DTQ)	-486.445931
H ₂ BClF ⁻	aVDZ	-585.442411
	aVTZ	-585.618634
	aVQZ	-585.673554
	CBS (DTQ)	-585.704577
H ₂ BBr ⁻	aVDZ	-2598.505114
	aVTZ	-2598.652460

	aVQZ	-2598.67848
	CBS (DTQ)	-2598.690958
H ₃ BBr ⁻	aVDZ	-2599.163370
	aVTZ	-2599.315805
	aVQZ	-2599.342776
	CBS (DTQ)	-2599.355715
H ₂ BBrF ⁻	aVDZ	-2698.294201
	aVTZ	-2698.530607
	aVQZ	-2698.584284
	CBS (DTQ)	-2698.612367
H ₂ BI ⁻	aVDZ	-321.171725
	aVTZ	-321.618081
	aVQZ	-321.814952
	CBS (DTQ)	-321.932623
H ₃ BI ⁻	aVDZ	-321.831477
	aVTZ	-322.282810
	aVQZ	-322.480516
	CBS (DTQ)	-322.598577
H ₂ BIF ⁻	aVDZ	-420.999358
	aVTZ	-421.557290
	aVQZ	-421.784663
	CBS (DTQ)	-421.919086
H ₃ B(NH ₂) ⁻	aVDZ	-82.405009
	aVTZ	-82.486809
	aVQZ	-82.508803
	CBS (DTQ)	-82.520835
H ₂ B(NH ₂)F ⁻	aVDZ	-181.548074
	aVTZ	-181.712075
	aVQZ	-181.759135
	CBS (DTQ)	-181.785265
H ₃ B(OH) ⁻	aVDZ	-102.267292
	aVTZ	-102.363957

	aVQZ	-102.391977
	CBS (DTQ)	-102.407570
H ₂ B(OH)F ⁻	aVDZ	-201.411653
	aVTZ	-201.591367
	aVQZ	-201.646115
	CBS (DTQ)	-201.676901
H ₃ B(SH) ⁻	aVDZ	-424.900905
	aVTZ	-424.983968
	aVQZ	-425.006870
	CBS (DTQ)	-425.019472
H ₂ B(SH)F ⁻	aVDZ	-524.032793
	aVTZ	-524.198788
	aVQZ	-524.24828
	CBS (DTQ)	-524.275991
HF ₂ ⁻	aVDZ	-224.763134
	aVTZ	-224.959751
	aVQZ	-225.021021
	CBS (DTQ)	-225.055631
HF ₃ ⁻	aVDZ	-324.576310
	aVTZ	-324.860448
	aVQZ	-324.948603
	CBS (DTQ)	-324.998355
HBCl ₂ ⁻	aVDZ	-944.798058
	aVTZ	-944.946151
	aVQZ	-944.993817
	CBS (DTQ)	-945.020912
H ₂ BCl ₂ ⁻	aVDZ	-945.459300
	aVTZ	-945.612325
	aVQZ	-945.660852
	CBS (DTQ)	-945.688358
HBCl ₂ F ⁻	aVDZ	-1044.594195
	aVTZ	-1044.831670

	aVQZ	-1044.906944
	CBS (DTQ)	-1044.949606
HBBr ₂ ⁻	aVDZ	-5170.499344
	aVTZ	-5170.766641
	aVQZ	-5170.811685
	CBS (DTQ)	-5170.832849
H ₂ BBr ₂ ⁻	aVDZ	-5171.160332
	aVTZ	-5171.433014
	aVQZ	-5171.478898
	CBS (DTQ)	-5171.500443
HBBr ₂ F ⁻	aVDZ	-5270.290899
	aVTZ	-5270.648209
	aVQZ	-5270.720826
	CBS (DTQ)	-5270.757512
HBI ₂ ⁻	aVDZ	-615.797463
	aVTZ	-616.646645
	aVQZ	-617.028776
	CBS (DTQ)	-617.257777
H ₂ BI ₂ ⁻	aVDZ	-616.458332
	aVTZ	-617.312803
	aVQZ	-617.695526
	CBS (DTQ)	-617.924743
HBI ₂ F ⁻	aVDZ	-715.623807
	aVTZ	-716.585317
	aVQZ	-716.997594
	CBS (DTQ)	-717.243079
H ₂ B(NH ₂) ₂ ⁻	aVDZ	-137.667691
	aVTZ	-137.798708
	aVQZ	-137.834913
	CBS (DTQ)	-137.854848
HB(NH ₂) ₂ F ⁻	aVDZ	-236.811597
	aVTZ	-237.025595

	aVQZ	-237.088322
	CBS (DTQ)	-237.123311
H ₂ B(OH) ₂ ⁻	aVDZ	-177.399416
	aVTZ	-177.560757
	aVQZ	-177.608939
	CBS (DTQ)	-177.635922
HB(OH) ₂ F ⁻	aVDZ	-276.551134
	aVTZ	-276.796034
	aVQZ	-276.871088
	CBS (DTQ)	-276.913343
H ₂ B(SH) ₂ ⁻	aVDZ	-822.646170
	aVTZ	-822.779528
	aVQZ	-822.817475
	CBS (DTQ)	-822.838506
HB(SH) ₂ F ⁻	aVDZ	-921.775514
	aVTZ	-921.992240
	aVQZ	-922.056683
	CBS (DTQ)	-922.092739
BF ₃ ⁻	aVDZ	-323.906361
	aVTZ	-324.189266
	aVQZ	-324.276986
	CBS (DTQ)	-324.326488
BF ₄ ⁻	aVDZ	-423.727171
	aVTZ	-424.096657
	aVQZ	-424.211710
	CBS (DTQ)	-424.276690
BCl ₃ ⁻	aVDZ	-1403.938959
	aVTZ	-1404.148443
	aVQZ	-1404.216577
	CBS (DTQ)	-1404.255383
HBCl ₃ ⁻	aVDZ	-1404.602198
	aVTZ	-1404.816064

	aVQZ	-1404.884876
	CBS (DTQ)	-1404.923989
BCl_3F^-	aVDZ	-1503.735464
	aVTZ	-1504.033796
	aVQZ	-1504.129363
	CBS (DTQ)	-1504.183637
BCl_4^-	aVDZ	-1863.736733
	aVTZ	-1864.011720
	aVQZ	-1864.100780
	CBS (DTQ)	-1864.151464
BBr_3^-	aVDZ	-7742.484658
	aVTZ	-7742.873407
	aVQZ	-7742.937540
	CBS (DTQ)	-7742.967388
HBBr_3^-	aVDZ	-7743.146288
	aVTZ	-7743.539645
	aVQZ	-7743.604308
	CBS (DTQ)	-7743.634354
BBr_3F^-	aVDZ	-7842.274873
	aVTZ	-7842.752643
	aVQZ	-7842.844033
	CBS (DTQ)	-7842.889223
BBr_4^-	aVDZ	-10315.122333
	aVTZ	-10315.636549
	aVQZ	-10315.719958
	CBS (DTQ)	-10315.758477
BI_3^-	aVDZ	-910.413403
	aVTZ	-911.666564
	aVQZ	-912.233927
	CBS (DTQ)	-912.574199
HBI_3^-	aVDZ	-911.072633
	aVTZ	-912.330136

	aVQZ	-912.897614
	CBS (DTQ)	-913.237813
BI ₃ F ⁻	aVDZ	-1010.235904
	aVTZ	-1011.599874
	aVQZ	-1012.196817
	CBS (DTQ)	-1012.553243
BI ₄ ⁻	aVDZ	-1205.678161
	aVTZ	-1207.337392
	aVQZ	-1208.089614
	CBS (DTQ)	-1208.540832
HB(NH ₂) ₃ ⁻	aVDZ	-192.937659
	aVTZ	-193.117644
	aVQZ	-193.168006
	CBS (DTQ)	-193.195813
B(NH ₂) ₃ F ⁻	aVDZ	-292.087305
	aVTZ	-292.349753
	aVQZ	-292.426602
	CBS (DTQ)	-292.469459
B(NH ₂) ₄ ⁻	aVDZ	-248.208915
	aVTZ	-248.437675
	aVQZ	-248.502113
	CBS (DTQ)	-248.537746
HB(OH) ₃ ⁻	aVDZ	-252.534235
	aVTZ	-252.760722
	aVQZ	-252.829284
	CBS (DTQ)	-252.867788
B(OH) ₃ F ⁻	aVDZ	-351.690267
	aVTZ	-351.999096
	aVQZ	-352.094436
	CBS (DTQ)	-352.148190
B(OH) ₄ ⁻	aVDZ	-327.678516
	aVTZ	-327.969055

	aVQZ	-328.057808
	CBS (DTQ)	-328.107741
HB(SH) ₃ ⁻	aVDZ	-1220.383766
	aVTZ	-1220.567227
	aVQZ	-1220.620051
	CBS (DTQ)	-1220.649404
B(SH) ₃ F ⁻	aVDZ	-1319.516264
	aVTZ	-1319.782730
	aVQZ	-1319.861979
	CBS (DTQ)	-1319.906320
B(SH) ₄ ⁻	aVDZ	-1618.121060
	aVTZ	-1618.354195
	aVQZ	-1618.421837
	CBS (DTQ)	-1618.459485

^a Dissociation is with respect to RCCSD(T) atoms for closed shell atoms and R/UCCSD(T) for open shell atoms. Symmetry equivalencing of the p_x , p_y , and p_z orbitals was not imposed in the atomic calculations. The I RECP has a 28 electron core respectively, leaving 25 electrons to be explicitly treated. ^b CBS (DTQ) values from Eq. 1 (see text) obtained with the aV n Z basis sets with $n = D, T, Q$.

Table A7.3. CCSD(T)/aVnZ-PP Total Energies (E_h) as a Function of the Basis Set.^{a,b}

Molecule	Basis Set	E_h
H ₂ BBr ⁻	aVDZ-PP	-441.608216
	aVTZ-PP	-441.697673
	aVQZ-PP	-441.722322
	CBS (DTQ)	-441.735884
H ₃ BBr ⁻	aVDZ-PP	-442.266272
	aVTZ-PP	-442.360920
	aVQZ-PP	-442.386550
	CBS (DTQ)	-442.400595
H ₂ BBrF ⁻	aVDZ-PP	-541.397258
	aVTZ-PP	-541.575927
	aVQZ-PP	-541.628229
	CBS (DTQ)	-541.657394
H ₂ BI ⁻	aVDZ-PP	-320.753071
	aVTZ-PP	-320.829028
	aVQZ-PP	-320.853797
	CBS (DTQ)	-320.867912
H ₃ BI ⁻	aVDZ-PP	-321.412200
	aVTZ-PP	-321.493288
	aVQZ-PP	-321.518896
	CBS (DTQ)	-321.533399
H ₂ BIF ⁻	aVDZ-PP	-420.540404
	aVTZ-PP	-420.705970
	aVQZ-PP	-420.758313
	CBS (DTQ)	-420.787963
HBBr ₂ ⁻	aVDZ-PP	-856.706061
	aVTZ-PP	-856.857608
	aVQZ-PP	-856.899860
	CBS (DTQ)	-856.923171
H ₂ BBr ₂ ⁻	aVDZ-PP	-857.366471
	aVTZ-PP	-857.523693

	aVQZ-PP	-857.566904
	CBS (DTQ)	-857.590665
HBBr ₂ F ⁻	aVDZ-PP	-956.497339
	aVTZ-PP	-956.739240
	aVQZ-PP	-956.809127
	CBS (DTQ)	-956.847989
HBI ₂ ⁻	aVDZ-PP	-614.990035
	aVTZ-PP	-615.114553
	aVQZ-PP	-615.156888
	CBS (DTQ)	-615.181196
H ₂ BI ₂ ⁻	aVDZ-PP	-615.649718
	aVTZ-PP	-615.779643
	aVQZ-PP	-615.822682
	CBS (DTQ)	-615.847279
HBI ₂ F ⁻	aVDZ-PP	-714.775267
	aVTZ-PP	-714.990149
	aVQZ-PP	-715.059860
	CBS (DTQ)	-715.099546
BBr ₃ ⁻	aVDZ-PP	-1271.794759
	aVTZ-PP	-1272.010234
	aVQZ-PP	-1272.070194
	CBS (DTQ)	-1272.103259
HBBr ₃ ⁻	aVDZ-PP	-1272.456100
	aVTZ-PP	-1272.676237
	aVQZ-PP	-1272.736901
	CBS (DTQ)	-1272.770281
BBr ₃ F ⁻	aVDZ-PP	-1371.584983
	aVTZ-PP	-1371.889558
	aVQZ-PP	-1371.976880
	CBS (DTQ)	-1372.025356
BBr ₄ ⁻	aVDZ-PP	-1687.536154
	aVTZ-PP	-1687.819313

	aVQZ-PP	-1687.897364
	CBS (DTQ)	-1687.940312
BI ₃ ⁻	aVDZ-PP	-909.215420
	aVTZ-PP	-909.390096
	aVQZ-PP	-909.450124
	CBS (DTQ)	-909.484658
HBI ₃ ⁻	aVDZ-PP	-909.874024
	aVTZ-PP	-910.052861
	aVQZ-PP	-910.113100
	CBS (DTQ)	-910.147631
BI ₃ F ⁻	aVDZ-PP	-1008.997109
	aVTZ-PP	-1009.260405
	aVQZ-PP	-1009.347290
	CBS (DTQ)	-1009.396910
BI ₄ ⁻	aVDZ-PP	-1204.088863
	aVTZ-PP	-1204.315461
	aVQZ-PP	-1204.393199
	CBS (DTQ)	-1204.437909

^a Dissociation is with respect to RCCSD(T) atoms for closed shell atoms and R/UCCSD(T) for open shell atoms. Symmetry equivalencing of the p_x, p_y, and p_z orbitals was not imposed in the atomic calculations. The Br and I RECP have a 10 and 28 electron core, respectively, leaving 25 electrons to be explicitly treated. ^b CBS (DTQ) values from Eq. 1 (see text) obtained with the aVnZ-PP basis sets with $n = D, T, Q$.

Table A7.4. Calculated Vibrational MP2/aVTZ Frequencies (cm⁻¹).

Molecule	Symmetry	Calculated
H ₃ B ⁻ (<i>D</i> _{3h}) ^a	a ₁ '	2415.4 (2516.0)
	e'	2325.4 (2422.3)
	e'	1150.7
	a ₂ ''	557.4
H ₃ BF ⁻ (<i>C</i> _{3v}) ^a	a ₁	2259.1
	a ₁	1212.9
	a ₁	854.8
	e	2217.2
	e	1182.6
	e	969.0
H ₂ BF ⁻ (<i>C</i> _{2v}) ^a	a ₁	2508.7
	a ₁	1234.7
	a ₁	981.2
	b ₁	497.6
	b ₂	2596.2
	b ₂	968.0
HBF ₂ ⁻ (<i>C</i> _s) ^a	a'	2479.7
	a'	1039.3
	a'	952.7
	a'	462.7
	a''	1141.6
	a''	1016.6
H ₂ BF ₂ ⁻ (<i>C</i> _{2v})	a ₁	2304.6
	a ₁	1250.5
	a ₁	903.2
	a ₁	433.3
	b ₁	2270.7
	b ₁	990.5
	b ₂	1212.5
	b ₂	889.7

	a ₂	991.8
BF ₃ ⁻ (C _{3v})	a ₁	741.1
	a ₁	574.6
	e	1078.4
	e	411.3
HBF ₃ ⁻ (C _{3v})	a ₁	2366.2
	a ₁	944.0
	a ₁	582.3
	e	1155.8
	e	948.3
	e	406.2
BF ₄ ⁻ (T _d)	a ₁	757.0
	e	344.3
	t ₂	1079.6
	t ₂	513.1
H ₂ BCl (C _s)	a'	2530.9
	a'	1151.1
	a'	630.5
	a'	438.9
	a''	2626.0
	a''	829.9
H ₃ BCl (C _{3v})	a ₁	2413.1
	a ₁	1148.9
	a ₁	506.9
	e	2448.9
	e	1204.0
	e	848.0
H ₂ BClF ⁻ (C _s)	a'	2428.6
	a'	1246.8
	a'	1143.5
	a'	958.7
	a'	520.5

	a'	295.8
	a''	2450.1
	a''	1006.0
	a''	851.9
HBCl ₂ ⁻ (C _s)	a'	2564.5
	a'	749.5
	a'	580.7
	a'	238.9
	a''	1001.3
	a''	651.7
H ₂ BCl ₂ ⁻ (C _{2v})	a ₁	2504.5
	a ₁	1207.0
	a ₁	584.8
	a ₁	228.9
	b ₁	2557.1
	b ₁	796.3
	b ₂	1095.8
	b ₂	574.4
	a ₂	939.0
HBCl ₂ F ⁻ (C _s)	a'	2547.6
	a'	1115.4
	a'	1022.1
	a'	620.3
	a'	382..2
	a'	220.9
	a''	1044.6
	a''	602.8
	a''	299.7
BCl ₃ ⁻ (C _{3v})	a ₁	521.7
	a ₁	323.7
	e	708.7
	e	218.9

HBCl ₃ ⁻ (C _{3v})	a ₁	2597.8
	a ₁	602.1
	a ₁	312.9
	e	1039.6
	e	647.0
	e	217.4
BCl ₃ F ⁻ (C _{3v})	a ₁	1081.4
	a ₁	468.4
	a ₁	294.4
	e	708.9
	e	341.5
	e	202.1
BCl ₄ ⁻ (T _d)	a ₁	410.2
	e	184.2
	t ₂	710.3
	t ₂	273.4
H ₂ BBr ⁻ (C _s)	a'	2532.1
	a'	1126.7
	a'	582.5
	a'	459.1
	a''	2634.5
	a''	786.5
H ₃ BBr ⁻ (C _{3v})	a ₁	2435.0
	a ₁	1118.0
	a ₁	424.0
	e	2484.6
	e	1199.7
	e	799.8
H ₂ BBrF ⁻ (C _s)	a'	2456.4
	a'	1244.8
	a'	1112.8
	a'	974.7

	a'	446.1
	a'	235.7
	a''	2489.8
	a''	1004.3
	a''	800.4
HBBr ₂ ⁻ (C _s)	a'	2593.0
	a'	705.3
	a'	493.2
	a'	145.8
	a''	962.4
	a''	578.8
H ₂ BBr ₂ ⁻ (C _{2v})	a ₁	2537.7
	a ₁	1183.0
	a ₁	496.8
	a ₁	140.2
	b ₁	2604.8
	b ₁	736.1
	b ₂	1050.2
	b ₂	512.0
	a ₂	905.4
HBBr ₂ F ⁻ (C _s)	a'	2574.9
	a'	1096.3
	a'	1036.7
	a'	546.5
	a'	307.6
	a'	138.0
	a''	1003.4
	a''	542.6
	a''	247.8
BBr ₃ ⁻ (C _{3v})	a ₁	423.7
	a ₁	203.1
	e	631.1

	e	133.0
HBBr ₃ ⁻ (C _{3v})	a ₁	2634.2
	a ₁	503.4
	a ₁	195.6
	e	994.1
	e	585.4
	e	132.1
BBr ₃ F ⁻ (C _{3v})	a ₁	1091.6
	a ₁	363.5
	a ₁	190.1
	e	640.3
	e	270.8
	e	127.6
BBr ₄ ⁻ (T _d)	a ₁	251.4
	e	111.3
	t ₂	638.9
	t ₂	167.5
H ₂ BI ⁻ (C _s)	a'	2533.7
	a'	1092.6
	a'	609.7
	a'	410.6
	a''	2642.7
	a''	730.2
H ₃ BI ⁻ (C _{3v})	a ₁	2465.4
	a ₁	1082.5
	a ₁	352.7
	e	2531.0
	e	1199.4
	e	742.4
H ₂ BIF ⁻ (C _s)	a'	2497.7
	a'	1252.1
	a'	1073.9

	a'	997.8
	a'	366.2
	a'	182.5
	a''	2547.5
	a''	1003.3
	a''	730.4
HBI ₂ ⁻ (C _s)	a'	2612.9
	a'	643.0
	a'	418.6
	a'	101.7
	a''	908.0
	a''	522.7
H ₂ BI ₂ ⁻ (C _{2v})	a ₁	2567.3
	a ₁	1157.1
	a ₁	423.9
	a ₁	98.5
	b ₁	2649.5
	b ₁	660.2
	b ₂	985.8
	b ₂	459.5
	a ₂	856.3
HBI ₂ F ⁻ (C _s)	a'	2889.4
	a'	1147.4
	a'	1068.9
	a'	602.2
	a'	277.7
	a'	97.0
	a''	1048.1
	a''	570.2
	a''	215.5
BI ₃ ⁻ (C _{3v})	a ₁	337.4
	a ₁	143.3

	e	574.8
	e	91.1
HBI ₃ ⁻ (C _{3v})	a ₁	2658.8
	a ₁	414.8
	a ₁	137.4
	e	937.4
	e	527.3
	e	91.8
BI ₃ F ⁻ (C _{3v})	a ₁	1100.1
	a ₁	297.7
	a ₁	132.3
	e	565.0
	e	233.2
	e	89.3
BI ₄ ⁻ (T _d)	a ₁	174.4
	e	76.2
	t ₂	560.0
	t ₂	114.1
H ₃ B(NH) ₂ ⁻ (C _s)	a'	3471.2
	a'	2300.3
	a'	2185.0
	a'	1584.4
	a'	1189.8
	a'	1174.3
	a'	977.6
	a'	840.7
	a'	679.6
	a''	3562.7
	a''	2296.9
	a''	1201.0
	a''	1119.6
	a''	757.7

	a''	243.4
H ₂ B(NH) ₂ F ⁻ (C _s)	a'	3495.3
	a'	2309.6
	a'	1593.6
	a'	1220.6
	a'	1173.7
	a'	915.9
	a'	818.9
	a'	692.1
	a'	372.2
	a''	3590.0
	a''	2298.5
	a''	1136.0
	a''	1020.8
	a''	735.9
	a''	301.3
H ₂ B(NH ₂) ₂ ⁻ (C ₂)	a	3581.1
	a	3479.4
	a	2209.2
	a	1568.0
	a	1227.3
	a	1092.1
	a	959.5
	a	792.8
	a	682.9
	a	404.0
	a	240.3
	b	3581.3
	b	3479.0
	b	2162.4
	b	1574.2
	b	1200.6

	b	1048.5
	b	896.5
	b	784.6
	b	667.9
	b	221.0
HB(NH ₂) ₂ F ⁻ (C _s)	a'	3578.4
	a'	3470.4
	a'	2295.0
	a'	1576.2
	a'	1190.7
	a'	1049.8
	a'	909.6
	a'	771.1
	a'	732.1
	a'	472.8
	a'	340.2
	a'	213.4
	a''	3576.9
	a''	3468.3
	a''	1570.1
	a''	1147.4
	a''	927.3
	a''	862.0
	a''	647.6
	a''	419.6
	a''	86.3
HB(NH ₂) ₃ ⁻ (C _s)	a'	3575.1
	a'	3508.0
	a'	3467.0
	a'	2205.6
	a'	1573.6
	a'	1567.2

	a'	1185.8
	a'	1035.7
	a'	921.0
	a'	765.6
	a'	728.1
	a'	683.6
	a'	453.2
	a'	333.9
	a'	287.2
	a''	3610.1
	a''	3575.3
	a''	3465.2
	a''	1564.1
	a''	1156.6
	a''	1049.0
	a''	875.6
	a''	834.9
	a''	650.4
	a''	411.3
	a''	277.2
	a''	209.6
B(NH ₂) ₃ F (C _s)	a'	3602.1
	a'	3519.3
	a'	3501.7
	a'	1580.3
	a'	1576.8
	a'	1165.0
	a'	1044.0
	a'	825.8
	a'	752.7
	a'	699.2
	a'	691.0

	a'	432.5
	a'	404.9
	a'	282.1
	a'	251.1
	a''	3622.1
	a''	3600.6
	a''	3498.9
	a''	1106.6
	a''	941.4
	a''	851.6
	a''	659.4
	a''	449.3
	a''	409.7
	a''	284.2
	a''	163.0
B(NH ₂) ₄ ⁻ (<i>D</i> _{2d})	a ₁	3497.7
	a ₁	1568.3
	a ₁	769.5
	a ₁	683.6
	a ₁	278.6
	a ₂	3599.3
	a ₂	893.9
	a ₂	225.1
	b ₁	3599.8
	b ₁	986.2
	b ₁	412.5
	b ₁	247.4
	b ₂	3496.9
	b ₂	1573.0
	b ₂	1040.4
	b ₂	715.0
	b ₂	393.6

	e	3599.5
	e	3495.5
	e	1567.3
	e	1147.7
	e	827.9
	e	662.8
	e	422.4
	e	303.4
H ₃ B(OH) ⁻ (C _s)	a'	3874.7
	a'	2326.6
	a'	2234.4
	a'	1209.3
	a'	1200.9
	a'	1119.8
	a'	846.5
	a'	861.4
	a''	2194.6
	a''	1186.0
	a''	954.7
	a''	219.8
H ₂ B(OH)F ⁻ (C ₁)	a	3873.5
	a	2328.3
	a	2227.3
	a	1236.2
	a	1196.8
	a	1139.9
	a	1012.6
	a	904.3
	a	855.8
	a	830.7
	a	445.5
	a	265.4

$\text{H}_2\text{B}(\text{OH})_2^- (\text{C}_2)$	a	3851.0
	a	2281.4
	a	1229.6
	a	1101.4
	a	947.0
	a	845.5
	a	481.1
	a	282.1
	b	3851.0
	b	2262.7
	b	1190.7
	b	1137.3
	b	863.1
	b	797.2
	b	289.7
	$\text{HB}(\text{OH})_2\text{F}^- (\text{C}_1)$	a
a		3847.8
a		2331.3
a		1203.9
a		1153.7
a		1091.2
a		1006.6
a		934.4
a		859.7
a		814.9
a		545.1
a		439.1
a		400.4
a		250.0
$\text{HB}(\text{OH})_3^- (\text{C}_3)$	a	3873.1
	a	2113.2

	a	1059.3
	a	810.3
	a	565.0
	a	259.9
	e	3876.8
	e	1195.9
	e	1009.3
	e	883.5
	e	403.9
	e	82.8
B(OH) ₃ F ⁻ (C ₃)	a	3882.3
	a	1085.2
	a	831.7
	a	730.8
	a	491.7
	a	270.2
	e	3886.5
	e	1184.0
	e	940.6
	e	484.8
	e	374.1
	e	112.3
B(OH) ₄ ⁻ (S ₄)	a	3875.7
	a	999.8
	a	729.7
	a	349.2
	a	176.9
	b	3884.5
	b	1046.5
	b	984.8
	b	507.6
	b	409.6

	b	221.8
	e	3880.2
	e	1195.5
	e	865.3
	e	474.1
	e	298.0
H ₃ B(SH) ⁻ (C _s)	a'	2743.0
	a'	2425.5
	a'	2389.1
	a'	1203.0
	a'	1124.1
	a'	921.1
	a'	606.0
	a'	528.7
	a''	2417.3
	a''	1187.1
	a''	817.1
	a''	218.7
H ₂ B(SH)F ⁻ (C ₁)	a	2748.1
	a	2414.7
	a	2395.3
	a	1215.8
	a	1131.9
	a	1022.0
	a	923.9
	a	899.0
	a	615.0
	a	527.9
	a	304.7
	a	239.8
H ₂ B(SH) ₂ ⁻ (C ₂)	a	2747.4
	a	2456.3

	a	1179.1
	a	983.4
	a	717.5
	a	525.9
	a	269.4
	a	184.4
	b	2747.4
	b	2499.2
	b	1061.3
	b	861.5
	b	605.3
	b	580.5
	b	237.2
HB(SH) ₂ F ⁻ (C _s)	a'	2744.7
	a'	2467.2
	a'	1109.2
	a'	972.8
	a'	827.6
	a'	493.1
	a'	348.9
	a'	248.0
	a'	168.1
	a''	2744.5
	a''	1057.0
	a''	680.0
	a''	615.8
	a''	305.5
	a''	137.1
HB(SH) ₃ ⁻ (C ₃)	a	2730.6
	a	2517.1
	a	787.6
	a	532.7

	a	305.7
	a	253.3
	e	2731.6
	e	1000.3
	e	792.6
	e	627.2
	e	224.0
	e	167.8
B(SH) ₃ F (C ₃)	a	2733.7
	a	1027.1
	a	734.9
	a	439.0
	a	243.1
	a	161.2
	e	2735.4
	e	834.6
	e	652.2
	e	321.1
	e	240.3
	e	161.2
B(SH) ₄ ⁻ (S ₄)	a	2732.5
	a	750.9
	a	379.4
	a	277.7
	a	130.9
	b	2736.0
	b	820.2
	b	677.6
	b	306.9
	b	232.5
	b	160.2
	e	2734.2

e	864.7
e	632.7
e	260.4
e	219.2

^a Calculated at the CCSD(T)/aVTZ level. Unscaled harmonic frequencies given in parentheses.

Table A7.5. Heats of Formation (kcal/mol) at 0 K and 298 K Calculated Based on CCSD(T)/aVnZ-PP ($n = D, T, Q$) Extrapolations.

Molecule	$\Delta H_f(0\text{ K})_{\text{theory}}$	$\Delta H_f(298\text{ K})_{\text{theory}}$
H ₂ BBr ⁻	-6.3	-8.8
H ₃ BBr ⁻	-51.3	-54.9
H ₂ BBrF ⁻	-143.2	-146.5
H ₂ BI ⁻	4.4	3.2
H ₃ BI ⁻	-41.2	-43.4
H ₂ BIF ⁻	-131.5	-133.3
H ₂ BBr ₂ ⁻	-84.1	-89.0
HBBr ₂ F ⁻	-177.0	-181.6
HBI ₂ ⁻	-12.1	-13.3
H ₂ BI ₂ ⁻	-58.6	-60.8
HBI ₂ F ⁻	-147.2	-149.0
BBr ₃ ⁻	-64.4	-69.6
HBBr ₃ ⁻	-111.3	-117.4
BBr ₃ F ⁻	-203.3	-208.9
BBr ₄ ⁻	-133.2	-140.2
BI ₃ ⁻	-23.8	-24.7
HBI ₃ ⁻	-68.5	-70.3
BI ₃ F ⁻	-156.7	-157.9
BI ₄ ⁻	-72.7	-74.6

Table A7.6. T_1 Diagnostics at the CCSD(T)/aVQZ Level.

Molecule	T_1 Diagnostics
H ₃ B ⁻	0.0795
H ₂ BF ⁻	0.0690
H ₃ BF ⁻	0.0114
H ₂ BF ₂ ⁻	0.0119
H ₂ BCl ⁻	0.0138
H ₃ BCl ⁻	0.0084
H ₂ BClF ⁻	0.0100
H ₂ BBr ⁻	0.0142
H ₃ BBr ⁻	0.0091
H ₂ BBrF ⁻	0.0104
H ₂ BI ⁻	0.0157
H ₃ BI ⁻	0.0083
H ₂ BIF ⁻	0.0088
H ₃ B(NH ₂) ⁻	0.0112
H ₂ B(NH ₂)F ⁻	0.0126
H ₃ B(OH) ⁻	0.0120
H ₂ B(OH)F ⁻	0.0124
H ₃ B(SH) ⁻	0.0105
H ₂ B(SH)F ⁻	0.0115
HBF ₂ ⁻	0.0421
HBF ₃ ⁻	0.0119
HBCl ₂ ⁻	0.0130
H ₂ BCl ₂ ⁻	0.0078
HBCl ₂ F ⁻	0.0113
HBBr ₂ ⁻	0.0141
H ₂ BBr ₂ ⁻	0.0087
HBBr ₂ F ⁻	0.0101
HBI ₂ ⁻	0.0159
H ₂ BI ₂ ⁻	0.0099
HBI ₂ F ⁻	0.0110

$\text{H}_2\text{B}(\text{NH}_2)_2^-$	0.0117
$\text{HB}(\text{NH}_2)_2\text{F}^-$	0.0121
$\text{H}_2\text{B}(\text{OH})_2^-$	0.0131
$\text{HB}(\text{OH})_2\text{F}^-$	0.0127
$\text{H}_2\text{B}(\text{SH})_2^-$	0.0110
$\text{HB}(\text{SH})_2\text{F}^-$	0.0117
BF_3^-	0.0157
BF_4^-	0.0139
BCl_3^-	0.0128
HBCl_3^-	0.0079
BCl_3F^-	0.0091
BCl_4^-	0.0080
BBr_3^-	0.0141
HBBr_3^-	0.0089
BBr_3F^-	0.0099
BBr_4^-	0.0090
BI_3^-	0.0160
HBI_3^-	0.0101
BI_3F^-	0.0101
BI_4^-	0.0104
$\text{HB}(\text{NH}_2)_3^-$	0.0123
$\text{B}(\text{NH}_2)_3\text{F}^-$	0.0117
$\text{B}(\text{NH}_2)_4^-$	0.0119
$\text{HB}(\text{OH})_3^-$	0.0130
$\text{B}(\text{OH})_3\text{F}^-$	0.0121
$\text{B}(\text{OH})_4^-$	0.0124
$\text{HB}(\text{SH})_3^-$	0.0114
$\text{B}(\text{SH})_3\text{F}^-$	0.0119
$\text{B}(\text{SH})_4^-$	0.0118

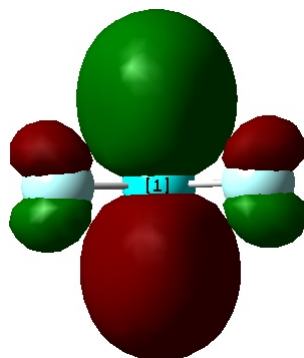
Table A7.7. Natural Bond Orbital Charges (units of electrons) of the Tri-substituted Boranes BX_3 at the B3LYP/aug-cc-pVDZ Level.

Molecule	B	X(group charge)
BH ₃	0.344	-0.115
BF ₃	1.529	-0.510
BCl ₃	0.412	-0.137
BBr ₃	0.048	-0.016
BI ₃	-0.399	0.133
B(OH) ₃	1.334	-0.445
B(SH) ₃	0.055	-0.018
B(NH ₂) ₃	1.078	-0.358

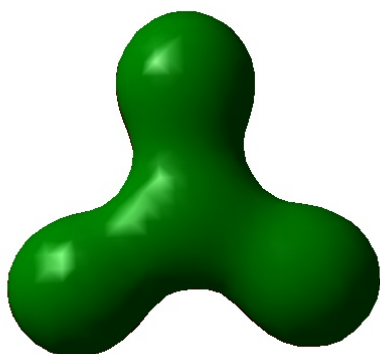
Figure A7.1. Top view of occupied out-of-plane lone pair orbital on BX_3 and side view of empty p orbital on BX_3 for X a halogen.



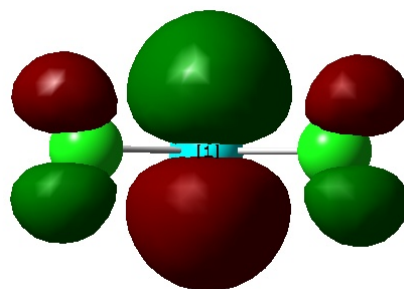
$BF_3(\text{HOMO-5})$



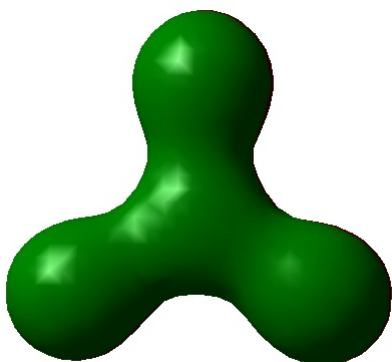
$BF_3(\text{LUMO+1})$



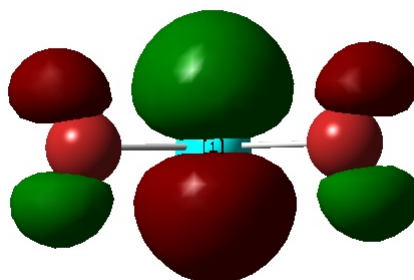
$BCl_3(\text{HOMO-5})$



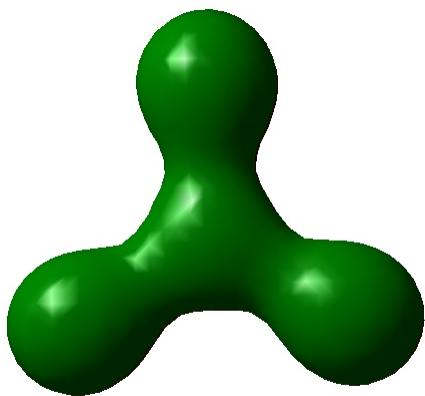
$BCl_3(\text{LUMO})$



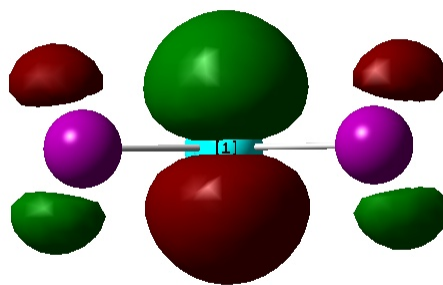
$BBr_3(\text{HOMO-5})$



$BBr_3(\text{LUMO})$



BI₃(HOMO-5)



BI₃(LUMO)

CHAPTER 8

DIAMMONIOSILANE: COMPUTATIONAL PREDICTION OF THE THERMODYNAMIC PROPERTIES OF A POTENTIAL CHEMICAL HYDROGEN STORAGE SYSTEM

From: Grant, D. J.; Arduengo, A. J., III; Dixon, D. A. *J. Phys. Chem. A* **2009**, *113*, 750-755.

8.1 Introduction

There is substantial interest in the discovery of potential molecules for chemical hydrogen storage systems in which dehydrogenation (hydrogen release) from these molecules is near thermoneutral. Near thermoneutral reactions facilitate both H₂ release and regeneration of the spent fuel. There is substantial interest in the use of amine complexes, such as ammonia borane, for use as chemical hydrogen storage systems.^{1,2,3,4,5,6,7,8,9} Another possibility for an amine complex would be to add NH₃ to SiH₄ to make a square planar SiH₄ with NH₃ molecules coordinating in the two apical positions. This is equivalent to stabilization of the edge inversion transition state for SiH₄ by two amines.^{10,11} We would expect that such a stabilized transition state is possible as the H atoms are electronegative with respect to Si, which is the case needed for edge inversion. Diammoniosilane if it could be made would have an excellent weight percent storage for hydrogen at 26 wt% if 8 molecules of H₂ are produced as compared to the amine boranes having 19% if 3 molecules of H₂ are produced.¹

There has also been considerable interest in understanding the chemistry of the edge inversion process, i.e., the formation of square planar AX₄ structures from tetrahedral AX₄ structures. For example, the isoelectronic species BH₄⁻, CH₄, and NH₄⁺, as well as AlH₄⁻, SiH₄,

and PH_4^+ , have been studied,¹² as have the Group IVA fluorides,¹⁰ four-coordinate Group IV centers,¹³ and the Group IVA hydrides.¹⁴ Edge inversion was first described and observed for tricoordinate pnictogen compounds.^{15, 16, 17, 18, 19} The possible effects that certain classes of substituents or solvents would have on stabilizing the edge inversion barrier have been described for PF_3O and PO_3OH .¹¹ Low-level calculations on $\text{SiF}_4(\text{NH}_3)_2$ have been reported.²⁰ Yoshizawa and Suzuki¹⁴ reported on the configurational inversion of tetrahedral molecules and predicted the activation energy for the inversion of silane to be 88.6 kcal/mol at the B3LYP/6-311G** level and 91.7 kcal/mol at the CAS(8,8)/6-311G** level. Earlier studies by Schleyer *et al.* report a silane inversion barrier of 114.1 kcal/mol at the HF/STO-3G* level.¹²

Modern computational chemistry methods implemented on high performance computer architectures can now provide reliable predictions of thermodynamic properties to within about 1 kcal/mol for most compounds that are not dominated by multireference character.²¹ We use the approach that we have been developing with collaborators at Pacific Northwest Laboratory and Washington State University for the prediction of accurate molecular thermochemistry²² to determine the atomization energies and the heats of formation of these compounds. Our approach is based on calculating the total atomization energy of a molecule and using this value with known heats of formation of the atoms to calculate the heat of formation at 0 K. The approach starts with coupled cluster theory with single and double excitations and including a perturbative triples correction (CCSD(T)),^{23, 24, 25} combined with the correlation-consistent basis sets²⁶ extrapolated to the complete basis set limit to treat the correlation energy of the valence electrons. This is followed by a number of smaller additive corrections including core-valence interactions and relativistic effects, both scalar and spin-orbit. The zero point energy can be obtained from experiment, theory, or a combination of the two. Corrections to 298 K can then be

calculated by using standard thermodynamic and statistical mechanics expressions in the rigid rotor-harmonic oscillator approximation²⁷ and appropriate corrections for the heat of formation of the atoms.²⁸ We now report reliable calculations on the interaction two NH₃ molecules with silane and the various dehydrogenation energies.

8.2 Computational Methods

The standard aug-cc-pVnZ basis sets were used for H and N. It has recently been found that tight *d* functions are necessary for calculating accurate atomization energies for 2nd row elements,²⁹ so we also included additional tight *d* functions in our calculations. Basis sets containing extra tight *d* functions are denoted aug-cc-pV(*n+d*)Z. We use aug-cc-pV(*n+d*)Z to represent the combination of aug-cc-pV(*n+d*)Z (on the 2nd row atom Si) and aug-cc-pVnZ (on H and N) basis sets and abbreviate this as aV(*n+d*)Z. Only the spherical component subset (e.g., 5-term *d* functions, 7-term *f* functions, etc.) of the Cartesian polarization functions were used. All CCSD(T) calculations were performed with the MOLPRO-2002³⁰ program system on an SGI Altix computer, the Cray XD-1, or the dense memory Linux cluster at the Alabama Supercomputer Center or the Dell Linux cluster at The University of Alabama. For the open shell atomic calculations, we used the restricted method for the starting Hartree-Fock wavefunction and then relaxed the spin restriction in the coupled cluster portion of the calculation. This method is conventionally labeled R/UCCSD(T). Our CBS estimates use a mixed exponential/Gaussian function of the form³¹

$$E(n) = E_{\text{CBS}} + Be^{-(n-1)} + Ce^{-(n-1)^2} \quad (1)$$

where $n = 2$ (aV(D+*d*)Z), 3 (aV(T+*d*)Z), 4 (aV(Q+*d*)Z). In order to achieve thermochemical properties within ± 1 kcal/mol of experiment, it is necessary to account for core-valence correlation energy effects. Core-valence (CV) calculations were carried out with the weighted

core-valence basis set cc-pwCVTZ.³² We need to account for relativistic effects in atoms and molecules. The first correction lowers the sum of the atomic energies (decreasing TAE) by replacing energies that correspond to an average over the available spin multiplets with energies for the lowest multiplets as most electronic structure codes produce only spin multiplet averaged wavefunctions. The atomic spin-orbit correction for Si is $\Delta E_{SO}(\text{Si}) = 0.43$ kcal/mol taken from the tables of Moore.³³ A second relativistic correction to the atomization energy accounts for molecular scalar relativistic effects, ΔE_{SR} . We evaluated ΔE_{SR} by using expectation values for the two dominant terms in the Breit-Pauli Hamiltonian, the so-called mass-velocity and one-electron Darwin (MVD) corrections from configuration interaction singles and doubles (CISD) calculations. The quantity ΔE_{SR} was obtained from CISD wavefunction with a VTZ basis set at the CCSD(T)/aV(T+d)Z or MP2/aV(T+d)Z geometry. The CISD(MVD) approach generally yields ΔE_{SR} values in good agreement (± 0.3 kcal/mol) with more accurate values from, for example, Douglas-Kroll-Hess calculations, for most molecules.

For all of the molecules, numerical geometry optimizations were performed with a convergence threshold on the gradient of approximately $10^{-4} E_h/\text{bohr}$ or smaller. For the smaller molecules, specifically SiH_4 , HNSiH_2 , and HNSiNH , geometries were optimized at the CCSD(T) level with the aV(D+d)Z and aV(T+d)Z basis sets. The geometries obtained with the aV(T+d)Z basis set were then used in single point CCSD(T)/aV(Q+d)Z calculations. The zero point energies (ΔE_{ZPE}) were calculated at the CCSD(T) level with the aV(T+d)Z basis set. For the larger molecules, geometry optimizations were performed at the MP2/aV(T+d)Z level, and the geometry obtained was further then used in single point CCSD(T) calculation with the aV(D+d)Z, aV(T+d)Z, and aV(Q+d)Z basis sets. The zero point energies (ΔE_{ZPE}) were calculated at the MP2 level with the aV(T+d)Z basis set. To calculate the zero point correction,

the calculated harmonic N-H and Si-H stretching frequencies were scaled by factors of 0.974 and 0.977, respectively, obtained by taking the average of the theoretical MP2/aV(T+d)Z values and the experimental values³⁴ for the N-H and Si-H stretches for NH₃ and SiH₄ and dividing the average by the theoretical value.

By combining our computed ΣD_0 values given by the following expression

$$\Sigma D_0 = \Delta E_{\text{elec}}(\text{CBS}) - \Delta E_{\text{ZPE}} + \Delta E_{\text{CV}} + \Delta E_{\text{SR}} + \Delta E_{\text{SO}} \quad (2)$$

with the known heats of formation at 0 K for the elements, we can derive ΔH_f^0 values for the molecules under study. The heats of formation of H and N are well-established as $\Delta H_f^0(\text{H}) = 51.63$ kcal/mol and $\Delta H_f^0(\text{N}) = 112.53$ kcal/mol.³⁵ The value for Si is not as well-established, and we use $\Delta H_f^0(\text{Si}) = 107.4 \pm 0.6$ kcal/mol from the work of Feller and Dixon on small Si containing molecules.³⁶ This value is within the error bars of the NIST value of $\Delta H_f^0(\text{Si}) = 106.6 \pm 1.9$ kcal/mol.³⁵ Heats of formation at 298 K were obtained by following the procedures outlined by Curtiss *et al.*²⁸

We have also calculated heats of formation and dehydrogenation energies employing a cheaper computational approach based on calculations performed at the G3(MP2) level of theory.³⁷ We wish to test the effectiveness of this method for use with larger molecules in the future.

8.3 Results and Discussion

The calculated geometries for the molecules are given as Supporting Information (Table A8.1), where they are compared with the available experimental values. The optimized molecular structures are depicted in Figure 8.1. The total CCSD(T) energies and calculated harmonic frequencies for the molecules are also given as Supporting Information in Table A8.2 and Table A 8.3, respectively.

8.3.1 *Geometries and Frequencies* The structure of diammoniosilane has C_i symmetry with ammonia groups in the apical positions above and below the square planar approximately D_{4h} SiH_4 molecule giving a pseudo octahedral structure at the Si. The lone pairs on the N atoms form dative bonds with the LUMO on Si, which is an empty p orbital of a_{2u} symmetry, similar to the dative bond of ammonia borane, $\text{H}_3\text{B-NH}_3$.¹ The Si-N bond distance at the MP2/aV(T+d)Z level is 0.29 Å longer than the Si-N single bond distance in $\text{H}_2\text{Si}(\text{NH}_2)_2$ at the same level. The Si-H distance of diammoniasilane is only 0.026 Å longer than the Si-H distance in SiH_4 (D_{4h}) at the MP2/aV(T+d)Z level, showing little perturbation of the Si-H bond distance upon binding of the two ammonia units. Similarly, there is only a small perturbation on the N-H bond distance upon complexation compared to NH_3 with that of the complex calculated to be 0.002 Å longer at the MP2/aV(T+d)Z level. The average $\angle\text{HNN}$ angle of the ammonia units of the complex is calculated to be 109.0° at the MP2/aV(T+d)Z level, only 2.2° larger than the $\angle\text{HNN}$ angle of the ammonia at the same level.

Diammoniosilane is characterized by all real harmonic frequencies at the MP2/aV(T+d)Z level. There are two very low modes in the diammoniosilane complex of 12 cm^{-1} (a_g mode) and 33 cm^{-1} (a_u mode) corresponding to torsions about the Si-N bonds. The next two largest modes at 197 cm^{-1} (a_u mode) and 204 cm^{-1} (a_g mode) correspond to wagging of the NH_3 subunits. The following two higher modes at 355 cm^{-1} (a_g mode) and 466 cm^{-1} (a_u mode) correspond to the symmetric and antisymmetric Si-N stretches, respectively, showing the stability of the complex. In addition, there is only a small perturbation in the N-H and Si-H stretching frequencies of $\text{H}_4\text{Si}(\text{NH}_3)_2$ when compared to that of NH_3 (C_{3v}) and SiH_4 (D_{4h}). The symmetric and antisymmetric N-H stretches of the diammoniosilane complex are $\sim 25\text{ cm}^{-1}$ less than the equivalent stretches in ammonia at the MP2/aV(T+d)Z level. Similarly, the symmetric and

antisymmetric Si-H stretches of the diammonio complex are 114 and 166 cm^{-1} less, respectively, compared to the equivalent stretches in SiH_4 (D_{4h}) at the MP2/aV(T+d)Z level.

The first dehydrogenated product of diammoniosilane is the complex $\text{H}_3\text{Si}(\text{NH}_2)(\text{NH}_3)$ (C_s). The Si-NH₂ bond distance is 0.013 Å longer than the Si-N bond distance in $\text{H}_3\text{Si}(\text{NH}_2)$ at the MP2/aV(T+d)Z level, showing minimal effect of the -NH₃ group. The Si-NH₃ bond distance at the MP2/aV(T+d)Z level is 1.00 Å longer than the equivalent bond distance in $\text{H}_4\text{Si}(\text{NH}_3)_2$ but only 0.16 Å shorter than the equivalent bond distance in $\text{H}_4\text{Si}(\text{NH}_3)$. Thus, this structure can be considered to be a weak complex of NH₃ with $\text{SiH}_3(\text{NH}_2)$, bound by only 1.0 kcal/mol at 0 K and 0.7 kcal/mol at 298 K at the CCSD(T) level. The Si-NH₃ stretching frequency is calculated to 88 cm^{-1} , much lower than the equivalent stretching frequency found for the diammoniosilane complex, but similar to that found in $\text{H}_4\text{Si}(\text{NH}_3)$. The structure of $\text{H}_3\text{Si}(\text{NH}_2)$ has C_s symmetry. The Si-H bond distances are calculated to be within 0.009 Å of that found in SiH_4 at the MP2/aV(T+d)Z level, showing only a small substituent effect of the NH₂ group on the Si-H bond distance. The N-H bond distance shows a small decrease of 0.008 Å compared to that of ammonia.

The second dehydrogenated product of diammoniosilane is $\text{H}_2\text{Si}(\text{NH}_2)_2$ of C_{2v} symmetry with normal tetrahedral bonding at the Si. The Si-N bond distance is 0.002 Å shorter than that in $\text{H}_3\text{Si}(\text{NH}_2)$. The Si-H and N-H bond distances are essentially the same as those found in $\text{H}_3\text{Si}(\text{NH}_2)$ with the largest difference predicted to be 0.001 Å found for the comparable Si-H bond. The Si-N symmetric stretching frequency is $\sim 60 \text{ cm}^{-1}$ less than that found in $\text{H}_3\text{Si}(\text{NH}_2)$. The N-H and Si-H symmetric and antisymmetric stretches are within 6 cm^{-1} of those found in $\text{H}_3\text{Si}(\text{NH}_2)$.

The third and fourth dehydrogenated products are $\text{HN}=\text{SiH}(\text{NH}_2)$ and $\text{HN}=\text{Si}=\text{NH}$, respectively. The structure of $\text{HN}=\text{Si}=\text{NH}$ has C_2 symmetry with the two $\text{Si}=\text{N}-\text{H}$ planes twisted by 83° . The $\text{Si}=\text{NH}$ bond distances are 0.013 and 0.021 Å shorter than that in $\text{H}_2\text{Si}=\text{NH}$, respectively, at the MP2/aV(T+d)Z level. The $\text{Si}-\text{NH}_2$ bond distance of $\text{HN}=\text{SiH}(\text{NH}_2)$ is calculated to be 0.033 Å shorter than the equivalent bond distance in $\text{H}_3\text{Si}(\text{NH}_2)$ at the MP2/aV(T+d)Z level. The structure of $\text{H}_2\text{Si}=\text{NH}$ is of C_s symmetry. The $\text{Si}=\text{N}$ bond distance shows a decrease of 0.117 Å compared to that of $\text{H}_3\text{Si}-\text{NH}_2$, consistent with the formation of a double bond.

Starting from a geometry derived from the diammoniosilane complex for $\text{H}_4\text{Si}(\text{NH}_3)$ leads to the formation of a very weak complex with C_3 symmetry. The complex is best described as the lone pair on the ammonia molecule loosely interacting with a tetrahedral SiH_4 along the C_3 axis pointing at the Si. The Si-N bond distance at the MP2/aV(T+d)Z level is 1.16 Å longer than the Si-N bond distance in the diammonio complex. The N-H and Si-H bond distances are only minimally perturbed compared to the equivalent distances in NH_3 (C_{3v}) and SiH_4 (T_d), respectively, with the largest difference calculated to be 0.005 Å for the Si-H bond distance. The $\text{H}_4\text{Si}(\text{NH}_3)$ complex is characterized by all real frequencies at the MP2/aV(T+d)Z level. The low Si-N stretching frequency is calculated to be at 86 cm^{-1} , within 2 cm^{-1} of the equivalent frequency in $\text{H}_3\text{Si}(\text{NH}_2)(\text{NH}_3)$ and about one fourth that in $\text{H}_4\text{Si}(\text{NH}_3)_2$.

The transition state for the edge inversion process of silane is characterized by one imaginary frequency at $2463.4i\text{ cm}^{-1}$ of B_{2u} symmetry and connects to one of the E modes of the T_d structure. As expected, the Si-H bond distance of the square planar D_{4h} structure of 1.532 Å is longer by 0.049 Å than that of the T_d structure of 1.483 Å^{22e} at the CCSD(T)/aV(T+d)Z level.

8.3.2 *Energies and Heats of Formation* The energetic components for predicting the total molecular dissociation energies are given in Table 8.1. The electronic states and symmetry labels for the molecules under study are included in Table 8.1. We first describe some general trends in the atomization energy components. The core-valence corrections for the molecules are all positive, except for that of $\text{SiH}_4 (D_{4h})$. The corrections are also small with values ranging from -0.90 [$\text{SiH}_4 (D_{4h})$] to 1.06 [$\text{H}_2\text{Si}(\text{NH}_2)_2$] kcal/mol. The scalar relativistic corrections are all small and negative, ranging from -0.65 [$\text{SiH}_4 (D_{4h})$] to -1.57 [$\text{H}_4\text{Si}(\text{NH}_3)_2$] kcal/mol. We estimate that the error bars for the calculated heats of formation are ± 1.0 kcal/mol considering errors in the energy extrapolation, frequencies, and other electronic energy components. An estimate of the potential for significant multireference character in the wavefunction can be obtained from the T_1 diagnostic³⁸ for the CCSD calculation. The values for the T_1 diagnostics are small (<0.03) showing that the wavefunction is dominated by a single configuration. The T_1 values are given as Supporting Information (Table A8.4).

The calculated heats of formation are given in Table 8.2 and are compared with experimental values^{35,39} where available. The agreement for silane is excellent as expected from previous work.³⁶ We first discuss the stability of diammoniosilane. Silane has T_d symmetry, and the edge inversion barrier passing through a transition state of D_{4h} symmetry is 89.0 kcal/mol at 0 K and 88.9 kcal/mol at 298 K at the CCSD(T) level. The corresponding value of the G3(MP2) inversion reaction is 89.5 kcal/mol at 0 K and 89.4 kcal/mol at 298 K, showing good agreement of the G3(MP2) value with the more accurate CCSD(T) value. Although the inversion barrier in SiH_4 is low compared to the edge inversion process of CH_4 predicted to be 109 kcal/mol at the B3LYP/6-311G** level,¹⁴ it is comparable to the Si-H bond dissociation energy (BDE) of 90 kcal/mol at 0 K.⁴⁰

Complexation with 2 NH₃ molecules recovers a substantial amount of the inversion barrier (63.6 kcal/mol at 298 K at the CCSD(T) level), so that the diammoniosilane complex is only 25.4 kcal/mol above the separated reactants SiH₄ + 2NH₃ at the CCSD(T) level at 298 K. The complex is a metastable species characterized by all real frequencies at the MP2/aV(T+d)Z level so it is a true intermediate.

The complexation energy of the first ammonia group to silane is only -0.5 kcal/mol at 0 K and -0.3 kcal/mol at 298 K relative to the separated reactants SiH₄ + NH₃ at the CCSD(T) level. At the G3(MP2) level, the complexation energy for H₄Si(NH₃) is predicted to be 1.1 kcal/mol at 0 K and 0.8 kcal/mol at 298 K. It is only upon introduction of the second ammonia group that a substantial amount of stabilization occurs, and the inversion barrier is recovered. The possibility of the stabilizing effect of electronegative groups such as OH, NH₂, and F on the planar-tetrahedral energy difference in SiH₄ and other isoelectronic molecules has been discussed by Dixon and Arduengo¹⁰ and by Schleyer *et al.*¹²

We can predict the heat of reaction for the dehydrogenation of diammoniosilane from the calculated heats of formation. The results for the various dehydrogenation reactions of diammoniosilane and its derivatives are presented in Table 8.3 at the CCSD(T) level and at the G3(MP2) level for comparison. The G3(MP2) result is typically within ± 4 kcal/mol of the more accurate CCSD(T) value. The overall dehydrogenation of diammoniosilane yielding 2 molecules of H₂ is predicted to be substantially exothermic at -45.8 kcal/mol at 298 K at the CCSD(T) level. The first loss of hydrogen from diammoniosilane to produce H₃Si(NH₂)(NH₃) is exothermic by 33.6 kcal/mol at 298 K at the CCSD(T) level. The sequential dehydrogenation reaction of H₃Si(NH₂)(NH₃) to produce H₂Si(NH₂)₂ is about a third less exothermic than the initial dehydrogenation reaction of diammoniosilane and is predicted to be -12.2 kcal/mol at 298

K at the CCSD(T) level. Further loss of H₂ to form HN=SiH(NH₂) and then HN=Si=NH result in dehydrogenation reactions that are substantially endothermic at 45.3 and 55.7 kcal/mol at the CCSD(T) level at 298 K. These dehydrogenation reactions are quite endothermic, and it is unlikely that one will be able to remove hydrogen from these species. If one can couple the endothermic and exothermic reactions effectively, one can remove three H₂ molecules from H₄Si(NH₃)₂.

An additional dehydrogenation reaction that must be considered is loss of hydrogen from H₃Si(NH₂), the deammoniated product of H₃Si(NH₂)(NH₃). The product of the first dehydrogenation reaction of diammoniosilane is H₃Si(NH₂)(NH₃), and there is the possibility of the loss of ammonia from this complex with the reaction calculated to be near thermoneutral at 1.0 kcal/mol at 0 K and 0.7 kcal/mol at 298 K at the CCSD(T) level. The loss of H₂ from H₃Si(NH₂) to yield H₂Si=NH is predicted to be substantially endothermic at 50.7 kcal/mol at the CCSD(T) at 298 K. Therefore, it will be unlikely that H₂ will be removed from the deammoniated product.

In our studies on the electronic structures of carbenes⁴¹ (and of others for silylenes⁴²), we found that experimental and calculated nuclear magnetic chemical shifts were extremely useful in characterizing bonding in terms of the chemical shift anisotropy. In order to aid the search for the hexacoordinate silicon species, we also calculated the nmr chemical shifts for SiH₄(*T_d*), SiH₄(*D_{4h}*) and SiH₄(NH₃)₂ at the density functional theory (DFT) level with the B3LYP gradient corrected hybrid exchange-correlation functional⁴³ and the Ahlrichs polarized triple zeta basis set⁴⁴ in the GIAO (gauge invariant atomic orbital) formalism.⁴⁵ The chemical shifts are given with respect to tetramethylsilane following our previous work on Si chemical shifts.⁴⁶ The calculated shifts are given in Table 8.4. The chemical shift for SiH₄(*T_d*) of -107.4 ppm is in the

range of other tetrahedrally coordinated silanes and matches well the experimentally determined gas phase values of -106.8 ppm⁴⁷ and -104.3 ppm.⁴⁸ A planar SiH₄ arrangement exhibits a very substantial downfield shift at the silicon somewhat reminiscent of the chemical shifts of carbenes and silylenes.⁴¹ The addition of two amines to produce an octahedral coordination environment at silicon leads to a substantial upfield shift which is generally expected for increased coordination numbers at main group centers.⁴⁹

8.4 Conclusions

We have predicted the heats of formation of diammoniosilane and its dehydrogenated derivatives at the CCSD(T) level plus additional corrections. The edge inversion barrier of silane is calculated to 88.9 kcal/mol at the CCSD(T) level and 89.4 kcal/mol at the G3(MP2) level at 298 K. A substantial amount of this edge inversion barrier (-63.6 kcal/mol at 298 K at the CCSD(T) level) is recovered upon complexation with 2 NH₃ molecules, so that the diammoniosilane complex is only 25.6 kcal/mol at 298 K above the separated reactants SiH₄ + 2NH₃. The complex is a metastable species characterized by all real frequencies at the MP2/aV(T+d)Z level so it is a true intermediate.

The dehydrogenation pathway of diammoniosilane yielding two molecules of H₂ and H₂Si(NH₂)₂ is exothermic at 298 K by -45.8 kcal/mol at the CCSD(T) and -48.2 kcal/mol at the G3(MP2) level. The sequential release of H₂ consequently yielding HN=SiH(NH₂) and HN=Si=NH are predicted to be largely endothermic reactions at 45.3 and 55.7 kcal/mol at the CCSD(T) level at 298 K and 42.9 and 51.9 kcal/mol at the G3(MP2) level, respectively. Coupling the exothermic first two dehydrogenation steps with the endothermic third step yields 3H₂ molecules and HN=SiH(NH₂) in an almost thermoneutral process at 298 K. The loss of H₂ from H₃Si(NH₂), the deammoniated product of H₃Si(NH₂)(NH₃), reaction is predicted to be

largely endothermic at 50.7 and 47.8 kcal/mol at the CCSD(T) and G3(MP2) levels at 298 K, respectively.

Acknowledgments Funding provided in part by the Department of Energy, Office of Energy Efficiency and Renewable Energy under the Hydrogen Storage Grand Challenge, Solicitation No. DE-PS36-03GO93013. This work was done as part of the Chemical Hydrogen Storage Center. D. A. Dixon is indebted to the Robert Ramsay Endowment and A. J. Arduengo, III to the Saxon Chair Foundation, both of the University of Alabama.

Appendix Calculated geometry parameters. Total CCSD(T) energies as a function of basis set. Calculated MP2 frequencies (cm^{-1}). T_1 diagnostics. This material is available free of charge via the internet at <http://pubs.acs.org>.

Table 8.1. CCSD(T) Atomization and Reaction Energies in kcal/mol.^a

Molecule	CBS ^b	$\Delta E_{\text{ZPE}}^{\text{c}}$	$\Delta E_{\text{CV}}^{\text{d}}$	$\Delta E_{\text{SR}}^{\text{e}}$	$\Delta E_{\text{SO}}^{\text{f}}$	$\Sigma D_0(0 \text{ K})^{\text{g}}$
SiH ₄ (¹ A _{1g} – D _{4h})	235.08	17.70	-0.90	-0.65	-0.43	215.41
H ₂ Si=NH (¹ A' – C _s)	352.55	17.98	0.24	-0.71	-0.43	333.66
HN=Si=NH (¹ A – C ₂)	385.66	16.06	0.85	-0.93	-0.43	369.08
H ₃ Si(NH ₂) (¹ A' – C _s)	518.64	31.48	0.35	-0.95	-0.43	486.14
H ₄ Si(NH ₃) (¹ A – C ₃)	625.10	42.17	0.27	-0.84	-0.43	581.92
HN=SiH(NH ₂) (¹ A' – C _s)	556.66	30.04	1.03	-1.16	-0.43	526.05
H ₂ Si(NH ₂) ₂ (¹ A ₁ – C _{2v})	716.90	42.83	1.06	-1.36	-0.43	673.35
H ₃ Si(NH ₂)(NH ₃) (¹ A' – C _s)	818.68	53.81	0.91	-1.25	-0.43	764.11
H ₄ Si(NH ₃) ₂ (¹ A _g – C _i)	901.04	68.68	0.70	-1.57	-0.43	831.05

^a The atomic asymptotes were calculated with the R/UCCSD(T) method. ^b Extrapolated by using eq. (1) with aV(D+d)Z, aV(T+d)Z, aV(Q+d)Z. ^c The zero point energies were taken as 0.5 the sum of the CCSD(T)/aV(T+d)Z or MP2/aV(T+d)Z scaled frequencies. ^d Core-valence corrections were obtained with the cc-pwCVTZ (N, Si) basis sets at the optimized CCSD(T)/aV(T+d)Z or MP2/aV(T+d)Z geometries. ^e The scalar relativistic correction is based on a CISD(FC)/VTZ MVD calculation and is expressed relative to the CISD result without the MVD correction, i.e. including the existing relativistic effects resulting from the use of a relativistic effective core potential. ^f Correction due to the incorrect treatment of the atomic asymptotes as an average of spin multiplets. Values are based on C. Moore's Tables, reference 33. ^g The theoretical value of $\Delta D_0(0 \text{ K})$ was computed with the CBS estimates.

Table 8.2. Calculated CCSD(T) Heats of Formation (kcal/mol).

Molecule	CCSD(T)		G3(MP2)	
	Theory (0 K)	Theory (298 K)	Theory (0 K)	Theory (298 K)
NH ₃ (<i>C</i> _{3v}) ^a	-9.6 ± 0.5 ^b	-11.3 ± 0.5 ^b	-8.3	-10.0
SiH ₄ (<i>T</i> _d) ^c	9.5 ± 0.6 ^d	7.2 ± 0.6 ^d	10.3	8.0
SiH ₄ (<i>D</i> _{4h})	98.5	96.1	99.8	97.4
H ₂ Si=NH (<i>C</i> _s)	41.2	39.1	41.5	39.4
HN=Si=NH (<i>C</i> ₂)	66.6	65.2	65.3	64.1
H ₃ Si(NH ₂) (<i>C</i> _s)	-8.1	-11.7	-6.0	-9.6
H ₄ Si(NH ₃) (<i>C</i> ₃)	-0.6	-4.4	0.9	-2.8
HN=SiH(NH ₂) (<i>C</i> _s)	12.9	9.5	14.4	11.1
H ₂ Si(NH ₂) ₂ (<i>C</i> _{2v})	-31.1	-35.8	-28.3	-32.9
H ₃ Si(NH ₂)(NH ₃) (<i>C</i> _s)	-18.6	-23.6	-16.1	-20.9
H ₄ Si(NH ₃) ₂ (<i>C</i> _i)	17.7	10.0	21.7	13.0

^a Experimental ΔH_f (NH₃) = -9.30 ± 0.10 kcal/mol at 0 K and -10.97 ± 0.10 kcal/mol at 298 K. Reference 35. ^b Reference 1. ^c

Experimental ΔH_f (SiH₄, *T*_d) = 9.5 ± 0.5 kcal/mol at 0 K. Reference 39. ^d Reference 22e.

Table 8.3. Dehydrogenation and NH₃ Stabilization Reactions at 0 K and 298 K (kcal/mol).

Reaction	CCSD(T)		G3(MP2)	
	(0 K)	(298 K)	(0 K)	(298 K)
H ₄ Si(NH ₃) ₂ → H ₃ Si(NH ₂)(NH ₃) + H ₂	-36.3	-33.6	-38.9	-35.0
H ₃ Si(NH ₂)(NH ₃) → H ₂ Si(NH ₂) ₂ + H ₂	-12.5	-12.2	-13.5	-13.1
H ₄ Si(NH ₃) ₂ → H ₂ Si(NH ₂) ₂ + 2H ₂	-48.8	-45.8	-52.4	-48.2
H ₂ Si(NH ₂) ₂ → HN=SiH(NH ₂) + H ₂	44.0	45.3	41.6	42.9
HN=SiH(NH ₂) → HN=Si=NH + H ₂	53.7	55.7	49.8	51.9
H ₃ Si(NH ₂) → H ₂ Si=NH + H ₂	49.2	50.7	46.3	47.8
H ₄ Si(NH ₃) ₂ → SiH ₄ (<i>T_d</i>) + 2NH ₃	-27.4	-25.4	-28.0	-25.0
H ₄ Si(NH ₃) ₂ → SiH ₄ (<i>D_{4h}</i>) + 2NH ₃	61.6	63.6	61.4	64.4
H ₄ Si(NH ₃) ₂ → H ₄ Si(NH ₃) + NH ₃	-27.9	-25.6	-29.1	-25.8
H ₄ Si(NH ₃) → SiH ₄ (<i>T_d</i>) + NH ₃	0.5	0.3	1.1	0.8
H ₃ Si(NH ₂)(NH ₃) → H ₃ Si(NH ₂) + NH ₃	1.0	0.7	1.7	1.3

Table 8.4. Calculated Si NMR Chemical Shifts for SiH_4 (T_d), SiH_4 (D_{4h}) and $\text{H}_4\text{Si}(\text{NH}_3)_2$ (C_i) at the B3LYP/Alrichs-VTZ+P level (ppm).^a

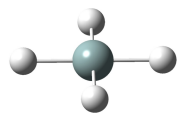
Molecule	δ
SiH_4 (T_d)	-107.9
SiH_4 (D_{4h})	323.4
$\text{H}_4\text{Si}(\text{NH}_3)_2$ (C_i)	-234.1

^a Calculated with respect to tetramethylsilane.

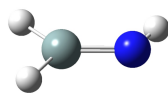
Figure Captions

Figure 8.1. Optimized molecular structures for SiH_4 , $\text{H}_2\text{Si}=\text{NH}$, $\text{HN}=\text{Si}=\text{NH}$, $\text{H}_3\text{Si}(\text{NH}_2)$, $\text{HN}=\text{SiH}(\text{NH}_2)$, $\text{H}_2\text{Si}(\text{NH}_2)_2$, $\text{H}_4\text{Si}(\text{NH}_3)$, $\text{H}_3\text{Si}(\text{NH}_2)(\text{NH}_3)$, and $\text{H}_4\text{Si}(\text{NH}_3)_2$.

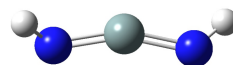
Figure 8.1.



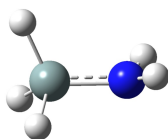
SiH_4 (D_{4h})



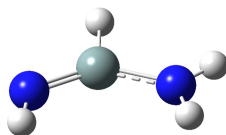
$\text{H}_2\text{Si}=\text{NH}$ (C_s)



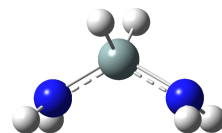
$\text{HN}=\text{Si}=\text{NH}$ (C_2)



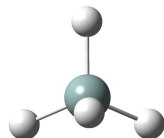
$\text{H}_3\text{Si}(\text{NH}_2)$ (C_s)



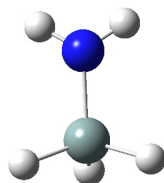
$\text{HN}=\text{SiH}(\text{NH}_2)$ (C_s)



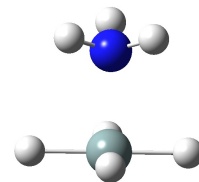
$\text{H}_2\text{Si}(\text{NH}_2)_2$ (C_{2v})



$\text{H}_4\text{Si}(\text{NH}_3)$ (C_3)



$\text{H}_3\text{Si}(\text{NH}_2)(\text{NH}_3)$ (C_s)



$\text{H}_4\text{Si}(\text{NH}_3)_2$ (C_i)

8.5 References

-
- ¹ Gutowski, M.; Dixon, D. A. *J. Chem. Phys. A* **2005**, *109*, 5129.
- ² Stephens, F. H.; Pons, V.; Baker, R. T. *Dalton Trans.* **2007**, 2613.
- ³ Nguyen, V. S.; Matus, M. H.; Grant, D. J.; Nguyen, M. T.; Dixon, D. A. *J. Phys. Chem. A* **2007**, *111*, 8844.
- ⁴ Matus, M. H.; Anderson, K. A.; Camaioni, D. M.; Autrey, S. T.; Dixon, D. A. *J. Phys. Chem. A* **2007**, *111*, 4411.
- ⁵ Matus, M. H.; Nguyen, M. T.; Dixon, D. A. *J. Phys. Chem. A* **2007**, *111*, 1726.
- ⁶ Nguyen, V. S.; Matus, M. H.; Nguyen, M. T.; Dixon, D. A. *J. Phys. Chem. C* **2007**, *111*, 9603.
- ⁷ Nguyen, M. T.; Matus, M. H.; Dixon, D. A. *Inorg. Chem.* **2007**, *46*, 7561.
- ⁸ Nguyen, V. S.; Matus, M. H.; Ngan, V. T.; Nguyen, M. T.; Dixon, D. A. *J. Phys. Chem. C* **2008**, *112*, 5662.
- ⁹ Nguyen, M. T.; Nguyen, V. S.; Matus, M. H.; Gopakumar, G.; Dixon, D. A. *J. Phys. Chem. A* **2007**, *111*, 679.
- ¹⁰ Dixon, D. A.; Arduengo III, A. J., *J. Phys. Chem.* **1987**, *91*, 3195.
- ¹¹ Dixon, D. A.; Arduengo III, A. J. *Inter. J. Quant. Chem: Quant. Chem. Symp.* **1988**, *22*, 85.
- ¹² Krogh-Jespersen, M-B.; Chandrasekhar, J.; Würthwein, E-U.; Collins, J. B.; Schleyer, P. v. R., *J. Am. Chem. Soc.* **1980**, *102*, 2263.
- ¹³ Arduengo III, A. J.; Dixon, D. A.; Roe, D. C.; Kline, M., *J. Am. Chem. Soc.* **1988**, *110*, 4437.
- ¹⁴ Yoshizawa, K.; Suzuki, A., *J. Chem. Phys.* **2001**, *271*, 41.
- ¹⁵ Dixon, D. A.; Arduengo III, A. J.; Fukunaga, T., *J. Am. Chem. Soc.* **1986**, *108*, 2461.
- ¹⁶ Arduengo III, A. J.; Dixon, D. A.; Roe, D. C., *J. Am. Chem. Soc.* **1986**, *108*, 6821.
- ¹⁷ Dixon, D. A.; Arduengo III, A. J., *J. Am. Chem. Soc.* **1987**, *109*, 338.
- ¹⁸ Arduengo III, A. J.; Stewart, C. A.; Davidson, F.; Dixon, D. A.; Becker, J. Y.; Culley, S. A.; Mizen, M. B., *J. Am. Chem. Soc.* **1987**, *109*, 628.
- ¹⁹ Arduengo III, A. J., *Pure & Appl. Chem.* **1987**, *59*, 1053.

-
- ²⁰ Hehre, W. J.; Radom, L.; Schleyer, P. v. R.; Pople, J. A. Wiley-Interscience, New York, **1986**, p. 436.
- ²¹ Dunning, T. H., Jr. *J. Phys. Chem.* **2000**, *104*, 9062.
- ²² (a) Peterson, K. A.; Xantheas, S. S.; Dixon, D. A.; Dunning, T. H. Jr., *J. Phys. Chem. A* **1998**, *102*, 2449; (b) Feller, D.; Peterson, K. A. *J. Chem. Phys.* **1998**, *108*, 154; (c) Dixon, D. A.; Feller, D. *J. Phys. Chem. A* **1998**, *102*, 8209; (d) Feller, D.; Peterson, K. A. *J. Chem. Phys.* **1999**, *110*, 8384; (e) Feller, D. *J. Chem. Phys.* **1999**, *111*, 4373; (f) Feller, D.; Dixon, D. A. *J. Phys. Chem. A* **2000**, *104*, 3048; (g) Feller, D.; Sordo, J. A. *J. Chem. Phys.* **2000**, *113*, 485; (h) Feller, D.; Dixon, D. A. *J. Chem. Phys.* **2001**, *115*, 3484; (i) Dixon, D. A.; Feller, D.; Sandrone, G. *J. Phys. Chem. A* **1999**, *103*, 4744; (j) Ruscic, B.; Wagner, A. F.; Harding, L. B.; Asher, R. L.; Feller, D.; Dixon, D. A.; Peterson, K. A.; Song, Y.; Qian, X.; Ng, C.; Liu, J.; Chen, W.; Schwenke, D. W. *J. Phys. Chem. A* **2002**, *106*, 2727; (k) Feller, D.; Dixon, D. A.; Peterson, K. A. *J. Phys. Chem. A*, **1998**, *102*, 7053; (l) Dixon, D. A.; Feller, D.; Peterson, K. A. *J. Chem. Phys.*, **2001**, *115*, 2576.
- ²³ Purvis III, G. D.; Bartlett, R. J. *J. Chem. Phys.* **1982**, *76*, 1910.
- ²⁴ Raghavachari, K.; Trucks, G. W.; Pople, J. A.; Head-Gordon, M. *Chem. Phys. Lett.* **1989**, *157*, 479.
- ²⁵ Watts, J. D.; Gauss, J.; Bartlett, R. J. *J. Chem. Phys.* **1993**, *98*, 8718.
- ²⁶ (a) Dunning, T. H., Jr. *J. Chem. Phys.* **1989**, *90*, 1007; (b) Kendall, R. A.; Dunning, T. H., Jr.; Harrison, R. J. *J. Chem. Phys.* **1992**, *96*, 6796; (c) Woon, D.E.; Dunning, T. H., Jr., *J. Chem. Phys.* **1993**, *98*, 1358; (d) Dunning, T. H., Jr.; Peterson, K. A.; Wilson, A. K. *J. Chem. Phys.* **2001**, *114*, 9244; (e) Wilson, A. K.; Woon, D.E.; Peterson, K. A.; Dunning, T. H., Jr., *J. Chem. Phys.* **1999**, *110*, 7667.
- ²⁷ McQuarrie, D. A. *Statistical Mechanics*, University Science Books: Sausalito, CA, 2001.
- ²⁸ Curtiss, L. A.; Raghavachari, K.; Redfern, P. C.; Pople, J. A. *J. Chem. Phys.* **1997**, *106*, 1063.
- ²⁹ Dunning, T. H. Jr., Peterson, K. A. Wilson, A. K. *J. Chem. Phys.* **2001**, *114*, 9244.
- ³⁰ MOLPRO a package of *ab initio* programs designed by Werner, H.-J.; and Knowles, P. J. version 2002.6, Universität Stuttgart, Stuttgart, Germany, University of Birmingham, Birmingham, United Kingdom, Amos, R. D.; Bernhardsson, A.; Berning, A.; Celani, P.; Cooper, D. L.; Deegan, M. J. O.; Dobbyn, A. J.; Eckert, F.; Hampel, C.; Hetzer, G.; Knowles, P. J.; Korona, T.; Lindh, R.; Lloyd, A. W.; McNicholas, S. J.; Manby, F. R.; Meyer, W.; Mura, M. E.; Nicklass, A.; Palmieri, P.; Pitzer, R.; Rauhut, G.; Schütz, M.; Schumann, U.; Stoll, H.; Stone, A. J.; Tarroni, R.; Thorsteinsson, T.; Werner, H.-J.
- ³¹ Peterson, K. A.; Woon, D. E.; Dunning, T. H., Jr. *J. Chem. Phys.* **1994**, *100*, 7410.

-
- ³² Peterson, K. A.; Dunning, T. H., Jr., *J. Chem. Phys.* **2002**, *117*, 10548.
- ³³ C. E. Moore "Atomic energy levels as derived from the analysis of optical spectra, Volume I, H to V," U.S. National Bureau of Standards Circular 467, U.S. Department of Commerce, National Technical Information Service, COM-72-50282, Washington, D.C.; **1949**.
- ³⁴ Shimanouchi, T. *Tables of Molecular Vibrational Frequencies Consolidated Volume I*, NSRDS-NBS 39; National Bureau of Standards: Washington DC, 1972.
- ³⁵ Chase, M. W., Jr.; NIST-JANAF Tables (4th Edition), *J. Phys. Chem. Ref. Data*, Mono. 9, Suppl. 1 (1998).
- ³⁶ Feller, D.; Dixon, D. A. *J. Phys. Chem. A* **1999**, *103*, 6413.
- ³⁷ Curtis, L. A.; Redfern, P. C.; Raghavachari, K.; Rassolov, V.; Pople, J. A. *J. Chem. Phys.* **1999**, *110*, 4703.
- ³⁸ Lee, T. J.; Taylor, P. R. *Int. J. Quantum Chem. Symp.* **1989**, *23*, 199
- ³⁹ Gunn, R. S.; Green, L. G. *J. Phys. Chem.* **1961**, *65*, 779.
- ⁴⁰ Based on the previously calculated heats of formation of silane of $\Delta H_f(\text{SiH}_4) = 8.7 \pm 0.6$ kcal/mol at 0 K^{22e} and of the silyl radical $\Delta H_f(\text{SiH}_3) = 47.3 \pm 0.5$ kcal/mol at 0 K^{22e} along with the experimental heat of formation of the hydrogen atom.³⁵
- ⁴¹ Arduengo, A. J., III; Dixon, D. A.; Kumashiro, K. K.; Lee, C.; Power, W. P.; Zilm, K. W. *J. Am. Chem. Soc.*, **1994**, *116*, 636.
- ⁴² Mueller, T. *J. Organometal. Chem.* **2003**, *686*, 251.
- ⁴³ Becke, A. D. *J. Chem. Phys.* **1993**, *98*, 1372, 5648; Lee, C.; Yang, W.; Parr, R. G. *Phys. Rev. B* **1988**, *37*, 785.
- ⁴⁴ Schafer, A.; Horn, H.; Ahlrichs, R. *J. Chem. Phys.* **1992**, *97*, 2571
- ⁴⁵ Wolinski, K.; Hinton, J.F.; Pulay, P. *J. Am Chem. Soc.* **1990**, *112*, 8251
- ⁴⁶ Cho, H.; Felmy, A. R.; Craciun, R.; Keenum, J. P.; Shah, N.; Dixon, D. A. *J. Am. Chem. Soc.*, **2006**, *128*, 2324.
- ⁴⁷ Jameson, C. J.; Jameson, A. K. *Chem. Phys. Lett.* **1988**, *149*, 300.
- ⁴⁸ Makulski, W.; Jackowski, K.; Antušek, A.; Jaszuński M. *J. Phys. Chem. A* **2006**, *110*, 11462

⁴⁹ Quin L.D.; Verkade, J.G. eds., *Phosphorus Chemistry, Proceedings of the 1981 International Conference*, American Chemical Society, Washington, D.C., 1981; Quin, L.D. *The Heterocyclic Chemistry of Phosphorus*, J. Wiley and Sons, New York, 1981; Quin L.D.; Verkade, J.G. eds. *Phosphorus-31 NMR spectral properties in compound characterization and structural analysis*. VCH Weinheim, New York, 1994; Quin, L.D. *A guide to organophosphorus chemistry* Wiley-IEEE, New York, 2000.

8.6 Appendix

Table A8.1. Calculated CCSD(T)/aV(T+d)Z Geometry Parameters. Bond Distances in Å and Bond Angles in Degrees.

Molecule	R _{Si-H}	R _{N-H}	R _{Si-N}	∠ HSiH	∠ HSiN	∠ HNSi	∠ HSiNH
SiH ₄ (<i>D</i> _{4h})	1.5322			90.0			
H ₂ Si=NH (<i>C</i> _s)	1.4717	1.0151	1.6106		117.8	119.5	180.0
	1.4842				129.6		
HN=Si=NH (<i>C</i> ₂) ^a		1.0098	1.5871			126.2	142.0
H ₃ Si(NH ₂) (<i>C</i> _s) ^b	1.4761	1.0077	1.7276	110.8	107.7	119.6	49.7
	1.4833			107.5	115.7		-70.6
H ₄ Si(NH ₃) (<i>C</i> ₃) ^b	1.4735	1.0127	3.1709	111.0	72.1	112.1	60.3
	1.4823			107.9	180.0		
HN=SiH(NH ₂) (<i>C</i> _s) ^b	1.4646	1.0102 (NH)	1.5959 (NH)		118.8 (NH)	126.1 (NH)	
		1.0072 (NH ₂)	1.6945 (NH ₂)			122.5 (NH ₂)	180.0
		1.0063 (NH ₂)				124.2 (NH ₂)	
H ₂ Si(NH ₂) ₂ (<i>C</i> _{2v}) ^b	1.4748	1.0074	1.7254	114.5	105.3	121.2	45.2
H ₃ Si(NH ₂)(NH ₃) (<i>C</i> _s) ^b	1.4737	1.0082 (NH ₂)	1.7406 (NH ₂)	113.4	105.6 (NH ₂)	119.3 (NH ₂)	50.2 (NH ₂)
	1.4817	1.0128 (NH ₃)	3.0155 (NH ₃)	109.3	72.1 (NH ₃)	110.4 (NH ₃)	59.6 (NH ₃)
						115.2 (NH ₃)	-61.4 (NH ₃)
H ₄ Si(NH ₃) ₂ (<i>C</i> _i) ^b	1.5487	1.0143	2.0136	90.0	90.0	110.3	179.6
		1.0136				109.8	59.6

^a ∠ HSiNH = ∠ HNSiN. ^b Calculated at the MP2/aV(T+d)Z level.

Table A8.2. CCSD(T) Total Energies (E_h) as a Function of the Basis Set.^{a,b}

Molecule	Basis Set	Energy
SiH ₄ (D_{4h})	aV(D+d)Z	-291.262451
	aV(T+d)Z	-291.300675
	aV(Q+d)Z	-291.309836
	CBS (DTQ)	-291.314703
H ₂ Si=NH (C_s)	aV(D+d)Z	-345.414872
	aV(T+d)Z	-345.495665
	aV(Q+d)Z	-345.518994
	CBS (DTQ)	-345.53197
HN=Si=NH (C_2)	aV(D+d)Z	-399.431701
	aV(T+d)Z	-399.557652
	aV(Q+d)Z	-399.594356
	CBS (DTQ)	-399.614803
H ₃ Si(NH ₂) (C_s)	aV(D+d)Z	-346.666796
	aV(T+d)Z	-346.757490
	aV(Q+d)Z	-346.782726
	CBS (DTQ)	-346.796643
H ₄ Si(NH ₃) (C_3)	aV(D+d)Z	-347.835945
	aV(T+d)Z	-347.926955
	aV(Q+d)Z	-347.952315
	CBS (DTQ)	-347.966304
HN=SiH(NH ₂) (C_s)	aV(D+d)Z	-400.691744
	aV(T+d)Z	-400.827208
	aV(Q+d)Z	-400.865863
	CBS (DTQ)	-400.887300
H ₂ Si(NH ₂) ₂ (C_{2v})	aV(D+d)Z	-401.936001
	aV(T+d)Z	-402.080445
	aV(Q+d)Z	-402.120555
	CBS (DTQ)	-402.142664
H ₃ Si(NH ₂)(NH ₃) (C_s)	aV(D+d)Z	-403.097587
	aV(T+d)Z	-403.242299
	aV(Q+d)Z	-403.282622
	CBS (DTQ)	-403.304864
H ₄ Si(NH ₃) ₂ (C_i)	aV(D+d)Z	-404.220478

aV(T+d)Z	-404.373877
aV(Q+d)Z	-404.414180
CBS (DTQ)	-404.436107

^a Dissociation is with respect to RCCSD(T) atoms for closed shell atoms and R/UCCSD(T) for open shell atoms. Symmetry equivalencing of the p_x , p_y , and p_z orbitals was not imposed in the atomic calculations. ^b CBS (DTQ) values from Eq. 1 (see text) obtained with the aV($n+d$)Z basis sets with $n = D, T, Q$.

Table A8.3. Calculated MP2 Frequencies (cm⁻¹).

Molecule	Symmetry	aV(T+d)Z
SiH ₄ (<i>D</i> _{4h}) ^a	a _{1g}	1986.6
	b _{1g}	1750.3
	b _{2g}	1440.4
	a _{2u}	1005.6
	b _{2u}	2463.4i
	e _u	1915.0
	e _u	1188.4
H ₂ Si=NH (<i>C</i> _s) ^a	a'	3467.8
	a'	2235.4
	a'	2163.0
	a'	1093.6
	a'	972.5
	a'	750.7
	a'	571.2
	a''	755.4
	a''	576.1
HN=Si=NH (<i>C</i> ₂) ^a	a	3545.2
	a	939.6
	a	545.4
	a	377.7
	a	192.2
	b	3544.7
	b	1310.8
	b	491.4
	b	298.3
H ₃ Si(NH ₂) (<i>C</i> _s)	a'	3505.6
	a'	2231.1
	a'	2184.2
	a'	1591.3
	a'	1012.4

	a'	958.3
	a'	846.6
	a'	714.8
	a'	401.7
	a''	3604.1
	a''	2233.0
	a''	1014.0
	a''	922.9
	a''	632.2
	a''	180.8
H ₄ Si(NH ₃) (C ₃)	a	3405.2
	a	2242.1
	a	2201.8
	a	1059.5
	a	934.2
	a	29.5
	e	3548.4
	e	2246.7
	e	1667.4
	e	1007.7
	e	275.9
	e	85.3
HN=SiH(NH ₂) (C _s)	a'	3622.8
	a'	3547.1
	a'	3511.4
	a'	2294.5
	a'	1576.6
	a'	1175.2
	a'	938.2
	a'	874.3
	a'	725.8
	a'	589.1

	a'	288.9
	a''	700.9
	a''	462.1
	a''	386.7
	a''	333.8
H ₂ Si(NH ₂) ₂ (C _{2v})	a ₁	3507.3
	a ₁	2232.2
	a ₁	1590.2
	a ₁	929.8
	a ₁	789.6
	a ₁	392.9
	a ₁	279.3
	b ₁	3609.5
	b ₁	2239.1
	b ₁	923.7
	b ₁	499.8
	b ₁	331.9
	b ₂	3507.7
	b ₂	1590.3
	b ₂	952.0
	b ₂	888.4
	b ₂	340.2
	a ₂	3609.5
	a ₂	941.1
	a ₂	722.5
	a ₂	104.6
H ₃ Si(NH ₂)(NH ₃) (C _s)	a'	3547.7
	a'	3498.9
	a'	3403.8
	a'	2228.3
	a'	2178.8
	a'	1666.6

	a'	1589.6
	a'	1062.6
	a'	989.6
	a'	933.3
	a'	821.2
	a'	774.0
	a'	414.5
	a'	210.5
	a'	88.4
	a'	78.0
	a''	3597.4
	a''	3547.8
	a''	2234.6
	a''	1666.4
	a''	994.6
	a''	931.5
	a''	671.3
	a''	247.5
	a''	160.2
	a''	80.3
	a''	47.9
H ₄ Si(NH ₃) ₂ (C _i)	a _g	3538.1
	a _g	3531.0
	a _g	3389.8
	a _g	1946.4
	a _g	1667.7
	a _g	1659.8
	a _g	1598.8
	a _g	1310.4
	a _g	1219.5
	a _g	928.5
	a _g	925.7

a _g	529.2
a _g	519.2
a _g	351.3
a _g	11.9
a _u	3537.9
a _u	3530.6
a _u	3389.3
a _u	1821.9
a _u	1821.8
a _u	1658.8
a _u	1641.6
a _u	1215.6
a _u	1110.7
a _u	1109.9
a _u	1090.5
a _u	754.9
a _u	707.0
a _u	661.0
a _u	466.1
a _u	203.6
a _u	197.4
a _u	33.4

^a Calculated at the CCSD(T)/aV(T+d)Z level.

Table A8.4. T_1 Diagnostics at the CCSD(T)/aV(Q+d)Z level.

Molecule	T_1 Diagnostics
SiH ₄ (D_{4h})	0.0093
H ₂ Si=NH (C_s)	0.0182
HN=Si=NH (C_2)	0.0202
H ₃ Si(NH ₂) (C_s)	0.0098
H ₄ Si(NH ₃) (C_3)	0.0099
HN=SiH(NH ₂) (C_s)	0.0149
H ₂ Si(NH ₂) ₂ (C_{2v})	0.0101
H ₃ Si(NH ₂)(NH ₃) (C_s)	0.0095
H ₄ Si(NH ₃) ₂ (C_i)	0.0085

CHAPTER 9

HEATS OF FORMATION AND BOND DISSOCIATION ENERGIES OF THE HALOSILANES, METHYLHALOSILANES AND HALOMETHYLSILANES

From: Grant, D. J.; Dixon, D. A. *J. Phys. Chem. A* **2009**, *113*, 3656-3661.

9.1 Introduction

There is substantial interest in the energetics of silanes for use in technological applications such as precursors for chemical vapor deposition processes or for regeneration schemes for chemical hydrogen storage systems. There is a limited quantity of experimental thermodynamic data available for the halosilanes, methylhalosilanes, and halomethylsilanes in terms of their heats of formation and bond dissociation energies (BDEs). Although the heats of formation of the silyl radical, the halosilanes, the methyl radical, and the halomethylradicals are known experimentally,^{1,2} there have been no experiments measuring the heats of formation for the methylhalosilanes, the halomethylsilanes, or the various radicals involved in the several of the bond breaking processes studied. Except for silane, the halosilanes, and methylsilane, there are limited experimental BDE data available for the molecules under study.³ Accurate thermodynamic data is essential in the design of regeneration process for chemical hydrogen storage systems. In addition, the heats of formation of simple model compounds are needed accurately for use in isodesmic reaction schemes in order to treat larger molecules.

Because it is difficult to measure BDEs, high-level theoretical calculations of these processes offer a unique opportunity to obtain accurate self-consistent values. Modern

computational chemistry methods implemented on high performance computer architectures can now provide reliable predictions of chemical bond energies to within about 1 kcal/mol for most reactants and products that are not dominated by multireference character.⁴ We can use the approach that we have been developing with collaborators at Washington State University for the prediction of accurate molecular thermochemistry⁵ to determine BDEs in these silane compounds. Our approach is based on calculating the total atomization energy (TAE) of a molecule and using this value with known heats of formation of the atoms to calculate the heat of formation at 0 K. The approach starts with coupled cluster theory with single and double excitations including a perturbative triples correction (CCSD(T)),^{6,7,8} in combination with the correlation-consistent basis sets⁹ extrapolated to the complete basis set limit to treat the correlation energy of the valence electrons. This is followed by a number of smaller additive corrections including core-valence interactions and relativistic effects, both scalar and spin-orbit. The zero point energy can be obtained from experiment, theory, or a combination of the two. Corrections to 298 K can then be calculated by using standard thermodynamic and statistical mechanics expressions in the rigid rotor-harmonic oscillator approximation¹⁰ and appropriate corrections for the heat of formation of the atoms.¹¹

In the current work, we have calculated the heats of formation of the halosilanes SiH_3X , the methylhalosilanes $\text{CH}_3\text{SiH}_2\text{X}$, and the halomethylsilanes XCH_2SiH_3 for $\text{X} = \text{F}, \text{Cl}, \text{Br},$ and I at the CCSD(T)/CBS level, as well as a range of radicals relevant to breaking the C-H, Si-H, Si-C, C-X, and Si-X bonds. This work was made possible by the availability of the new effective core potential/correlation consistent basis sets developed by Peterson and co-workers.¹² These basis sets were developed in combination with effective core potentials from the Stuttgart/Köln

group and allow us to study all of the main-group elements with high quality basis sets that can be extrapolated to the CBS limit.

9.2 Computational Methods

The standard aug-cc-pVnZ basis sets were used for H, C, and F. It has recently been found that tight d functions are necessary for calculating accurate atomization energies for 2nd row elements,^{9d} so we also included additional tight d functions in our calculations. Basis sets containing extra tight d functions are denoted aug-cc-pV($n+d$)Z in analogy to the original augmented correlation consistent basis sets. We use aug-cc-pV($n+d$)Z to represent the combination of aug-cc-pV($n+d$)Z (on the 2nd row atoms Si and Cl) and aug-cc-pVnZ (on H, C, F) basis sets and abbreviate this as aV($n+d$)Z. For heavier elements, the effects of relativity need to be included in the basis sets. A small core relativistic effective core potential (RECP) was used for Br and I. For Br, the RECP subsumes the ($1s^2$, $2s^2$, and $2p^6$) orbital space into the 10-electron core set, leaving the ($3s^2$, $3p^6$, $4s^2$, $3d^{10}$, and $4p^5$) space with 25 electrons to be handled explicitly; only the ($4s^2$, $4p^5$) electrons are active in our valence correlation treatment. For I, the RECP subsumes the ($1s^2$, $2s^2$, $2p^6$, $3s^2$, $3p^6$, and $3d^{10}$) orbital space into the 28-electron core set, leaving the ($4s^2$, $4p^6$, $5s^2$, $4d^{10}$, and $5p^5$) space with 25 electrons to be handled explicitly; only the ($5s^2$, $5p^5$) electrons are active in our valence correlation treatment. Even though the 4s and 4p inner shell occupied orbitals may have similar energies with the inner shell occupied 3d orbitals, there is good spatial separation between the 3d and the 4s and 4p orbitals so the 3d electrons are included in the RECP and the 4s and 4p are included as active electrons with the 4d in the inner core-valence region for the small core RECPs.¹³ The polarized relativistic basis sets are labeled as aug-cc-pVnZ-PP.¹² We use the shorthand notation of aVnZ-PP to denote the combination of the aug-cc-pVnZ basis set on H, C, and F, the aug-cc-pV($n+d$)Z basis set on Cl and Si, and the

aug-cc-pVnZ-PP basis set on Br and I. Only the spherical component subset (e.g., 5-term d functions, 7-term f functions, etc.) of the Cartesian polarization functions were used. All CCSD(T) calculations were performed with the MOLPRO-2002¹⁴ program system on a single processor of an SGI Origin computer, the Cray XD-1 at the Alabama Supercomputer Center, or on a Dell Cluster at the University of Alabama.

For the open shell atomic calculations, we used restricted Hartree-Fock for the starting wavefunction and then relaxed the spin restriction in the coupled cluster portion of the calculation; this method is conventionally labeled R/UCCSD(T). Our CBS estimates use a mixed exponential/Gaussian function of the form¹⁵

$$E(n) = E_{\text{CBS}} + Be^{-(n-1)} + Ce^{-(n-1)^2} \quad (1)$$

where $n = 2$ (aVDZ-PP), 3 (aVTZ-PP), 4 (aVQZ-PP).

Most correlated electronic structure calculations based on molecular orbital theory are done in the frozen core approximation with the energetically lower lying orbitals, e.g., the 1s in fluorine, excluded from the correlation treatment. In order to achieve thermochemical properties within ± 1 kcal/mol of experiment, it is necessary to account for core-valence correlation energy effects. Core-valence (CV) calculations were carried out with the weighted core-valence basis set cc-pwCVTZ.¹⁶ The cc-pwCVTZ-PP basis set for Br and I is based on the cc-pVTZ-PP basis set and accompanying small core RECP. For Br and I, the cc-pwCVTZ-PP basis set includes up through g -functions in order to provide a consistent degree of angular correlation for the active 4d electrons.¹⁷ Core-valence calculations for Br and I involve all 25 electrons outside the RECP core, i.e. $3s^2$, $3p^6$, $4s^2$, $3d^{10}$, and $4p^5$ and $4s^2$, $4p^6$, $5s^2$, $4d^{10}$, and $5p^5$, respectively.

Two adjustments to the total atomization energy (TAE = ΣD_0) are necessary in order to account for relativistic effects in atoms and molecules. The first correction lowers the sum of the

atomic energies (decreasing TAE) by replacing energies that correspond to an average over the available spin multiplets with energies for the lowest multiplets as most electronic structure codes produce only spin multiplet averaged wavefunctions. The atomic spin-orbit corrections are $\Delta E_{\text{SO}}(\text{C}) = 0.09$ kcal/mol, $\Delta E_{\text{SO}}(\text{F}) = 0.39$ kcal/mol, $\Delta E_{\text{SO}}(\text{Si}) = 0.43$ kcal/mol, $\Delta E_{\text{SO}}(\text{Cl}) = 0.84$ kcal/mol, $\Delta E_{\text{SO}}(\text{Br}) = 3.50$ kcal/mol, and $\Delta E_{\text{SO}}(\text{I}) = 7.24$ kcal/mol from the tables of Moore.¹⁸ A second relativistic correction to the atomization energy accounts for molecular scalar relativistic effects, ΔE_{SR} . We evaluated ΔE_{SR} by using expectation values for the two dominant terms in the Breit-Pauli Hamiltonian, the so-called mass-velocity and one-electron Darwin (MVD) corrections from configuration interaction singles and doubles (CISD) calculations. The quantity ΔE_{SR} was obtained from CISD wavefunction with a VTZ-PP basis set at the CCSD(T)/aVTZ-PP geometry. The CISD(MVD) approach generally yields ΔE_{SR} values in good agreement (± 0.3 kcal/mol) with more accurate values from, for example, Douglas-Kroll-Hess calculations, for most molecules. A potential problem arises in computing the scalar relativistic corrections for the molecules in this study as there is the possibility of “double counting” the relativistic effect on Br and I when applying a MVD correction to an energy which already includes most of the relativistic effects via the RECP. Because the MVD operators mainly sample the core region where the pseudo-orbitals are small, we assume any double counting to be small.

Numerical geometry optimizations were performed with a convergence threshold on the gradient of approximately $10^{-4} E_{\text{h}}/\text{bohr}$ or smaller. Geometries were optimized at the aVDZ-PP and aVTZ-PP. The geometry obtained with the aVTZ-PP basis set was then used in single point aVQZ-PP calculations. The harmonic frequencies for use in the zero point energy (ΔE_{ZPE}) calculations were obtained at the CCSD(T) level with the aVTZ-PP basis set. The C-H and Si-H stretching frequencies contain the most anharmonicity so to calculate the ΔE_{ZPE} correction, the

calculated harmonic C-H and Si-H stretching frequencies were scaled by factors of 0.980 and 0.990, respectively. The scale factors for the C-H and Si-H bonds are obtained by taking the average of the theoretical CCSD(T)/aVTZ-PP values and the experimental values¹⁹ for the C-H and Si-H stretches for CH₄ and SiH₄ and dividing the average by the theoretical value. In the ΔE_{ZPE} calculations, the remaining calculated harmonic frequencies were not scaled. ΔE_{ZPE} was calculated as 0.5 the sum of the calculated frequencies with the C-H and Si-H frequencies scaled.

By combining our computed ΣD_0 values given by the following expression

$$\Sigma D_0 = \Delta E_{\text{elec}}(\text{CBS}) - \Delta E_{\text{ZPE}} + \Delta E_{\text{CV}} + \Delta E_{\text{SR}} + \Delta E_{\text{SO}} \quad (2)$$

with the known¹ heats of formation at 0 K for the elements, $\Delta H_f^0(\text{H}) = 51.63$ kcal/mol, $\Delta H_f^0(\text{C}) = 169.98$ kcal/mol, $\Delta H_f^0(\text{F}) = 18.47 \pm 0.07$ kcal/mol, $\Delta H_f^0(\text{Si}) = 107.4 \pm 0.6$ kcal/mol,^{5e} $\Delta H_f^0(\text{Cl}) = 28.59$ kcal/mol, $\Delta H_f^0(\text{Br}) = 28.18$ kcal/mol, and $\Delta H_f^0(\text{I}) = 25.61$ kcal/mol, we can derive ΔH_f^0 values for the molecules under study at 0 and 298 K.¹¹ The experimental heat of formation of Si is not as well-established as one would like with significant error bars in the standard tabulations. The NIST-JANAF Tables¹ list $\Delta H_f^0(0 \text{ K, Si}) = 106.6 \pm 1.9$ kcal/mol, while the CODATA Tables contain a slightly smaller value, at 106.5 ± 1.9 kcal/mol.²⁰ For the present work, we have chosen to use a value of 107.4 ± 0.6 kcal/mol for $\Delta H_f^0(0\text{K,Si})$, as recommended by Feller and Dixon^{5e} in a computational study of small silicon-containing molecules. This value is in excellent agreement with the value of 107.2 ± 0.2 kcal/mol value of Karton and Martin,²¹ which was derived from W4 calculations of the total atomization energies for SiH₄, Si₂H₆, and SiF₄, whose experimental values can be obtained separately without referencing the gaseous heat of formation of the Si atom. These values all fall within our estimated error bars of ± 1.0 kcal/mol for the heats of formation.

9.3 *Results and Discussion*

The total energies used in this study are given as Supporting Information (Table A9.1). The calculated geometries and frequencies are also given as Supporting Information in Tables A9.2 to A9.5 and Table A9.6, respectively, where they are compared with the available experimental values.

9.3.1 *Geometries and Frequencies* The experimental molecular structure data is available for a few of the molecules under study,^{22,23} and they are in excellent agreement with our calculated theoretical values. Comparing the CCSD(T)/aVTZ-PP calculations with experiment, the C-X bond distances for the fluoromethyl and chloromethyl radicals are too long by ~ 0.01 Å. For the H_3SiX compounds, the largest error is for the Si-X bond distance, with the largest error for SiH_3I , where the Si-I bond distance was predicted to be too long by 0.021 Å. Structural data for the methylhalosilanes also show good agreement with experiment, and in general, the Si-C and Si-X (halogen) bond distances are calculated to be too long by 0.01 to 0.03 Å. The calculated theoretical data are also in excellent agreement with the available experimental structure data for $\text{SiH}_3\text{CH}_2\text{Cl}$ and $\text{SiH}_3\text{CH}_2\text{Br}$ with the largest difference for the Si-Cl bond distance.

The experimental vibrational frequencies are available for the silyl radical,^{24,25,26} the halosilanes¹⁹ (other than iodosilane), methylsilane,²⁷ and the halomethyl radicals, other than the iodomethyl radical,^{28,29,30,31} and allow us to benchmark our calculated values. The largest difference for SiH_3 is for the e Si-H stretch. The biggest differences for the halosilanes are for the Si-H stretches as expected due to the fact that the calculated values are harmonic and the experimental values include anharmonic effects. For methylsilane, the largest differences between the calculated and experimental values are for the C-H and Si-H stretches as expected. The CH_3 asymmetric deformation e mode was calculated to be 71 cm^{-1} greater than the

experimental value.²⁷ For the halomethyl radicals, the largest differences between the calculated and experimental values are for the umbrella out-of-plane mode, which could be due to the measurements being in an Ar matrix.

9.3.2 Heats of Formation The energetic components for predicting the TAEs are given in Table 9.1 with the electronic state symmetry labels. The core-valence corrections (ΔE_{CV}) for the molecules are positive, except for those of SiH_3 , SiH_2F , SiH_2Cl , SiH_3F , and SiH_3Cl . The ΔE_{CV} range from -0.41 (SiH_3) to 2.06 (SiH_2ICH_3) kcal/mol. The scalar relativistic corrections (ΔE_{SR}) are all negative with values that range from -0.17 (CH_3) to -1.18 (SiH_2FCH_3) kcal/mol. We estimate that the error bars for the calculated heats of formation are ± 1.0 kcal/mol considering errors in the energy extrapolation, frequencies, and other electronic energy components. An estimate of the potential for significant multireference character in the wavefunction can be obtained from the T_1 diagnostic³² for the CCSD calculation. The value for the T_1 diagnostics are small (<0.02) showing that the wavefunction is dominated by a single configuration.

The calculated heats of formation are presented in Table 9.2 where they are compared with available experimental data. The estimated¹ heats of formation of SiH_3X for X a halogen are all within 1.5 kcal/mol of our calculated values. The calculated values for $\Delta H_f(\text{SiH}_3)$ and $\Delta H_f(\text{CH}_3)$ are the same as those previously reported^{5e,5g} and in excellent agreement with experiment.^{1,33} The experimental heats of formation of the halomethyl radicals have been reported, and our calculated theoretical values are in excellent agreement with experiment² within 1 kcal/mol. Calculations of the heat of formation of CH_2F and CH_2Cl from isodesmic reactions at the MP2 level with a polarized double zeta basis set (MP2/DZP)³⁴ are in good agreement with the current high level value. Our calculated values for the heats of formation of

the halosilanes are also in excellent agreement with the reported experimental values¹ within the error bar limits and, as noted above, we expect our values to be accurate to ± 1 kcal/mol.

9.3.3 Bond Dissociation Energies We can use our calculated heats of formation to predict a wide range of various BDEs in the halosilanes, methylhalosilanes, and halomethylsilanes, specifically the C-H, Si-H, Si-C, C-X, and Si-X BDEs (Table 9.3). The adiabatic BDE is defined as dissociation to the ground state of the separated species. For the BDEs under consideration, the adiabatic BDE is equal to the diabatic BDE, which represents dissociation to a configuration most representing the actual bonding in the reactant;^{35,36} the BDE for these molecules is from a closed-shell singlet species to two open-shell doublets as the products. The calculated adiabatic BDEs at 0 K for the halosilanes, methylhalosilanes, halomethanes,³⁷ and halomethylsilanes as a function of the electronegativity³⁸ and the covalent radii³⁸ of the halogen substituent are provided in Figures 9.1 and 9.2, respectively.

As expected, the Si-H BDE in SiH₄ is in excellent agreement with the various reported experimental Si-H BDEs.^{3,33,39,40,41,42} Substitution of a halogen atom for H leads to only a small change (<3 kcal/mol) in the Si-H BDE. Substitution of a fluorine atom leads to a slight increase, of a chlorine or bromine atom to no change, and of an iodine atom to a small decrease. The experimental Si-X BDEs are available and the calculated Si-X BDEs are in excellent agreement with the reported experimental values.⁴² The Si-F BDE in SiH₃F is 60 kcal/mol larger than the Si-H BDE in SiH₄ or SiH₃F. The Si-Cl BDE in SiH₃Cl is 42 kcal/mol less than the H₃Si-F BDE and is larger by 17 kcal/mol than the ClSiH₂-H BDE. In SiH₃Br, the Si-Br BDE is comparable to the Si-H BDE in SiH₄ and SiH₃Br. The Si-Br BDE in SiH₃Br is 59 kcal/mol smaller than the H₃Si-F BDE. The Si-I BDE in SiH₃I is the smallest of the halosilanes, 78 kcal/mol less than the Si-F BDE in SiH₃F. In contrast to the other halosilanes, the Si-I BDE in SiH₃I is smaller by 16

kcal/mol when compared to the equivalent Si-H BDE in SiH₃I. There is a direct correlation between the increase in the H₃Si-X bond distance and the decrease in H₃Si-X BDE. As illustrated in Figure 9.1, there is a direct correlation (R^2 value of 0.987) between the decrease in the H₃Si-X BDE and the decrease in the electronegativity of the halogen substituent.³⁸ There is also an excellent correlation (R^2 value of 0.995) between the H₃Si-X BDE and the covalent radii of the halogen substituent (Figure 9.2).³⁸

The effect of substituting a methyl group for H on the Si-H and Si-X BDEs was also studied. The Si-H BDE in CH₃SiH₃ increases by 1.3 kcal/mol as compared to the Si-H BDE in SiH₄, in excellent agreement with the reported experimental values.^{3,41,43} The slight increase in the Si-H BDE can be accounted for by the electron donating effect of the methyl group. Except for CH₃SiH₂I, methyl substitution leads to an increase in the Si-X BDE by 4 to 5 kcal/mol when compared to the analogous halosilane, again consistent with the electron donating ability of the methyl group. In CH₃SiH₂I, methyl substitution has no effect on the Si-I BDE compared to SiH₃I. The corresponding H₃Si-X bond distances are all shorter on average by ~0.01 Å compared to the CH₃SiH₂-X bond distance. This is opposite to what would be expected given the larger Si-X BDEs of the CH₃SiH₂X molecules showing that bond strength near the minimum may not directly correlate with the adiabatic BDE. The H₃Si-X and CH₃SiH₂-X stretching frequencies (Table 9.4) decrease with increasing atomic number with the H₃Si-X stretching frequencies on average 14 cm⁻¹ larger than those of CH₃SiH₂-X, which is again not consistent with the larger Si-X BDE found for the methylhalosilanes but is consistent with the change in the geometry. There are excellent correlations of the electronegativity³⁸ and covalent radii³⁸ (Figures 9.1 and 9.2) of the halogen substituent with the CH₃SiH₂-X BDE.

For the methylhalosilanes, the effect of halide substitution at the silyl group on the Si-C BDE can be studied. The calculated Si-C BDE in methylsilane is in good agreement with the reported experimental value.⁴² Except for CH₃SiH₂I, halide substitution leads to increases in the Si-C BDEs in CH₃SiH₂X (X = F, Cl, and Br) by 6.1, 3.3, and 2.6 kcal/mol, respectively. In CH₃SiH₂I, the Si-C BDE decreases by 3.2 kcal/mol. The trends in the Si-C BDEs are not consistent with the change in the Si-C bond distance in the H₃C-SiH₂X molecules, which are longer than in H₃Si-CH₃. The trends in the Si-C BDEs are consistent with the Si-C stretching frequencies in the methylhalosilanes, which are all larger than the equivalent frequency in methylsilane (Table 9.4). The largest difference in the Si-C stretching frequency was predicted to be 67 cm⁻¹ for H₃C-SiH₂F at the CCSD(T)/aVTZ-PP level, consistent with H₃CSiH₂F having the largest Si-C BDE predicted.

The effect of silyl substitution for H on the C-H and C-X BDEs in methylsilane and the halomethanes and the halomethylsilanes can also be studied. The C-H BDE decreases by 4 kcal/mol compared to the C-H BDE in methane on substitution of the electropositive silyl group, SiH₃ for H.^{5g} In the halomethylsilanes, the C-F BDE in SiH₃CH₂F is the largest of the halide substituents. The C-I BDE in SiH₃CH₂I is the smallest of the C-X BDEs in the halomethylsilanes, 50 kcal/mol less than the C-F BDE in SiH₃CH₂F. Only for fluoromethylsilane is the C-X BDE larger than the corresponding C-H BDE in methylsilane. Using the previously calculated heats of formation of the halomethanes,³⁷ we have calculated the H₃C-X BDEs and predict that the electropositive silyl group decreases the strength of the C-X BDEs in the halomethylsilanes by an average of 4.3 kcal/mol. The largest effect was predicted for the SiH₃CH₂-F BDE, which was calculated to be 6.1 kcal/mol less than the H₃C-F BDE. There is an excellent correlation (Figure 9.1) between the decrease in electronegativity ($R^2 = 0.976$) of the halide substituent and the

increase in SiH₃CH₂-X bond distance, as well as between the BDE and the covalent radii ($R^2 = 0.998$) (Figure 9.2). The halomethanes³⁷ exhibit the same dependence on the electronegativity and covalent radii of the halogen substituent (Figures 9.1 and 9.2).

We investigated the effect of halide substitution at the methyl group on the Si-C BDE in the halomethylsilanes. Unlike the methylhalosilanes, the halomethylsilanes all show a decrease in the Si-C BDE when compared to the Si-C BDE in methylsilane. In addition to the electropositive silyl unit, each respective halide substituent has a larger electronegativity compared to that of H leading to a further weakening of the Si-C BDE with the largest effect of halide substitution found for fluouromethylsilane. For the halomethylsilanes, the larger the electronegativity of the halide, the larger is the decrease in the Si-C BDE. The predicted trends in the Si-C BDE are consistent with the Si-C bond distances in the H₃SiCH₂X molecules, which are all longer than the corresponding Si-C bond distance in H₃Si-CH₃. The predicted trends in the Si-C BDEs are not consistent with the Si-C stretching frequencies in the methylhalosilanes as those for the halomethylsilanes are all consistently larger than that of methylsilane (Table 9.4).

The SiH₃CH₂X isomers are always less stable than the SiH₂XCH₃ isomers, and this energy difference correlates linearly with the electronegativity of the halogen as shown in Figure 9.3. The difference in the isomer energies is due to the fact that the C-H BDE is 8.3 kcal/mol larger than the Si-H BDE in CH₃SiH₃ and that the Si-X BDEs are much larger than the C-X BDEs. For the isomer pairs SiH₃CH₂X/SiH₂XCH₃, the difference in the Si-X and C-X BDEs is 52.5, 33.6, 29.6, and 19.9 kcal/mol for X = F, Cl, Br, and I, respectively. The larger Si-X BDE as compared to the C-X BDE is consistent with the smaller electronegativity of Si leading to a larger electronegativity difference between Si and X and a larger BDE with more ionic character. The respective isomer energy differences of 60.8, 41.9, 37.8, and 28.1 kcal/mol for X = F, Cl, Br,

and I, respectively, are to a good approximation given by 8.3 kcal/mol plus the difference in the Si-X and C-X BDEs given above.

9.4 *Conclusions*

We have predicted the heats of formation of the halosilanes, the methylhalosilanes, and the halomethylsilanes, as well as radicals involved in the various bond breaking processes, at the CCSD(T)/CBS level plus additional corrections. The calculated values should be good to ± 1.0 kcal/mol, and are in excellent agreement with the available experimental data. Our accurately calculated heats of formation allow us to predict the various adiabatic BDEs for all of the substituted silane compounds to within ± 1.0 kcal/mol, dramatically improving the estimates of these important quantities. The Si-H BDE in SiH₃F is the largest of the halosilanes. Only in iodosilane is the Si-H BDE larger than the corresponding Si-X BDE. Except for methyliodosilane, methyl substitution leads to an increase in the Si-X BDE when compared to the Si-X BDE in the halosilanes. Except for methyliodosilane, halide substitution leads to an increase in the Si-C BDE when compared to the Si-C BDE in methylsilane. Fluoromethylsilane has the strongest Si-X BDE of 155.1 kcal/mol at 0 K. Unlike the methylhalosilanes, the halomethylsilanes all show a decrease in the Si-C BDE when compared to the Si-C BDE in methylsilane. The various trends can be explained in terms of the electronegativity of the substituent, the atomic sizes, and the electron donating properties of the methyl substituent.

Acknowledgments Funding provided in part by the Department of Energy, Office of Energy Efficiency and Renewable Energy under the Hydrogen Storage Grand Challenge, Solicitation No. DE-PS36-03GO93013. This work was done as part of the Chemical Hydrogen Storage

Center. DAD is indebted to the Robert Ramsay Endowment of the University of Alabama. We thank Prof. Kirk Peterson, Washington State University, for providing some of the basis sets.

Appendix Total CCSD(T) energies as a function of basis set. CCSD(T) geometry parameters for CH₂X, SiH₃, SiH₂X, SiH₃CH₂, and SiH₂CH₃; SiH₃X; SiH₃CH₃ and SiH₂XCH₃; and SiH₃CH₂X where (X = F, Cl, Br, and I). CCSD(T) calculated frequencies (cm⁻¹). This material is available free of charge via the internet at <http://pubs.acs.org>.

Table 9.1. CCSD(T) Atomization and Reaction Energies in kcal/mol.^a

Molecule	CBS ^b	$\Delta E_{\text{ZPE}}^{\text{c}}$	$\Delta E_{\text{CV}}^{\text{d}}$	$\Delta E_{\text{SR}}^{\text{e}}$	$\Delta E_{\text{SO}}^{\text{f}}$	$\Sigma D_0(0 \text{ K})^{\text{g}}$
CH ₃ (² A ₂ ' - D _{3h})	306.80	18.38	0.94	-0.17	-0.09	289.10
CH ₂ F (² A' - C _s)	313.32	15.37	0.96	-0.45	-0.48	297.97
CH ₂ Cl (² A' - C _s)	287.95	14.00	1.11	-0.41	-0.93	273.71
CH ₂ Br (² A' - C _s)	274.64	13.72	1.33	-0.22	-3.89	258.13
CH ₂ I (² A' - C _s)	263.33	13.39	1.67	-0.18	-7.33	244.11
SiH ₃ (² A ₁ - C _{3v})	228.75	13.25	-0.41	-0.48	-0.43	214.18
SiH ₂ F (² A' - C _s)	284.59	11.00	-0.36	-0.86	-0.82	271.56
SiH ₂ Cl (² A' - C _s)	244.21	10.36	-0.28	-0.71	-1.27	231.60
SiH ₂ Br (² A' - C _s)	229.95	9.99	0.05	-0.58	-3.93	215.49
SiH ₂ I (² A' - C _s)	215.81	9.86	0.61	-0.49	-7.67	198.40
SiH ₃ F (¹ A ₁ - C _{3v})	383.96	17.20	-0.31	-0.95	-0.82	364.69
SiH ₃ Cl (¹ A ₁ - C _{3v})	341.22	16.43	-0.24	-0.80	-1.27	322.47
SiH ₃ Br (¹ A ₁ - C _{3v})	326.30	16.12	0.19	-0.67	-3.93	305.76
SiH ₃ I (¹ A ₁ - C _{3v})	310.57	15.85	0.69	-0.58	-7.67	287.15
SiH ₃ CH ₃ (¹ A ₁ - C _{3v})	628.54	37.92	0.87	-0.78	-0.52	590.18
SiH ₃ CH ₂ (² A' - C _s)	520.21	29.17	0.65	-0.77	-0.52	490.39
SiH ₂ CH ₃ (² A' - C _s)	531.00	31.89	0.77	-0.71	-0.52	498.65
SiH ₂ FCH ₃ (¹ A' - C _s)	689.64	35.14	1.37	-1.18	-0.91	653.77
SiH ₂ ClCH ₃ (¹ A' - C _s)	646.75	34.38	0.99	-1.03	-1.36	610.97
SiH ₂ BrCH ₃ (¹ A' - C _s)	631.78	34.17	1.44	-0.91	-4.02	594.12
SiH ₂ ICH ₃ (¹ A' - C _s)	611.70	33.90	2.06	-0.79	-7.76	571.30
SiH ₃ CH ₂ F (¹ A' - C _s)	627.51	33.82	1.28	-1.05	-0.91	593.01
SiH ₃ CH ₂ Cl (¹ A' - C _s)	603.60	33.03	0.93	-1.01	-1.36	569.13
SiH ₃ CH ₂ Br (¹ A' - C _s)	592.57	32.70	1.24	-0.83	-4.02	556.26
SiH ₃ CH ₂ I (¹ A' - C _s)	582.43	32.38	1.71	-0.78	-7.76	543.22

^a The atomic asymptotes were calculated with the R/UCCSD(T) method. ^b Extrapolated by using eq. (1) with the aVDZ-PP, aVTZ-PP, and aVQZ-PP basis sets. ^c The zero point energies were taken as 0.5 the sum of the CCSD(T) harmonic frequencies. ^d Core-valence corrections were obtained with the cc-pwCVTZ (for C, F, Si, and Cl) and cc-pwCVTZ-PP (for Br and I) basis sets

at the optimized CCSD(T)/aVTZ-PP geometries.^e The scalar relativistic correction is based on a CISD(FC)/VTZ MVD calculation and is expressed relative to the CISD result without the MVD correction, i.e. including the existing relativistic effects resulting from the use of a relativistic effective core potential.^f Correction due to the incorrect treatment of the atomic asymptotes as an average of spin multiplets. Values are based on C. Moore's Tables, reference 18.^g The theoretical value of $\Delta D_0(0\text{ K})$ was computed with the CBS estimates.

Table 9.2. Calculated Heats of Formation (kcal/mol).

Molecule	Theory (0 K)	Theory (298 K)	Expt/Other Calc (298 K)
CH ₃ (<i>C_s</i>)	35.8	35.0	34.8 ^a
CH ₂ F (<i>C_s</i>)	-6.3	-6.9	-7.6 ± 2 ^b , (-6.8 ± 1.3) ^d
CH ₂ Cl (<i>C_s</i>)	28.1	27.4	28.0 ± 0.7 ^b , 29.4 ± 0.8
CH ₂ Br (<i>C_s</i>)	43.3	40.8	40.4 ± 2 ^b
CH ₂ I (<i>C_s</i>)	54.7	53.8	
SiH ₃ (<i>C_{3v}</i>)	48.1	46.8	(47.7 ± 1.2) ^c
SiH ₂ F (<i>C_s</i>)	-42.4	-43.7	
SiH ₂ Cl (<i>C_s</i>)	7.6	6.4	
SiH ₂ Br (<i>C_s</i>)	23.3	20.4	
SiH ₂ I (<i>C_s</i>)	37.9	36.3	
SiH ₃ F (<i>C_{3v}</i>)	-83.8	-88.8	-90 ± 5 ^a
SiH ₃ Cl (<i>C_{3v}</i>)	-31.6	-33.8	-33.9 ± 2 ^a
SiH ₃ Br (<i>C_{3v}</i>)	-15.3	-19.2	-19 ± 4 ^a
SiH ₃ I (<i>C_{3v}</i>)	0.7	-1.8	-0.5 ± 4 ^a
SiH ₃ CH ₃ (<i>C_{3v}</i>)	-3.0	-6.9	
SiH ₃ CH ₂ (<i>C_s</i>)	45.1	42.5	
SiH ₂ CH ₃ (<i>C_s</i>)	36.9	34.0	
SiH ₂ FCH ₃ (<i>C_s</i>)	-99.8	-103.4	
SiH ₂ ClCH ₃ (<i>C_s</i>)	-46.9	-50.3	
SiH ₂ BrCH ₃ (<i>C_s</i>)	-30.4	-35.6	
SiH ₂ ICH ₃ (<i>C_s</i>)	-10.2	-14.0	
SiH ₃ CH ₂ F (<i>C_s</i>)	-39.0	-42.6	
SiH ₃ CH ₂ Cl (<i>C_s</i>)	-5.0	-8.5	
SiH ₃ CH ₂ Br (<i>C_s</i>)	7.4	2.1	
SiH ₃ CH ₂ I (<i>C_s</i>)	17.9	14.0	

^a Reference 1. ^b Reference 2. ^c Experimental heat of formation given is at 0 K. Reference 33. ^d

Reference 34.

Table 9.3 Calculated Bond Dissociation Energies (BDEs) at 0 K (kcal/mol).

BDE	Theory	Expt.
$\text{SiH}_4 \rightarrow \text{SiH}_3 + \text{H}$	90.2	90.3 ± 1.2 , ^a 91.8 ± 0.5 , ^b 91.7 ± 0.5 , ^c 91.5 ± 2 , ^d 91.8 ± 0.5 ^e
$\text{SiH}_3\text{F} \rightarrow \text{SiH}_2\text{F} + \text{H}$	93.1	
$\text{SiH}_3\text{Cl} \rightarrow \text{SiH}_2\text{Cl} + \text{H}$	90.9	
$\text{SiH}_3\text{Br} \rightarrow \text{SiH}_2\text{Br} + \text{H}$	90.3	
$\text{SiH}_3\text{I} \rightarrow \text{SiH}_2\text{I} + \text{H}$	88.8	
$\text{SiH}_3\text{F} \rightarrow \text{SiH}_3 + \text{F}$	150.5	152.5 ± 1.2 ^e
$\text{SiH}_3\text{Cl} \rightarrow \text{SiH}_3 + \text{Cl}$	108.3	109.5 ± 1.7 ^e
$\text{SiH}_3\text{Br} \rightarrow \text{SiH}_3 + \text{Br}$	91.6	89.9 ± 2.2 ^e
$\text{SiH}_3\text{I} \rightarrow \text{SiH}_3 + \text{I}$	73.0	71.5 ± 2.0 ^e
$\text{CH}_3\text{SiH}_3 \rightarrow \text{CH}_3\text{SiH}_2 + \text{H}$	91.5	89.6 ± 2 , ^f 92.3 ± 3 , ^d 92.7 ± 1.2 ^e
$\text{CH}_3\text{SiH}_2\text{F} \rightarrow \text{CH}_3\text{SiH}_2 + \text{F}$	155.1	
$\text{CH}_3\text{SiH}_2\text{Cl} \rightarrow \text{CH}_3\text{SiH}_2 + \text{Cl}$	112.3	
$\text{CH}_3\text{SiH}_2\text{Br} \rightarrow \text{CH}_3\text{SiH}_2 + \text{Br}$	95.5	
$\text{CH}_3\text{SiH}_2\text{I} \rightarrow \text{CH}_3\text{SiH}_2 + \text{I}$	72.7	
$\text{CH}_3\text{SiH}_3 \rightarrow \text{SiH}_3 + \text{CH}_3$	86.9	89.6 ± 1.2 ^e
$\text{CH}_3\text{SiH}_2\text{F} \rightarrow \text{SiH}_2\text{F} + \text{CH}_3$	93.0	
$\text{CH}_3\text{SiH}_2\text{Cl} \rightarrow \text{SiH}_2\text{Cl} + \text{CH}_3$	90.2	
$\text{CH}_3\text{SiH}_2\text{Br} \rightarrow \text{SiH}_2\text{Br} + \text{CH}_3$	89.5	
$\text{CH}_3\text{SiH}_2\text{I} \rightarrow \text{SiH}_2\text{I} + \text{CH}_3$	83.7	
$\text{CH}_3\text{SiH}_3 \rightarrow \text{SiH}_3\text{CH}_2 + \text{H}$	99.8	
$\text{SiH}_3\text{CH}_2\text{F} \rightarrow \text{SiH}_3\text{CH}_2 + \text{F}$	102.6	
$\text{SiH}_3\text{CH}_2\text{Cl} \rightarrow \text{SiH}_3\text{CH}_2 + \text{Cl}$	78.7	
$\text{SiH}_3\text{CH}_2\text{Br} \rightarrow \text{SiH}_3\text{CH}_2 + \text{Br}$	65.9	
$\text{SiH}_3\text{CH}_2\text{I} \rightarrow \text{SiH}_3\text{CH}_2 + \text{I}$	52.8	
$\text{SiH}_3\text{CH}_2\text{F} \rightarrow \text{CH}_2\text{F} + \text{SiH}_3$	80.9	
$\text{SiH}_3\text{CH}_2\text{Cl} \rightarrow \text{CH}_2\text{Cl} + \text{SiH}_3$	81.2	
$\text{SiH}_3\text{CH}_2\text{Br} \rightarrow \text{CH}_2\text{Br} + \text{SiH}_3$	83.9	
$\text{SiH}_3\text{CH}_2\text{I} \rightarrow \text{CH}_2\text{I} + \text{SiH}_3$	84.9	

^a Reference 33. ^b Reference 39. ^c Reference 40. ^d Reference 41. ^e Reference 42. ^f Reference 43.

Table 9.4. Calculated Si-X and Si-C Stretching Frequencies at the CCSD(T)/aVTZ-PP level (cm⁻¹).

Molecule	Frequency
H ₃ Si-F	870.9
H ₃ Si-Cl	546.6
H ₃ Si-Br	427.2
H ₃ Si-I	361.6
H ₃ CSiH ₂ -F	861.2
H ₃ CSiH ₂ -Cl	524.3
H ₃ CSiH ₂ -Br	412.6
H ₃ CSiH ₂ -I	356.3
H ₃ Si-CH ₃	703.7
H ₃ Si-CH ₂ F	770.7
H ₃ Si-CH ₂ Cl	758.1
H ₃ Si-CH ₂ Br	752.1
H ₃ Si-CH ₂ I	738.0

Figure Captions

Figure 9.1. Plot of the calculated adiabatic BDE (kcal/mol) at 0 K as a function of the electronegativity of the halogen substituent.

Figure 9.2. Plot of the calculated adiabatic BDE (kcal/mol) at 0 K as a function of the covalent radii (Å) of the halogen substituent.

Figure 9.3. Plot of the magnitude of the energy difference between the calculated $\Delta H_f(\text{CH}_3\text{SiH}_2\text{X})$ and $\Delta H_f(\text{SiH}_3\text{CH}_2\text{X})$ of the different isomers in kcal/mol at 0 K as a function of the electronegativity of the halogen substituent.

Figure 9.1.

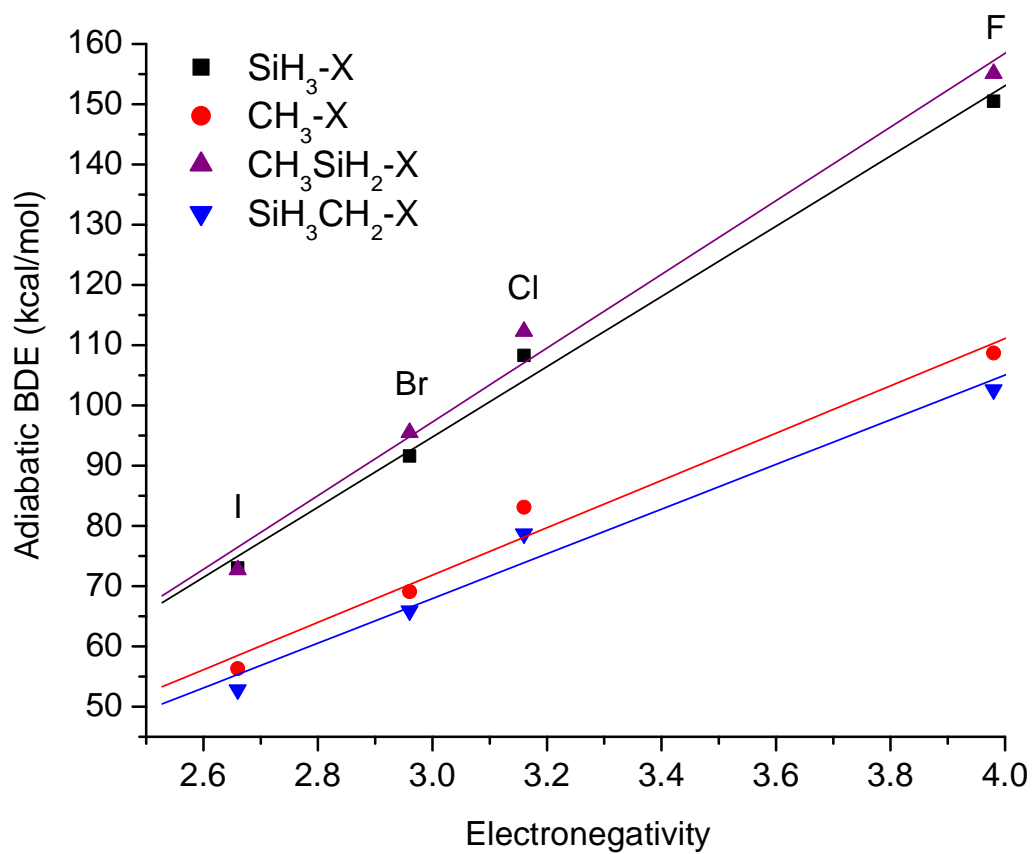


Figure 9.2.

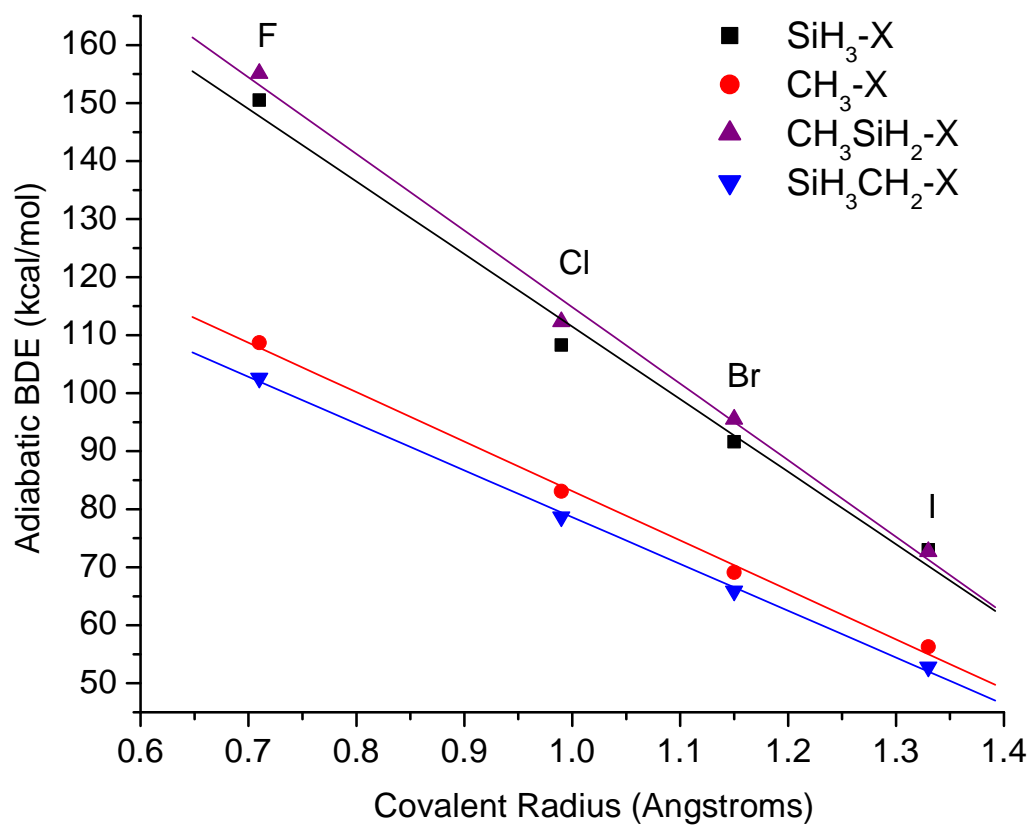
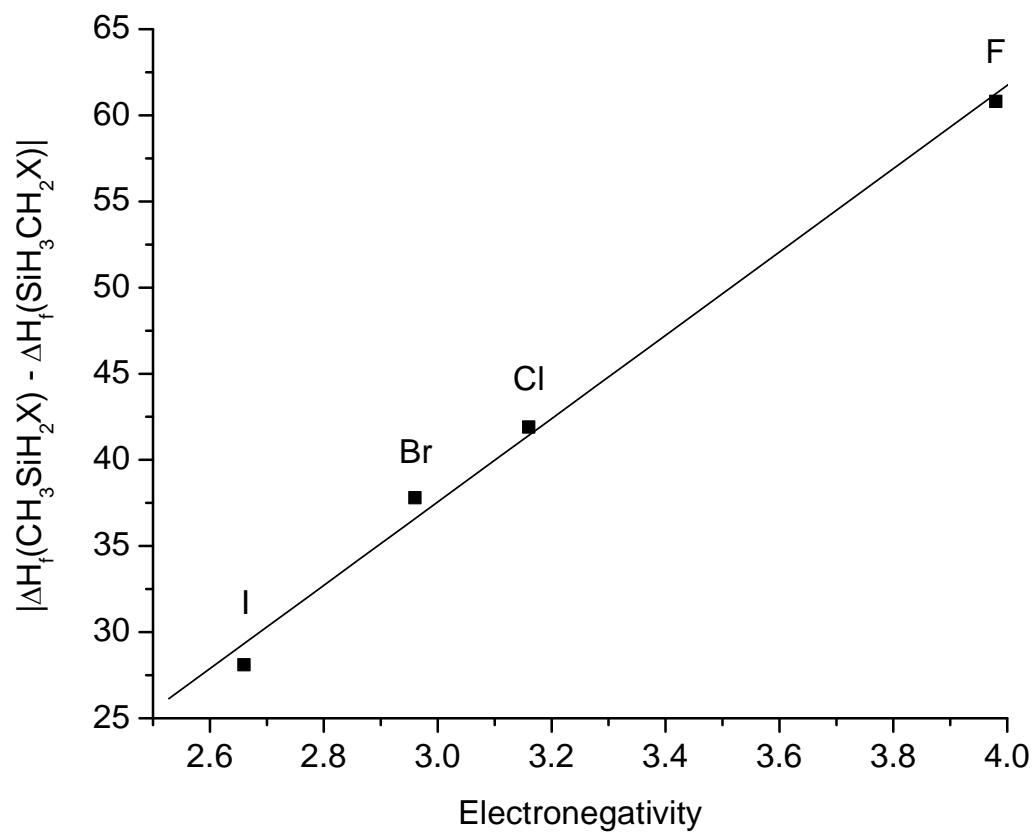


Figure 9.3.



9.5 References

¹ Chase, M. W., Jr. *NIST-JANAF Thermochemical Tables, Fourth Edition, J. Phys. Chem. Ref. Data, Monograph 9, 1998*, 1-1951.

² Sander, S. P.; Friedl, R. R.; Ravishankara, A. R.; Golden, D. M.; Kolb, C. E.; Kurylo, M. J.; Molina, M. J.; Moortgat, G. K.; Finlayson-Pitts, B. J. Wine, P.H.; Huie, R. E.; Orkin, V. L. *Chemical Kinetics and Photochemical Data for Use in Atmospheric Studies: Evaluation Number 15*; JPL Publication 06-2, National Aeronautics and Space Administration, Jet Propulsion Laboratory, California Institute of Technology: Pasadena, CA 2006. http://jpldataeval.jpl.nasa.gov/pdf/JPL_15_AllInOne.pdf

³ Luo, T.-R. *Comprehensive Handbook of Chemical Bond Energies*; CRC Press, Taylor & Francis Group: Boca Raton, FL, 2007.

⁴ Dunning, T.H., Jr. *J. Phys. Chem.* **2000**, *104*, 9062.

⁵ (a) Peterson, K. A.; Xantheas, S. S.; Dixon, D. A.; Dunning, T. H. Jr., *J. Phys. Chem. A* **1998**, *102*, 2449; (b) Feller, D.; Peterson, K. A. *J. Chem. Phys.* **1998**, *108*, 154; (c) Dixon, D. A.; Feller, D. *J. Phys. Chem. A* **1998**, *102*, 8209; (d) Feller, D.; Peterson, K. A. *J. Chem. Phys.* **1999**, *110*, 8384; (e) Feller, D.; Dixon, D. A. *J. Phys. Chem. A* **1999**, *103*, 6413; (f) Feller, D. *J. Chem. Phys.* **1999**, *111*, 4373; (g) Feller, D.; Dixon, D. A. *J. Phys. Chem. A* **2000**, *104*, 3048; (h) Feller, D.; Sordo, J. A. *J. Chem. Phys.* **2000**, *113*, 485; (i) Feller, D.; Dixon, D. A. *J. Chem. Phys.* **2001**, *115*, 3484; (j) Dixon, D. A.; Feller, D.; Sandrone, G. *J. Phys. Chem. A* **1999**, *103*, 4744; (k) Ruscic, B.; Wagner, A. F.; Harding, L. B.; Asher, R. L.; Feller, D.; Dixon, D. A.; Peterson, K. A.; Song, Y.; Qian, X.; Ng, C.; Liu, J.; Chen, W.; Schwenke, D. W. *J. Phys. Chem. A* **2002**, *106*, 2727; (l) Feller, D.; Dixon, D. A.; Peterson, K. A. *J. Phys. Chem. A*, **1998**, *102*, 7053; (m) Dixon, D. A.; Feller, D.; Peterson, K. A. *J. Chem. Phys.*, **2001**, *115*, 2576.

⁶ Purvis III, G. D.; Bartlett, R. J. *J. Chem. Phys.* **1982**, *76*, 1910.

⁷ Raghavachari, K.; Trucks, G. W.; Pople, J. A.; Head-Gordon, M. *Chem. Phys. Lett.* **1989**, *157*, 479.

⁸ Watts, J. D.; Gauss, J.; Bartlett, R. J. *J. Chem. Phys.* **1993**, *98*, 8718.

⁹ (a) Dunning, T. H., Jr. *J. Chem. Phys.* **1989**, *90*, 1007; (b) Kendall, R. A.; Dunning, T. H., Jr.; Harrison, R. J. *J. Chem. Phys.* **1992**, *96*, 6796; (c) Woon, D.E.; Dunning, T. H., Jr., *J. Chem. Phys.* **1993**, *98*, 1358; (d) Dunning, T. H., Jr.; Peterson, K. A.; Wilson, A. K. *J. Chem. Phys.* **2001**, *114*, 9244; (e) Wilson, A. K.; Woon, D.E.; Peterson, K. A.; Dunning, T. H., Jr., *J. Chem. Phys.* **1999**, *110*, 7667.

¹⁰ McQuarrie, D. A. *Statistical Mechanics*, University Science Books: Sausalito, CA, 2001.

¹¹ Curtiss, L. A.; Raghavachari, K.; Redfern, P. C.; Pople, J. A. *J. Chem. Phys.* **1997**, *106*, 1063.

-
- ¹² (a) Peterson, K. A. *J. Chem. Phys.* **2003**, *119*, 11099; (b) Peterson, K. A.; Figgen, D.; Goll, E.; Stoll, H.; Dolg, M. *J. Chem. Phys.* **2003**, *119*, 11113.
- ¹³ Peterson, K. A.; Figgen, D.; Dolg, M.; Stoll, H. *J. Chem. Phys.* **2007**, *126*, 124101
- ¹⁴ MOLPRO a package of *ab initio* programs designed by Werner, H.-J.; and Knowles, P. J. version 2002.6, Universität Stuttgart, Stuttgart, Germany, University of Birmingham, Birmingham, United Kingdom, Amos, R. D.; Bernhardsson, A.; Berning, A.; Celani, P.; Cooper, D. L.; Deegan, M. J. O.; Dobbyn, A. J.; Eckert, F.; Hampel, C.; Hetzer, G.; Knowles, P. J.; Korona, T.; Lindh, R.; Lloyd, A. W.; McNicholas, S. J.; Manby, F. R.; Meyer, W.; Mura, M. E.; Nicklass, A.; Palmieri, P.; Pitzer, R.; Rauhut, G.; Schütz, M.; Schumann, U.; Stoll, H.; Stone, A. J.; Tarroni, R.; Thorsteinsson, T.; Werner, H.-J.
- ¹⁵ Peterson, K. A.; Woon, D. E.; Dunning, T. H., Jr. *J. Chem. Phys.* **1994**, *100*, 7410.
- ¹⁶ Peterson, K. A.; Dunning, T. H., Jr., *J. Chem. Phys.* **2002**, *117*, 10548.
- ¹⁷ The initial cc-pwCVTZ-PP basis sets used in this work are available on request from Prof. K. Peterson at Washington State University. See. <http://tyr0.chem.wsu.edu/~kipeters/>
- ¹⁸ Moore, C. E. "Atomic energy levels as derived from the analysis of optical spectra, Volume I, H to V," U.S. National Bureau of Standards Circular 467, U.S. Department of Commerce, National Technical Information Service, COM-72-50282, Washington, D.C.; **1949**.
- ¹⁹ Shimanouchi, T. *Tables of Molecular Vibrational Frequencies Consolidated Volume I, National Bureau of Standards*, **1972**, 1-160.
- ²⁰ Cox, D. J. D.; Wagman, D.; Medvedev, V. A. *CODATA Key Values for Thermodynamics*. Hemisphere, New York, 1989.
- ²¹ Karton, A.; Martin, J. M. L. *J. Phys. Chem. A* **2007**, *111*, 5936.
- ²² Kuchitsu, K. Ed. *Structure of Free Polyatomic Molecules - Basic Data*; Springer: Berlin, 1998.
- ²³ Harmony, M. D.; Laurie, V. W.; Kuczkowski, R. L.; Schwendeman, R. H.; Ramsey, D. A.; Lovas, F. J.; Lafferty, W. J.; Maki, A. G. *J. Phys. Chem. Ref. Data* **1979**, *8*, 619.
- ²⁴ Yamada, C.; Hirota, E.; *Phys. Rev. Lett.* **1986**, *56*, 923.
- ²⁵ Sumiyoshi, Y.; Tanaka, K.; Tanaka, T.; *Appl. Surf. Sci.* **1994**, *79/80*, 471.
- ²⁶ Andrews, L.; Wang, X.; *J. Phys. Chem. A* **2002**, *106*, 7696.
- ²⁷ Shimanouchi, T. *Tables of Molecular Vibrational Frequencies Consolidated Volume II, J. Phys. Chem. Ref. Data*, **1972**, *6*, 3, 993-1102.

-
- ²⁸ Whitney, E. S.; Dong, F.; Nesbitt, D. J. *J. Chem. Phys.* **2006**, *125*, 054304.
- ²⁹ Jacox, M. E. *Vibrational and Electronic Energy Levels of Polyatomic Transient Molecules, Monograph No. 3*, I. PH.s Chem. Ref. Data, **1994**.
- ³⁰ Whitney, E. S.; Haeber, T.; Schuder, M. D.; Blair, A. C.; Nesbitt, D. J., *J. Chem. Phys.* **2006**, *125*, 054303.
- ³¹ Fridgen, T. D.; Zhang, X. K.; Parnis, J. M.; March, R. E. *J. Phys. Chem. A* **2000**, *104*, 3487.
- ³² Lee, T. J.; Taylor, P. R. *Int. J. Quantum Chem. Symp.* **1989**, *23*, 199.
- ³³ Doncaster, A. M.; Walsch, R. *Int. J. Chem. Kinet.* **1981**, *13*, 1503.
- ³⁴ Kumaran, S. S.; Su, M. -C.; Lim, K. P.; Michael, J. V.; Wagner, A. F.; Harding, L. B.; Dixon, D. A. *J. Phys. Chem.* **1996**, *100*, 7541.
- ³⁵ Grant, D. J.; Matus, M. H.; Switzer, J. S.; Dixon, D. A.; Francisco, J. S.; Christe, K. O. *J. Phys. Chem. A.*, **2008**, *112*, 3145.
- ³⁶ Grant, D. J.; Dixon, D. A. *J. Phys. Chem. A* **2006**, *110*, 12955.
- ³⁷ Feller, D.; Peterson, K. A.; de Jong, W. A.; Dixon, D. A. *J. Chem. Phys.* **2003**, *118*, 3510.
- ³⁸ Lide, R. D. *Reference Handbook of Chemistry and Physics* 86th Edition, Taylor and Francis Group, Boca Rotan, FL, 2005.
- ³⁹ Seetula, J. A.; Feng, Y.; Gutman, D.; Seakins, P. W.; Pilling, M. J. *J. Phys. Chem.* **1991**, *95*, 1658.
- ⁴⁰ Berkowitz, J.; Ellison, G. B.; Gutman, D. *J. Phys. Chem.* **1994**, *98*, 2744.
- ⁴¹ Chatgililoglu, C. *Chem. Rev.* **1995**, *95*, 1229.
- ⁴² Beccerra, R.; Walsh, R. *The Chemistry of Organic Silicon Compounds* Vol. 2, Eds. Wiley, New York, 1998, Chap. 4, pp. 153.
- ⁴³ Walsh, R. *The Chemistry of Organosilicon Compounds, Part 1*, Eds., Wiley, New York, 1989, Chap. 5, pp. 371.

9.6 Appendix

Table A9.1. CCSD(T) Total Energies (E_h) as a Function of the Basis Set.^{a,b}

Molecule	Basis Set	Energy
CH ₃ (D_{3h})	aVDZ-PP	-39.724697
	aVTZ-PP	-39.763644
	aVQZ-PP	-39.773323
	CBS (DTQ)	-39.778515
CH ₂ F (C_s)	aVDZ-PP	-138.779999
	aVTZ-PP	-138.899479
	aVQZ-PP	-138.935673
	CBS (DTQ)	-138.956001
CH ₂ Cl (C_s)	aVDZ-PP	-498.808014
	aVTZ-PP	-498.908450
	aVQZ-PP	-498.937967
	CBS (DTQ)	-498.954441
CH ₂ Br (C_s)	aVDZ-PP	-454.761242
	aVTZ-PP	-454.863288
	aVQZ-PP	-454.889740
	CBS (DTQ)	-454.904084
CH ₂ I (C_s)	aVDZ-PP	-333.904961
	aVTZ-PP	-333.993118
	aVQZ-PP	-334.019523
	CBS (DTQ)	-334.034270
SiH ₃ (C_{3v})	aVDZ-PP	-290.760091
	aVTZ-PP	-290.790882
	aVQZ-PP	-290.799713
	CBS (DTQ)	-290.804615
SiH ₂ F (C_s)	aVDZ-PP	-389.887123
	aVTZ-PP	-390.00287
	aVQZ-PP	-390.039761
	CBS (DTQ)	-390.060695
SiH ₂ Cl (C_s)	aVDZ-PP	-749.893452
	aVTZ-PP	-749.98842
	aVQZ-PP	-750.018300

	CBS (DTQ)	-750.035212
SiH ₂ Br (C _s)	aVDZ-PP	-705.845636
	aVTZ-PP	-705.941863
	aVQZ-PP	-705.968604
	CBS (DTQ)	-705.983346
SiH ₂ I (C _s)	aVDZ-PP	-584.983970
	aVTZ-PP	-585.066588
	aVQZ-PP	-585.093610
	CBS (DTQ)	-585.109017
SiH ₃ F (C _{3v})	aVDZ-PP	-390.537764
	aVTZ-PP	-390.659124
	aVQZ-PP	-390.697395
	CBS (DTQ)	-390.719063
SiH ₃ Cl (C _{3v})	aVDZ-PP	-750.540352
	aVTZ-PP	-750.640678
	aVQZ-PP	-750.672060
	CBS (DTQ)	-750.689800
SiH ₃ Br (C _{3v})	aVDZ-PP	-706.491061
	aVTZ-PP	-706.592600
	aVQZ-PP	-706.621122
	CBS (DTQ)	-706.636884
SiH ₃ I (C _{3v})	aVDZ-PP	-585.62767
	aVTZ-PP	-585.715309
	aVQZ-PP	-585.743799
	CBS (DTQ)	-585.760023
SiH ₃ CH ₃ (C _{3v})	aVDZ-PP	-330.62339
	aVTZ-PP	-330.700175
	aVQZ-PP	-330.720343
	CBS (DTQ)	-330.731315
SiH ₃ CH ₂ (C _s)	aVDZ-PP	-329.958057
	aVTZ-PP	-330.028637
	aVQZ-PP	-330.048018
	CBS (DTQ)	-330.058674
SiH ₂ CH ₃ (C _s)	aVDZ-PP	-329.975438
	aVTZ-PP	-330.046977
	aVQZ-PP	-330.065701

	CBS (DTQ)	-330.075878
SiH ₂ FCH ₃ (<i>C_s</i>)	aVDZ-PP	-429.759022
	aVTZ-PP	-429.920904
	aVQZ-PP	-429.968932
	CBS (DTQ)	-429.995791
SiH ₂ ClCH ₃ (<i>C_s</i>)	aVDZ-PP	-789.761692
	aVTZ-PP	-789.90222
	aVQZ-PP	-789.943359
	CBS (DTQ)	-789.966298
SiH ₂ BrCH ₃ (<i>C_s</i>)	aVDZ-PP	-745.712369
	aVTZ-PP	-745.854042
	aVQZ-PP	-745.892330
	CBS (DTQ)	-745.913302
SiH ₂ I CH ₃ (<i>C_s</i>)	aVDZ-PP	-624.848982
	aVTZ-PP	-624.976512
	aVQZ-PP	-625.010764
	CBS (DTQ)	-625.029497
SiH ₃ CH ₂ F (<i>C_s</i>)	aVDZ-PP	-429.66965
	aVTZ-PP	-429.82459
	aVQZ-PP	-429.870868
	CBS (DTQ)	-429.896783
SiH ₃ CH ₂ Cl (<i>C_s</i>)	aVDZ-PP	-789.699240
	aVTZ-PP	-789.835975
	aVQZ-PP	-789.875529
	CBS (DTQ)	-789.897530
SiH ₃ CH ₂ Br (<i>C_s</i>)	aVDZ-PP	-745.65585
	aVTZ-PP	-745.79425
	aVQZ-PP	-745.83086
	CBS (DTQ)	-745.850812
SiH ₃ CH ₂ I (<i>C_s</i>)	aVDZ-PP	-624.801619
	aVTZ-PP	-624.925931
	aVQZ-PP	-624.962468
	CBS (DTQ)	-624.982860

^a Dissociation is with respect to RCCSD(T) atoms for closed shell atoms and R/UCCSD(T) for open shell atoms. Symmetry equivalencing of the p_x, p_y, and p_z orbitals was not imposed in the

atomic calculations. The Br and I RECP have a 10 and 28 electron core respectively, leaving 25 electrons to be explicitly treated.

^b CBS (DTQ) values from Eq. 1 (see text) obtained with the $aVnZ$ -PP basis sets with $n = D, T, Q$.

Table A9.2. Calculated CCSD(T) Geometry Parameters for CH₂X, SiH₃, SiH₂X, SiH₃CH₂, and SiH₂CH₃ compounds where (X = F, Cl, Br, and I). Bond Distances in Å and Bond Angles in Degrees.

Molecule	Basis Set	R _{C-H}	R _{Si-H}	R _{C-X}	R _{Si-X}	∠XCH	∠XSiH	∠HCXH	∠HSiXH
CH ₂ F (² A' - C _s) ^a	aVDZ-PP	1.0942		1.3648		114.0	124.3	151.1	
	aVTZ-PP	1.0805		1.3427		114.5	124.1	152.3	
	expt. ^b	1.09(±1)		1.3337(49)			126.3(21)		
CH ₂ Cl (² A' - C _s)	aVDZ-PP	1.0908		1.7147		117.5	123.9	172.3	
	aVTZ-PP	1.0772		1.6995		117.7	124.2	172.6	
	expt. ^b	1.09(±1)		1.6917(4)			122.6(20)		
CH ₂ Br (² A' - C _s)	aVDZ-PP	1.0913		1.8738		117.3	-	167.6	
	aVTZ-PP	1.0775		1.8561		117.4	-	168.6	
CH ₂ I (² A' - C _s)	aVDZ-PP	1.0920		2.0749		118.1	-	172.0	
	aVTZ-PP	1.0783		2.0535		118.4	-	174.3	
SiH ₃ (² A ₁ - C _{3v})	aVDZ-PP		1.4891				111.1		120.0
	aVTZ-PP		1.4814				111.2		120.0
SiH ₂ F (² A' - C _s)	aVDZ-PP		1.4902		1.6431		107.7		120.7
	aVTZ-PP		1.4833		1.6079		108.7		120.8
SiH ₂ Cl (² A' - C _s)	aVDZ-PP		1.4889		2.0918		108.4		121.0
	aVTZ-PP		1.4813		2.0653		108.7		121.1
SiH ₂ Br (² A' - C _s)	aVDZ-PP		1.4892		2.2502		108.6		120.9

	aVTZ-PP		1.4820		2.2270		108.9		121.2
SiH ₂ I (² A' - C _s)	aVDZ-PP		1.4903		2.4751		108.9		120.8
	aVTZ-PP		1.4828		2.4508		109.2		121.0
SiH ₃ CH ₂ (² A' - C _s)	aVDZ-PP	1.0990	1.4931		1.8662		111.3		119.6
			1.4890				110.0		
	aVTZ-PP	1.0853	1.4862		1.8525		111.3		119.7
			1.4823				110.1		
SiH ₂ CH ₃ (² A' - C _s)	aVDZ-PP	1.1078	1.4938	1.9005		110.7		119.9	
			1.1055			110.9			
	aVTZ-PP	1.0948	1.4863	1.8860		110.5		119.9	
			1.0924			110.7			

^a For CH₂F, ∠XSiH = ∠HCH. ^b Reference 21.

Table A9.3. Calculated CCSD(T) Geometry Parameters for SiH₃X where (X = F, Cl, Br, and I). Bond Distances in Å and Bond Angles in Degrees.

Molecule	Basis Set	R _{Si-H}	R _{Si-X}	∠XSiH	∠HSiXH
SiH ₃ F (¹ A ₁ - C _{3v})	aVDZ-PP	1.4816	1.6374	108.0	120.0
	aVTZ-PP	1.4754	1.6003	108.0	120.0
	expt. ^a	1.485 ± 0.005	1.593 ± 0.005	108.4 ± 1.0	120.0
	expt. ^b	1.47608(19)	1.59450(13)	108.269(21)	120.0
SiH ₃ Cl (¹ A ₁ - C _{3v})	aVDZ-PP	1.4813	2.0890	108.2	120.0
	aVTZ-PP	1.4746	2.0653	108.4	120.0
	expt. ^a	1.485 ± 0.01	2.049 ± 0.002	108.7 ± 0.5	120.0
	expt. ^b	1.47496(11)	2.05057(6)	108.295(12)	120.0
SiH ₃ Br (¹ A ₁ - C _{3v})	aVDZ-PP	1.4814	2.2504	108.2	120.0
	aVTZ-PP	1.4750	2.2291	108.4	120.0
	expt. ^a	1.481 ± 0.005	2.210 ± 0.005	107.9 ± 0.5	120.0
	expt. ^b	1.47425(18)	2.21227(9)	108.161(20)	120.0
SiH ₃ I (¹ A ₁ - C _{3v})	aVDZ-PP	1.4823	2.4810	108.2	120.0
	aVTZ-PP	1.4754	2.4584	108.4	120.0
	expt. ^a	1.487 ± 0.005	2.437 ± 0.002	108.4 ± 0.5	120.0
	expt. ^b	1.4741(14)	2.43835(59)	108.16(17)	120.0

^a Reference 22. ^b Reference 21.

Table A9.4. Calculated CCSD(T) Geometry Parameters for SiH₃CH₃ and SiH₂XCH₃ where (X = F, Cl, Br, and I). Bond Distances in Å and Bond Angles in Degrees.

Molecule	Basis Set	R _{C-H}	R _{Si-H}	R _{Si-C}	R _{Si-X}	∠HSiC	∠HCSi	∠XSiC
SiH ₃ CH ₃ (¹ A ₁ - C _{3v}) ^a	aVDZ-PP	1.1061	1.4904	1.8931		108.4	107.9	
						110.5	110.8	
	aVTZ-PP	1.0929	1.4835	1.8797		108.3	108.1	
						110.6	110.8	
	expt. ^b	1.093 ± 0.005	1.485 ± 0.005	1.869 ± 0.002		108.2 ± 1.0	107.7 ± 1.0	
	expt. ^c	1.0957(5)	1.4832(4)	1.8686(4)		-	-	
						110.50(3)	110.88(3)	
SiH ₂ FCH ₃ (¹ A' - C _s)	aVDZ-PP	1.1072	1.4847	1.8720	1.6415	111.8	110.4	108.7
		1.1057					111.0	
	aVTZ-PP	1.0943	1.4789	1.8610	1.6074	111.5	110.2	109.1
		1.0928					110.9	
	expt. ^b	1.099 ± 0.005	1.477 ± 0.005	1.849 ± 0.005	1.597 ± 0.005	112.5 ± 2.0	-	108.9 ± 0.5
	expt. ^c	1.105(5)	1.478(2)	1.847(5)	1.597(9)	112.3(3)	108.7(7)	109.2(7)
		1.089(1)					111.3(4)	
SiH ₂ ClCH ₃ (¹ A' - C _s)	aVDZ-PP	1.1072	1.4840	1.8761	2.0950	111.6	110.3	109.3
		1.1055					110.8	
	aVTZ-PP	1.0942	1.4778	1.8650	2.0728	111.6	110.1	109.3
		1.0927					110.6	

	expt. ^c	1.060(10)			2.051(10)		113.0(4)	
		1.088(4)					110.0(6)	
	expt. ^c	1.0666(107)	1.4766(21)	1.8541(35)	2.0547(27)	111.17(26)	111.96(119)	108.97(10)
		1.1047(50)					110.32(25)	
SiH ₂ BrCH ₃	aVDZ-PP	1.1072	1.4843	1.8782	2.2574	111.8	110.3	109.2
(¹ A' - C _s)		1.1054					110.8	
	aVTZ-PP	1.0942	1.4778	1.8661	2.2370	111.7	110.1	109.3
		1.0925					110.5	
SiH ₂ ICH ₃	aVDZ-PP	1.1073	1.4852	1.8809	2.4888	111.9	110.3	109.5
(¹ A' - C _s)		1.1053					110.7	
	aVTZ-PP	1.0943	1.4783	1.8688	2.4669	111.8	110.1	109.4
		1.0923					110.5	
	expt. ^c	1.070(1)	1.474(1)	1.857(3)	2.444(2)	111.50(18)	110.85(17)	109.53(18)
		1.088(2)					110.77(25)	

^a For SiH₃CH₃, the first \angle HSiC given = \angle HSiH and the first given \angle HCSi = \angle HCH. ^b Reference 22. ^c Reference 21.

Table A9.5. Calculated CCSD(T) Geometry Parameters for SiH₃CH₂X where (X = F, Cl, Br, and I). Bond Distances in Å and Bond Angles in Degrees.

Molecule	Basis Set	R _{C-H}	R _{Si-H}	R _{Si-C}	R _{C-X}	∠HSiC	∠HCSi	∠XCSi
SiH ₃ CH ₂ F (¹ A' - C _s)	aVDZ-PP	1.1065	1.4902 1.4859	1.9123	1.4297	112.6	107.9 109.5	108.9
	aVTZ-PP	1.0940	1.4831 1.4795	1.9017	1.4067	111.9	108.0 109.6	109.4
SiH ₃ CH ₂ Cl (¹ A' - C _s)	aVDZ-PP	1.1037	1.4908 1.4856	1.9059	1.8181	112.5	108.5 109.1	109.4
	aVTZ-PP	1.0900	1.4838 1.4788	1.8921	1.8029	112.3	108.8 109.2	109.2
	expt. ^a	1.096(10)	1.477(5)	1.889(10)	1.788(10)	-	109.3(5)	109.3(3)
SiH ₃ CH ₂ Br (¹ A' - C _s)	aVDZ-PP	1.1027	1.4913 1.4854	1.9021	1.9838	113.1	108.6 109.2	109.2
	aVTZ-PP	1.0892	1.4842 1.4789	1.8887	1.9626	112.9	108.9 109.2	109.0
	expt. ^a	1.0896(10)	1.477(10)	1.889(10)	1.950(5)	-	109.3(10)	109.3(5)
SiH ₃ CH ₂ I (¹ A' - C _s)	aVDZ-PP	1.1027	1.4919 1.4857	1.8990	2.1931	113.1	108.8 109.3	109.9
	aVTZ-PP	1.0893	1.4847	1.8860	2.1641	112.9	109.1	109.9

1.4793

109.4

^a Reference 21.

Table A9.6 Calculated CCSD(T)/aVTZ-PP Frequencies (cm⁻¹).^a

Molecule	Symmetry	Calc.	Expt.
CH ₂ F (² A' - C _s)	a'	3144.1 (3081.8)	3044.4 ^b
	a'	1475.3	
	a'	1183.2	1170.4, ^c 1163 ^c
	a'	607.2	300(30), ^c 260(30) ^c
	a''	3297.2 (3231.9)	3183.9 ^b
	a''	1177.9	
CH ₂ Cl (² A' - C _s)	a'	3176.9 (3114.1)	3055.1 ^e
	a'	1419.5	1391 ^{c,e}
	a'	846.2	827, ^{c,e} 829 ^e
	a'	167.5	402, ^{c,e} 395, ^e 389 ^e
	a''	3323.5 (3257.7)	
	a''	996.8	
CH ₂ Br (² A' - C _s)	a'	3173.9 (3111.1)	
	a'	1390.9	1355.7 ^c
	a'	708.4	693.4 ^c
	a'	208.6	368 ^c
	a''	3324.1 (3258.3)	
	a''	928.7	953 ^c
CH ₂ I (² A' - C _s)	a'	3169.6 (3106.8)	3050 ^c
	a'	1365.3	1330, ^c 1331.5 ^c
	a'	626.0	611 ^c
	a'	174.3	375 ^c
	a''	3315.8 (3250.2)	
	a''	847.2	
SiH ₃ (² A ₁ - C _{3v})	a ₁	2211.6 (2189.1)	
	a ₁	768.3	727.9 ^f
	e	2245.4 (2222.6)	2185.2 ^g
	e	937.0	928.6 ^h
SiH ₂ F (² A' - C _s)	a'	2196.8 (2174.5)	
	a'	931.9	

	a'	867.8	
	a'	802.6	
	a''	2232.5 (2209.8)	
	a''	711.0	
SiH ₂ Cl (² A' - C _s)	a'	2205.8 (2183.3)	
	a'	921.8	
	a'	733.6	
	a'	545.0	
	a''	2240.4 (2217.6)	
	a''	648.7	
SiH ₂ Br (² A' - C _s)	a'	2165.1 (2143.1)	
	a'	922.0	
	a'	715.8	
	a'	407.3	
	a''	2201.3 (2178.9)	
	a''	627.6	
SiH ₂ I (² A' - C _s)	a'	2198.4 (2176.0)	
	a'	912.0	
	a'	661.5	
	a'	364.0	
	a''	2232.7 (2210.0)	
	a''	581.9	
SiH ₃ F (¹ A ₁ - C _{3v})	a ₁	2271.0 (2247.9)	2206(15) ⁱ
	a ₁	999.2	990(6) ⁱ
	a ₁	870.9	872(3) ⁱ
	e	2274.2 (2251.1)	2196(6) ⁱ
	e	975.6	956(6) ⁱ
	e	734.6	728(3) ⁱ
SiH ₃ Cl (¹ A ₁ - C _{3v})	a ₁	2266.3 (2243.2)	2201(15) ⁱ
	a ₁	955.6	949(15) ⁱ
	a ₁	546.6	551(6) ⁱ
	e	2275.5 (2252.3)	2195(3) ⁱ

	e	963.3	954(3) ⁱ
	e	663.0	664(3) ⁱ
SiH ₃ Br (¹ A ₁ - C _{3v})	a ₁	2263.5 (2238.7)	2200(15) ⁱ
	a ₁	937.4	930(6) ⁱ
	a ₁	427.2	430(6) ⁱ
	e	2275.7 (2250.0)	2196(6) ⁱ
	e	959.4	950(3) ⁱ
	e	631.9	633(3) ⁱ
SiH ₃ I (¹ A ₁ - C _{3v})	a ₁	2256.5 (2233.6)	
	a ₁	913.7	
	a ₁	361.6	
	e	2270.8 (2247.7)	
	e	953.7	
	e	592.9	
SiH ₃ CH ₃ (¹ A ₁ - C _{3v})	a ₁	3031.8 (2971.7)	2898(30) ^j
	a ₁	2231.4 (2208.7)	2169(6) ^j
	a ₁	1297.0	1260(6) ^j
	a ₁	951.2	940(6) ^j
	a ₁	703.7	700(6) ^j
	a ₂	199.4	187(15) ^j
	e	3115.5 (3053.8)	2982(1) ^j
	e	2229.3 (2206.6)	2166(1) ^j
	e	1473.9	1403(6) ^j
	e	966.8	980(15) ^j
	e	889.3	868(3) ^j
	e	517.2	540(6) ^j
SiH ₂ CH ₃ (² A' - C _s)	a'	3102.6 (3041.2)	
	a'	3023.6 (2963.7)	
	a'	2196.0 (2173.7)	
	a'	1469.8	
	a'	1287.1	
	a'	938.1	

	a'	849.6
	a'	696.4
	a'	569.9
	a''	3120.7 (3058.9)
	a''	2215.82193.3
	a''	1467.0
	a''	891.9
	a''	524.3
	a''	197.0
SiH ₂ FCH ₃ (¹ A' - C _s)	a'	3111.0 (3049.4)
	a'	3029.6 (2969.7)
	a'	2253.9 (2231.0)
	a'	1471.7
	a'	1298.4
	a'	988.0
	a'	961.4
	a'	861.2
	a'	770.7
	a'	687.0
	a'	244.5
	a''	3120.9 (3059.1)
	a''	2252.6 (2229.7)
	a''	1465.9
	a''	890.5
	a''	745.0
	a''	505.7
	a''	172.2
SiH ₂ ClCH ₃ (¹ A' - C _s)	a'	3111.5 (3049.9)
	a'	3028.3 (2968.4)
	a'	2252.2 (2229.3)
	a'	1468.9
	a'	1296.2

	a'	971.3
	a'	918.3
	a'	758.1
	a'	701.5
	a'	524.3
	a'	196.1
	a''	3121.5 (3059.7)
	a''	2255.4 (2232.5)
	a''	1463.6
	a''	891.0
	a''	682.3
	a''	493.3
	a''	160.2
SiH ₂ BrCH ₃ (¹ A' - C _s)	a'	3113.3 (3051.6)
	a'	3029.8 (2969.8)
	a'	2251.1 (2228.2)
	a'	1469.2
	a'	1296.7
	a'	969.4
	a'	909.2
	a'	752.1
	a'	696.3
	a'	412.6
		173.9
	a''	3124.6 (3062.7)
	a''	2256.7 (2233.7)
	a''	1463.5
	a''	894.6
	a''	662.8
	a''	490.6
	a''	180.2
SiH ₂ ICH ₃ (¹ A' - C _s)	a'	3111.9 (3050.3)

	a'	3028.4 (2968.5)
	a'	2233.9 (2211.2)
	a'	1467.1
	a'	1294.7
	a'	912.0
	a'	880.4
	a'	738.0
	a'	691.5
	a'	356.3
	a'	157.5
	a''	3125.8 (3063.9)
	a''	2265.2 (2242.2)
	a''	1463.0
	a''	899.8
	a''	677.6
	a''	492.9
	a''	164.3
SiH ₃ CH ₂ (² A' - C _s)	a'	3126.8 (3064.9)
	a'	2238.6 (2210.9)
	a'	2207.4 (2185.0)
	a'	1411.3
	a'	955.8
	a'	947.7
	a'	834.2
	a'	752.9
	a'	666.9
	a''	3218.7 (3155.0)
	a''	2238.8 (2216.0)
	a''	967.8
	a''	525.1
	a''	511.4
	a''	17.4

SiH ₃ CH ₂ F (¹ A' - C _s)	a'	3037.7 (2977.5)
	a'	2251.8 (2228.9)
	a'	2234.4 (2211.6)
	a'	1479.6
	a'	1327.3
	a'	1033.6
	a'	957.7
	a'	928.7
	a'	745.2
	a'	579.0
	a'	231.2
	a''	3090.7 (3029.5)
	a''	2255.7 (2232.7)
	a''	1245.8
	a''	950.2
	a''	865.6
	SiH ₃ CH ₂ Cl (¹ A' - C _s)	a'
a'		2254.0 (2209.4)
a'		2229.5 (2206.8)
a'		1451.1
a'		1208.4
a'		957.1
a'		933.6
a'		772.8
a'		724.6
a'		557.0
a'		186.5
a''		3135.1 (3073.1)
a''		2259.3 (2236.3)
a''		1134.2

	a''	954.3
	a''	830.5
	a''	506.0
	a''	162.3
SiH ₃ CH ₂ Br (¹ A' - C _s)	a'	3086.3 (3025.2)
	a'	2253.3 (2230.4)
	a'	2226.2 (2203.5)
	a'	1439.2
	a'	1159.8
	a'	954.9
	a'	934.1
	a'	745.1
	a'	687.5
	a'	510.5
	a'	160.2
	a''	3150.1 (3087.7)
	a''	2258.9 (2235.9)
	a''	1081.1
	a''	954.9
	a''	815.1
	a''	504.7
	a''	161.8
SiH ₃ CH ₂ I (¹ A' - C _s)	a'	3086.4 (3025.3)
	a'	2250.4 (2227.5)
	a'	2222.2 (2199.6)
	a'	1427.0
	a'	1105.5
	a'	952.7
	a'	935.2
	a'	739.8
	a'	666.9
	a'	470.2

a'	148.3
a''	3152.1 (3089.7)
a''	2255.7 (2232.8)
a''	1037.4
a''	955.6
a''	793.0
a''	497.9
a''	159.0

^a C-H and Si-H scaled frequencies are given in parentheses. ^b Reference 27. ^c Reference 28. ^d Reference 29. ^e Reference 30. ^f Reference 23. ^g Reference 24. ^h Reference 25. ⁱ Reference 19. ^j Reference 26.

CHAPTER 10

BOND DISSOCIATION ENERGIES IN SECOND ROW COMPOUNDS

From: Grant, D. J.; Matus, M. H.; Switzer, J. R.; Dixon, D. A. *J. Phys. Chem. A* **2008**, *1112*, 3145-3156.

10.1 Introduction

There is substantial interest in the bond dissociation energies in compounds containing second and higher row main group elements with coordination numbers beyond the standard values. These types of compounds have many practical applications and are of substantial interest as model systems.¹ In addition, they are broadly used as examples in basic chemistry courses. In a diatomic molecule, there is only one bond, and the dissociation products are the two atoms. In polyatomic molecules, the situation is more complicated as each bond dissociation energy (BDE) can be quite different as one product is an atom and the other is a molecule, which may have a substantially different electronic structure than the reactant molecule. The BDEs for individual steps in the stepwise dissociation of a polyatomic binary compound can be very different as they depend on the relative stabilities of the starting compound and the products, and can differ significantly from the average bond energy (total atomization energy divided by the number of broken bonds) in the molecule. In addition, there are different ways to define the BDE. The diabatic BDE is dissociation to the configurations most closely representing the bonding configuration in the reactant and the adiabatic BDE is dissociation to the ground state of the separated species. The adiabatic BDE will always be equal to or less than the diabatic BDE.

The adiabatic BDE may not be representative of the bonding near the minimum, and so when comparing different BDEs, it may be more appropriate to compare diabatic BDEs, especially when addressing bond distances, stretching frequencies, and bond force constants, which are representative of the minimum, not the lowest energy dissociation channel. Note that for the diabatic BDE, we require that the spin be conserved whereas in the adiabatic BDE, the process may not occur on the same spin surface. We also constrain the diabatic BDE to correlate with no more than one excited state of the product atoms and molecules. The difference in the adiabatic and diabatic BDEs represents a reorganization or relaxation energy of the product atom or molecule. The difference in diabatic and adiabatic BDEs has been discussed relative to the strength of π -bonds in olefins and main group compounds.^{2,3,4}

Because the separate experimental measurement of each individual step often is either very difficult (often due to the formation of atomic and polyatomic radicals) or cannot be measured under comparable conditions, high-level theoretical calculations of these processes offer a unique opportunity to obtain accurate self-consistent values for these processes.⁵ Modern computational chemistry methods implemented on high-performance computer architectures can now provide reliable predictions of chemical bond energies to within about 1 kcal/mol for most compounds that are not dominated by multireference character. We can use the approach that we have been developing with collaborators at Pacific Northwest Laboratory and Washington State University for the prediction of accurate molecular thermochemistry⁶ to determine BDEs in compounds containing a second row element as the central atom. Our approach is based on calculating the total atomization energy of a molecule and using this value with known heats of formation of the atoms to calculate the heat of formation at 0 K. The approach starts with coupled cluster theory with single and double excitations and including a perturbative triples

correction (CCSD(T)),^{7,8,9} combined with the correlation-consistent basis sets^{10,11} extrapolated to the complete basis set limit to treat the correlation energy of the valence electrons. This is followed by a number of smaller additive corrections including core-valence interactions and relativistic effects, both scalar and spin-orbit. The zero point energy can be obtained from experiment, theory, or a combination of the two. Corrections to 298 K can then be calculated by using standard thermodynamic and statistical mechanics expressions in the rigid rotor-harmonic oscillator approximation¹² and appropriate corrections for the heat of formation of the atoms.¹³

Due to their large range of possible oxidation states, sulfur and phosphorus fluorides and oxofluorides are ideally suited for such an investigation. There have been numerous theoretical and experimental studies of the thermochemistry and BDEs of PF_xO_y and SF_xO_y compounds, but many of them have not been as accurate as one would hope for, and there are not as many reliable main group dissociation energies known as one would like. Many of the results are derived from the heats of formation in the JANAF Tables or the updated values from the NIST web site¹⁴ and have recently been compiled by Luo.¹⁵ The experimental P-F and S-F bond energies for a number of compounds are summarized in Table 10.1. Ahlrichs *et al.*¹⁶ reported mass spectrometric and matrix isolation infrared investigations of PFO and obtained a value of -96.7 kcal/mol for the heat of formation at 298 K. They also reported *ab initio* calculations at the SCF (self consistent field), CISD (single and double configuration interaction), and CPF (coupled pair functional) levels. Beckers *et al.*¹⁷ further studied PFO by millimeter-wave spectroscopy, high-resolution infrared spectroscopy, and high-level *ab initio* calculations at the MP2 (2nd order Møller-Plesset) and CCSD(T) levels with a series of correlation-consistent basis sets including additional diffuse functions and *d*-functions. Gustev¹⁸ has studied the structure and stability of the phosphorus fluorides PF_n and their singly charged anions PF_n^- ($n = 1 - 6$) using

density functional theory (DFT). Tschumper *et al.*¹⁹ studied these systems with a range of density functional methods (four exchange-correlation functionals using DZP and DZP++ basis sets). Gu and Leszczynski²⁰ also studied the $\text{PF}_n/\text{PF}_n^-$ series for ($n = 1 - 6$) with G2 theory and several of its modified versions and predicted bond dissociation energies, as well as the atomization energies, enthalpies of formation, and adiabatic electron affinities.

There have been a number of experiments measuring the thermochemistry of the sulfur fluorides. Bott and Jacobs²¹ performed shock-tube experiments, and used RRK reaction rate theory to determine the first S-F bond dissociation energy in SF_6 to be 75.9 kcal/mol. Thynne and Harland²² studied negative ion formation of sulfur tetrafluoride and estimated the $\text{SF}_3\text{-F}$ BDE to be ≤ 83.9 kcal/mol. Hildebrand²³ reported mass spectrometric studies of gaseous sulfur fluorides measuring the heats of formation of SF, SF_2 , and SF_4 . Coupled with other data, this gives the step-wise BDE of SF_6 . Lyman²⁴ reanalyzed their data for the thermal dissociation of SF_6 using RRKM unimolecular reaction rate theory and found a value of 92 kcal/mol for the S-F BDE. Benson²⁵ reviewed the thermochemistry of sulfur containing molecules and provided estimates for the heats of formation of SF_5 , SF_4O and SF_5O as well as the $\text{SF}_4=\text{O}$ BDE. Kiang *et al.*^{26,27} studied the chemiluminescent reactions of SF_6 and SF_4 with metastable calcium and strontium atoms under single-collision conditions. Their experiments allowed them to determine the $\text{F}_5\text{S-F}$ (91.1 ± 3.2 kcal/mol) and $\text{F}_3\text{S-F}$ (84.1 ± 3.0 kcal/mol) BDEs, and when combined with known heats of formation, they obtained the step-wise BDEs for SF_6 . Babcock *et al.*²⁸ measured the first BDE of SF_6 from ion-molecule reactions and found a value of 94.5 ± 3.0 kcal/mol at 298 K. Tsang and Herron²⁹ reevaluated most of the data for the $\text{F}_5\text{S-F}$ BDE and derived a new value for the BDE of 100.4 ± 2.4 kcal/mol at 298 K. Fisher *et al.*³⁰ used collision-induced dissociation and charge transfer experiments to measure ionization energies of the sulfur fluoride ions and

combined with BDEs were able to derive heats of formation for both ionic and neutral species. Later, Stevens-Miller *et al.*³¹ used negative ion-molecule reactions in a selected ion flow tube and determined a SF₃-F BDE of 86.2 ± 7.8 kcal/mol. Endo *et al.*³² studied the FSO radical by microwave spectroscopy and obtained geometrical parameters and vibrational frequencies. Kronberg *et al.*³³ reported the spectroscopic characterization of the SF₅, SF₅O, and SF₅OO radicals, as well as quantum chemical calculations at the DFT [B3LYP/6-311++G(3df,3pd)] level. Their experiments examined the species resulting from the atmospheric oxidation of SF₆, a long-lived atmospheric species, initiated by photodissociation, which breaks an S-F bond.

Ziegler and Gustev³⁴ studied the molecular and electronic structure of the sulfur fluorides using DFT. Irikura³⁵ used G2 theory to predict the molecular structure and thermochemistry of the sulfur fluorides SF_n (n = 1 – 5). Cheung *et al.*³⁶ have also reported G2 and G2(MP2) results for the heats of formation of the neutral, cationic, and anionic sulfur fluorides and their corresponding BDEs. King *et al.*³⁷ reported the BDEs of SF_n (n = 1 – 6) at the DFT level with a DZP++ basis set. Bauschlicher and Ricca³⁸ predicted the heats of formation of the SF_n (n = 1 – 6), series together with the corresponding ions SF_n⁺ and SF_n⁻ at the CCSD(T) level of theory with extrapolation to the complete basis set limit. Miller *et al.*³⁹ also investigated the thermochemistry, specifically bond enthalpies and electron affinities, of the sulfur fluoride neutrals SF_n and anions SF_n⁻ (n = 1 – 6) at the G3 and G2 level of theory, as well as at the G3(MP2) and G2(MP2) levels.

10.2 Computational Approach

For the current study, we started with the augmented correlation consistent basis sets aug-cc-pVnZ for O, F, P, and S (n = D, T, Q, 5).^{10,11} For the sake of brevity, we abbreviate the names to aVnZ. Only the spherical components (5-d, 7-f, 9-g, 11-h) of the Cartesian basis functions

were used. It has recently been found that tight d functions are necessary for calculating accurate atomization energies for 2nd row elements,⁴⁰ so additional tight d functions on P and S were included in our calculations. Basis sets containing extra tight d functions are denoted aug-cc-pV($n+d$)Z in analogy with the original augmented correlation consistent basis sets. We use aug-cc-pV($n+d$)Z to represent the combination of aug-cc-pV($n+d$)Z (on the 2nd row atoms P and S) and aug-cc-pVnZ (on O and F) basis sets and abbreviate this as aV($n+d$)Z.

All of the current work was performed with the MOLPRO suite of programs.⁴¹ The open-shell CCSD(T) calculations for the atoms were carried out at the R/UCCSD(T) level. In this approach, a restricted open shell Hartree-Fock (ROHF) calculation was initially performed, and the spin constraint was relaxed in the coupled cluster calculation.^{42,43,44} All of the calculations were done on a massively parallel HP Linux cluster with 1970 Itanium-2 processors in the Molecular Sciences Computing Facility in the William R. Wiley Environmental Molecular Sciences Laboratory or on the 144 processor Cray XD-1 computer system at the Alabama Supercomputer Center.

The geometries were optimized numerically at the frozen core CCSD(T) level with the aVDZ and aVTZ, as well as the aV(D+ d)Z and aV(T+ d)Z correlation-consistent basis sets. The geometries of the diatomics were also optimized at the aV(Q+ d)Z level. The CCSD(T)/aV(Q+ d)Z geometries were then used in single point CCSD(T)/aV(5+ d)Z calculations. For the polyatomic molecules, the CCSD(T)/aV(T+ d)Z geometries were then used in single point CCSD(T)/aV(Q+ d)Z and CCSD(T)/aV(5+ d)Z calculations. For the large open shell molecules due to the computational expense of open shell CCSD(T) calculations, the largest basis set used for the CBS extrapolations for PF₄, SF₅, and SF₅O was the aV(Q+ d) basis set.

Frequencies for the polyatomic molecules were calculated at the MP2/aug-cc-pV(T+d)Z level using the Gaussian program system⁴⁵ in order to obtain zero point energies and thermal corrections at 298 K. Zero point energies were obtained either directly from the experimental values or from the calculated frequencies if experimental values were not available. Bond distances, harmonic frequencies, and anharmonic constants for the diatomics were obtained from a 5th order fit⁴⁶ of the potential energy curve at the CCSD(T)/aug-cc-pV(Q+d)Z level.

The CCSD(T) total energies were extrapolated to the CBS limit by using a mixed exponential/Gaussian function of the form:

$$E(n) = E_{\text{CBS}} + A \exp[-(n-1)] + B \exp[-(n-1)^2] \quad (1)$$

with $n = 2$ (DZ), 3 (TZ) and 4 (QZ), as first proposed by Peterson *et al.*⁴⁷ This extrapolation method has been shown, when combined with the other corrections given below, to yield atomization energies in the closest agreement with experiment (by a small amount) as compared to other extrapolation approaches up through $n = 4$.⁶ The total atomization energies for the molecules were also obtained by extrapolating the aug-cc-pV(Q+d)Z and aug-cc-pV(5+d)Z values using the formula

$$E(l_{\text{max}}) = E_{\text{CBS}} + B/l_{\text{max}}^3 \quad (2)$$

We abbreviate the extrapolation with Eq (1) as the DTQ extrapolation and that with Eq (2) as the Q5 extrapolation. The T_1 diagnostics⁴⁸ (Supporting Information) are small with the largest values being 0.025 for the diatomics PO and SO, suggesting that our CCSD(T) approach based on a single configuration should provide good results.

Core-valence corrections, ΔE_{CV} , were obtained at the CCSD(T)/cc-pwCVTZ level of theory.⁴⁹ Scalar relativistic corrections (ΔE_{SR}), which account for changes in the relativistic contributions to the total energies of the molecule and the constituent atoms, were included at the

CISD level of theory using the cc-pVTZ basis set. ΔE_{SR} is taken as the sum of the mass-velocity and 1-electron Darwin (MVD) terms in the Breit-Pauli Hamiltonian.⁵⁰ ΔE_{SR} were also calculated at the MP2 level with the cc-pVTZ DK basis set and the spin-free, one-electron Douglas-Kroll-Hess (DKH) Hamiltonian for some molecules.^{51,52,53} As shown below, the two approaches for ΔE_{SR} are in agreement within better than 0.5 kcal/mol in the worst case and usually within 0.3 kcal/mol.^{6i,n} Most calculations using available electronic structure computer codes do not correctly describe the lowest energy spin multiplet of an atomic state as spin-orbit in the atom is usually not included. Instead, the energy is a weighted average of the available multiplets. For P in the ^4S state, no spin-orbit correction is needed, but corrections of 0.22, 0.38, and 0.56 kcal/mol for O, F, and S, respectively, are needed and are taken from the excitation energies of Moore.⁵⁴ The spin-orbit corrections for the diatomic molecules PO and SF were taken from Huber and Herzberg.⁵⁵

By combining our computed ΣD_0 (total atomization energies) values with the known heats of formation¹⁴ at 0 K for the elements, $\Delta H_f^0(\text{O}) = 58.99$ kcal/mol, $\Delta H_f^0(\text{F}) = 18.47$ kcal/mol, $\Delta H_f^0(\text{P}) = 75.42$ kcal/mol, and $\Delta H_f^0(\text{S}) = 65.66$ kcal/mol, we can derive ΔH_f^0 values for the molecules under study in the gas phase. We obtain heats of formation at 298 K by following the procedures outlined by Curtiss *et al.*¹³

10.3 Results and Discussion

10.3.1 *Geometries* The optimized geometry parameters for the P derivatives are shown in Table 10.2 and for the S derivatives in Table 10.3. The point groups and ground state symmetry labels are given in these tables for the molecules under study. For the P derivatives, the P-F and P-O bond distances are too long as compared to experiment by >0.013 Å at the CCSD(T)/aug-cc-pV(T+d)Z level, and by >0.006 at the CCSD(T)/aug-cc-pV(Q+d)Z level. In fact, we found that it

was very important to include the tight d functions in the geometry optimizations of these species as the bond lengths were much too long without their inclusion. For PFO, even larger calculations showed that inclusion of core-valence correlation, as well as large basis sets up to aV5Z with a correction for the tight d functions, was required to obtain the best agreement with experiment.¹⁷ Similar results are found for the MP2 optimizations for the S derivatives.

For the diatomics PO ($^2\Pi$), PF ($^3\Sigma^-$), SF ($^2\Pi$), and SO ($^3\Sigma^-$), our calculated values are in agreement with the experimental data⁵⁵ with the largest discrepancy in the S-F distance, which is 0.0073 Å longer than experiment. High-level calculations on SO has been discussed in detail previously, and we note that it is important to include tight d functions in the description of the structures and energetics.^{40, 56, 57} Our values, which are included for completeness, are in agreement with the previous calculations.

The P-F distance in PF₃ was found to be 0.01 Å longer than the experimental value of 1.561 Å,⁵⁸ whereas the \angle FPF was slightly smaller by 0.3° than the experimental value of 97.7°.⁵⁸ In PF₃O, the calculated P-F and P-O distances of 1.531 Å and 1.443 Å are in agreement with experiment being only 0.007 and 0.008 Å longer, respectively, whereas the bond angles \angle FPF and \angle FPO are 0.5° smaller and 0.4° larger compared to experiment.^{59,60} In PF₅, the P-F_{eq} bond is slightly longer by 0.008 Å than the experimental value of 1.534 Å,⁶¹ and the P-F_{ax} bond is also slightly longer by 0.004 Å as compared to the experimental value of 1.577 Å.⁶¹

For SF₂ the geometrical parameters are in agreement with experiment with the S-F bond distance being only 0.009 Å longer than the experimental value of 1.58745(12) Å⁶² and the \angle FSF being only 0.3° larger. The S-F and S-O distances in SF₂O are both slightly longer by 0.01 Å compared to experiment while the \angle FSF and \angle FSO angles are within 0.2° of experiment.⁶³ For SF₄, the calculated S-F_{eq} bond of 1.553 Å is slightly longer by 0.008 Å as compared to

experiment, whereas the S-F_{ax} bond of 1.654 Å is only 0.008 Å longer than the experimental value. The ∠FSF_{eq} bond angle is practically the same as the experimental value of 101.5° (with only a 0.01 difference), whereas the ∠FSF_{ax} angle is 0.7° larger than experiment.^{64,65} In SF₂O₂, the S-F and S-O bond distances are slightly longer than experiment by 0.015 Å and 0.007 Å, respectively.⁶⁶ The ∠FSF bond angle is slightly smaller than the experimental value of 96.1° by 0.8° whereas the ∠OSO angle is 1.2° larger than experiment. There have been several experimental studies^{65,67,68} into the molecular geometry of SF₄O. The S-F bond of 1.567 Å in SF₆ is in agreement with the experimental bond distance of 1.561 Å.⁵⁸

10.3.2 Vibrational Frequencies The calculated MP2 frequencies for the P derivatives are in excellent agreement with the experimental values^{17,55,69,70,71,72} considering the level of the calculations presented in Supporting Information (Table A10.3). Most of the stretching frequencies are too low by a few wave numbers due to the fact that the calculated bond distances are slightly too long. The largest discrepancy is found for PFO with about 30 cm⁻¹ difference in the P-O stretch. CCSD(T) calculations with an augmented aVQZ basis set yield values within a few cm⁻¹ of experiment.¹⁷ For the S derivatives shown in Supporting Information (Table A10.4), there is overall excellent agreement with experiment for most of the modes.^{55,73,74,75,76,77,78,79,80,81} The largest discrepancy is for the S-O stretch in FSO, but we note that this mode has never been measured and that the “experimental” frequency uses an estimated force constant to fit centrifugal distortion constants.⁷⁴ We suggest that our value is substantially more accurate. Overall, the excellent agreement between theory and experiment for the frequencies suggests that our calculated frequencies for the compounds whose frequencies have not been measured should be good to better than 30 to 40 cm⁻¹. In addition, the anharmonic contributions for the diatomics

and for PFO are not large so we can estimate that our zero point energies should have an accuracy of ± 0.2 kcal/mol.

10.3.3 Calculated Heats of Formation The contributions to the total dissociation energy are given in Table 10.4. We first describe some trends in various contributions. For the P derivatives, the agreement between the DTQ and Q5 extrapolations with only F as a substituent are essentially the same within ~ 0.2 kcal/mol. When one of the substituents is O, the difference grows to as large as ~ 0.7 kcal/mol for PO with the Q5 value being larger. This is similar to what was observed in the acid oxides of S. Use of a larger basis set (aug-cc-pV5Z) in the CBS extrapolation improves the agreement with experiment for both H_2SO_4 and FSO_3H .⁸² Compounds with a second row atom, where there is a large change in oxidation state from the atom in the molecules to the bare atom, may require use of very large basis sets to recover the valence correlation energy for the total dissociation energy. The compounds with the largest basis set effect have the largest effective charges on the P as seen in Table A10.6 (Supporting Information) containing both the Mulliken atomic charges and NBO charges from a Natural Bond Orbital (NBO) analysis⁸³ for the closed shell PF_xO_y and SF_xO_y molecules calculated at the density functional theory B3LYP/DGDZVP2 level.^{84,85} The NBO charges predict the molecules to be more ionic than do the Mulliken charges, consistent with previous observations.^{83f} The molecules are all predicted to have significant ionic character with larger negative charges on the O than on the F balanced by a positive charge on P or S. A summary of the NBO results is given in Supporting Information. There is, of course, some dependence of the NBO charges on the basis set and computational method,⁸³ but we are simply using these values as qualitative guidelines. The dipole moments calculated at the MP2/aV(T+d) level are given as Supporting Information.

For the S derivatives, the same trends in the energy components are observed. When only F is present as a substituent, the difference between the DTQ and Q5 extrapolations is a maximum for SF₆ with a difference of 0.4 kcal/mol. However, for the compounds with O as a substituent, the difference is as large as 1.8 kcal/mol for SF₂O₂, just as found for SO₄H₂. Again, the largest effective charges are on the S with these substituents. For these compounds, the second row sulfur atom is in a high oxidation state of +6. In terms of the atomization energy, the S atom is in oxidation state 0, and the difference between the two oxidation states requires the use of a very large basis set to recover the valence correlation energy for the total dissociation energy.

The core valence corrections are small with the largest value being 0.8 kcal/mol for SF₂O₂. The scalar relativistic corrections are substantially larger than the core-valence corrections. The scalar relativistic effects increase with the number of substituents. For the P derivatives, the DK correction is larger than the MD correction by up to 0.37 kcal/mol for PF₅. For the S derivatives, the DK and MD values are within 0.3 kcal/mol of each other with the largest difference found for SF₂O₂. The fact that the DKH corrections are in general more negative than the CI-SD MVD corrections is consistent with previously observed differences.^{82,86} The large values for ΔE_{SR} are consistent with the large change in the character of the P or S atom going from the free atom to the nominal +5/+6 charge on that atom in PF₃O or SF₂O₂.

The heats of formation (Table 10.5) of the diatomics are in good agreement with the experimental values,¹⁴ and our values are expected to provide lower error limits. The heats of formation of PF₃ and PF₅ are in good agreement with the experimental values.¹⁴ The value for PF₃ is more positive than the experimental value as expected and within the error bars. For PF₅, the calculated value is 1 kcal/mol higher than the experimental value and just outside the

experimental error limits. The calculated heat of formation of PF_2 is within the experimental error limits,¹⁴ and our value is more precise with an estimated error limit of ± 1 kcal/mol. For PF_3O , our calculated value is more negative than the experimental value,¹⁴ and just outside the experimental error limits. For H_2SO_4 , the calculated value⁸² was above the experimental value suggesting that our analysis of the experimental value for PF_3O is correct. This suggests that the value for PF_3O needs to be revised downwards. The good agreement that we find for our calculated values with experiment for the P derivatives, and our own assessment of the errors in the calculations, leads us to estimate error bars of ± 1 kcal/mol for the calculated heats of formation. The G2 method underestimates the heats of formation of PF_3 and PF_5 by 5 to 6 kcal/mol, whereas G2MP2 and G2M(CC5) methods show best agreement compared to experiment for the entire series.²⁰

The heat of formation of SO is in excellent agreement with the experimental⁵⁵ and other high-level theoretical values.^{40,56} The result for $\Delta H_f(\text{SF}_6)$ is in excellent agreement with the highly accurate experimental value.¹⁴ The calculated values for the heats of formation of SF_2 and SF_4 are within the quite large experimental error limits,¹⁴ and our values should be more reliable. For the SF_3 and SF_5 radicals, our calculated values differ from the best experimental values¹⁴ by more than the error bars. However, the experimental values are not very reliable, and our calculated values should be more reliable. The best experimental value for the heat of formation of SF_5 comes from an analysis of a number of experiments for the bond dissociation energy for SF_6 and is -210.2 ± 2.7 kcal/mol at 298 K²⁹ in comparison to our value of -204.6 kcal/mol, which should be good to ± 1 kcal/mol. The heat of formation of SF_3 is predicted to be -107.0 , which is above the experimental value¹⁴ of -120 ± 8 kcal/mol. The heat of formation of SF_2O is within the very large experimental error limits,¹⁴ and our value should be much better.

10.3.4 *Bond Dissociation Energies* The BDEs are given in Table 10.1 where they are compared to experiment. The BDEs for a given central atom are compared to each other in Figures 10.1 and 10.3 for the perfluorocompounds and in Figures 10.2, 10.4, and 10.5 for the oxofluorides. For consistency, the BDEs in the figures are from the CBS(DTQ) values with Eq. 1.

The value for $D_0^0(\text{PO})$ from the JANAF Tables¹⁴ is 140.7 ± 1 kcal/mol and from Huber and Herzberg⁵⁵ is 141.18 kcal/mol. Our value of 141.4 is in excellent agreement with both. The reaction for the adiabatic BDE of PO, $\text{PO}(^2\Pi) \rightarrow \text{P}(^4\text{S}) + \text{O}(^3\text{P})$, is the same as the diabatic BDE, i.e., two of the unpaired electrons on the P can bond with the two unpaired electrons on the O leaving an extra unpaired electron on P. The ^2PO molecule cannot correlate on the same spin surface with the singlet excited state of O and ^4P . The bond dissociation energy for PF has been estimated to be 4.60 ± 0.2 eV (106 ± 5 kcal/mol).¹⁴ Our best calculated value of 107.0 kcal/mol is in excellent agreement with this value. The reaction for the adiabatic BDE of PF, $\text{PF}(^3\Sigma^-) \rightarrow \text{P}(^4\text{S}) + \text{F}(^2\text{P})$, is the same as the diabatic BDE.

For SF, the heat of formation was measured from Knudsen cell mass spectrometry experiments,¹⁴ and a bond energy of 81.2 ± 2.0 kcal/mol can be derived in excellent agreement with our best value of 83.0 kcal/mol. Our best calculated value for the total dissociation energy of SO is 123.7 kcal/mol in excellent agreement with the experimental value of 123.58 kcal/mol.⁵⁵ Our extrapolated CBS(Q5) value for the valence correlation energy is in excellent agreement with Martin's best estimated value⁵⁶ of 126.03 kcal/mol obtained with a somewhat different basis sets for the tight d functions and differs by 0.4 kcal/mol from the extrapolated value of 125.62 kcal/mol obtained by Dunning *et al.*⁴⁰ at the RCCSD(T) level using the aug-cc-pV(n+d)Z basis sets up through $n = 6$. If ^2SF correlates with $\text{S}(^1\text{D})$, then the S-F diabatic BDE would be 109.6 kcal/mol using a singlet-triplet splitting in S of 26.4 kcal/mol.⁵⁴ If ^3SO correlates with the excited

singlet state of O and ground state 3S , the diabatic BDE would be 168.4 kcal/mol using singlet-triplet splitting in O (45.3 kcal/mol).⁵⁴ If 3SO correlates with 1S and 3O , then the diabatic BDE would be 149.5 kcal/mol.

The best experimental value for the first bond dissociation energy for SF_6 from the analysis of a number of experiments is a value of 100.4 ± 2.4 kcal/mol at 298 K.²⁹ Our calculated value is 106.8 kcal/mol, somewhat larger than this value, and our value should be good to ± 1 kcal/mol. Our value confirms the conclusions of Tsang and Herron²⁹ that the value of the SF_5-F BDE is higher than that determined by Zare and coworkers,^{26,27} and that the reaction of $Sr + SF_5 \rightarrow SrF + SF_4$ may play a role. Our predicted value for the exothermicity of this reaction is -89.9 ± 4 kcal/mol at 298 K (using experimental values¹⁴ for the heats of formation of Sr and SrF) consistent with the maximum observed in the chemiluminescence corresponding to 87.2 kcal/mol.

Our calculated heats of formation enable us to calculate a wide range of BDEs. All possible P-F and P-O BDEs are given in Table 10.1 and are compared graphically in Figures 10.1 and 10.2. The first P-F adiabatic BDEs of all the binary phosphorus fluorides are all quite strong except for that of PF_4 , which is much lower due to the relative instability of the PF_4 radical and the stability of the product PF_3 . For PF_5 , PF_3 , PF_2 , and PF , the adiabatic and diabatic BDEs are the same. The adiabatic P-F BDE for 2PF_4 produces 1PF_3 and $F(^2P)$. In order to compare the BDEs, it may be more appropriate to consider the diabatic BDE with the formation of 3PF_3 where there are two unpaired electrons, one from the unpaired electron on PF_4 and one from the P-F bond that was broken (see Figure 10.1). Addition of the singlet-triplet splitting in PF_3 obtained at the CCSD(T)/CBS//MP2/aVTZ level (Table 10.6) (an estimate of the reorganization energy) gives 146.5 kcal/mol, which is more in line with the other P-F BDEs. The

reorganization energy in this case is the pairing of the two electrons to form the lone pair on PF₃ (see the spin density in Figure 10.1). The P-F bonds in PF₅ and PF₃ are comparable to the first C-F BDE in CF₄ (129.6 ± 1.0), and are slightly lower than the first Si-F BDE in SiF₄.¹⁵

The first PF adiabatic BDE in PF₃O is higher than the adiabatic BDE for the P-O bond because the POF₂ radical is energetically less stable than the closed shell PF₃ molecule. Note that the adiabatic P-O BDE is defined by the reaction ${}^1\text{POF}_3 \rightarrow {}^1\text{PF}_3 + \text{O}({}^3\text{P})$ (Figure 10.2). The situation is reversed when the diabatic BDE for O is considered on the singlet surface for the reaction ${}^1\text{POF}_3 \rightarrow {}^1\text{PF}_3 + \text{O}({}^1\text{D})$. Addition of the singlet-triplet splitting in O (45.3 kcal/mol)⁵⁴ to the P-O adiabatic BDE yields a diabatic BDE of 176.9 (CBS(DTQ)) kcal/mol, consistent with the differences in the bond distances and force constants at the minimum in PF₃O. The adiabatic P-F BDE in PF₂O is about half that in PF₃O, whereas the P-O BDE is only 12 kcal/mol lower than that in PF₃O, again reflecting the different stabilities of the reactants and products. Use of the singlet-triplet splitting in FPO (Table 10.6) leads to a diabatic P-F bond energy of 159.4 kcal/mol. This is probably not the best model for the P-F diabatic BDE because much of the spin is on the O. One can also correlate the P-O bond in PF₂O with the singlet excited state of O. This yields a diabatic P-O BDE of 165.0 kcal/mol, very similar to the adiabatic value in PFO and PF₃O. We note that the spin density in PF₂O is not fully localized on the P as there is some on the O atom. The adiabatic P-O BDE in PFO is ~24 kcal/mol higher than in PO and ~33 kcal/mol higher than the adiabatic P-O BDE in PF₃O. The adiabatic P-O BDE in PFO correlates with the products PF (${}^3\Sigma^-$) + F(${}^2\text{P}$) as does the diabatic value. The PFO molecule cannot correlate on the same spin surface with the singlet excited state of O and ${}^3\text{PF}$. Thus, it may be more appropriate to compare the diabatic P-O BDE in PF₃O with that in PFO and the diabatic BDE in the latter is then lower than that in the former. The P-F BDE in PFO is comparable to the first BDE in PF₃ or

PF₅, consistent with the result that the adiabatic and diabatic asymptotes are the same in these molecules.

On average, S-F bonds are weaker than P-F bonds, which results in lower BDEs. The adiabatic S-F BDE in SF₆ is the highest adiabatic BDE for the SF_x compounds, as expected from the exceptional stability of octahedral closed shell SF₆ and the relative instability of the SF₅ radical. Similarly, the closed shell SF₄ and SF₂ molecules exhibit much larger adiabatic BDEs than do the SF₅ and SF₃ radicals. In these cases, the adiabatic and diabatic BDEs for the closed shell species are the same as they dissociate to a doublet SF_x radical and F(²P). For the radical SF_x species, the first S-F adiabatic BDEs increase in the opposite order with SF₅ having the lowest adiabatic BDE (38 kcal/mol) and S-F the highest. The adiabatic BDEs of the doublet SF_x radicals correlate with a closed shell singlet species and F(²P). As for the BDE in ²PF₄, it is more appropriate to compare the diabatic BDEs where ³SF₄ and ³SF₂ are formed from ²SF₅ and ²SF₃ (Figure 10.3). Use of the singlet-triplet splittings in SF₄ and SF₂ (Table 10.6) yields respective diabatic S-F BDEs for SF₅ and SF₃ of 104.7 and 104.6 kcal/mol, consistent with the adiabatic S-F BDEs of the closed shell molecules and essentially the same as that in SF₆. These results are consistent with the inherent instability of the sulfur radicals, as compared to the closed shell species, and show the reorganization of electron density that occurs on spin pairing to form the lone pairs in SF₄ and SF₂.

By analogy with PF₃O, the S-F and S=O adiabatic BDEs in SF₄O are similar (Figure 10.4). This contrasts with the BDEs in the diatomics, where the S=O double bond is much stronger (123.1 kcal/mol, CBS(DTQ)) than the S-F single bond (83.2 kcal/mol, CBS(DTQ)). The similarity of the S-F and S=O adiabatic BDEs in SF₄O is due to the fact that oxygen loss results in the energetically favored closed shell SF₄ molecule, whereas fluorine loss produces an

unstable SF_3O radical. If we perform the same correlation with $\text{O}(^1\text{D})$ as done for PF_3O , the diabatic S-O BDE on the singlet surface for SF_4O is 133.3 kcal/mol, substantially higher than the adiabatic value and more consistent with the diatomic BDE (Figure 10.4). This is representative of the BDE of an S=O double bond and is consistent with the geometry and the S-O stretching force constants. The S-O BDE in SF_2O is substantially larger than the S-F bond even though the stable SF_2 molecule is being formed for the former as compared to the SFO radical for the latter. The diabatic value for the S-O BDE in SF_2O correlating to $\text{O}(^1\text{D}) + ^1\text{SF}_2\text{O}$ is even higher, 174.1 kcal/mol and comparable to the diabatic BDE for SO correlating with ^1O and ^3S . The adiabatic S-O BDE in SF_2O is comparable to that for diatomic SO.

The S-O adiabatic BDE in SF_5O is much lower (71.6 kcal/mol) than the S-O adiabatic BDE in SF_4O , consistent with an S-O single bond, as would be expected from the simplest description of the structure with the unpaired electron on the O (Figure 10.4). For SF_5O , the adiabatic and diabatic limits ($^2\text{SF}_5 + \text{O}(^3\text{P})$) are the same on the basis of the spin density. The adiabatic S-O BDE in the radical SF_3O is 94 kcal/mol and is larger than the adiabatic S-O BDE in SF_5O . The adiabatic S-O BDE in SF_3O is similar to the adiabatic BDEs in SF_2O_2 (see below) and in SF_4O . The spin density in SF_3O shows little excess on O so it may have some double bond character. In this case, the diabatic S-O BDE arising from $^2\text{SF}_3 + ^1\text{O}$ is 139.3 kcal/mol, very similar to the diabatic SO BDE in SF_4O or SF_2O_2 .

As for PF_xO , the loss of a fluorine atom from a closed shell SF_xO molecule to give a radical results in a large adiabatic BDE whereas the loss of a fluorine atom from a radical to give a stable closed shell molecule gives rise to a much smaller adiabatic BDE. The first adiabatic S-F BDE in the radical SF_5O is very low, 21 kcal/mol. If we consider the diabatic S-F BDE in SF_5O to form $^3\text{SF}_4\text{O} + \text{F}(^2\text{P})$, we obtain a value of 101.8 kcal/mol using the singlet-triplet splitting

(Table 10.6 and Figure 10.4). The S-F diabatic BDE is higher than the adiabatic S-O single BDE as expected. The adiabatic S-F BDE in the radical SF₃O is also small, 20 kcal/mol. The diabatic S-F BDE in SF₃O correlates with ³SF₂O + F(²P) and is 104.9 kcal/mol with the singlet-triplet splitting from Table 10.6. Thus, the diabatic S-F BDEs in SF₃O and SF₅O are comparable to the diabatic S-F BDEs for SF₃ and SF₅ and the adiabatic BDEs of the closed shell SF_x and SF_xO compounds.

The adiabatic S-F BDE in SF₂O₂ is larger than the adiabatic S-O BDE by ~8 kcal/mol, again reflecting the stability of the radicals. If we consider the diabatic BDE for the S-O bond correlating with O(¹D) + ¹SF₂O, we obtain a value of 144.0 kcal/mol (Figure 10.5), slightly higher than the diabatic value in SF₄O and again consistent with the geometry and force constants. The adiabatic S-O BDE in SFO₂ is 85.4 kcal/mol and is in the range of an S-O single bond, consistent with the spin distribution and the S-O single bond values given above. The adiabatic S-O BDE in SO₂ is consistent with the other S=O BDEs. Note that in SO₂, the excited state of O or SO is not appropriate for use in the diabatic BDE calculation as the reaction no longer occurs on a single spin state and we do not want to include two excited states in the calculation.

The adiabatic S-F BDE in SFO₂ is relatively low, 40 kcal/mol, but is higher than the adiabatic S-F bond in SF₃O. This BDE was evaluated using the experimental heat of formation of SO₂ at 0 K ($\Delta H_f(\text{SO}_2) = -70.34 \pm 0.05$ kcal/mol).¹⁴ Extensive calculations on SO₂ show that it is possible to calculate the heat of formation reliably using the above approaches as long as tight *d* functions are included.^{56,57} The diabatic value for the S-F BDE in FSO₂ correlating with SO₂(³B₁) + F(²P) is 114.0 kcal/mol using the experimental singlet-triplet splitting⁸⁷ of 73.6

kcal/mol in SO_2 . The adiabatic S-O BDE in SFO_2 is much larger than the adiabatic S-F BDE and is comparable to the adiabatic S-O BDE in SF_4O .

The various bond energies provide insights into the stability of the various species. The non-radical species are very stable with large adiabatic BDEs, and the radicals tend to be less stable with smaller adiabatic BDEs. There is a difference in the effective stability between the radicals with P and S as the central atom. For the PF_n series, PF_4 has the lowest adiabatic P-F BDE, 54 kcal/mol. For PF_2O , the adiabatic P-F BDE is smaller than the P-O BDE, but the radical is still quite stable with respect to bond breaking with a P-F bond energy of 74 kcal/mol. In the SF_n series, the S-F adiabatic BDE is the lowest in SF_5 , 38 kcal/mol. The adiabatic S-F BDEs in SF_5O and SF_3O are small, ~ 20 kcal/mol, showing that these radicals will be highly reactive with respect to loss of an F atom. The S-O BDEs are much larger in the S radicals just as found for the P radicals. The fact the SF_xO radicals are less stable with respect to breaking an S-F bond as compared to breaking a P-F bond in the PF_xO radicals is consistent with the fact that overall the P-F BDEs are larger than the S-F BDEs.

10.4 *Conclusions*

The heats of formation at 0 K and 298 K are predicted for PF_3 , PF_5 , PF_3O , SF_2 , SF_4 , SF_6 , SF_2O , SF_2O_2 , and SF_4O , as well as a number of radicals derived from these stable compounds on the basis of coupled cluster theory (CCSD(T)) calculations extrapolated to the complete basis set limit. The calculated values should be good to ± 1 kcal/mol. The calculated heats of formation are in excellent agreement with the available experimental data for the closed shell molecules. The calculated values allow us to predict the adiabatic bond dissociation energies for all of the compounds to within ± 1 kcal/mol, dramatically improving the estimates of these important quantities, particularly for the radicals.

The calculated BDEs provide important insight into the reactivity of these molecules. For example, the adiabatic BDEs in the closed shell phosphorus fluorides are quite high, 130 to 140 kcal/mol. In PF_3O , the $\text{P}=\text{O}$ bond is more easily broken than the $\text{P}-\text{F}$ bond, a surprising result, but in the PF_2O radical and the closed shell PFO molecule, the situation is reversed.

The first S-F adiabatic BDEs are predicted to be substantially smaller than those of the P-F bonds with the largest first S-F BDE being 105 kcal/mol in SF_6 . The calculated value for the S-F bond dissociation energy in SF_6 is about 6 kcal/mol higher than the most recent value based on analyzing a range of experiments and substantially higher than earlier estimates by up to 30 kcal/mol. Thus, SF_5 is predicted to be a less stable radical than previously thought, and the calculated S-F BDE in SF_5 is substantially lower than the estimated experimental values. Similarly, the S-F bond dissociation energy in SF_4 is higher than the experimental estimates and the SF_3 radical is less stable than previously thought. The calculated values for the bond dissociation energies in SF_2 and SF are in good agreement with the experimental estimates. The S-O BDE is stronger than the first S-F BDE in SF_2O , weaker than the first S-F BDE in SF_2O_2 and comparable to the first S-F BDE in SF_4O .

The results in combination with singlet-triplet splittings enable us to compare the adiabatic and diabatic BDEs. In diatomics, the BDE is a direct measure for the bond strength, and frequently the same assumption is applied incorrectly to polyatomic species for which reorganization energies in the product are important. Therefore, for polyatomic species, adiabatic bond dissociation energies and bond strengths are not the same and a clear distinction must be made between the two. The measurement of the strength or stiffness of a given bond involves only a small displacement of its atoms and no reorganization of the molecule. Appropriate criteria for judging the bond strength include the curvature of the bond energy plots, bond

lengths, vibrational frequencies, force constants, bond orders, etc, and it is these that form the basis for writing representative valence bond structures for polyatomic molecules in their ground states. The differences between the adiabatic and diabatic BDEs, which are related to the reorganization energy in the products, can be estimated in the molecules under study from singlet-triplet splittings. The reorganization energies can account for the large fluctuations in adiabatic BDEs observed during the stepwise loss of fluorine atoms. In contrast, the diabatic BDEs of a given type are often very similar in size to each other and thus exhibit more regular trends.

Acknowledgments This work was supported by the Chemical Sciences, Geosciences and Biosciences Division, Office of Basic Energy Sciences, U.S. Department of Energy (DOE) under grant no. DE-FG02-03ER15481 (catalysis center program) and the National Science Foundation under Grant No CHE-0456343. DAD also thanks the Robert Ramsay Chair Fund of The University of Alabama for support. Part of this work was performed at the W. R. Wiley Environmental Molecular Sciences Laboratory, a national scientific user facility sponsored by DOE's Office of Biological and Environmental Research and located at Pacific Northwest National Laboratory, operated for the DOE by Battelle. KOC also thanks the Air Force Office of Scientific Research and the Office of Naval Research for financial support.

Appendix Total CCSD(T) energies, CBS energies (in Hartrees). CCSD(T)/aV(D+d)Z geometry parameters for the PF_xO_y compounds. Calculated MP2/aug-cc-pV(T+d)Z frequencies (cm⁻¹) for the PF_xO_y compounds. Calculated MP2/aug-cc-pV(T+d)Z frequencies (cm⁻¹) for the SF_xO_y compounds. *T*₁ diagnostics for PF_xO_y and SF_xO_y compounds. Mulliken and natural charges, Natural bond orbital analysis for closed shell PF_xO_y and SF_xO_y compounds. Summary of NBO

analysis. Dipole moments at the MP2/aV(T+d)Z level. Total CCSD(T) energies, CBS energies (in Hartrees), for triplets. MP2/aV(D+d)Z geometry parameters for the triplets. Calculated MP2/aug-cc-pV(T+d)Z frequencies (cm^{-1}) for the triplets. T_1 diagnostics for the triplets. Spin densities for the triplets. Spin densities for the PF_xO doublets. Spin densities for the SF_xO_y doublets. This material is available free of charge via the Internet at <http://pubs.acs.org>.

Table 10.1. Experimental and Calculated Bond Dissociation Energies in kcal/mol at 0 K.^a

Bond Energy Reaction	Experiment	Calc (DTQ)	Calc (Q5)
PF ₅ → PF ₄ + F		132.8	
PF ₄ → PF ₃ + F		54.5	
PF ₃ → PF ₂ + F	130.2 ± 5.9 ^b	132.0	131.8
PF ₂ → PF + F	(123.2) ^c	119.2	119.1
PF → P + F	106 ± 5 ^b	107.2 [107.1]	107.1 [107.0]
PF ₃ O → PF ₃ + O	129.0 ± 2.8 ^b	131.6 [131.4]	132.4 [132.2]
PF ₃ O → PF ₂ O + F		143.8	143.9
PF ₂ O → PF ₂ + O		119.7	120.3
PF ₂ O → PFO + F		74.3	74.2
PFO → PF + O		164.6 [164.5]	165.2 [165.2]
PFO → PO + F		130.9 [130.8]	130.8 [130.7]
PO → P + O	141.8 ± 1 ^b	140.9 [140.8]	141.6 [141.4]
SF ₆ → SF ₅ + F	92.2 ± 3.8 ^b	104.8	
	(100.4 ± 2.4) ^d		
	75.92 ^e		
	78 ^f		
	92.0 ^g		
	(91.1 ± 3.2) ^h		
	88.1 ± 3.2 ⁱ		
	(94.5 ± 3.0) ^j		
SF ₅ → SF ₄ + F	72 ^f	37.7	
	(53.1 ± 6.0) ^h		
	57.9 ± 3.0 ⁱ		
SF ₄ → SF ₃ + F	80 ± 13 ^b	95.5	95.7
	≤ 83.9 ± 1.2 ^k		
	83 ^f		
	(84.1 ± 3.0) ^h		
	89.2 ± 2.3 ⁱ		
	86.2 ± 7.8 ^l		

$\text{SF}_3 \rightarrow \text{SF}_2 + \text{F}$	63 ^f (63.7 ± 7.1) ^h 60.9 ± 2.8 ⁱ	54.8	54.6
$\text{SF}_2 \rightarrow \text{SF} + \text{F}$	91.8 ± 5.5 ^b 94 ^f (91.7 ± 4.3) ^h 94.3 ± 4.6 ⁱ	89.1 [89.2]	89.3 [89.3]
$\text{SF} \rightarrow \text{S} + \text{F}$	81.0 ± 1.6 ^b 82 ^f (81.2 ± 1.6) ^h 77.5 ± 4.2 ⁱ	83.2 [83.1]	83.2 [83.1]
$\text{SF}_5\text{O} \rightarrow \text{SF}_5 + \text{O}$		71.6	
$\text{SF}_5\text{O} \rightarrow \text{SF}_4\text{O} + \text{F}$		21.1	
$\text{SF}_4\text{O} \rightarrow \text{SF}_4 + \text{O}$	(102 ± 6) ^m	88.2 [88.0]	88.9 [88.7]
$\text{SF}_4\text{O} \rightarrow \text{SF}_3\text{O} + \text{F}$		89.7	89.8
$\text{SF}_3\text{O} \rightarrow \text{SF}_2\text{O} + \text{F}$		20.0	20.0
$\text{SF}_3\text{O} \rightarrow \text{SF}_3 + \text{O}$		94.0	94.8
$\text{SF}_2\text{O} \rightarrow \text{SFO} + \text{F}$		93.6	93.7
$\text{SF}_2\text{O} \rightarrow \text{SF}_2 + \text{O}$	118 ± 29.0 ^b	128.8 [128.7]	129.4 [129.5]
$\text{SFO} \rightarrow \text{SO} + \text{F}$		85.4	86.2
$\text{SFO} \rightarrow \text{SF} + \text{O}$		124.3	125.0
$\text{SF}_2\text{O}_2 \rightarrow \text{SF}_2\text{O} + \text{O}$	(109 ± 27) ^b (110 ± 5) ^m	98.7 [98.5]	99.7 [99.3]
$\text{SF}_2\text{O}_2 \rightarrow \text{SFO}_2 + \text{F}$		106.9	107.2
$\text{SFO}_2 \rightarrow \text{SO}_2 + \text{F}$		40.4 ⁿ	
$\text{SFO}_2 \rightarrow \text{SFO} + \text{O}$		85.4	86.2
$\text{SO} \rightarrow \text{S} + \text{O}$	123.58 ^o	123.1 [123.0]	123.7 [123.6]

^a Values in parentheses are at 298 K. ^b Reference 14. ^c Reference 15. ^d Reference 29. ^e Reference 21. ^f Reference 23. ^g Reference 24. ^h References 26 and 27. ⁱ Reference 30. ^j Reference 28. ^k Reference 22. ^l Reference 31. ^m Reference 25. ⁿ Calculated using the experimental heat of formation of SO_2 from Ref. 14. ^o Reference 55.

Table 10.2. Optimized Bond Lengths (Å) and Angles (degrees) for PF_xO_y Equilibrium Geometries.^a

Molecule	Basis Set	R_{PF}	R_{PO}	$\angle FPF$	$\angle FPO$
PO (${}^2\Pi$, $C_{\infty v}$)	aV(T+d)Z		1.4889		
	aV(Q+d)Z		1.4828		
	exp ^b		1.4759		
PF (${}^3\Sigma^-$, $C_{\infty v}$)	aV(T+d)Z	1.6028			
	aV(Q+d)Z	1.5960			
	exp ^b	1.589 ₇			
PFO (${}^1A_1'$, C_s)	aV(T+d)Z	1.5855	1.4646		110.1
	exp ^c	1.5727 ± 0.0002	1.4528 ± 0.0001		110.16 ± 0.02
PF ₂ (2B_1 , C_{2v})	aV(T+d)Z	1.5883		98.2	
PF ₃ (1A_1 , C_{3v})	aV(T+d)Z	1.5723		97.5	
	exp ^d	1.561(1)		97.7(2)	
PF ₂ O (C_s)	aV(T+d)Z	1.5581	1.4654	98.93	115.9
PF ₃ O (1A_1 , C_{3v})	aV(T+d)Z	1.5314	1.4429	100.84	117.1
	exp ^e	1.522	1.437	101.14	
	exp ^f	1.524 ₀ ± 0.003	1.435 ₆ ± 0.006	101.3 ± 0.2	116.8
PF ₄ (2A_1 , C_{2v})	aV(T+d)Z	1.5470 _{eq}		94.6 _{eq}	
		1.6023 _{ax}		104.5 _{ax}	
PF ₅ (${}^1A_1'$, D_{3h})	aV(T+d)Z	1.5415 _{eq}		120.0 _{eq}	
		1.5813 _{ax}		90.0 _{ax}	
	exp ^g	1.5340 _{eq}			
		1.5770 _{ax}			

^a CCSD(T) optimizations on the PF_xO_y compounds up to aug-cc-pV(T+d)Z and up to aug-cc-pV(Q+d)Z for diatomics. ax = axial and eq = equatorial. ^b PF and PO electronic spectroscopy; Reference 55. ^c Millimeter-wave and high resolution infrared spectroscopies. Reference 17. ^d Microwave R_e. Reference 58. ^e Microwave. Reference 60. ^f Electron diffraction, Reference 59. ^g Electron diffraction, Reference 61.

Table 10.3. Optimized Bond Lengths (Å) and Angles (degrees) for SF_xO_y Equilibrium Geometries.^a

Molcecule	Basis Set	R _{SF}	R _{SO}	∠FSF	∠FSO	∠OSO	∠F _{eq} SF _{eq} F _{ax}	∠FSFO
							∠F _{ax} SF _{ax} F _{eq}	∠OSOF
SF (² Π, C _{∞v})	aV(T+d)Z	1.6057						
	aV(Q+d)Z exp ^b	1.6013 1.600574						
SO (³ Σ ⁻ , C _{∞v})	aV(T+d)Z		1.4932					
	aV(Q+d)Z exp ^b		1.4866 1.481087					
SF ₂ (¹ A ₁ , C _{2v})	aV(T+d)Z	1.5969		98.4				
	exp ^c	1.58745 (12)		98.048(13)				
SFO (² A'', C _s)	aV(T+d)Z	1.6139	1.4474		109.2			
SF ₃ (² A', C _s)	aV(T+d)Z	1.5695 _{eq} 1.6632 _{ax}		88.0 _{eq} 162.0 _{ax}			-77.0	
SF ₂ O (¹ A', C _s)	aV(T+d)Z	1.5958	1.4268	92.6	106.7			108.3
	exp ^d	1.5854 ± 0.0002	1.4127 ± 0.0003	92.83 ± 0.02	106.82 ± 0.03			
SFO ₂ (² A', C _s)	aV(T+d)Z	1.5885	1.4356		106.9	124.6		-125.3
SF ₄ (¹ A ₁ , C _{2v})	aV(T+d)Z	1.5531 _{eq} 1.6536 _{ax}		101.5 _{eq} 187.6 _{ax}			50.8 -50.8	
	exp ^e	1.545 ± 0.003 _{eq}		101.5 ± 0.5 _{eq}				

		$1.646 \pm 0.003_{\text{ax}}$		$186.9 \pm 0.5_{\text{ax}}$			
	exp ^f	$1.542 \pm 0.005_{\text{eq}}$		$103.8 \pm 0.6_{\text{eq}}$			
		$1.643 \pm 0.005_{\text{ax}}$		$176.8 \pm 2.5_{\text{ax}}$			
SF ₃ O (² A',C _s)	aV(T+d)Z	1.5526_{eq}	1.4188	90.3_{eq}	111.2_{eq}		-90.9
		1.6362_{ax}		147.5_{ax}	105.0_{ax}		
SF ₂ O ₂ (¹ A ₁ ,C _{2v})	aV(T+d)Z	1.5447	1.4117	95.3	108.1	125.2	
	exp ^g	1.530	1.405	96.1		124.0	
SF ₅ (² A ₁ ,C _{4v})	aV(T+d)Z	1.5983_{eq}		89.9_{eq}			91.6
		1.5467_{ax}		91.6_{ax}			
SF ₄ O (¹ A ₁ ,C _{2v})	aV(T+d)Z	1.5475_{eq}	1.4155	112.5_{eq}	123.8_{eq}		83.5
		1.6046_{ax}		164.4_{ax}	97.8_{ax}		-83.5
				$85.7_{\text{eq-ax}}$			
	exp ^h	$1.535(4)_{\text{eq}}$	1.406(3)	$114.9(3.4)_{\text{eq}}$	122.5_{eq}		
		$1.593(4)_{\text{ax}}$		$164.4(6)_{\text{ax}}$	97.8_{ax}		
				$85.8_{\text{eq-ax}}$			
	exp ⁱ	$1.552(4)_{\text{eq}}$	1.403(3)	$110.1(1.8)_{\text{eq}}$	$124.9(9)_{\text{eq}}$		
		$1.575(3)_{\text{ax}}$		$89.6(2)_{\text{eq-ax}}$	$90.6(4)_{\text{ax}}$		
	exp ^j	$1.550 \pm 0.003_{\text{eq}}$	1.413 ± 0.001	$110.01 \pm 0.74_{\text{eq}}$			
		$1.583 \pm 0.003_{\text{ax}}$		$178.35 \pm 0.48_{\text{ax}}$			
	exp ^f	$1.539 \pm 0.005_{\text{eq}}$	1.422 ± 0.008	$122.8 \pm 1.8_{\text{eq}}$			

		$1.602 \pm 0.005_{\text{ax}}$		$182.8 \pm 0.7_{\text{ax}}$		
SF ₅ O (² B ₁ , C _{2v})	aV(T+d)Z	1.5785 _{eq}	1.6175	90.1 _{eq}	92.1 _{eq}	87.9
		1.5699 _{eq}		87.9 _{eq}	88.0 _{eq}	92.0
		1.5673 _{ax}		92.0 _{eq}	180.0 _{ax}	
SF ₆ (¹ A _{1g} , O _h)	aV(T+d)Z	1.5666		90.0 _{eq}		
				180.0 _{ax}		
	exp ^k	1.56072(7)		90.0 _{eq}		
				180.0 _{ax}		

^a CCSD(T) optimizations on SF, and MP2 optimizations on the SF_xO_y compounds. ax = axial and eq = equatorial ^b SF and SO, Microwave; Reference 55. ^c Microwave R_e. Reference 62. ^d Microwave, R⁰, Reference 63. ^e Microwave. Reference 64. ^f Electron diffraction. Reference 65. ^g Microwave. Reference 66. ^h Electron Diffraction, Structure D. Reference 67. Used by Oberhammer, H.; Boggs, J.E. *J. Mol. Spectrosc.*, **1979**, *56*, 107 in their computational study. ⁱ Electron Diffraction, Structure B, Reference 67. ^j Electron diffraction, Reference 68. ^k R₀. Computed in Reference 58 from rotational constant from Patterson, C.W.; Herlemont, F.; Azzizi, M.; LeMaire, K. *J. Mol. Spectrosc.*, **1984**, *108*, 31; Doppler-free two-photon spectroscopy of the 2ν₃ band.

Table 10.4. Components for Calculating the Atomization Energies in kcal/mol.^a

Molecule	CBS ^b	CBS ^c	ΔE_{ZPE}	$\Delta E_{\text{CV}}^{\text{d}}$	$\Delta E_{\text{SR-DK}}^{\text{e}}$	$\Delta E_{\text{SR}}^{\text{f}}$	$\Delta E_{\text{SO}}^{\text{g}}$	$D_0(0\text{K})^{\text{h}}$	$D_0(0\text{K})^{\text{h}}$
	(DTQ)	(Q5)						(DTQ)	(Q5)
PO (² Π)	142.36	143.03	1.75 ^k	0.51	-0.44	-0.29	0.10 ⁱ	140.93 [140.77]	141.59 [141.44]
PF (³ Σ ⁻)	108.91	108.81	1.20 ^k	0.25	-0.45	-0.34	-0.38	107.23 [107.12]	107.13 [107.02]
PFO	276.10	276.68	3.62 ^l	0.67	-0.96	-0.75	-0.60	271.80 [271.60]	272.38 [272.18]
PF ₂	230.49	230.28	2.94 ^l	0.41		-0.80	-0.76	226.40	226.19
PF ₃	365.86	365.51	5.41 ^l	0.44	-1.56	-1.37	-1.14	358.38 [358.19]	358.03 [357.84]
PF ₂ O	354.65	355.06	6.18 ^l	0.43		-1.79	-0.98	346.12	346.54
PF ₃ O	502.06	502.54	9.11 ^l	0.55	-3.03	-2.61	-0.92	489.96 [489.55]	490.44 [490.02]
PF ₄	424.32		7.56 ^l	0.11		-2.45	-1.52	412.90	
PF ₅	561.72	561.62	10.70 ^l	0.04	-3.79	-3.42	-1.90	545.75 [545.37]	545.64 [545.27]
SF (² Π)	84.87	84.93	1.20 ^k	0.20	-0.40	-0.31	-0.37 ^j	83.19 [83.11]	83.24 [83.16]
SO (³ Σ ⁻)	125.36	126.04	1.64 ^k	0.44	-0.47	-0.37	-0.94	123.00 [122.90]	123.68 [123.58]
SF ₂	176.99	177.11	2.85 ^l	0.30	-0.84	-0.76	-1.32	172.35 [172.27]	172.47 [172.39]
SFO	212.54	213.31	3.66 ^m	0.60		-0.83	-1.16	207.48	208.25
SF ₃	233.98	234.02	4.56 ^m	0.39		-1.05	-1.70	227.06	227.11
SF ₂ O	309.46	310.33	5.99 ^l	0.58	-1.49	-1.46	-1.54	301.05 [301.01]	302.92 [302.89]
SFO ₂	302.40	303.93	6.86 ^m	0.74		-1.97	-1.39	292.92	294.45
SF ₄	333.49	333.71	7.40	0.32	-1.78	-1.81	-2.08	322.52 [322.55]	322.75 [322.77]
SF ₃ O	332.92	333.68	8.05 ^m	0.48		-2.37	-1.92	321.06	321.82
SF ₂ O ₂	413.61	415.38	9.89 ^l	0.80	-3.30	-2.99	-1.77	399.76 [399.45]	401.53 [401.23]
SF ₅	375.76		9.98 ^l	0.10		-3.19	-2.46	360.24	

SF ₄ O	426.73	427.66	11.24 ^m	0.33	-3.83	-3.63	-2.30	409.72 [410.53]	411.65 [411.46]
SF ₅ O	461.65		13.07	0.13	-4.19		-2.68	431.84	
SF ₆	485.57	485.98	13.40 ^l	0.03	-4.63	-4.40	-2.84	464.96 [464.74]	465.37 [465.15]

^a $\Sigma D_0 = \Delta E_{\text{elec}}(\text{CBS}) - \Delta E_{\text{ZPE}} + \Delta E_{\text{CV}} + \Delta E_{\text{SR}} + \Delta E_{\text{SO}}$. ^b Valence electron dissociation energy extrapolated to the CBS limit by using

Equation (1) with $n = D, T, Q$. ^c Valence electron dissociation energy extrapolated to the CBS limit by using Equation (2) with $n = Q$,

5. ^d Core-valence corrections were obtained with the cc-pwCVTZ basis sets at the optimized geometries. ^e The scalar relativistic

correction is based on Douglas-Kroll method. ^f The scalar relativistic correction is based on a CISD(FC)/cc-pVTZ MVD calculation. ^g

Correction due to the incorrect treatment of the atomic asymptotes as an average of spin multiplets. Values are based on C. Moore's

Tables, ref. 54. ^h The theoretical value of the dissociation energy to atoms $\Sigma D_0(0 \text{ K})$. Values in square brackets are using Douglas-

Kroll relativistic correction. ⁱ Includes the spin orbit correction for the diatomic = 0.32 kcal/mol (112 cm⁻¹). ^j Includes the SO

stabilization of the molecule (199 cm⁻¹). ^k Zero point energy obtained from the fifth order fitting of the PES at the

CCSD(T)/aV(Q+d)Z geometry. ^l Zero point energy obtained from the experimental values. ^m Zero point energy obtained from the

calculated MP2/aV(T+d)Z value.

Table 10.5. Heats of Formation (kcal/mol) at 0 K and 298 K.^a

Molecule	$\Delta H_f(0\text{K})_{\text{theory}}$	$\Delta H_f(0\text{K})_{\text{theory}}$	$\Delta H_f(0\text{K})_{\text{exp}}$	$\Delta H_f(298\text{K})_{\text{theory}}$	$\Delta H_f(298\text{K})_{\text{theory}}$	$\Delta H_f(298\text{K})_{\text{exp}}$
	(DTQ)	(Q5)		(DTQ)	(Q5)	
PO (² Π)	-6.5 [-6.4]	-7.2 [-7.0]	-5.6 ± 4	-6.8 [-6.6]	-7.4 [-7.3]	-5.6 ± 1
PF (³ Σ ⁻)	-13.3 [-13.2]	-13.2 [-13.1]	-12.3 ± 5	-13.6 [-13.4]	-13.5 [-13.3]	-12.5 ± 5
PFO	-118.9 [-118.7]	-119.5 [-119.3]		-119.7 [-119.5]	-120.2 [-120.0]	
PF ₂	-114.0	-113.8	-116.0 ± 5.0	-114.8	-114.5	-116.6 ± 5.0
PF ₃	-227.6 [-227.4]	-227.2 [-227.0]	-227.7 ± 0.9	-228.9 [-228.7]	-228.5 [-228.3]	-229.0 ± 0.9
PF ₂ O	-174.8	-175.2		-176.2	-176.6	
PF ₃ O	-300.1 [-299.7]	-300.6 [-300.2]	-297.7 ± 1.9	-302.2 [-301.8]	-302.7 [-302.3]	-299.6 ± 1.9
PF ₄	-263.6			-265.4		
PF ₅	-378.0 [-377.6]	-377.9 [-377.5]	-378.5 ± 0.7	-380.5 [-380.2]	-380.4 [-380.1]	-380.9 ± 0.7
SF (² Π)	0.9 [1.0]	0.9 [1.0]	2.9 ± 1.5	1.0 [1.0]	0.9 [1.0]	3.1 ± 1.5
SO (³ Σ ⁻)	1.6 [1.7]	1.0 [1.1]	1.2 ± 0.3	1.6 [1.7]	1.0 [1.1]	1.2 ± 0.3
SF ₂	-69.7 [-69.7]	-69.9 [-69.8]	-70.4 ± 4.0	-70.2 [-70.1]	-70.3 [-70.3]	-70.9 ± 4.0
SFO	-64.4	-65.1		-64.9	-65.6	
SF ₃	-106.0	-106.0	-119.3 ± 8.0	-106.9	-106.9	-120.2 ± 8.0
SF ₂ O	-139.5 [-139.4]	-140.3 [-140.3]	-129 ± 25	-140.6 [-140.6]	-141.5 [-141.5]	-130 ± 25
SFO ₂	-90.8	-92.3		-92.1	-93.6	
SF ₄	-183.0 [-183.0]	-183.2 [-183.2]	-180.9 ± 5.0	-184.7 [-184.7]	-184.9 [-184.9]	-182.3 ± 5.0
SF ₃ O	-141.0	-141.8		-142.7	-143.4	
SF ₂ O ₂	-179.2 [-178.9]	-181.0 [180.6]	-179.3 ± 2.0	-181.2 [-180.9]	-182.9 [-182.6]	-181.2 ± 2.0
SF ₅	-202.2		-214.7 ± 3.6	-204.6		-217.0 ± 3.6

			-207.9 ± 2.7^b			-210.2 ± 2.7^b
SF ₄ O	-212.2 [-212.0]	-213.1 [-212.9]		-214.7 [-214.5]	-215.6 [-215.4]	
SF ₅ O	-214.8			-218.0		
SF ₆	-288.5 [-288.3]	-288.9 [-288.7]	-288.4 ± 0.2	-291.8 [-291.6]	-292.2 [-292.0]	-291.6 ± 0.2

^a Values in square brackets use Douglas-Kroll method for the scalar relativistic correction. Experimental data from Reference 14. ^b

Reference 29.

Table 10.6. Electronic Contribution to the CCSD(T) Singlet-Triplet Splitting (kcal/mol) for SF_xO_y and PF_xO_y compounds.

Molecule	aV(D+d)Z	aV(T+d)Z	aV(Q+d)Z	CBS	CBS + ZPE^a
PFO	79.3	83.5	85.1	86.0	85.1
PF ₃	88.4	90.4	91.7	92.5	92.0
SF ₂	44.8	48.5	49.5	50.1	49.8
SF ₂ O	78.0	84.0	85.1	85.6	84.9
SF ₄	61.0	65.9	66.9	67.4	67.0
SF ₄ O	67.6	78.4	81.0	82.3	80.7

^a ZPE for singlets in Table 10.4. ZPE for triplets from MP2/aV(T+d)Z calculations.

Figure Captions

Figure 10.1 Adiabatic and diabatic BDEs for PF_x in kcal/mol. Unique diabatic BDEs in red. Spin density contour level = 0.05 a.u. in radicals except for PF_2 with a contour level of 0.035 a.u. Orange = P, blue-green = F, red = O and yellow = S. Contour levels obtained with density functional theory at the B3LYP/DZVP2 level.

Figure 10.2 Adiabatic and diabatic BDEs for PF_xO in kcal/mol. See Figure 10.1 caption.

Figure 10.3 Adiabatic and diabatic BDEs for SF_x in kcal/mol. See Figure 10.1 caption.

Figure 10.4 Adiabatic and diabatic BDEs for SF_xO in kcal/mol. See Figure 10.1 caption.

Figure 10.5 Adiabatic and diabatic BDEs for SF_xO_2 in kcal/mol. See Figure 10.1 caption.

Figure 10.1.

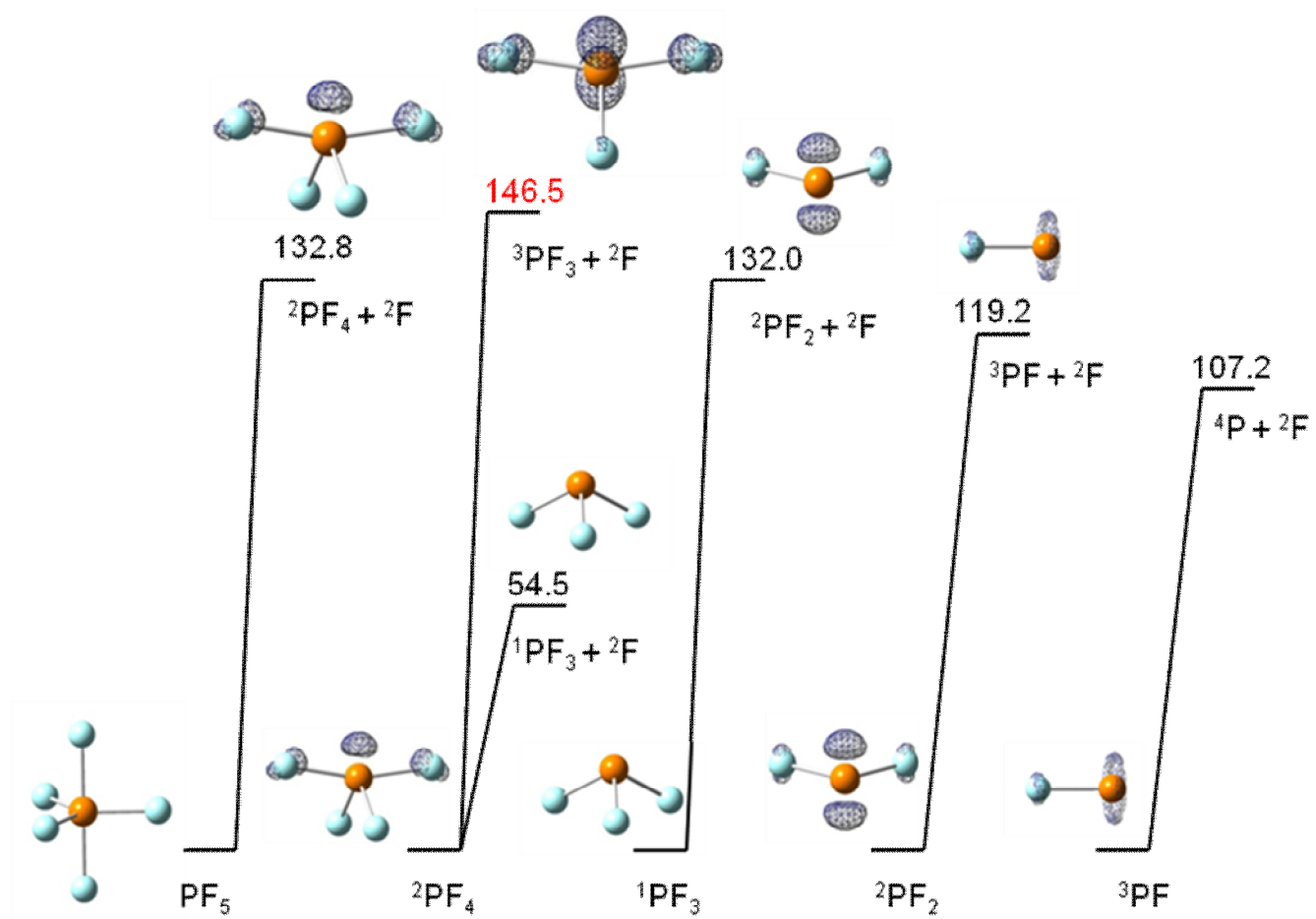


Figure 10.2.

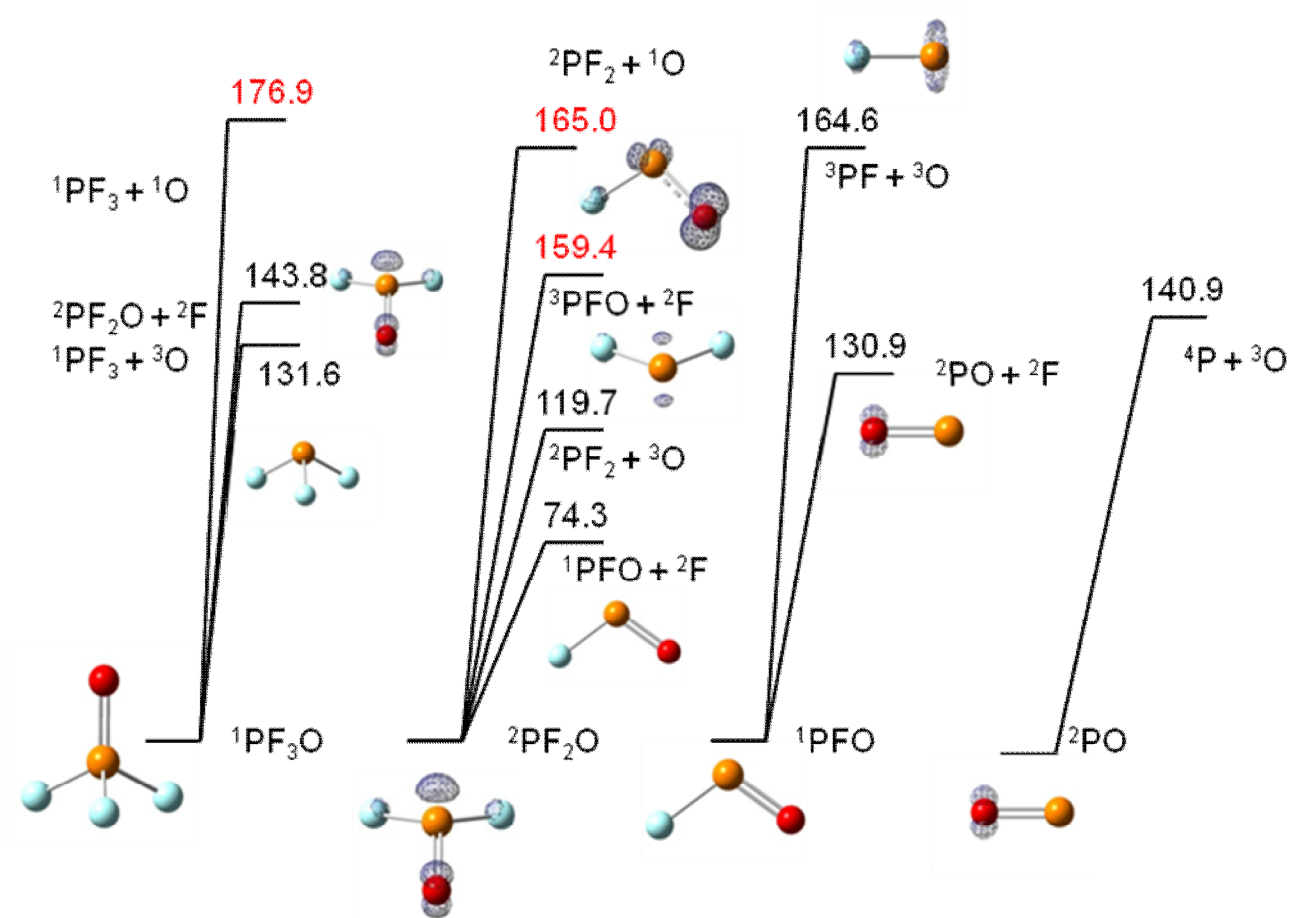


Figure 10.3.

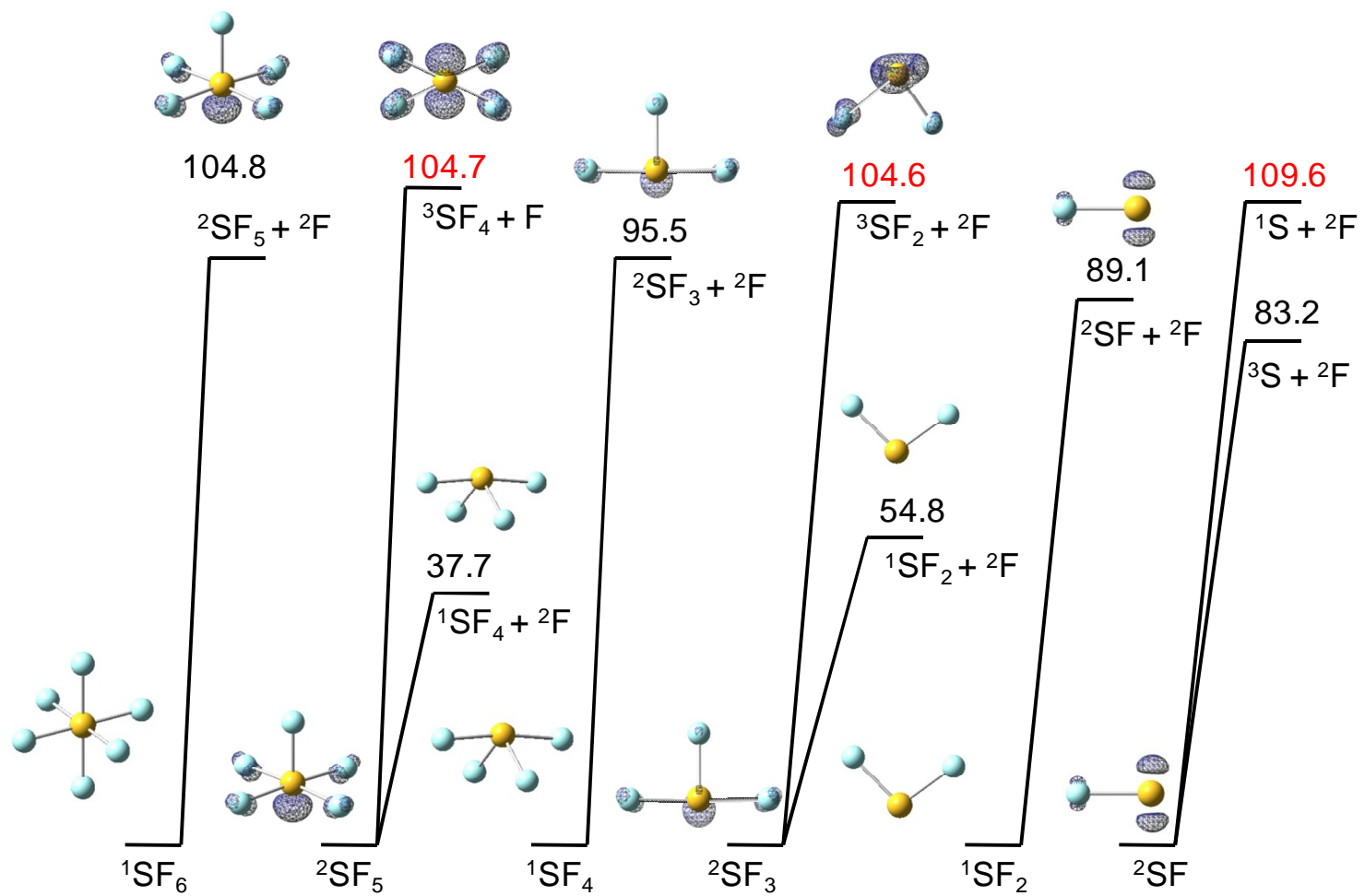


Figure 10.4.

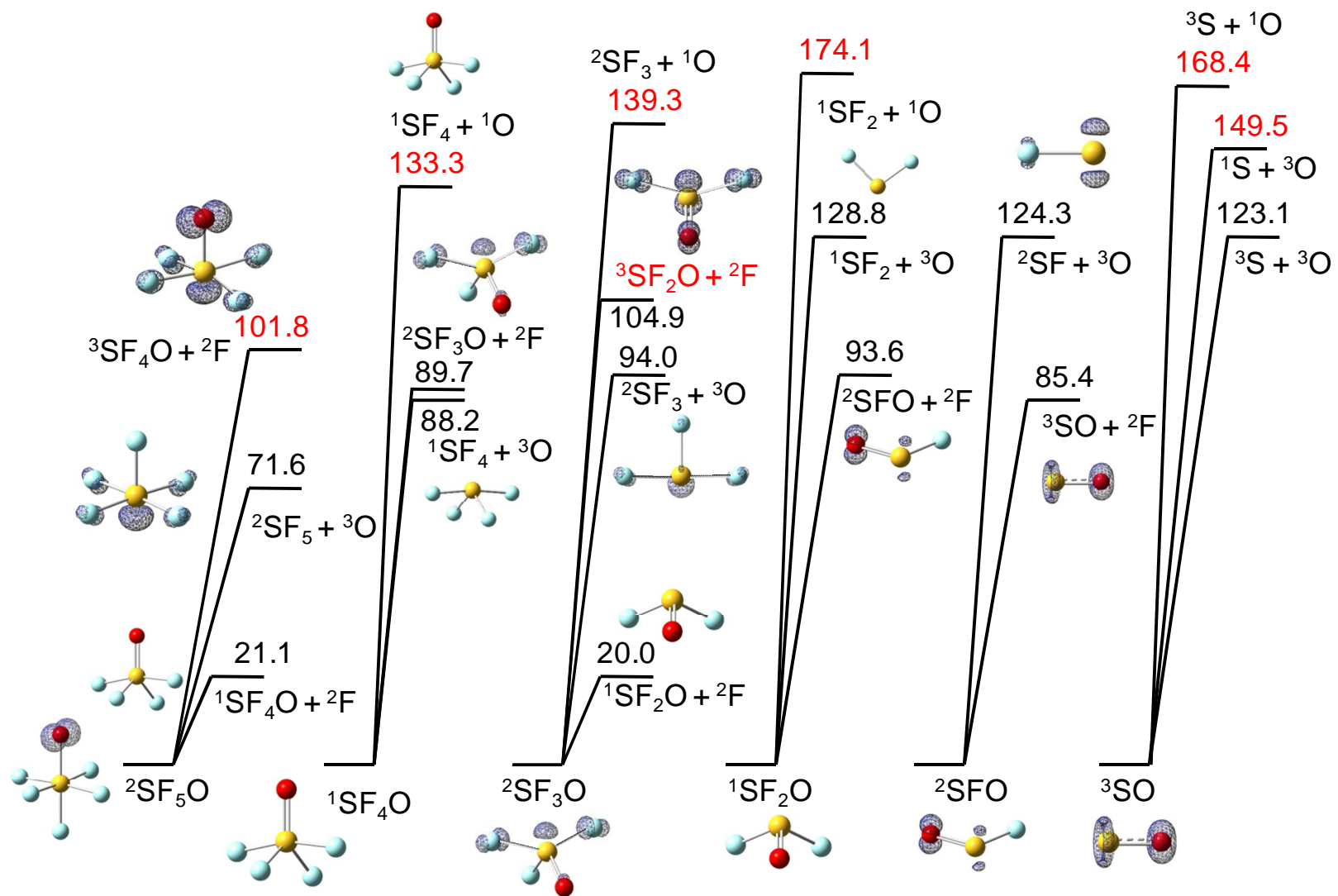
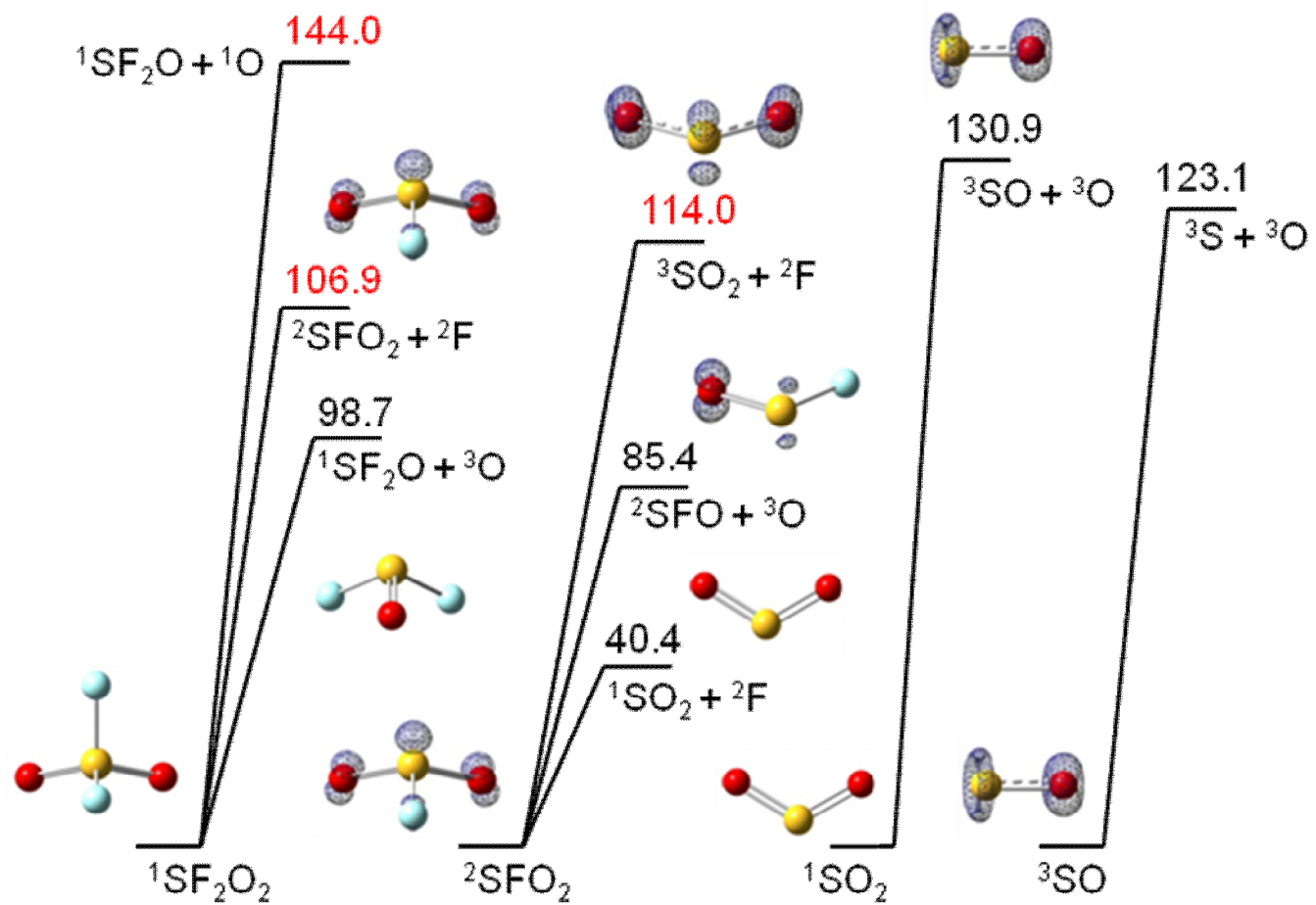


Figure 10.5.



10.5 References

- ¹ Greenwood, N. N.; Earnshaw, A. *Chemistry of the Elements*, Pergamon Press, Oxford, 1984.
- ² (a) Nicolaides, A.; Borden, W. T. *J. Am. Chem. Soc.* **1991**, *113*, 6750; (b) Wang, S. Y.; Borden, W. T. *J. Am. Chem. Soc.* **1989**, *111*, 7282.
- ³ (a) Carter, E. A.; Goddard, W. A., III, *J. Am. Chem. Soc.* **1988**, *110*, 4077; (b) Carter, E. A.; Goddard, W. A., III, *J. Phys. Chem.* **1986**, *90*, 998.
- ⁴ Grant, D. J.; Dixon, D. A. *J. Phys. Chem.* **2006**, *110*, 12955.
- ⁵ Dunning, T. H., Jr. *J. Phys. Chem.* **2000**, *104*, 9062.
- ⁶ (a) Peterson, K. A.; Xantheas, S. S.; Dixon, D. A.; Dunning, T. H. Jr., *J. Phys. Chem. A* **1998**, *102*, 2449; (b) Feller, D.; Peterson, K. A. *J. Chem. Phys.* **1998**, *108*, 154; (c) Dixon, D. A.; Feller, D. *J. Phys. Chem. A* **1998**, *102*, 8209; (d) Feller, D.; Peterson, K. A. *J. Chem. Phys.* **1999**, *110*, 8384; (e) Feller, D.; Dixon, D. A. *J. Phys. Chem. A* **1999**, *103*, 6413; (f) Feller, D. *J. Chem. Phys.* **1999**, *111*, 4373; (g) Feller, D.; Dixon, D. A. *J. Phys. Chem. A* **2000**, *104*, 3048; (h) Feller, D.; Sordo, J. A. *J. Chem. Phys.* **2000**, *113*, 485; (i) Feller, D.; Dixon, D. A. *J. Chem. Phys.* **2001**, *115*, 3484; (j) Dixon, D. A.; Feller, D.; Sandrone, G. *J. Phys. Chem. A* **1999**, *103*, 4744; (k) Ruscic, B.; Wagner, A. F.; Harding, L. B.; Asher, R. L.; Feller, D.; Dixon, D. A.; Peterson, K. A.; Song, Y.; Qian, X.; Ng, C.; Liu, J.; Chen, W.; Schwenke, D. W. *J. Phys. Chem. A* **2002**, *106*, 2727; (l) Feller, D.; Dixon, D. A.; Peterson, K. A. *J. Phys. Chem. A*, **1998**, *102*, 7053; (m) Dixon, D. A.; Feller, D.; Peterson, K. A. *J. Chem. Phys.*, **2001**, *115*, 2576; (n) Pollack, L.; Windus, T. L.; de Jong, W. A.; Dixon, D. A. *J. Phys. Chem. A* **2005**, *109*, 6934.
- ⁷ Purvis III, G. D.; Bartlett, R. J. *J. Chem. Phys.* **1982**, *76*, 1910.
- ⁸ Raghavachari, K.; Trucks, G. W.; Pople, J. A.; Head-Gordon, M. *Chem. Phys. Lett.* **1989**, *157*, 479.
- ⁹ Watts, J. D.; Gauss, J.; Bartlett, R. J. *J. Chem. Phys.* **1993**, *98*, 8718.
- ¹⁰ Dunning, T. H. *J. Chem. Phys.* **1989**, *90*, 1007.
- ¹¹ Kendall, R. A.; Dunning Jr., T. H.; Harrison, R. J. *J. Chem. Phys.* **1992**, *96*, 6796.
- ¹² McQuarrie, D. A. *Statistical Mechanics*, University Science Books: Sausalito, CA, 2001.
- ¹³ Curtiss, L. A.; Raghavachari, K.; Redfern, P. C.; Pople, J. A. *J. Chem. Phys.* **1997**, *106*, 1063.
- ¹⁴ Chase, M. W., Jr. NIST-JANAF Tables (4th Edition), *J. Phys. Chem. Ref. Data*, Mono. 9, Suppl. 1 (1998). See also Linstrom, P. J.; Mallard, W. G., Eds., *NIST Chemistry WebBook*, NIST Standard Reference Database Number 69, June 2005, National Institute of Standards and Technology, Gaithersburg MD, 20899, (<http://webbook.nist.gov/chemistry/>).

-
- ¹⁵ Luo, T. -R. *Comprehensive Handbook of Chemical Bond Energies*; CRC Press, Taylor & Francis Group: Boca Raton, FL, 2007.
- ¹⁶ Ahlrichs, R.; Becherer, R.; Binnewies, M.; Borrmann, H.; Lakenbrink, M.; Schunck, S.; Schnöckel, H. *J. Am. Chem. Soc.* **1986**, *108*, 7905.
- ¹⁷ Beckers, H.; Bürger, H.; Papelewski, P.; Bogey, M.; Demaison, J.; Dréan, P.; Walters, A.; Breidung, J.; Thiel, W. *Phys. Chem. Chem. Phys.* **2001**, *3*, 4247.
- ¹⁸ Gustev, G. L. *J. Chem. Phys.* **1993**, *98*, 444.
- ¹⁹ Tschumper, G. S.; Fermann, J. T.; Schaefer III, H. F. *J. Chem. Phys.* **104**, *10*, 3676.
- ²⁰ Gu, J.; Leszczynski, J. *J. Phys. Chem. A* **1999**, *103*, 7856.
- ²¹ Bott, J. F.; Jacobs, T. A. *J. Chem. Phys.* **1969**, *50*, 3850.
- ²² Harland, P. W.; Thynne, J. C. *J. Phys. Chem.* **1971**, *75*, 3517.
- ²³ Hildebrand, D. L. *J. Phys. Chem.* **1973**, *77*, 897.
- ²⁴ Lyman, J. L. *J. Chem. Phys.* **1977**, *67*, 1868.
- ²⁵ Benson, S. W. *J. Am. Chem. Soc.* **1978**, *78*, 23.
- ²⁶ Kiang, T.; Estler, R. C.; Zare, R. N. *J. Chem. Phys.* **1979**, *70*, 5925.
- ²⁷ Kiang, T.; Zare, R. N. *J. Am. Chem. Soc.* **1980**, *102*, 4024.
- ²⁸ Babcock, L. M.; Streit, G. E. *J. Chem. Phys.* **1981**, *74*, 5700.
- ²⁹ Tsang, W.; Herron, J. T. *J. Chem. Phys.* **1992**, *96*, 4272.
- ³⁰ Fisher, E. R.; Kickel, B. L.; Armentrout, P. B. *J. Chem. Phys.* **1992**, *97*, 4859.
- ³¹ Stevens-Miller, A. E.; Miller, T. M.; Viggiano, A. A.; Morris, R. A.; Van Doren, J. M.; Arnold, S. T.; Paulson, J. F. *J. Chem. Phys.* **1995**, *102*, 8865.
- ³² Endo, Y.; Saito, S.; Hirota, E. *J. Chem. Phys.* **1981**, *74*, 1568.
- ³³ Kronberg, M.; Ahsen von, S.; Willner, H.; Francisco, J. S. *Angew. Chem. Int. Ed.* **2005**, *44*, 253.
- ³⁴ Ziegler, T.; Gustev, G. L. *J. Chem. Phys.* **1992**, *96*, 7623.

-
- ³⁵ Irikura, K. K. *J. Chem. Phys.* **1995**, *102*, 5357.
- ³⁶ Cheung, Y. -S.; Chen, Y. -J.; Ng, C. Y.; Chiu, See-Wing; Li, Wai-Kee *J. Am. Chem. Soc.* **1995**, *117*, 9725.
- ³⁷ King, R. A.; Galbraith, J. M.; Schaefer III, H. F. *J. Phys. Chem.* **1996**, *100*, 6061.
- ³⁸ Bauschlicher Jr., C. W.; Ricca, A. *J. Phys. Chem.* **1998**, *102*, 4722.
- ³⁹ Miller, T. M.; Arnold, S. T.; Viggiano, A. A. *Inter. J. Mass. Spec.* **2003**, *227*, 413.
- ⁴⁰ Dunning, T. H. Jr., Peterson, K. A. Wilson, A. K. *J. Chem. Phys.* **2001**, *114*, 9244.
- ⁴¹ Werner, H.-J.; Knowles, P. J.; Amos, R. D.; Bernhardsson, A.; Berning, A.; Celani, P.; Cooper, D. L.; Deegan, M. J. O.; Dobbyn, A. J.; Eckert, F.; Hampel, C.; Hetzer, G.; Korona, T.; Lindh, R.; Lloyd, A. W.; McNicholas, S. J.; Manby, F. R.; Meyer, W.; Mura, M. E.; Nicklass, A.; Palmieri, P.; Pitzer, R. M.; Rauhut, G.; Schütz, M.; Stoll, H.; Stone, A. J.; Tarroni, R.; Thorsteinsson, T. MOLPRO-2002, a package of initio programs written by, Universität Stuttgart, Stuttgart, Germany, University of Birmingham, Birmingham, United Kingdom, 2002.
- ⁴² Rittby, M.; Bartlett, R. J. *J. Phys. Chem.* **1988**, *92*, 3033.
- ⁴³ Knowles, P. J.; Hampel, C.; Werner, H. -J. *J. Chem. Phys.* **1994**, *99*, 5219.
- ⁴⁴ Deegan, M. J. O.; Knowles, P. J. *Chem. Phys. Lett.* **1994**, *227*, 321.
- ⁴⁵ Gaussian 03, Revision C.02, Frisch, M. J.; Trucks, G. W.; Schlegel, H. B.; Scuseria, G. E.; Robb, M. A.; Cheeseman, J. R.; Montgomery, Jr., J. A.; Vreven, T.; Kudin, K. N.; Burant, J. C.; Millam, J. M.; Iyengar, S. S.; Tomasi, J.; Barone, V.; Mennucci, B.; Cossi, M.; Scalmani, G.; Rega, N.; Petersson, G. A.; Nakatsuji, H.; Hada, M.; Ehara, M.; Toyota, K.; Fukuda, R.; Hasegawa, J.; Ishida, M.; Nakajima, T.; Honda, Y.; Kitao, O.; Nakai, H.; Klene, M.; Li, X.; Knox, J. E.; Hratchian, H. P.; Cross, J. B.; Bakken, V.; Adamo, C.; Jaramillo, J.; Gomperts, R.; Stratmann, R. E.; Yazyev, O.; Austin, A. J.; Cammi, R.; Pomelli, C.; Ochterski, J. W.; Ayala, P. Y.; Morokuma, K.; Voth, G. A.; Salvador, P.; Dannenberg, J. J.; Zakrzewski, V. G.; Dapprich, S.; Daniels, A. D.; Strain, M. C.; Farkas, O.; Malick, D. K.; Rabuck, A. D.; Raghavachari, K.; Foresman, J. B.; Ortiz, J. V.; Cui, Q.; Baboul, A. G.; Clifford, S.; Cioslowski, J.; Stefanov, B. B.; Liu, G.; Liashenko, A.; Piskorz, P.; Komaromi, I.; Martin, R. L.; Fox, D. J.; Keith, T.; Al-Laham, M. A.; Peng, C. Y.; Nanayakkara, A.; Challacombe, M.; Gill, P. M. W.; Johnson, B.; Chen, W.; Wong, M. W.; Gonzalez, C.; and Pople, J. A.; Gaussian, Inc., Wallingford CT, 2004.
- ⁴⁶ Dunham, J. L. *Phys. Rev.* **1932**, *41*, 721.
- ⁴⁷ Peterson, K. A.; Woon, D. E.; Dunning, T. H., Jr. *J. Chem. Phys.* **1994**, *100*, 7410.
- ⁴⁸ Lee, T. J.; Rice, J. E.; Scuseria, G. E.; Schaefer, H. F., III, *Theor. Chim. Acta* **1989**, *75*, 81.

-
- ⁴⁹ (a) Peterson, K. A.; Dunning, T. H., Jr., *J. Chem. Phys.* **2002**, *117*, 10548; (b) Woon, D. E.; Dunning, T. H., Jr., *J. Chem. Phys.* **1993**, *98*, 1358.
- ⁵⁰ Davidson, E. R.; Ishikawa, Y.; Malli, G. L. *Chem. Phys. Lett.* **1981**, *84*, 226.
- ⁵¹ (a) Douglas, M.; Kroll, N. M. *Ann. Phys.* **1974**, *82*, 89-155. (b) Hess, B. A. *Phys. Rev. A* **1985**, *32*, 756-763. (c) Hess, B. A. *Phys. Rev. A* **1986**, *33*, 3742-3748.
- ⁵² de Jong, W.A.; Harrison, R.J.; Dixon, D.A. *J. Chem. Phys.* **2001**, *114*, 48.
- ⁵³ EMSL basis set library. <http://www.emsl.pnl.gov/forms/basisform.html>
- ⁵⁴ Moore, C. E. *Atomic Energy Levels*; Vol. U.S. National Bureau of Standards Circular: Washington, D.C., 1949, 467, NBS.
- ⁵⁵ Huber, K.P.; Herzberg, G., *Molecular Spectra and Molecular Structure. IV. Constants of Diatomic Molecules*, Van Nostrand Reinhold Co., New York, 1979.
- ⁵⁶ (a) Martin, J. M. L.; Uzan, O. *Chem. Phys. Lett.* **1998**, *282*, 16; (b) Martin, J. M. L. *J. Chem. Phys.* **1998**, *108*, 2791.
- ⁵⁷ (a) Bauschlicher, C. W., Jr.; Partridge, H. *Chem. Phys. Lett.* **1995**, *240*, 533; (b) Bauschlicher, C. W., Jr.; Ricca, A. *J. Phys. Chem.* **1998**, *102*, 8044.
- ⁵⁸ Kuchitsu, K. Ed. *Structure of Free Polyatomic Molecules - Basic Data*; Springer: Berlin, 1998.
- ⁵⁹ Hellwege, K. H.; Hellwege A. M., Eds. *Landolt-Bornstein: Group II: Atomic and Molecular Physics Volume 7: Structure Data of Free Polyatomic Molecules*; Springer-Verlag: Berlin, 1976; Moritani, T.; Kuchitsu, K.; Morino, Y. *Inorg. Chem.* **1971**, *10*, 344.
- ⁶⁰ (a) Harmony, M. D.; Laurie, V. W.; Kuczkowski, R. L.; Schwendeman, R. H.; Ramsey, D. A.; Lovas, F. J.; Lafferty, W. J.; Maki, A. G. *J. Phys. Chem. Ref. Data* **1979**, *8*, 619; (b) Kagann, R. H.; Ozier, I.; Gerry, M. C. L. *Chem. Phys. Lett.* **1977**, *47*, 572; (c) Smith, J. G. *Mol. Phys.* **1976**, *32*, 621.
- ⁶¹ Gurvich, L.V.; Veyts, I. V.; Alcock, C. B., *Thermodynamic Properties of Individual Substances*, Fourth Edition; Hemisphere Pub. Co.: New York, 1989.
- ⁶² Endo, Y.; Saito, S.; Hirota, E.; Chikaraishi, T. *J. Mol. Spectrosc.* **1979**, *77*, 222.
- ⁶³ (a) Ferguson, R. C. *J. Am. Chem. Soc.* **1954**, *76*, 850; (b) Lucas, N. J. D.; Smith, J. G. *J. Mol. Spectrosc.* **1972**, *43*, 327.
- ⁶⁴ Tolles, W. M.; Gwinn, W. D. *J. Chem. Phys.* **1962**, *36*, 1119.

-
- ⁶⁵ Kimura, K.; Bauer, S. H. *J. Chem. Phys.* **1963**, *39*, 3172.
- ⁶⁶ Lide, D. R.; Mann, D. E.; Fristom, R. M. *J. Chem. Phys.* **1957**, *26*, 734.
- ⁶⁷ Gundersen, G.; Hedberg, K. *J. Chem. Phys.* **1969**, *51*, 2500.
- ⁶⁸ Hencher, J. L.; Cruickshank, D. W. J.; Bauer, S. H. *J. Chem. Phys.* **1968**, *48*, 518.
- ⁶⁹ Zhao, Y.; Setser, D. W. *Chem. Phys. Lett.*, **1993**, *210*, 362.
- ⁷⁰ Saito, S.; Endo, Y.; Hirota, E. *J. Chem. Phys.* **1986**, *85*, 1778.
- ⁷¹ Shimanouchi, T. *Tables of Molecular Vibrational Frequencies Consolidated Volume I*, NSRDS-NBS 39; National Bureau of Standards: Washington DC, 1972.
- ⁷² Shimanouchi, T. *J. Phys. Chem. Ref. Data*, **1977**, *6*, 993.
- ⁷³ Haas, A.; Willner, H. *Spectrochim. Acta*, **1978**, *34A*, 541.
- ⁷⁴ Endo, Y.; Saito, S.; Hirota, E. *J. Chem. Phys.*, **1981**, *74*, 1568.
- ⁷⁵ Hassanzadeh, P.; Andrews, L. *J. Phys. Chem.*, **1992**, *96*, 79.
- ⁷⁶ Christe, K. O.; Willner, H.; Sawodny, W. *Spectrochim. Acta, Part A* **1979**, *35A*, 1347.
- ⁷⁷ Sawodny, W.; Birk, K.; Fogarasi, G.; Christe, K. O. *Z. Naturforsch., B* **1980**, *358*, 1137.
- ⁷⁸ Kronberg, M.; von Ahsen, S.; Willner, H.; Francisco, J. S. *Angew. Chem. Int. Ed.*, **2005**, *44*, 253.
- ⁷⁹ Christe, K. O.; Schack, C. J.; Curtis, E. C. *Spectrochim. Acta, Part A* **1977**, *33A*, 323.
- ⁸⁰ Christe, K. O.; Dixon, D. A.; Goldberg, I. B.; Schack, C. J.; Walther, B. W.; Wang, J. T.; Williams, F. *J. Am. Chem. Soc.* **1993**, *115*, 1129.
- ⁸¹ McDowell, R. S.; Aldridge, J. P.; Holland, R. F. *J. Phys. Chem.* **1976**, *80*, 1203.
- ⁸² Gutowski, K. E.; Dixon, D. A. *J. Phys. Chem. A*, **2006**, *110*, 12044.
- ⁸³ (a) Reed, A. E.; Curtiss, L. A.; Weinhold, F. *Chem. Rev.* **1988**, *88*, 899; (b) Foster, J. P.; Weinhold, F. *J. Am. Chem. Soc.* **1980**, *102*, 7211; (c) Reed, A. E.; Weinhold, F. *J. Chem. Phys.*, **1983**, *78*, 4066; (d) Reed, A. E.; Weinstock, R. B.; Weinhold, F. *J. Chem. Phys.*, **1985**, *83*, 735; (e) Reed, A. E.; Weinhold, F. *J. Chem. Phys.*, **1985**, *83*, 1736; (f) Weinhold, F.; Landis, C. R. *Valency and Bonding: A Natural Bond Orbital Donor-Acceptor Perspective*; Cambridge U. Press, 2003.

⁸⁴ (a) Becke, A. D. *J. Chem. Phys.* **1993**, *98*, 5648; (b) Lee, C.; Yang, W.; Parr, R. G. *Phys. Rev. B*, **1988**, *37*, 785.

⁸⁵ Godbout, N.; Salahub, D. R.; Andzelm, J.; Wimmer, E. *Can. J. Chem.* **1992**, *70*, 560.

⁸⁶ Bauschlicher, C. W., Jr. *J. Phys. Chem A* **2000**, *104*, 2281.

⁸⁷ Herzberg, G., *Molecular Spectra and Molecular Structure. III. Electronic Spectra and Electronic Structure of Polyatomic Molecules*, Van Nostrand Reinhold Co., New York, 1966.

10.6 Appendix

Table A10.1. Total CCSD(T) Energies (E_h) as a Function of Basis Set.

Molecule	Basis Set					
	aV(D+d)Z	aV(T+d)Z	aV(Q+d)Z	aV(5+d)Z	CBS (DTQ)	CBS (Q5)
PO ($^2\Pi$)	-415.916101	-416.017132	-416.046494	-416.056280	-416.062842	-416.066548
PF ($^3\Sigma^-$)	-440.499816	-440.616017	-440.652014	-440.663934	-440.672323	-440.676441
PFO	-515.657795	-515.850608	-515.909765	-515.929554	-515.943077	-515.950317
PF ₂	-540.221101	-540.430049	-540.495900	-540.517815	-540.533180	-540.540808
PF ₃	-639.963634	-640.266594	-640.362005	-640.393763	-640.416011	-640.427083
PF ₂ O	-615.311025	-615.597339	-615.685601	-615.715079	-615.735350	-615.746007
PF ₃ O	-751.068133	-751.452832	-715.570861	-715.610364	-715.637374	-715.651810
PF ₄	-739.590118	-739.983535	-740.106665		-740.176277	
PF ₅	-839.335209	-839.824266	-839.976420	-840.027534	-840.062339	-840.081163
SF	-497.281440	-497.413252	-497.454133	-497.467670	-497.477204	-497.481872
SO ($^3\Sigma^-$)	-472.713608	-472.827065	-472.860362	-472.871392	-472.878940	-472.882965
SF ₂	-596.958878	-597.181618	-597.251546	-597.274976	-597.291104	-597.299559
SFO	-572.380615	-572.586576	-572.649536	-572.670657	-572.684963	-572.692817
SF ₃	-696.589960	-696.897215	-696.994142	-697.026786	-697.049025	-697.061035
SF ₂ O	-672.063366	-672.362338	-672.454543	-672.485616	-672.506519	-672.518218
SFO ₂	-647.416417	-647.698933	-647.784453	-647.813310	-647.832479	-647.843586
SF ₄	-796.274905	-796.677343	-796.803420	-796.846004	-796.874712	-796.890682
SF ₃ O	-771.636689	-772.023501	-772.143376	-772.183796	-772.211015	-772.226204
SF ₂ O ₂	-747.115652	-747.496564	-747.611981	-747.651022	-747.676808	-747.691983

SF ₅	-895.875986	-896.368593	-896.522315		-896.609171	
SF ₄ O	-871.312267	-871.794871	-871.943709	-871.993997	-872.027609	-872.046758
SF ₅ O	-970.902065	-971.463086	-971.636574		-971.734422	
SF ₆	-995.578681	-996.165955	-996.348325	-996.410094	-996.451269	-996.474900

Table A10.2. Optimized Bond Lengths (\AA) and Angles (degrees) for the PF_xO_y compounds.^a

Molecule	Basis Set	R_{PF}	R_{PO}	$\angle\text{FPF}$	$\angle\text{FPO}$
PO ($^2\Pi$)	aV(D+d)Z		1.5147		
PF ($^3\Sigma^-$)	aV(D+d)Z	1.6514			
PFO	aV(D+d)Z	1.6384	1.4861		109.77
PF ₂	aV(D+d)Z	1.6336		97.79	
PF ₃	aV(D+d)Z	1.6144		97.04	
PF ₂ O	aV(D+d)Z	1.6038	1.4883	98.03	116.22
PF ₃ O	aV(D+d)Z	1.5685	1.4607	99.93	117.86
PF ₄	aV(D+d)Z	1.5843 eq		94.53 eq	
		1.6425 ax		165.23 ax	
PF ₅	aV(D+d)Z	1.5729 eq		120.0 eq	
		1.6088 ax		90.0 ax	

Table A10.3. Calculated vibrational MP2/aug-cc-pV(T+d)Z frequencies (cm^{-1}) for the PF_xO_y compounds.

Molecule	Symmetry	Calculated	Experimental
PO ($^2\Pi$) ^a	ω_e	1230.8 ^b	1233.34
	$\omega_e\chi_e$	6.4 ^c	6.56
PF ($^3\Sigma$) ^a	ω_e	845.5 ^b	846.75
	$\omega_e\chi_e$	4.5 ^c	4.489
PFO	a'	1269.5	1297.5 ^e
	a'	808.7	819.6 ^e
	a'	400.4	416.0 ^f
PF ₂	a_1	859.0	841(4) ^g
	a_1	363.9	366 ^g
	b_2	839.2	848(24) ^h
PF ₃ ⁱ	a_1	889.4	892
	a_1	480.8	487
	e	856.7	860
	e	342.6	344
PF ₂ O	a'	1355.5	
	a'	860.9	
	a'	486.5	
	a''	902.8	
	a''	354.2	
PF ₃ O ^j	a_1	1415.1	1417
	a_1	868.1	873
	a_1	473.7	472
	e	987.9	991
	e	465.5	482
	e	329.2	336
PF ₄	a_1	913.3	
	a_1	489.6	
	a_2	396.3	

	b ₁	952.9	
	b ₁	284.9	
	b ₂	879.9	
	b ₂	483.4	
PF ₅ ^j	a ₁ '	814.4	816
	a ₁ '	646.3	648
	a ₂ "	950.7	947
	a ₂ "	569.5	575
	e'	1023.3	1024
	e'	525.2	533
	e'	172.8	174
	e"	507.1	520

^a Huber, K.P.; Herzberg, G., *Molecular Spectra and Molecular Structure. IV. Constants of Diatomic Molecules*, Van Nostrand Reinhold Co., 1979. ^b Harmonic frequency obtained from the fifth order fitting of the PES at the CCSD(T)/aV(Q+d)Z geometry. ^c Anharmonic constant, $\omega_e\chi_e$, obtained from the fifth order fitting of the PES at the CCSD(T)/aV(Q+d)Z geometry. ^e Beckers, H.; Bürger, H.; Paplewski, P.; Bogey, M.; Demaison, J.; Dréan, P.; Walters, A.; Breidung, J.; Thiel, W. *Phys. Chem. Chem. Phys.* **2001**, *3*, 4247. ^f Ahlrichs, R.; Becherer, R.; Binnewies, M.; Borrmann, H.; Lakenbrink, M.; Schunck, S.; Schnöckel, H.. *J. Am. Chem. Soc.* **1986**, *108*, 7905. ^g Zhao, Y.; Setser, D. W. *Chem. Phys. Lett.*, **1993**, *210*, 362. ^h Saito, S.; Endo, Y.; Hirota, E. *J. Chem. Phys.* **1986**, *85*, 1778. ⁱ Shimanouchi, T. *Tables of Molecular Vibrational Frequencies Consolidated Volume I*, NSRDS-NBS 39; National Bureau of Standards: Washington DC, 1972. ^j Shimanouchi, T. *J. Phys. Chem. Ref. Data*, **1977**, *6*, 993.

Table A10.4. Calculated vibrational MP2/aug-cc-pV(T+d)Z frequencies (cm^{-1}) for the SF_xO_y compounds.

Molecule	Symmetry	Calculated	Experimental
SF ($^2\Pi$) ^a	ω_e	839.3 ^b	820
	$\omega_e\chi_e$	4.4 ^c	
SO ($^3\Sigma^-$) ^a	ω_e	1152.6 ^b	1149.2
	$\omega_e\chi_e$	6.2 ^c	5.6
SF ₂ ^d	a ₁	848.3	832
	a ₁	352.2	358
	b ₂	819.5	804
SFO ^e	a'	1412.0	1215
	a'	754.6	763
	a'	394.0	396
SF ₃ ^f	a'	865.2	843.8
	a'	581.6	
	a'	369.0	
	a'	177.6	
	a''	718.5	681.8
	a''	475.9	
SF ₂ O ^g	a'	1359.3	1333
	a'	799.0	808
	a'	522.0	530
	a'	372.6	378
	a''	733.4	747
	a''	385.9	393
SFO ₂	a'	1188.2	
	a'	764.2	
	a'	546.7	
	a'	425.4	
	a''	1462.8	
	a''	406.9	

SF ₄ ^h	a ₁	898.6	892
	a ₁	557.2	558
	a ₁	530.4	532
	a ₁	225.5	228
	a ₂	466.5	[437]
	b ₁	733.6	730
	b ₁	535.7	475 ⁱ
	b ₂	870.7	867
	b ₂	352.8	353
SF ₃ O	a'	1369.5	
	a'	853.3	
	a'	623.3	
	a'	511.9	
	a'	342.5	
	a'	229.9	
	a''	779.4	
	a''	504.1	
	a''	412.2	
SF ₂ O ₂ ^g	a ₁	1285.4	1269
	a ₁	843.2	848
	a ₁	544.2	544
	a ₁	381.1	385
	a ₂	378.5	388
	b ₁	1528.7	1502
	b ₁	535.0	553
	b ₂	876.8	885
	b ₂	531.9	539
SF ₅ ^j	a ₁	897.4	891.7
	a ₁	662.6	633.0
	a ₁	566.6	553.4
	b ₁	472.4	
	b ₂	599.5	

	b ₂	244.3	
	e	863.5	817.8
	e	535.7	524.7
	e	366.0	387.2
SF ₄ O ^k	a ₁	1405.8	1380
	a ₁	800.2	795
	a ₁	589.0	587
	a ₁	565.7	566, ^l 455
	a ₁	180.0	174
	a ₂	560.3	
	b ₁	926.4	924
	b ₁	560.2	566
	b ₁	266.9	265
	b ₂	819.9	815
	b ₂	636.0	640
	b ₂	549.8	558
SF ₆	a _{1g}	778.9	774 ^m /773.6 ± 0.5 ⁿ
	e _g	643.5	642 ^m /642.1 ± 0.5 ⁿ
	t _{1u}	952.1	948 ^m /947.968 ± 0.001 ⁿ
	t _{1u}	613.1	616 ^m /615.03 ± 0.02 ⁿ
	t _{2g}	521.4	525 ^m /522.9 ± 0.5 ⁿ
	t _{2u}	345.0	347 ^m /346 ± 1 ⁿ

^a Huber, K.P.; Herzberg, G., *Molecular Spectra and Molecular Structure. IV. Constants of Diatomic Molecules*, Van Nostrand Reinhold Co., 1979. ^b Harmonic frequency obtained from the fifth order fitting of the PES at the CCSD(T)/aV(Q+d)Z geometry. ^c Anharmonic constant, $\omega_e\chi_e$, obtained from the fifth order fitting of the PES at the CCSD(T)/aV(Q+d)Z geometry. ^d Haas, A.; Willner, H. *Spectrochim. Acta*, **1978**, 34A, 541.. ^e Endo, Y.; Saito, S.; Hirota, E. *J. Chem. Phys.*, **1981**, 74, 1568. ^f Hassanzadeh, P.; Andrews, L. *J. Phys. Chem.*, **1992**, 96, 79. ^g Shimanouchi, T. *J. Phys. Chem. Ref. Data*, **1977**, 6, 993. ^h Christe, K. O.; Willner, H.; Sawodny, W. *Spectrochim. Acta, Part A* **1979**, 35A, 1347. ⁱ An alternative assignment for ν_7 , 532 cm⁻¹, has been given,

Sawodny, W.; Birk, K.; Fogarasi, G.; Christe, K. O. *Z. Naturforsch., B* **1980**, 358, 1137.^j
Kronberg, M.; von Ahsen, S.; Willner, H.; Francisco, J. S. *Angew. Chem. Int. Ed.*, **2005**, 44, 253.
^k Christe, K. O.; Schack, C. J.; Curtis, E. C. *Spectrochim. Acta, Part A* **1977**, 33A, 323 unless
noted.^l Christe, K. O.; Dixon, D. A.; Goldberg, I. B.; Schack, C. J.; Walther, B. W.; Wang, J. T.;
Williams, F. *J. Am. Chem. Soc.* **1993**, 115, 1129.^m Shimanouchi, T. *Tables of Molecular*
Vibrational Frequencies Consolidated Volume I, NSRDS-NBS 39; National Bureau of
Standards: Washington DC, 1972.ⁿ McDowell, R. S.; Aldridge, J. P.; Holland, R. F. *J. Phys.*
Chem. **1976**, 80, 1203.

Table A10.5. T_1 diagnostics from CCSD(T) calculations with the aug-cc-pV(T+d)Z basis set.

Molecule	T_1 Diagnostics
PO ($^2\Pi$)	0.0254
PF ($^3\Sigma^-$)	0.0161
PFO	0.0183
PF ₂	0.0167
PF ₃	0.0151
PF ₂ O	0.0210
PF ₃ O	0.0141
PF ₄	0.0166
PF ₅	0.0116
SF	0.0179
SO	0.0248
SF ₂	0.0152
SFO	0.0189
SF ₃	0.0216
SF ₂ O	0.0181
SFO ₂	0.0220
SF ₄	0.0155
SF ₃ O	0.0188
SF ₂ O ₂	0.0154
SF ₅	0.0158
SF ₄ O	0.0142
SF ₅ O	0.0143
SF ₆	0.0122

Table A10.6. Mulliken Charges and Natural Charges of the PF_xO_y and SF_xO_y Compounds at the B3LYP/DZVP2 Level.

Molecule	Mulliken Charges	Natural Charges
PFO	q _P (0.879)	q _P (1.519)
	q _O (-0.518)	q _O (-0.929)
	q _F (-0.361)	q _F (-0.590)
PF ₃ O	q _P (1.476)	q _P (2.664)
	q _O (-0.580)	q _O (-1.022)
	q _F (-0.299)	q _F (-0.547)
PF ₃	q _P (1.065)	q _P (1.744)
	q _F (-0.355)	q _F (-0.581)
PF ₅	q _P (1.605)	q _P (2.775)
	q _{Fax} (-0.352)	q _{Fax} (-0.579)
	q _{Feq} (-0.300)	q _{Feq} (-0.539)
SF ₂	q _S (0.647)	q _S (0.913)
	q _F (-0.323)	q _F (-0.457)
SF ₄	q _S (1.331)	q _S (1.995)
	q _F (-0.395)	q _F (-0.553)
	q _F (-0.270)	q _F (-0.445)
SF ₆	q _S (1.777)	q _S (2.820)
	q _F (-0.296)	q _F (-0.470)
SF ₂ O	q _S (1.183)	q _S (1.818)
	q _F (-0.330)	q _F (-0.497)
	q _O (-0.522)	q _O (-0.824)
SF ₄ O	q _S (1.692)	q _S (2.709)
	q _F (-0.339)	q _F (-0.504)
	q _F (-0.257)	q _F (-0.440)
	q _O (-0.501)	q _O (-0.820)
SF ₂ O ₂	q _S (1.599)	q _S (2.621)
	q _F (-0.282)	q _F (-0.471)
	q _O (-0.517)	q _O (-0.839)

Table S-7. Natural Bond Orbital Analysis of the PF_xO_y and SF_xO_y Compounds at the B3LYP/DZVP2 Level.

Molecule	Occupancies		Valence Lewis Structure			Hybridization		%Polarization ^a	Occupancy
	Lewis	Non-Lewis	Core	Bond	Lone Pair				
PFO ^b	31.71	0.29	7	3	6	P(sp ^{4.39} d ^{1.37})	O(sp ^{3.62})	18.9/81.1	1.943
						P(p)	O(p)	22.5/77.5	2.000
						P(sp ^{3.77} d ^{2.02})	F(sp ^{3.68})	12.3/87.7	1.941
PF ₃ O ^c	49.33	0.67	9	4	12	P(sp ^{1.77})	O(sp ^{2.75})	27.3/72.7	1.988
						P(sp ^{2.01} d ^{1.64})	F(sp ^{3.15})	14.7/85.3	1.926
PF ₃	41.69	0.31	8	3	10	P(sp ^{8.81})	F(sp ^{3.79})	16.6/83.4	1.992
PF ₅	59.29	0.71	10	5	15	P(sp ^{2.71} d ^{1.71})	F _{ax} (sp ^{3.94})	15.3/84.7	1.937
						P(sp ^{3.05} d ^{0.71})	F _{eq} (sp ^{3.72})	17.5/82.5	1.963
SF ₂	33.84	0.16	7	2	8	S(sp ^{10.45})	F(sp ^{5.59})	24.0 /76.0	1.997
SF ₄	51.42	0.58	9	4	13	S(sp ^{6.92} d ^{4.10})	F(sp ^{6.35})	16.3/83.7	1.927
						S(sp ^{7.69} d ^{1.23})	F(sp ^{5.49})	23.1/76.9	1.961
SF ₆	68.98	1.02	11	6	18	S(sp ^{3.00} d ^{2.00})	F(sp ^{5.28})	20.7/79.3	1.905
SF ₂ O	41.36	0.64	8	4	9	S(sp ^{7.62} d ^{3.19})	F(sp ^{5.85})	19.3/80.7	1.924
						S(sp ^{3.84})	O(sp ^{3.34})	33.5/66.5	1.992
						S(p ^{1.00} d ^{0.89})	O(p)	14.1/85.9	1.922
SF ₄ O	58.93	1.07	10	5	15	S(sp ^{3.01} d ^{1.92})	F(sp ^{6.19})	19.7/80.3	1.912
						S(sp ^{2.43} d ^{2.26})	F(sp ^{5.47})	19.4/80.6	1.877
						S(sp ^{1.94} d ^{0.26})	O(sp ^{3.64})	34.4/65.6	1.956
						S(sp ^{1.00} d ^{0.96})	O(p)	14.1/85.9	1.922

SF ₂ O ₂ ^c	48.75	1.25	9	4	12	S(sp ^{2.14} d ^{2.36})	F(sp ^{5.25})	17.6/82.6	1.869
						S(sp ^{1.40} d ^{1.22})	O(sp ^{4.29})	26.2/73.9	1.862

^a Polarization in the order P or S/O. ^b description of lone pairs on O. Hybridization: P(sp^{5.76}d^{3.58}) O(sp^{11.23}); %Polarization: 9.54/90.46;

Occupancy: 1.960. ^c description of lone pairs on O. Hybridization:P(p) O(p); %Polarization: 9.37/90.63; Occupancy: 1.956. ^d

description of lone pairs on O. Hybridization: S(sp^{8.84}d^{9.30}) O(sp^{28.43}); %Polarization: 12.2/87.8; Occupancy: 1.919

Summary of NBO analysis. For PFO, the Lewis structure of a P-F single bond, a P=O double bond, and a lone pair on P is consistent with the NBO analysis shown in Table S-7, which contains the NBO analysis for all of the closed shell molecules. One of the O atom lone pairs also exhibits about 10% backbonding onto the P. The NBO analysis of PF₃O shows the structure to have four bonds (three P-F bonds and one P-O bond) and 12 lone pairs of electrons consistent with a charge separated Lewis structure. Two of the electron lone pairs on O show about 10% back-bonding onto the P, consistent with a P=O bond and an expanded octet. The P-O bond is shorter than the P-F bond and has a much higher force constant, in agreement with this result. Noury et al. (Noury, S.; Silvi, B.; Gillespie, R. J. *Inorg. Chem.* **2002**, *41*, 2164) have used ELF analysis (Becke, A. D.; Edgecombe, K. E. *J. Chem. Phys.* **1990**, *92*, 5397) with the density generated at the B3LYP/6-311+G(2d,f) level of DFT to analyze the bonding in a number of main group compounds. For PF₃O, they find a valence population of 5.13 e on P, less than the Lewis value of 8 e and consistent with a charge separated Lewis structure.

PF₃ has a normal Lewis octet structure with a lone pair and three P-F bonds, whereas PF₅ has an expanded octet to accommodate 5 bonds. Both simple Lewis structures are consistent with the NBO analysis. The NBO analysis shows that the P-F bonds in PF₃ and PF₅ are quite ionic and that the ionicities are comparable within about 2%. The axial P-F bonds in PF₅ are predicted to be slightly more ionic than the equatorial P-F bonds. These results are consistent with those of the ELF analysis of Noury *et al.* (Noury, S.; Silvi, B.; Gillespie, R. J. *Inorg. Chem.* **2002**, *41*, 2164) with valence shell populations on P of 4.64 e and 5.33 e for PF₃ and PF₅ respectively.

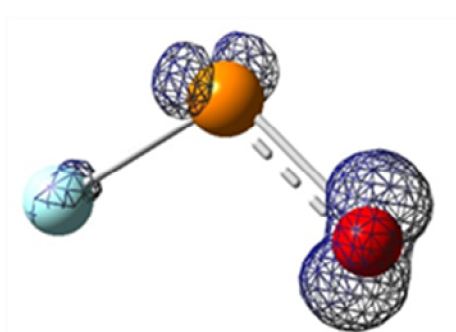
Similar results are found for the sulfur compounds. For SF₂, the NBO analysis is consistent with a normal Lewis structure. The NBO analysis for SF₂O can be interpreted in two

ways. The first is that there are two S-F bonds, an S-O bond and a delocalized lone pair with 14% of the population on the S. The second way is to describe this delocalized lone pair as a very ionic π -bond between the S and O. For SF₂O, the expanded Lewis octet with the S=O double bond is a better description of the geometry and force constants. The addition of another O atom to form SF₂O₂ leads to the same observations as for PF₃O. The NBO analysis shows that SF₂O₂ contains four bonds and 12 lone pairs of electrons. Two of the lone pairs on O are about 12% back-bonded to the S, intermediate between the 10% backbonding found in PF₃O and the 14% used to describe the ionic π -bond in SF₂O. In SF₄O, the S-O bond distances are clearly shorter than the S-F bonds so the expanded Lewis structure with a double S=O bond provides a good description of the geometry. The NBO analysis of SF₄O can be interpreted as having 6 bonds depending on the cut-off for delocalization. There are four S-F bonds, one S-O bond, and a lone pair on O with 14% delocalization onto the S representing an ionic π -bond between S and O.

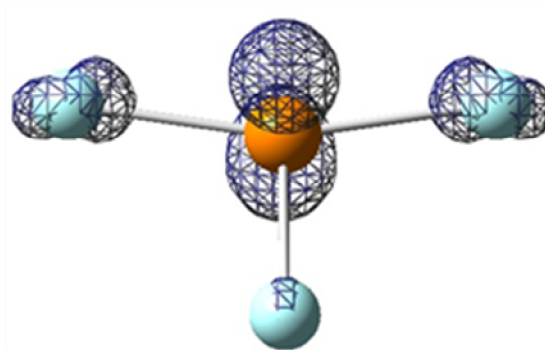
Table A10.8. Calculated MP2/aug-cc-pV(T+d)Z dipole moments (Debye) for SF_xO_y and PF_xO_y compounds.

Molecule	μ	Molecule	μ
PF	1.09	SF	1.14
PO	2.66	SO	1.90
PF ₂	1.29	SF ₂	1.35
PFO	2.42	SFO	1.94
PF ₃	1.22	SF ₃	0.88
PF ₂ O	2.27	SF ₂ O	2.06
		SFO ₂	1.45
PF ₄	0.74	SF ₄	0.80
PF ₃ O	2.05	SF ₃ O	1.44
		SF ₂ O ₂	1.22
PF ₅	0.00	SF ₅	0.49
		SF ₄ O	1.37
		SF ₆	0.00

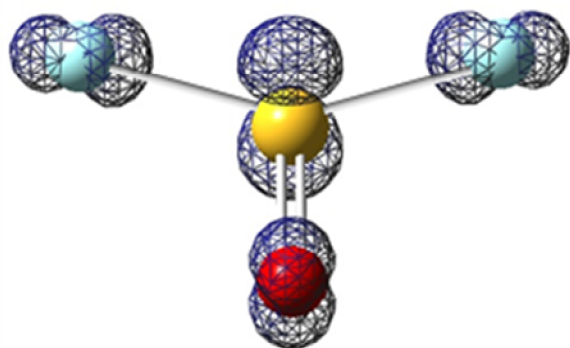
Triplet Spin Densities



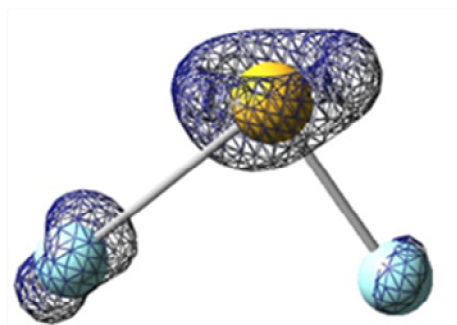
a



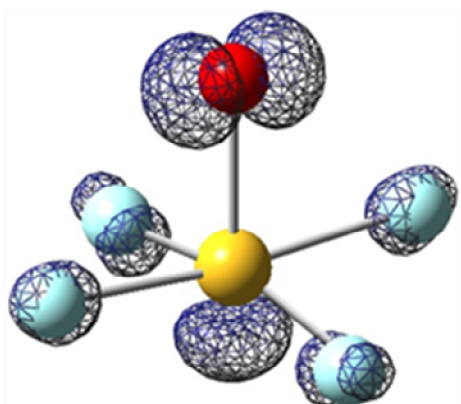
b



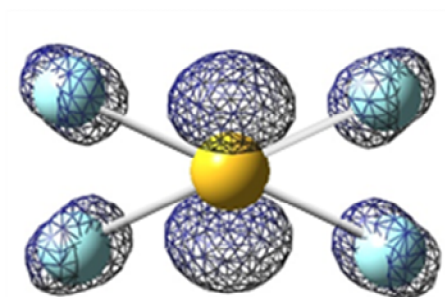
c



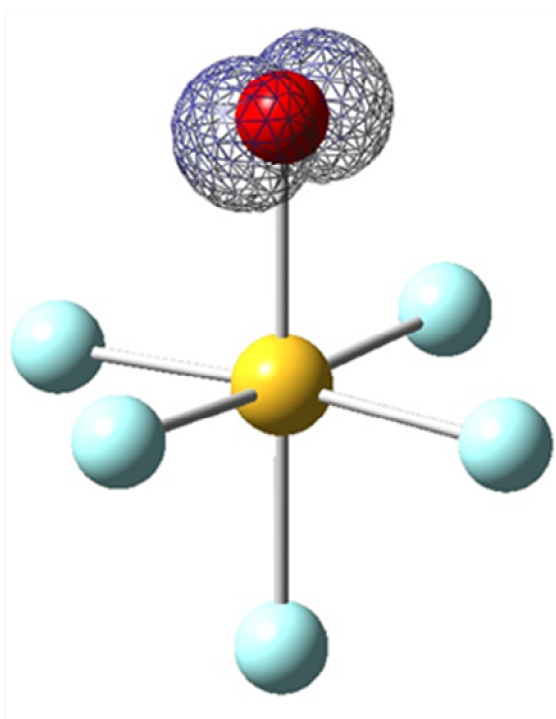
d



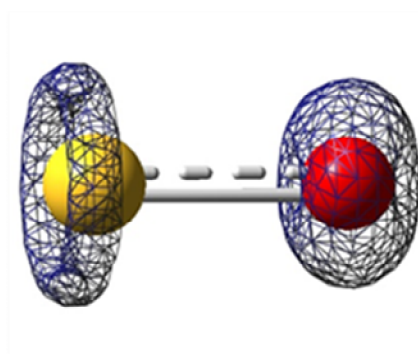
e



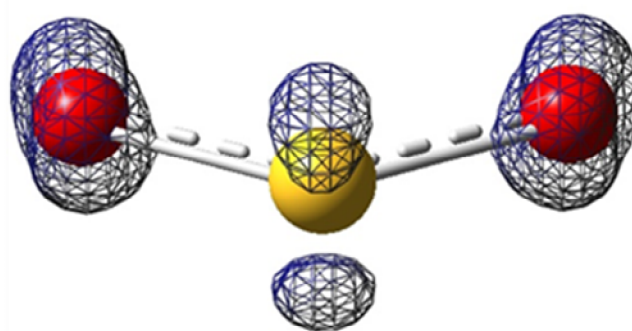
f



g

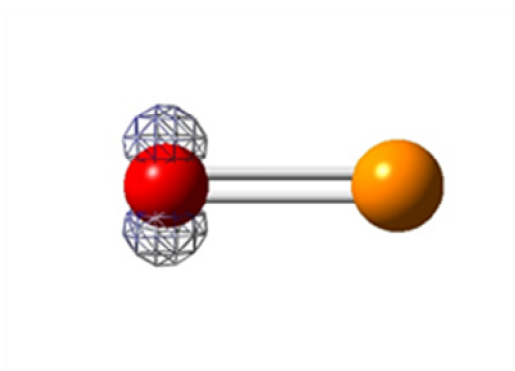


h

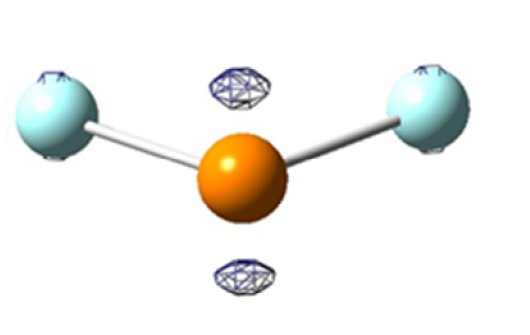


i

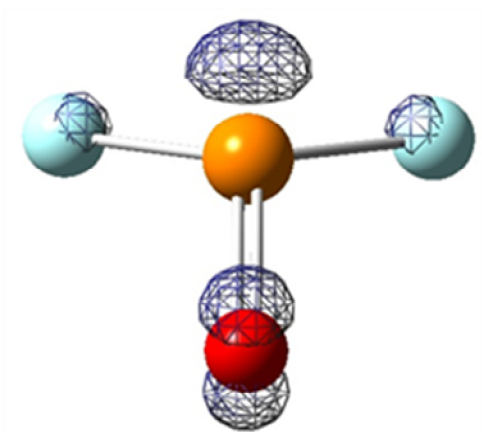
PF_xO Doublet Spin Densities



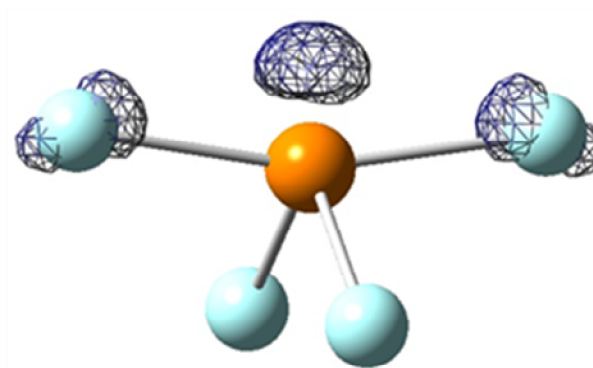
a



b

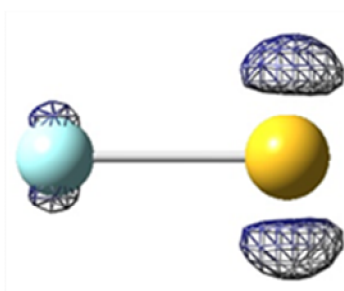


c

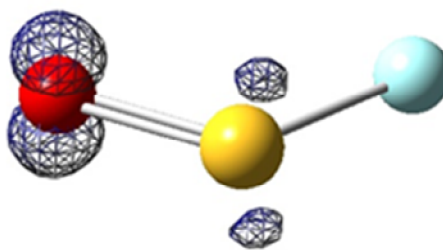


d

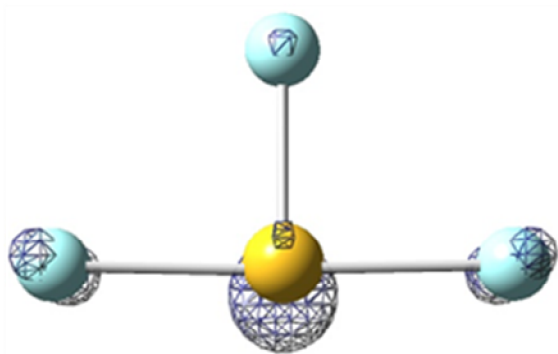
SF_xO_y Doublet Spin Densities



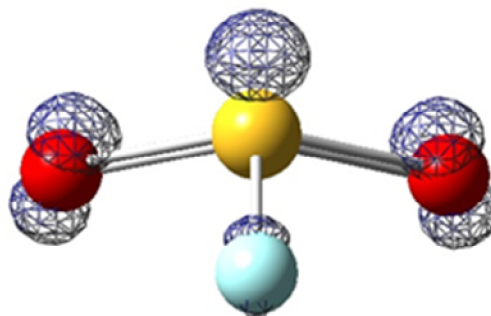
a



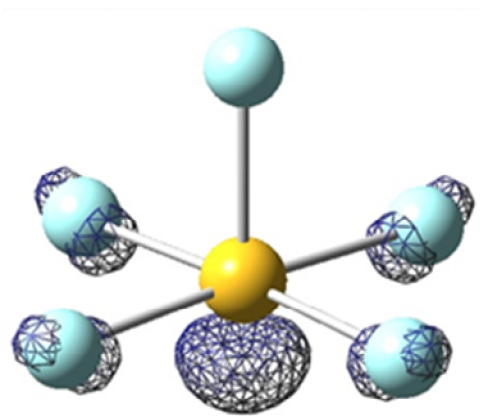
b



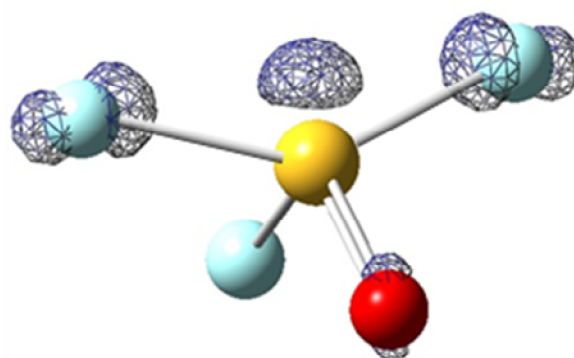
c



d



e



f

CHAPTER 11

CONCLUSIONS

There has been substantial interest in the discovery of potential molecules for chemical hydrogen storage systems in which hydrogen storage and release are near thermoneutral processes. In order to predict the thermodynamic properties of the potential hydrogen storage materials, namely their total atomization energies (TAE), heats of formation, bond dissociation energies (BDEs), hydride affinities (HA), fluoride affinities (FA), electron affinities (EA), and proton affinities (PA), within chemical accuracy of ± 1.0 kcal/mol, we have developed an additive combination method using *ab initio* molecular orbital theory at the frozen core CCSD(T) level in conjunction with the augmented correlation consistent basis sets.

In Chapter 3, the heats of formation for BH_3PH_3 , BH_2PH_2 , BPH_2 , AlH_3NH_3 , AlH_2NH_2 , AlH_2NH , AlH_3PH_3 , AlH_2PH_2 , AlH_2PH , AlH_4^- , PH_3 , PH_4 , and PH_4^+ ; the diatomics BP , AlN , and AlP ; and the salts $[\text{BH}_4^-][\text{PH}_4^+](\text{s})$, $[\text{AlH}_4^-][\text{NH}_4^+](\text{s})$, and $[\text{AlH}_4^-][\text{PH}_4^+](\text{s})$, which have been estimated by using a combined computational chemistry and empirical modeling expression for the lattice energy and the calculated heats of formation of the component ions, have been calculated. The calculations show that both $\text{AlH}_3\text{NH}_3(\text{g})$ and the $[\text{AlH}_4^-][\text{NH}_4^+](\text{s})$ salt can serve as good hydrogen storage systems, releasing H_2 in a slightly exothermic process and that $\text{AlH}_3\text{PH}_3(\text{g})$ and the $[\text{AlH}_4^-][\text{PH}_4^+]$ and $[\text{BH}_4^-][\text{PH}_4^+]$ salts also have the potential to serve as H_2 storage systems. The HA of AlH_3 , defined as $-\Delta\text{H}$ for the $\text{AlH}_3 + \text{H}^-$ reaction, is calculated to be 70.4 kcal/mol. The PA of PH_3 , defined as $-\Delta\text{H}$ for the $\text{PH}_3 + \text{H}^+$ reaction, is calculated to be

187.8 kcal/mol, in excellent agreement with the experimental value of 188 kcal/mol. In addition, PH_4 is calculated to be barely stable with respect to loss of hydrogen to form PH_3 .

In Chapter 4, the novel electronic structure of the isoelectronic borane amines has led to significant interest in their overall energetics in order to obtain an improved understanding of their chemistry in terms of stability, reactivity, and thermodynamic forces driving H_2 release. The σ - and π -bond strengths for the molecules BH_2NH_2 , BH_2PH_2 , AlH_2NH_2 , and AlH_2PH_2 have been calculated. The adiabatic π -bond energy is defined as the rotational barrier between the equilibrium ground state configuration and the C_s symmetry transition state for torsion about the A-X bond, while the intrinsic π -bond energy corresponds to the adiabatic rotational barrier that is corrected for the inversion barrier at N or P in the ground state and rotated transition state structures. The adiabatic σ -bond energy is defined as the adiabatic dissociation energy of $\text{AH}_2\text{XH}_2 \rightarrow \text{AH}_2 + \text{XH}_2$ in their ground states minus the adiabatic π -bond energy. The adiabatic σ -bond strengths for BH_2NH_2 , BH_2PH_2 , AlH_2NH_2 , and AlH_2PH_2 are 109.8, 98.8, 77.6, and 68.3 kcal/mol, respectively, and the corresponding adiabatic π -bond strengths are 29.9, 10.5, 9.2, and 2.7 kcal/mol, respectively.

In Chapter 5, we have predicted the thermodynamic properties including the heats of formations, bond dissociation energies, and dehydrogenation energies of the methyl-substituted ammonia borane at both B and N, as well as their dehydrogenated derivatives. The thermodynamic properties of the single methyl substituted compounds were calculated at the composite CCSD(T)/CBS level. The heats of formation of the dimethyl- and trimethyl-substituted ammonia boranes, their dehydrogenated derivatives, and various molecules involved in the different bond breaking processes, were predicted based on G3(MP2) isodesmic reaction schemes. The thermodynamics for dehydrogenation pathways show that dehydrogenation across

the B-N bond is more favorable as opposed to dehydrogenation across the B-C and N-C bonds. Methylation at N reduces the exothermicity of the dehydrogenation reaction and makes the reaction more thermoneutral, whereas methylation at B moves it further away from thermoneutral. Methyl substitution at N leads to increased stability of the B-N dative σ -bond whereas methyl substitution at B leads to decreased stability of the B-N dative σ -bond due to a combination of hyperconjugation and steric effects, which are stabilizing on N and destabilizing on B. Methyl substitution on N destabilizes the product ($\sigma + \pi$) binding energy, and assuming the N-H and B-H bonds are approximately equal, makes hydrogen elimination closer to thermoneutral. The second methyl substituent at N has an additive effect and leads to further stabilization of the B-N dative σ -bond and destabilization of the product ($\sigma + \pi$) binding energy, making dehydrogenation even more thermoneutral. In contrast, methylation at B destabilizes the B-N dative σ -bond and the product ($\sigma + \pi$) binding energy, making dehydrogenation further away from thermoneutral.

There is substantial interest in the energetics of substituted boranes, as intermediates in the regeneration cycle of spent fuel derived from ammonia borane. In Chapter 6, we predicted the B-X and B-H BDEs to provide insight into the reactivity and stability of these substituted borane compounds $H_{3-n}BX_n$ for ($X = F, Cl, Br, I, NH_2, OH, \text{ and } SH$), as well as the radicals derived from the various BDE processes. The calculated heats of formation are in excellent agreement with the available experimental data for the closed shell molecules, but show larger differences with the reported “experimental” values for the BX_2 radicals. The heats of formation of the BX_2 radicals were also calculated at the G3(MP2) level of theory, and the G3(MP2) values were in excellent agreement with the more accurate CCSD(T) values. On the basis of extensive comparisons with experiment for a wide range of compounds, our calculated CCSD(T) values

for these radicals should be good to ± 1.5 kcal/mol, and thus, are to be preferred over the experimental values. Comparing the various B-X adiabatic BDEs, we find that the B-F BDEs in the $\text{H}_{3-n}\text{BF}_n$ compounds and in $\text{BF} (^1\Sigma^+)$ are the largest. The second and third largest B-X BDEs in the $\text{H}_{3-n}\text{BX}_n$ and BX compounds are predicted for $\text{X} = \text{OH}$ and NH_2 , respectively. The substituents were found to have a minimal effect on the B-H BDEs in HBX_2 and H_2BX compared to the first B-H BDE of BH_3 . The differences in the adiabatic and diabatic BDEs, which are related to the reorganization energy in the product, were estimated from molecular singlet-triplet splittings, and account for the large fluctuations in the adiabatic BDEs observed, specifically for the BX_2 and HBX radicals, during the stepwise loss of the respective substituents.

In order to provide a further understanding of the chemistry of these substituted borane ($\text{BH}_{3-n}\text{X}_n$) compounds, we have calculated the hydride, fluoride, and X^- affinities, offering a unique measure of the Lewis acidity and providing insight into the reactivity and periodic behavior of the substituents, as described in Chapter 7. Although the H^- and F^- affinities differ somewhat in their magnitudes, they show very similar trends and are both suitable for judging the Lewis acidities of compounds. The only significant differences in their acidity strength orders are found for the boranes substituted with the strongly electron withdrawing and back donating F and OH ligands. The highest H^- and F^- affinities are found for BI_3 and the lowest ones for $\text{B}(\text{NH}_2)_3$. Within the boron trihalide series, the Lewis acidity increases monotonically with increasing atomic weight of the halogen, i.e., BI_3 is a considerably stronger Lewis acid than BF_3 . For the X^- affinities in the BX_3 , HBX_2 , and H_2BX series, the fluorides show the highest values, whereas the amino and mercapto compounds show the lowest ones. The HA and FA of the $\text{BH}_{3-n}\text{X}_n$ compounds exhibit linear correlations with the PA of X^- for most X ligands, except for F and

H. Therefore, since the PAs for a number of anions are known or readily calculated, the H^- or F^- affinity of the $\text{BH}_{3-n}\text{X}_n$ compounds with other X groups can be readily estimated. In addition, a detailed analysis of the various contributions to the strength of the Lewis acid shows the dominant effect in determining the magnitude of the acidity to be the strength of the BX_3^- -A bond. It has also been shown that BI_3 is a considerably stronger Lewis acid than BF_3 , and the main contributor to the relative differences in the Lewis acidities of BX_3 for X a halogen is the difference in the EA of BX_3 with a secondary contribution from the distortion energy of BX_3 from planar to pyramidal. The B-F BDE of $\text{X}_3\text{B-F}^-$ and the distortion energy from pyramidal to tetrahedral BX_3^- are of less importance in determining the relative acidities. Since the EA of BX_3 is strongly influenced by the charge density in the empty p_z LUMO of boron, the amount of π -back donation from the halogen to boron is crucial and explains why the Lewis acidity of BF_3 is significantly lower than those of BX_3 with X = Cl, Br, and I.

In Chapter 8, we have studied a potential class of chemical hydrogen storage materials based on diammoniosilane $\text{SiH}_4(\text{NH}_3)_2$ and predicted their thermodynamics for H_2 release. The edge inversion barrier of silane is predicted to be 88.9 kcal/mol, and a substantial amount, -63.6 kcal/mol, is recovered upon complexation with 2 NH_3 molecules, so that the diammoniosilane complex is only 25.6 kcal/mol above the separated reactants $\text{SiH}_4 + 2\text{NH}_3$. The diammoniosilane complex is a metastable species characterized by all real frequencies at the MP2/aV(T+d)Z level. We predict the heat of reaction for the sequential dehydrogenation of diammoniosilane to yield $\text{H}_3\text{Si}(\text{NH}_2)(\text{NH}_3)$ and $\text{H}_2\text{Si}(\text{NH}_2)_2$ to be exothermic by 33.6 and 12.2 kcal/mol, respectively, so the cumulative dehydrogenation reaction yielding two molecules of hydrogen is -45.8 kcal/mol. The sequential release of two molecules of H_2 from $\text{H}_2\text{Si}(\text{NH}_2)_2$, consequently yielding $\text{HN}=\text{SiH}(\text{NH}_2)$ and $\text{HN}=\text{Si}=\text{NH}$, are predicted to be largely endothermic reactions at 45.3 and

55.7 kcal/mol, respectively. However, if the endothermic reaction for the third step and the exothermic reactions for the release of the first two hydrogen molecules were coupled effectively, loss of three hydrogen molecules from $\text{H}_4\text{Si}(\text{NH}_3)_2$ would be almost thermoneutral at 0 K.

There is substantial interest in the energetics of silanes for use in regeneration schemes for chemical hydrogen storage systems. In Chapter 9, we have predicted the heats of formation of the SiH_3X , SiH_2XCH_3 , and $\text{SiH}_3\text{CH}_2\text{X}$ compounds and the various C-H, Si-H, Si-C, C-X, and Si-X (X = F, Cl, Br, and I) BDEs. Our results indicate that, except for methyl iodosilane, methyl substitution leads to an increase in the Si-X BDE when compared to the Si-X BDE in the halosilanes. Except for methyl iodosilane also, halide substitution leads to an increase in the Si-C BDE in comparison to the Si-C BDE in methylsilane of 86.9 kcal/mol. Unlike the methylhalosilanes, the halomethylsilanes all show a decrease in the Si-C BDE when compared to the Si-C BDE in methylsilane. The trends correlate with the electronegativity and covalent radii of the substituent.

In Chapter 10, we have investigated and expanded our understanding of chemical BDEs in second row compounds with high oxidation states beyond a normal Lewis octet, specifically PF_3 , PF_5 , PF_3O , SF_2 , SF_4 , SF_6 , SF_2O , SF_2O_2 , and SF_4O , as well as a number of radicals derived from these stable compounds through various bond breaking processes. The experimental BDEs are often not readily available due to difficulty in the measurements of such quantities, especially when radicals are formed in the bond breaking process; however, theoretically calculated BDEs allow for the prediction of a consistent set of values that substantially reduce the error limits for these species. A detailed comparison of adiabatic and diabatic BDEs is made and used to explain trends in the BDEs. Since the adiabatic BDEs of polyatomic molecules represent not only the

energy required for breaking a specific bond, but also contain any reorganization energies of the bonds in the resulting products, these adiabatic BDEs can be quite different for each step in the stepwise loss of ligands in binary compounds. For example, the adiabatic BDE for the removal of one fluorine ligand from the very stable closed shell SF_6 molecule to give the unstable SF_5 radical is 2.8 times the BDE needed for the removal of one fluorine ligand from the unstable SF_5 radical to give the stable closed shell SF_4 molecule. Similarly, the BDE for the removal of one fluorine ligand from the stable closed shell PF_3O molecule to give the unstable PF_2O radical is higher than the BDE needed to remove the oxygen atom to give the stable closed shell PF_3 molecule. The same principles govern the BDEs of the phosphorous fluorides and the sulfur oxofluorides. In polyatomic molecules, significant care must be exercised not to equate BDEs with the bond strengths of given bonds. The measurement of the bond strength or stiffness of a given bond represented by its force constant involves only a small displacement of the atoms near equilibrium and, therefore, does not involve any reorganization energies, i.e., it may be more appropriate to correlate with the diabatic product states when considering the stepwise loss of respective substituents.

References

-
- ¹ Grant, P. M. *Nature* **2003**, *424*, 129.
- ² U.S. Department of Energy Hydrogen Program. April 2006. www.hydrogen.energy.gov
- ³ U.S. Department of Energy Hydrogen Program. *Hydrogen Production*. March 2006. www.hydrogen.energy.gov
- ⁴ U.S. Department of Energy Hydrogen Program. *Hydrogen Safety*. April 2006. www.hydrogen.energy.gov
- ⁵ U.S. Department of Energy Hydrogen Program. *Hydrogen Storage*. May 2006. www.hydrogen.energy.gov
- ⁶ U.S. Department of Energy Hydrogen Program. *Hydrogen Fuel Cells*. July 2006. www.hydrogen.energy.gov
- ⁷ Petrucci, R. H.; Harwood, W. S. *General Chemistry: Principles and Modern Applications*. 7th Edition. Prentice-Hall, Inc. 1997.
- ⁸ U.S. Department of Energy. Energy Efficiency and Renewable Energy. Hydrogen, Fuel Cells, and Infrastructure Technologies Program. *Materials-based Hydrogen Storage*. September 2009. www.eere.energy.gov/hydrogenandfuelcells/storage/materials
- ⁹ U.S. Department of Energy Hydrogen Program. *Hydrogen Distribution and Delivery Infrastructure*. July 2006. www.hydrogen.energy.gov
- ¹⁰ U.S. Department of Energy. Energy Efficiency and Renewable Energy. Hydrogen, Fuel Cells, and Infrastructure Technologies Program. *Hydrogen Storage: Current Technology*. September 2006. www.eere.energy.gov/hydrogenandfuelcells/storage/current_technology
- ¹¹ Lewis, N. S. *Engineering. and Science* **2007**, *2*, 13.
- ¹² “Basic Energy Needs for the Hydrogen Economy,” Dresselhaus, M.; Crabtree, G.; Buchanan, M., Eds., Basic Energy Sciences, Office of Science, U.S. Department of Energy, Washington, D.C., 2003; Maelund, A.J.; Hauback, B.C. in “Advanced Materials for the Energy Conversion II,” Ed. Chandra, D.; Bautista, R.G.; Schlapbach, L. The Minerals, Metals and Material Society, 2004.
- ¹³ Stephens, F. H.; Pons, V.; Baker, R. T. *Dalton Trans.* **2007**, 2613
- ¹⁴ Karkamkar, A. J., Aardahl, C. L.; Autrey, T. *Material Matters* **2007**, *2*, 6.

-
- ¹⁵ (a) Wolf, G.; van Miltenburg, R. A.; Wolf, U. *Thermochim. Acta* **1998**, *317*, 111. (b) Wolf, G.; Baumann, J.; Baitalow, F.; Hoffmann, F. P. *Thermochim. Acta* **2000**, *343*, 19. (c) Baitalow, F.; Baumann, J.; Wolf, G.; Jaenicke-Rlobler, K.; Leitner, G. *Thermochim. Acta* **2002**, *391*, 159.
- ¹⁶ Parvanov, V. M.; Schenter, G. K.; Hess, N. J.; Daemen, L. L.; Hartl, A.; Stowe, A. C.; Camaioni, D. M.; Autrey, T. *Dalton Trans.* **2008**, 4514.
- ¹⁷ Stowe, A. C.; Shaw, W. J.; Linehan, J. C.; Schmid, B.; Autrey, T. *Phys. Chem. Chem. Phys.* **2007**, *9*, 1831.
- ¹⁸ Shaw, W. J.; Linehan, J. C.; Szymczak, N. K.; Heldebrant, D. J.; Yonker, C.; Camaioni, D. M.; Baker, R. T.; Autrey, T. *Angew. Chem. Int. Ed.* **2008**, *47*, 7493.
- ¹⁹ Stephens, F. H.; Baker, R. T.; Matus, M. H.; Grant, D. J.; Dixon, D. A. *Angew Chem. Int. Ed.*, **2007**, *46*, 746.
- ²⁰ Pons, V.; Baker, R. T.; Szymczak, N. K.; Heldebrant, D. J.; Linehan, J. C.; Matus, M. H.; Grant, D. J.; Dixon, D. A. *Chem Comm.* **2008**, 6597.
- ²¹ Gutowska, A.; Li, L.; Shin, Y.; Wang, Ch.; Li, S.; Linehan, J.; Smith, R. S.; Kay, B.; Schmid, B.; Shaw, W.; Gutowski, M.; Autrey, T. *Angew. Chem. Int. Ed.* **2005**, *44*, 2.
- ²² Parry, R. W.; Schultz, D. R.; Girardot, P. R. *J. Am. Chem. Soc.* **1958**, *80*, 1.
- ²³ Sorokin, V. P.; Vesina, B. I.; Klimova, N. S. *Russ. J. Inorg. Chem.* **1963**, *8*, 32.
- ²⁴ Dixon, D. A.; Gutowski, M. *J. Phys. Chem. A* **2005**, *109*, 5129.
- ²⁵ Klooster, W. T.; Koetzle, T. F.; Siegbahn, P. E. M.; Richardson, T. B.; Crabtree, R. H. *J. Am. Chem. Soc.* **1999**, *121*, 6337.
- ²⁶ Morrison, C. A.; Siddick, M. M. *Angew. Chem.-Int. Edit.* **2004**, *43*, 4780.
- ²⁷ Richardson, T. B.; de Gala, S.; Crabtree, R. H.; Siegbahn, P. E. M. *J. Am. Chem. Soc.* **1995**, *117*, 12875.
- ²⁸ Pauling, L. *General Chemistry*; Dover Publications: New York, **1988**; p 182.
- ²⁹ Karkamkar, A.; Kathmann, S. M.; Schenter, G. K.; Heldebrant, D. J.; Hess, N. Gutowski, M.; Autrey T. *Chem. Mater.* **2009**, *21*, 4356.
- ³⁰ Wolf, G.; Baumann, J.; Baitalow, F.; Hoffman, F. P. *Thermochim. Acta* **2000**, *343*, 19.
- ³¹ Amendola, S. C.; Sharp-Goldman, S. L.; Janjua, M. S.; Spencer, N. C.; Kelly, M. T.; Petillo, P. J.; Binder, Michael. *Int. J. Hydrogen Energy*, 2000, *25*, 969.

-
- ³² Gutowska, A.; Li, L.; Shin, Y.; Wang, Ch.; Li, S.; Linehan, J.; Smith, R. S.; Kay, B.; Schmid, B.; Shaw, W.; Gutowski, M.; Autrey, T. *Angew. Chem. Int. Ed.*, **2005**, *44*, 2.
- ³³ Dixon, D. A.; Grant, D. J. *J. Phys. Chem. A* **2005**, *109*, 10138.
- ³⁴ Sander, S. P.; Friedl, R. R.; Ravishankara, A. R.; Golden, D. M.; Kolb, C. E.; Kurylo, M. J.; Huie, R. E.; Orkin, V. L.; Molina, M. J.; Moortgat, G. K.; Finlayson-Pitts, B. J. *Chemical Kinetics and Photochemical Data for Use in Atmospheric Studies: Evaluation Number 14*; JPL Publication 02-25, National Aeronautics and Space Administration, Jet Propulsion Laboratory, California Institute of Technology: Pasadena, California 2003.
http://jpldataeval.jpl.nasa.gov/pdf/JPL_02-25_rev02.pdf.
- ³⁵ Ervin, K.M.; Gronert, S.; Barlow, S.E.; Gilles, M.K.; Harrison, A.G.; Bierbaum, V.M.; DePuy, C.H.; Lineberger, W.C.; Ellison, G.B. *J. Am. Chem. Soc.* **1990**, *112*, 5750.
- ³⁶ Schimdt, M. W.; Truong, P. N.; Gordon, M. S. *J. Am. Chem. Soc.* **1987**, 5217.
- ³⁷ Ervin, K. M.; Gronert, S.; Barlow, S. E.; Gilles, M. K.; Harrison, A. G.; Bierbaum, V. M.; DePuy, C. H.; Lineberger, W. C.; Ellison, G. B. *J. Am. Chem. Soc.* **1990**, *112*, 5750.
- ³⁸ Nguyen, M. T.; Matus, M. H.; Lester, Jr., W. A.; Dixon, D. A. *J. Phys. Chem. A*, **2008**, *112*, 2082.
- ³⁹ Douglas, J. E.; Rabinovitch, B. S.; Looney, F. S. *J. Chem. Phys.* **1955**, *23*, 315.
- ⁴⁰ (a) Geanangel, R. A.; Shore, S. G. *Prep. Inorg. React.* **1966**, *3*, 123; (b) Framery, E.; Vaultier, M. *Heteroatom Chem.* **2000**, *11*, 218; (c) See also Lane, C.F. *Ammonia-Borane and Related N-B-H Compounds and Materials: Safety Aspects, Properties and Applications*, (2005).
http://www1.eere.energy.gov/hydrogenandfuelcells/pdfs/nbh_h2_storage_survey.pdf
- ⁴¹ Lane, C.; Baker, S.; "Applied Research on the Use of Amine-Borane Materials for Hydrogen Storage," DOE Hydrogen Program Annual Merit Review, Project ID # STP8, May 2007, Arlington, Va. http://www.hydrogen.energy.gov/pdfs/review07/stp_8_lane.pdf; Lane, C. F., "Safety Analysis and Applied Research on the Use of Borane-Amines for Hydrogen Storage," DOE Hydrogen Program Annual Progress Report, Contract No. DE-FC36-05GO15060, November 2007, Washington, D.C.
http://www.hydrogen.energy.gov/pdfs/progress07/iv_b_5j_lane.pdf
- ⁴² Grant, D. J.; Dixon, D. A. *J. Phys. Chem. A* **2006**, *110*, 12955.
- ⁴³ Matus, M. H.; Anderson, K. A.; Camaioni, D. M.; Autrey, S. T.; Dixon, D. A. *J. Phys. Chem. A* **2007**, *111*, 4411.
- ⁴⁴ Luo, T.-R. *Comprehensive Handbook of Chemical Bond Energies*; CRC Press, Taylor & Francis Group: Boca Raton, FL, 2007.

-
- ⁴⁵ Grant, D. J.; Matus, M. H.; Switzer, J. S.; Dixon, D. A.; Francisco, J. S.; Christe, K. O. *J. Phys. Chem., J. Phys. Chem. A.*, **2008**, *112*, 3145.
- ⁴⁶ Christe, K. O.; Dixon, D. A.; McLemore, D.; Wilson, W. W.; Sheehy, J. A.; Boatz, J. A., *J. Fluor. Chem.* **2000**, *101*, 151.
- ⁴⁷ Vianello, R.; Maccic, Z. B. *Inorg. Chem.* **2005**, *44*, 1095, and references cited therein.
- ⁴⁸ Dixon, D. A.; Arduengo III, A. J., *J. Phys. Chem.* **1987**, *91*, 3195.
- ⁴⁹ Dixon, D. A.; Arduengo III, A. J. *Inter. J. Quant. Chem: Quant. Chem. Symp.* **1988**, *22*, 85.
- ⁵⁰ Dunning, T.H., Jr. *J. Phys. Chem.* **2000**, *104*, 9062.
- ⁵¹ (a) Peterson, K. A.; Xantheas, S. S.; Dixon, D. A.; Dunning, T. H. Jr., *J. Phys. Chem. A.* **1998**, *102*, 2449; (b) Feller, D.; Peterson, K. A. *J. Chem. Phys.* **1998**, *108*, 154; (c) Dixon, D. A.; Feller, D. *J. Phys. Chem. A* **1998**, *102*, 8209; (d) Feller, D.; Peterson, K. A. *J. Chem. Phys.* **1999**, *110*, 8384; (e) Feller, D.; Dixon, D. A. *J. Phys. Chem. A* **1999**, *103*, 6413; (f) Feller, D. *J. Chem. Phys.* 1999, *111*, 4373; (g) Feller, D.; Dixon, D. A. *J. Phys. Chem. A* **2000**, *104*, 3048; (h) Feller, D.; Sordo, J. A. *J. Chem. Phys.* **2000**, *113*, 485; (i) Feller, D.; Dixon, D. A. *J. Chem. Phys.* **2001**, *115*, 3484; (j) Dixon, D. A.; Feller, D.; Sandrone, G. *J. Phys. Chem. A* **1999**, *103*, 4744; (k) Ruscic, B.; Wagner, A. F.; Harding, L. B.; Asher, R. L.; Feller, D.; Dixon, D. A.; Peterson, K. A.; Song, Y.; Qian, X.; Ng, C.; Liu, J.; Chen, W.; Schwenke, D. W. *J. Phys. Chem. A* **2002**, *106*, 2727; (l) Feller, D.; Dixon, D.A.; Peterson, K.A. *J. Phys. Chem. A*, **1998**, *102*, 7053; (m) Dixon, D.A.; Feller, D. ; Peterson, K.A. *J. Chem. Phys.*, **2001**, *115*, 2576; (n) Feller, D.; Dixon, D. A., *J. Phys. Chem. A*, **2003**, *107*, 9641 (o) Dixon, D.A.; Feller, D.; Christe, K. O.; Wilson, W. W.; Vij, A.; Vij, V.; Jenkins, H. D. B.; Olson, R. M.; Gordon, M. S. *J. Am. Chem. Soc.*, **2004**, *126*, 834; (p) Dixon, D. A.; Gutowski, M. *J. Phys. Chem. A*, **2005**, *109*, 5129; (q) Pollack, L.; Windus, T. L.; de Jong, W. A.; Dixon, D.A. *J. Phys. Chem. A*, **2005**, *109*, 6934 (r) Feller, D.; Peterson, K.A.; Dixon, D.A. *J. Chem. Phys.*, **2008**, *129*, 204015.
- ⁵² Purvis III, G.D.; Bartlett, R.J. *J. Chem. Phys.* **1982**, *76*, 1910.
- ⁵³ Raghavachari, K.; Trucks, G. W.; Pople, J. A.; Head-Gordon, M. *Chem. Phys. Lett.* **1989**, *157*, 479.
- ⁵⁴ Watts, J. D.; Gauss, J.; Bartlett, R. J. *J. Chem. Phys.* **1993**, *98*, 8718.
- ⁵⁵ Dunning, T. H. *J. Chem. Phys.* **1989**, *90*, 1007.
- ⁵⁶ Kendall, R. A.; Dunning Jr., T. H.; Harrison, R. J. *J. Chem. Phys.* **1992**, *96*, 6796.
- ⁵⁷ Peterson, K. A.; Woon, D. E.; Dunning, T. H., Jr. *J. Chem. Phys.* **1994**, *100*, 7410.
- ⁵⁸ McQuarrie, D. A. *Statistical Mechanics*, University Science Books: Sausalito, CA, 2001.

-
- ⁵⁹ Curtiss, L. A.; Raghavachari, K.; Redfern, P. C.; Pople, J. A. *J. Chem. Phys.* **1997**, *106*, 1063.
- ⁶⁰ Born, M.; Oppenheimer, J. R. *Ann. Phys.* **1927**, *70*, 361.
- ⁶¹ Cramer, C. J. *Essentials of Computational Chemistry. Theories and Models*, John Wiley & Sons Ltd., England, 2002.
- ⁶² Hehre, W. J.; Stewart, R. F.; Pople, J. A. *J. Chem. Phys.* **1969**, *51*, 2657.
- ⁶³ Huzinaga, S. *J. Chem. Phys.* **1965**, *42*, 1293; Dunning, T. H. *J. Chem. Phys.* **1971**, *55*, 716.
- ⁶⁴ Almlöf, J.; Taylor, P. R. *J. Chem. Phys.* **1990**, *92*, 551; Almlöf, J.; Taylor, P. R. *Adv. Quantum. Chem.* **1991**, *22*, 301.
- ⁶⁵ Dunning, T. H. Jr., Peterson, K. A. Wilson, A. K. *J. Chem. Phys.* **2001**, *114*, 9244.
- ⁶⁶ (a) Peterson, K. A.; Dunning, T. H., Jr., *J. Chem. Phys.* **2002**, *117*, 10548; (b) Woon, D. E.; Dunning, T. H., Jr., *J. Chem. Phys.* **1993**, *98*, 1358.
- ⁶⁷ (a) Peterson, K. A. *J. Chem. Phys.* **2003**, *119*, 11099; (b) Peterson, K. A.; Figgien, D.; Goll, E.; Stoll, H.; Dolg, M. *J. Chem. Phys.* **2003**, *119*, 11113.
- ⁶⁸ Dixon, D. A.; Grant, D. J.; Christie, K. O.; Peterson, K. A. *Inorg. Chem.* **2008**, *47*, 5485
- ⁶⁹ Pople, J. A.; Seeger, R.; Krishnan, R. *Int. J. Quant. Chem. Symp.* **1977**, *11*, 149; Krishnan, R.; Schlegel, H. B.; Pople, J. A. *J. Chem. Phys.* **1980**, *72*, 4654; Raghavachari, K.; Pople, J. A. *Int. J. Quant. Chem.* **1981**, *20*, 167.
- ⁷⁰ Møller, C.; Plesset, M. S. *Phys. Rev.* **1934**, *46*, 618; Pople, J. A.; Binkley, J. S.; Seeger, R. *Int. J. Quantum Chem. Symp.* **1976**, *10*, 1.
- ⁷¹ Schaeffer, H.F., III, *The Electronic Structure of Atoms and Molecules: A Survey of Rigorous Quantum Mechanical Results*, Addison-Wesley, Reading MA 1972, p. 10.
- ⁷² Werner, H.-J.; Knowles, P. J.; Amos, R. D.; Bernhardsson, A.; Berning, A.; Celani, P.; Cooper, D. L.; Deegan, M. J. O.; Dobbyn, A. J.; Eckert, F.; Hampel, C.; Hetzer, G.; Korona, T.; Lindh, R.; Lloyd, A. W.; McNicholas, S. J.; Manby, F. R.; Meyer, W.; Mura, M. E.; Nicklass, A.; Palmieri, P.; Pitzer, R. M.; Rauhut, G.; Schütz, M.; Stoll, H.; Stone, A. J.; Tarroni, R.; Thorsteinsson, T. MOLPRO-2002, a package of initio programs written by, Universität Stuttgart, Stuttgart, Germany, University of Birmingham, Birmingham, United Kingdom, 2002.
- ⁷³ Rittby, M.; Bartlett, R. J. *J. Phys. Chem.* **1988**, *92*, 3033.
- ⁷⁴ Knowles, P. J.; Hampel, C.; Werner, H.-J. *J. Chem. Phys.* **1994**, *99*, 5219.

-
- ⁷⁵ Deegan, M. J. O.; Knowles, P. J. *Chem. Phys. Lett.* **1994**, *227*, 321.
- ⁷⁶ Dunham, J. L. *Phys. Rev.* **1932**, *41*, 721.
- ⁷⁷ Gaussian 03, Revision C.02, Frisch, M. J.; Trucks, G. W.; Schlegel, H. B.; Scuseria, G. E.; Robb, M. A.; Cheeseman, J. R.; Montgomery, Jr., J. A.; Vreven, T.; Kudin, K. N.; Burant, J. C.; Millam, J. M.; Iyengar, S. S.; Tomasi, J.; Barone, V.; Mennucci, B.; Cossi, M.; Scalmani, G.; Rega, N.; Petersson, G. A.; Nakatsuji, H.; Hada, M.; Ehara, M.; Toyota, K.; Fukuda, R.; Hasegawa, J.; Ishida, M.; Nakajima, T.; Honda, Y.; Kitao, O.; Nakai, H.; Klene, M.; Li, X.; Knox, J. E.; Hratchian, H. P.; Cross, J. B.; Bakken, V.; Adamo, C.; Jaramillo, J.; Gomperts, R.; Stratmann, R. E.; Yazyev, O.; Austin, A. J.; Cammi, R.; Pomelli, C.; Ochterski, J. W.; Ayala, P. Y.; Morokuma, K.; Voth, G. A.; Salvador, P.; Dannenberg, J. J.; Zakrzewski, V. G.; Dapprich, S.; Daniels, A. D.; Strain, M. C.; Farkas, O.; Malick, D. K.; Rabuck, A. D.; Raghavachari, K.; Foresman, J. B.; Ortiz, J. V.; Cui, Q.; Baboul, A. G.; Clifford, S.; Cioslowski, J.; Stefanov, B. B.; Liu, G.; Liashenko, A.; Piskorz, P.; Komaromi, I.; Martin, R. L.; Fox, D. J.; Keith, T.; Al-Laham, M. A.; Peng, C. Y.; Nanayakkara, A.; Challacombe, M.; Gill, P. M. W.; Johnson, B.; Chen, W.; Wong, M. W.; Gonzalez, C.; and Pople, J. A.; Gaussian, Inc., Wallingford CT, 2004.
- ⁷⁸ Peterson, K. A.; Dunning, T. H., Jr., *J. Chem. Phys.* **2002**, *117*, 10548.
- ⁷⁹ Moore, C. E. "Atomic energy levels as derived from the analysis of optical spectra, Volume 1, H to V," U.S. National Bureau of Standards Circular 467, U.S. Department of Commerce, National Technical Information Service, COM-72-50282, Washington, D.C.; **1949**.
- ⁸⁰ Davidson, E. R.; Ishikawa, Y.; Malli, G. L. *Chem. Phys. Lett.* **1981**, *84*, 226.
- ⁸¹ (a) Douglas, M.; Kroll, N. M. *Ann. Phys.* **1974**, *82*, 89-155. (b) Hess, B. A. *Phys. Rev. A* **1985**, *32*, 756-763. (c) Hess, B. A. *Phys. Rev. A* **1986**, *33*, 3742-3748.
- ⁸² de Jong, W. A.; Harrison, R. J.; Dixon, D. A. *J. Chem. Phys.* **2001**, *114*, 48.
- ⁸³ EMSL basis set library. <http://www.emsl.pnl.gov/forms/basisform.html>
- ⁸⁴ Chase, M.W., Jr.; NIST-JANAF Tables (4th Edition), *J. Phys. Chem. Ref. Data*, Mono. 9, Suppl. 1, 1998.
- ⁸⁵ Karton, A.; Martin, J. M. L. *J. Phys. Chem. A* **2007**, *111*, 5936.
- ⁸⁶ Storms E.; Mueller, B. *J. Phys. Chem.* **1977**, *81*, 318.
- ⁸⁷ Ruscic, B.; Mayhew, C. A.; Berkowitz, J. *J. Chem. Phys.* **1988**, *88*, 5580.
- ⁸⁸ Martin, J. M. L.; Taylor, P. R. *J. Phys. Chem. A* **1998**, *102*, 2995.

⁸⁹ Cox, J. D.; Wagman, D. D.; Medvedev, V. A. *CODATA Key Values for Thermodynamics*, Hemisphere Publishing Corp., New York, 1989.

⁹⁰ Gurvich, L. V.; Veyts, I. V.; Alcock, C. B. *Thermodynamic Properties of Individual Substances*, Vol. 3, Begell House, New York, 1996.

⁹¹ Feller, D.; Dixon, D.A. *J. Phys. Chem. A* **1999**, *103*, 6413.